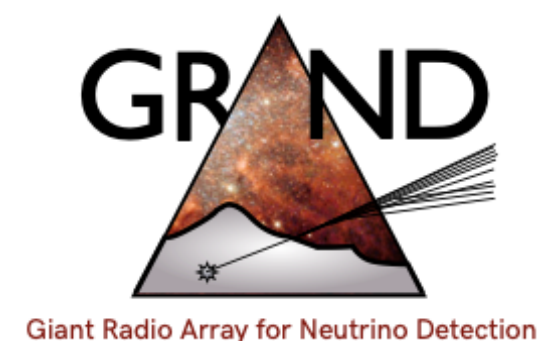
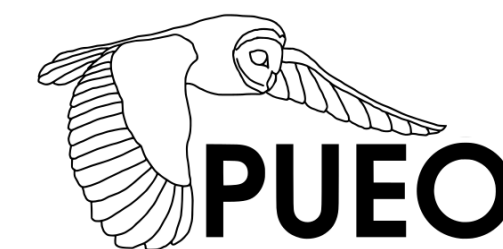
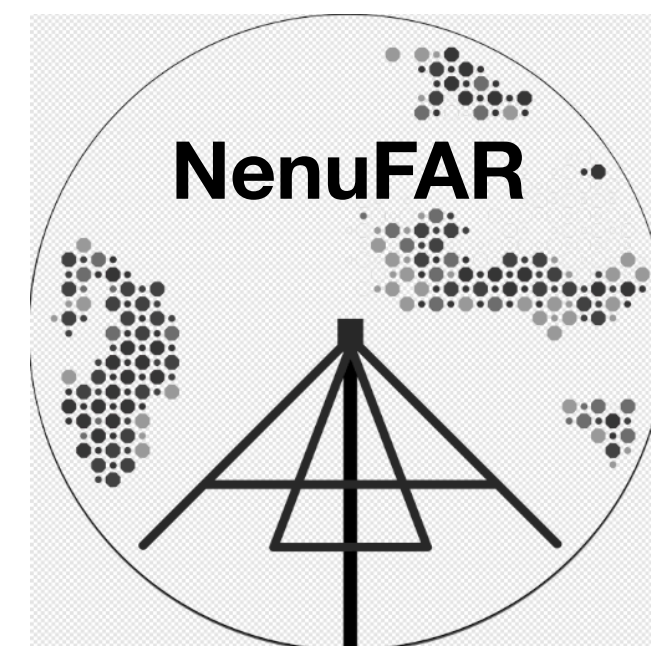
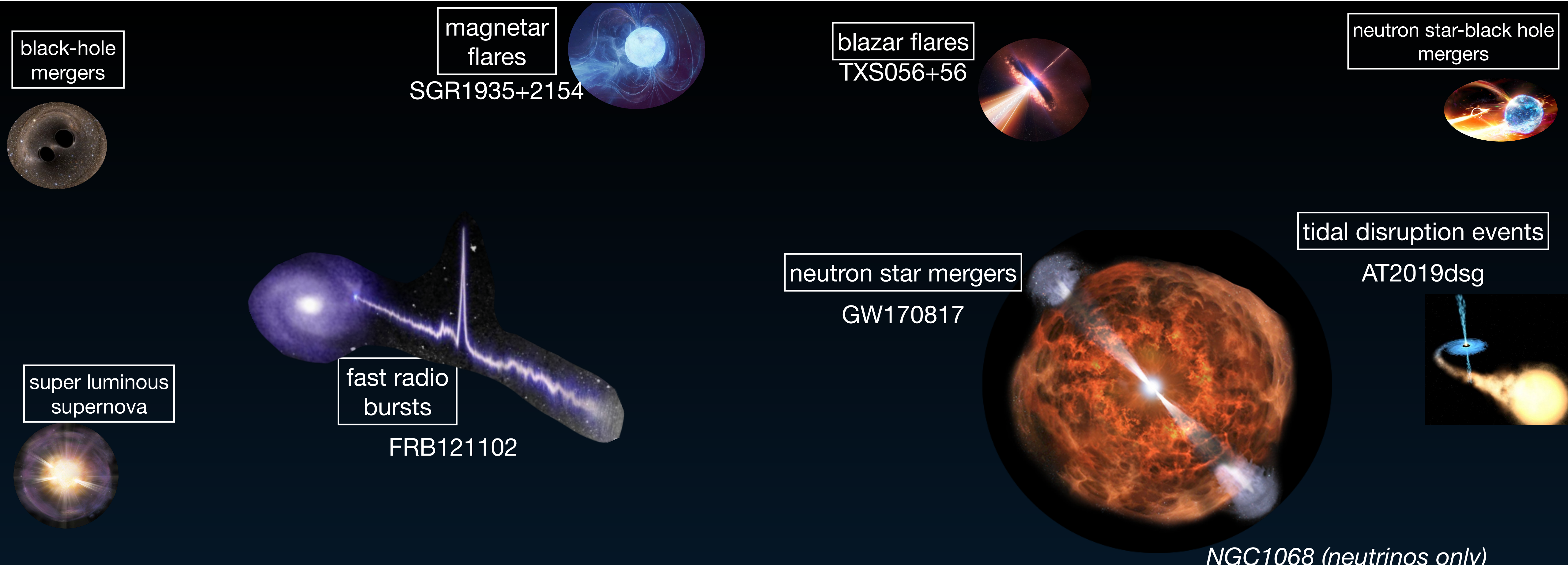


# Sources and detection of high-energy cosmic events: a journey through neutrinos and fast radio bursts.





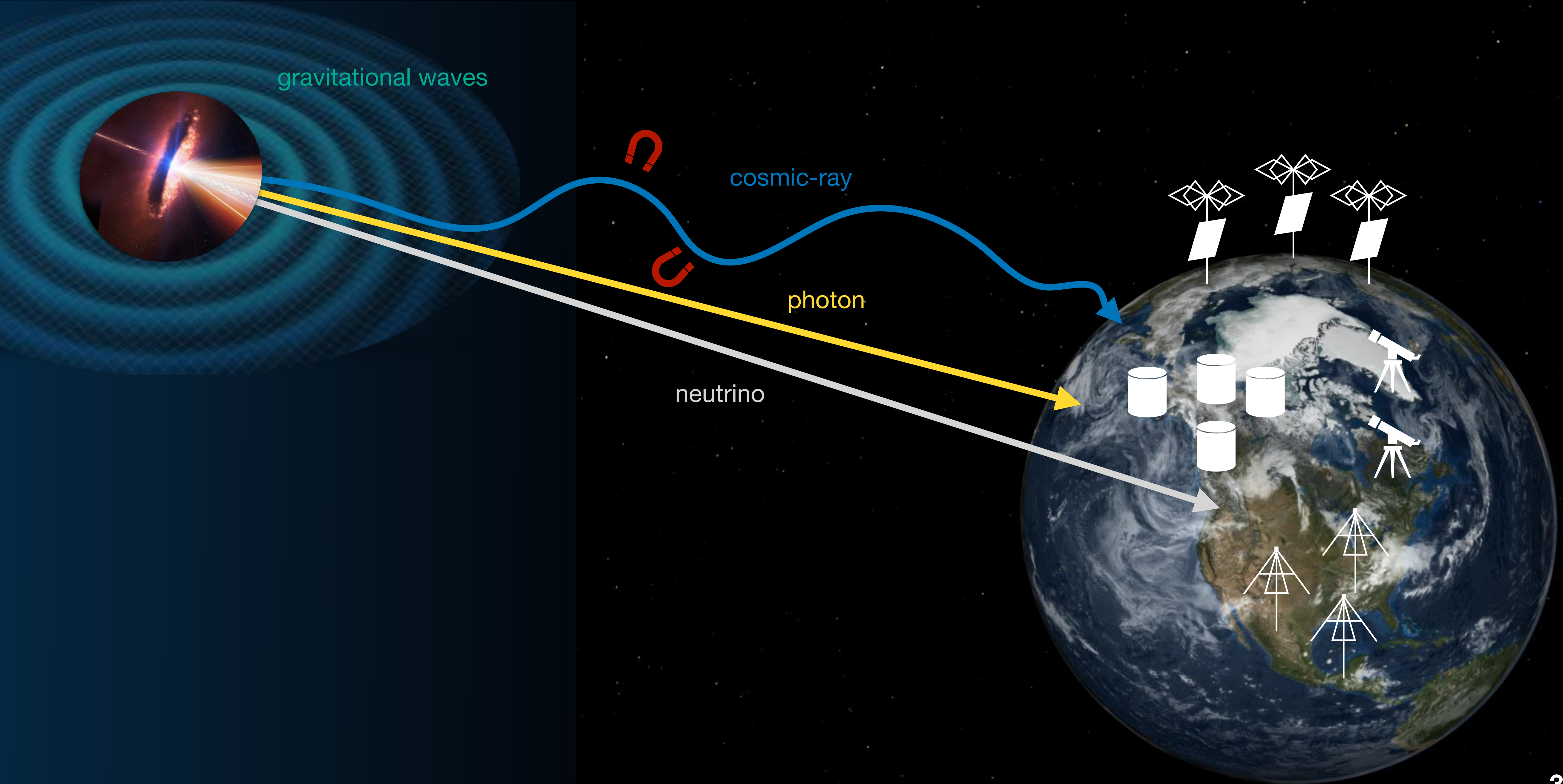
# The high-energy Universe and the advent of multimessenger astronomy



TXS0506+056  
NGC1068 (neutrinos only)



# Multi-messenger astronomy





# The cosmic neutrino enigma

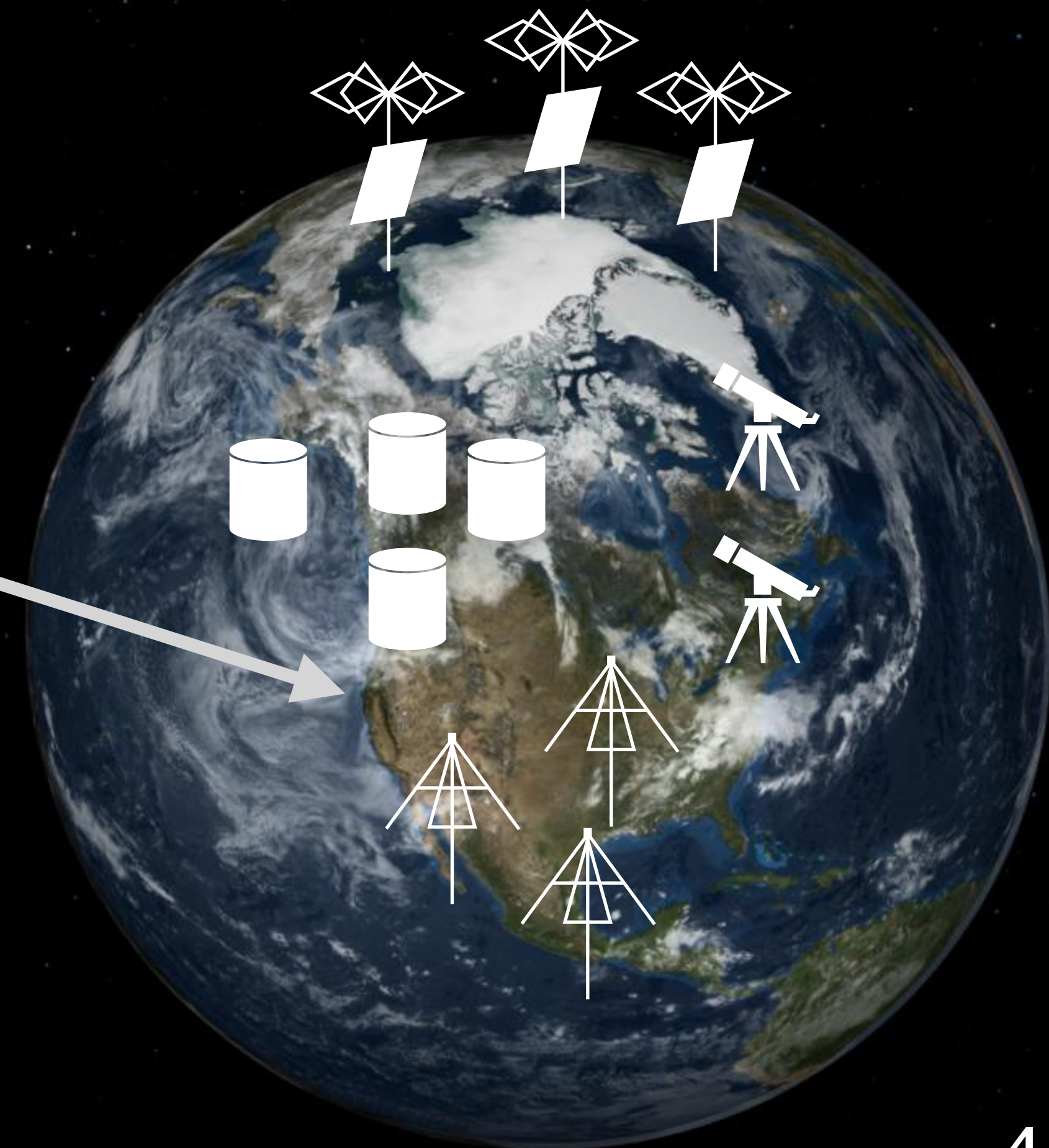
in the high-energy and ultra high-energy regime

Neutrinos pros:

- low cross section  $\rightarrow$  low interaction length  $\rightarrow$  astronomy
- neutral  $\rightarrow$  not deflected by B-fields  $\rightarrow$  astronomy
- hadronic processes  $\rightarrow$  good probe of high energy processes



$\nu$





# The cosmic neutrino enigma

in the high-energy and ultra high-energy regime



Neutrinos pros:

- low cross section  $\rightarrow$  low interaction length  $\rightarrow$  astronomy
- neutral  $\rightarrow$  not deflected by B-fields  $\rightarrow$  astronomy
- hadronic processes  $\rightarrow$  good probe of high energy processes

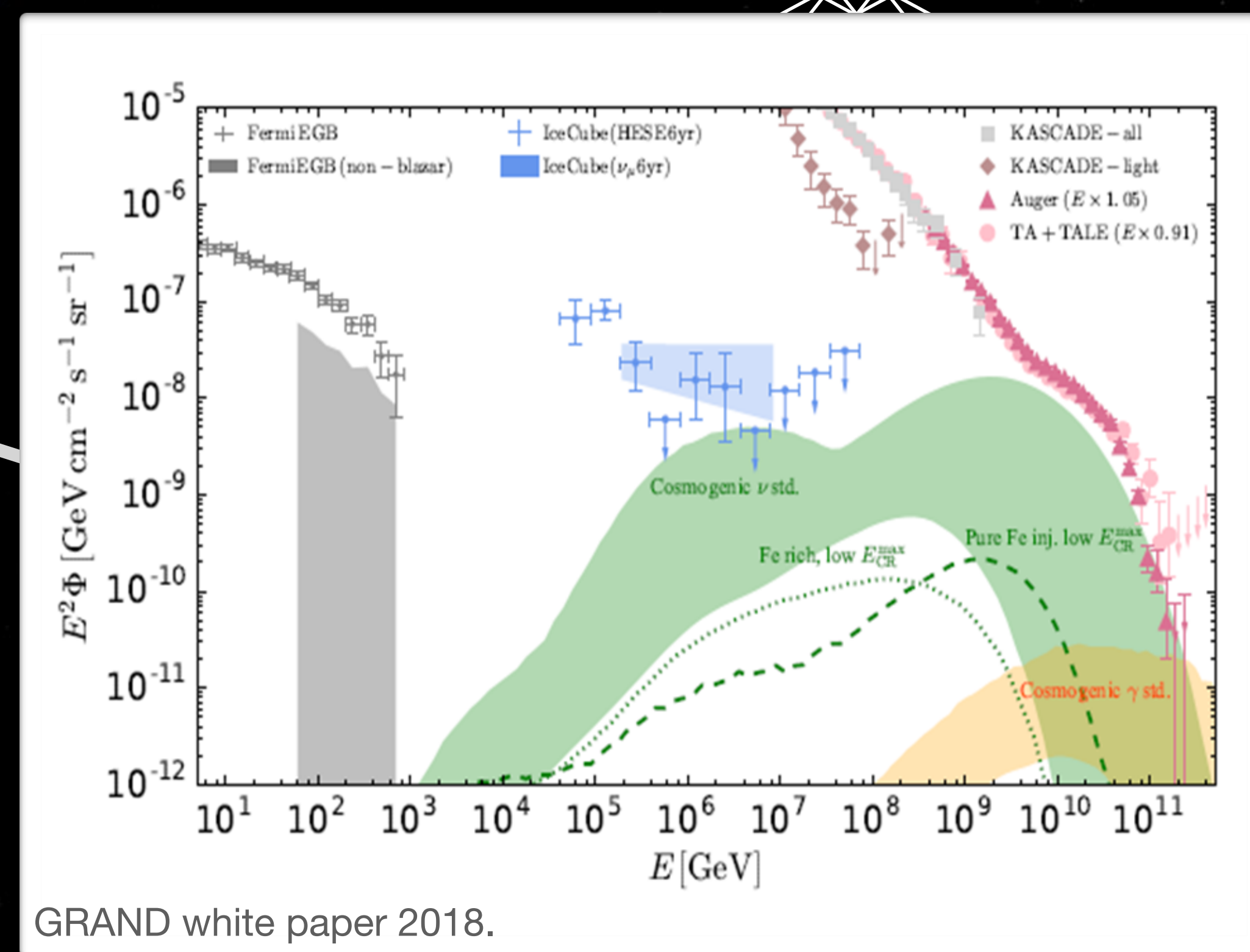
$\nu$

## • Sources?

- what are the sources of observed neutrinos?
- what could be the sources of more energetic neutrinos?
- can we detect neutrinos from new transients events?

## • How to detect them?

- new generation of detector?
- detector optimisation?
- reconstruction methods?





# Is GW170817 a neutrino source ?

- highly energetic  $L \approx 10^{52} \text{ erg.s}^{-1}$
- high baryon loading

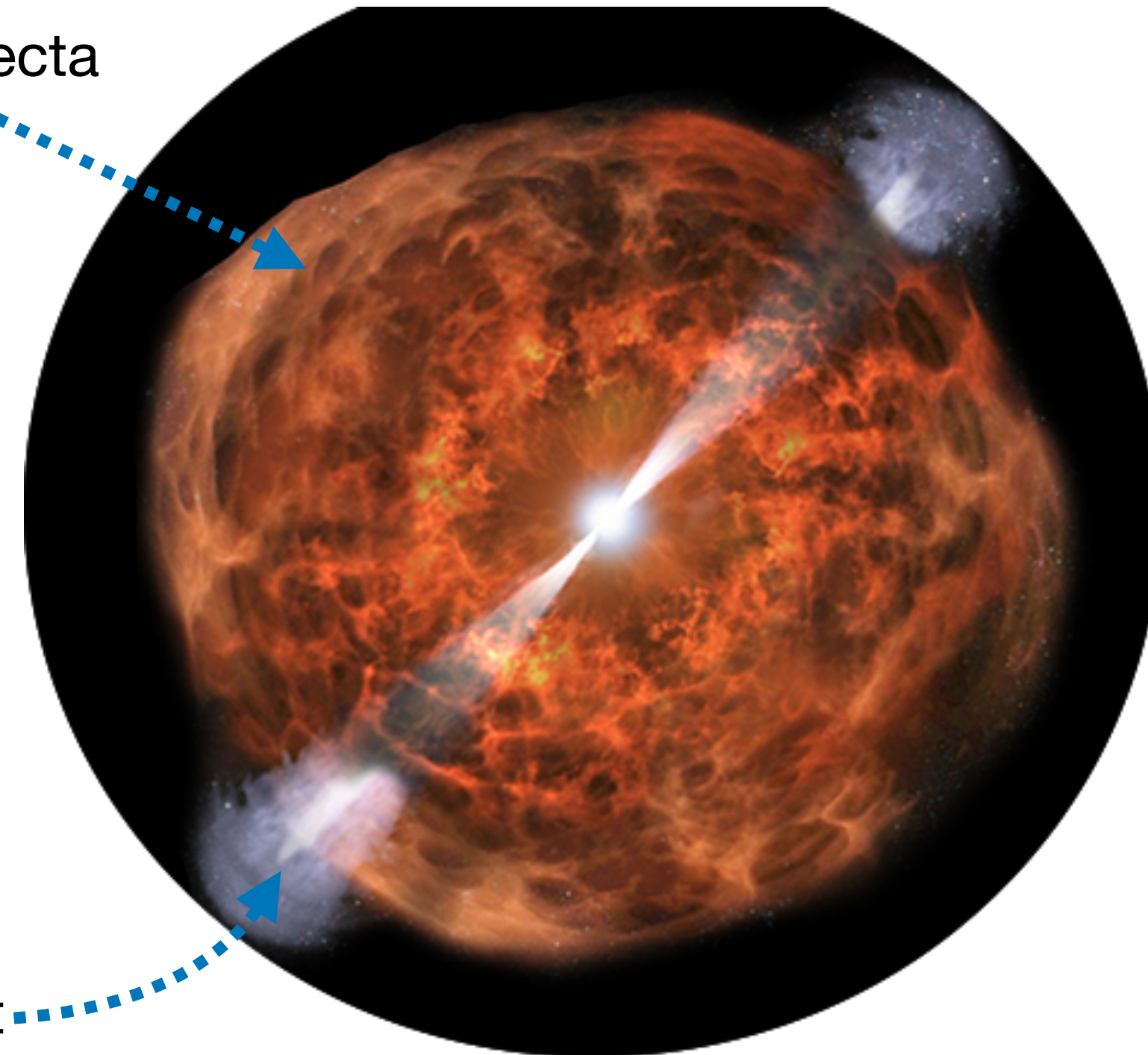
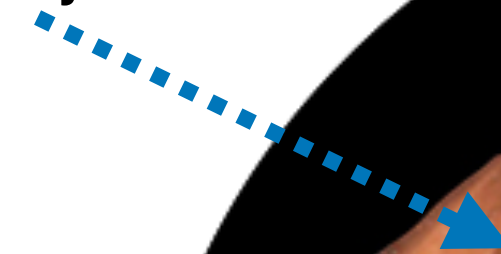
good candidates for



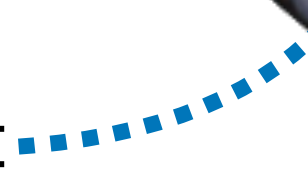
- photons (EM) ✓
- gravitational waves (GW) ✓
- ultra high-energy cosmic rays (UHECR)
- neutrinos

## GW170817: neutron star merger (NSM)

radioactive ejecta



relativistic jet





# Is GW170817 a neutrino source ?

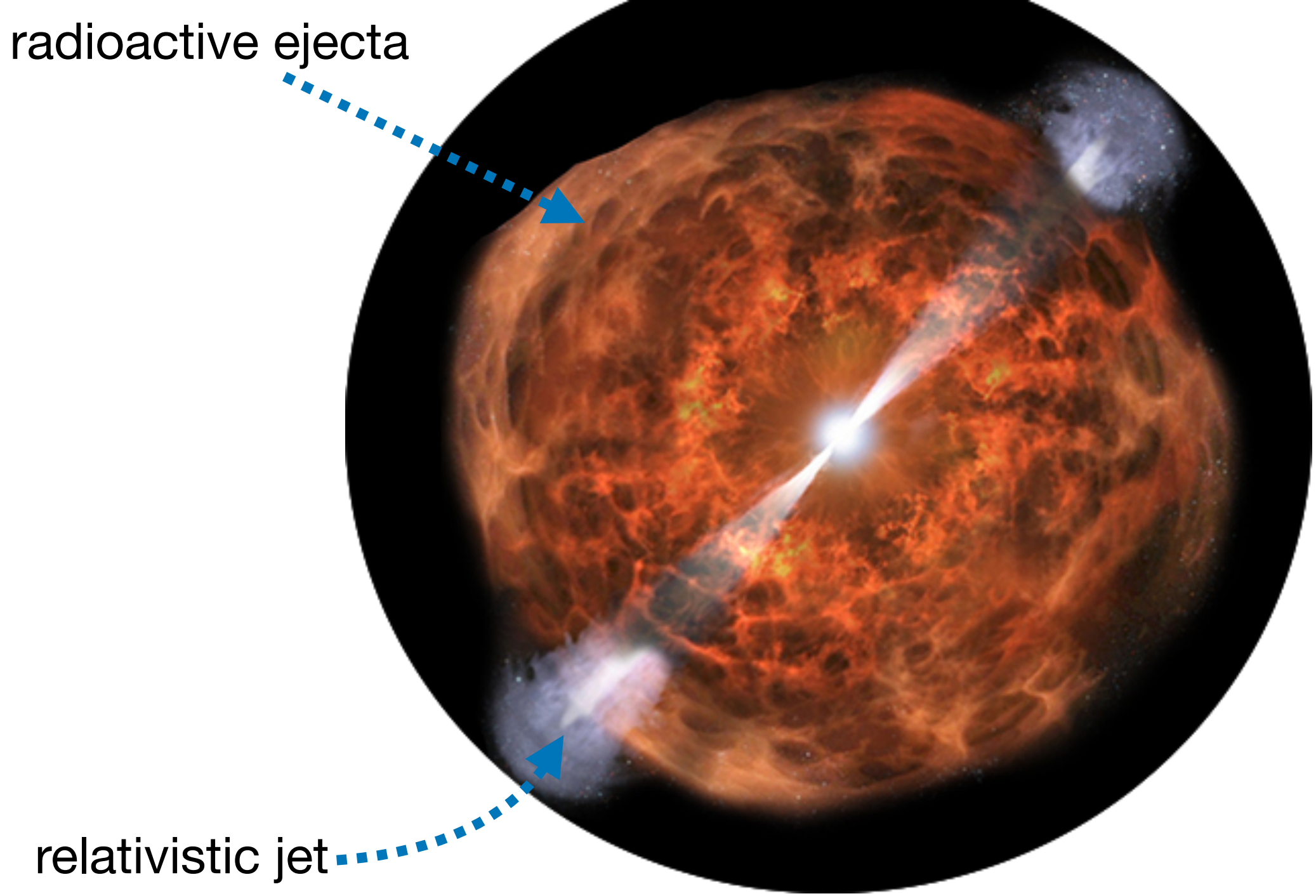
- highly energetic  $L \approx 10^{52} \text{ erg.s}^{-1}$
- high baryon loading

good candidates for



- photons (EM) ✓
- gravitational waves (GW) ✓
- ultra high-energy cosmic rays (UHECR)
- neutrinos

## GW170817: neutron star merger (NSM)



high photon density medium  
 high baryon density medium

cosmic rays interactions:

- photo hadronic interactions
- purely hadronic interactions

$$p + \gamma \rightarrow p + \pi^\pm \rightarrow \mu^\pm + \bar{\nu}_\mu$$

\*pion production\*

$$\rightarrow e^\pm + \bar{\nu}_e$$
  

$$p + p \rightarrow p + \pi^\pm \rightarrow \mu^\pm + \bar{\nu}_\mu$$

$$\rightarrow e^\pm + \bar{\nu}_e$$



# Is GW170817 a neutrino source ?

- highly energetic  $L \approx 10^{52} \text{ erg.s}^{-1}$
- high baryon loading

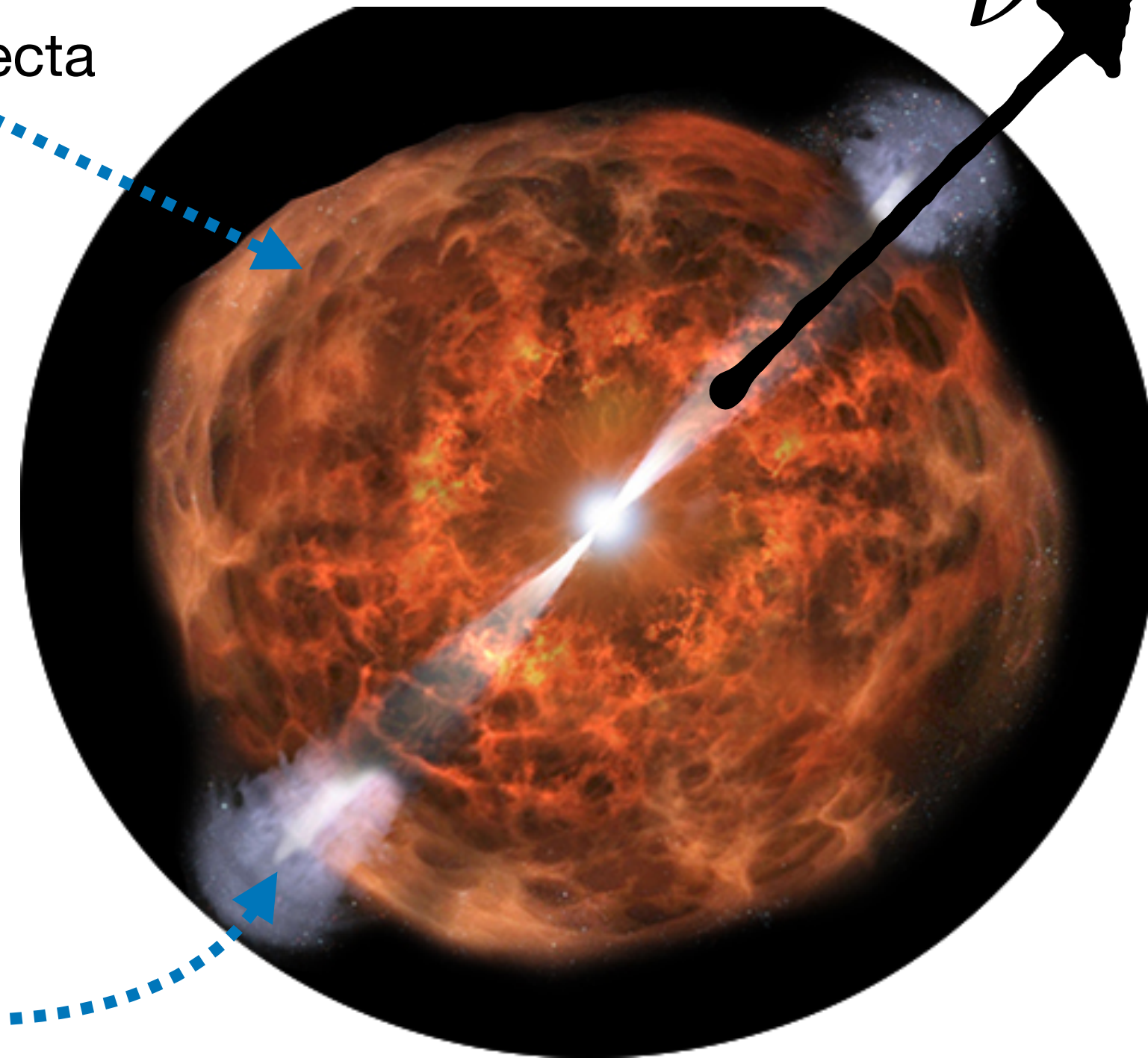
good candidates for



- photons (EM) ✓
- gravitational waves (GW) ✓
- ultra high-energy cosmic rays (UHECR)
- neutrinos

## GW170817: neutron star merger (NSM)

radioactive ejecta



relativistic jet

previous works

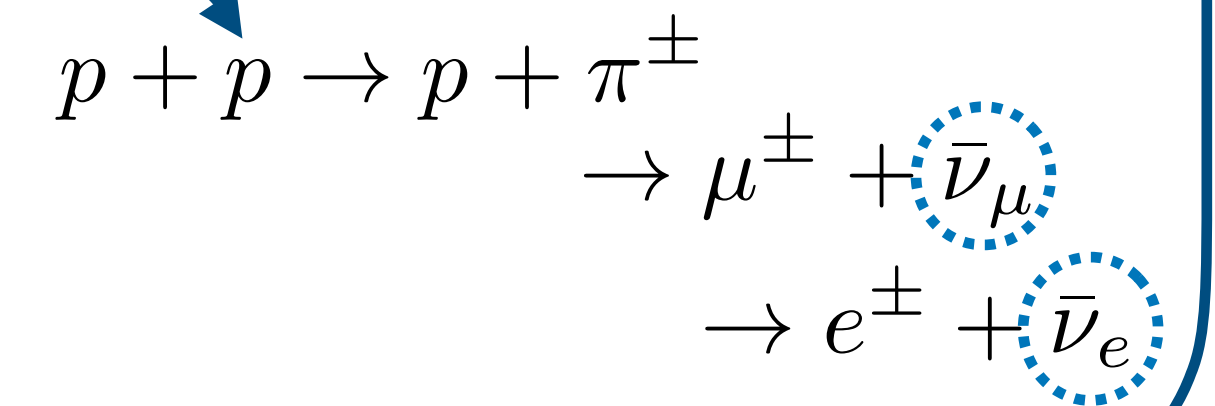
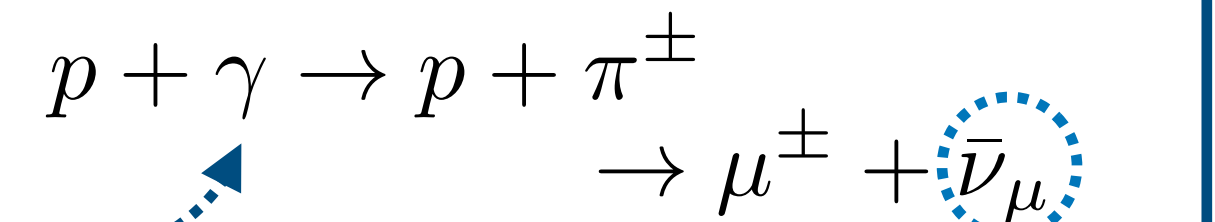
- Kimura et al. (2017)
- Biehl et al. (2018)
- Ahlers et Halser (2019)

high photon density  
medium

high baryon density  
medium

cosmic rays interactions:

- photo hadronic interactions
- purely hadronic interactions



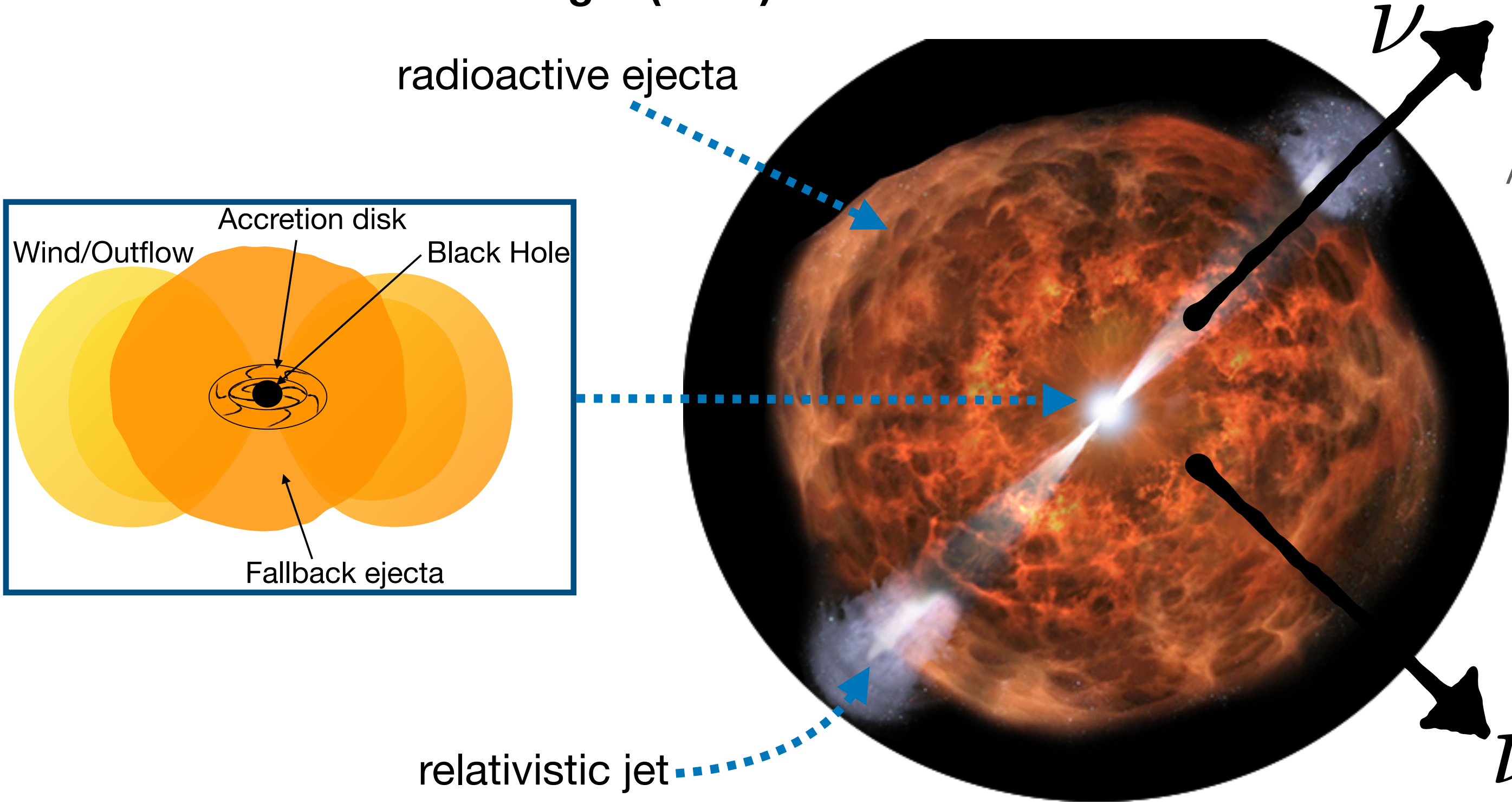


# Is GW170817 a neutrino source ?

- highly energetic  $L \approx 10^{52} \text{ erg.s}^{-1}$
  - high baryon loading
- good candidates for

- photons (EM) ✓
- gravitational waves (GW) ✓
- ultra high-energy cosmic rays (UHECR)
- neutrinos

## GW170817: neutron star merger (NSM)



previous works  
 Kimura et al. (2017)  
 Biehl et al. (2018)  
 Ahlers et Halser (2019)

high photon density medium  
 high baryon density medium

cosmic rays interactions:

- photo hadronic interactions
- purely hadronic interactions

$$p + \gamma \rightarrow p + \pi^\pm \rightarrow \mu^\pm + \bar{\nu}_\mu \rightarrow e^\pm + \bar{\nu}_e$$

\*pion production\*

$$p + p \rightarrow p + \pi^\pm \rightarrow \mu^\pm + \bar{\nu}_\mu \rightarrow e^\pm + \bar{\nu}_e$$

my work

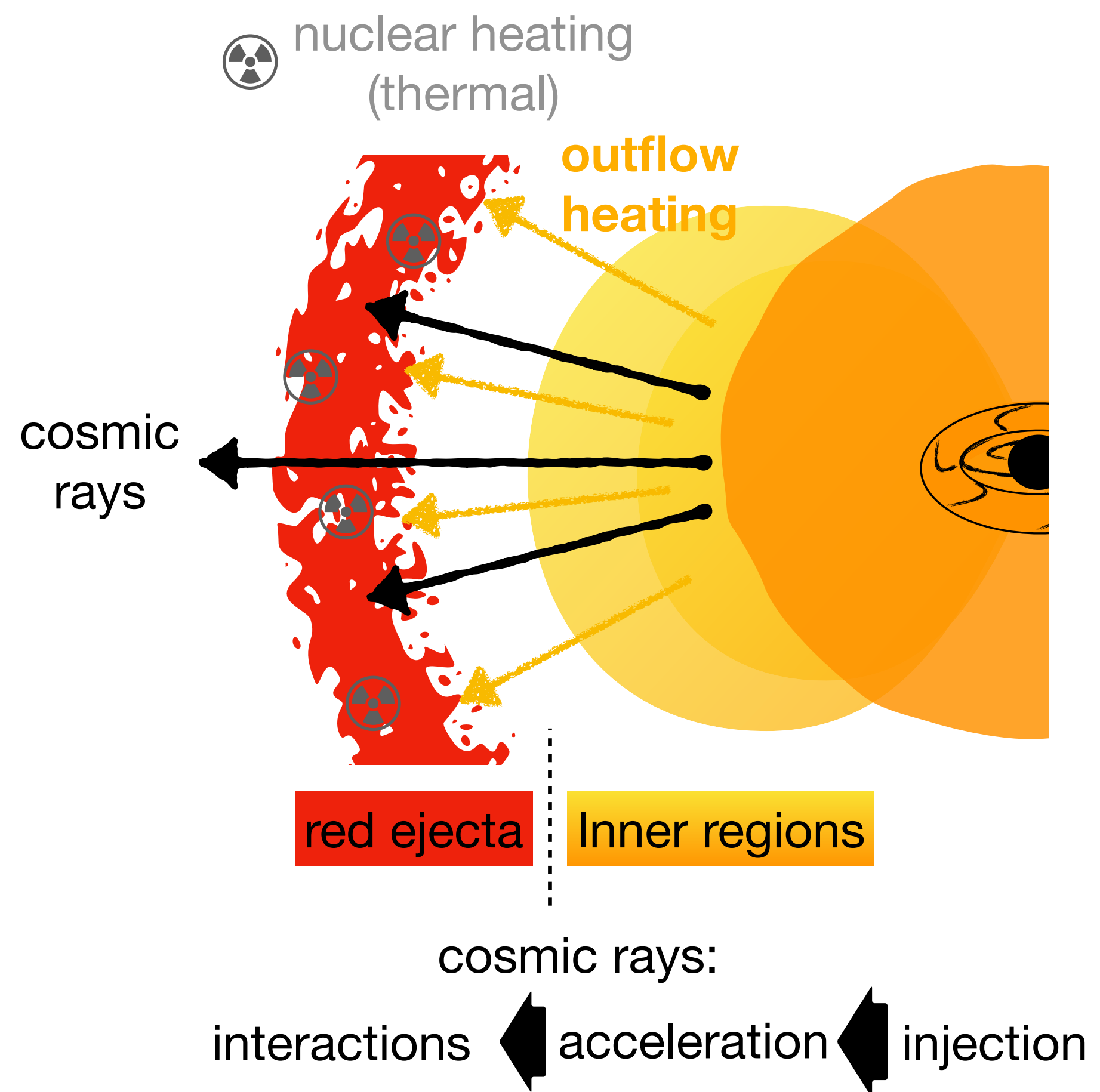
We want to compute the neutrino flux from NSM: radiative background + particle interactions



# High-energy neutrinos from fallback accretion of binary neutron star merger remnants

V. D., Guépin (UChicago), Fang (Berkeley), Kotera (IAP) and Metzger (Columbia) (JCAP 2019)

## 1) A model for the radiative background inside the ejecta:





# High-energy neutrinos from fallback accretion of binary neutron star merger remnants

V. D., Guépin (UChicago), Fang (Berkeley), Kotera (IAP) and Metzger (Columbia) (JCAP 2019)

## 1) A model for the radiative background inside the ejecta:

- Thermodynamical equilibrium** Metzger et al. 2011

$$\frac{d\mathcal{E}}{dt} = -3 \frac{\mathcal{E}}{R} \frac{dR}{dt} - \frac{\mathcal{E}}{t_{\text{esc}}} + \dot{Q}_r + \dot{Q}_{\text{fb}}$$

energy evolution    mechanical losses    radiative losses
- $$t_{\text{esc}} \approx \left( \frac{3M\kappa}{4\pi R^2} + 1 \right) \frac{R}{c}$$

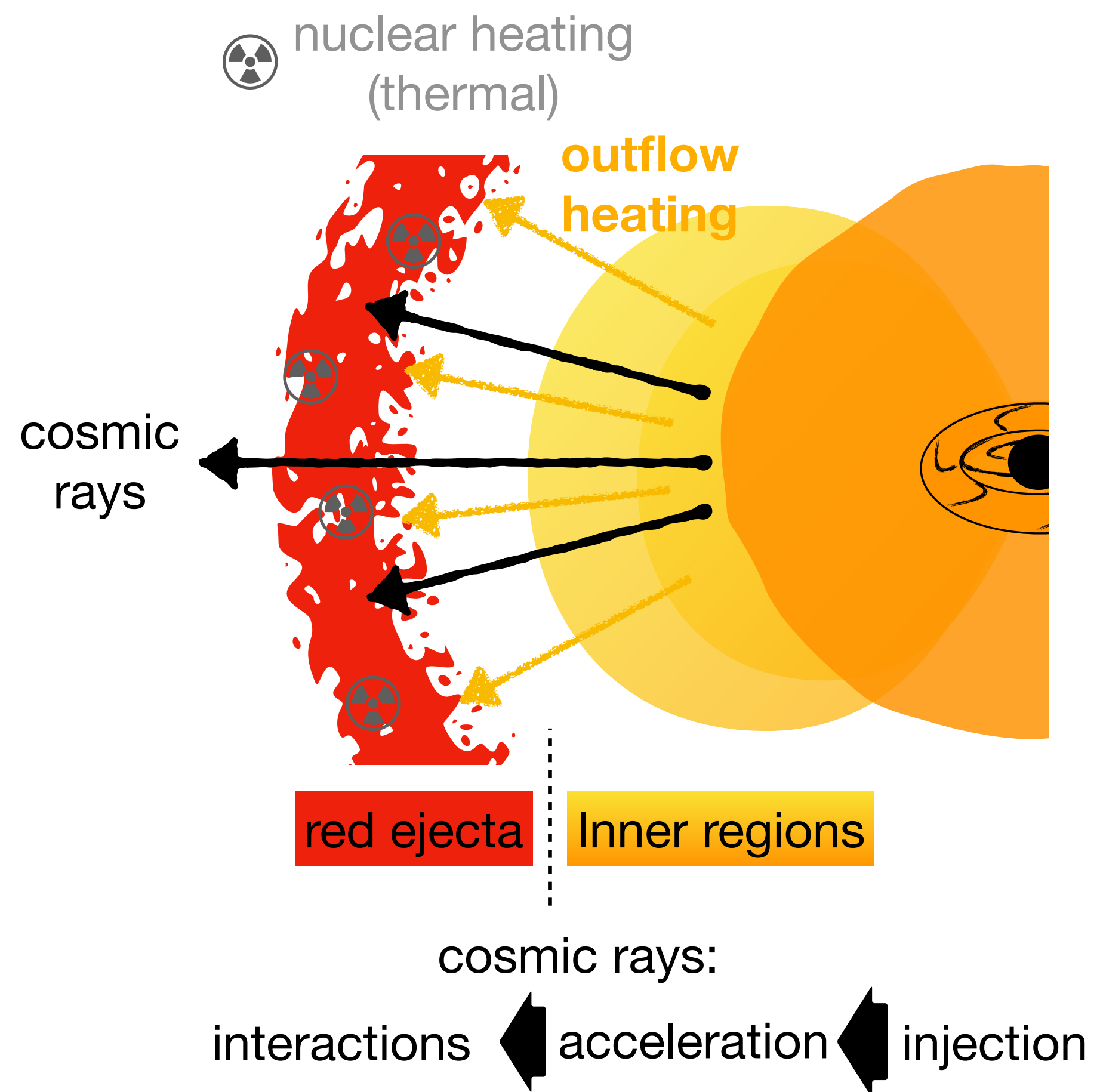
opacity (lanthanides)
- Fall-back**

$$\dot{Q}_{\text{fb}} = \epsilon_{\text{fb}} \dot{M}_{\text{fb}} c^2$$

mass accretion rate
- Nuclear reaction** Barnes et al. 2016  
M. R. Drout et al, 2017

$$\dot{Q}_r = M X_r \dot{e}_r(t)$$

nuclear mass energy  
 lanthanides mass fraction





# High-energy neutrinos from fallback accretion of binary neutron star merger remnants

V. D., Guépin (UChicago), Fang (Berkeley), Kotera (IAP) and Metzger (Columbia) (JCAP 2019)

## 1) A model for the radiative background inside the ejecta:

- Thermodynamical equilibrium** Metzger et al. 2011  

$$\frac{d\mathcal{E}}{dt} = -3 \frac{\mathcal{E}}{R} \frac{dR}{dt} - \frac{\mathcal{E}}{t_{\text{esc}}} + \dot{Q}_r + \dot{Q}_{\text{fb}}$$

energy evolution    mechanical losses    radiative losses
- $$t_{\text{esc}} \approx \left( \frac{3M\kappa}{4\pi R^2} + 1 \right) \frac{R}{c}$$

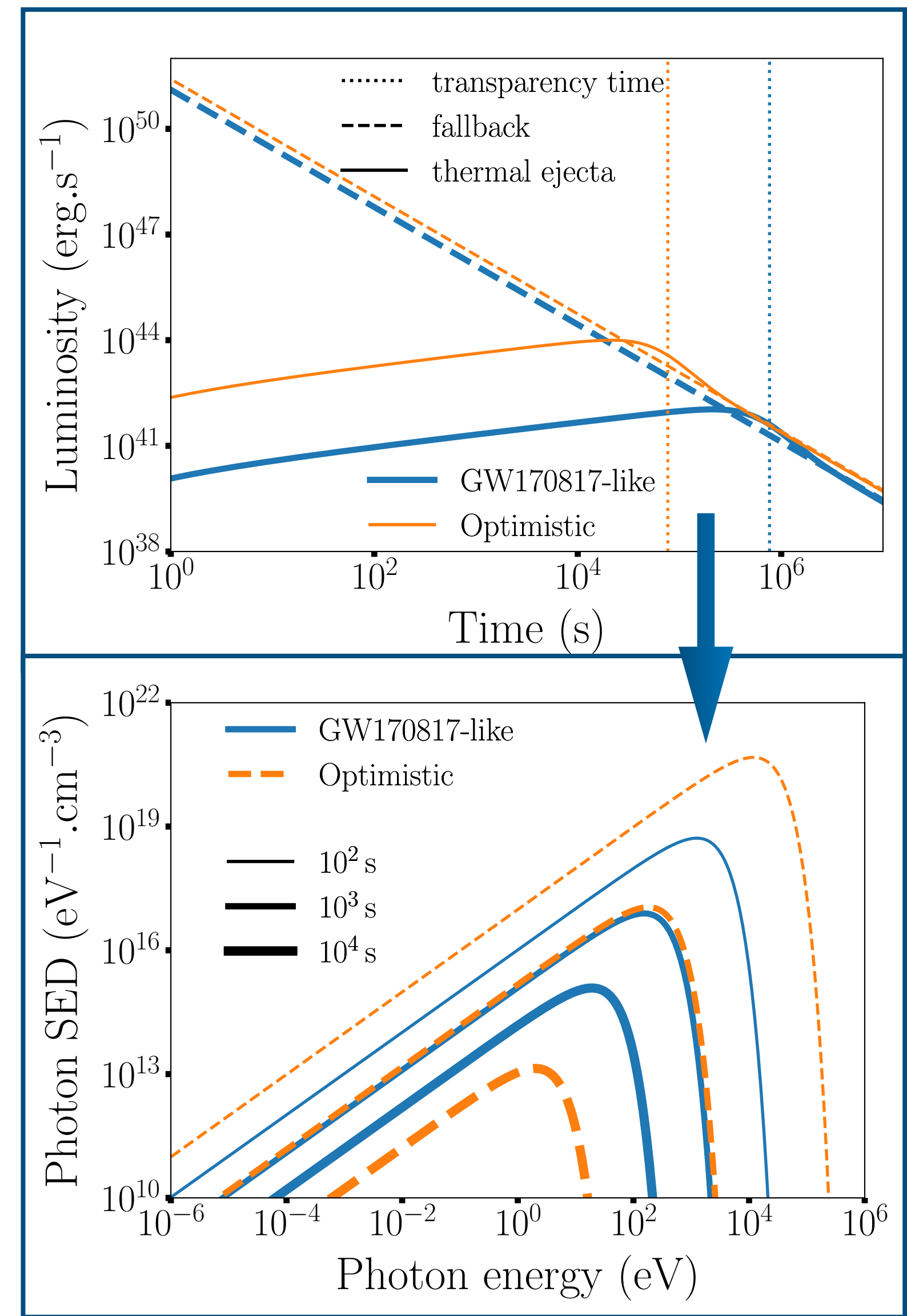
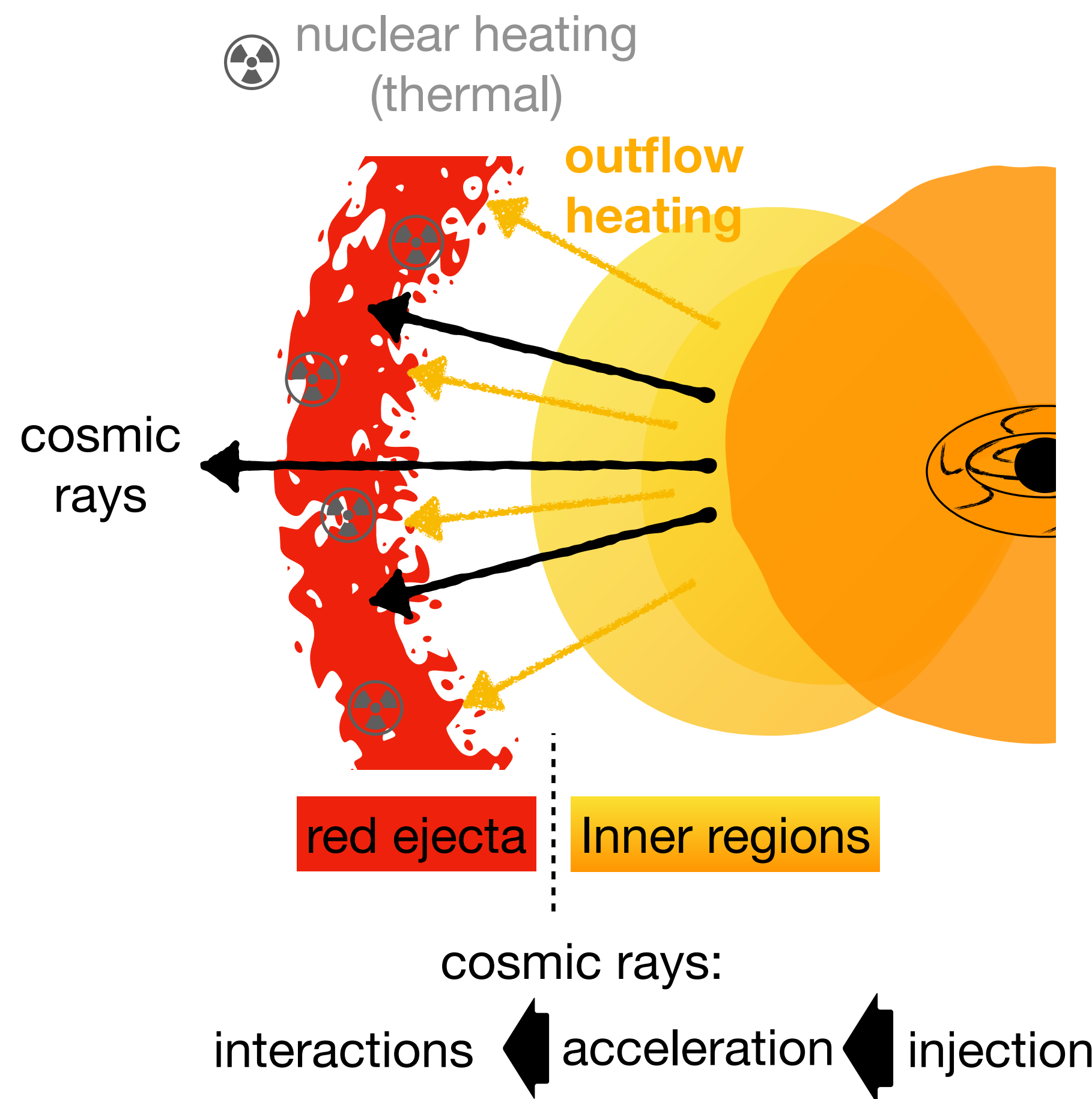
opacity (lanthanides)
- Fall-back**  

$$\dot{Q}_{\text{fb}} = \epsilon_{\text{fb}} \dot{M}_{\text{fb}} c^2$$

mass accretion rate
- Nuclear reaction** Barnes et al. 2016  

$$\dot{Q}_r = M X_r \dot{e}_r(t)$$

M. R. Drout et al, 2017  
 nuclear mass energy  
 lanthanides mass fraction





## 2) Particle interactions computations:

Numerical Mont-Carlo computation (EPOS/TALYS/SOPHIA)

Guépin et al. (2017) Mücke, et al. (2000) Koning, et al. (2005) Werner, et al. (2006)

$$p + \gamma \rightarrow p + \pi^{\pm}$$



## 2) Particle interactions computations:

---

Numerical Mont-Carlo computation (EPOS/TALYS/SOPHIA)

Guépin et al. (2017) Mücke, et al. (2000) Koning, et al. (2005) Werner, et al. (2006)

$$p + \gamma \rightarrow p + \pi^{\pm}$$

$$\begin{aligned} &\rightarrow \mu^{\pm} + \bar{\nu}_{\mu} \\ &\rightarrow e^{\pm} + \bar{\nu}_e \end{aligned}$$



HE neutrino production



## 2) Particle interactions computations:

Numerical Mont-Carlo computation (EPOS/TALYS/SOPHIA)

Guépin et al. (2017) Mücke, et al. (2000) Koning, et al. (2005) Werner, et al. (2006)

$$p + \gamma \rightarrow p + \pi^{\pm}$$

$$\begin{aligned} &\rightarrow \mu^{\pm} + \bar{\nu}_{\mu} \\ &\rightarrow e^{\pm} + \bar{\nu}_e \end{aligned}$$



HE neutrino production

or

$$\begin{aligned} &\rightarrow \text{Cascades} \\ &\pi^{\pm} + \gamma \\ &\pi^{\pm} + p \\ &\dots \end{aligned}$$

special  
implementations

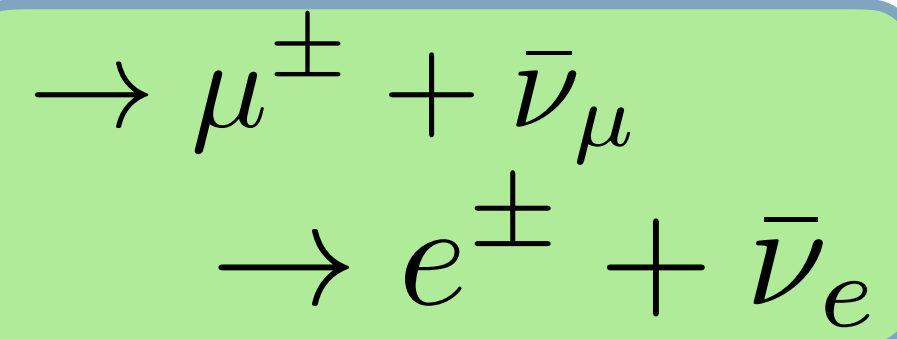
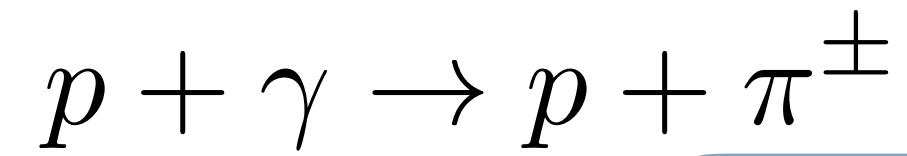


HE neutrino suppression

## 2) Particle interactions computations:

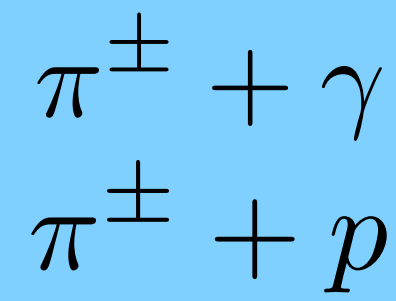
Numerical Mont-Carlo computation (EPOS/TALYS/SOPHIA)

Guépin et al. (2017) Mücke, et al. (2000) Koning, et al. (2005) Werner, et al. (2006)



or

$\rightarrow$  Cascades



special implementations



HE neutrino production



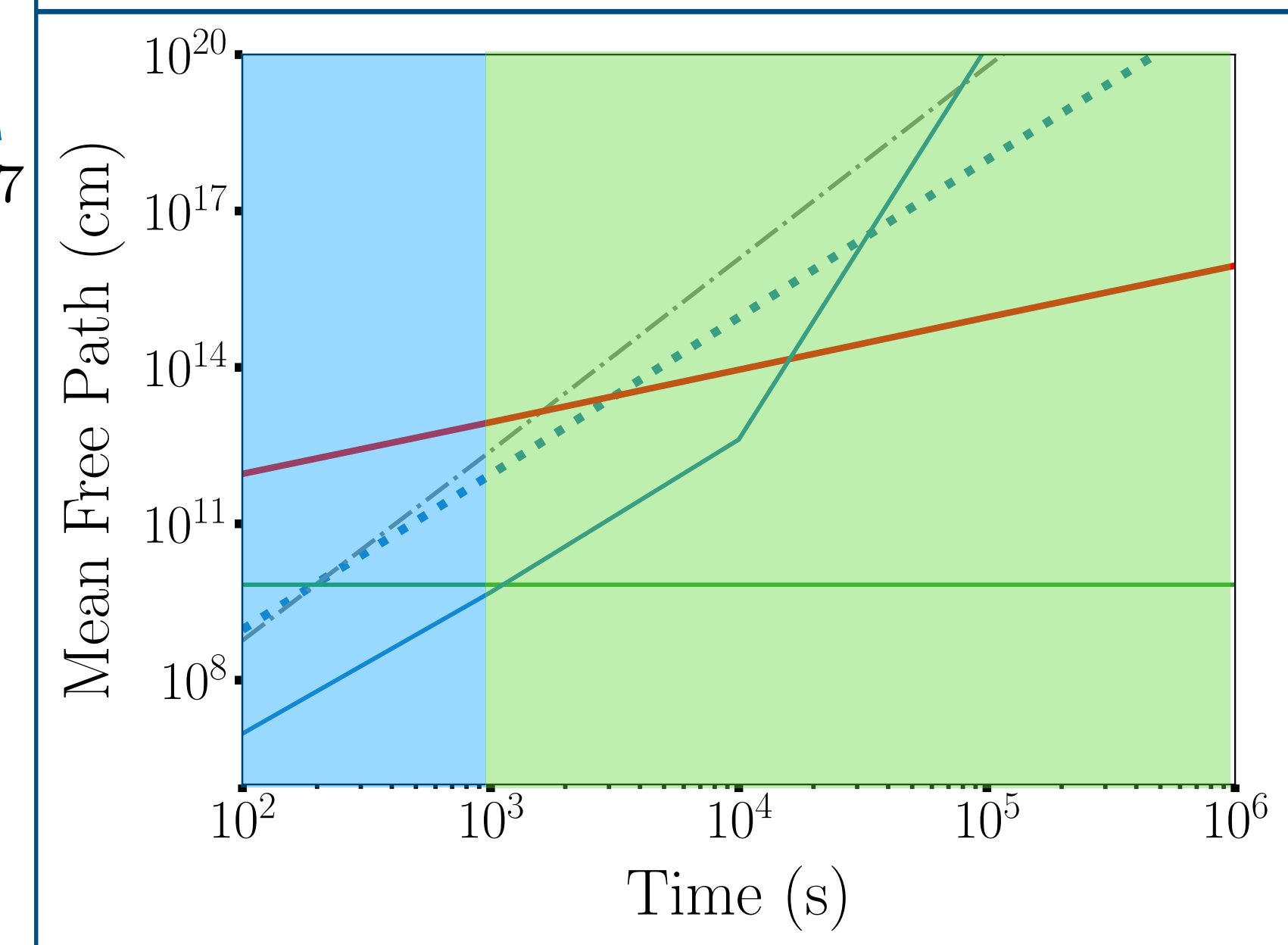
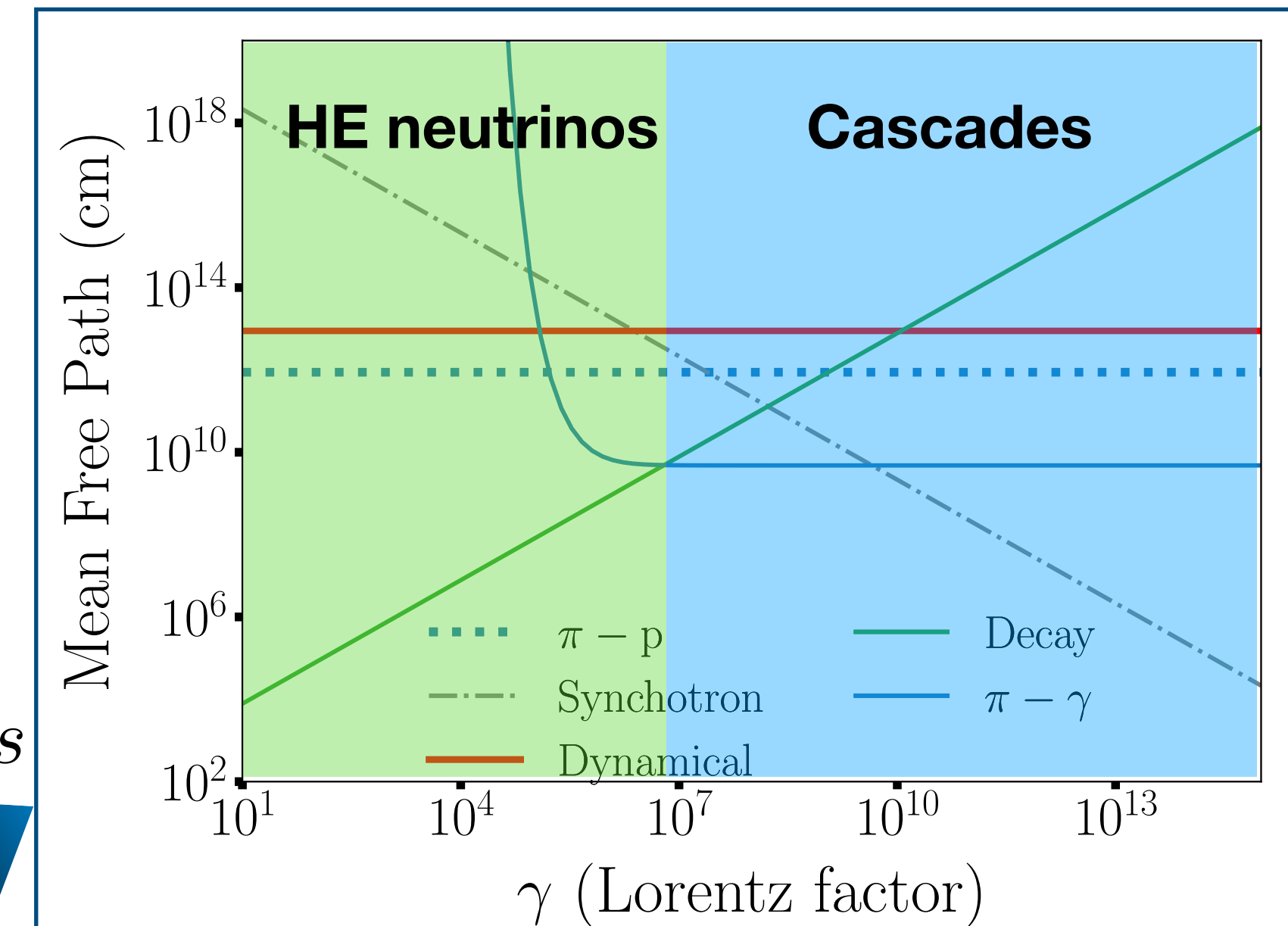
HE neutrino suppression

Optimum neutrino production depends on:

- neutrino energy
- production time

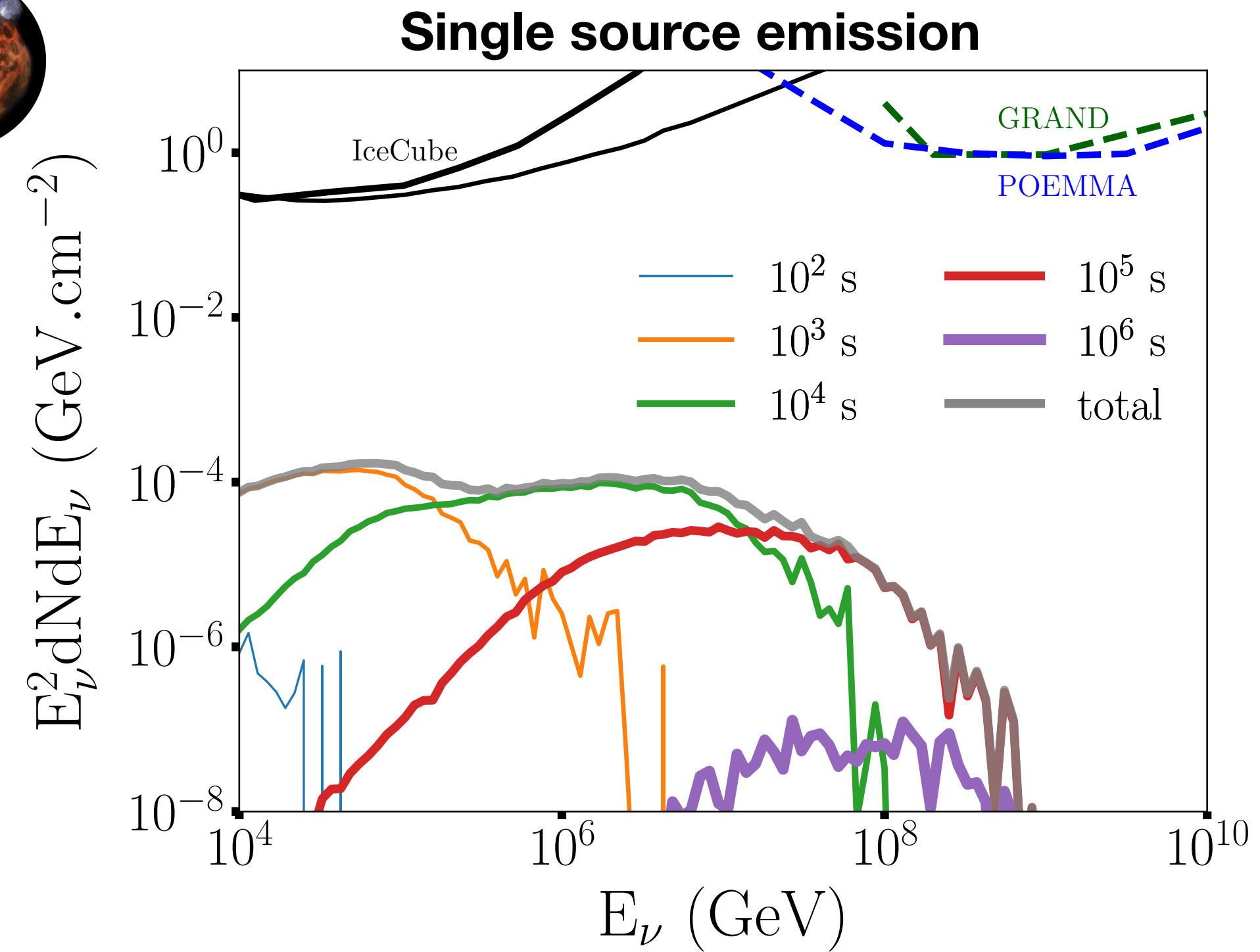
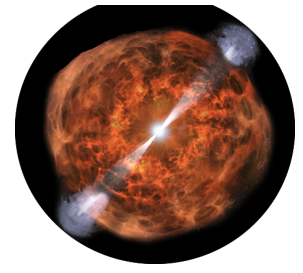
$t = 10^3 \text{ s}$

$\gamma = 10^7$



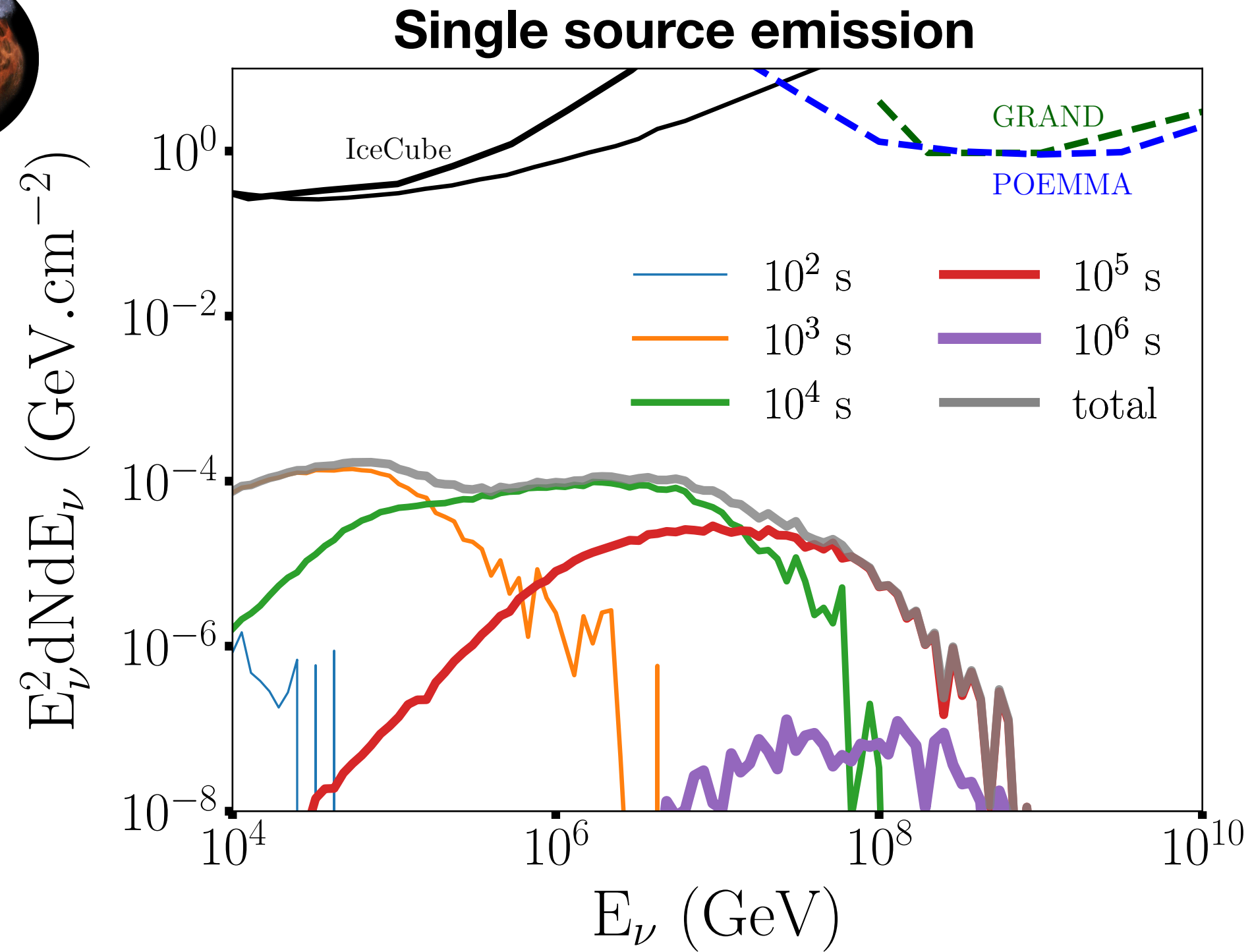
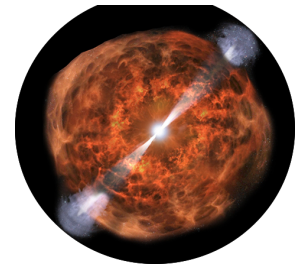


# Neutrino fluxes

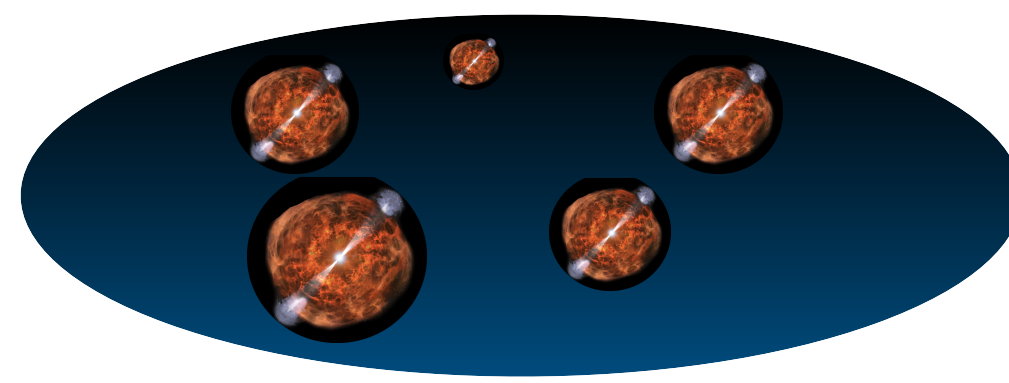


- Maximum neutrino energy increases with time
- Maximum neutrino flux decreases with time

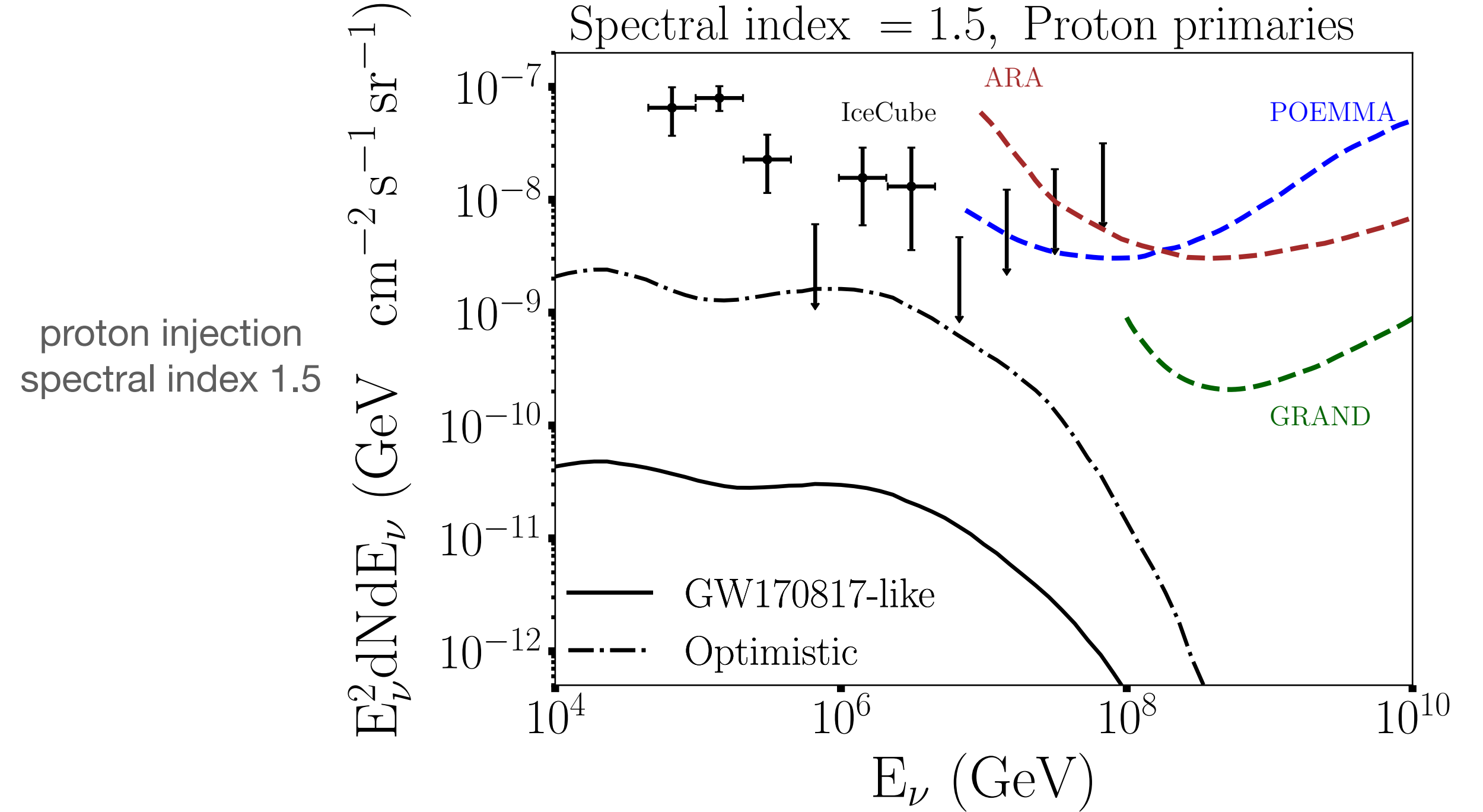
# Neutrino fluxes



- Maximum neutrino energy increases with time
- Maximum neutrino flux decreases with time



## Diffuse emission



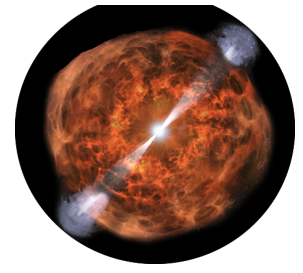
| Scenario      | $M_{\text{ej}}$<br>[ $M_\odot$ ] | $\beta_{\text{ej}}$ | $M_{\text{fb}}$<br>[ $M_\odot$ ] | $\beta_{\text{wind}}$ | $\epsilon_{\text{fb}}$ | $\dot{n}_0$<br>[ $\text{Gpc}^{-3} \text{yr}^{-1}$ ] | $\mathcal{R}(z)$              |
|---------------|----------------------------------|---------------------|----------------------------------|-----------------------|------------------------|---|-------------------------------|
| GW170817-like | $10^{-2}$                        | 0.3                 | $5 \times 10^{-2}$               | 0.1                   | 0.1                    | 600   | 1                             |
| Optimistic    | $10^{-4}$                        | 0.3                 | $1 \times 10^{-1}$               | 0.1                   | 0.1                    | 3000  | $\mathcal{R}_{\text{SFR}}(z)$ |

Two scenarii:

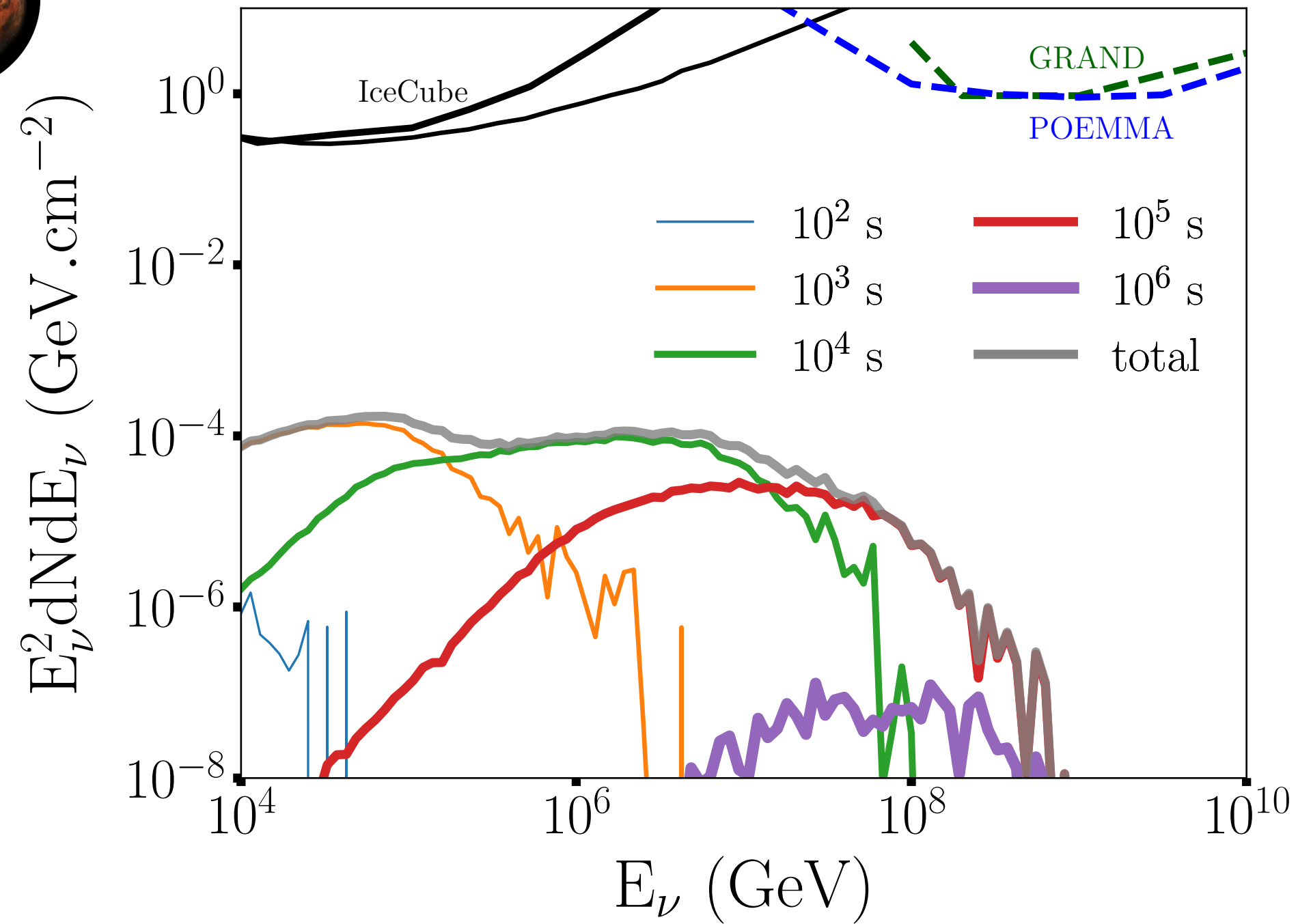
- GW170817 parameters
- optimistic simulated parameters



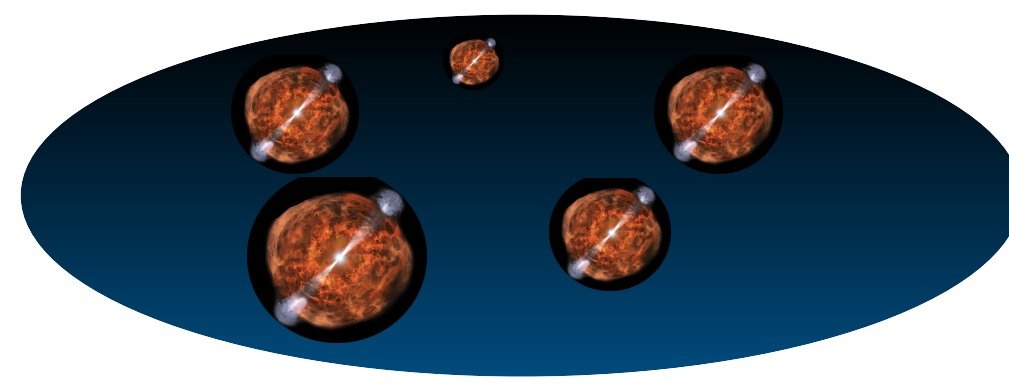
# Neutrino fluxes



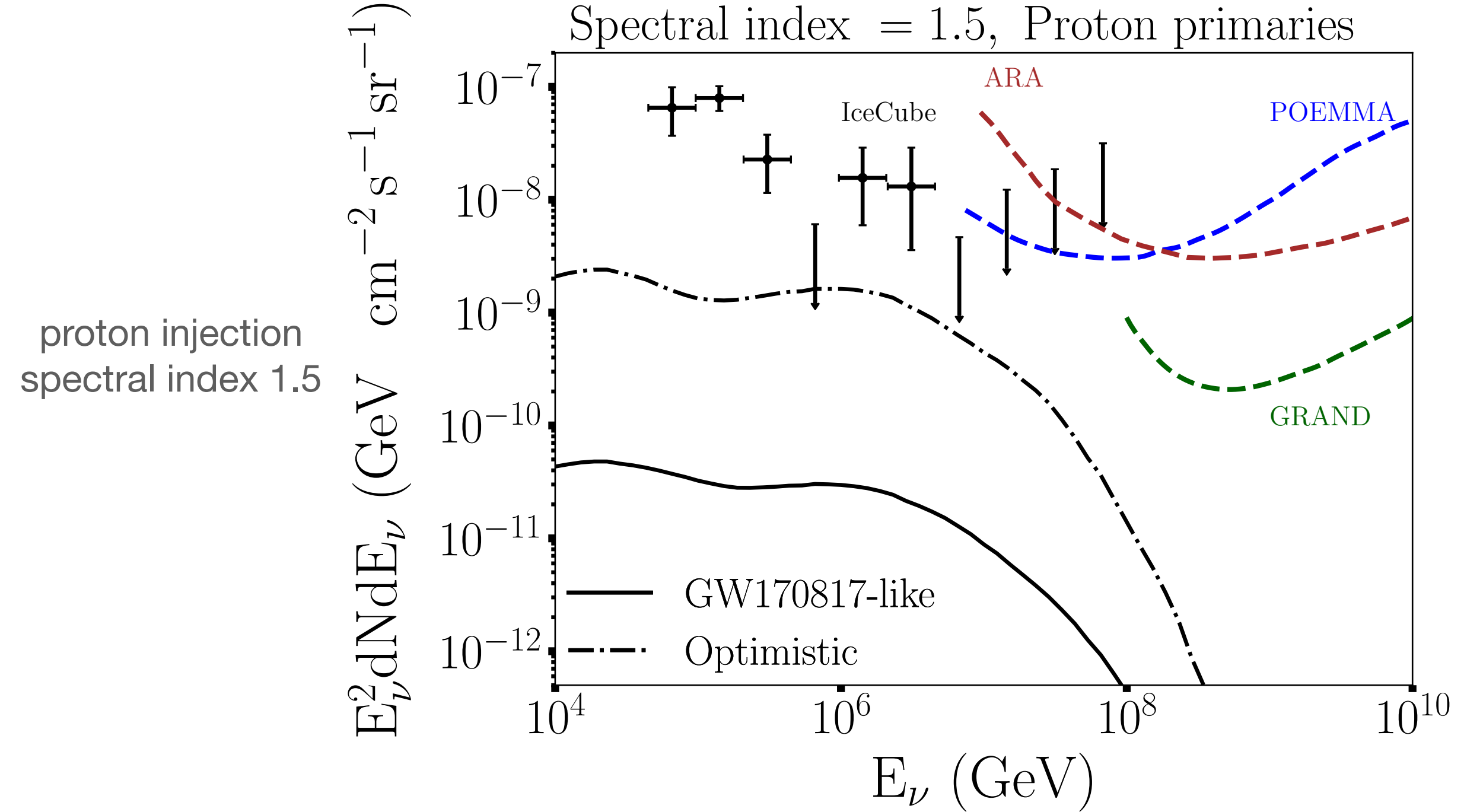
## Single source emission



- Maximum neutrino energy increases with time
- Maximum neutrino flux decreases with time



## Diffuse emission



| Scenario      | $M_{\text{ej}}$<br>[ $M_\odot$ ] | $\beta_{\text{ej}}$ | $M_{\text{fb}}$<br>[ $M_\odot$ ] | $\beta_{\text{wind}}$ | $\epsilon_{\text{fb}}$ | $\dot{n}_0$<br>[ $\text{Gpc}^{-3} \text{yr}^{-1}$ ] | $\mathcal{R}(z)$              |
|---------------|----------------------------------|---------------------|----------------------------------|-----------------------|------------------------|---|-------------------------------|
| GW170817-like | $10^{-2}$                        | 0.3                 | $5 \times 10^{-2}$               | 0.1                   | 0.1                    | 600   | 1                             |
| Optimistic    | $10^{-4}$                        | 0.3                 | $1 \times 10^{-1}$               | 0.1                   | 0.1                    | 3000  | $\mathcal{R}_{\text{SFR}}(z)$ |

Two scenarii:

- GW170817 parameters
- optimistic simulated parameters

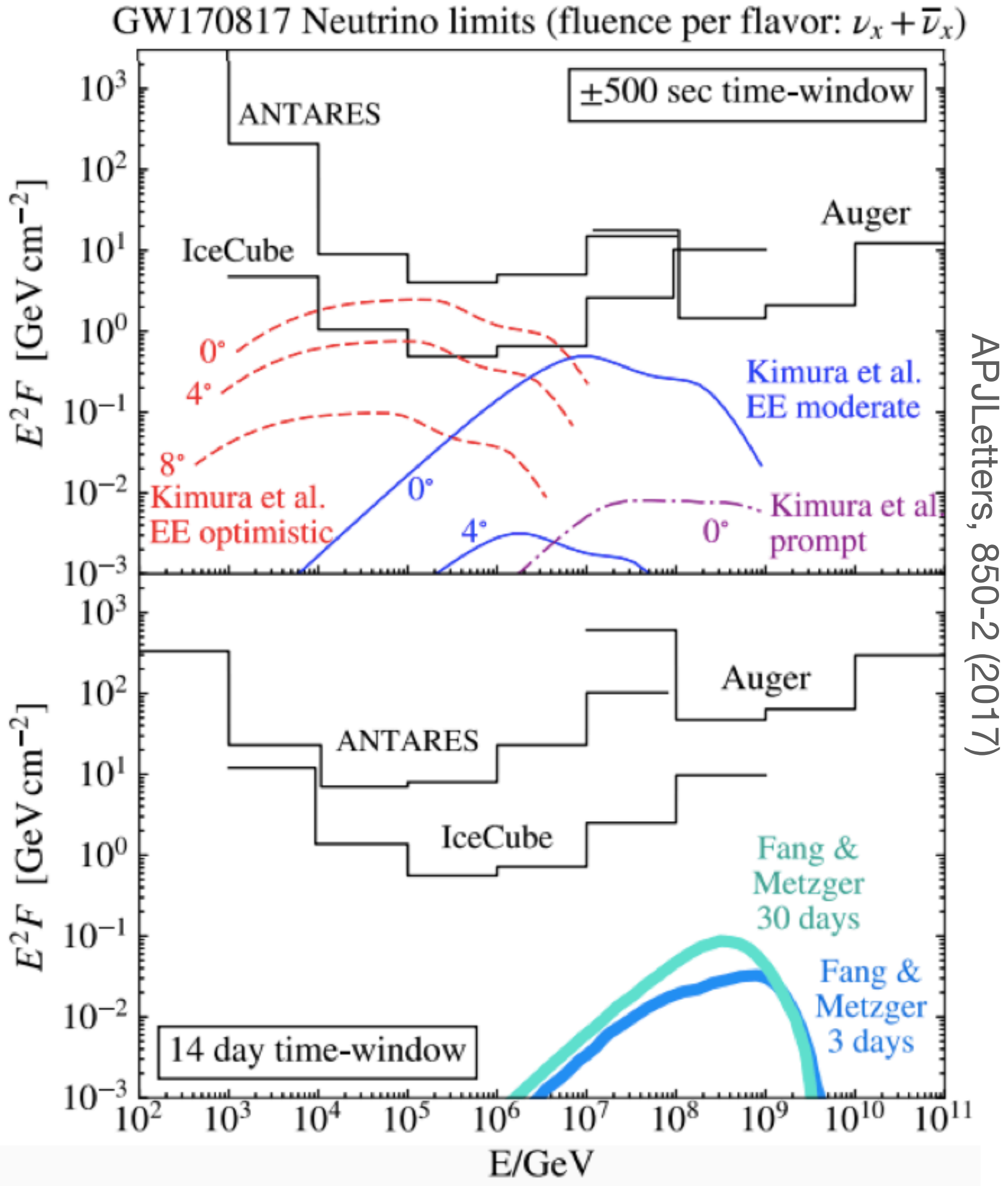
The diffuse neutrino flux from binary neutron stars mergers can contribute up to 10% of the IceCube measured flux

# **Neutrino sources are challenging to detect**



# Neutrino sources are challenging to detect

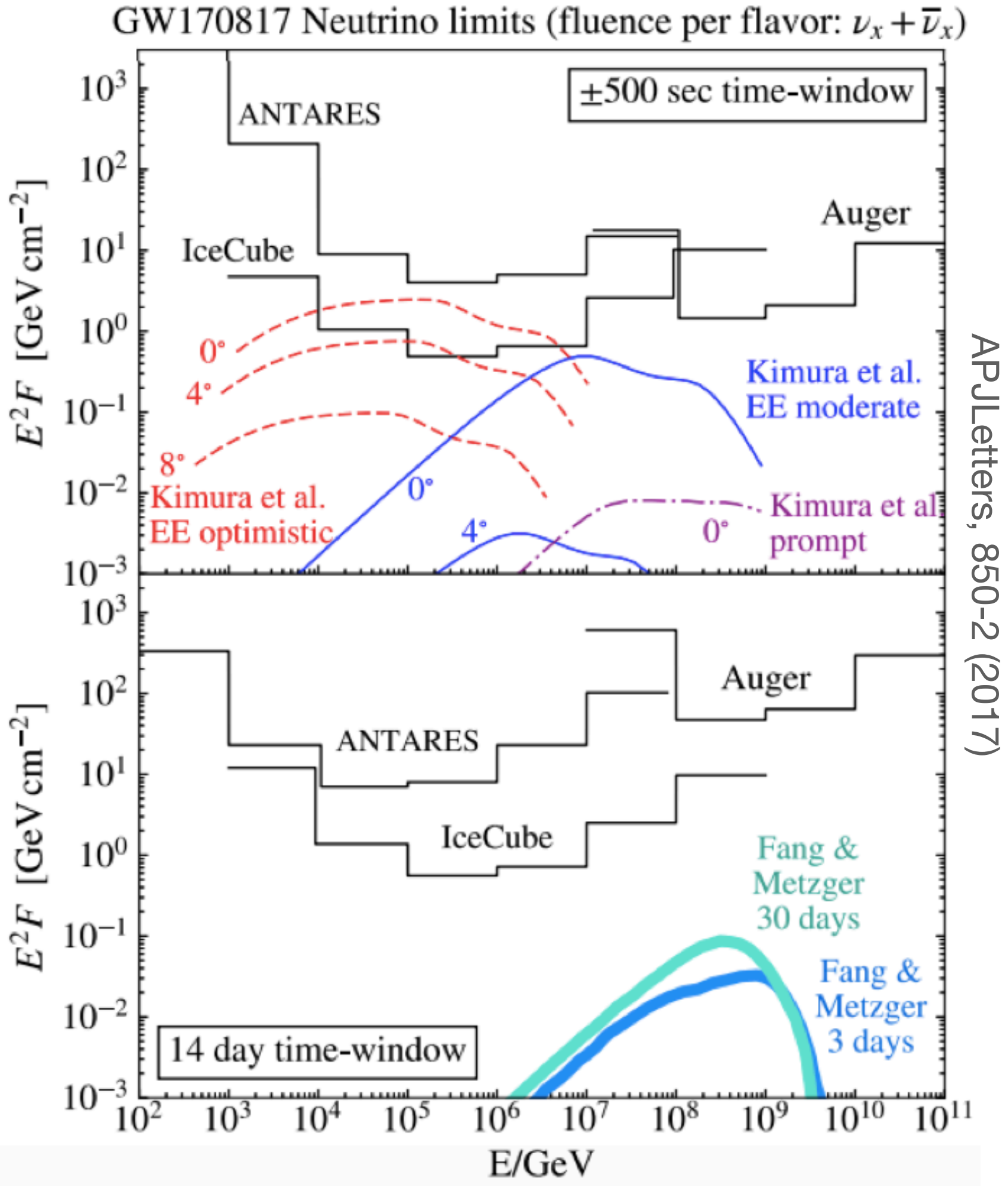
Even for jet emissions!



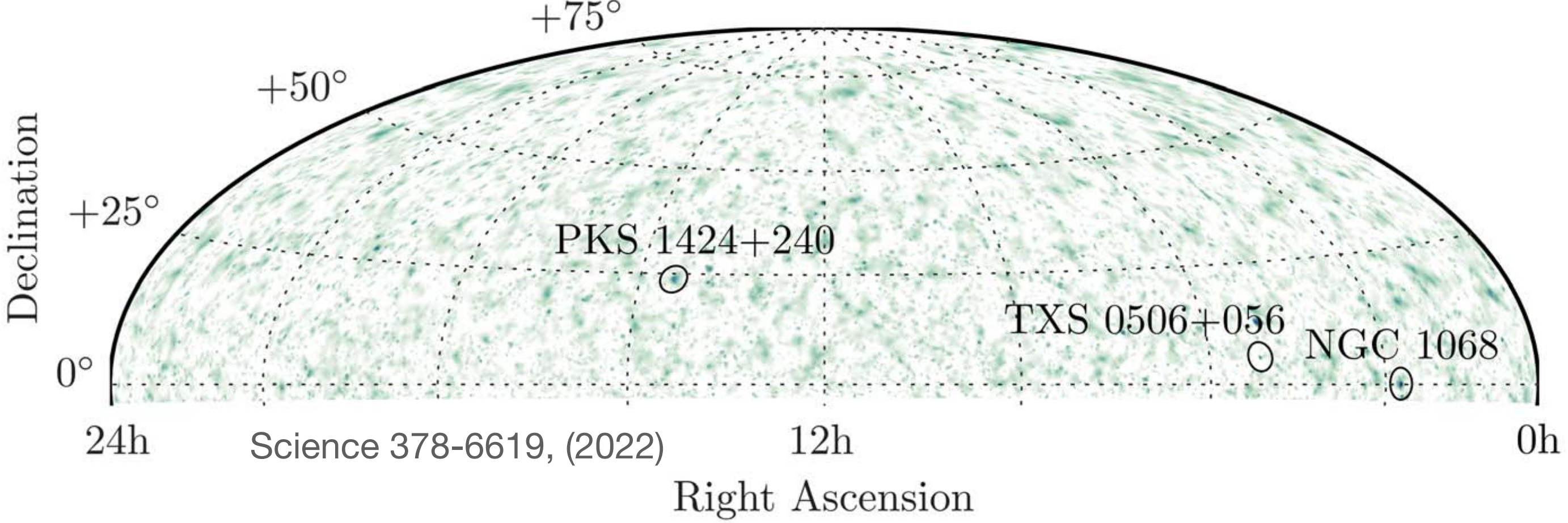
APJ Letters, 850-2 (2017)

# Neutrino sources are challenging to detect

Even for jet emissions!



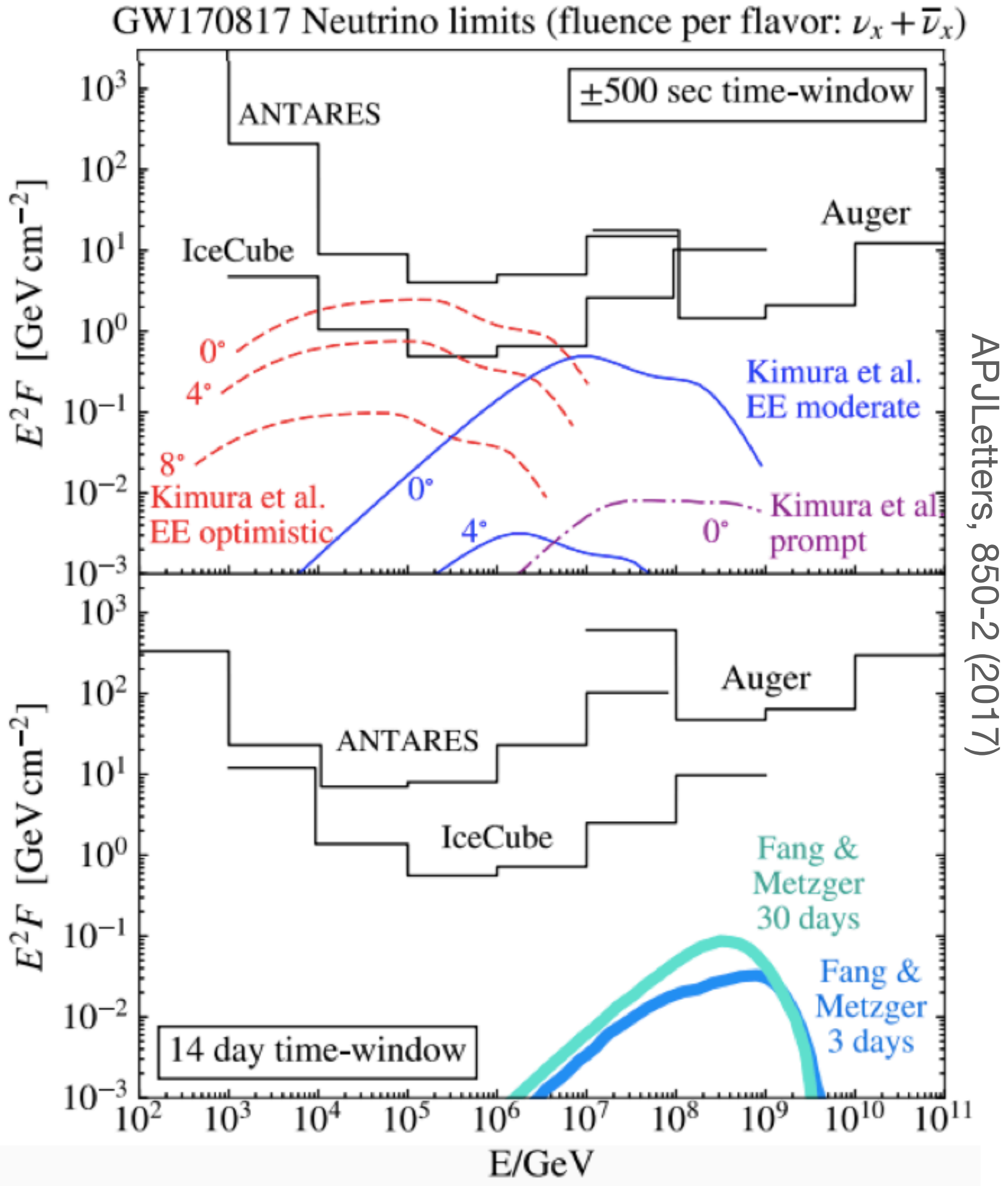
IceCube 19 years of data: 3 candidates



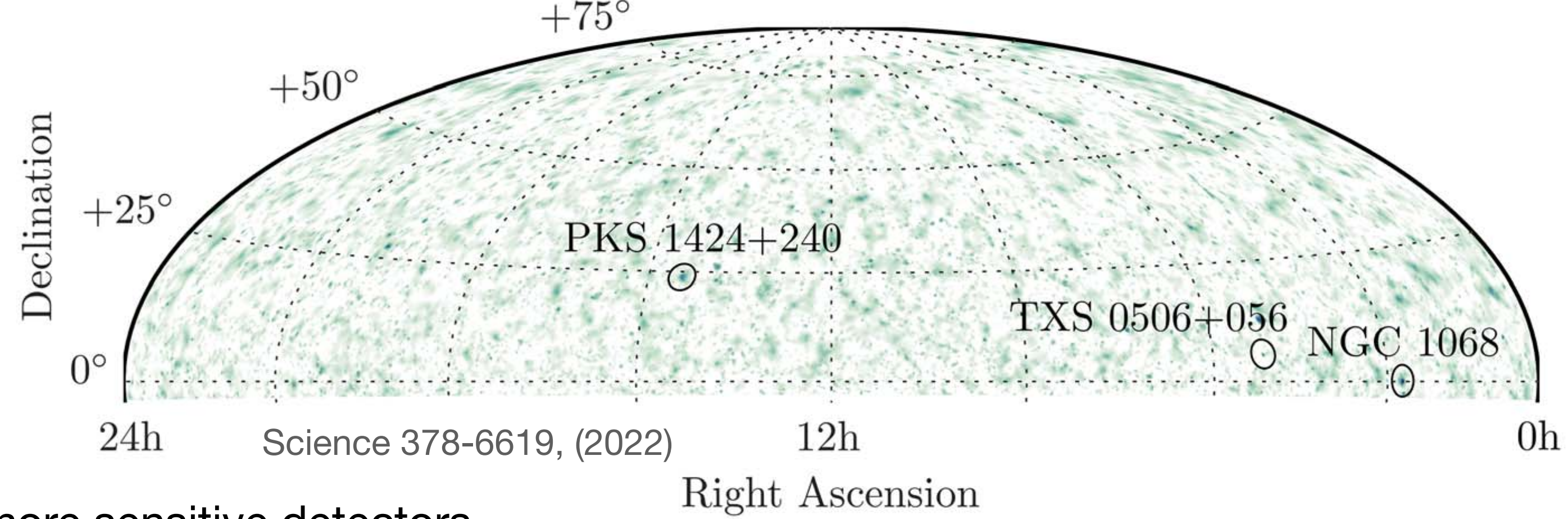


# Neutrino sources are challenging to detect

Even for jet emissions!



IceCube 19 years of data: 3 candidates

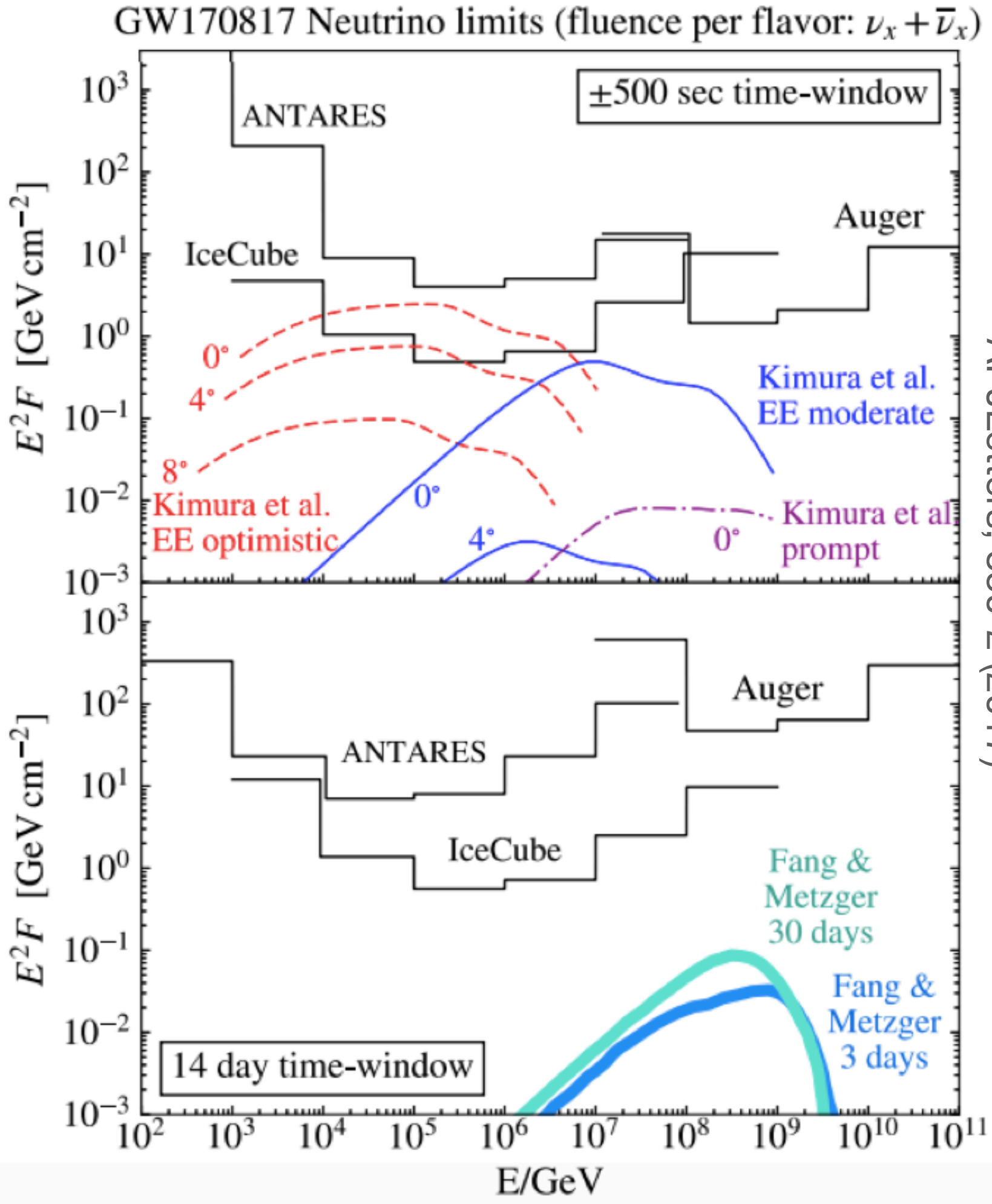


→ we need more sensitive detectors



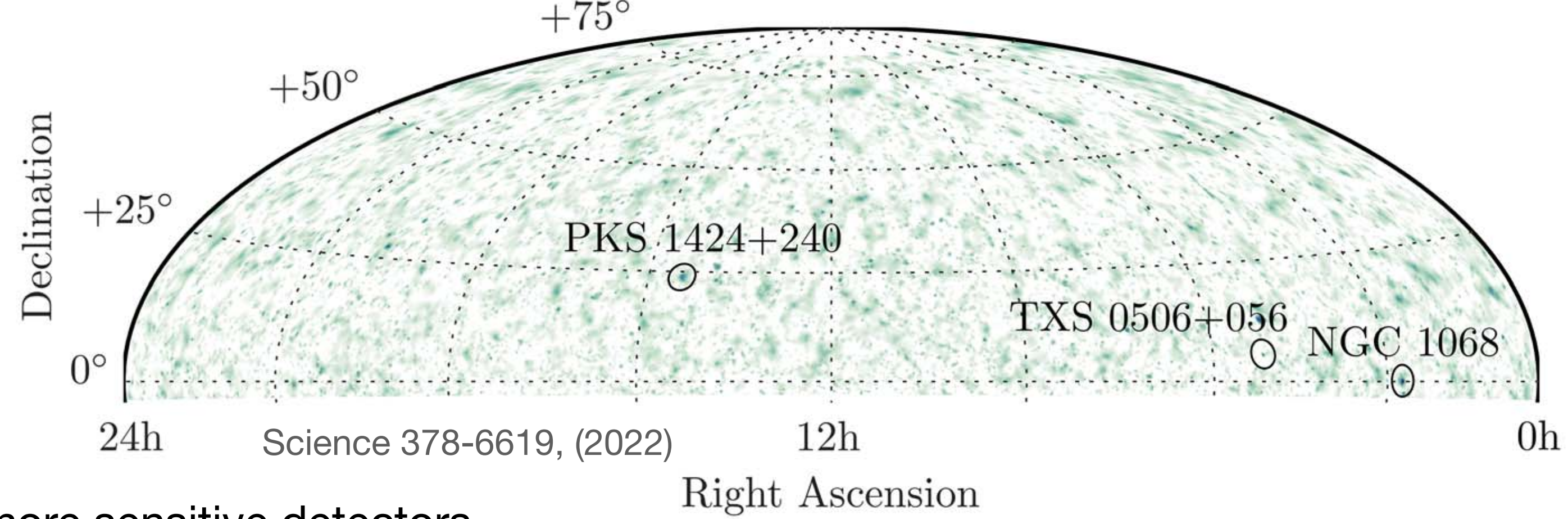
# Neutrino sources are challenging to detect

Even for jet emissions!



APJLetters, 850-2 (2017)

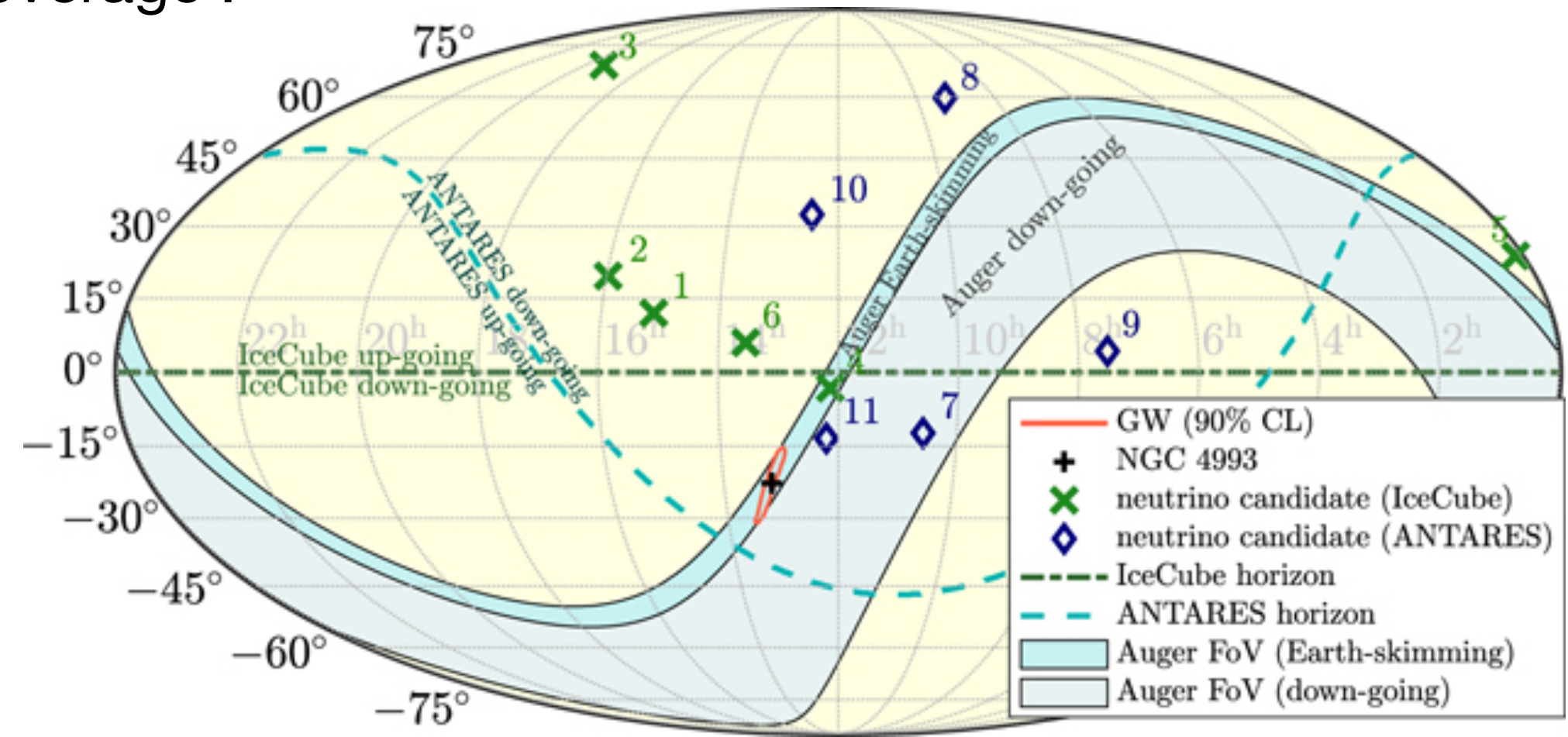
IceCube 19 years of data: 3 candidates



→ we need more sensitive detectors

→ and a better sky coverage !

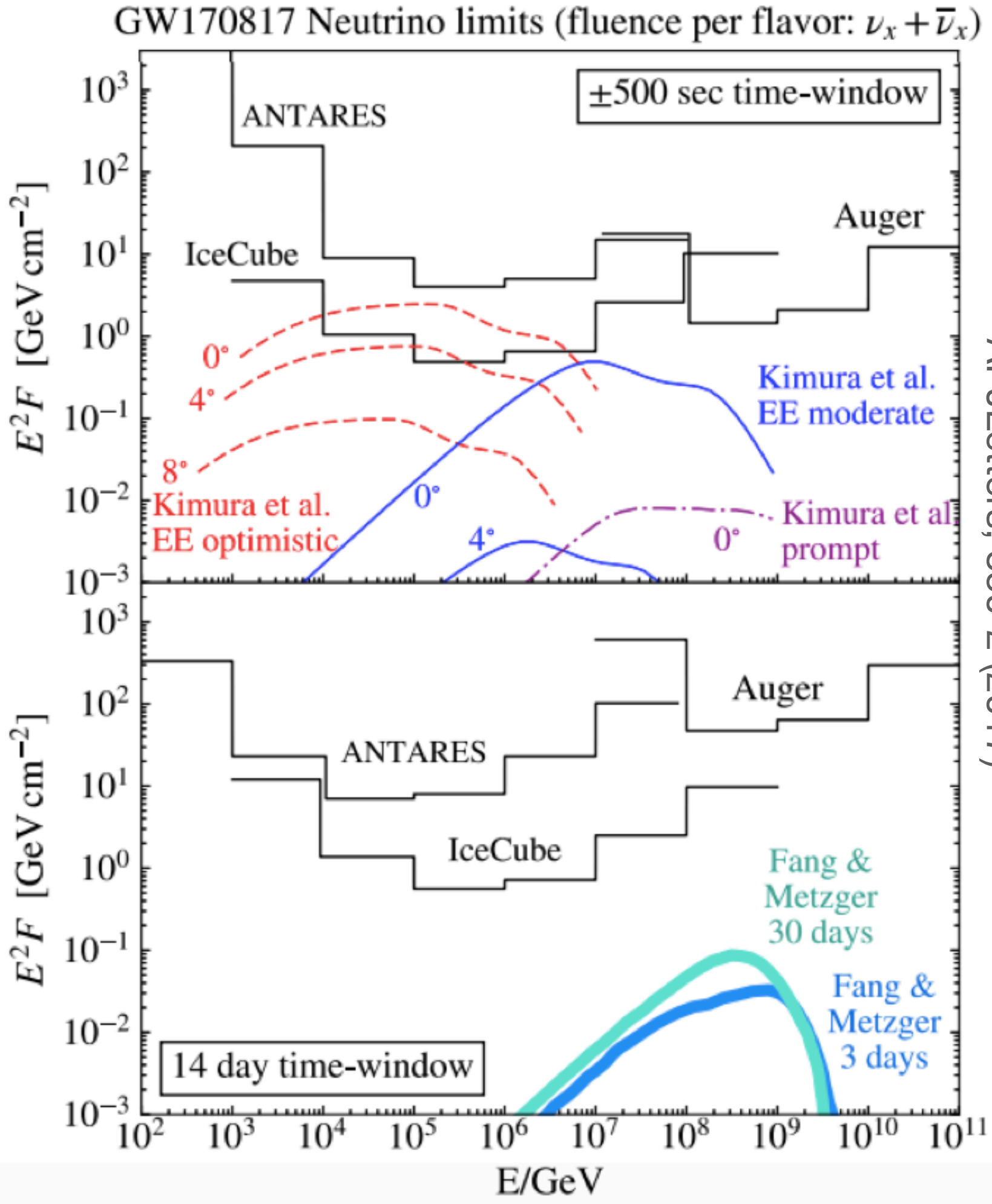
APJLetters, 850-2 (2017)



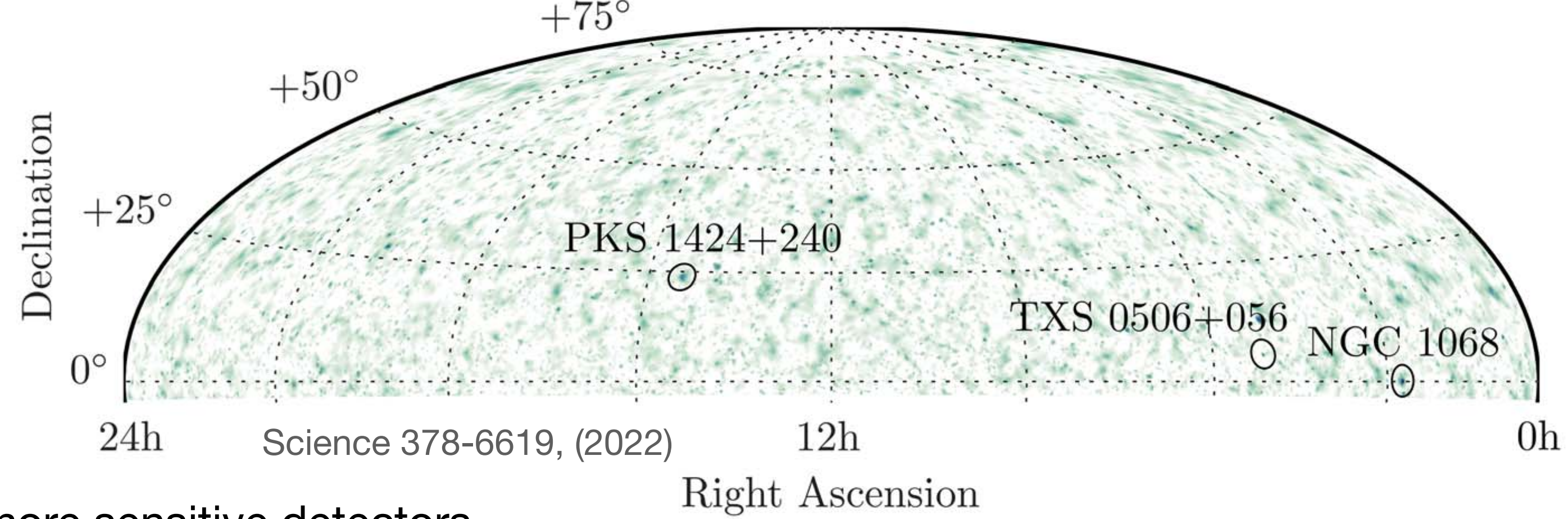


# Neutrino sources are challenging to detect

Even for jet emissions!

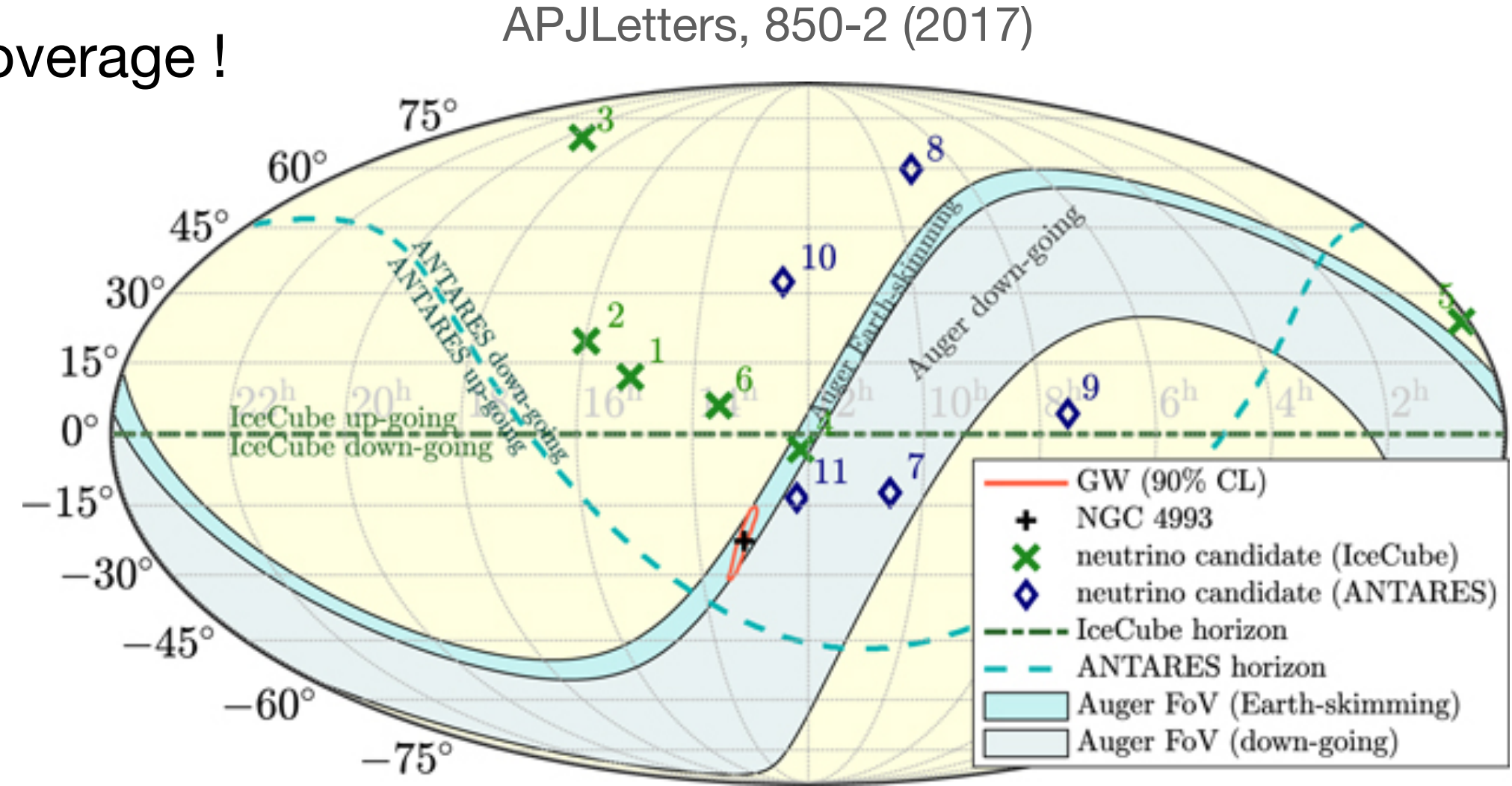


IceCube 19 years of data: 3 candidates



→ we need more sensitive detectors

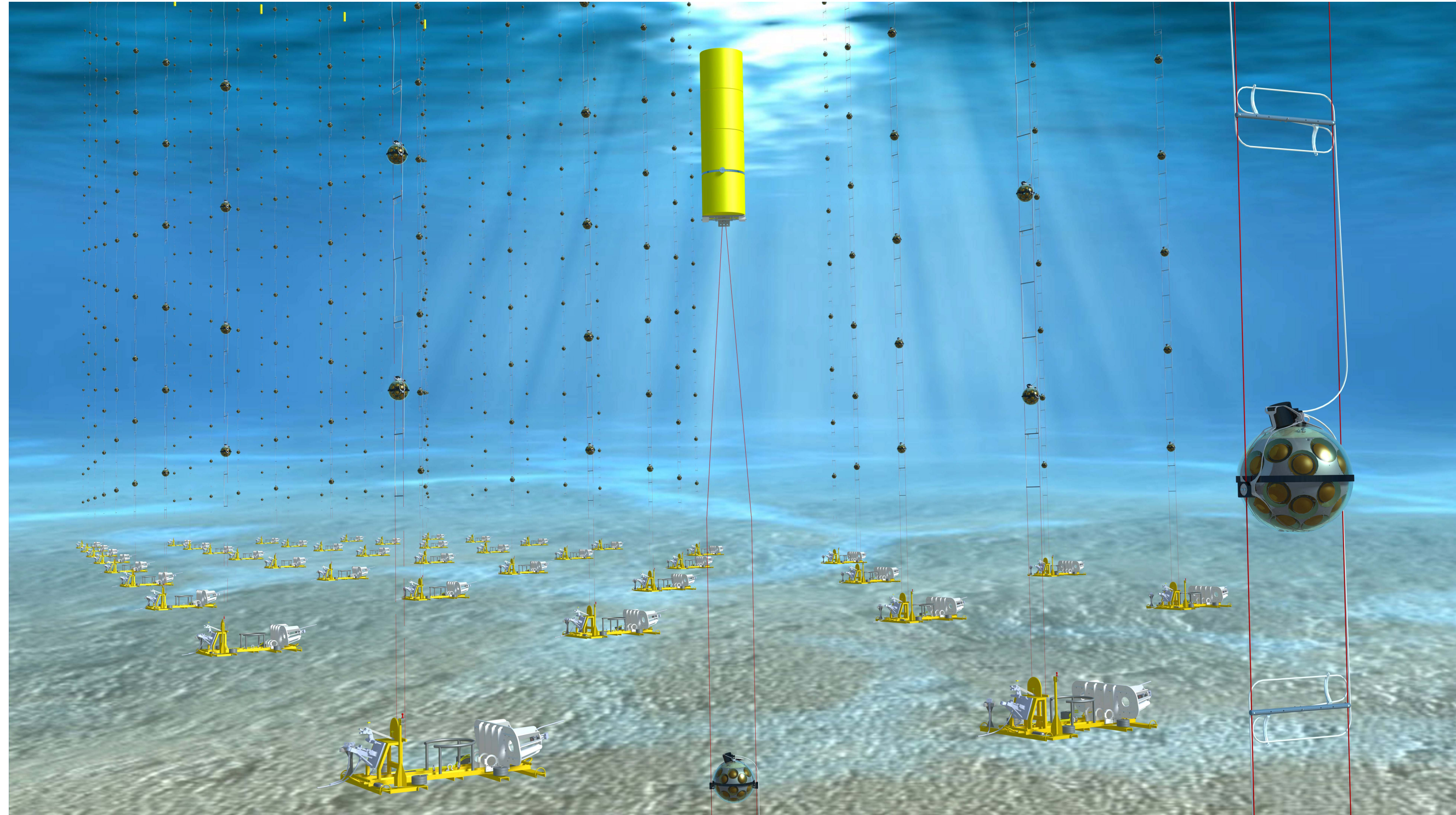
→ and a better sky coverage !



**KM3NeT!**



# The KM3NeT project (in a nutshell)

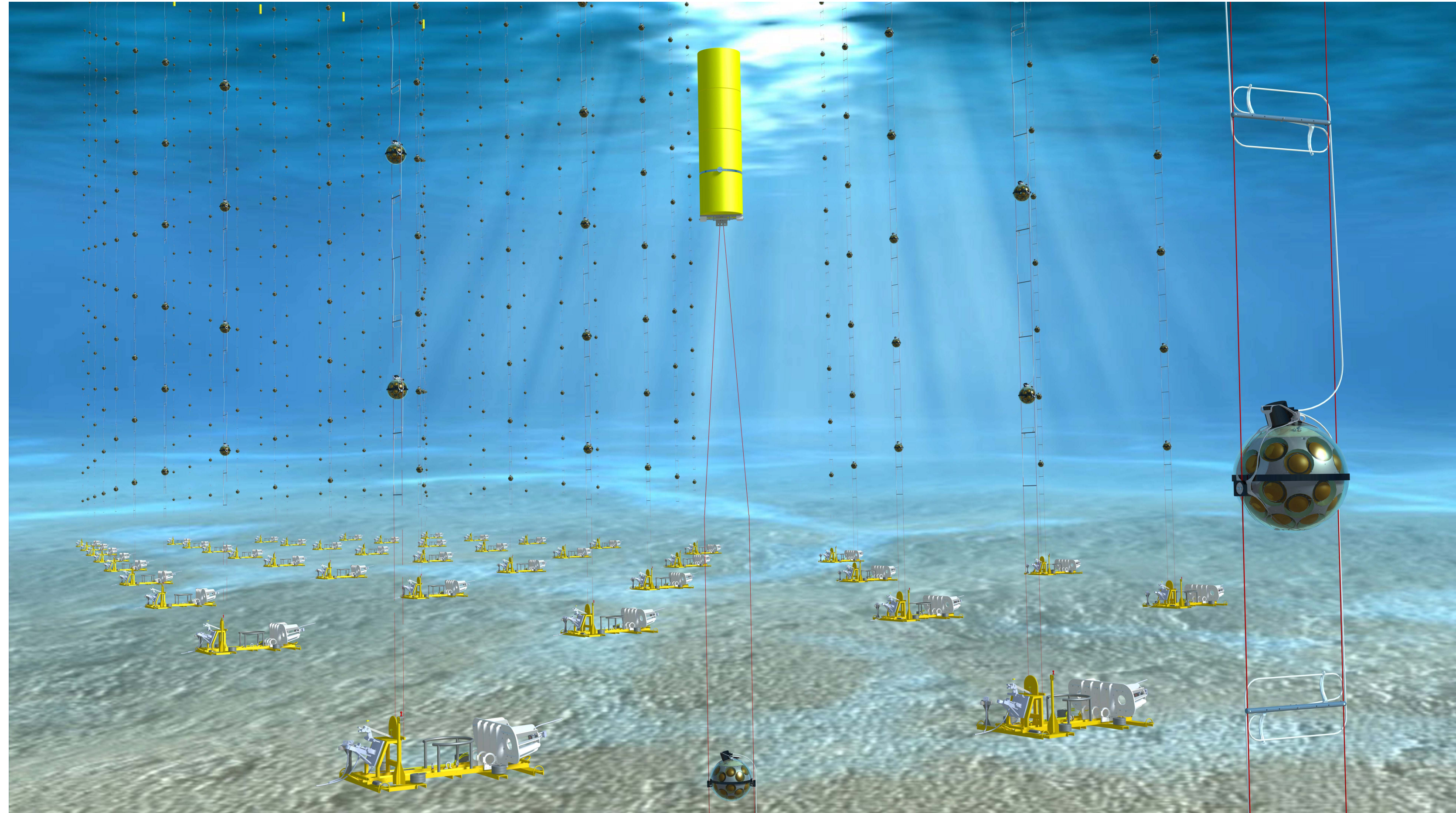




# The KM3NeT project (in a nutshell)

→ Successor of Antares

- two Cherenkov detectors (a la IceCube)
- ORCA (compact) and ARCA (sparse)
- in Mediterranean deep sea (~2500-3500m)
- detector volume envisioned of ~1km<sup>3</sup>

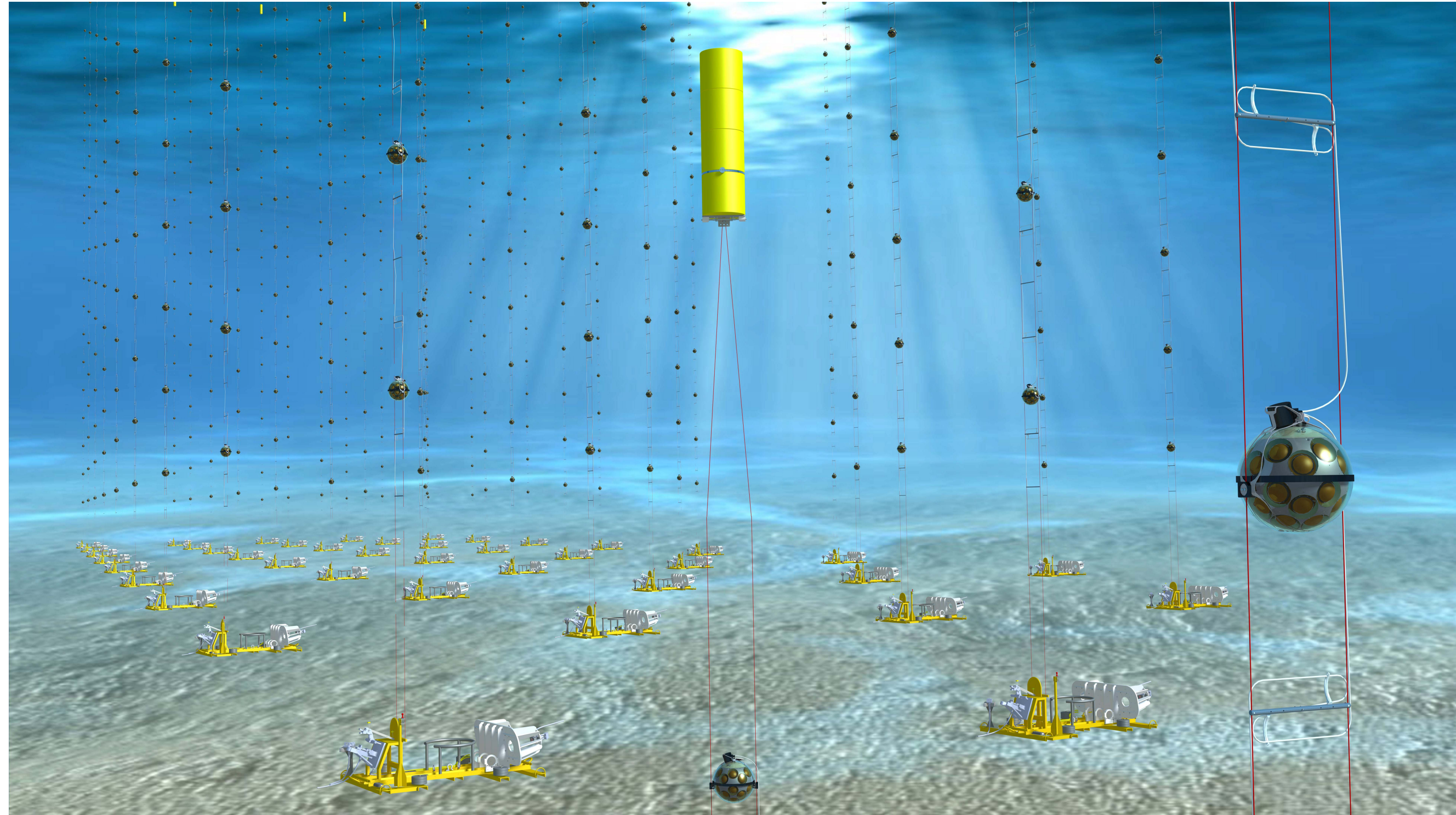




# The KM3NeT project (in a nutshell)

→ Successor of Antares

- two Cherenkov detectors (a la IceCube)
- ORCA (compact) and ARCA (sparse)
- in Mediterranean deep sea (~2500-3500m)
- detector volume envisioned of ~1km<sup>3</sup>



Technical configuration:

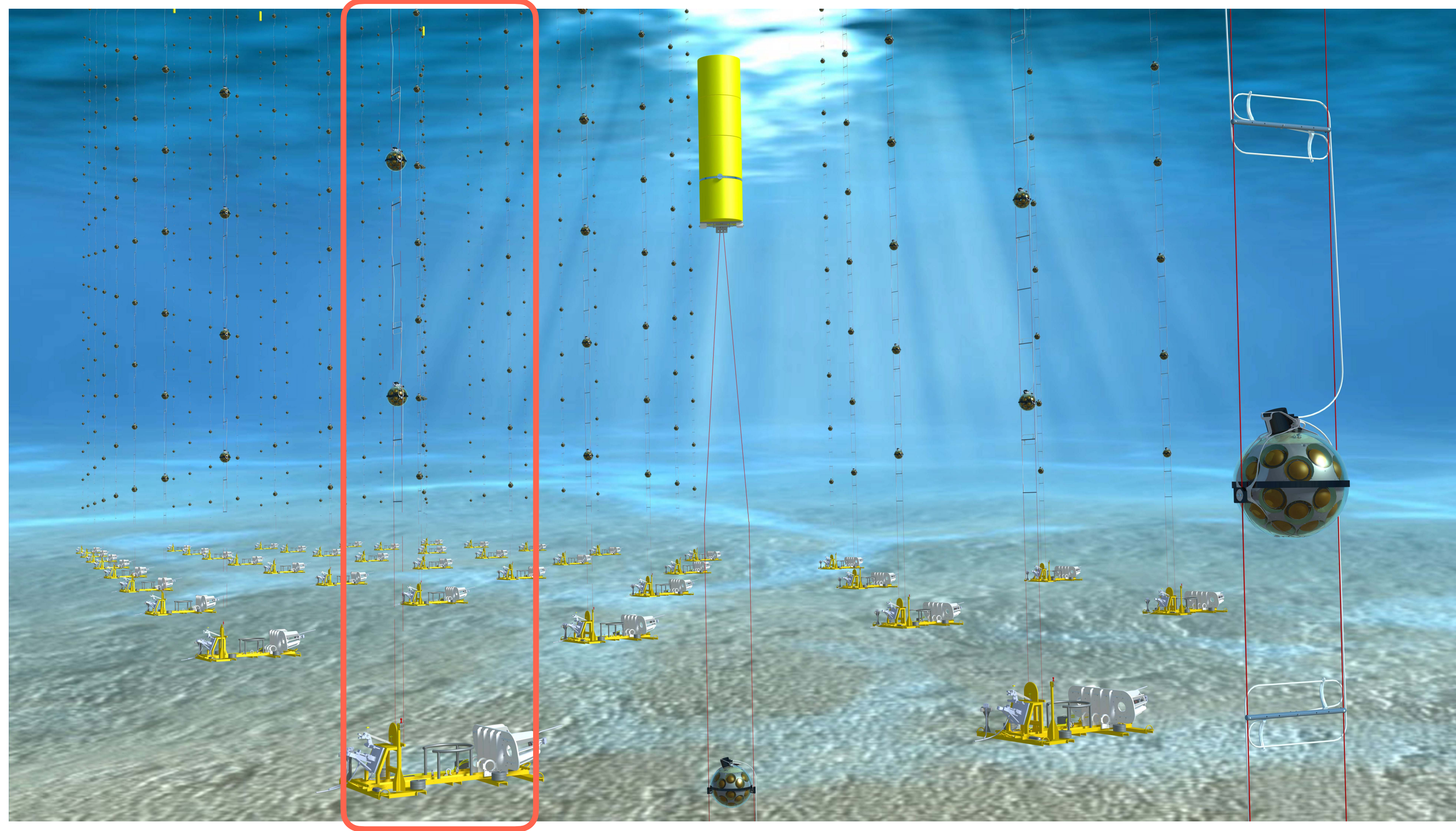
- each **Detection Unit** (DU) is a line made of 18 DOMs
- each **DOMs** is made of 31 **PMTs**



# The KM3NeT project (in a nutshell)

→ Successor of Antares

- two Cherenkov detectors (a la IceCube)
- ORCA (compact) and ARCA (sparse)
- in Mediterranean deep sea (~2500-3500m)
- detector volume envisioned of ~1km<sup>3</sup>



Technical configuration:

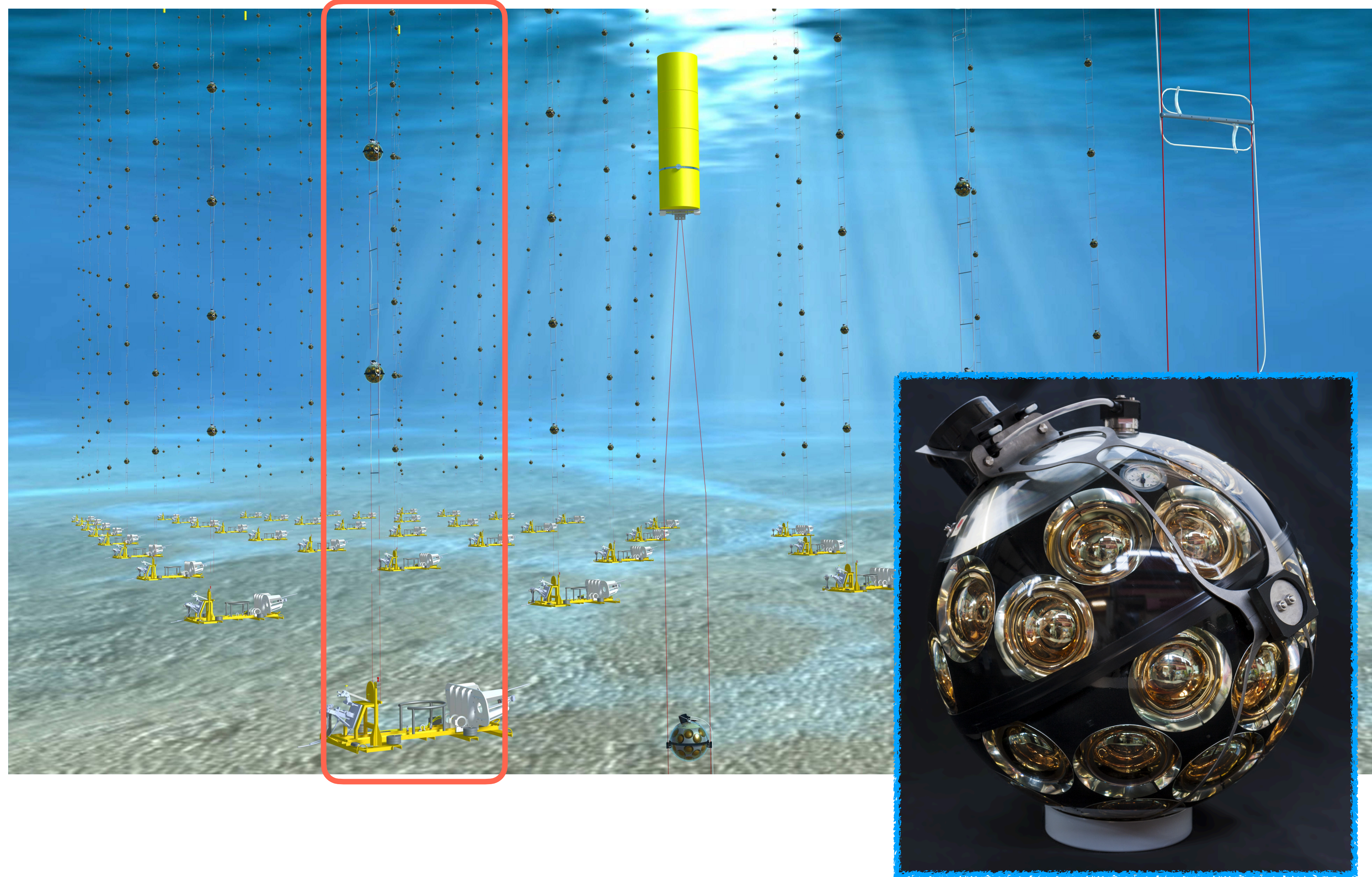
- each **Detection Unit** (DU) is a line made of 18 DOMs
- each **DOMs** is made of 31 **PMTs**



# The KM3NeT project (in a nutshell)

→ Successor of Antares

- two Cherenkov detectors (a la IceCube)
- ORCA (compact) and ARCA (sparse)
- in Mediterranean deep sea (~2500-3500m)
- detector volume envisioned of ~1km<sup>3</sup>



Technical configuration:

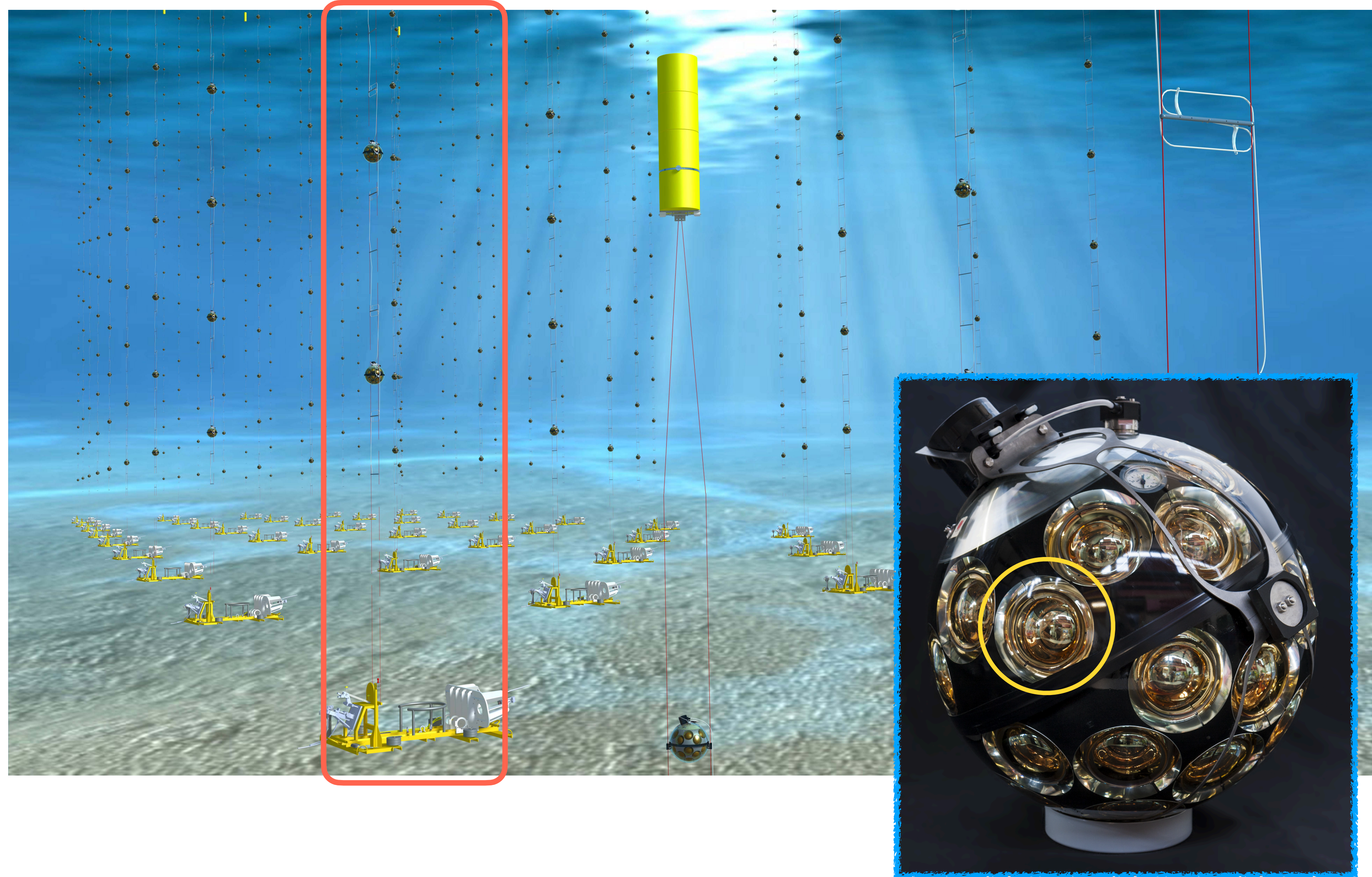
- each **Detection Unit** (DU) is a line made of 18 DOMs
- each **DOMs** is made of 31 **PMTs**



# The KM3NeT project (in a nutshell)

→ Successor of Antares

- two Cherenkov detectors (a la IceCube)
- ORCA (compact) and ARCA (sparse)
- in Mediterranean deep sea (~2500-3500m)
- detector volume envisioned of ~1km<sup>3</sup>



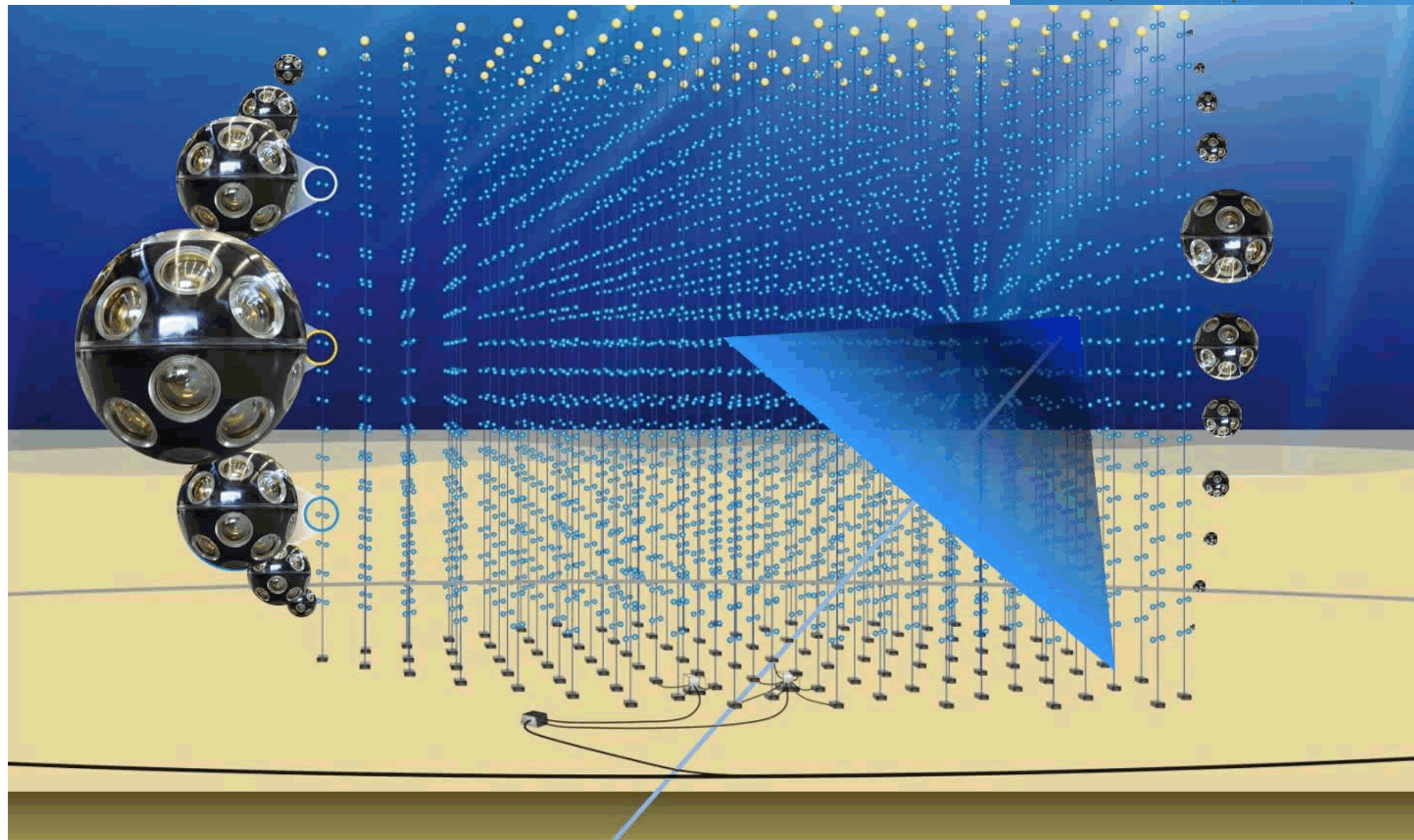
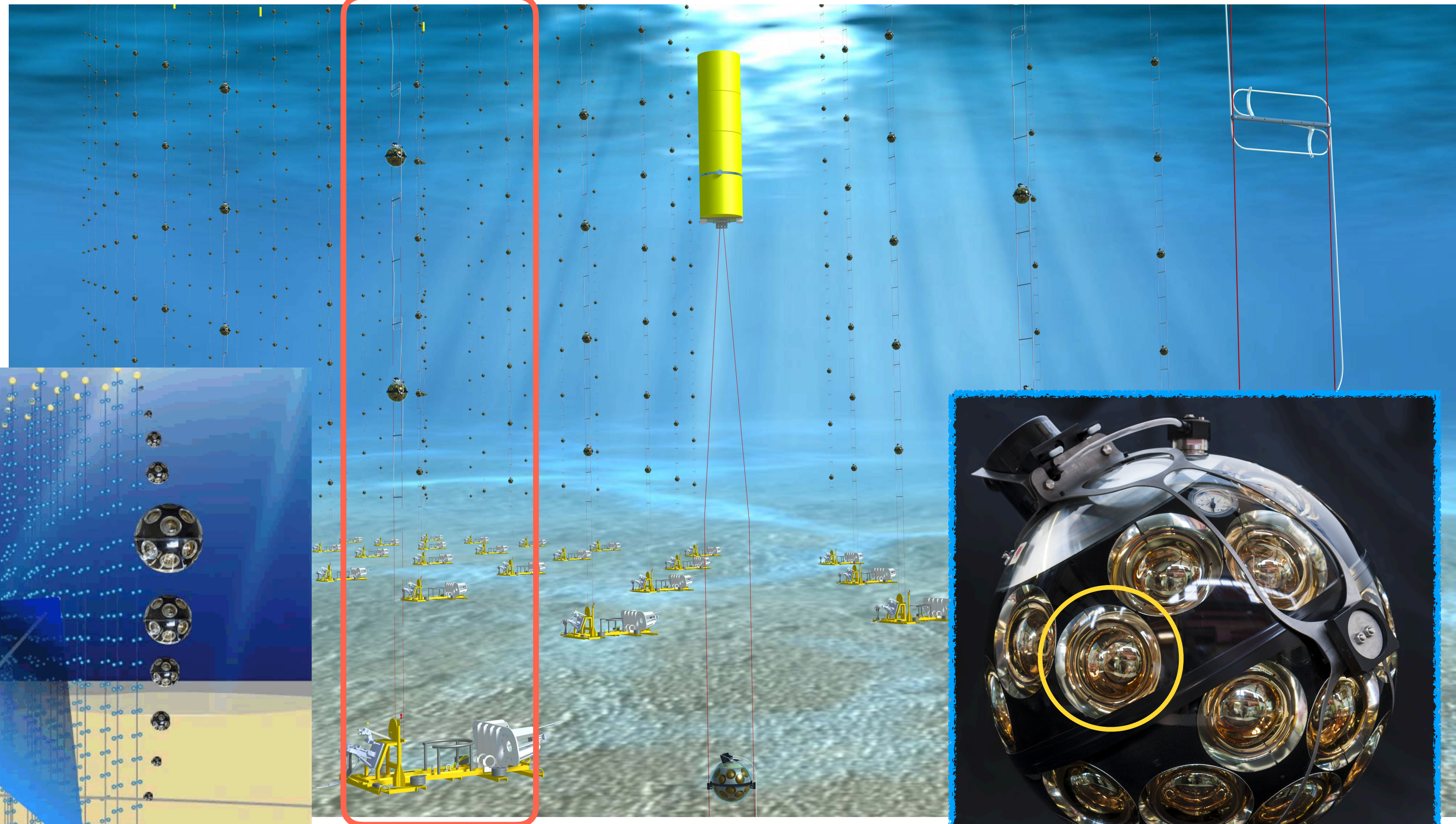
Technical configuration:

- each **Detection Unit** (DU) is a line made of 18 DOMs
- each **DOMs** is made of 31 **PMTs**

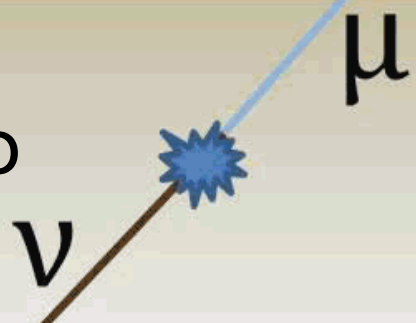


# The KM3NeT project (in a nutshell)

- Successor of Antares
- two Cherenkov detectors (a la IceCube)
- ORCA (compact) and ARCA (sparse)
- in Mediterranean deep sea (~2500-3500m)
- detector volume envisioned of ~1km<sup>3</sup>



Science case from  
neutrino physics to  
astronomy



Detect Cherenkov lights from:

- muon tracks
- neutrino cascades

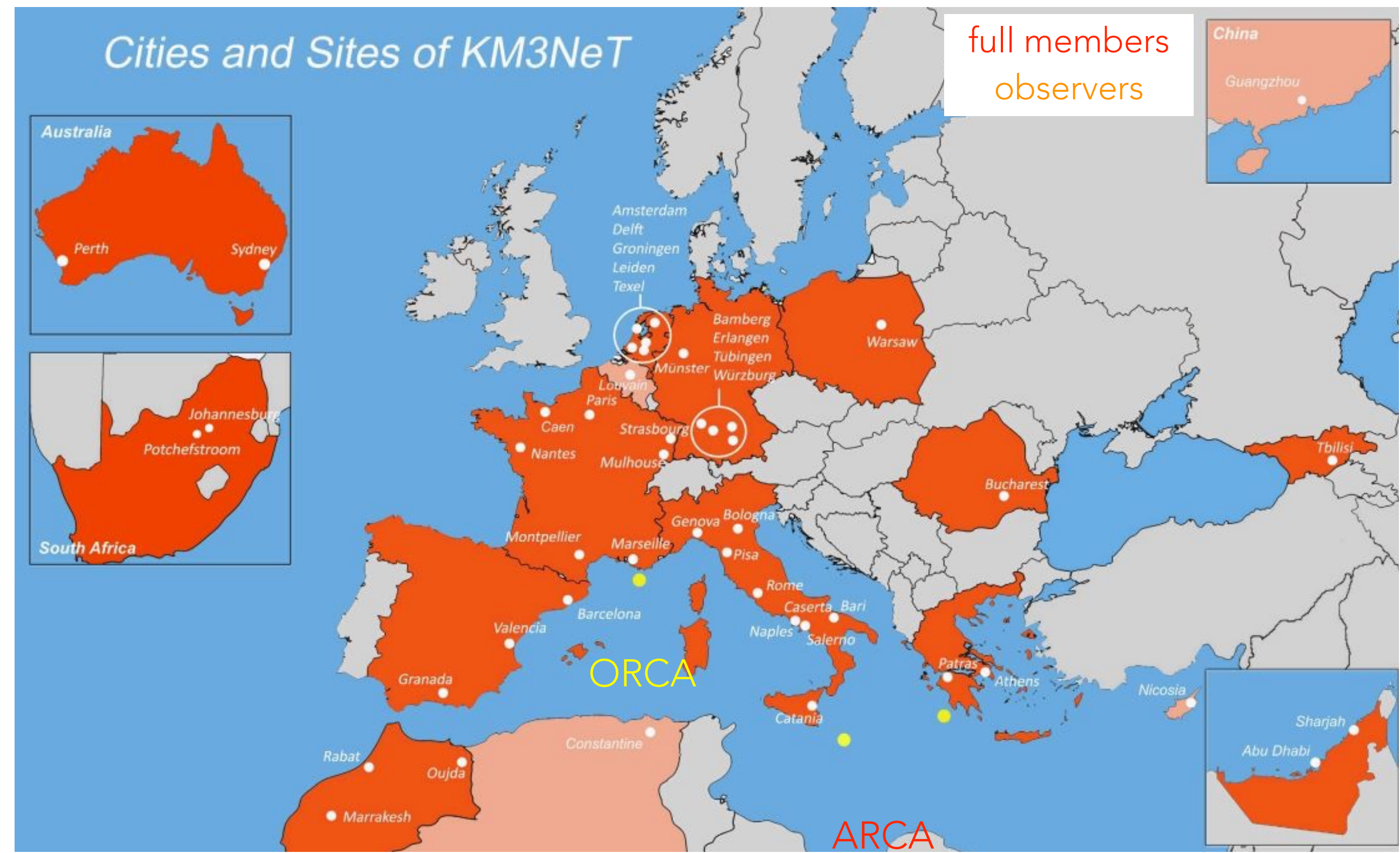
Technical configuration:

- each **Detection Unit** (DU) is a line made of 18 DOMs
- each **DOMs** is made of 31 **PMTs**



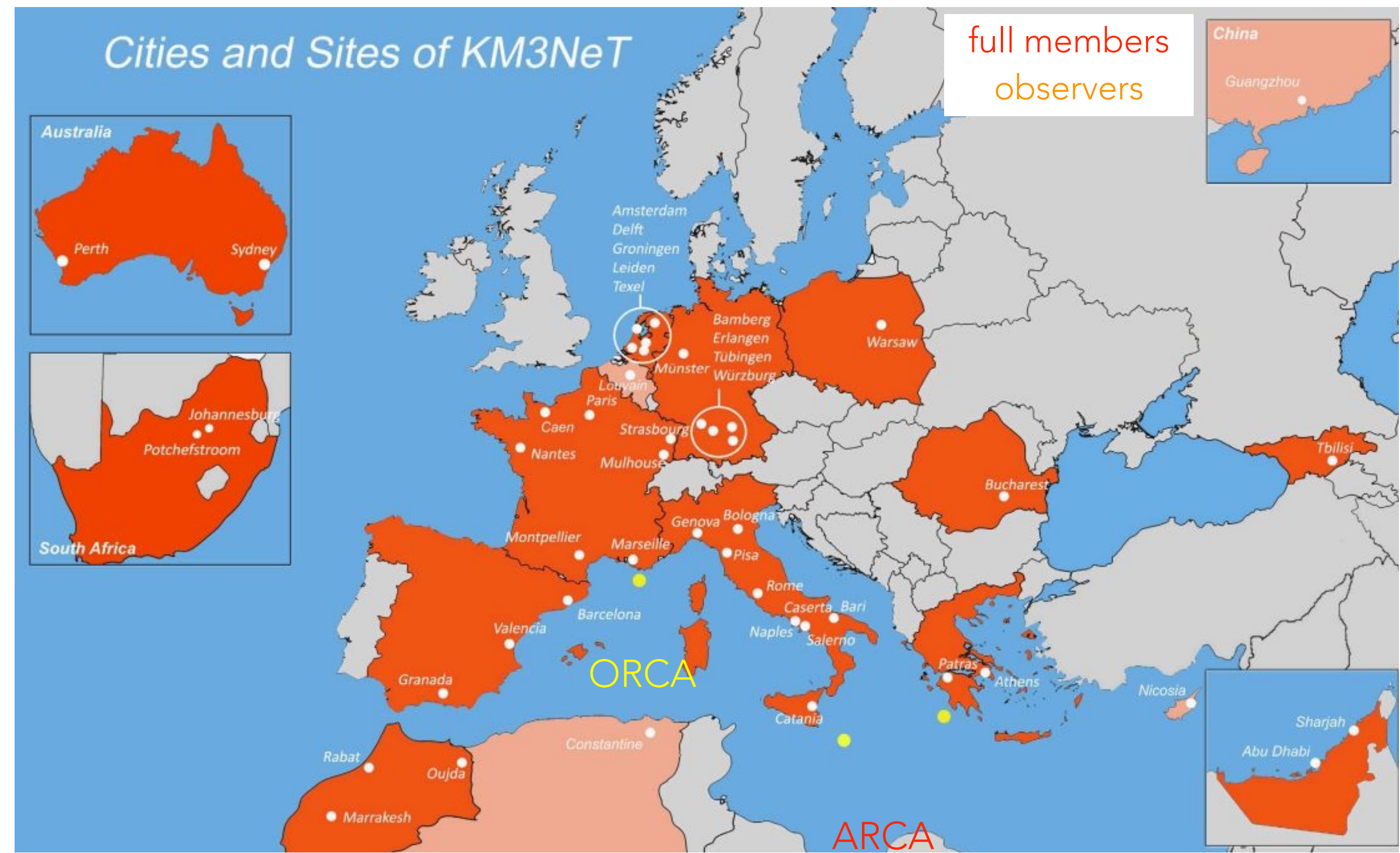
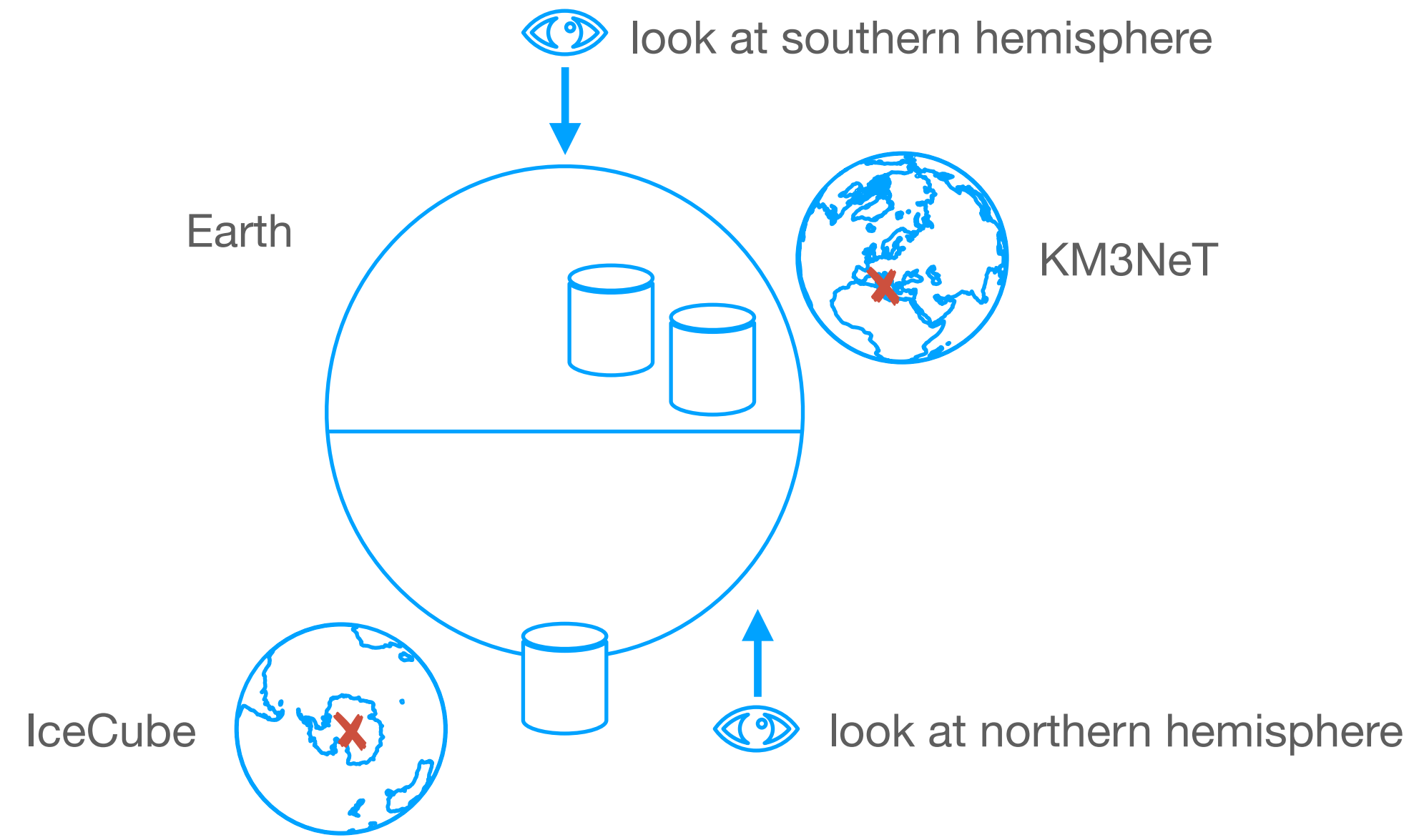


# Astronomy potential with KM3NeT



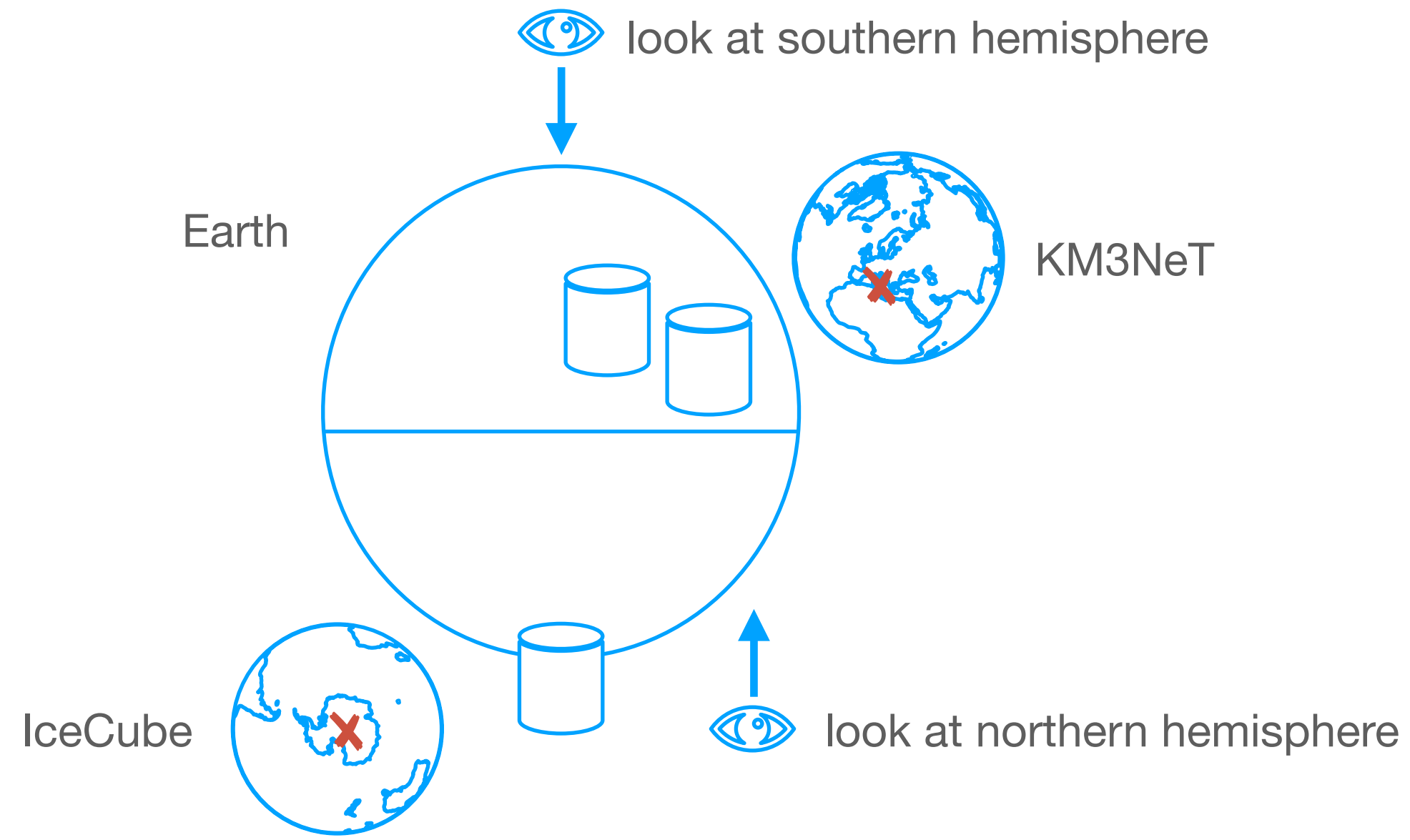


# Astronomy potential with KM3NeT

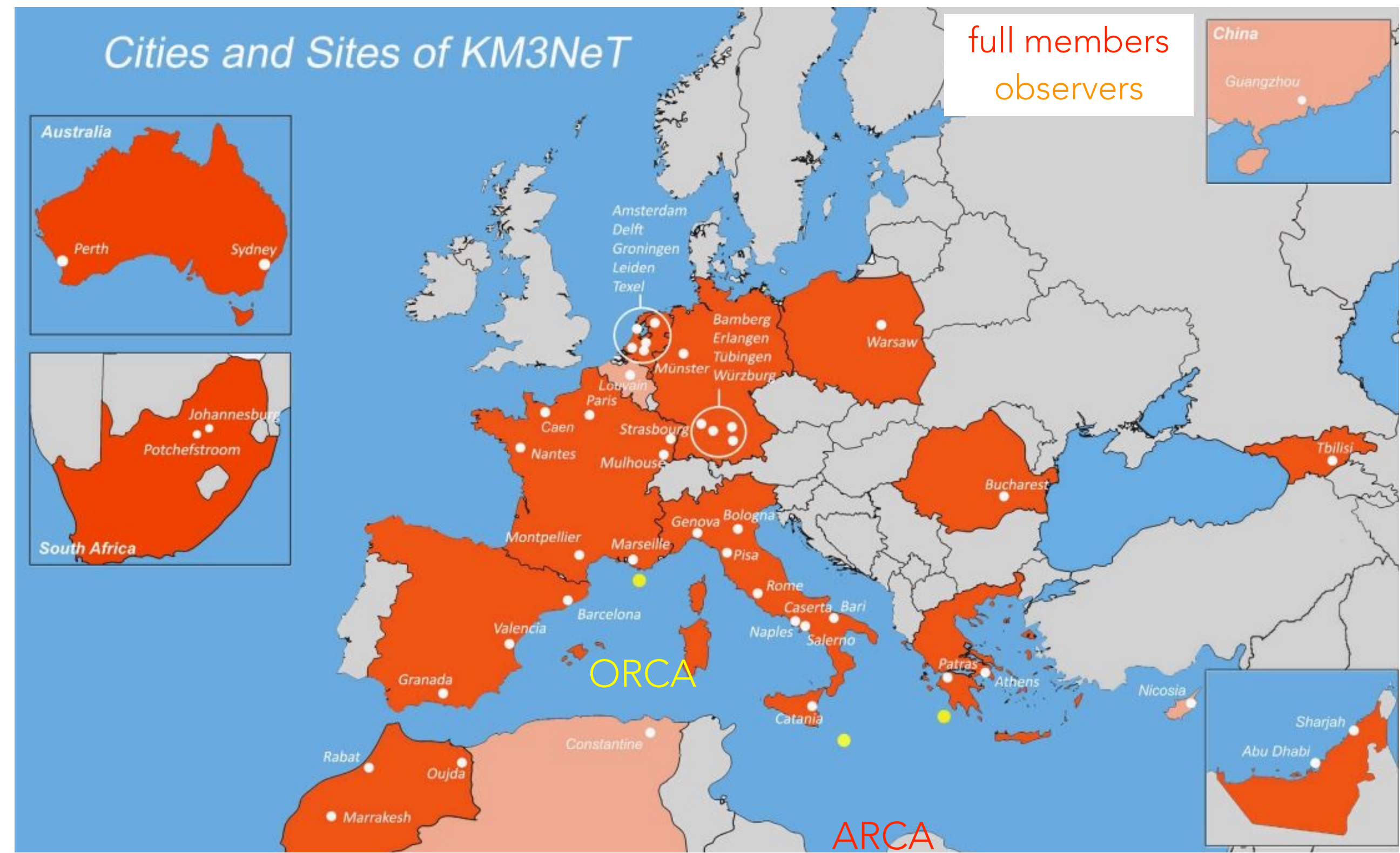




# Astronomy potential with KM3NeT

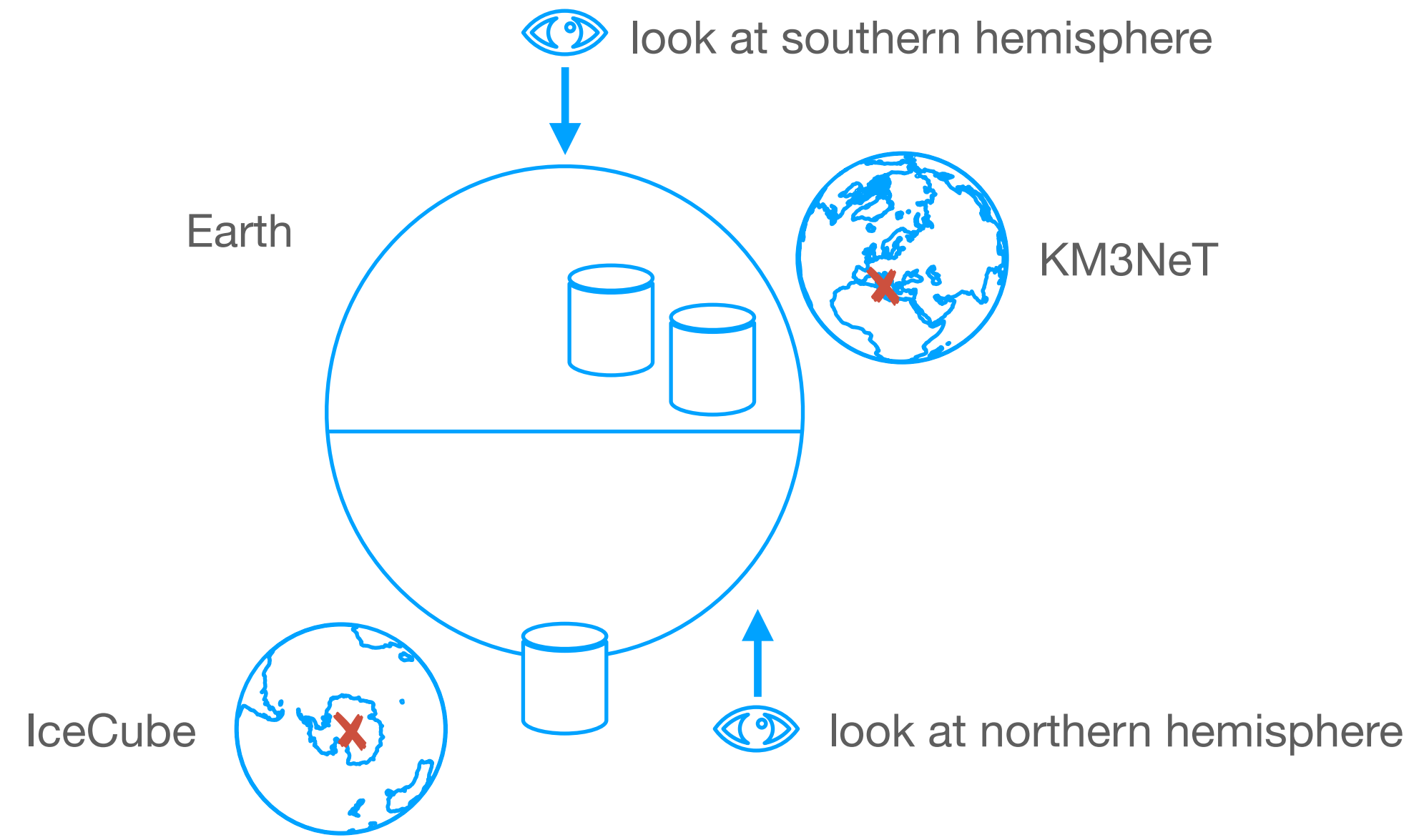


Galaxy centre visible from southern hemisphere!



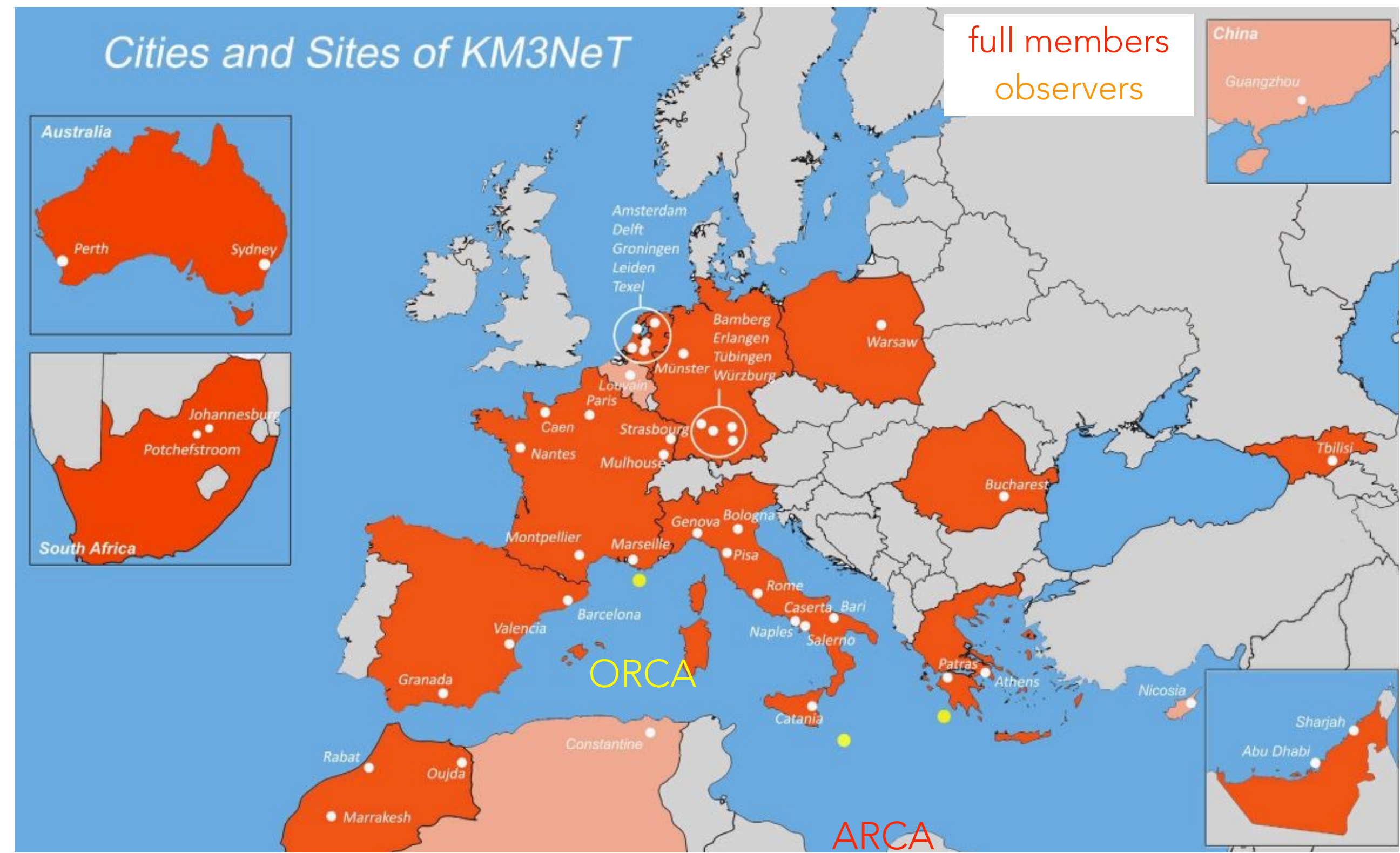


# Astronomy potential with KM3NeT



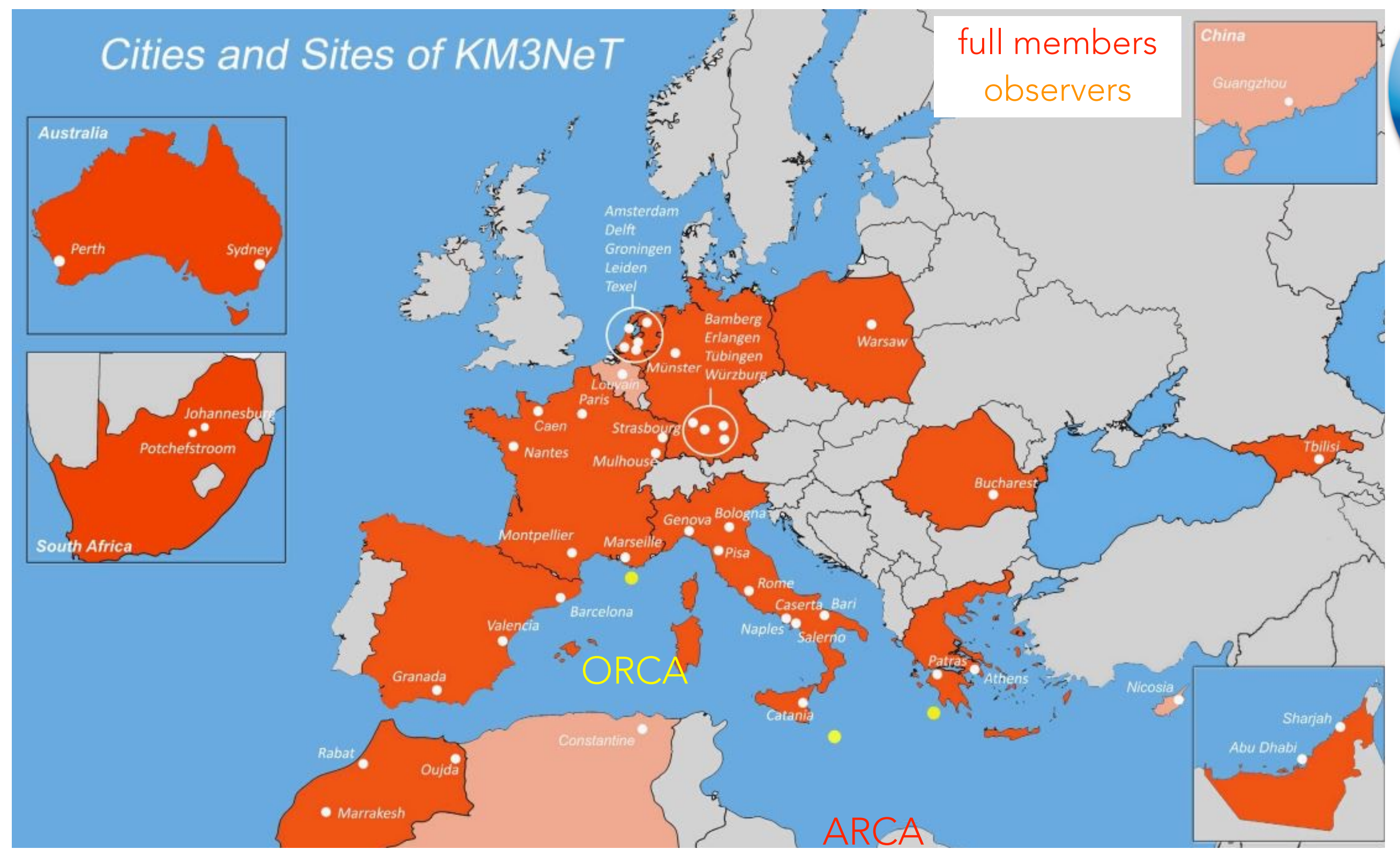
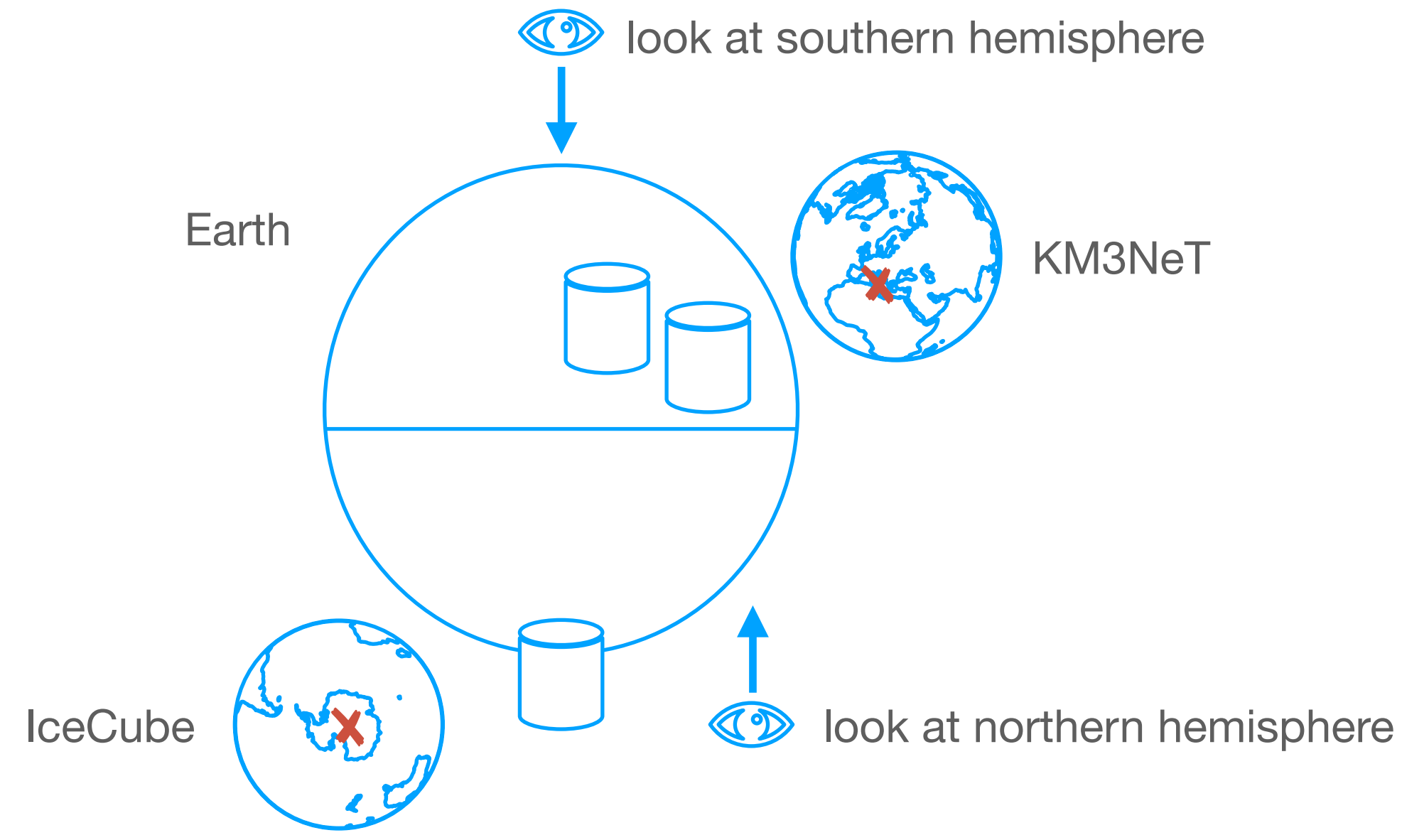
Galaxy centre visible from southern hemisphere!

strong assets of KM3NeT





# Astronomy potential with KM3NeT

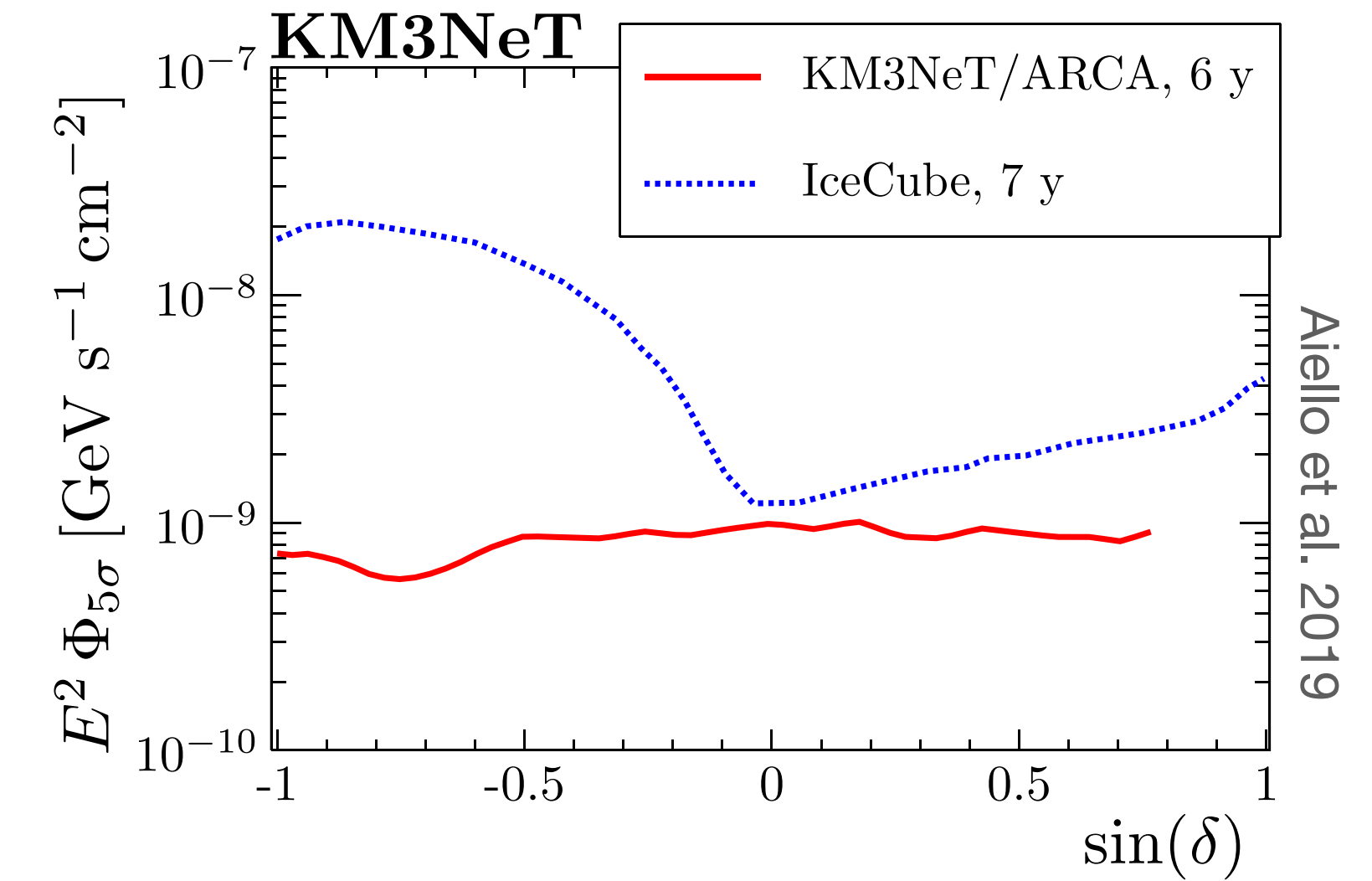
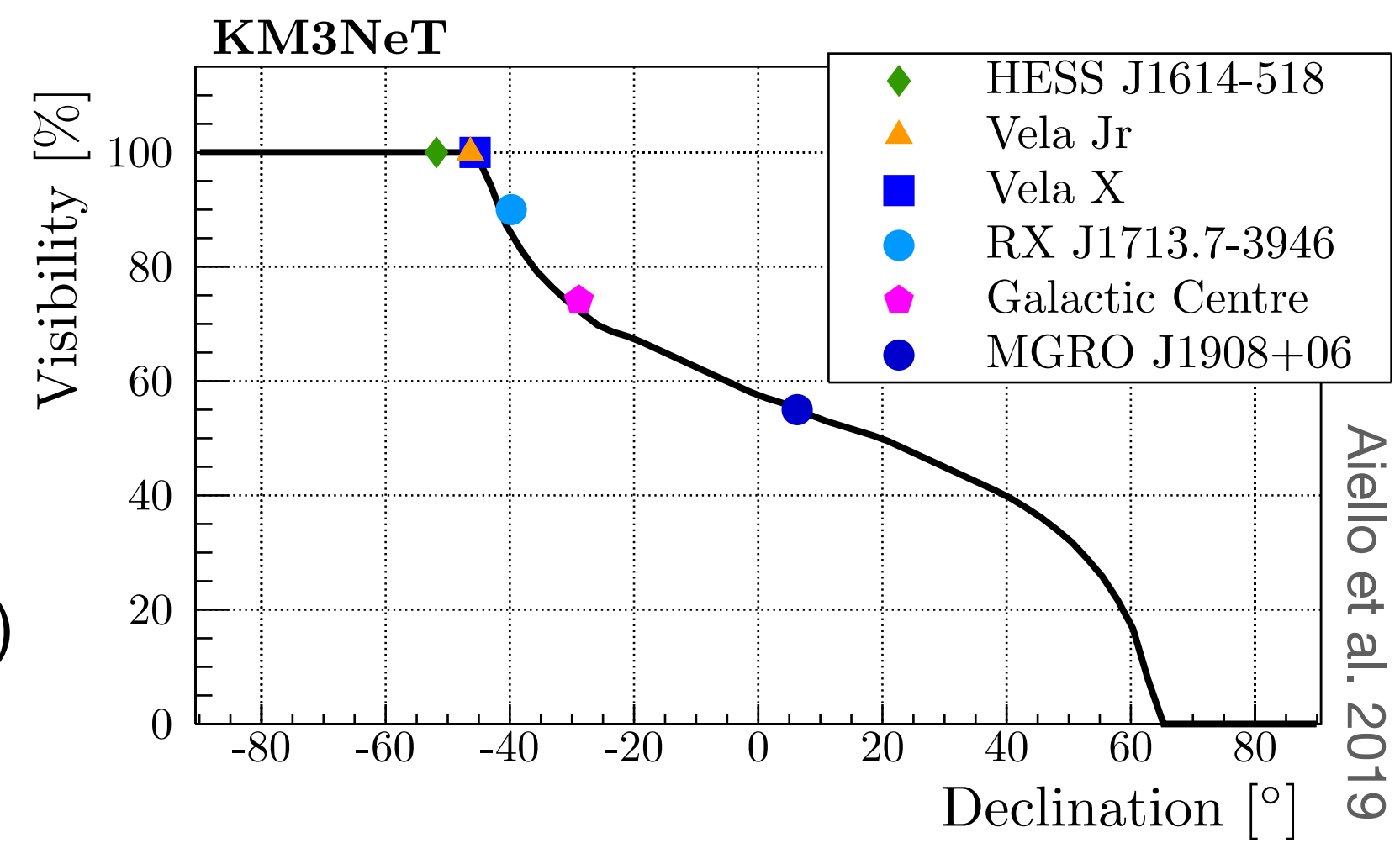


Galaxy centre visible from southern hemisphere!



strong assets of KM3NeT

1. field of view
2. sensitivity (over the whole sky)





# KM3NeT activities at Subatech

---

Our team is involved in the astronomy analysis

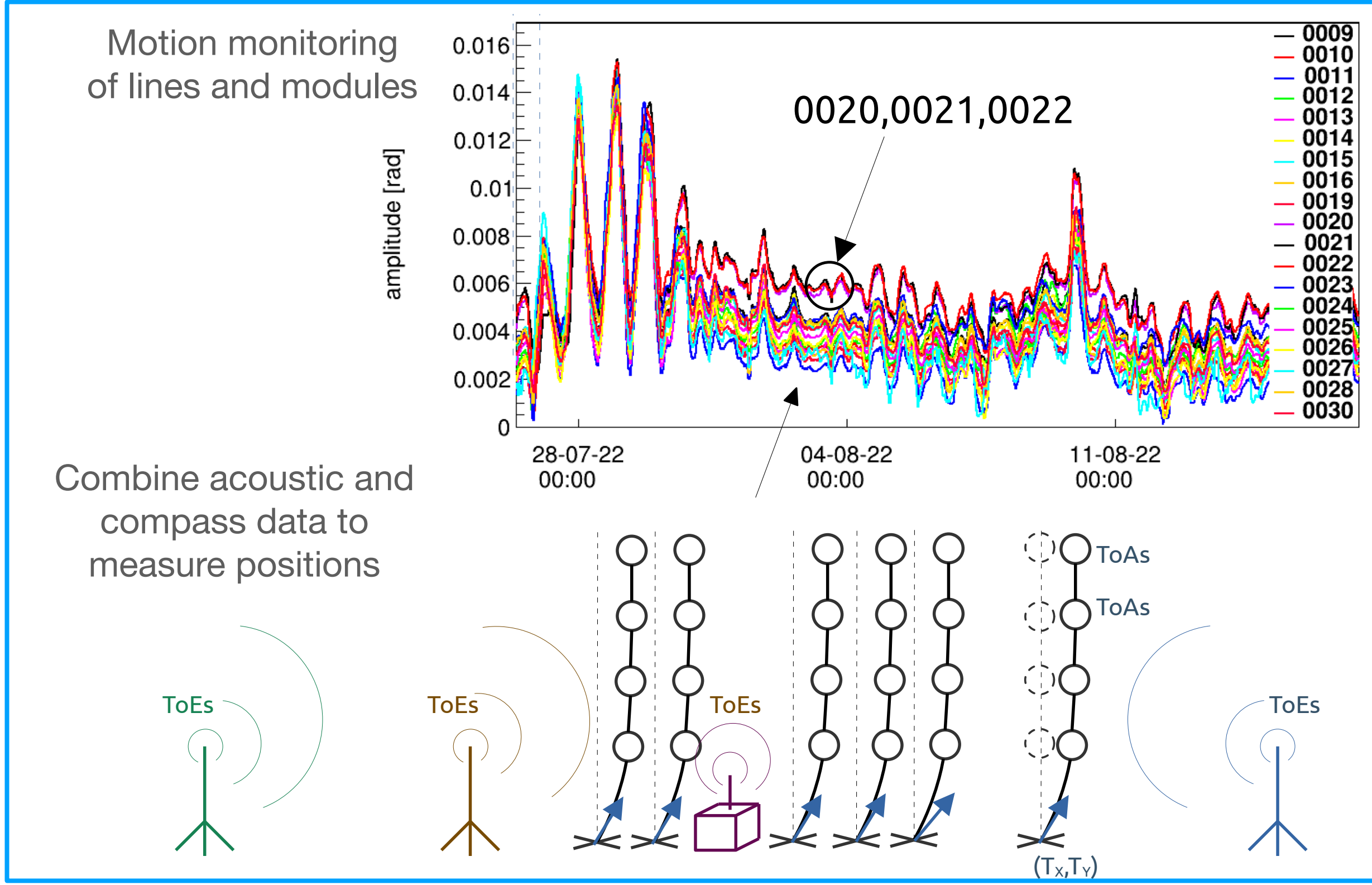
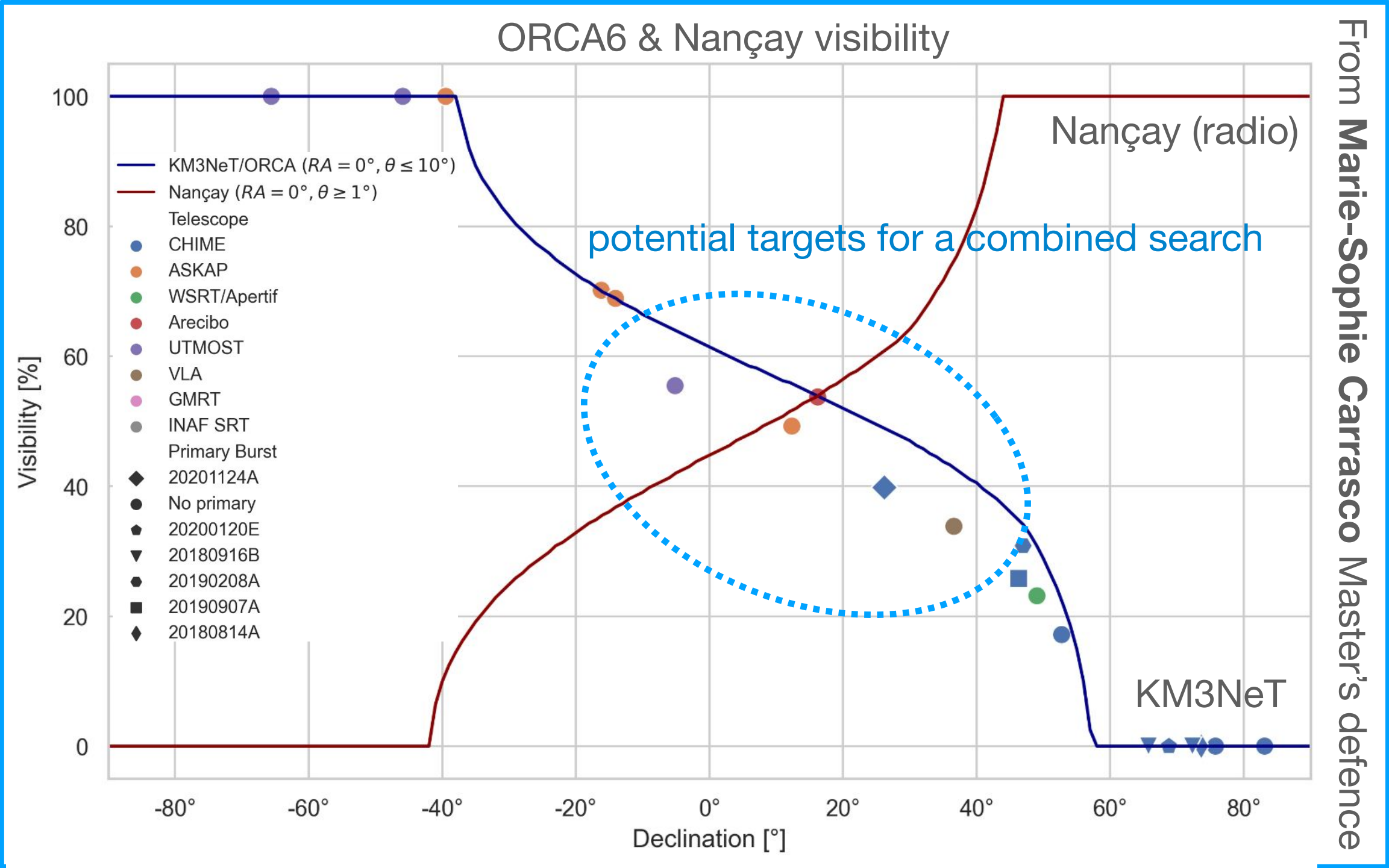




Our team is involved in the astronomy analysis

## Main (current) projects :

- neutrino analysis with FRB catalogs → visibility studies / binned & ON-OFF searches (work lead by **Félix Bretaudeau** PhD student)
- positioning calibration → critical for angular resolution → astronomy (work lead by **Lilian Martin**)





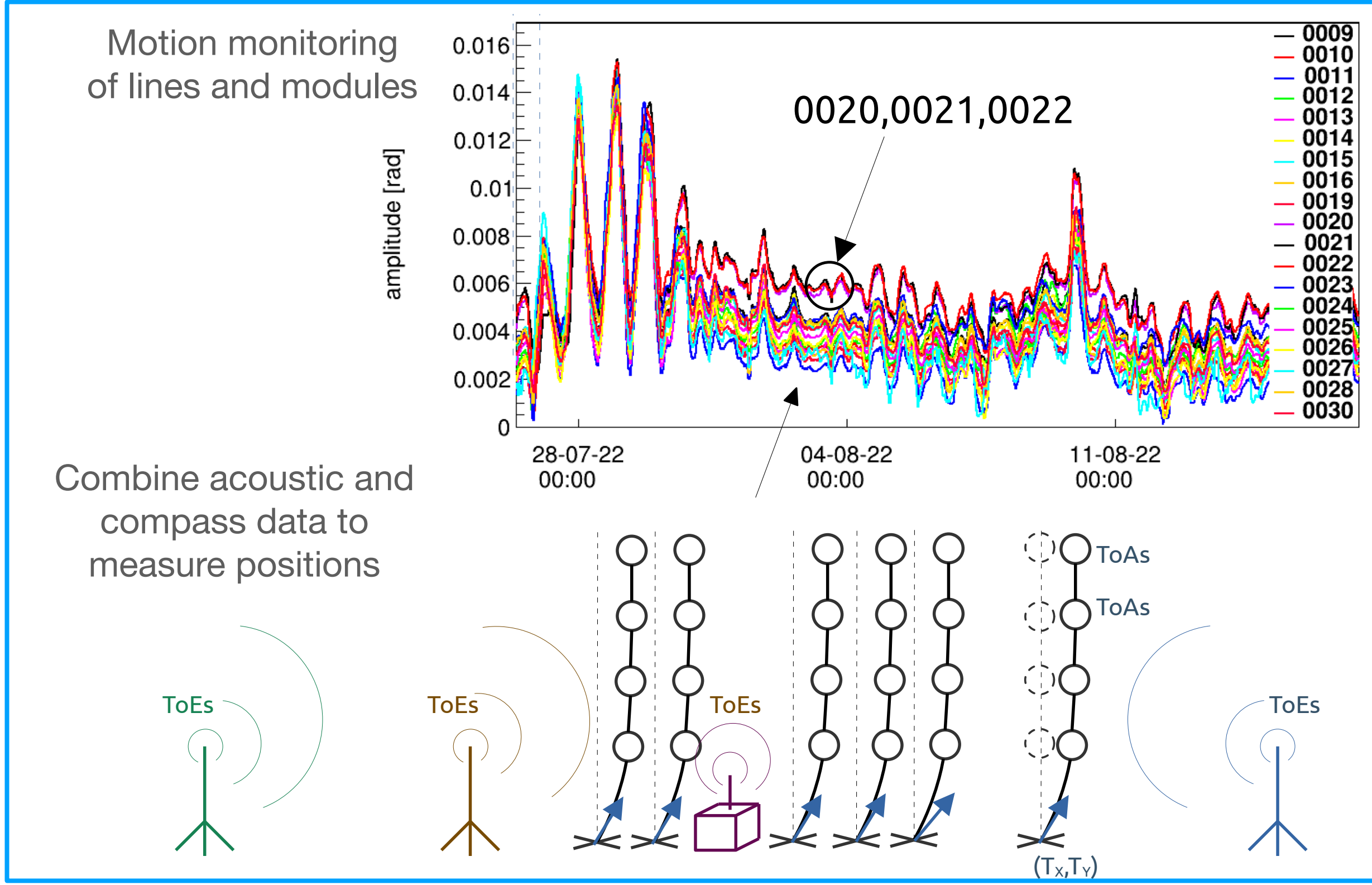
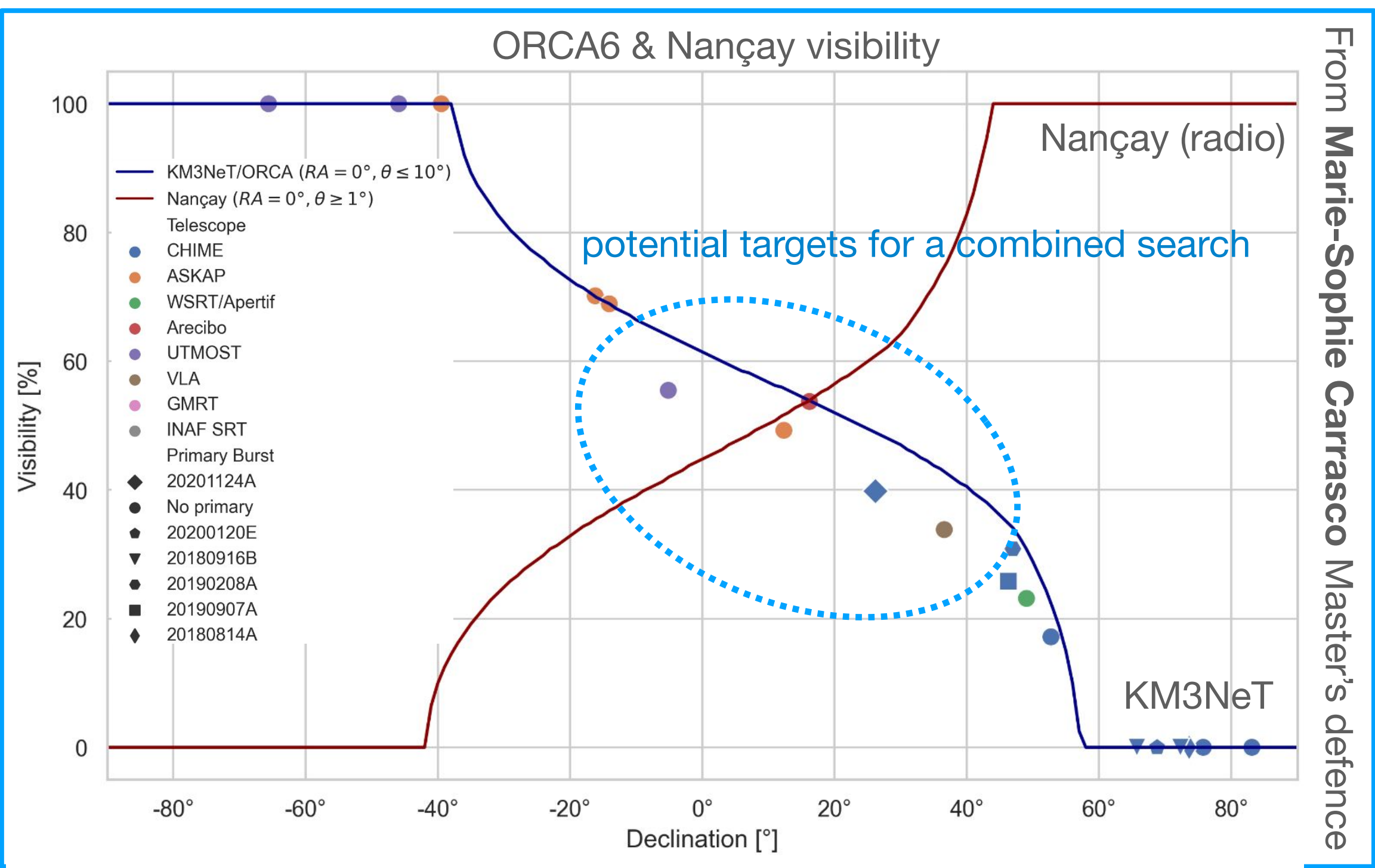
# KM3NeT activities at Subatech



Our team is involved in the astronomy analysis

## Main (current) projects :

- neutrino analysis with FRB catalogs → visibility studies / binned & ON-OFF searches (work lead by **Félix Bretaudeau** PhD student)
- positioning calibration → critical for angular resolution → astronomy (work lead by **Lilian Martin**)



## (some) futurs projects :

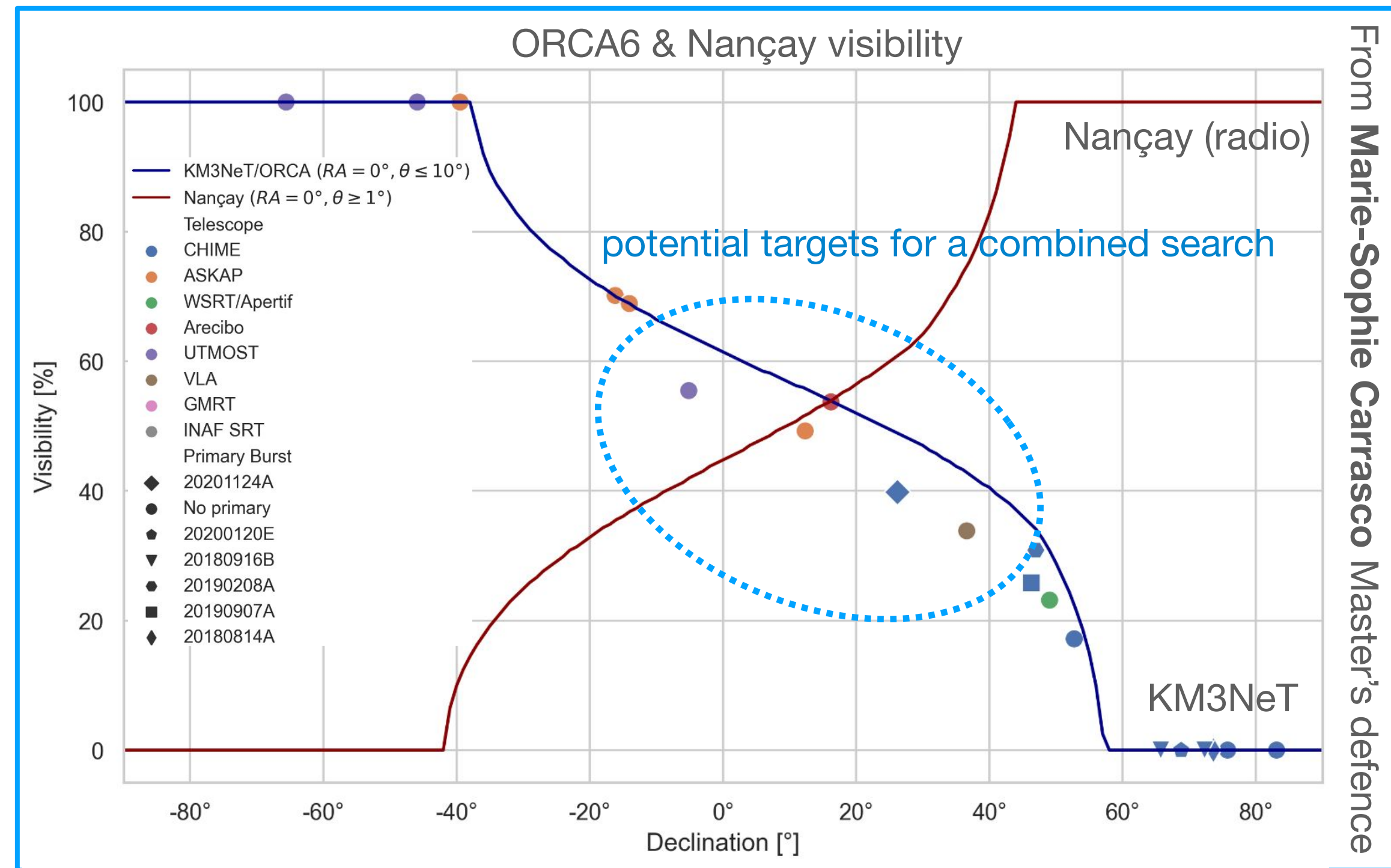
- extension to southern radio-telescopes (Meerkat, MWA, SKA?)
- alert and observation strategies with radio-telescope (online analysis)
- model développements for multi-messenger fast radio transients sources (iterative with alerts and strategies)



Our team is involved in the astronomy analysis

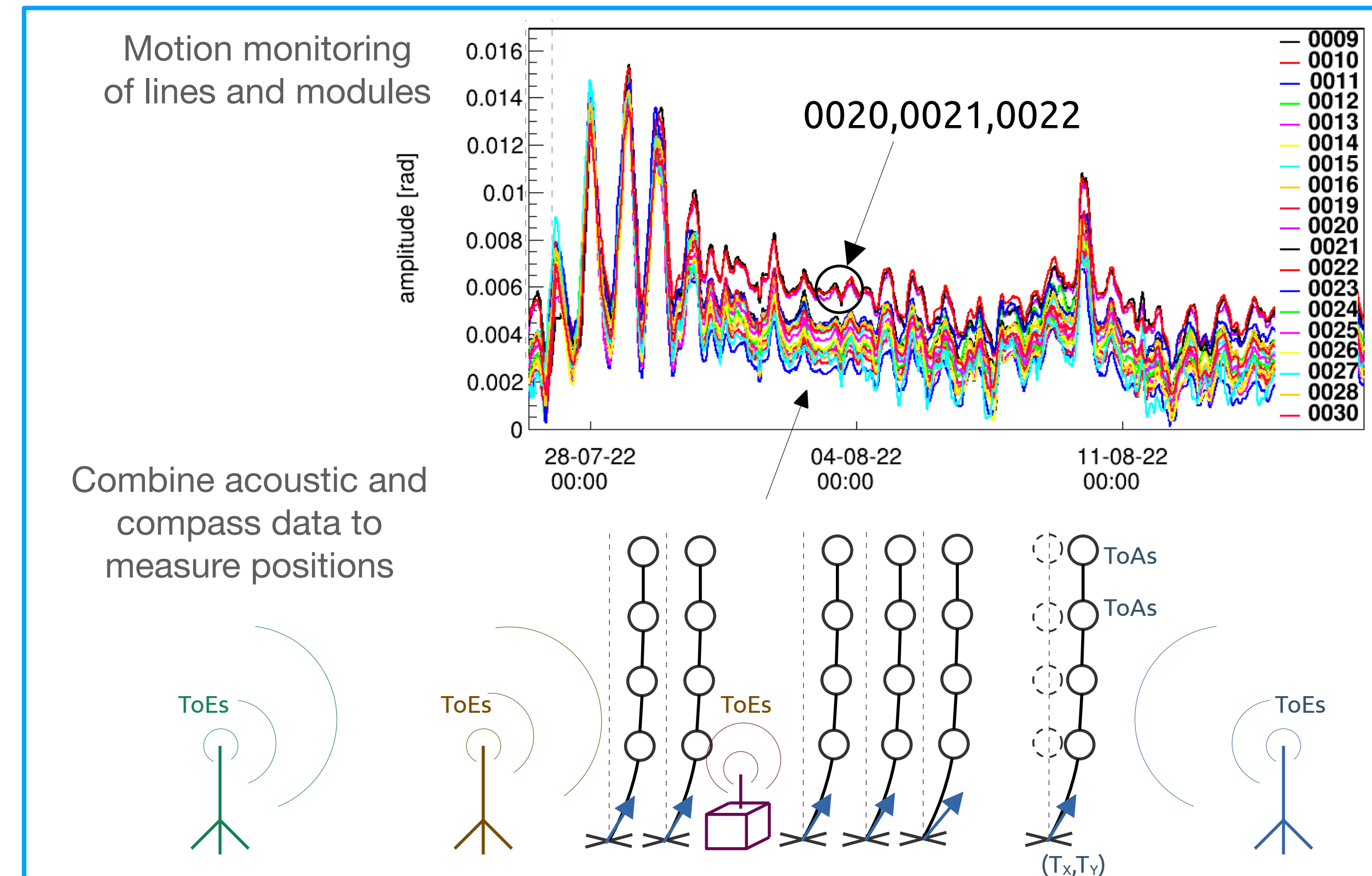
## Main (current) projects :

- neutrino analysis with FRB catalogs → visibility studies / binned & ON-OFF searches (work lead by **Félix Bretaudeau** PhD student)
- positioning calibration → critical for angular resolution → astronomy (work lead by **Lilian Martin**)



## (some) futurs projects :

- extension to southern radio-telescopes (Meerkat, MWA, SKA?)
- alert and observation strategies with radio-telescope (online analysis)
- model développements for multi-messenger fast radio transients sources (iterative with alerts and strategies)

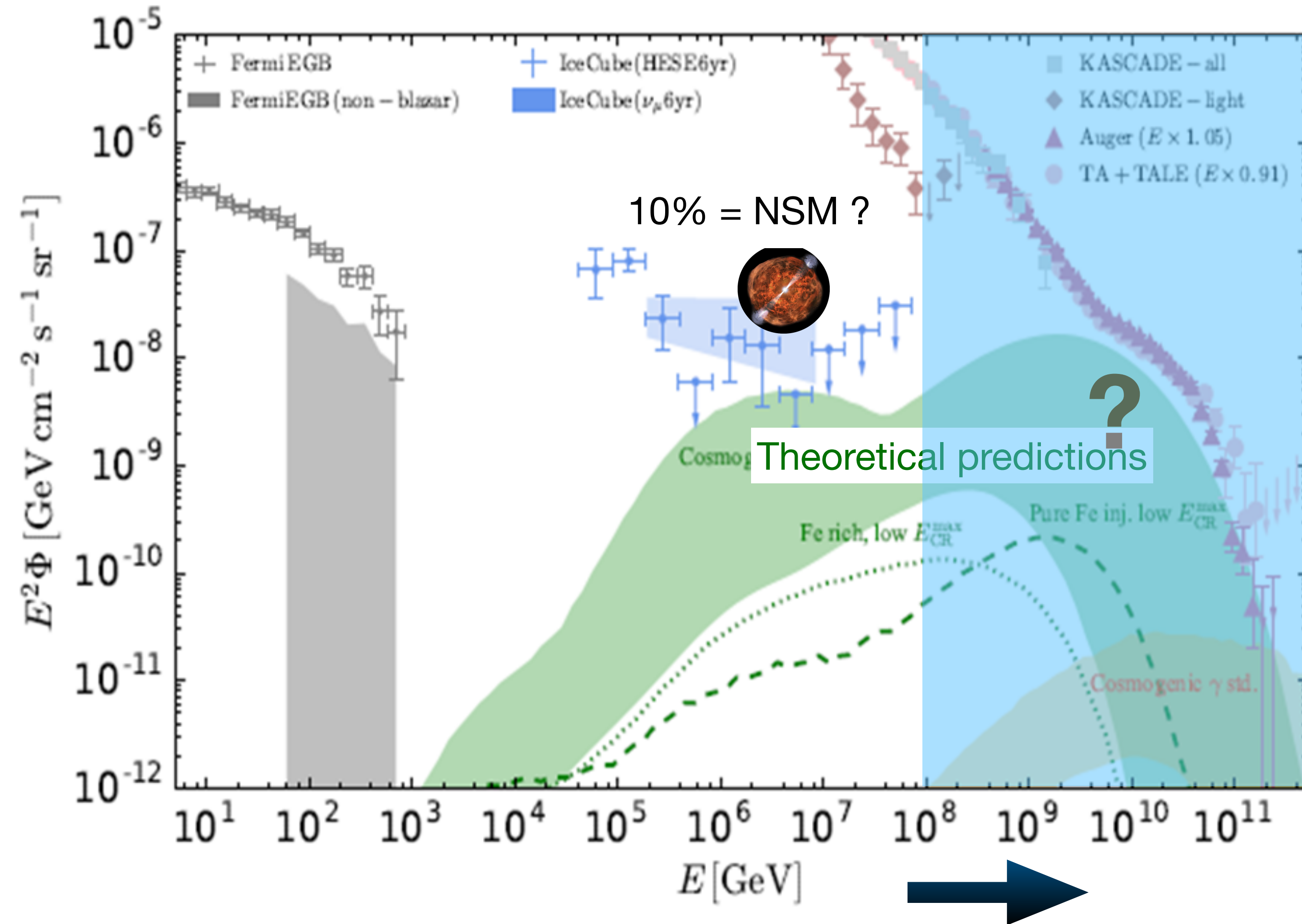


Work in progress, new results are coming soon!



# Predicted ultra high-energy neutrinos

- Expand the measurements of the neutrino spectrum
- Reach the cosmogenic flux of ultra high-energy (UHE) neutrinos



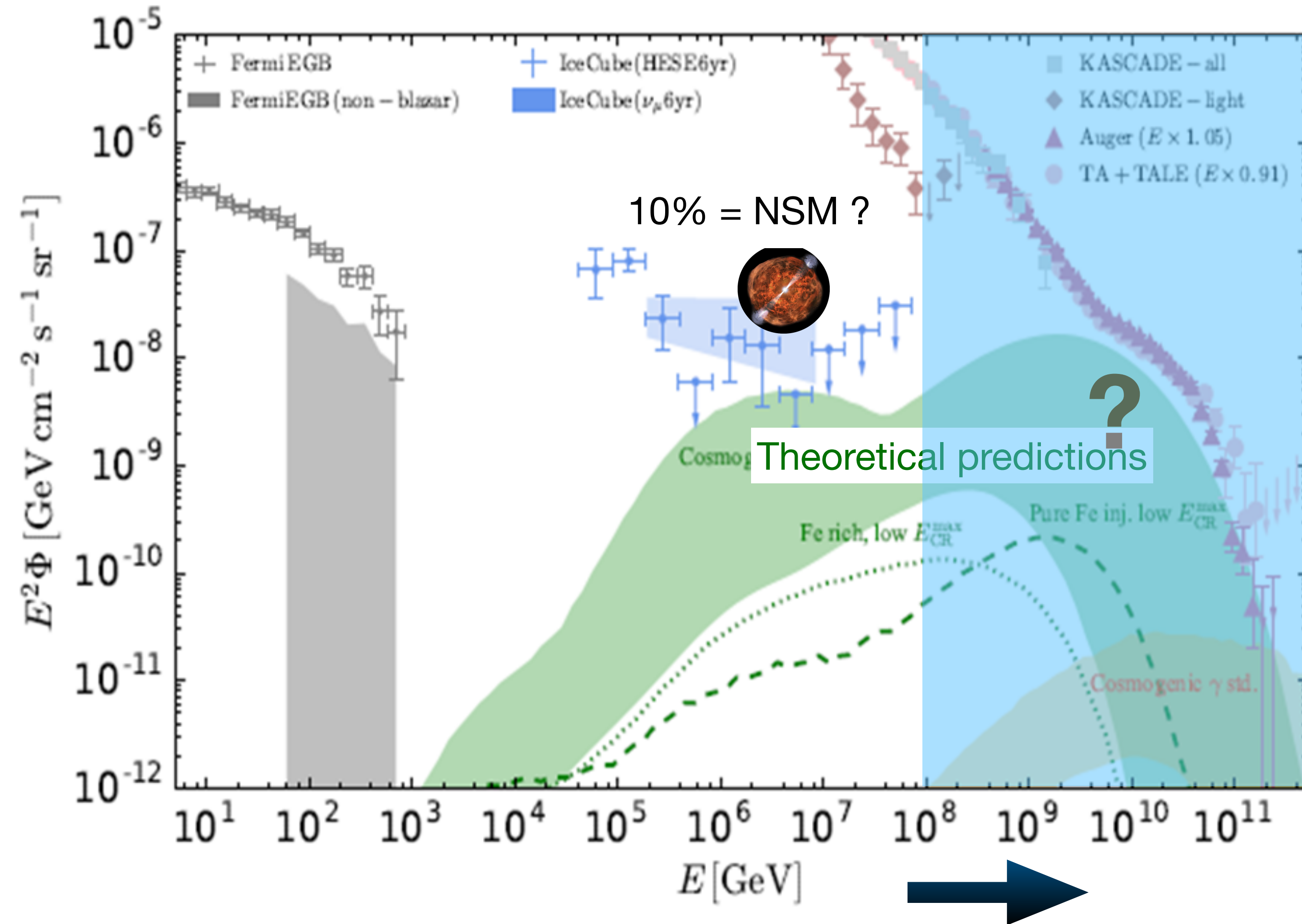
Guaranteed  
cosmogenic neutrinos

UHECR + cosmic photons → UHE neutrinos  
+ neutrinos from astrophysical sources



# Predicted ultra high-energy neutrinos

- Expand the measurements of the neutrino spectrum
- Reach the cosmogenic flux of ultra high-energy (UHE) neutrinos



Guaranteed  
cosmogenic neutrinos

UHECR + cosmic photons → UHE neutrinos  
+ neutrinos from astrophysical sources

Which sources and where ?



# Constraining the possible sources of cosmogenic neutrinos

---

V. D., Romero-Wolf (JPL), Deaconu (UChicago), and Wissel (PSU) (in progress)

**Which cosmogenic sources are we going to see with which instrument?**



# Constraining the possible sources of cosmogenic neutrinos

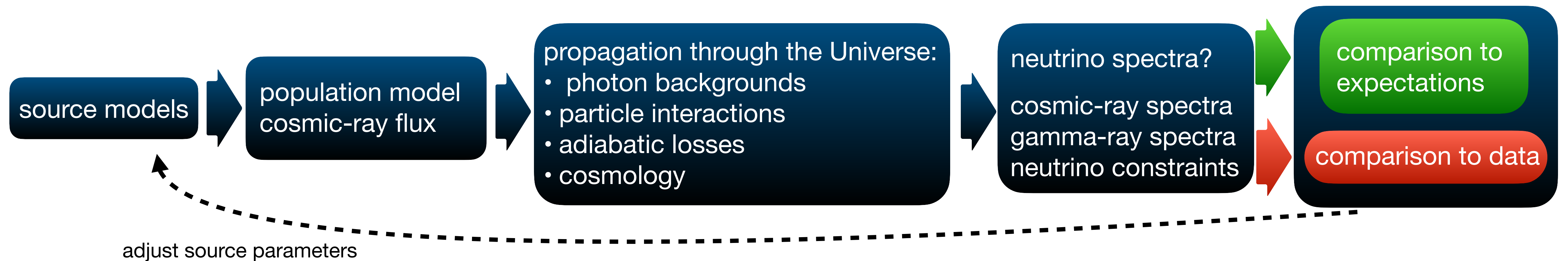
V. D., Romero-Wolf (JPL), Deaconu (UChicago), and Wissel (PSU) (in progress)

Which cosmogenic sources are we going to see with which instrument?

Study based on the initial works of *Andres Romero-Wolf and Maximo Ave 2018*

Extended to multimessenger constraints: cosmic-ray, gamma-ray, neutrino

+ constraint from possible futur detection of planned experiments: here PUEO





# Constraining the possible sources of cosmogenic neutrinos

V. D., Romero-Wolf (JPL), Deaconu (UChicago), and Wissel (PSU) (in progress)

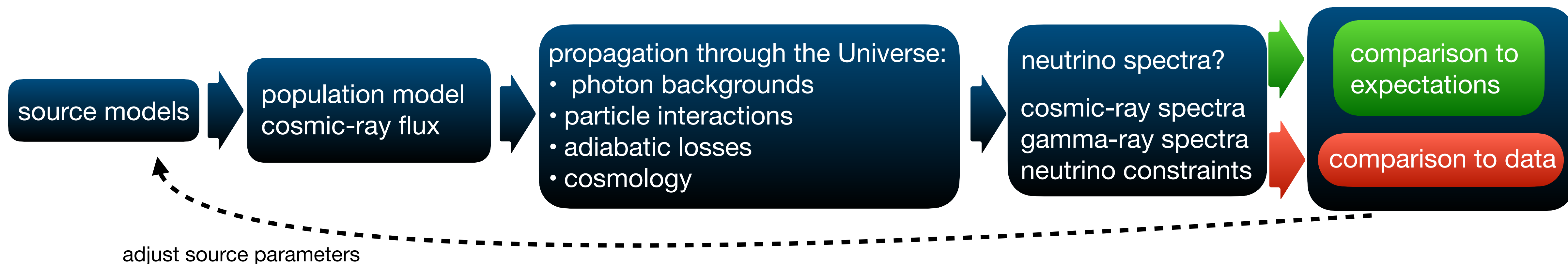
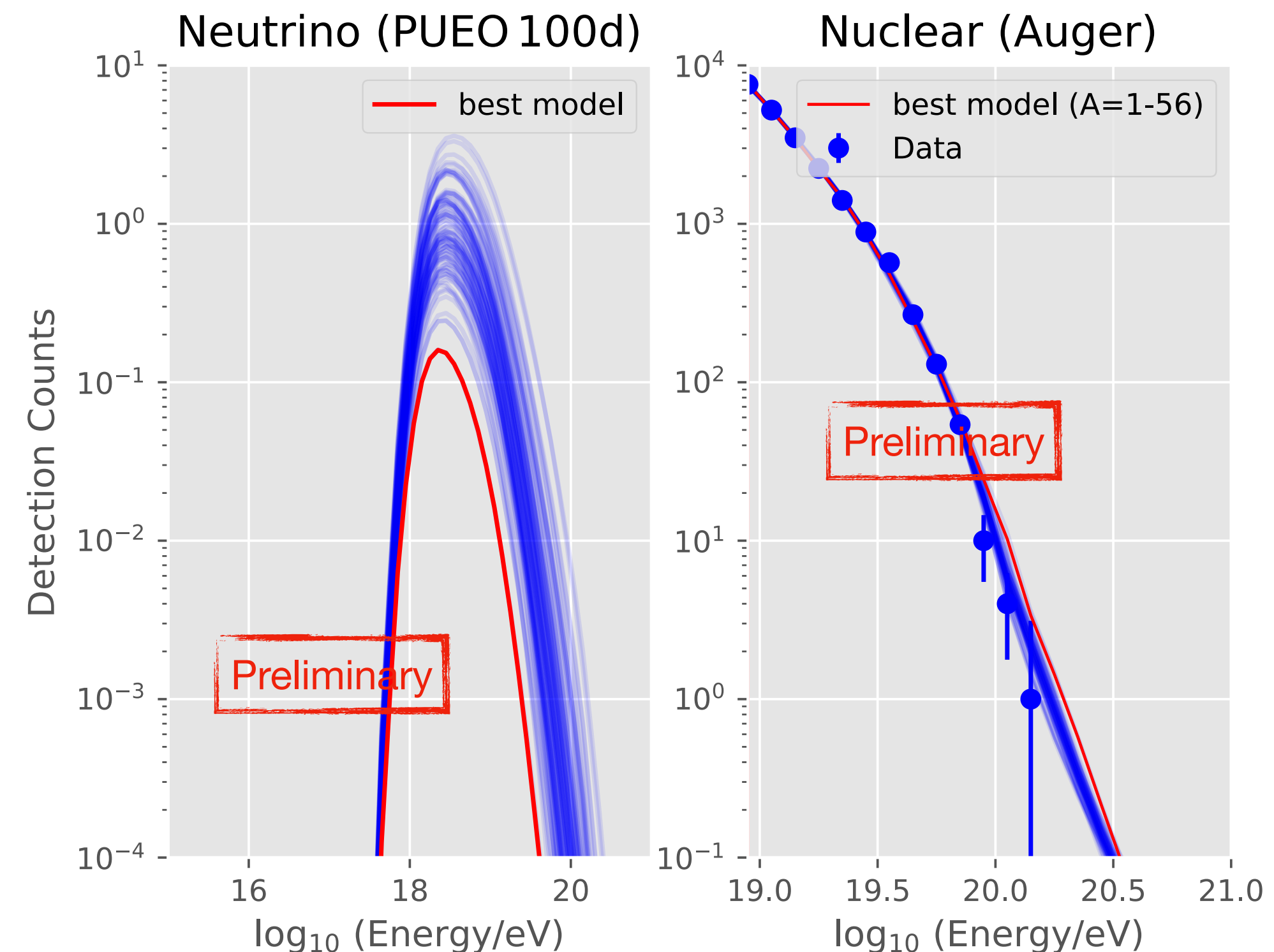
## Which cosmogenic sources are we going to see with which instrument?

Study based on the initial works of *Andres Romero-Wolf and Maximo Ave 2018*

Extended to multimessenger constraints: cosmic-ray, gamma-ray, neutrino

+ constraint from possible futur detection of planned experiments: here PUEO

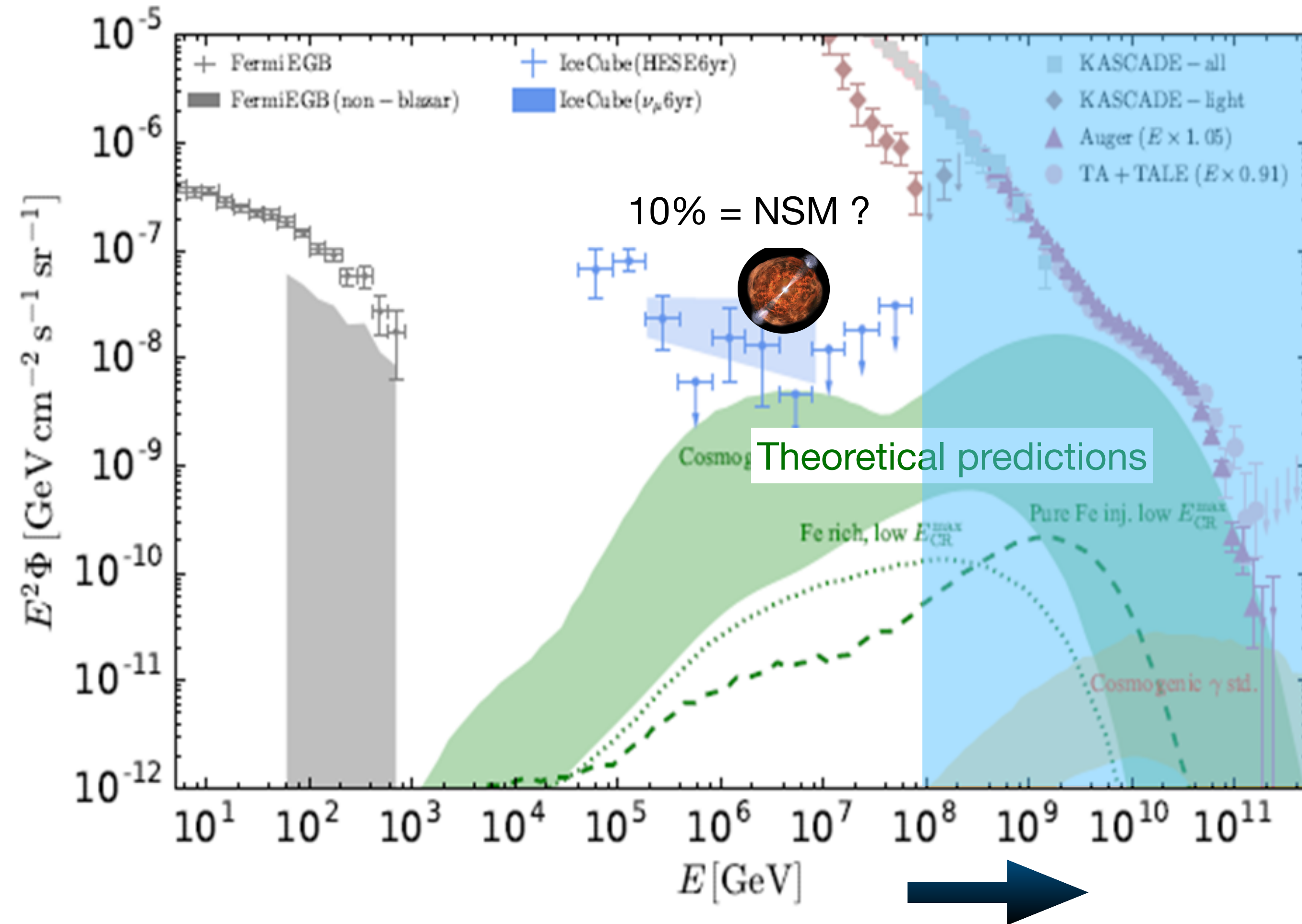
→ Goal is to probe the parameter space from the experimental point of view





# Predicted ultra high-energy neutrinos

- Expand the measurements of the neutrino spectrum
- Reach the cosmogenic flux of ultra high-energy (UHE) neutrinos



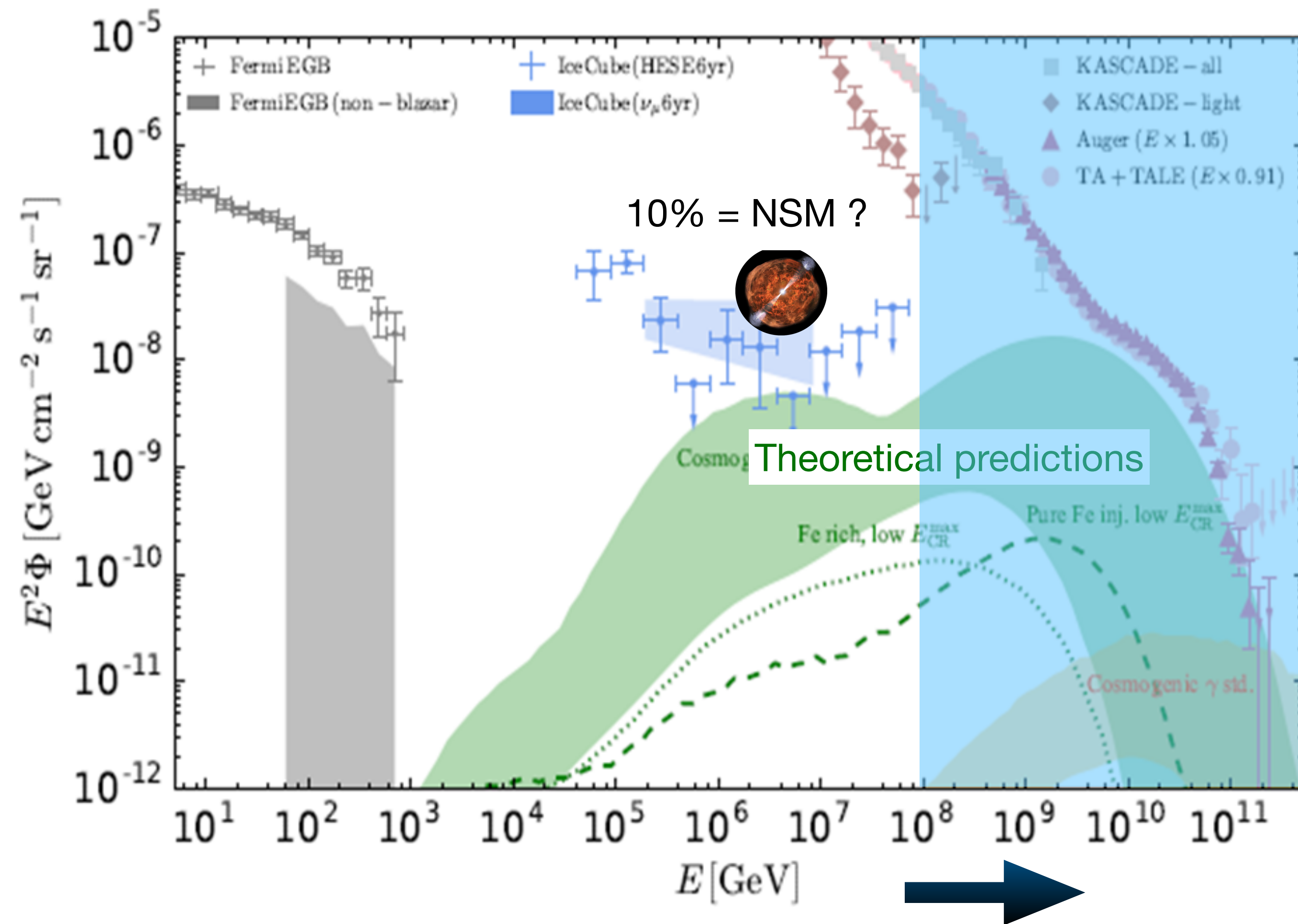
Guaranteed  
cosmogenic neutrinos

UHECR + cosmic photons  $\rightarrow$  UHE neutrinos  
+ neutrinos from astrophysical sources



# Predicted ultra high-energy neutrinos

- Expand the measurements of the neutrino spectrum
- Reach the cosmogenic flux of ultra high-energy (UHE) neutrinos



Guaranteed  
cosmogenic neutrinos

UHECR + cosmic photons → UHE neutrinos  
+ neutrinos from astrophysical sources

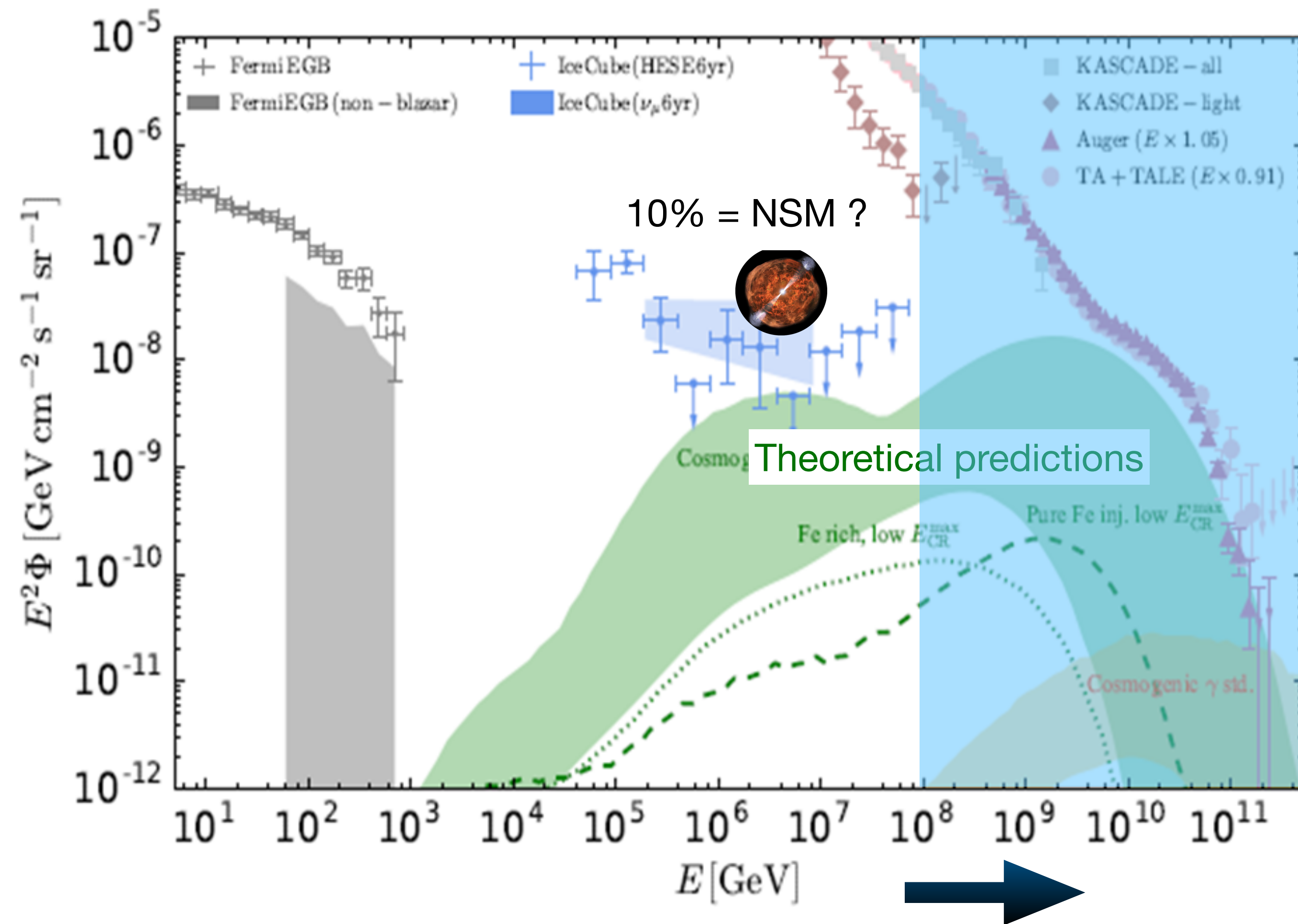
How to detect them ?

- low fluxes
- low cross sections → large volume of target



# Predicted ultra high-energy neutrinos

- Expand the measurements of the neutrino spectrum
- Reach the cosmogenic flux of ultra high-energy (UHE) neutrinos



Guaranteed  
cosmogenic neutrinos

UHECR + cosmic photons → UHE neutrinos  
+ neutrinos from astrophysical sources

How to detect them ?

- low fluxes
  - low cross sections
- large volume of target

One possibility:

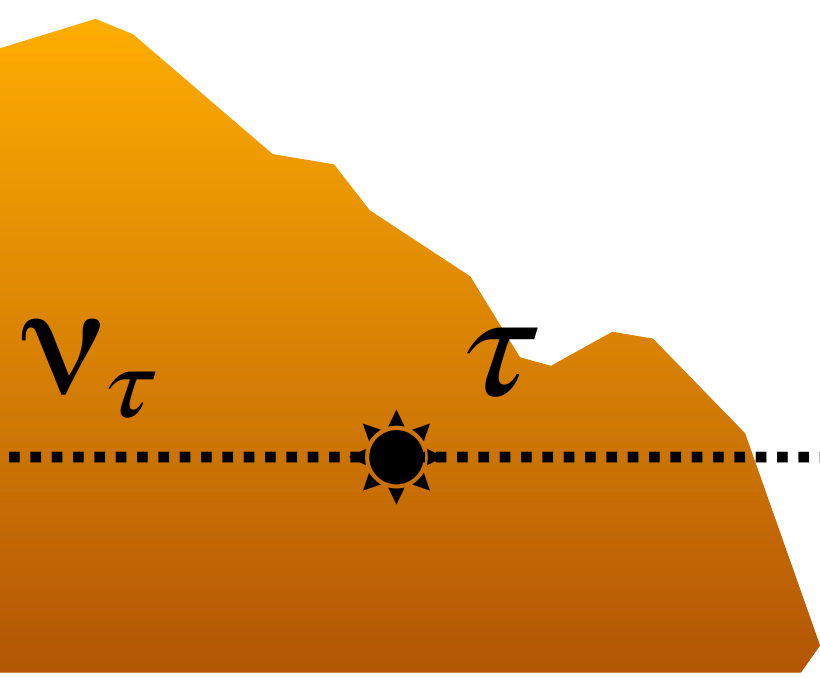
- use Earth as target
- detect product of interactions → extensive air showers
- radio detection of extensive air showers



# Extensive air showers (EAS)

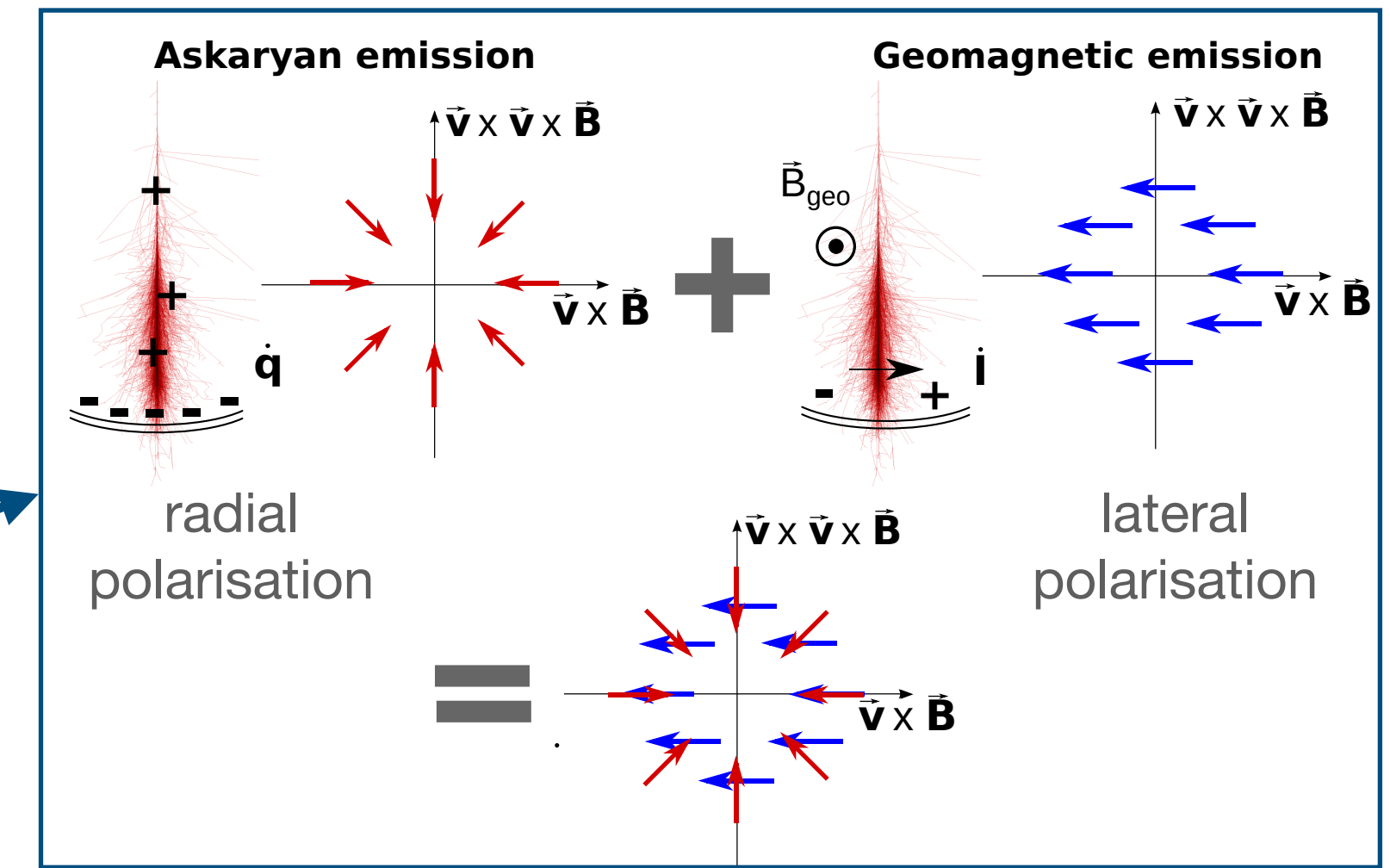
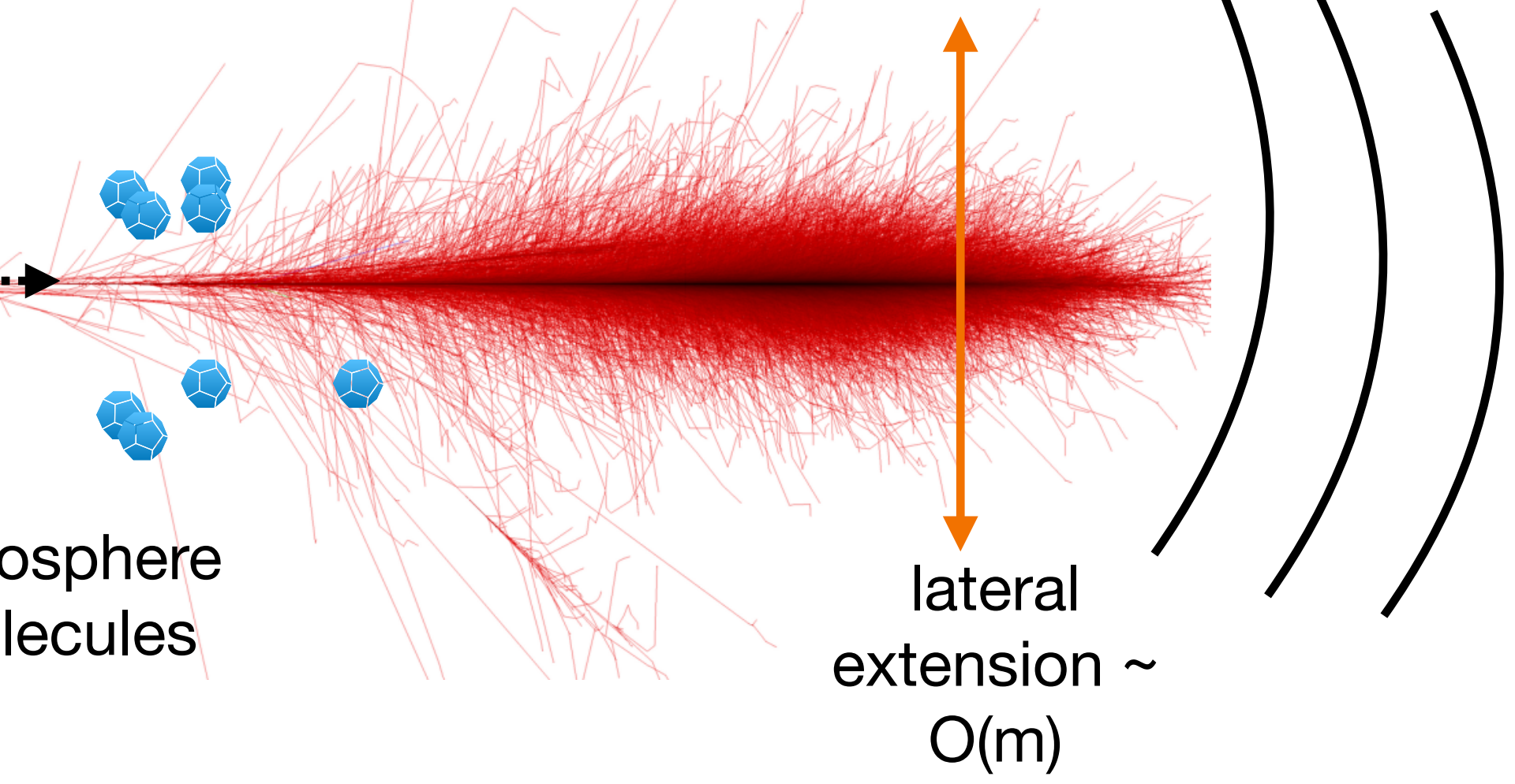
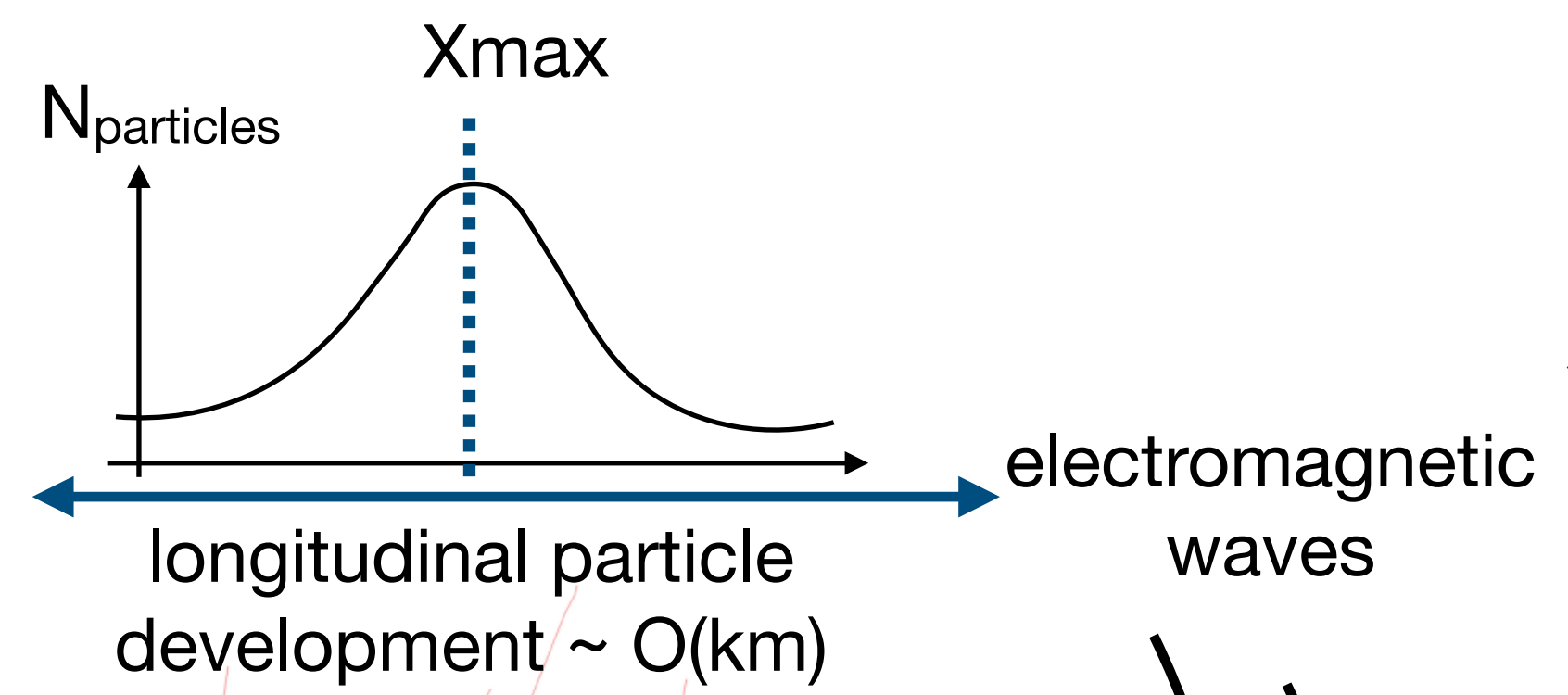
for UHE neutrino!

Earth/mountains



$\tau$  decay

atmosphere molecules



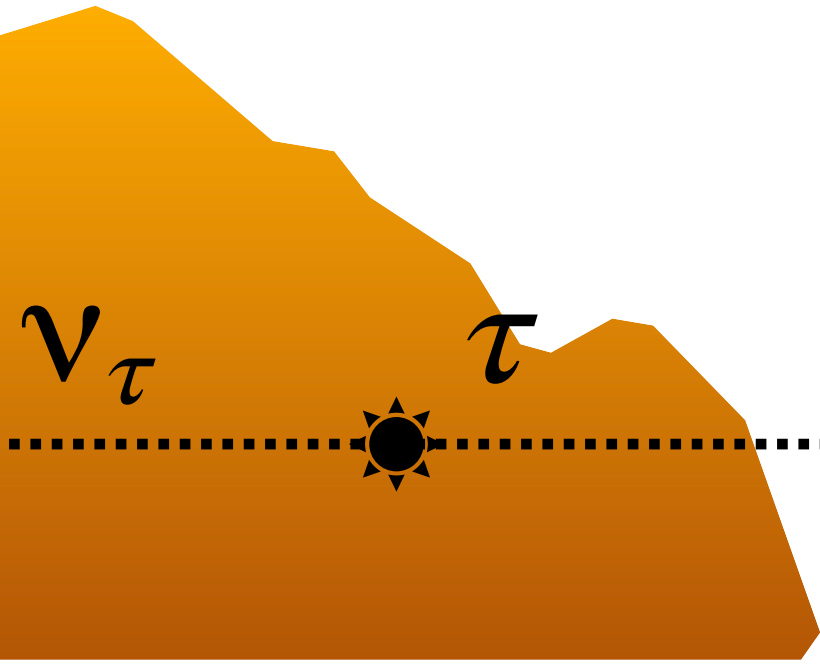
$e^+$  and  $e^-$  (in motion) + geomagnetic field = radiation  
 collective effects lead to two main mechanisms of emission



# Extensive air showers (EAS)

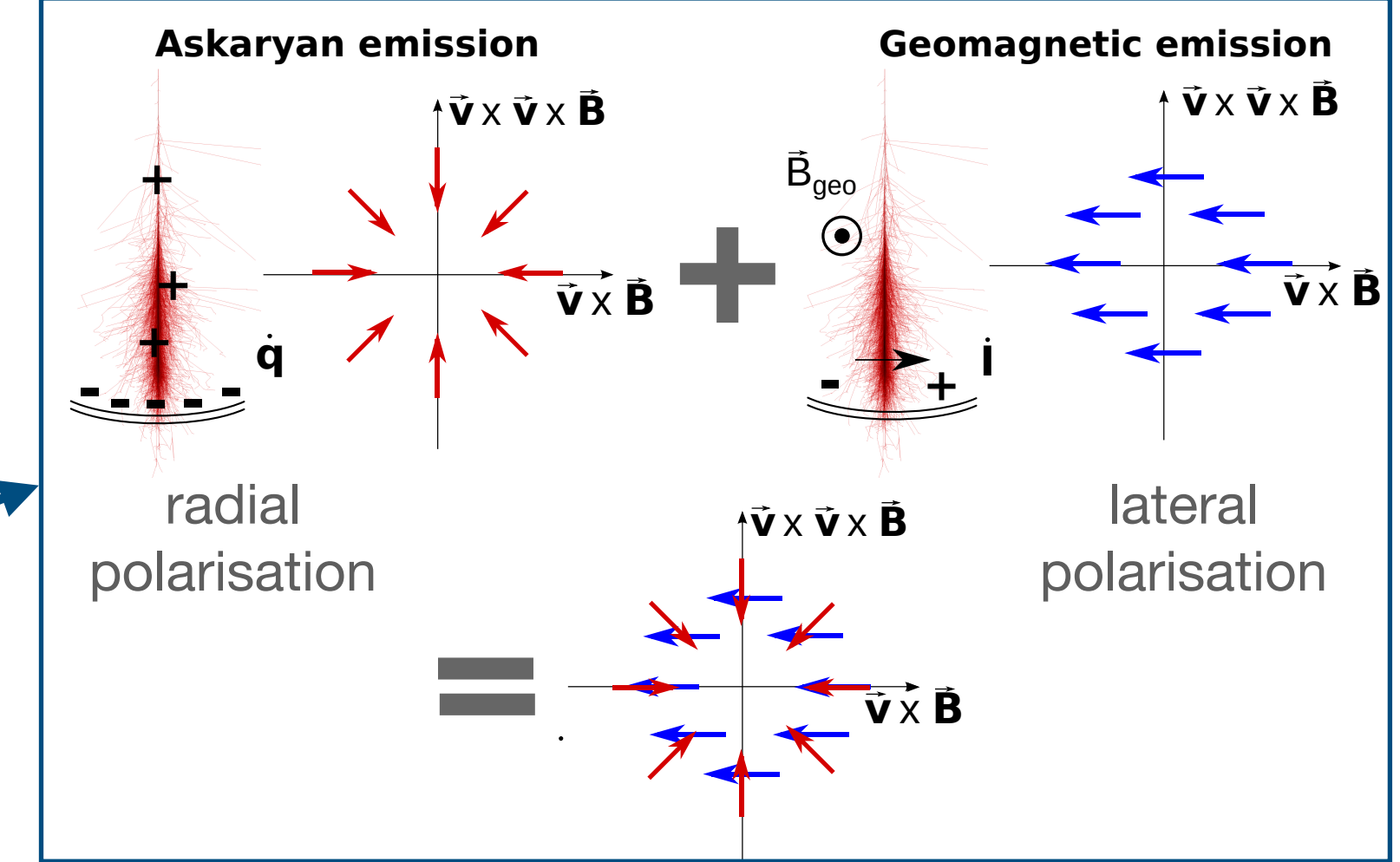
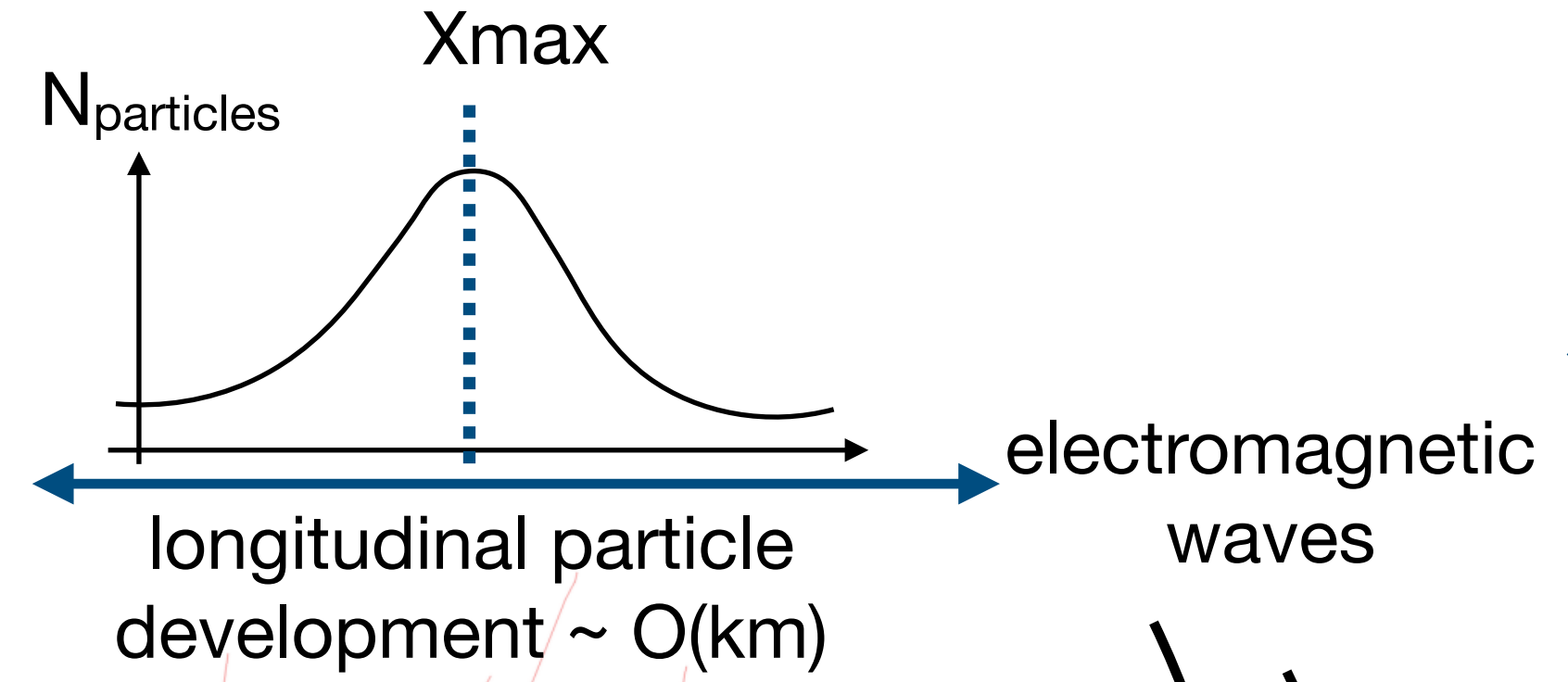
for UHE neutrino!

Earth/mountains



$\tau$  decay

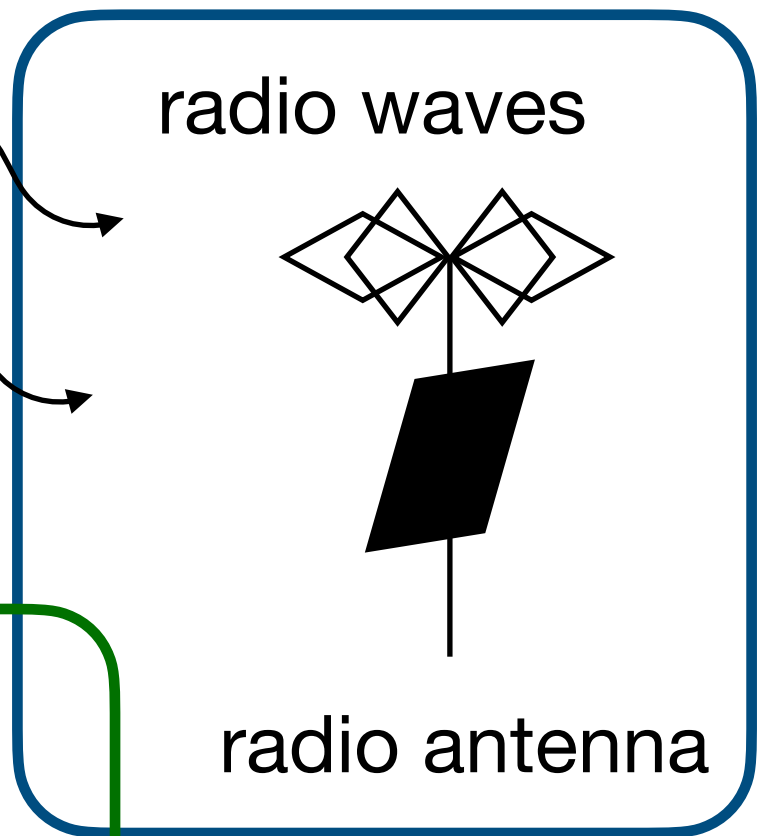
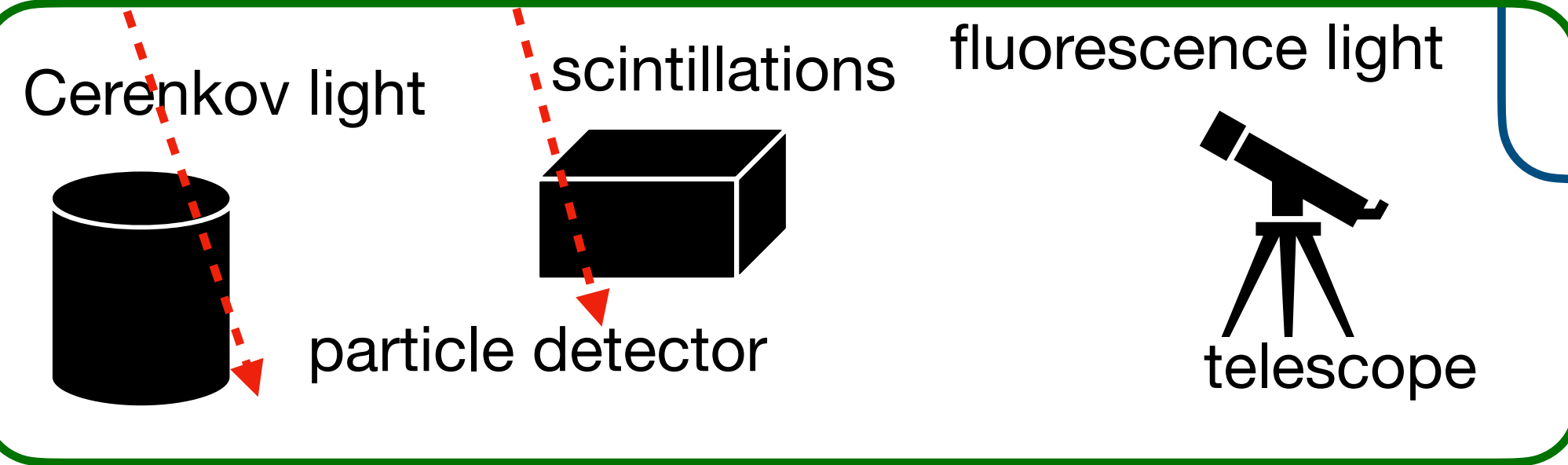
atmosphere molecules



$e^+$  and  $e^-$  (in motion) + geomagnetic field = radiation  
collective effects lead to two main mechanisms of emission

lateral extension ~ O(m)

ex: Pierre Auger Observatory/  
Telescope Array



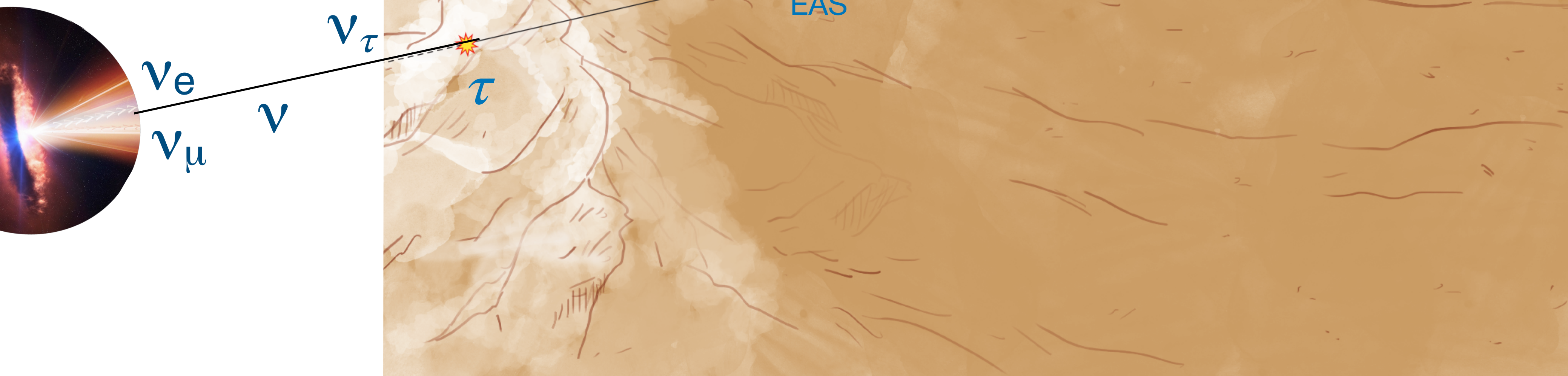
ex: CODALEMA / LOFAR / AERA...



# Some Radio Detectors (on which I worked on)

one goal → maximise effective volume!

Use the Earth as a target  
→ Earth skimming neutrinos trajectories

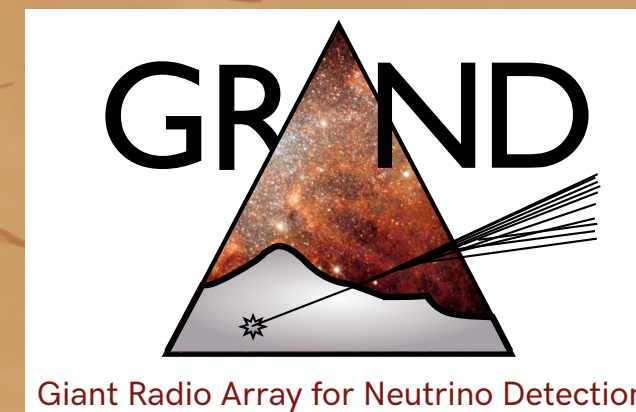
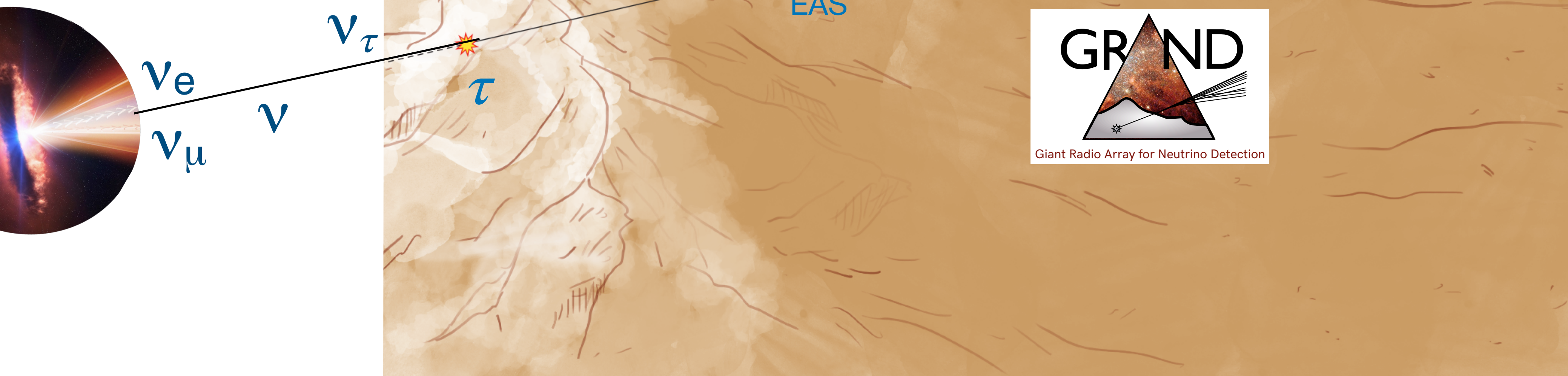




# Some Radio Detectors (on which I worked on)

one goal → maximise effective volume!

Use the Earth as a target  
→ Earth skimming neutrinos trajectories





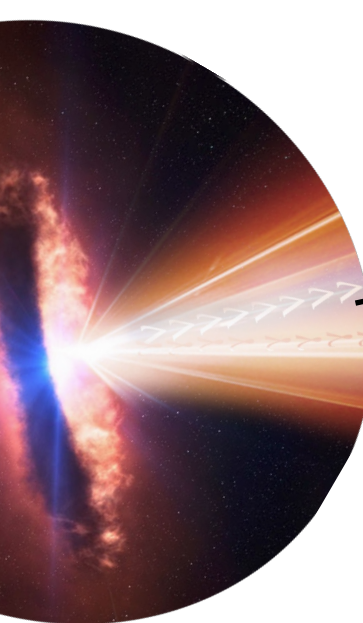
# Some Radio Detectors (on which I worked on)

one goal → maximise effective volume!

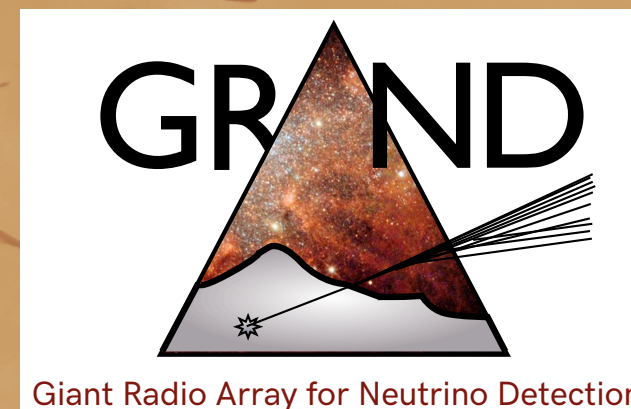
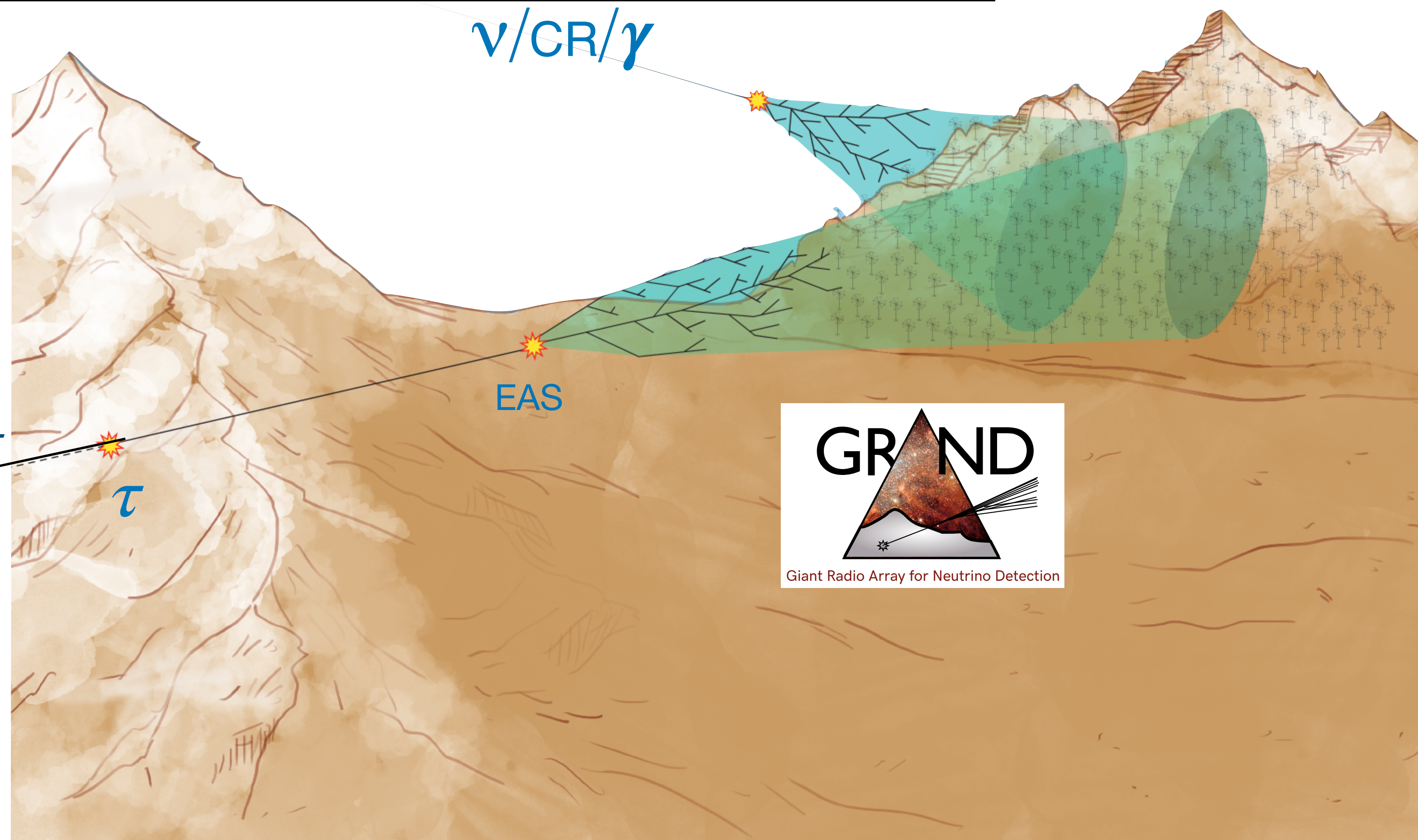
GRAND concept:

- 200,000 antennas over 200,000 km<sup>2</sup> = 20 sub-arrays of 10,000 km<sup>2</sup>
- in radio quiet mountainous regions around the world (half in China)
- autonomous radio detection of inclined air-showers in 50-200 MHz band

Use the Earth as a target  
→ Earth skimming neutrinos trajectories



$\nu_e$   
 $\nu_\mu$   
 $\nu_\tau$   
 $\nu$





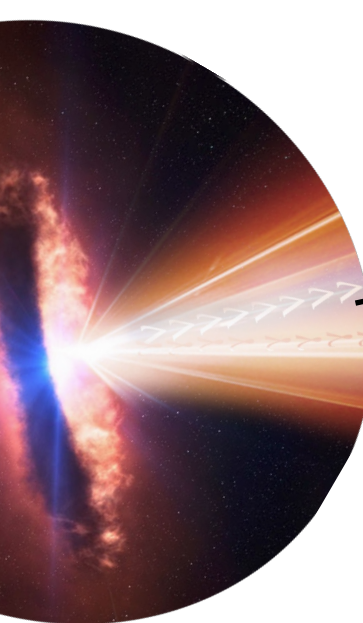
# Some Radio Detectors (on which I worked on)

one goal → maximise effective volume!

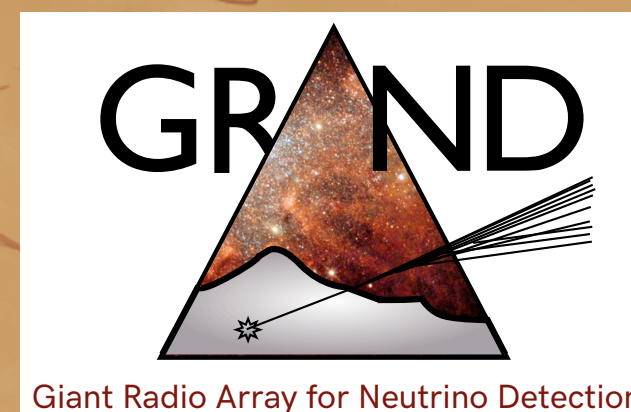
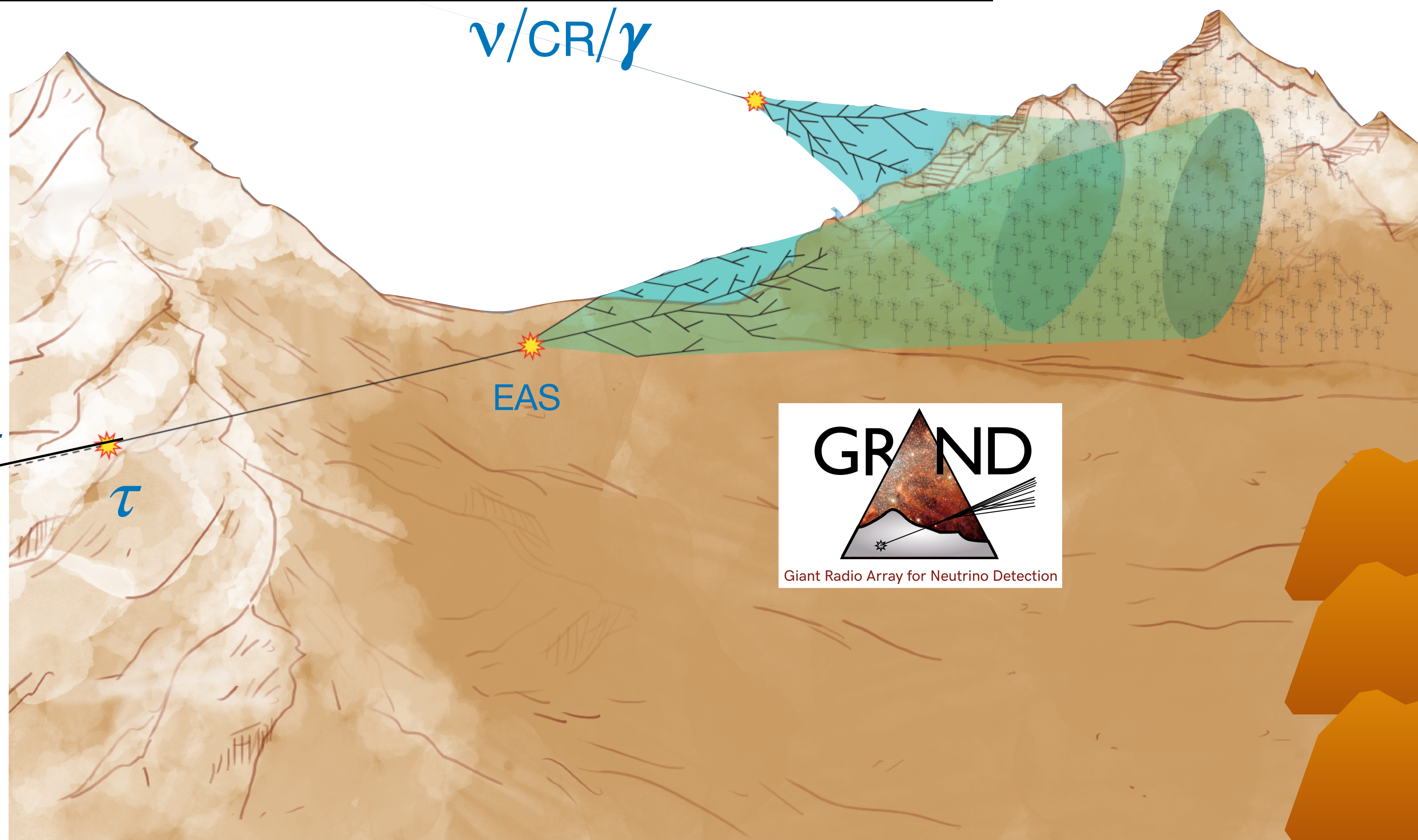
GRAND concept:

- 200,000 antennas over 200,000 km<sup>2</sup> = 20 sub-arrays of 10,000 km<sup>2</sup>
- in radio quiet mountainous regions around the world (half in China)
- autonomous radio detection of inclined air-showers in 50-200 MHz band

Use the Earth as a target  
→ Earth skimming neutrinos trajectories



$\nu_e$   
 $\nu_\mu$   
 $\nu$   
 $\nu_\tau$





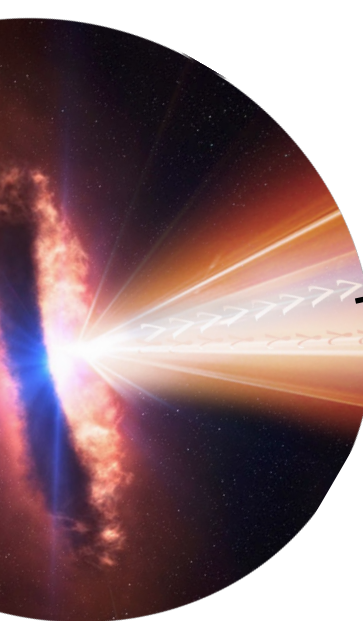
# Some Radio Detectors (on which I worked on)

one goal → maximise effective volume!

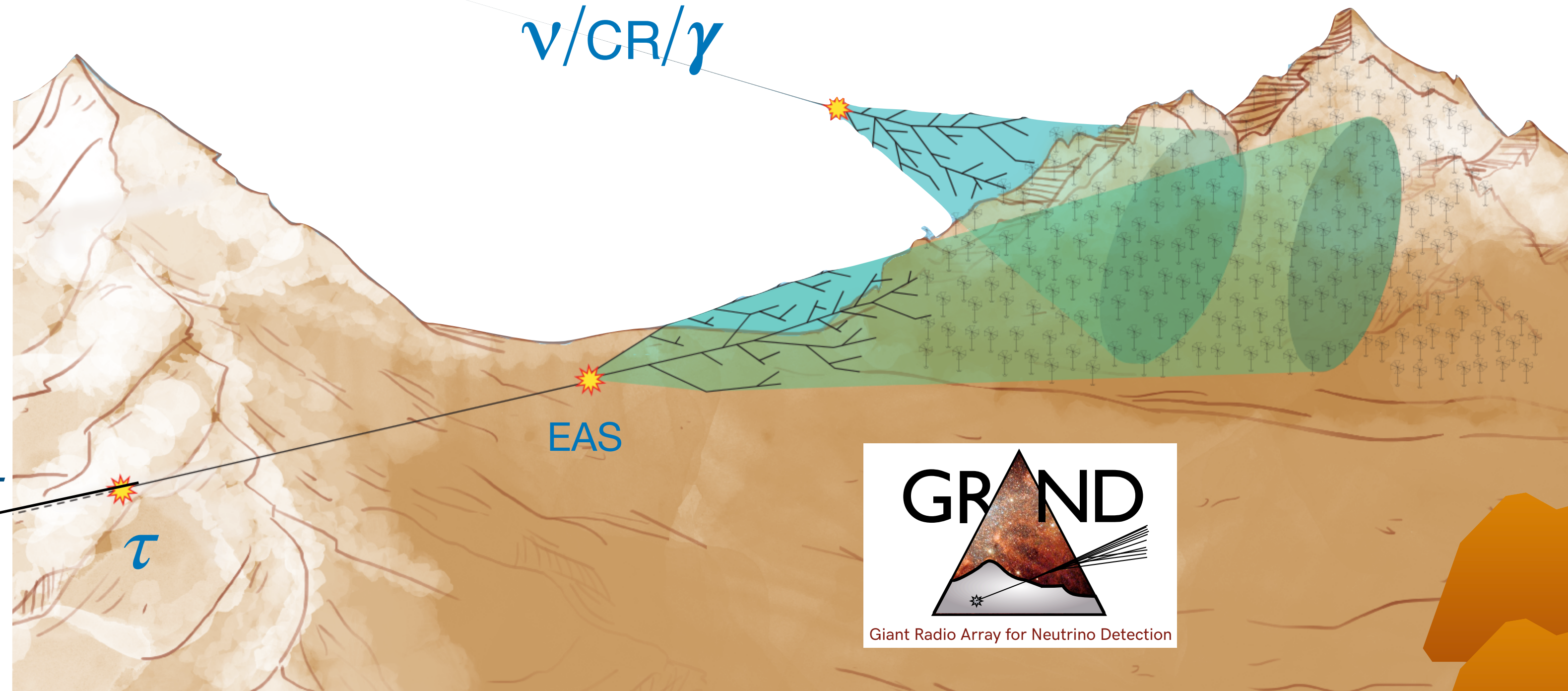
GRAND concept:

- 200,000 antennas over 200,000 km<sup>2</sup> = 20 sub-arrays of 10,000 km<sup>2</sup>
- in radio quiet mountainous regions around the world (half in China)
- autonomous radio detection of inclined air-showers in 50-200 MHz band

Use the Earth as a target  
→ Earth skimming neutrinos trajectories



$\nu_e$   
 $\nu_\mu$   
 $\nu$   
 $\nu_\tau$



BEACON concept:

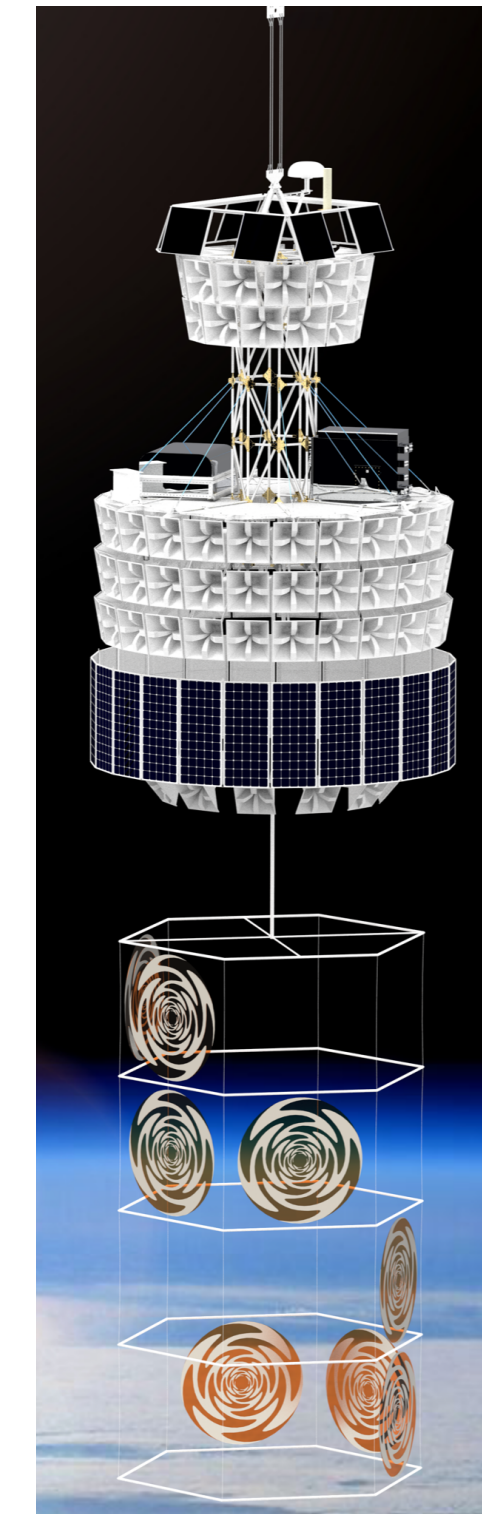
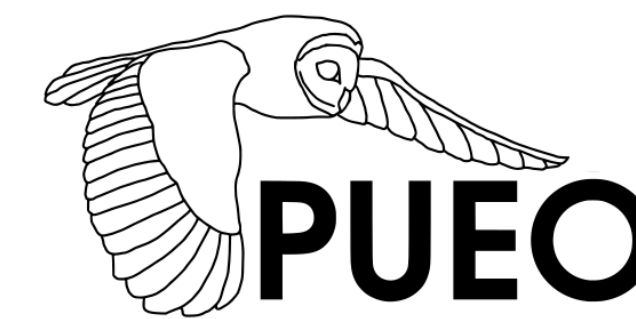
- deploy antenna stations in high altitude mountains → very large effective area!
- autonomous radio detection in 30-80 MHz
- beamforming radio technique → increase SNR in specific directions!





# Some Radio Detectors (on which I worked on)

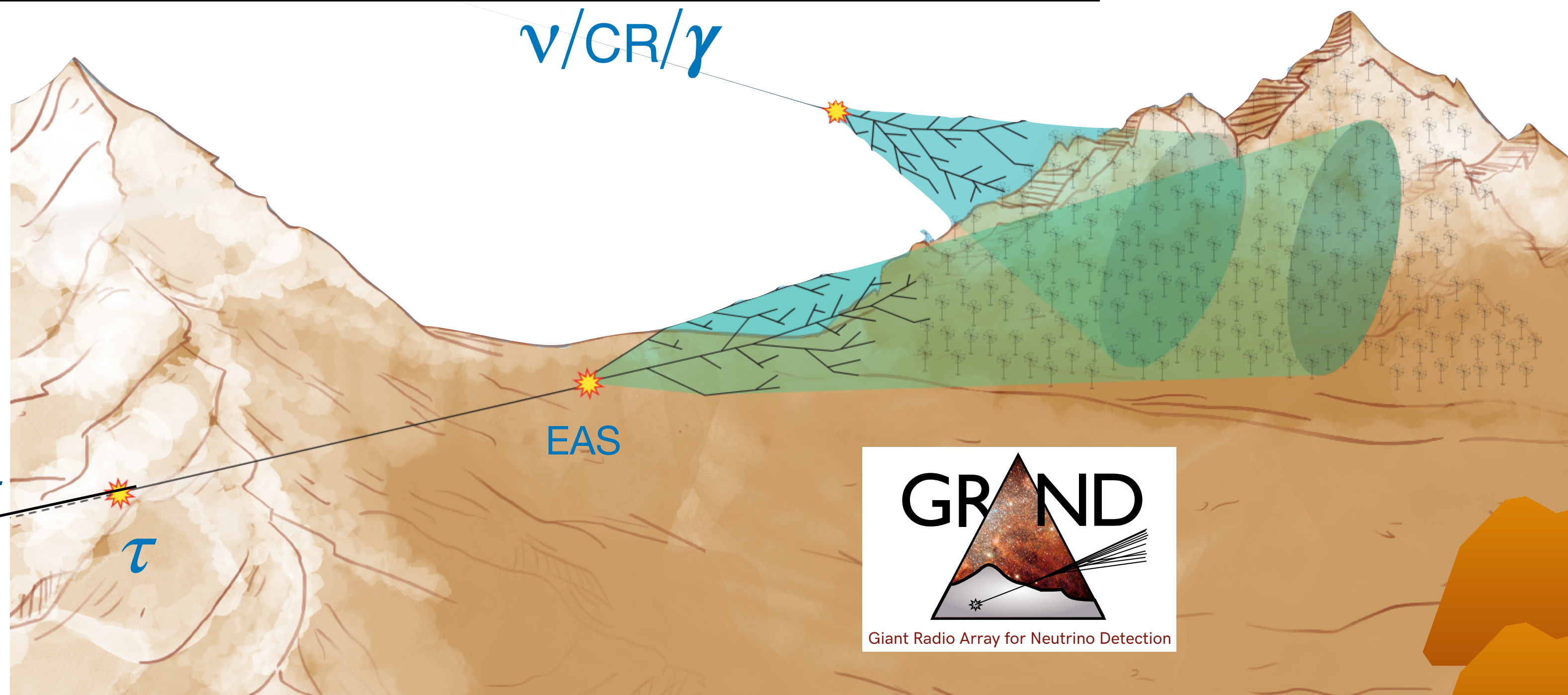
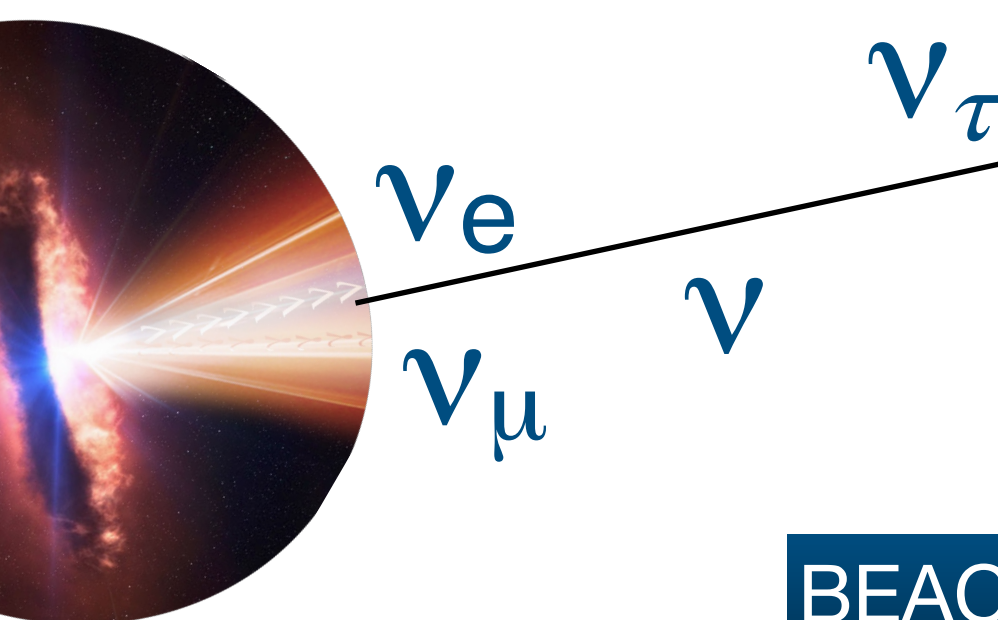
one goal → maximise effective volume!



GRAND concept:

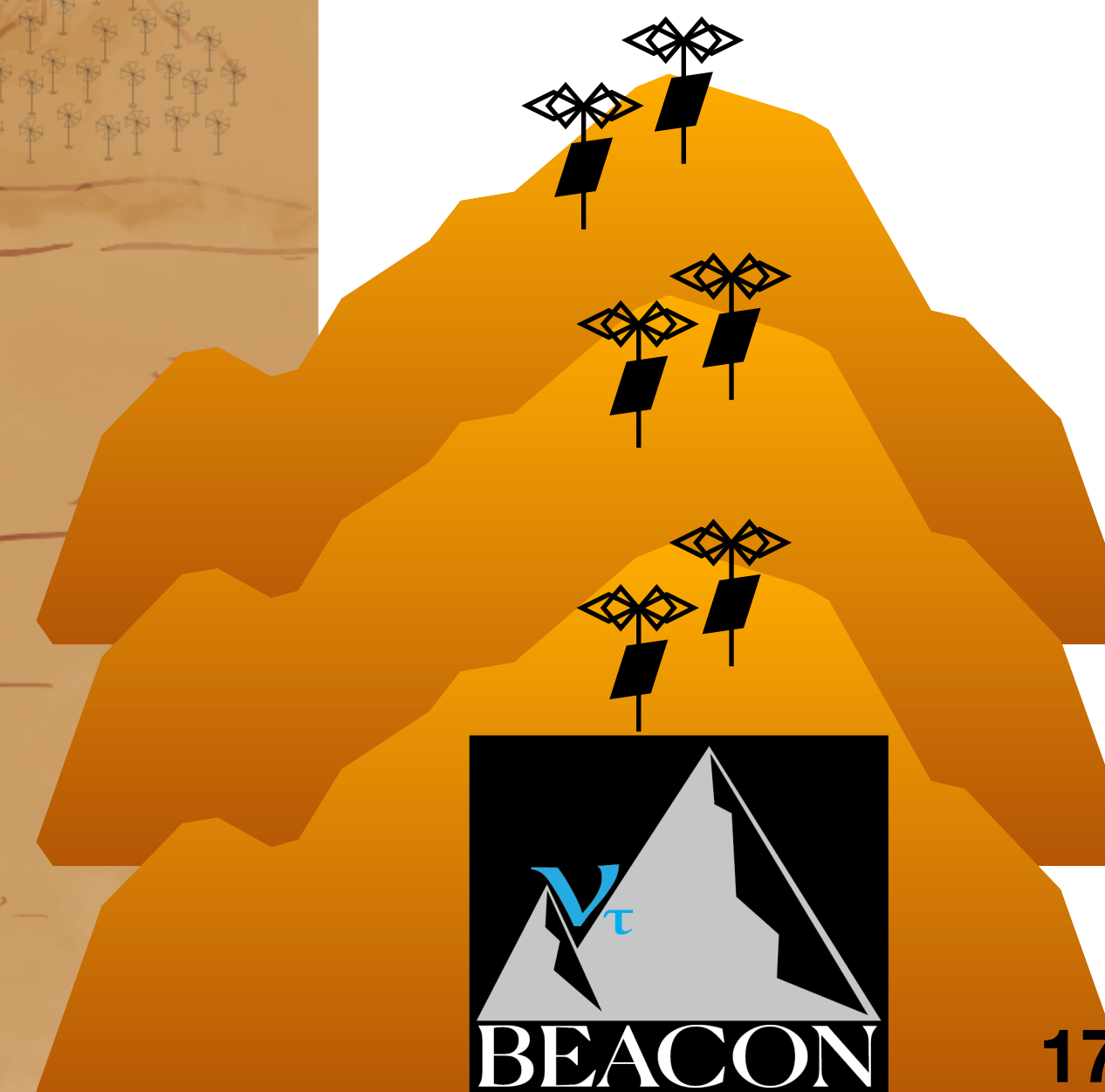
- 200,000 antennas over 200,000 km<sup>2</sup> = 20 sub-arrays of 10,000 km<sup>2</sup>
- in radio quiet mountainous regions around the world (half in China)
- autonomous radio detection of inclined air-showers in 50-200 MHz band

Use the Earth as a target  
→ Earth skimming neutrinos trajectories



BEACON concept:

- deploy antenna stations in high altitude mountains → very large effective area!
- autonomous radio detection in 30-80 MHz
- beamforming radio technique → increase SNR in specific directions!



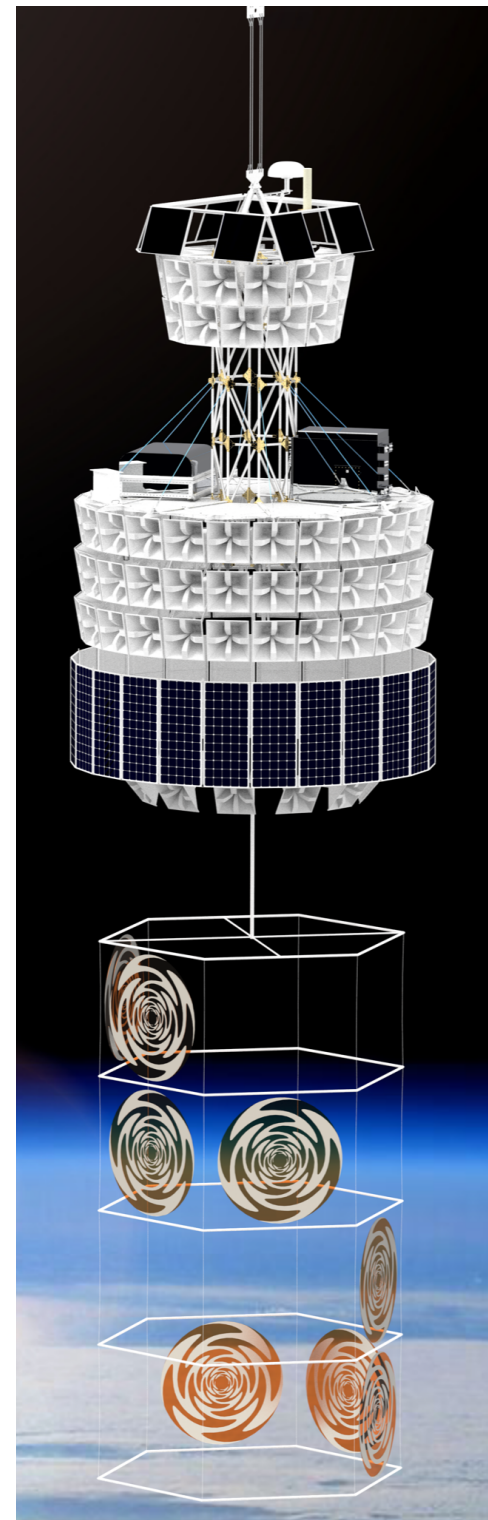
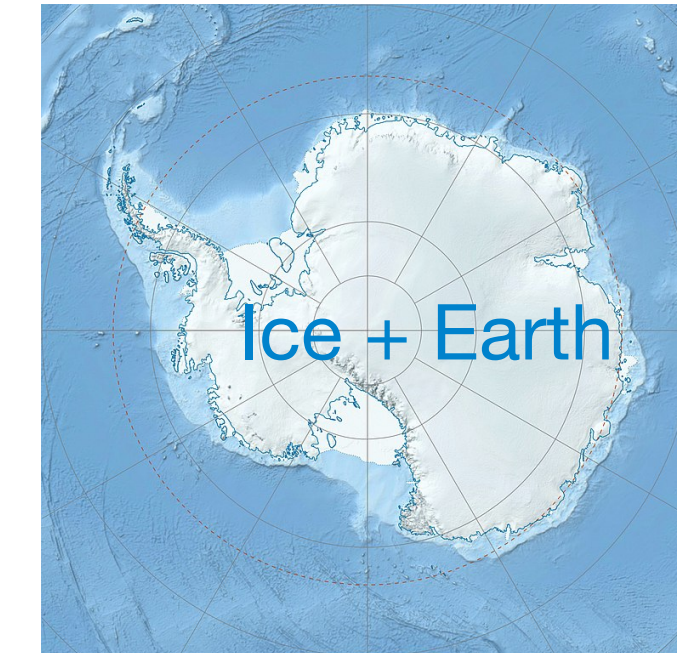
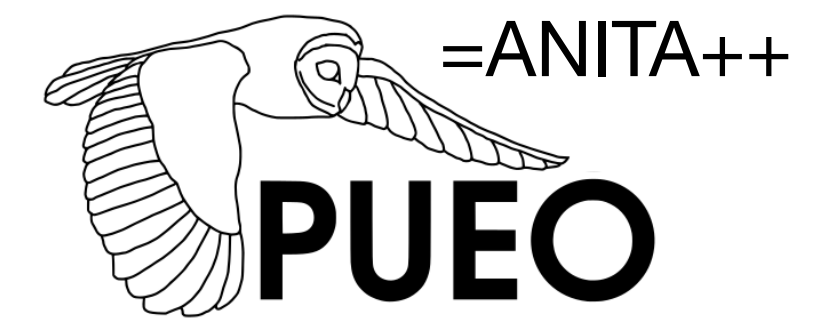


# Some Radio Detectors (on which I worked on)

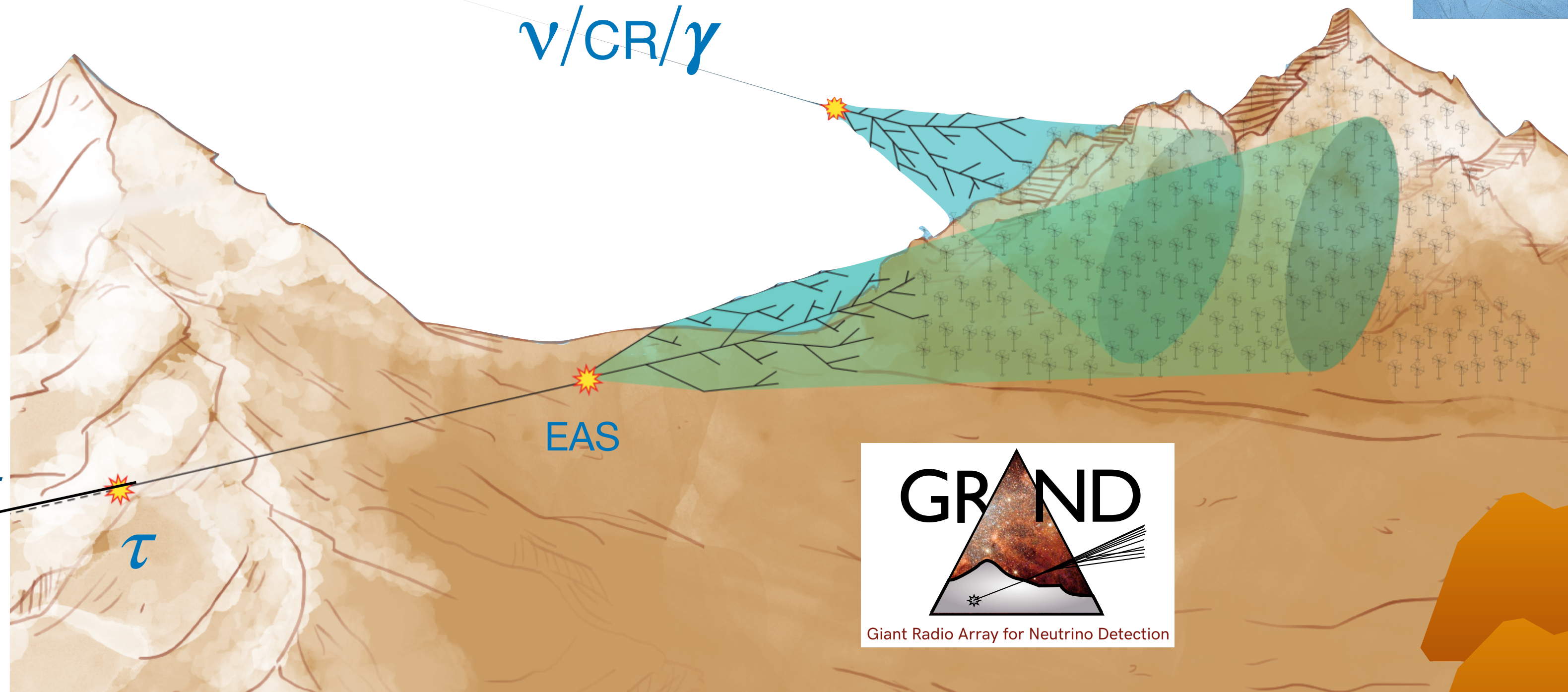
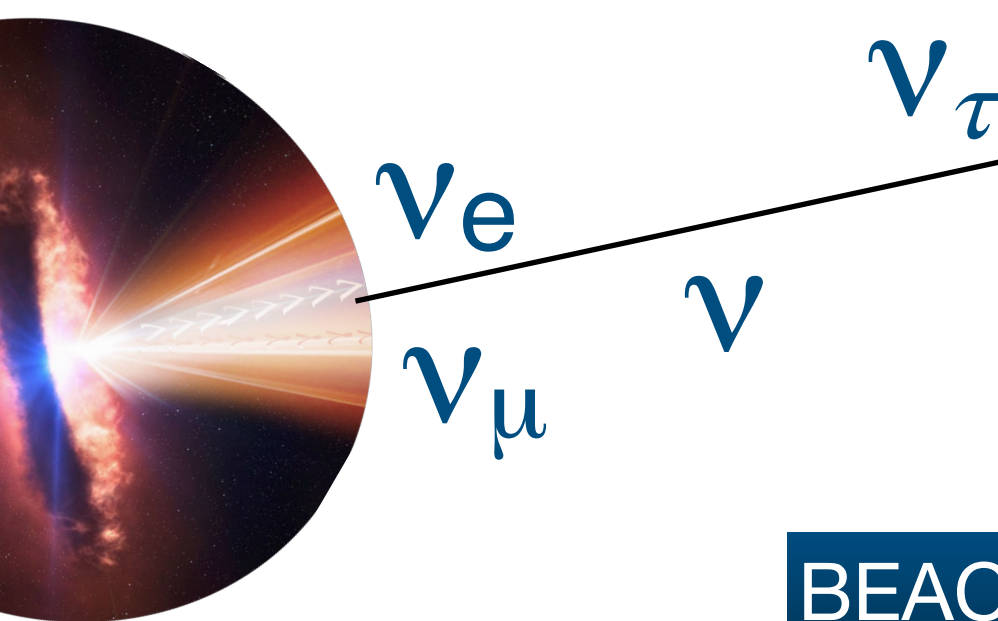
one goal → maximise effective volume!

GRAND concept:

- 200,000 antennas over 200,000 km<sup>2</sup> = 20 sub-arrays of 10,000 km<sup>2</sup>
- in radio quiet mountainous regions around the world (half in China)
- autonomous radio detection of inclined air-showers in 50-200 MHz band

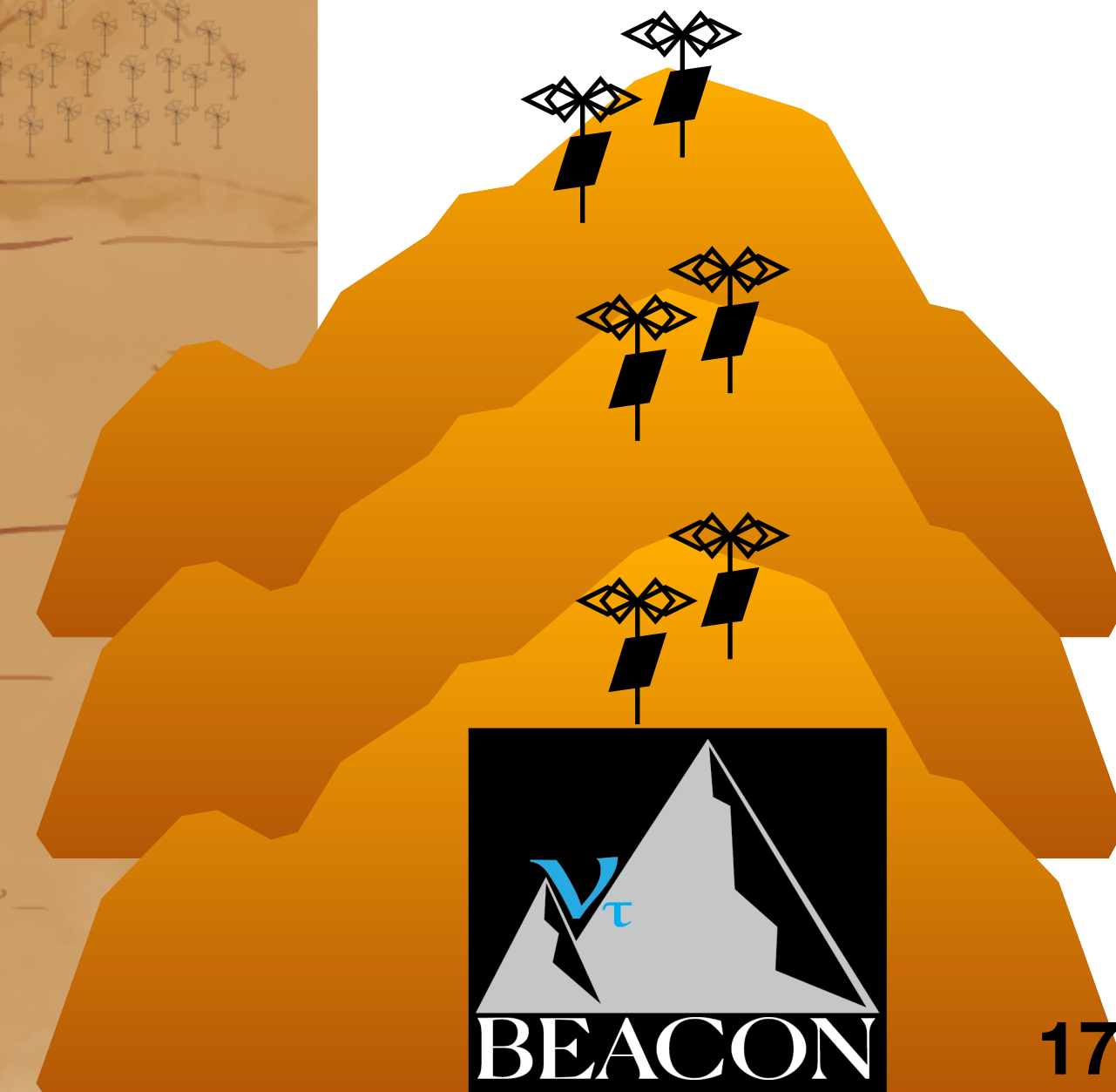


Use the Earth as a target  
→ Earth skimming neutrinos trajectories



BEACON concept:

- deploy antenna stations in high altitude mountains → very large effective area!
- autonomous radio detection in 30-80 MHz
- beamforming radio technique → increase SNR in specific directions!

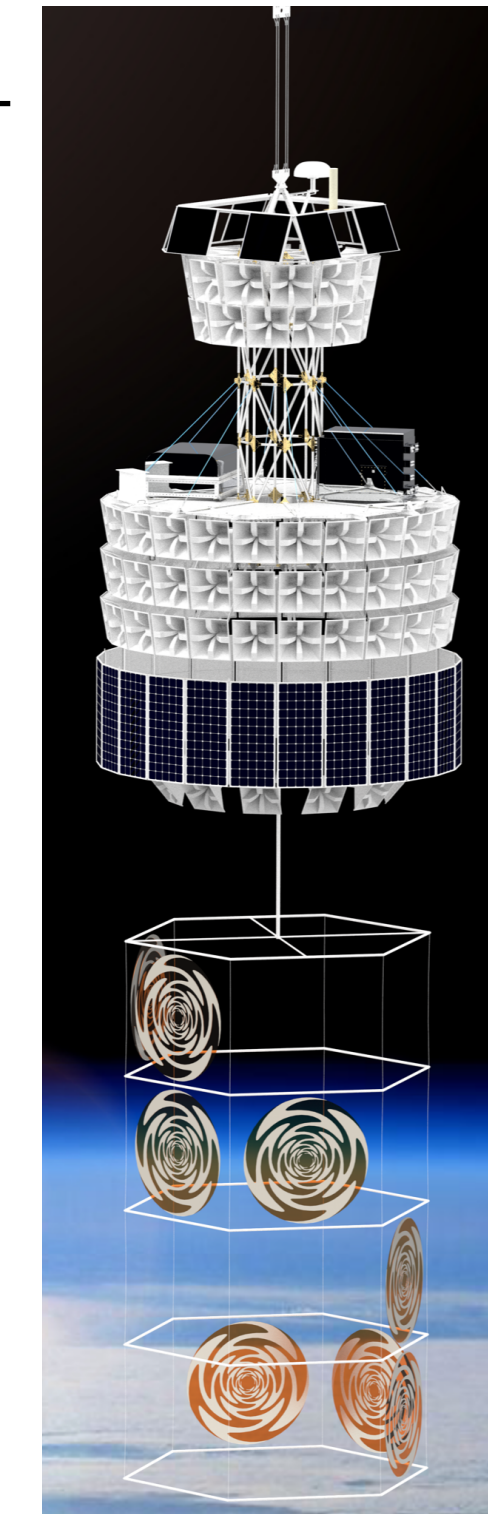
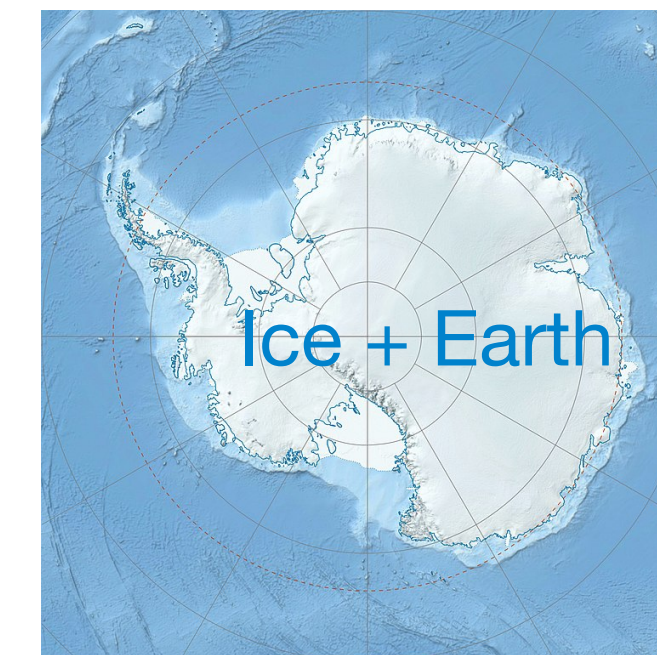
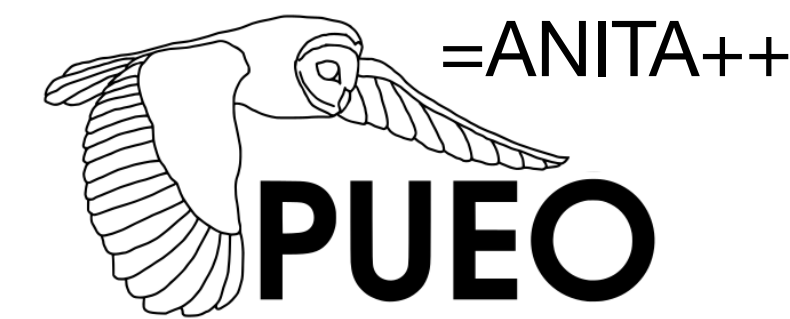




# Some Radio Detectors (on which I worked on)

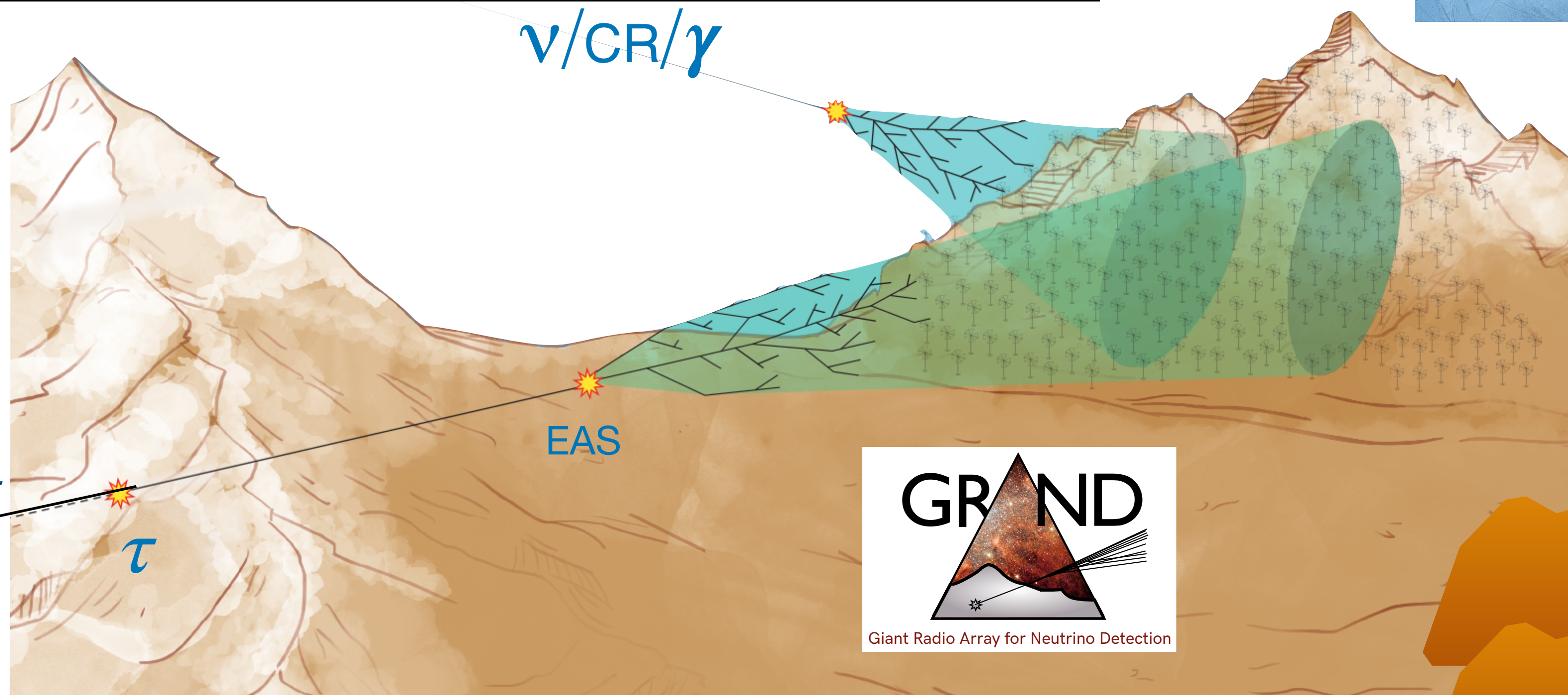
one goal → maximise effective volume!

**PUEO concept: (50-300 + 300-1200MHz)**  
 - long duration balloon flying in antartica  
 - payload made of 3 distinct radio instrument  
 - targeting all EAS configurations!



**GRAND concept:**

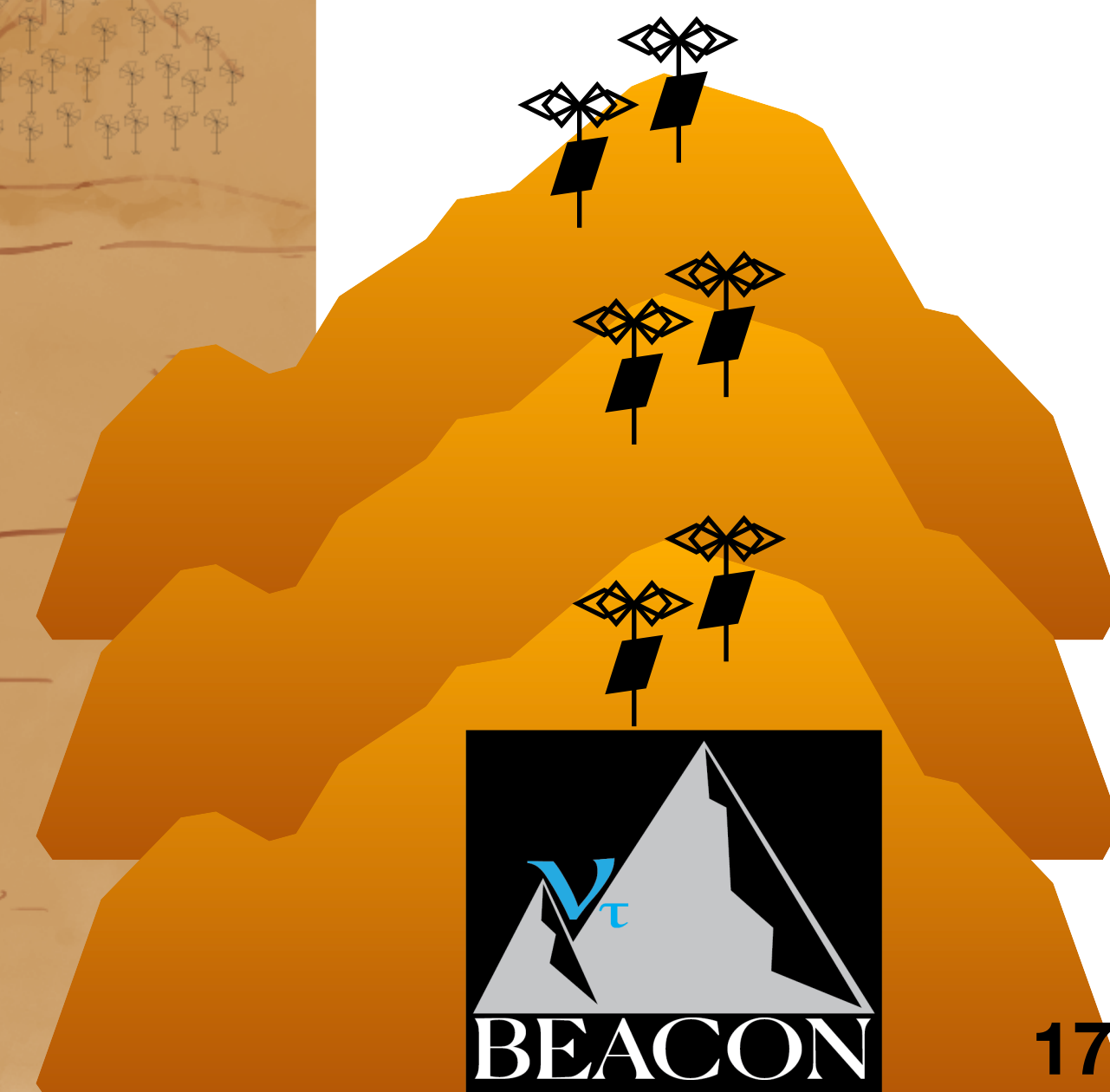
- 200,000 antennas over 200,000 km<sup>2</sup> = 20 sub-arrays of 10,000 km<sup>2</sup>  
 - in radio quiet mountainous regions around the world (half in China)  
 - autonomous radio detection of inclined air-showers in 50-200 MHz band



Use the Earth as a target  
 → Earth skimming neutrinos trajectories

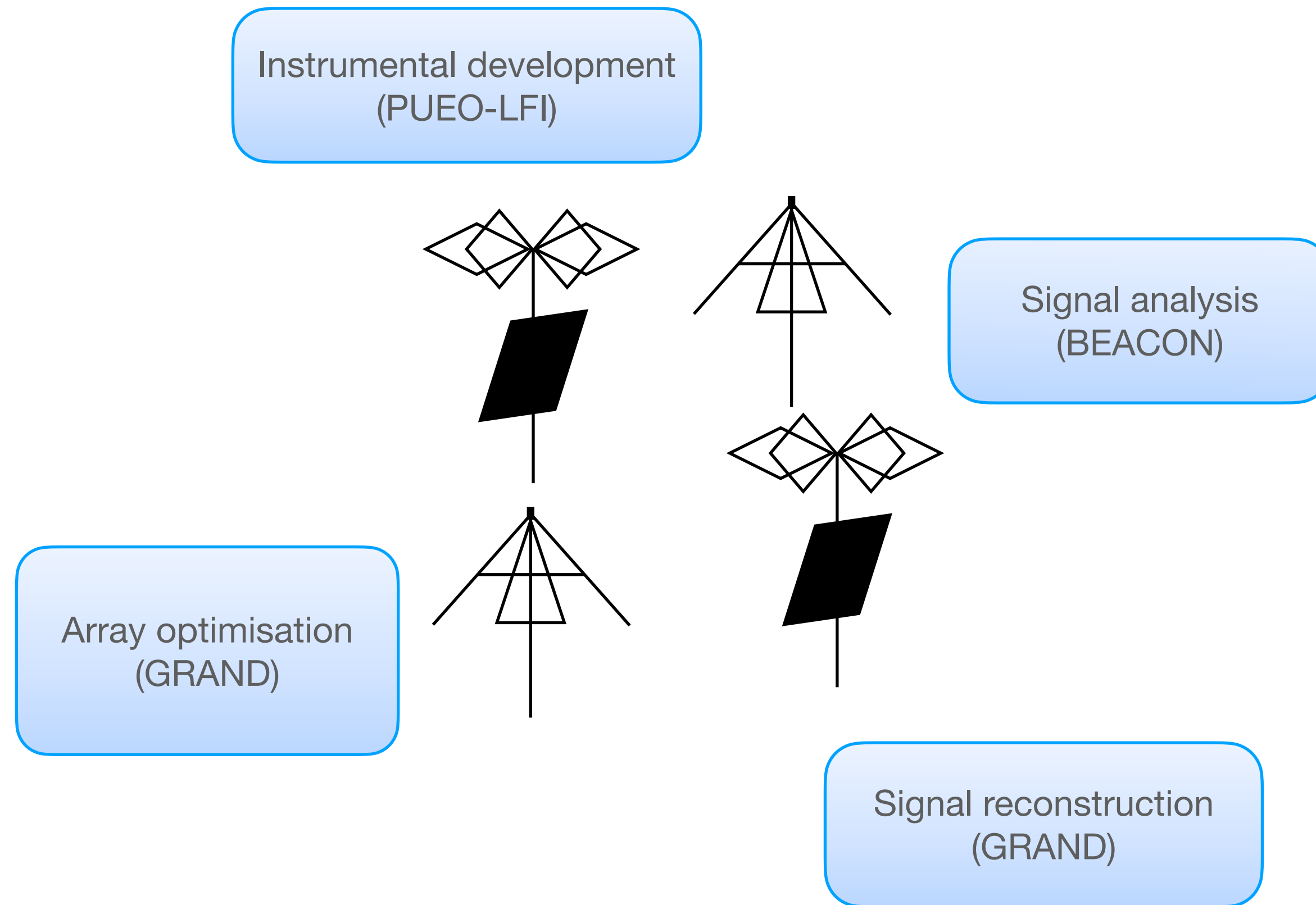
**BEACON concept:**

- deploy antenna stations in high altitude mountains → very large effective area!  
 - autonomous radio detection in 30-80 MHz  
 - beamforming radio technique → increase SNR in specific directions!





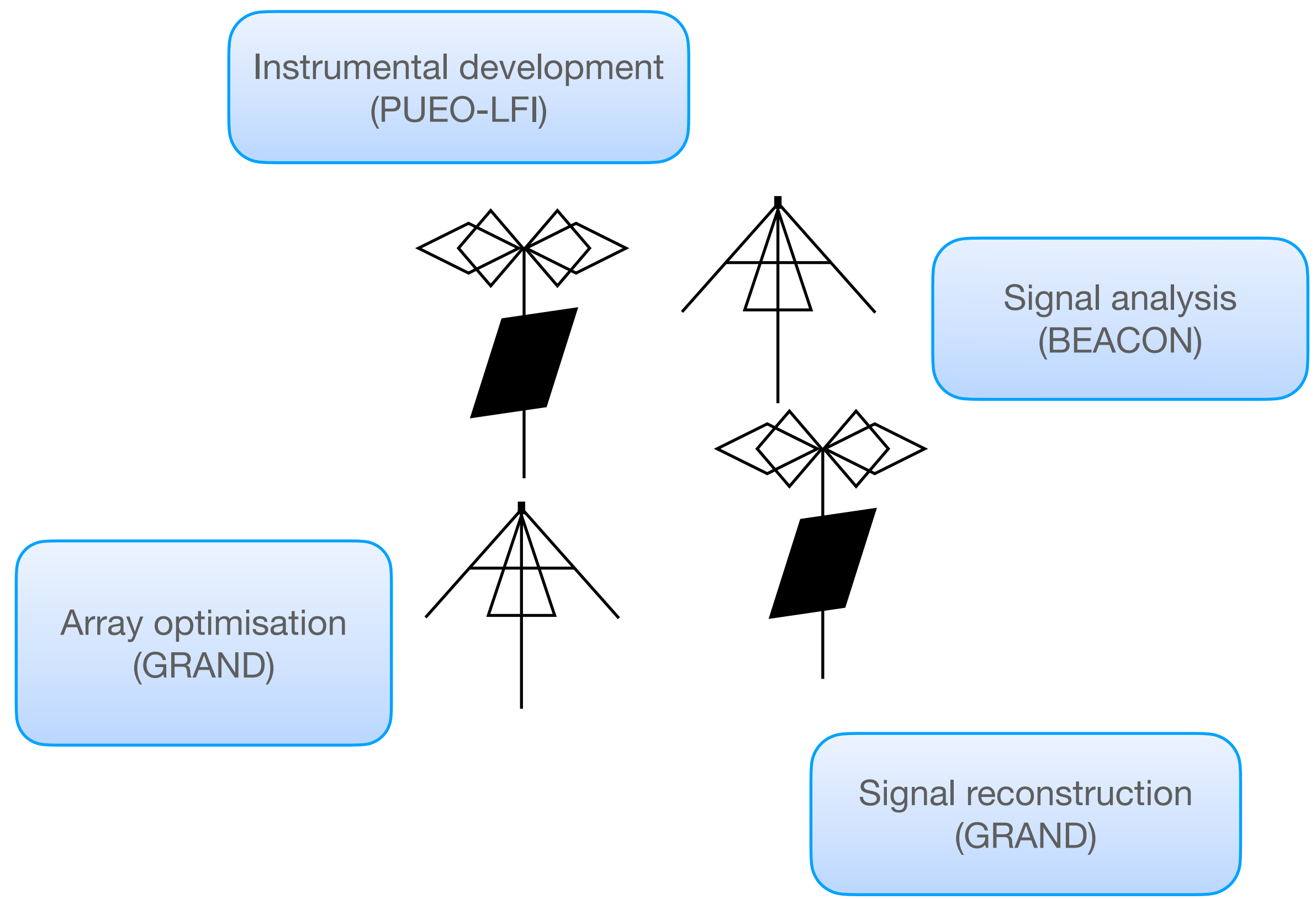
# Some challenges of the radio detection of **UHE** (on which I worked on)





# Some challenges of the radio detection of UHE (on which I worked on)

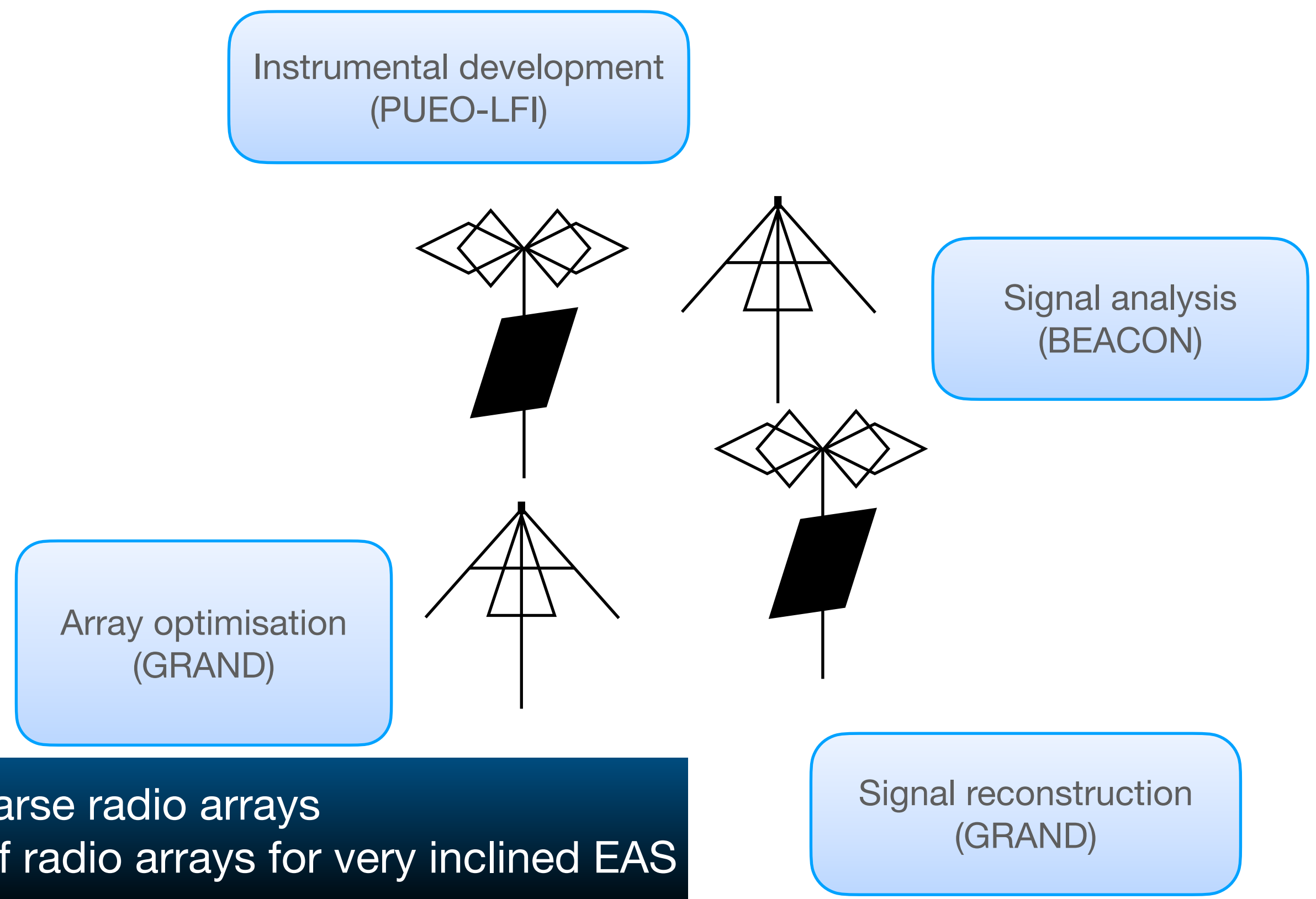
Context: low frequency instrument dedicated to Earth-skimming UHE neutrinos  
Goals: optimise antenna and RF chain to neutrino induced EAS





# Some challenges of the radio detection of UHE (on which I worked on)

Context: low frequency instrument dedicated to Earth-skimming UHE neutrinos  
Goals: optimise antenna and RF chain to neutrino induced EAS



Context: very extended and sparse radio arrays  
Goals: study the optimisation of radio arrays for very inclined EAS



# Some challenges of the radio detection of UHE (on which I worked on)

Context: low frequency instrument dedicated to Earth-skimming UHE neutrinos  
Goals: optimise antenna and RF chain to neutrino induced EAS

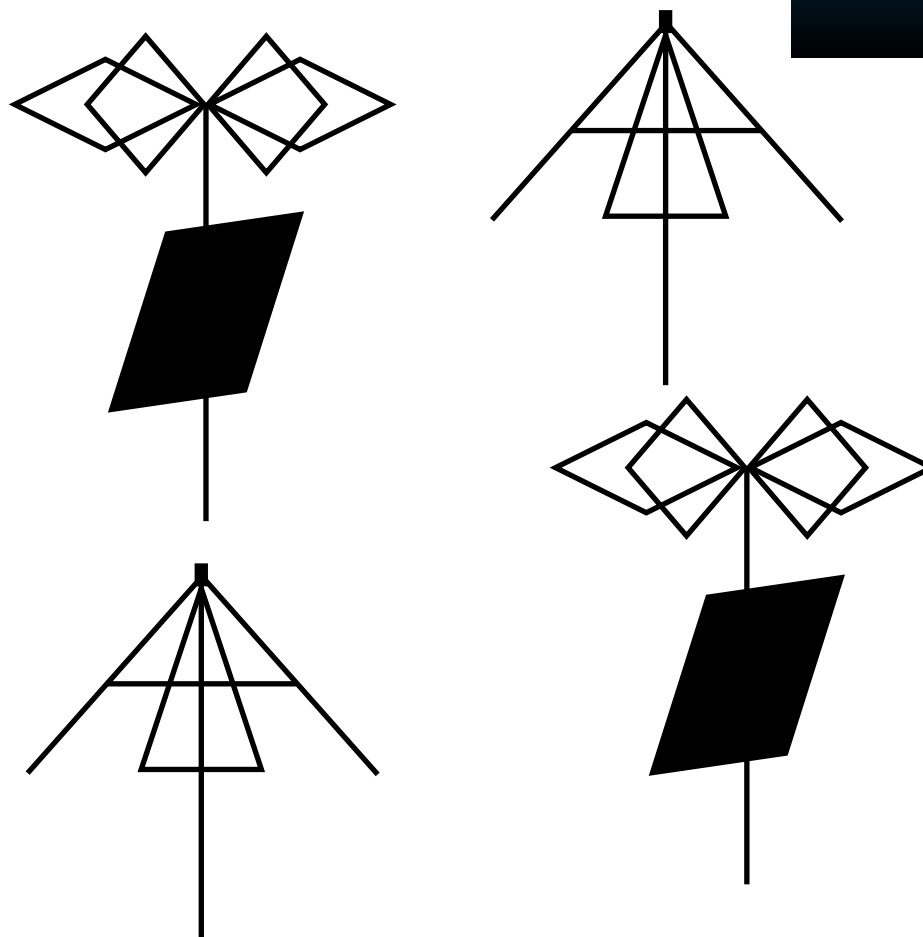
Instrumental development  
(PUEO-LFI)

Context: prototype of a beamformed radio detector  
Goals: show understanding of background and EAS identification

Array optimisation  
(GRAND)

Signal analysis  
(BEACON)

Signal reconstruction  
(GRAND)



Context: very extended and sparse radio arrays  
Goals: study the optimisation of radio arrays for very inclined EAS



# Some challenges of the radio detection of UHE (on which I worked on)

Context: low frequency instrument dedicated to Earth-skimming UHE neutrinos  
Goals: optimise antenna and RF chain to neutrino induced EAS

Instrumental development  
(PUEO-LFI)

Context: prototype of a beamformed radio detector  
Goals: show understanding of background and EAS identification

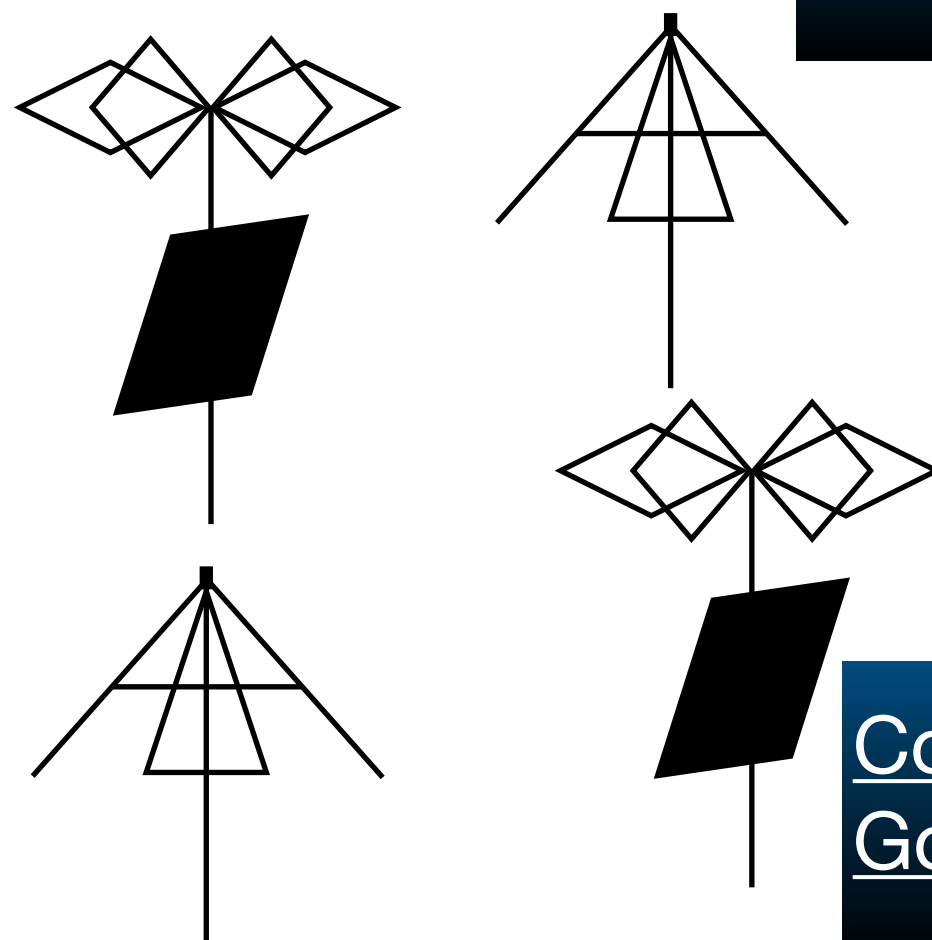
Signal analysis  
(BEACON)

Array optimisation  
(GRAND)

Context: very extended and sparse radio arrays  
Goals: develop a reconstruction procedure for very inclined EAS

Signal reconstruction  
(GRAND)

Context: very extended and sparse radio arrays  
Goals: study the optimisation of radio arrays for very inclined EAS

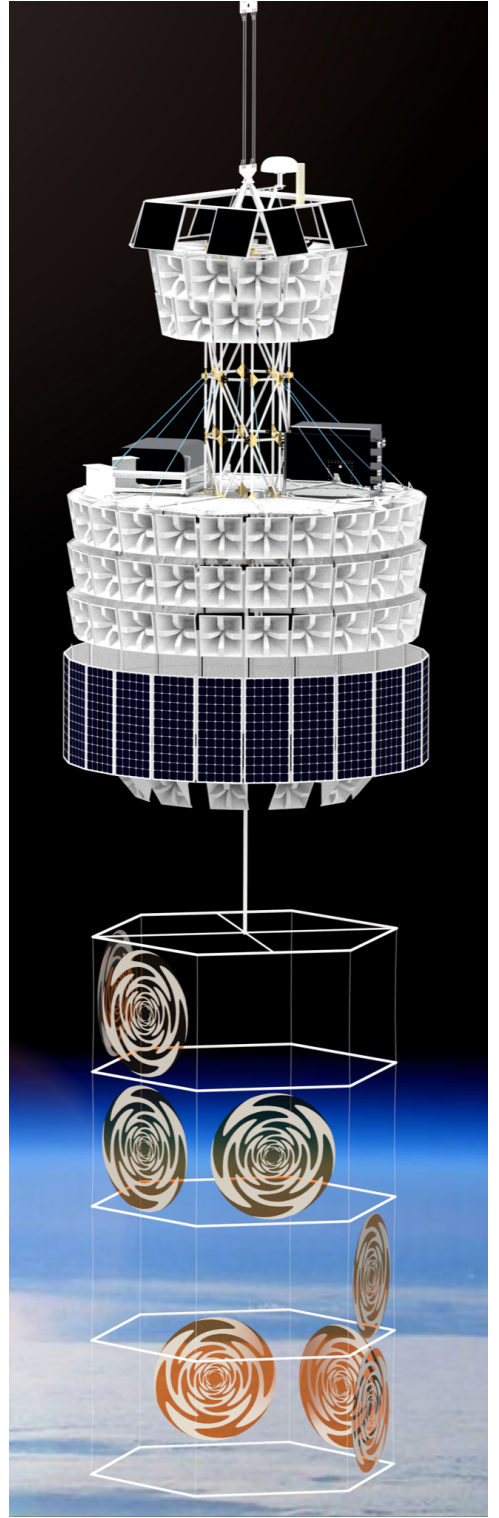




# Low Frequency Instrument

---

Target radio emission from EAS in the 50-300 MHz → larger radio beam → larger FoV → better sensitivity

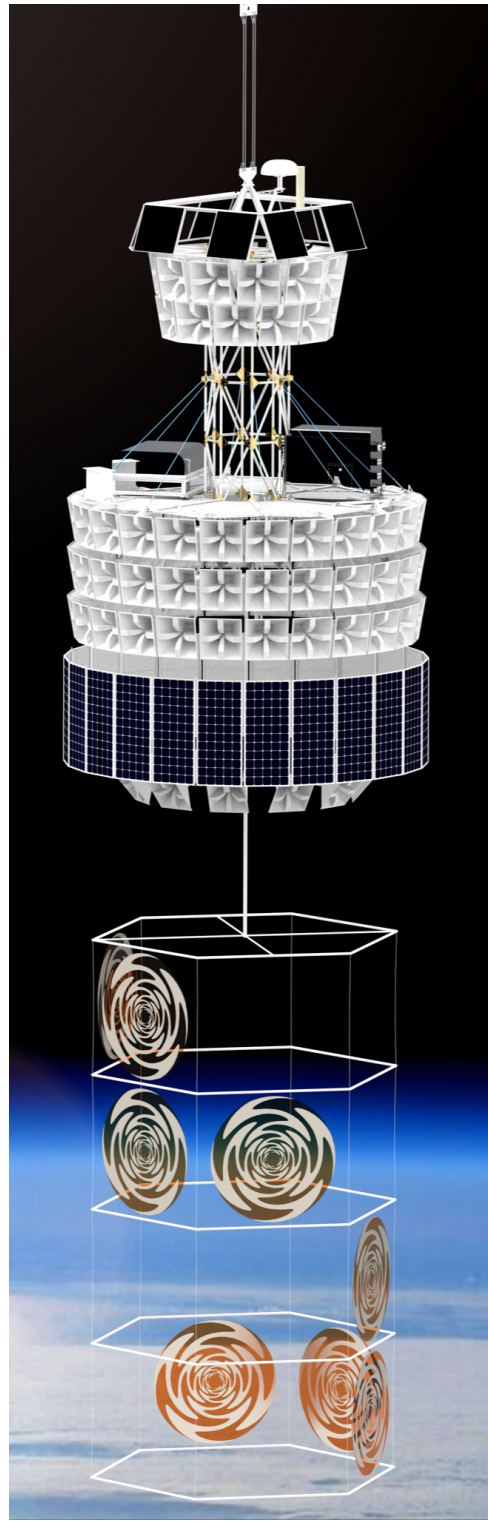
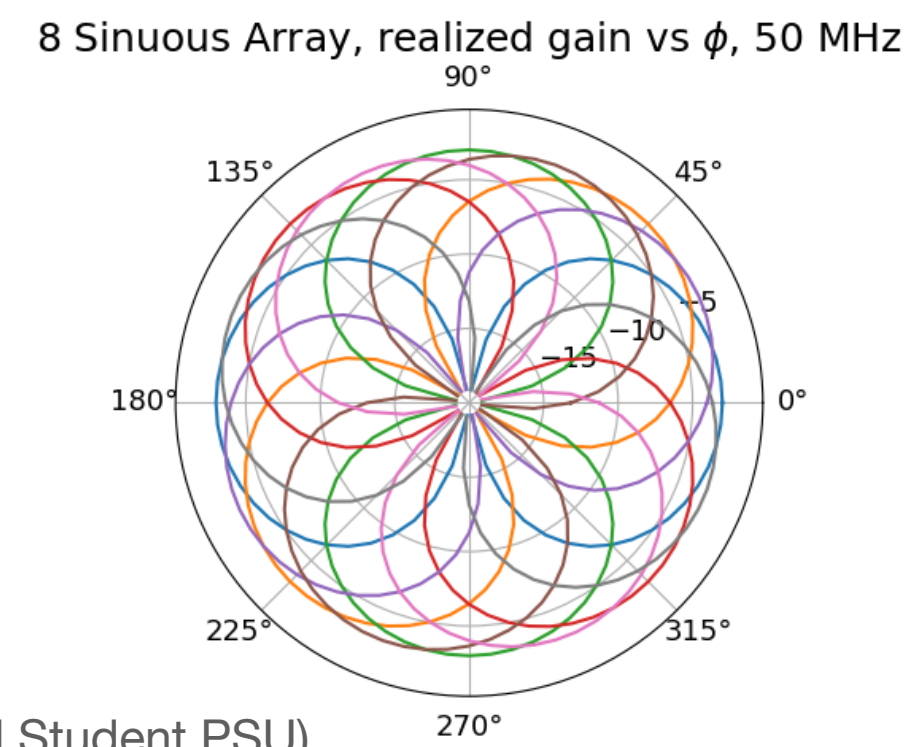
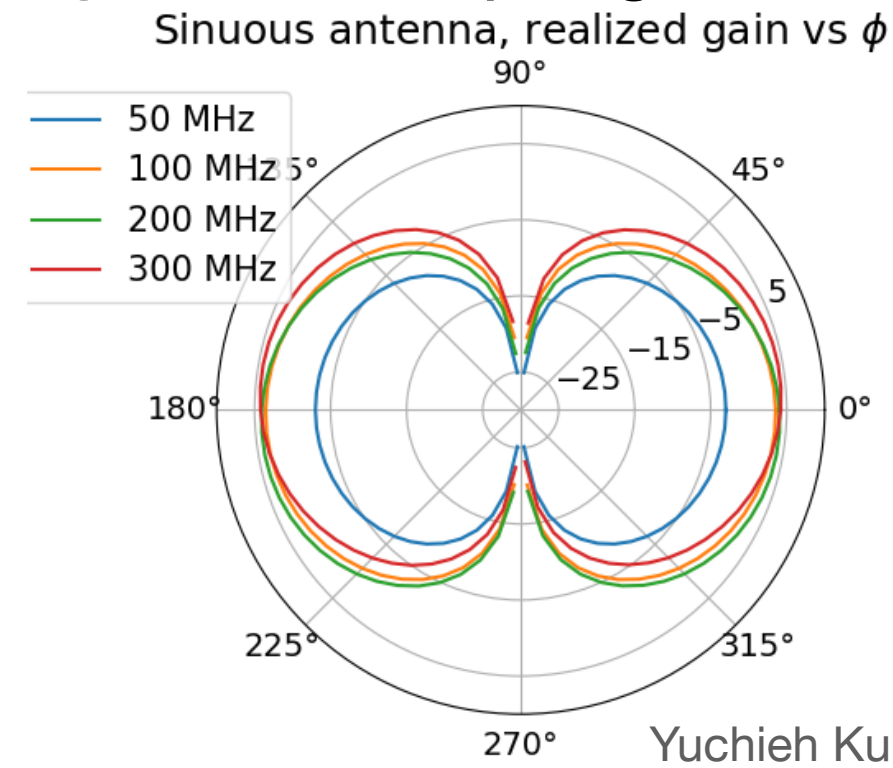
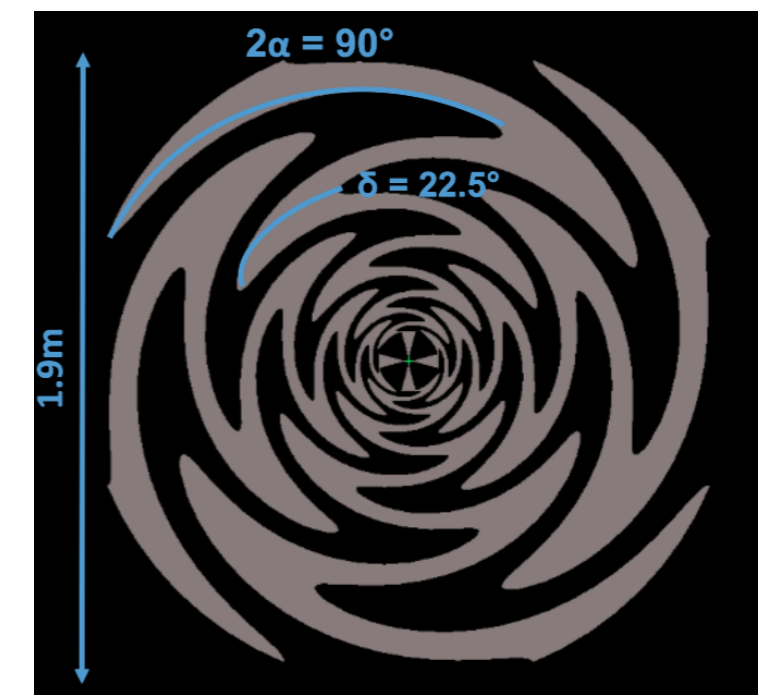




# Low Frequency Instrument

Target radio emission from EAS in the 50-300 MHz → larger radio beam → larger FoV → better sensitivity

**Sinuuous antenna design** → isotropic gain response of the array → maximise FoV

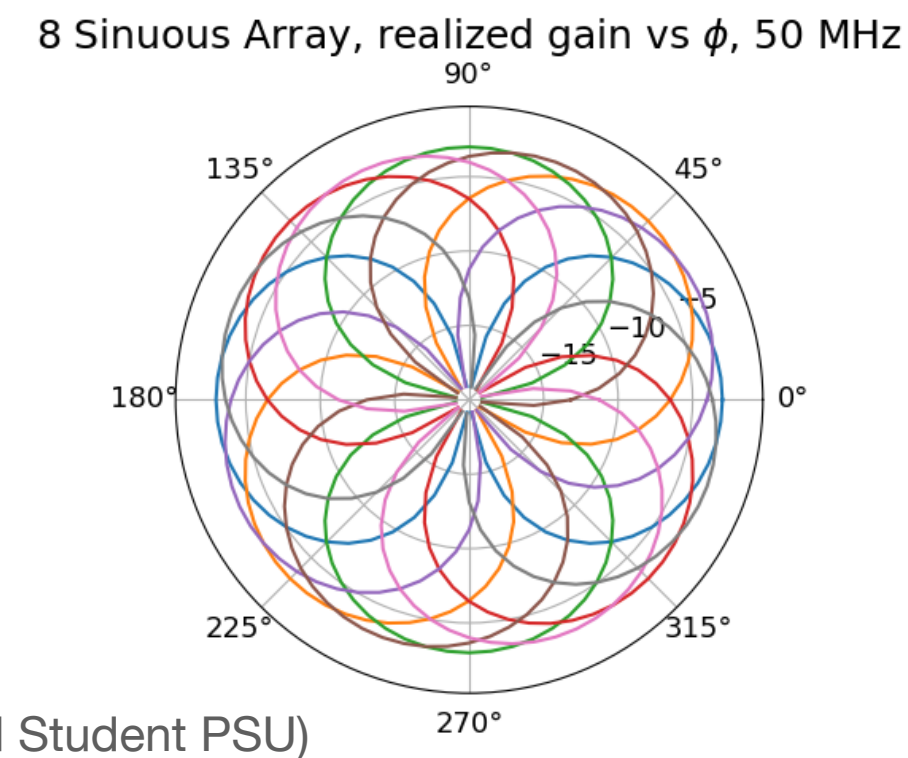
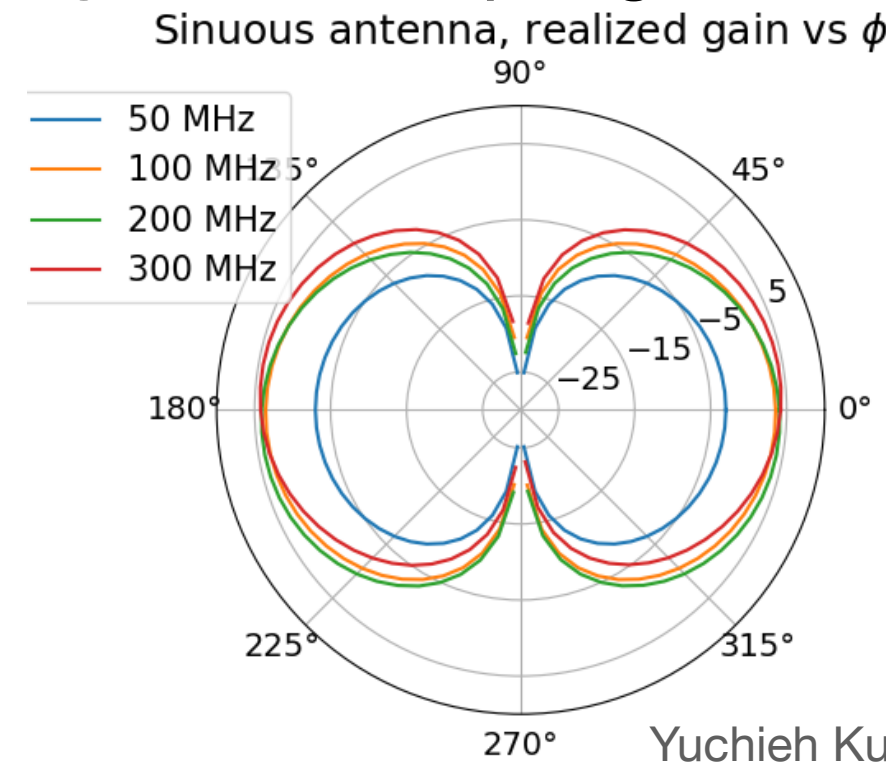
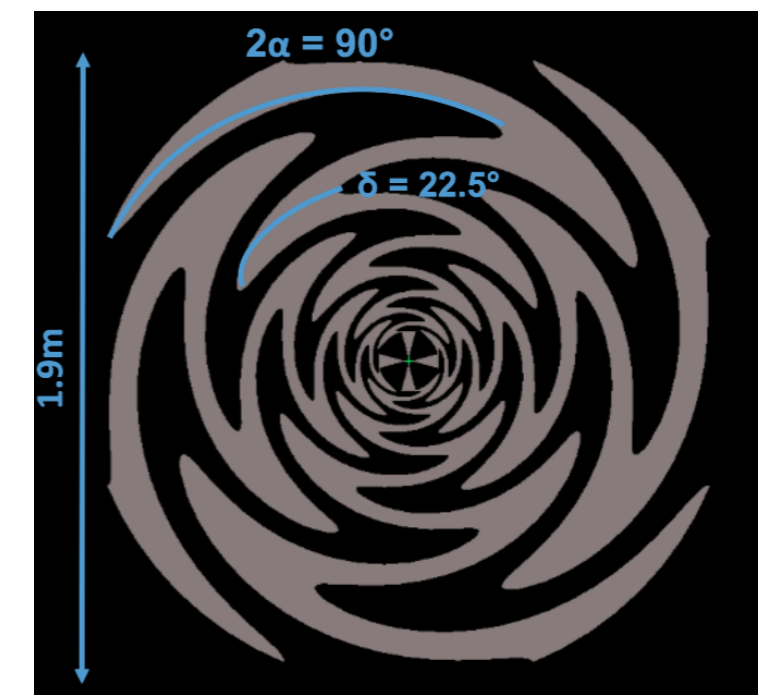




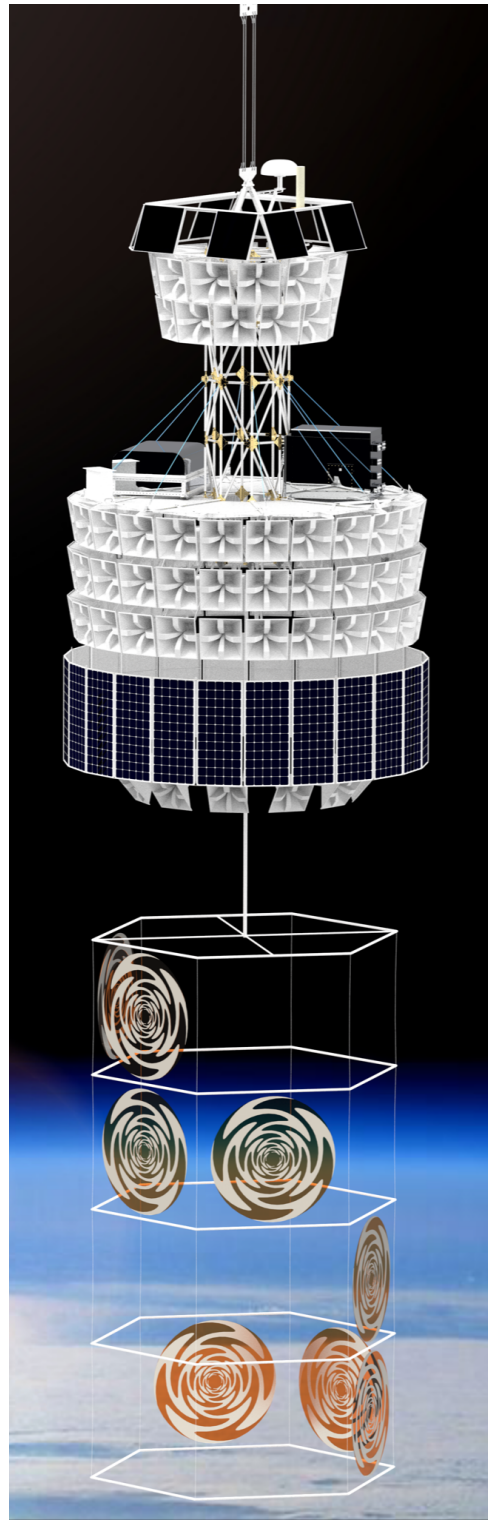
# Low Frequency Instrument

Target radio emission from EAS in the 50-300 MHz → larger radio beam → larger FoV → better sensitivity

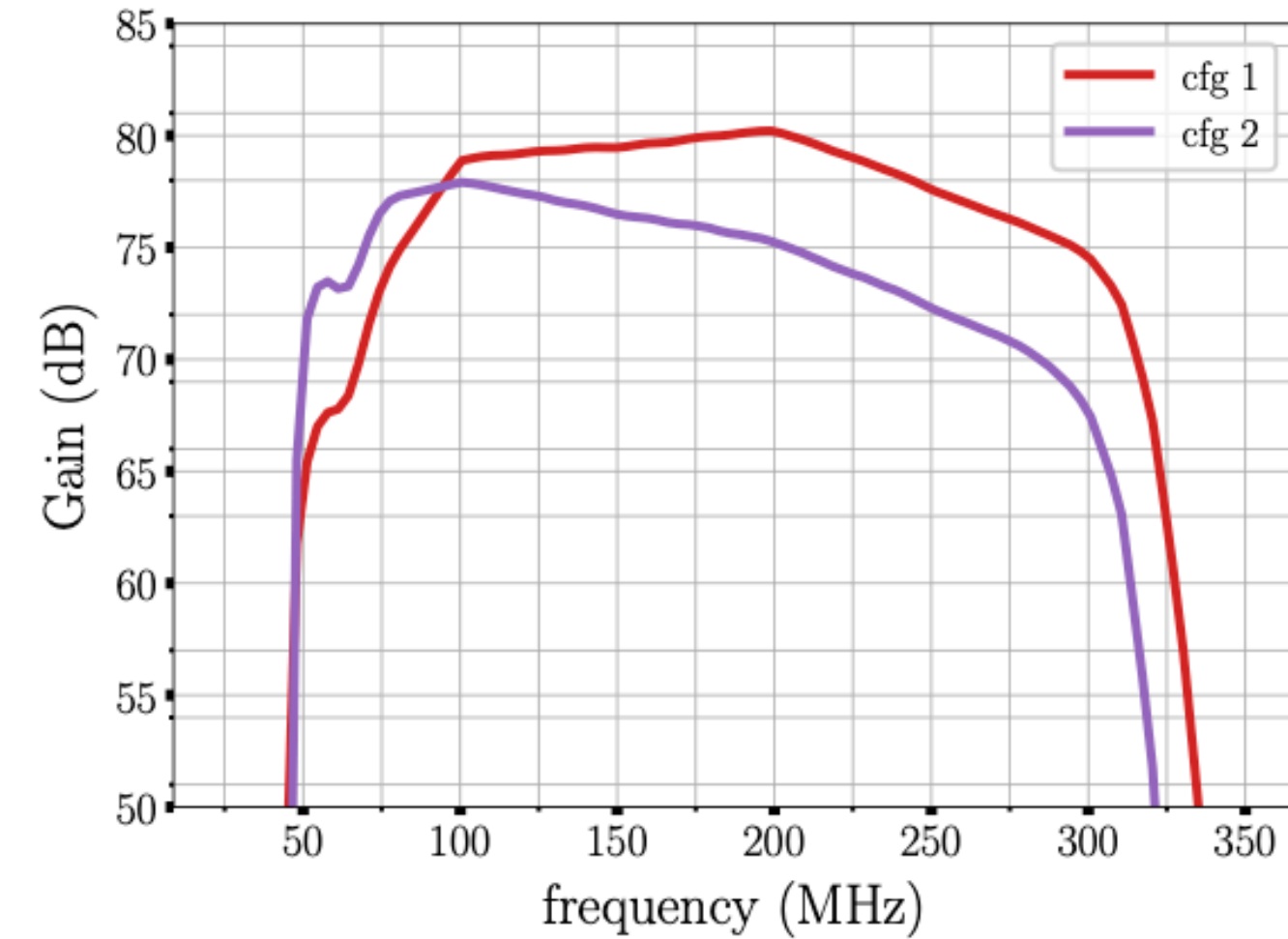
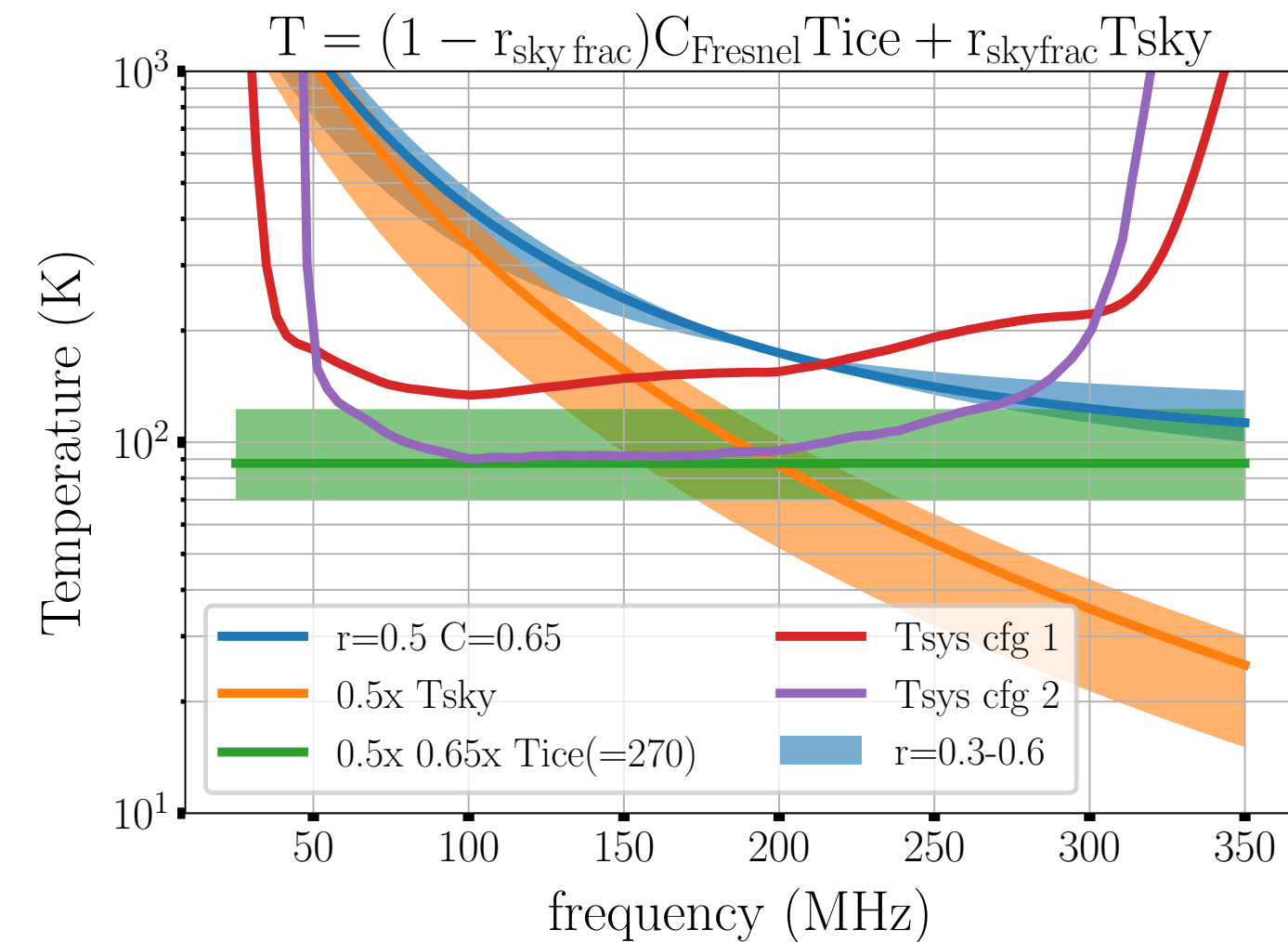
**Sinuuous antenna design** → isotropic gain response of the array → maximise FoV



Yuchieh Ku (Grad Student PSU)



**RF chain** → sensitive down to ice and sky background + TRL6 requirements (pressure/temp)

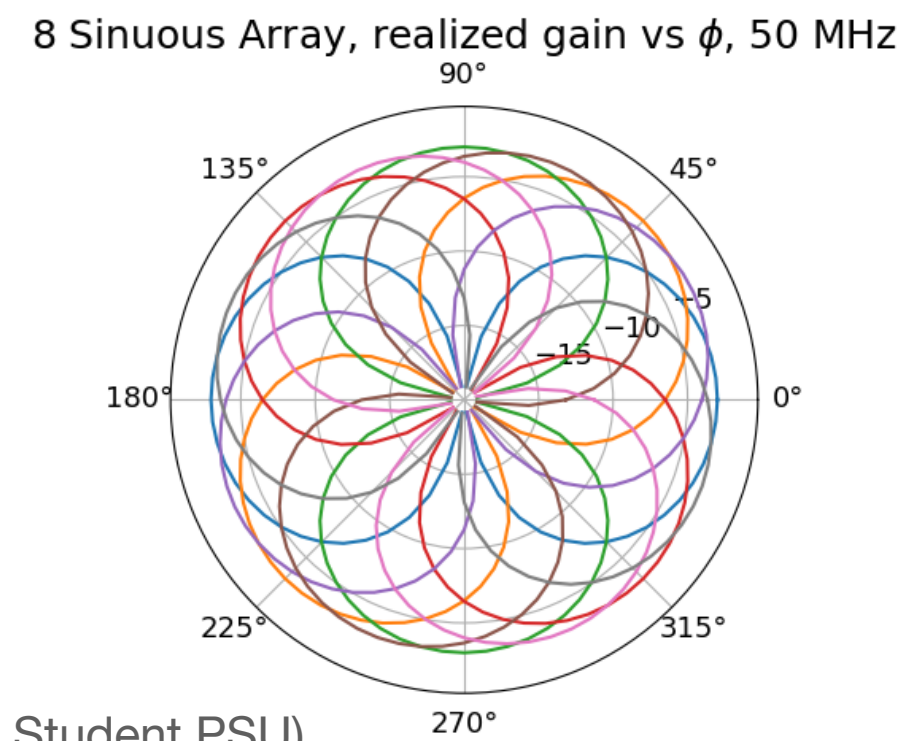
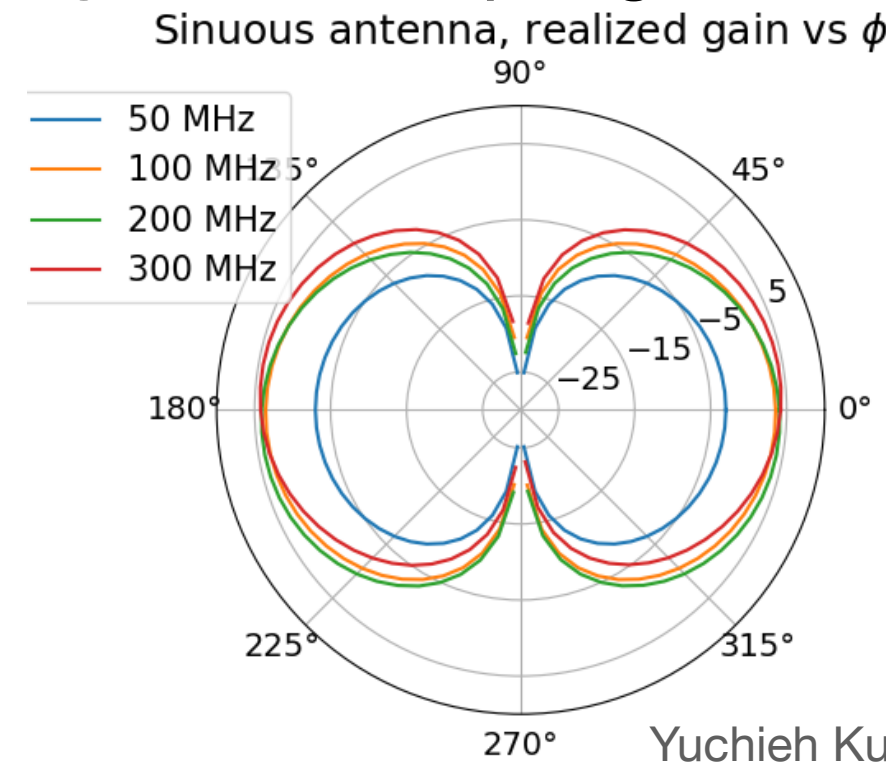
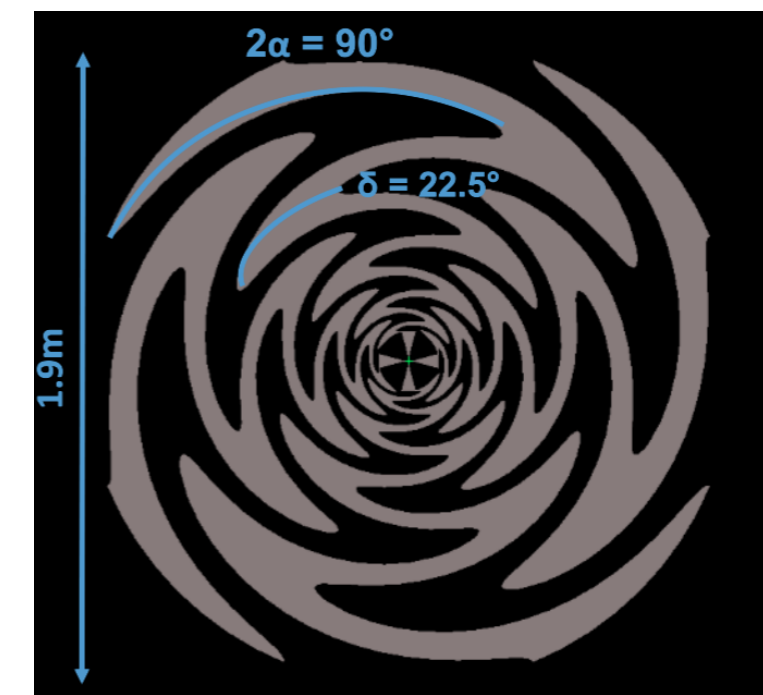




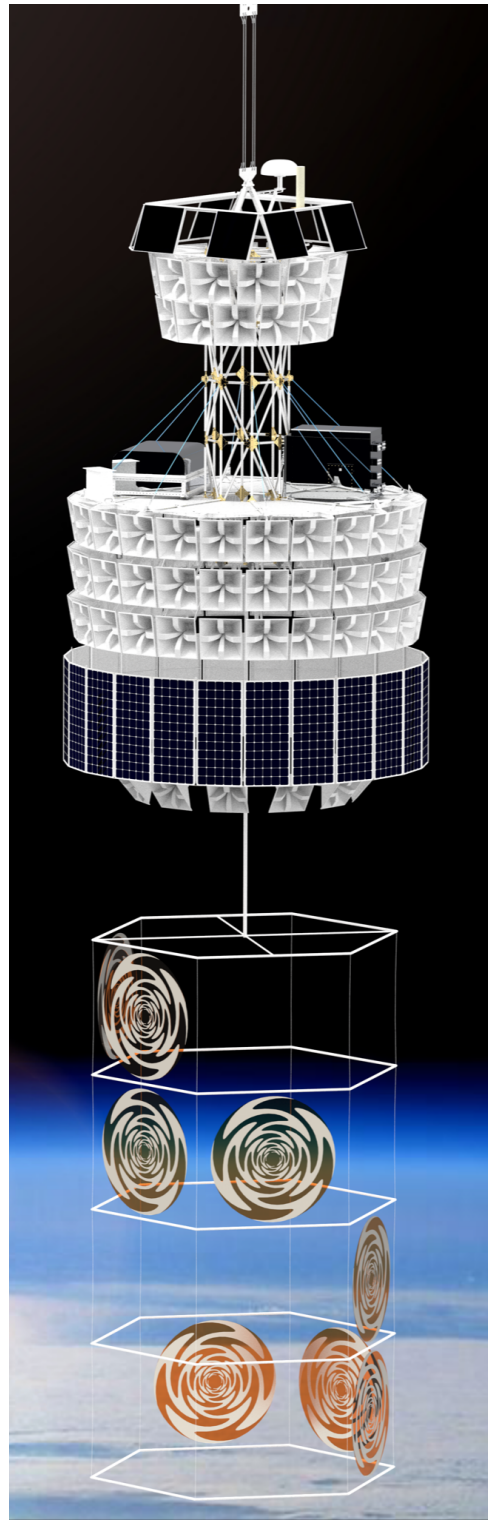
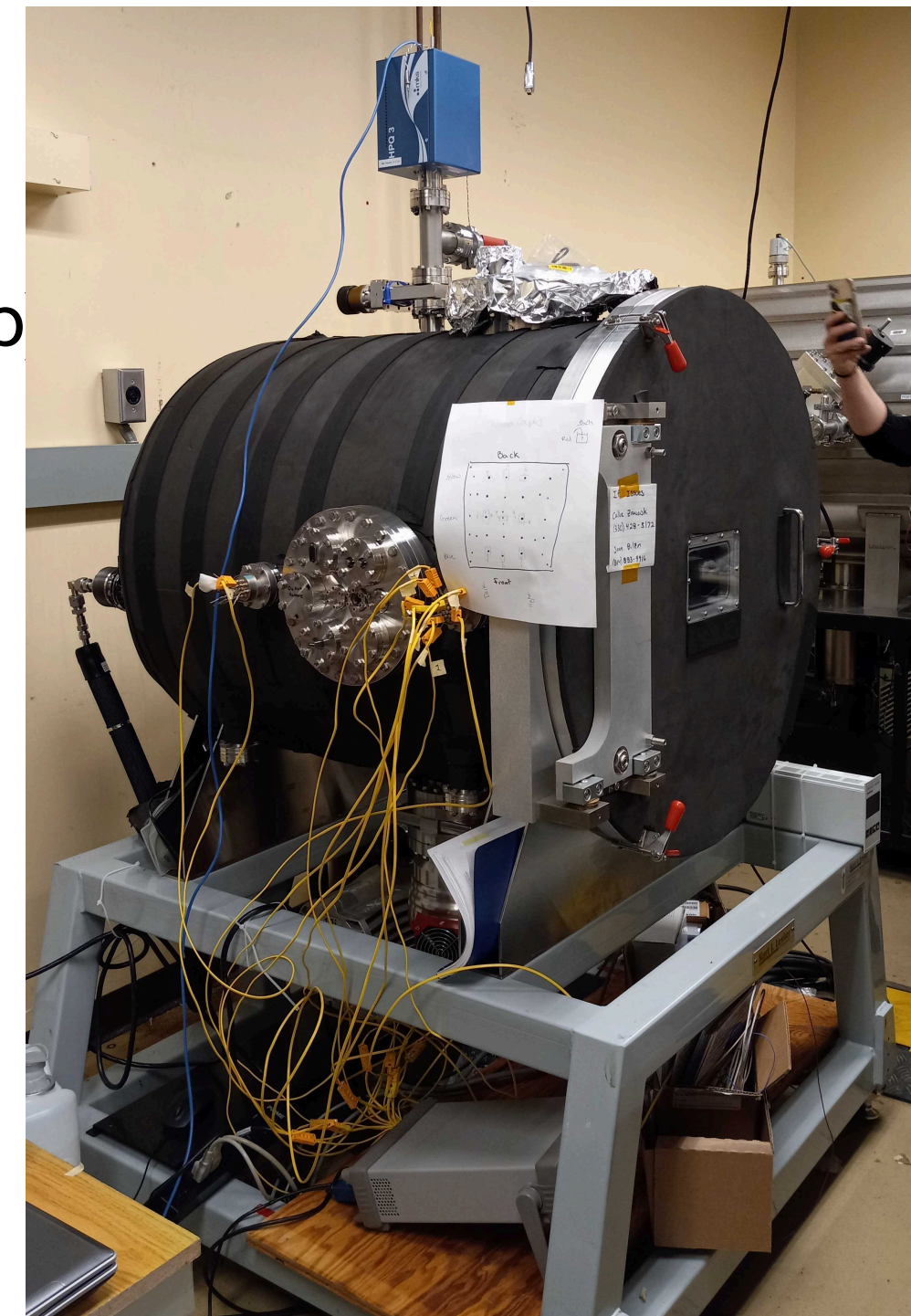
# Low Frequency Instrument

Target radio emission from EAS in the 50-300 MHz → larger radio beam → larger FoV → better sensitivity

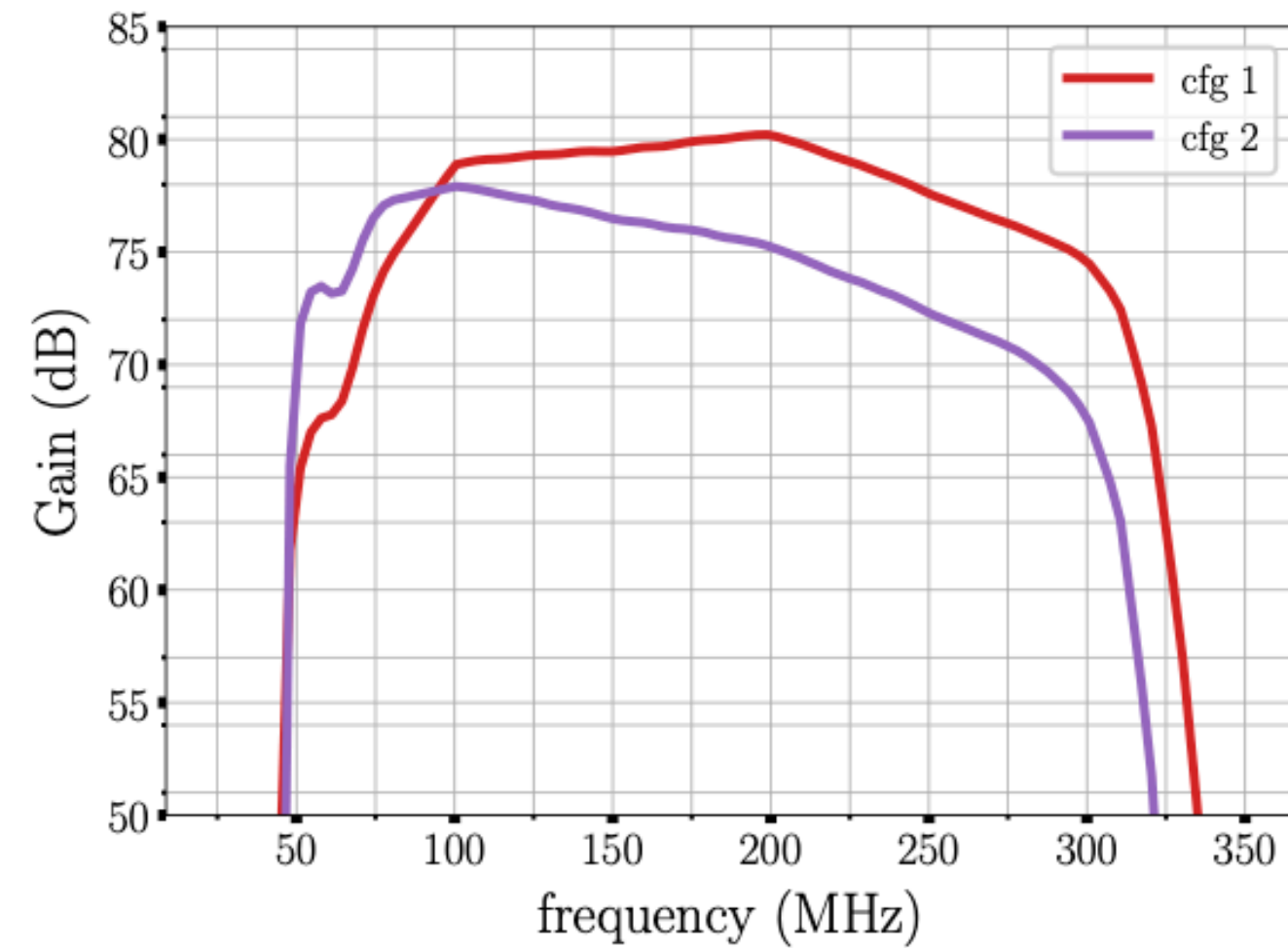
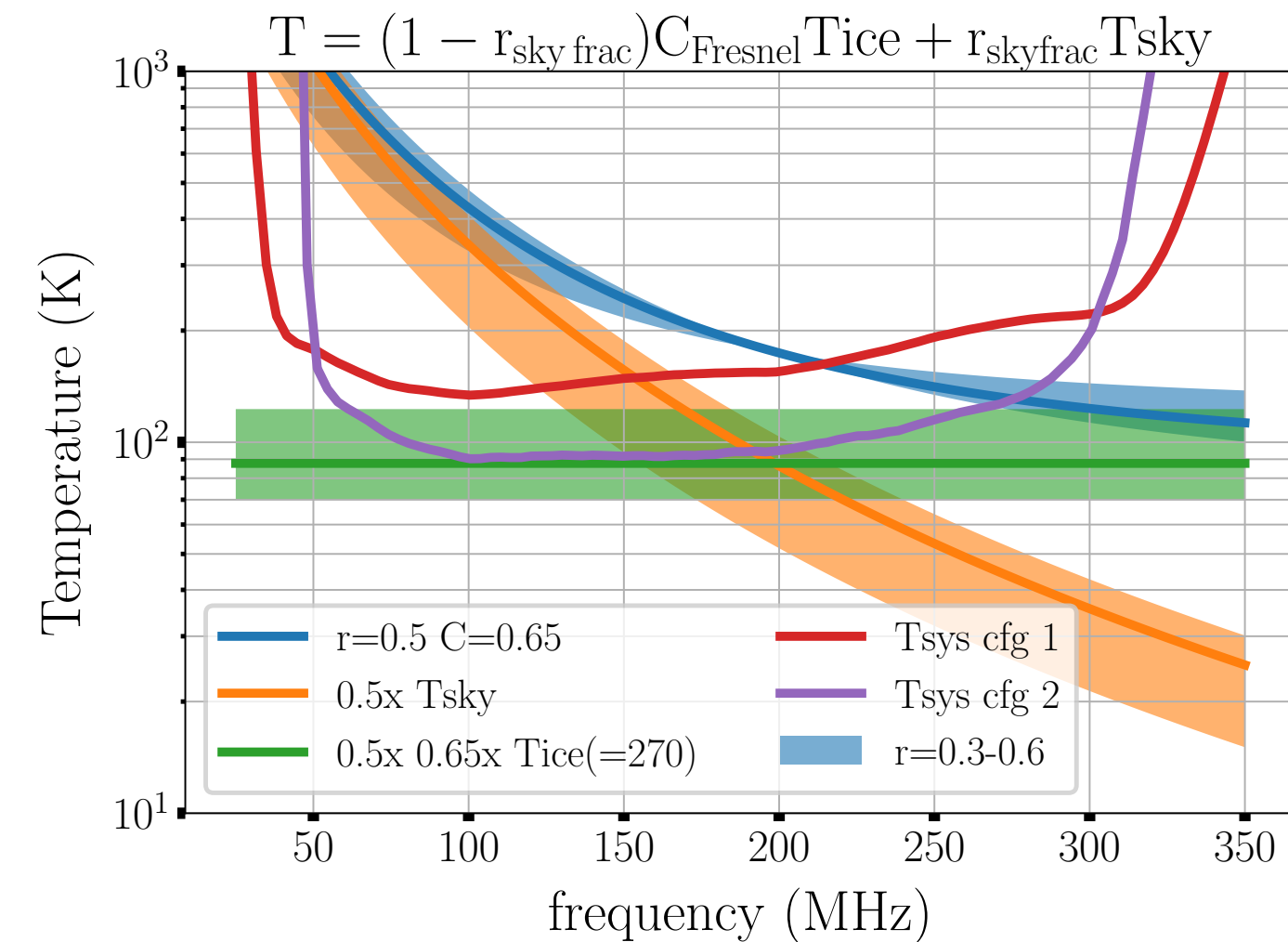
**Sinuuous antenna design** → isotropic gain response of the array → maximise FoV



Thermal vacuum chamber (PSU)



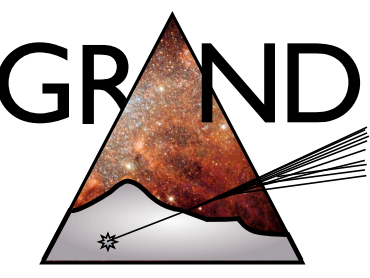
**RF chain** → sensitive down to ice and sky background + TRL6 requirements (pressure/temp





# Influence of the topography on the radio detection of neutrino induced air showers

---



V. D., Renault-Tinacci (IAP), Martineau (LPNHE), Charrier (Subatech), Kotera (IAP), Le Coz (NAOC), Niess (UCA), Tueros (CONICET), Zilles (IAP) (NIMA 2021)

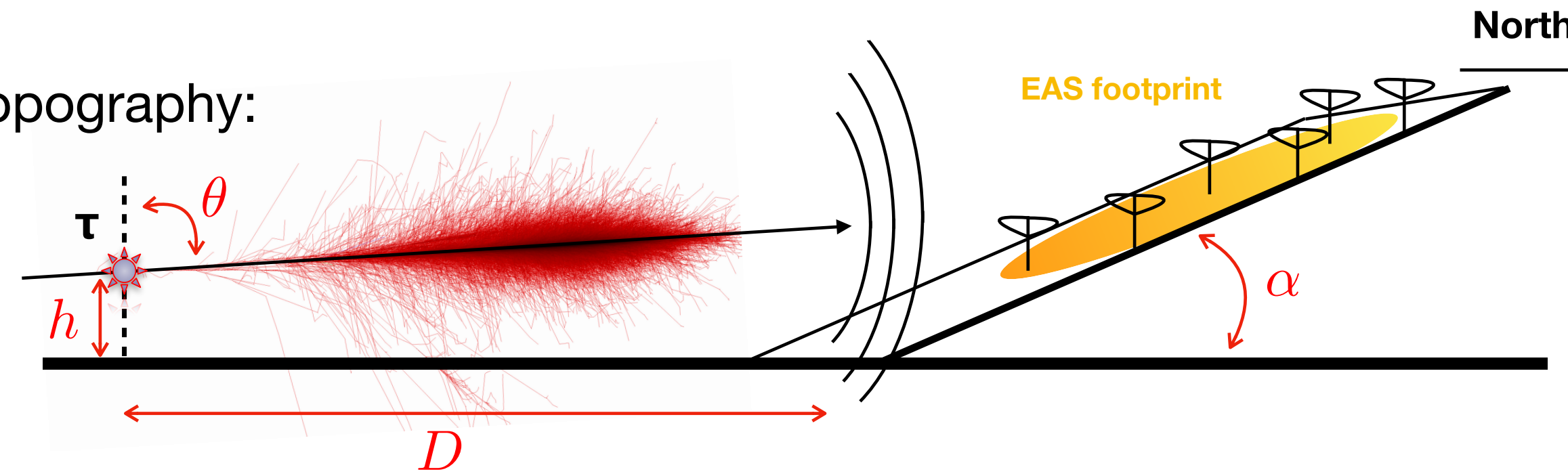


# Influence of the topography on the radio detection of neutrino induced air showers

V. D., Renault-Tinacci (IAP), Martineau (LPNHE), Charrier (Subatech), Kotera (IAP), Le Coz (NAOC), Niess (UCA), Tueros (CONICET), Zilles (IAP) (NIMA 2021)

Two parameters to model the topography:

- $D$  = valley depth
- $\alpha$  = the mountain slope



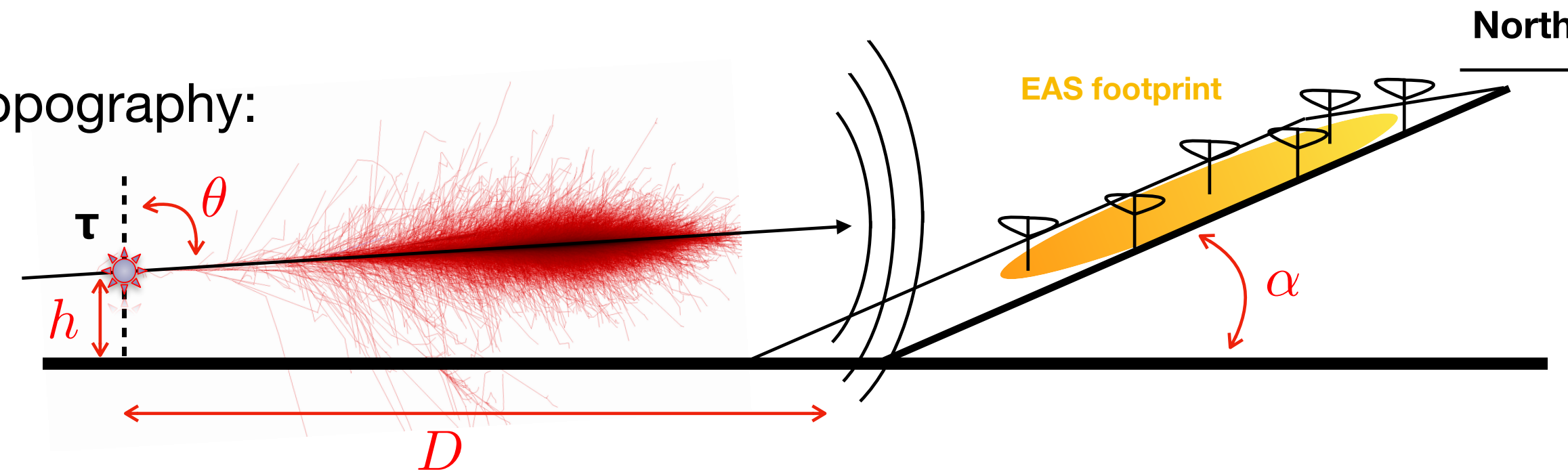


# Influence of the topography on the radio detection of neutrino induced air showers

V. D., Renault-Tinacci (IAP), Martineau (LPNHE), Charrier (Subatech), Kotera (IAP), Le Coz (NAOC), Niess (UCA), Tueros (CONICET), Zilles (IAP) (NIMA 2021)

Two parameters to model the topography:

- $D$  = valley depth
- $\alpha$  = the mountain slope



## 3 tools:

- microscopic simulation (MC - ZHAireS) A. Zilles, et al. 2019 (including V.D.)
- semi-analytic simulation (Radio Morphing)
- analytic computation (cone modelling of the trigger volume)

- 3 computation speeds → from several hours to tens of seconds
- consistent results (within  $\pm 10\%$  for Radio Morphing and  $[-30\%, 0\%]$  for Cone)

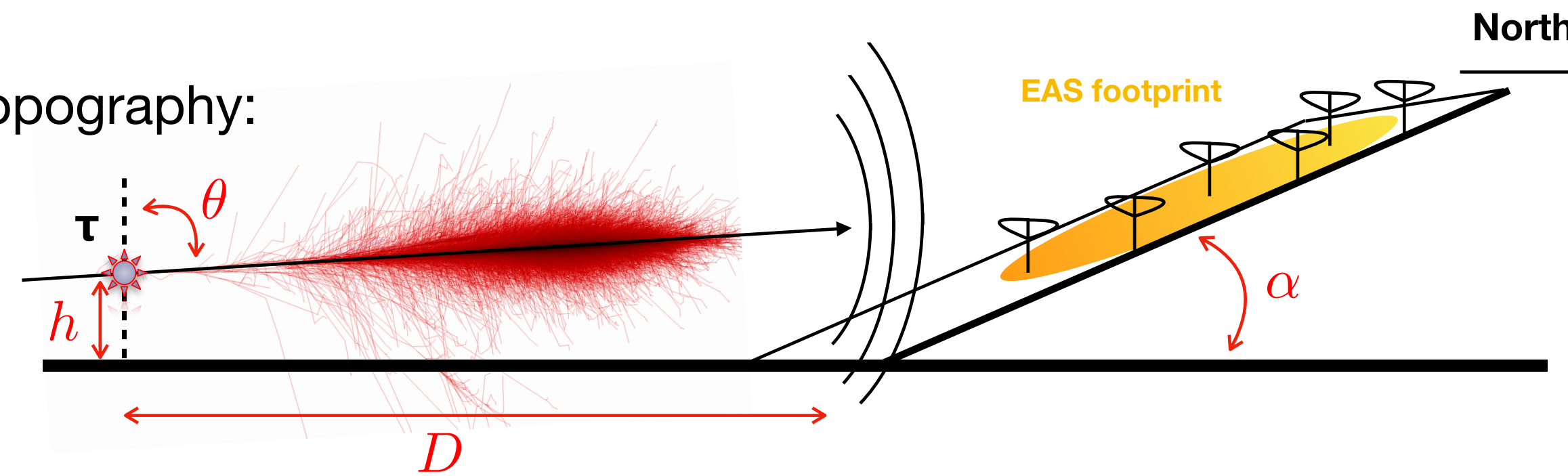


# Influence of the topography on the radio detection of neutrino induced air showers

V. D., Renault-Tinacci (IAP), Martineau (LPNHE), Charrier (Subatech), Kotera (IAP), Le Coz (NAOC), Niess (UCA), Tueros (CONICET), Zilles (IAP) (NIMA 2021)

Two parameters to model the topography:

- $D$  = valley depth
- $\alpha$  = the mountain slope



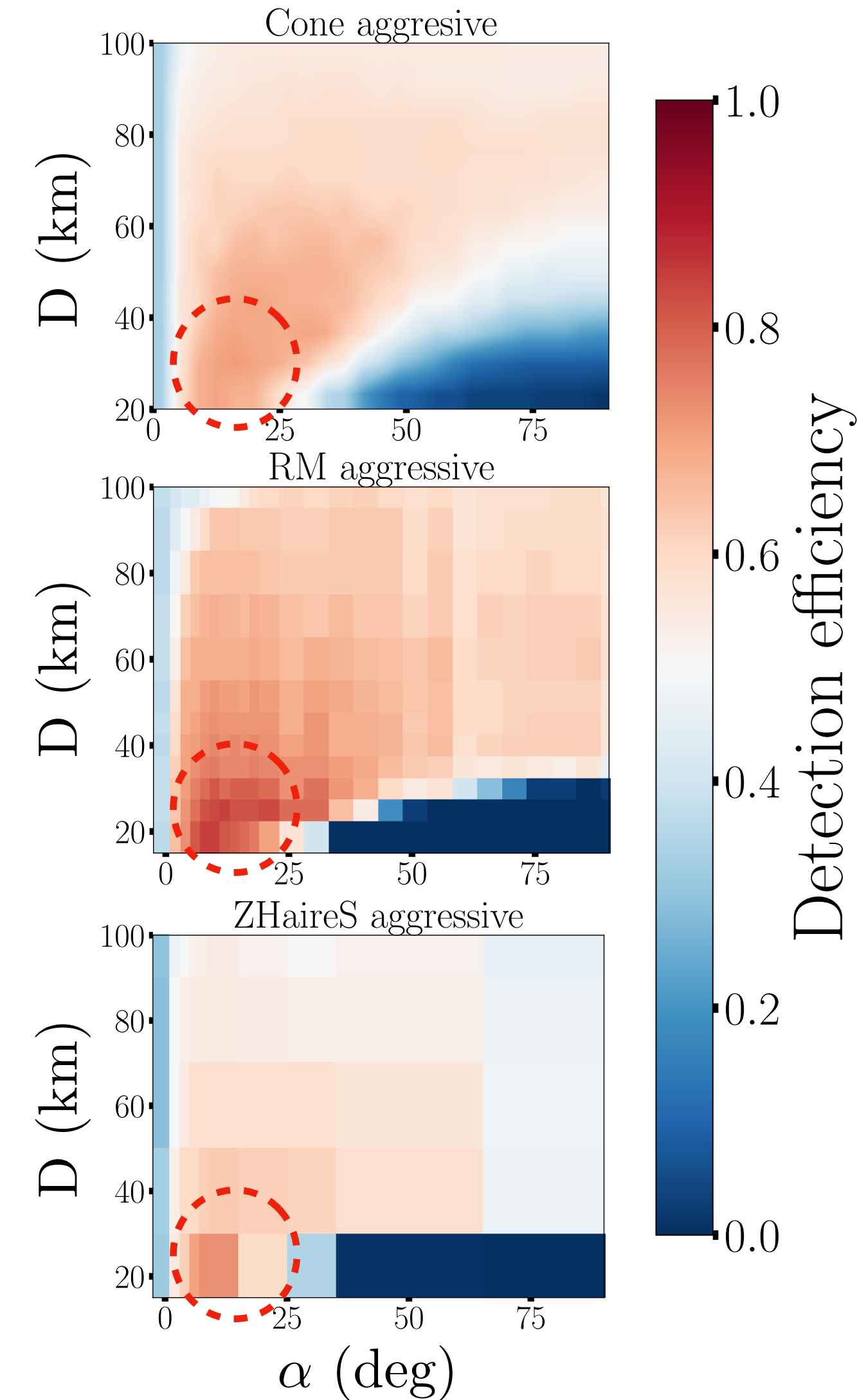
3 tools:

- microscopic simulation (MC - ZHAireS) A. Zilles, et al. 2019 (including V.D.)
- semi-analytic simulation (Radio Morphing)
- analytic computation (cone modelling of the trigger volume)

- ▶ 3 computation speeds → from several hours to tens of seconds
- ▶ consistent results (within  $\pm 10\%$  for Radio Morphing and  $[-30\%, 0\%]$  for Cone)

Result:

- inclined topographies increase the detection efficiency up to a factor of 3
- the effect remains constant over angles ranging from  $5^\circ$  to  $20^\circ$



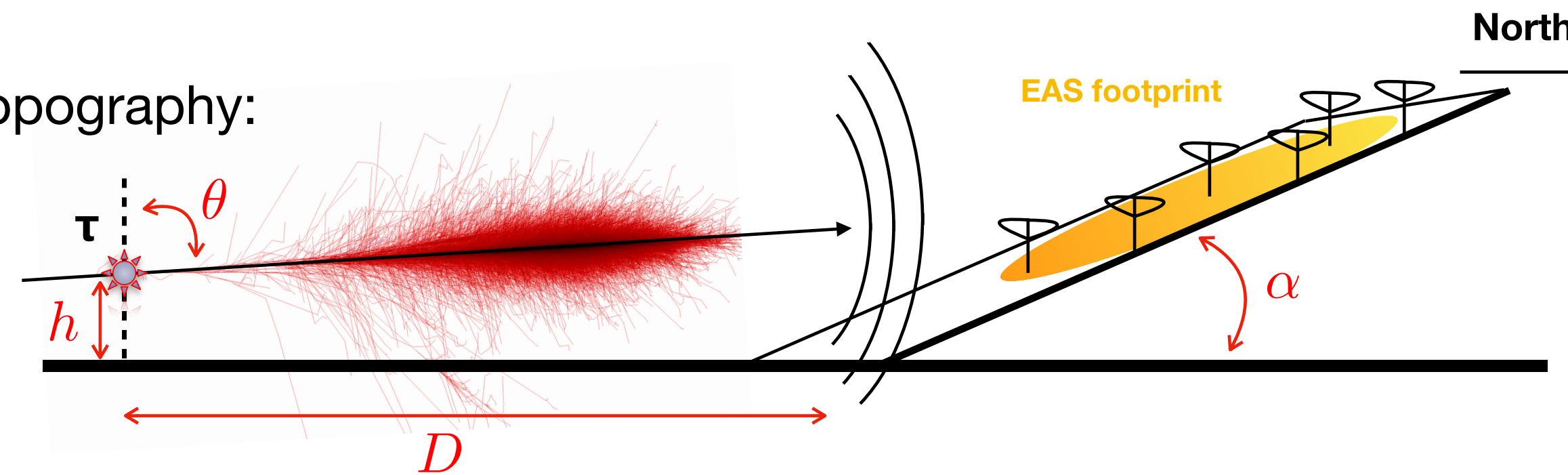


# Influence of the topography on the radio detection of neutrino induced air showers

V. D., Renault-Tinacci (IAP), Martineau (LPNHE), Charrier (Subatech), Kotera (IAP), Le Coz (NAOC), Niess (UCA), Tueros (CONICET), Zilles (IAP) (NIMA 2021)

Two parameters to model the topography:

- $D$  = valley depth
- $\alpha$  = the mountain slope



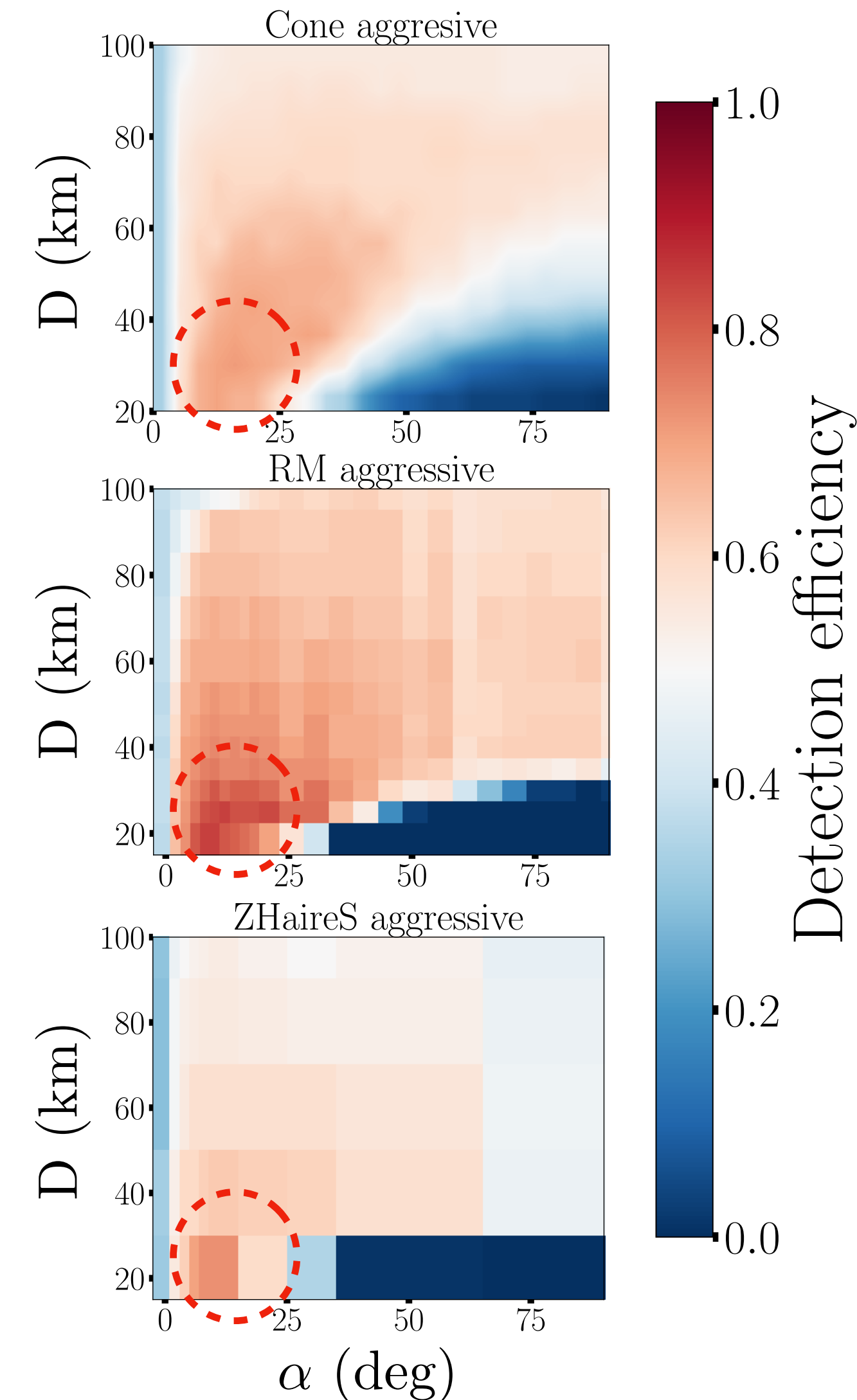
3 tools:

- microscopic simulation (MC - ZHAireS) A. Zilles, et al. 2019 (including V.D.)
- semi-analytic simulation (Radio Morphing)
- analytic computation (cone modelling of the trigger volume)

- 3 computation speeds → from several hours to tens of seconds
- consistent results (within  $\pm 10\%$  for Radio Morphing and  $[-30\%, 0\%]$  for Cone)

Result:

- inclined topographies increase the detection efficiency up to a factor of 3
- the effect remains constant over angles ranging from  $5^\circ$  to  $20^\circ$



Consequences: Very mild slopes of wide valleys or large basins could offer optimal topographies for the detection of neutrinos.



# The BEACON prototype

---



Southall (UChicago), Deaconu (UChicago), V. D., et al. (accepted in NIMA)

Prototype deployed (8 antennas x4 pol) and taking data at Barcroft Field Station, in the White Mountains in California





# The BEACON prototype

---

Southall (UChicago), Deaconu (UChicago), V. D., et al. (accepted in NIMA)

Prototype deployed (8 antennas x4 pol) and taking data at Barcroft Field Station, in the White Mountains in California

**Goal:** to assess the potential of radio beam detectors (similar to radio-astronomy) for EAS on cosmic rays:

- understand background (Las Vegas, planes, snow storm, wind,...)
- trigger and identify EAS (reconstruction and Monte-Carlo comparison)





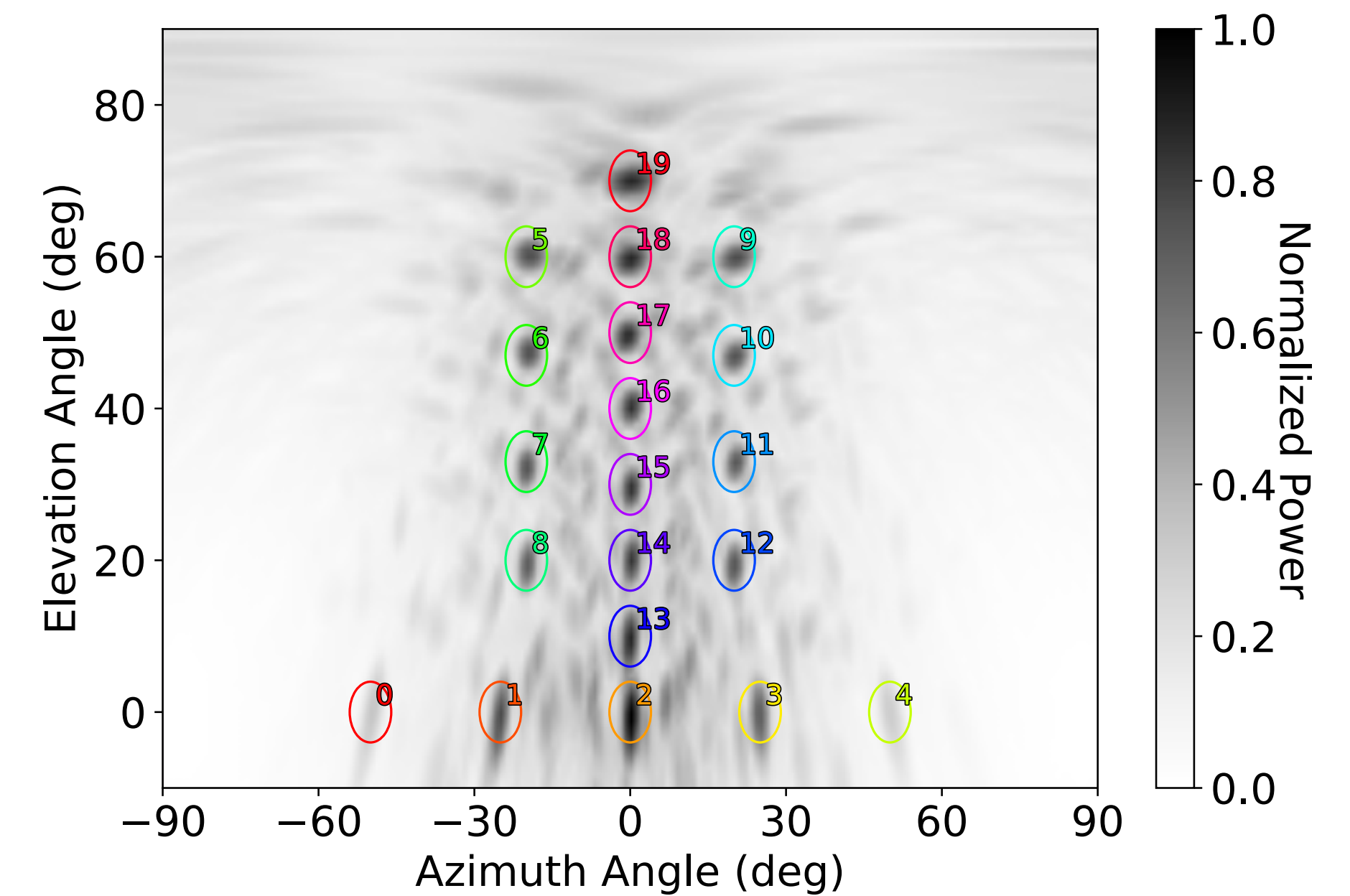
# The BEACON prototype

Southall (UChicago), Deaconu (UChicago), V. D., et al. (accepted in NIMA)

Prototype deployed (8 antennas x4 pol) and taking data at Barcroft Field Station, in the White Mountains in California

**Goal:** to assess the potential of radio beam detectors (similar to radio-astronomy) for EAS on cosmic rays:

- understand background (Las Vegas, planes, snow storm, wind,...)
- trigger and identify EAS (reconstruction and Monte-Carlo comparison)





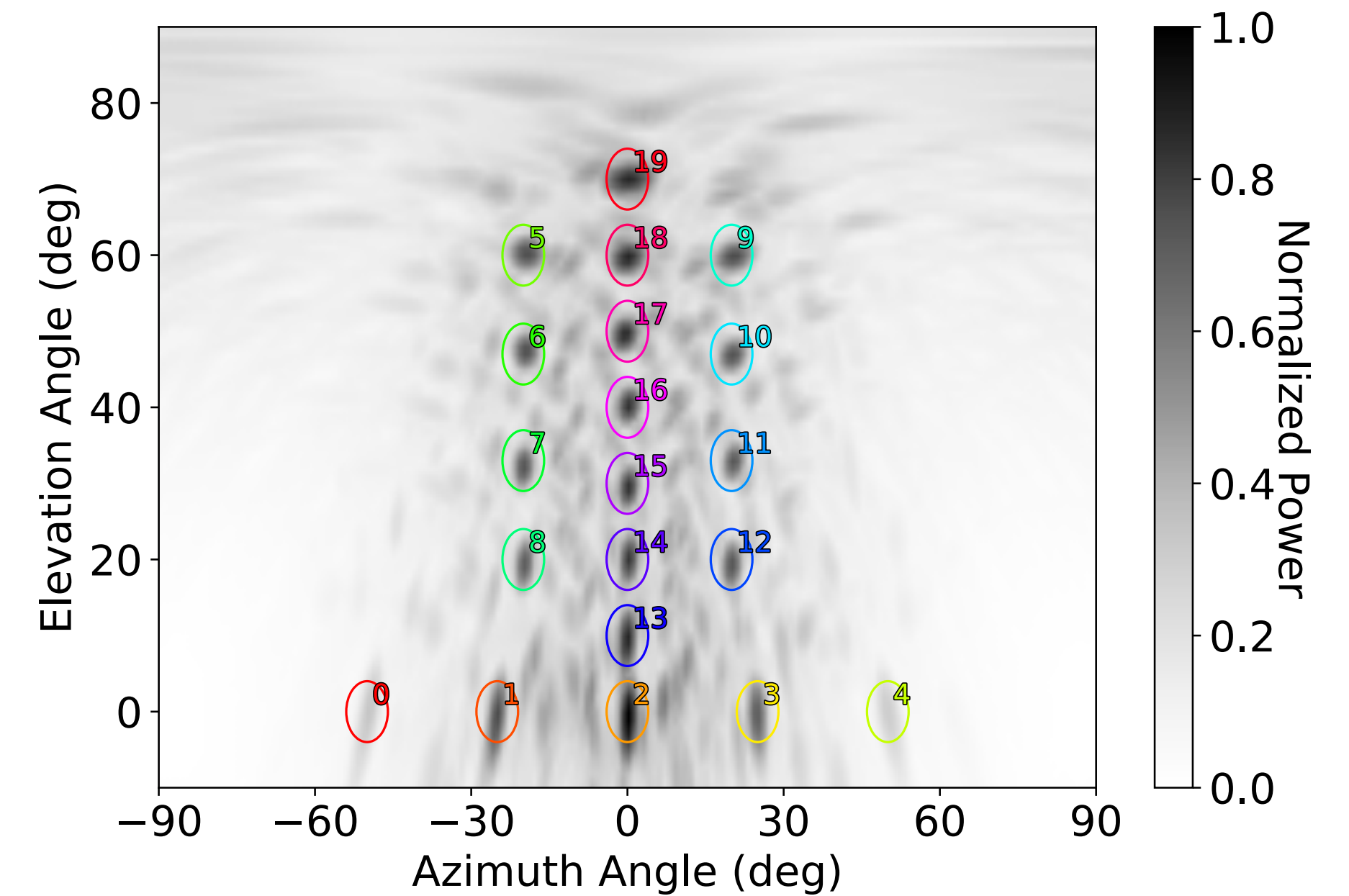
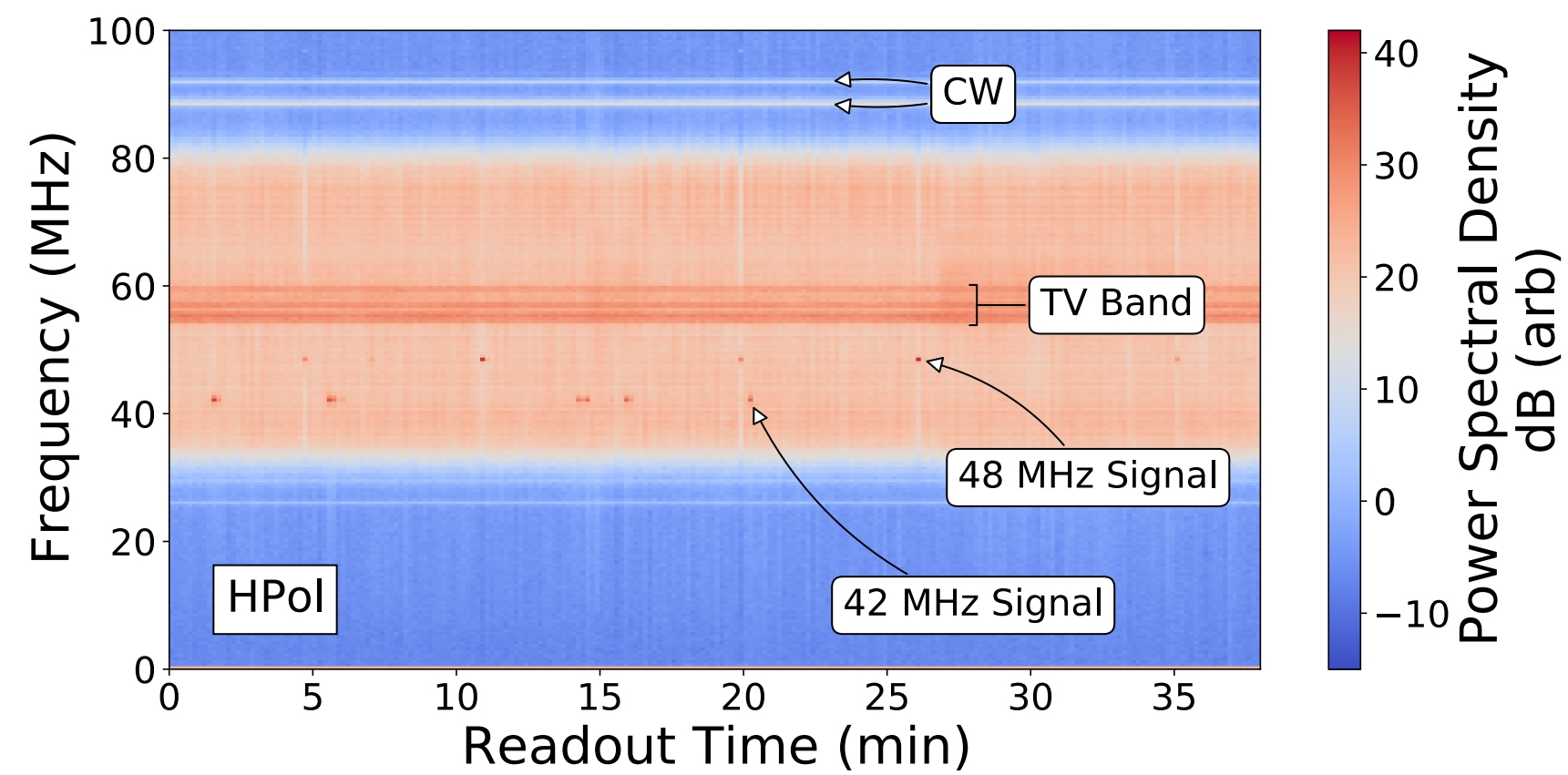
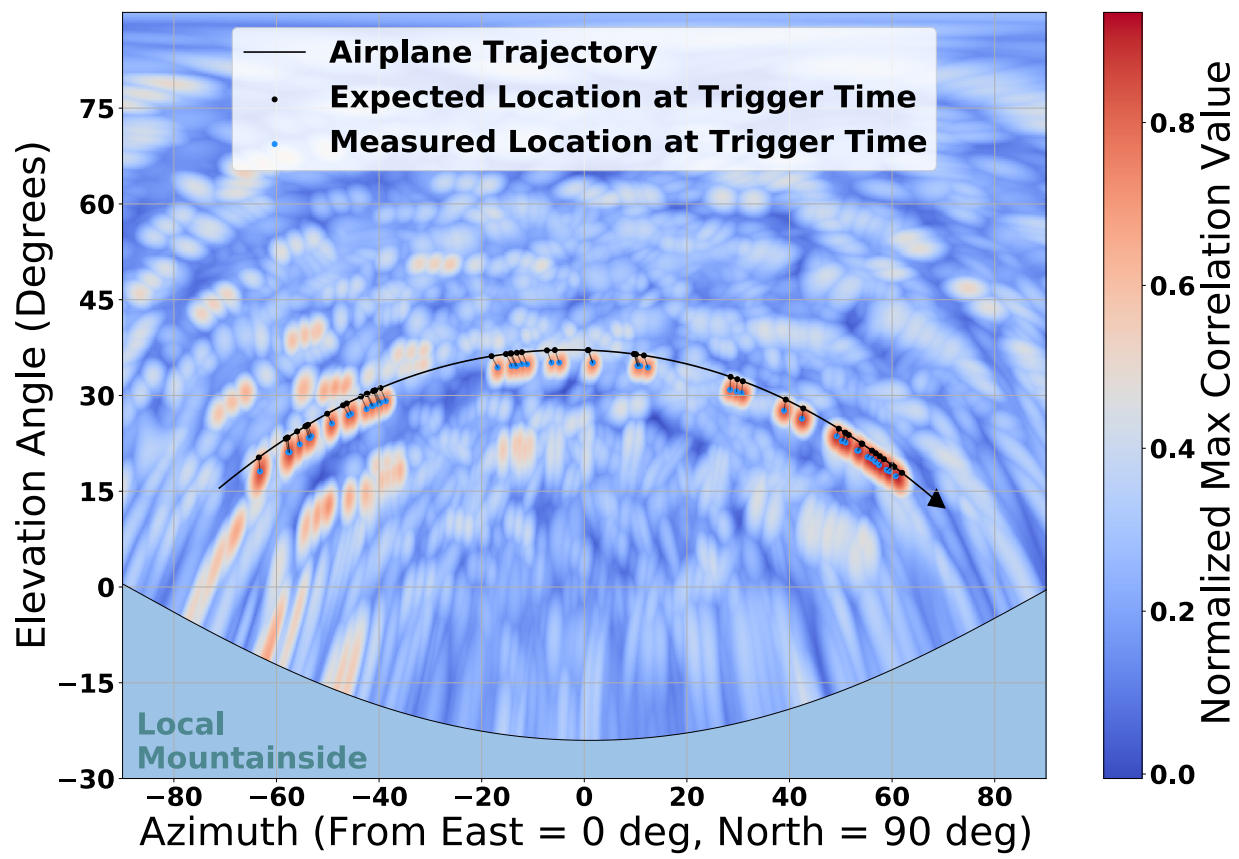
# The BEACON prototype

Southall (UChicago), Deaconu (UChicago), V. D., et al. (accepted in NIMA)

Prototype deployed (8 antennas x4 pol) and taking data at Barcroft Field Station, in the White Mountains in California

**Goal:** to assess the potential of radio beam detectors (similar to radio-astronomy) for EAS on cosmic rays:

- understand background (Las Vegas, planes, snow storm, wind,...)
- trigger and identify EAS (reconstruction and Monte-Carlo comparison)





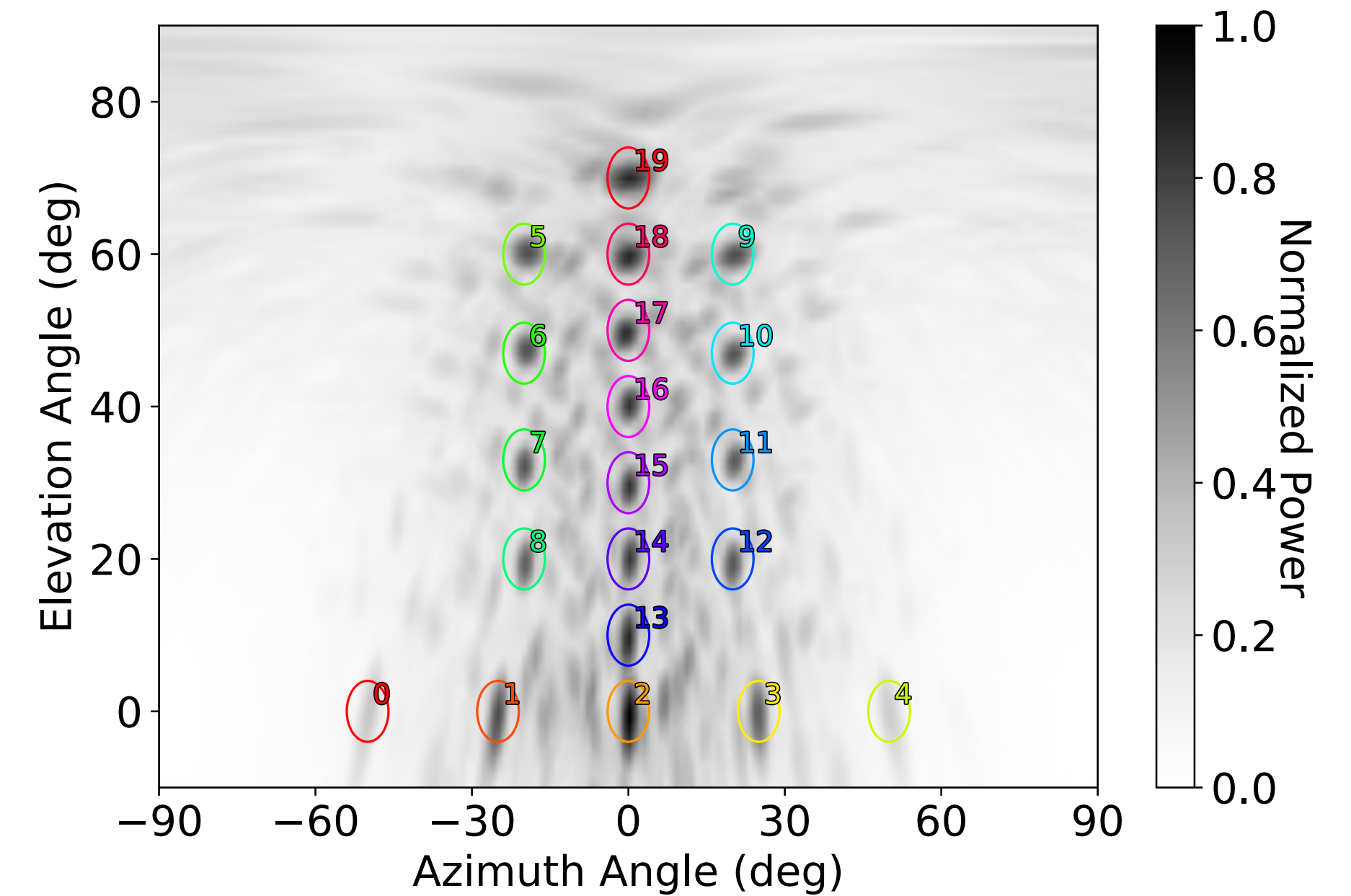
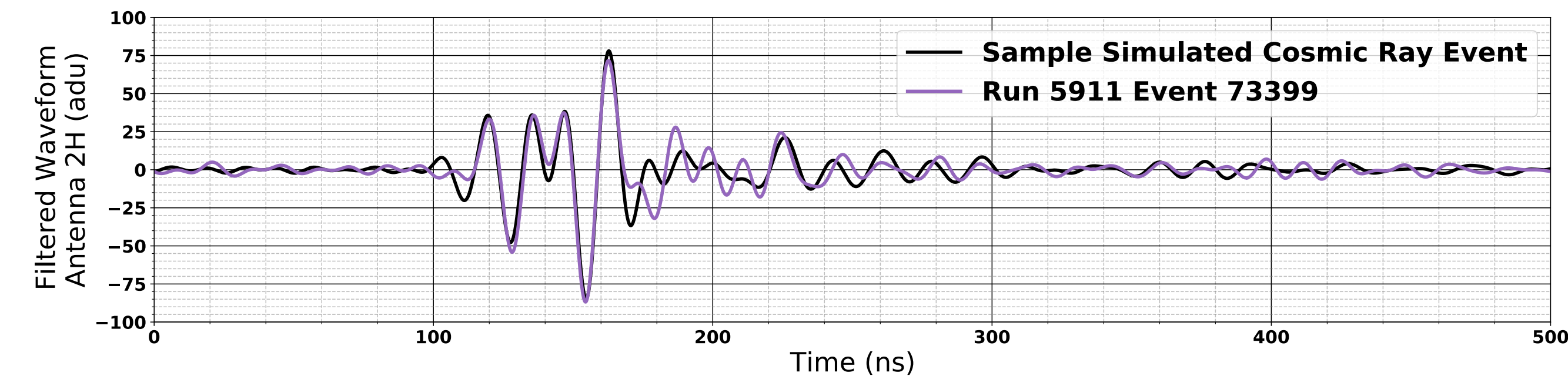
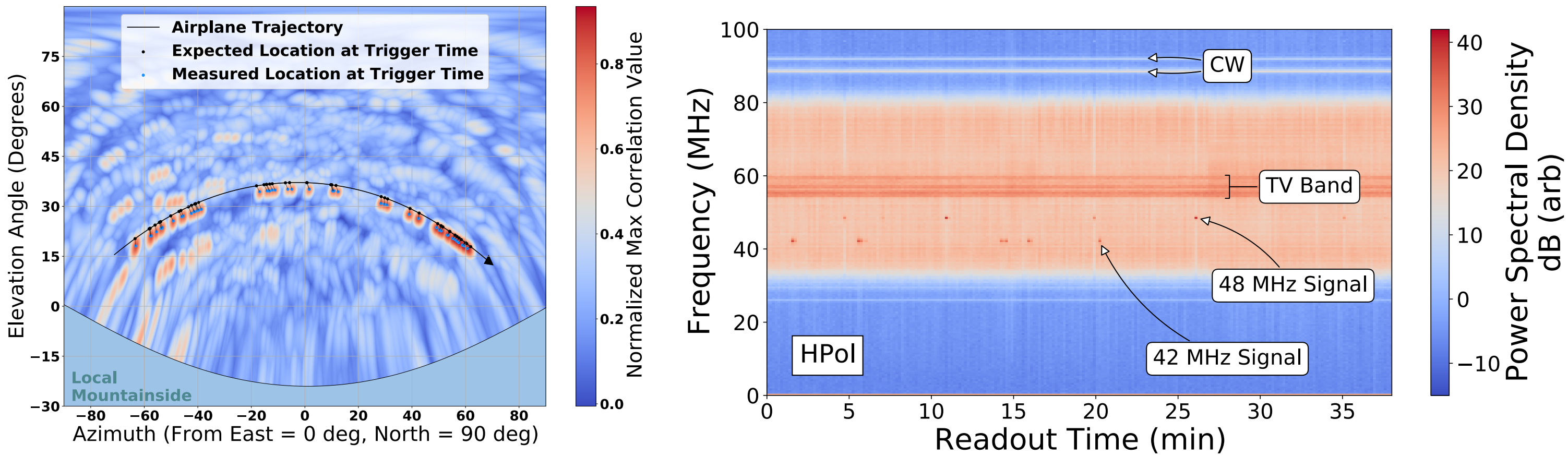
# The BEACON prototype

Southall (UChicago), Deaconu (UChicago), V. D., et al. (accepted in NIMA)

Prototype deployed (8 antennas x4 pol) and taking data at Barcroft Field Station, in the White Mountains in California

**Goal:** to assess the potential of radio beam detectors (similar to radio-astronomy) for EAS on cosmic rays:

- understand background (Las Vegas, planes, snow storm, wind,...)
- trigger and identify EAS (reconstruction and Monte-Carlo comparison)





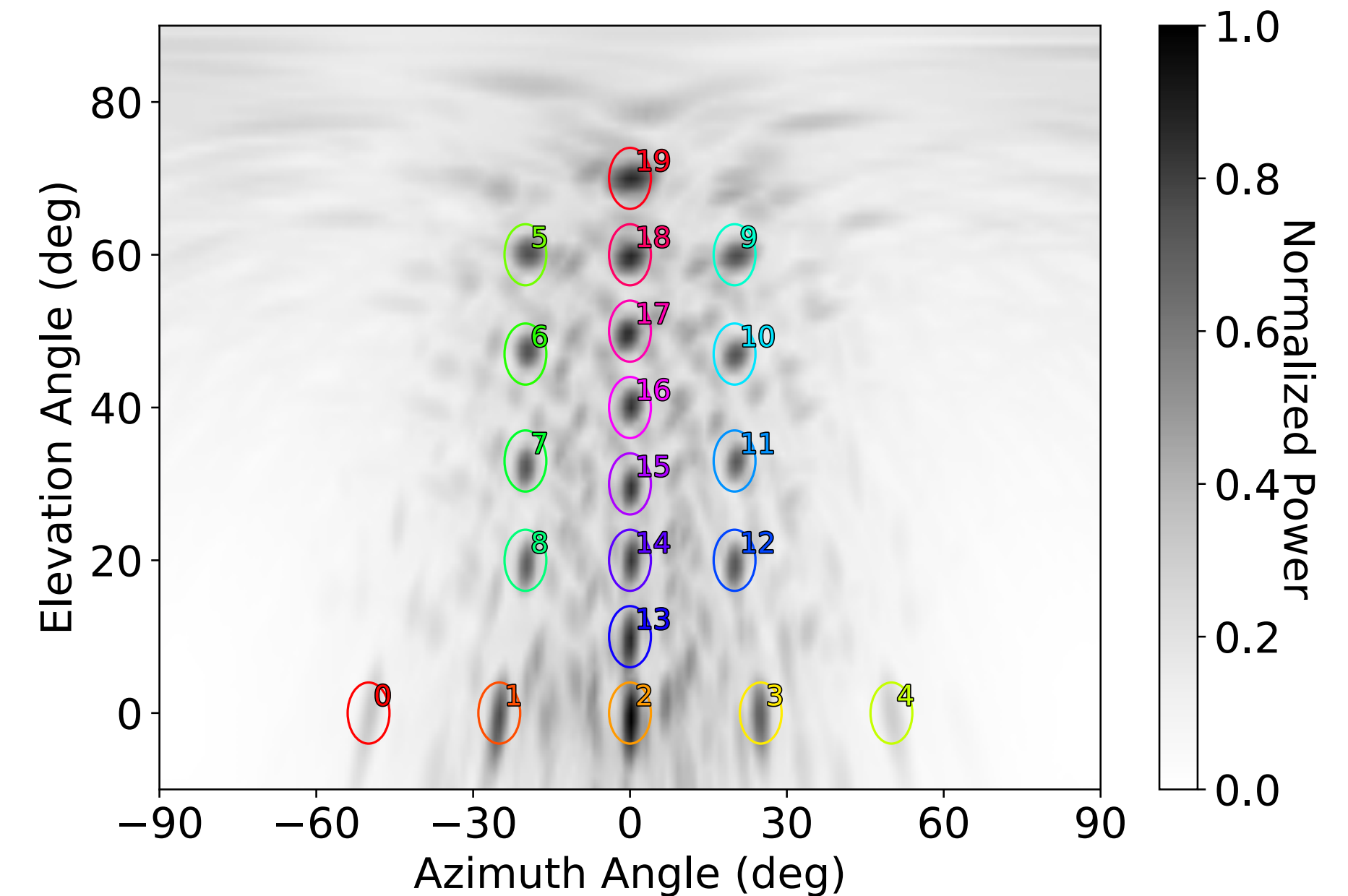
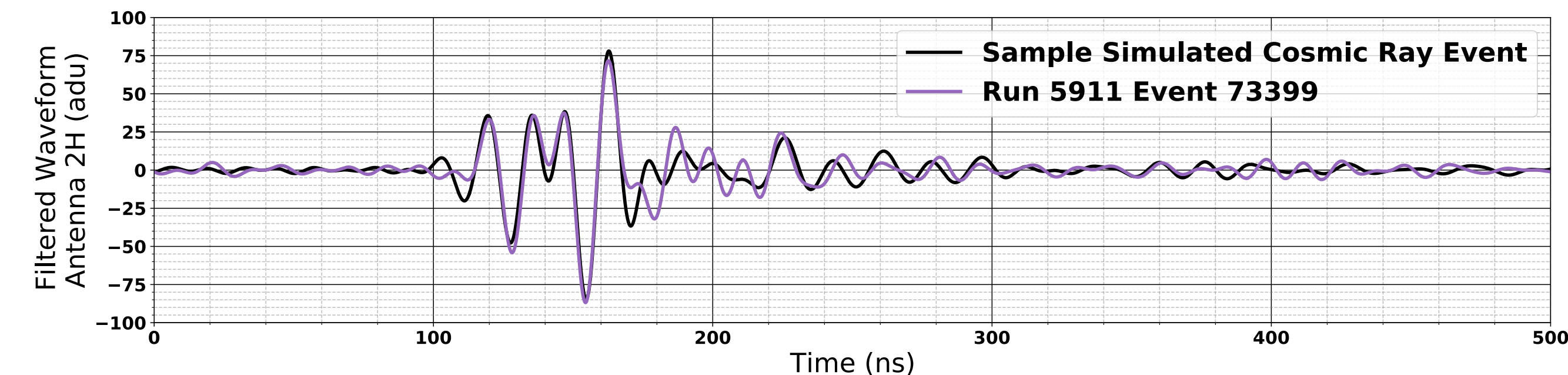
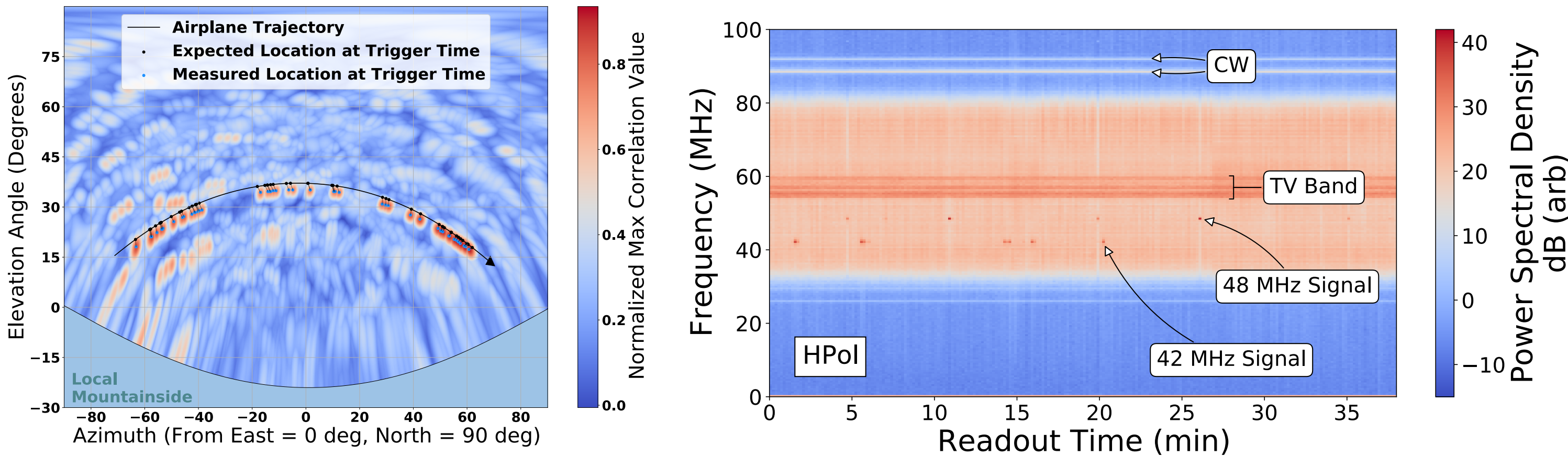
# The BEACON prototype

Southall (UChicago), Deaconu (UChicago), V. D., et al. (accepted in NIMA)

Prototype deployed (8 antennas x4 pol) and taking data at Barcroft Field Station, in the White Mountains in California

**Goal:** to assess the potential of radio beam detectors (similar to radio-astronomy) for EAS on cosmic rays:

- understand background (Las Vegas, planes, snow storm, wind,...)
- trigger and identify EAS (reconstruction and Monte-Carlo comparison)



The cosmic-ray search is an excellent test bench for signal analysis development for future neutrino searches!



# EAS reconstruction

---

V.D., Martineau-Huynh and Tueros (published in Astroparticle Physics)

V.D., Martineau-Huynh, Tueros and Chiche (in prep.)

*Goal : develop a reconstruction procedure for very inclined EAS  
(UHE neutrino induced configuration)*



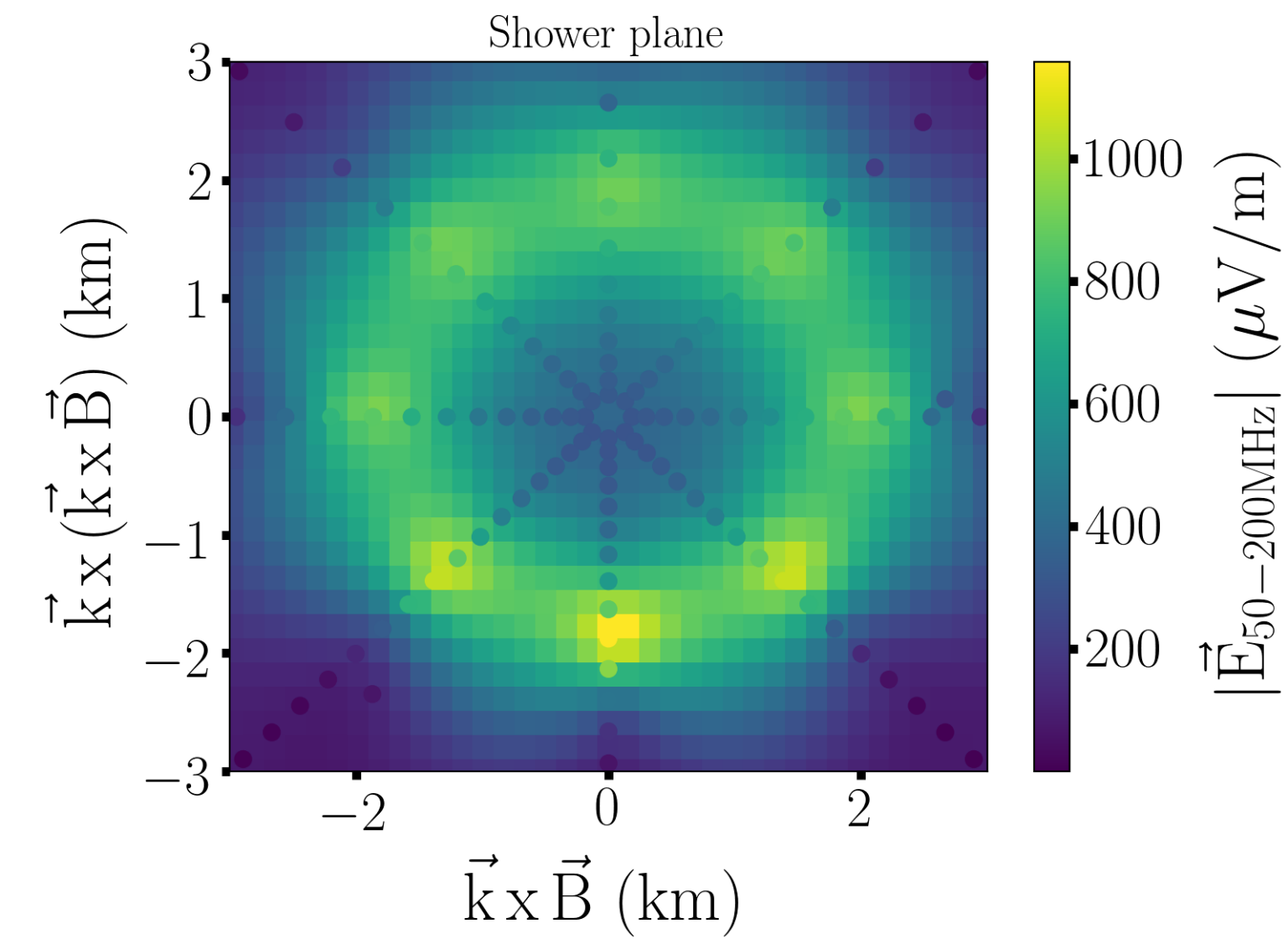
# EAS reconstruction

V.D., Martineau-Huynh and Tueros (published in Astroparticle Physics)

V.D., Martineau-Huynh, Tueros and Chiche (in prep.)

*Goal : develop a reconstruction procedure for very inclined EAS  
(UHE neutrino induced configuration)*

- **hybrid reconstruction** : combine arrival times and signal amplitude within the footprint
- modélisation sphérique du **front d'onde**
- **analytical description** of the footprint amplitude signal :
  - **signal asymmetries** (early-late / charge excess) and **Cherenkov asymmetry** (1<sup>st</sup> evidence !)





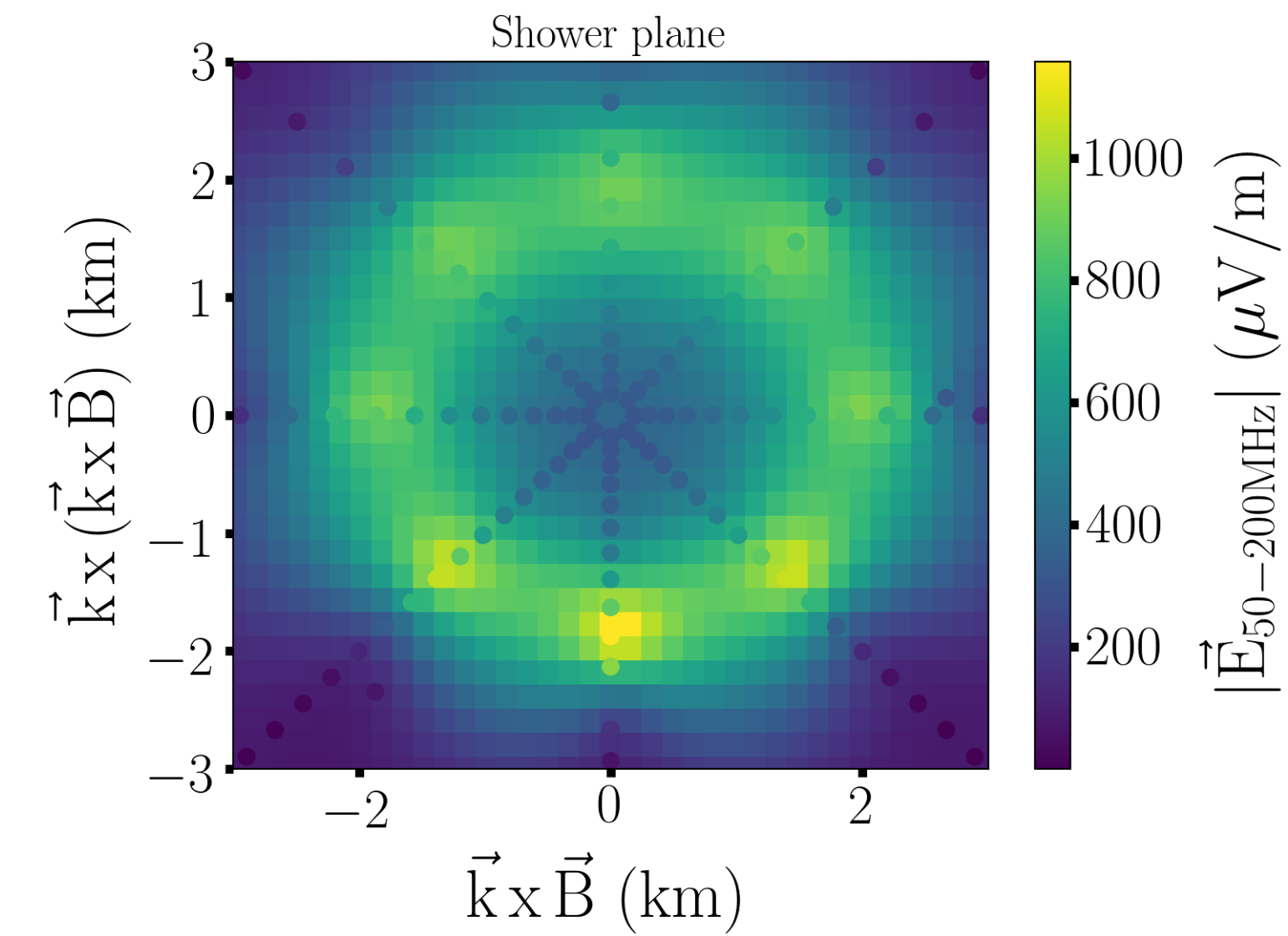
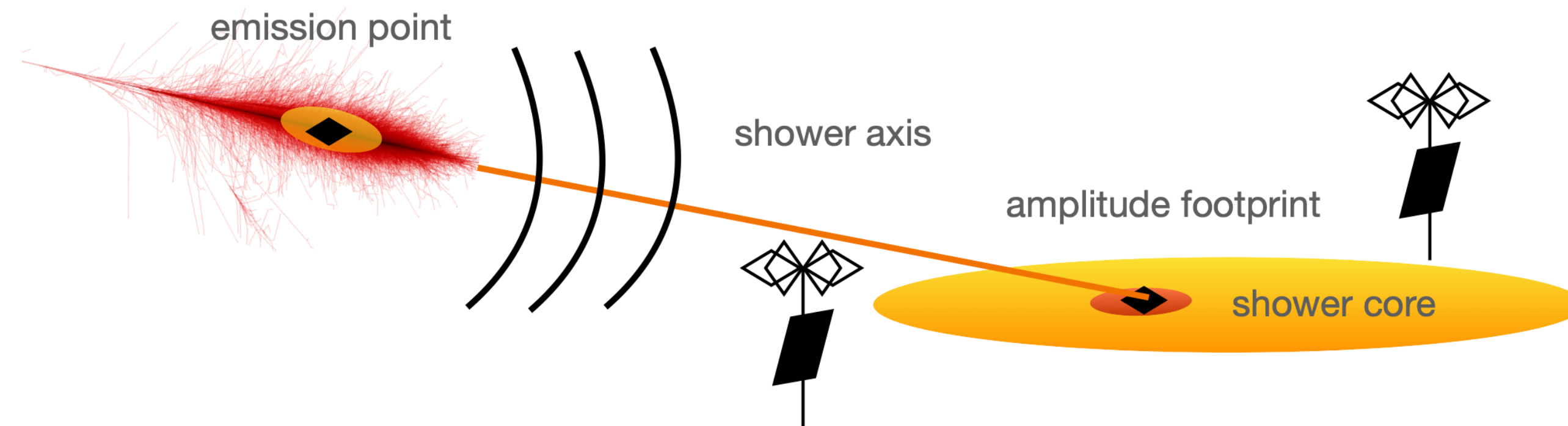
# EAS reconstruction

V.D., Martineau-Huynh and Tueros (published in Astroparticle Physics)

V.D., Martineau-Huynh, Tueros and Chiche (in prep.)

*Goal : develop a reconstruction procedure for very inclined EAS  
(UHE neutrino induced configuration)*

- **hybrid reconstruction** : combine arrival times and signal amplitude within the footprint
- modélisation sphérique du **front d'onde**
- **analytical description** of the footprint amplitude signal :
  - **signal asymmetries** (early-late / charge excess) and **Cherenkov asymmetry** (1<sup>st</sup> evidence !)





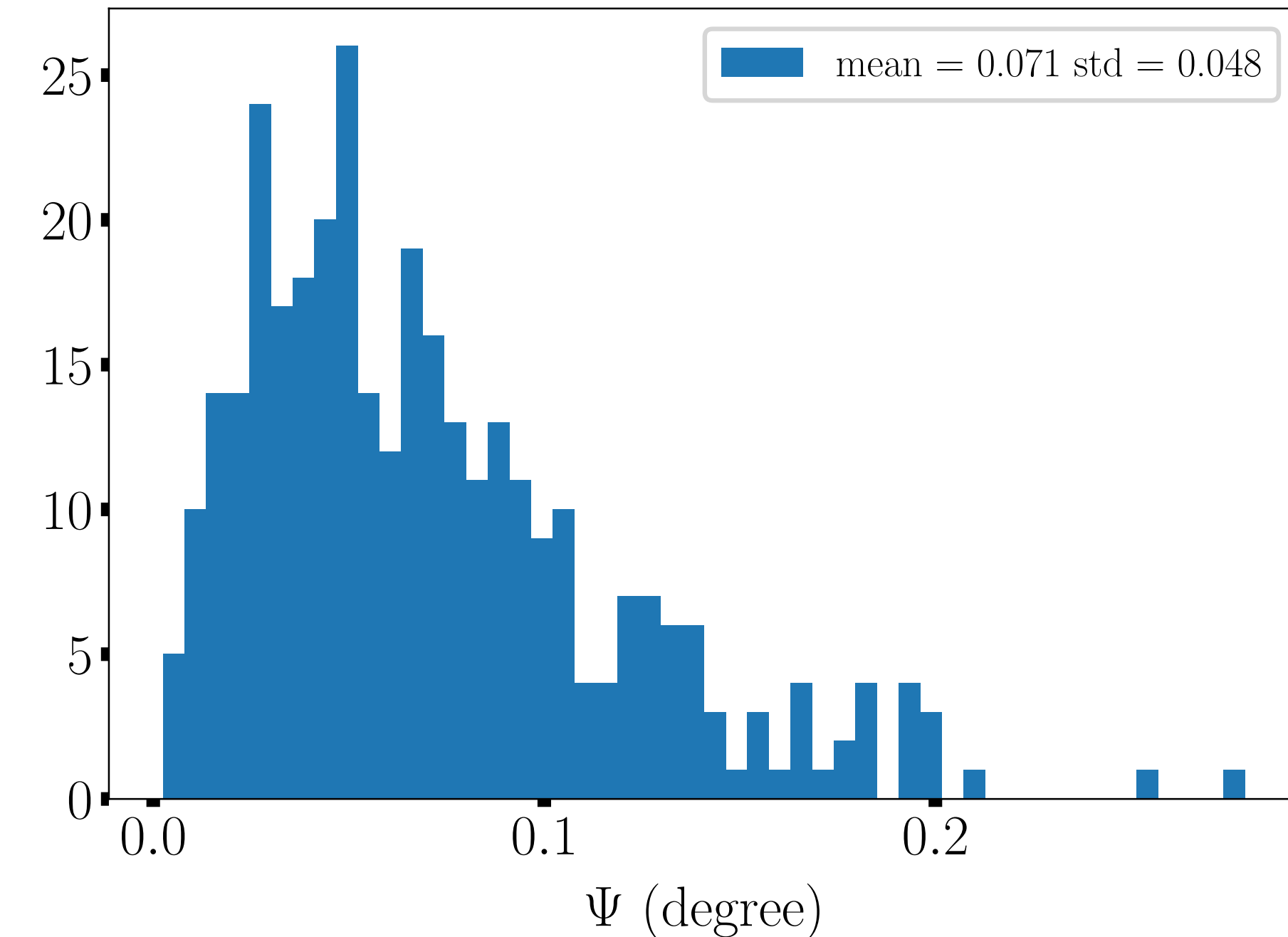
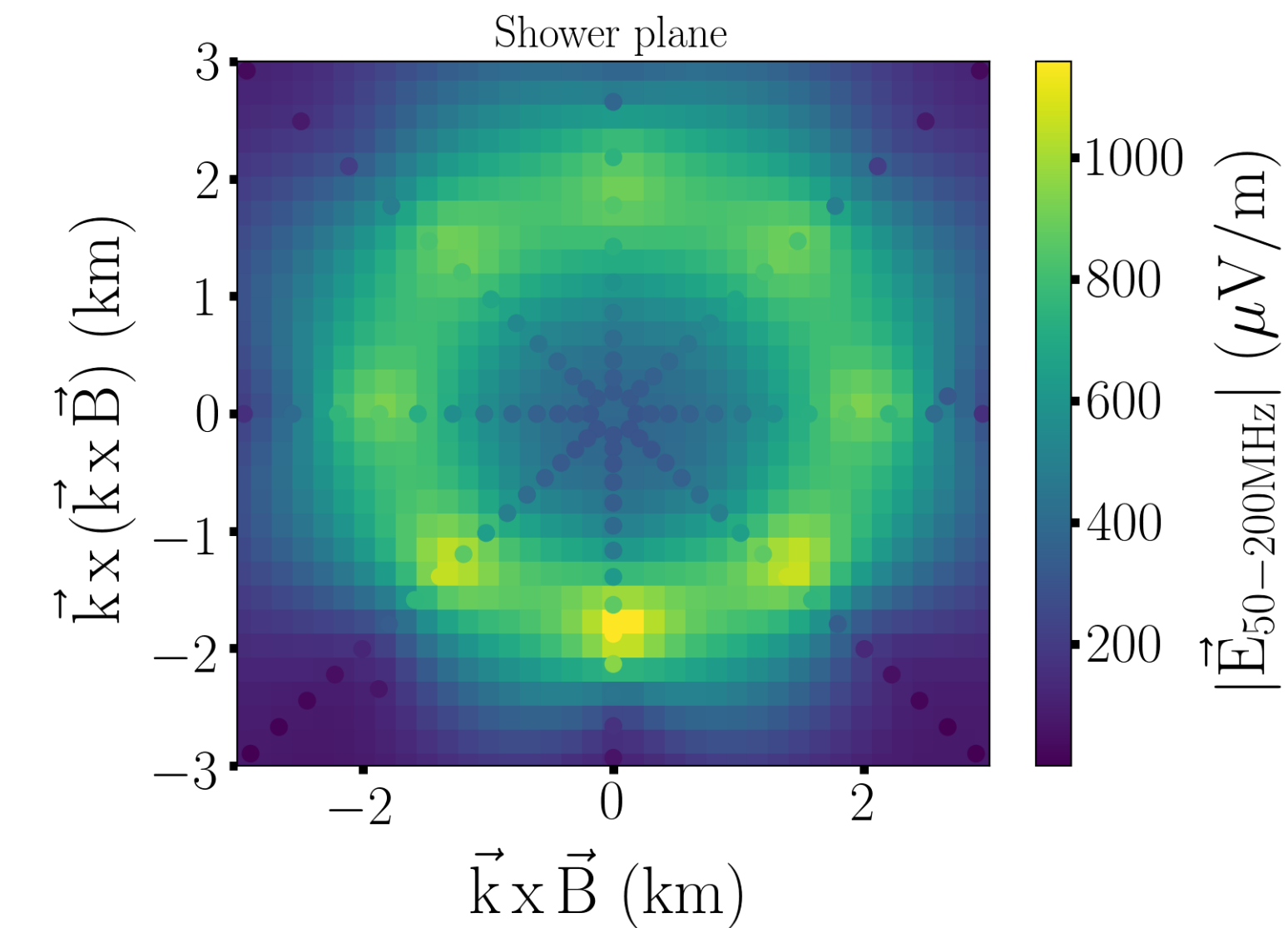
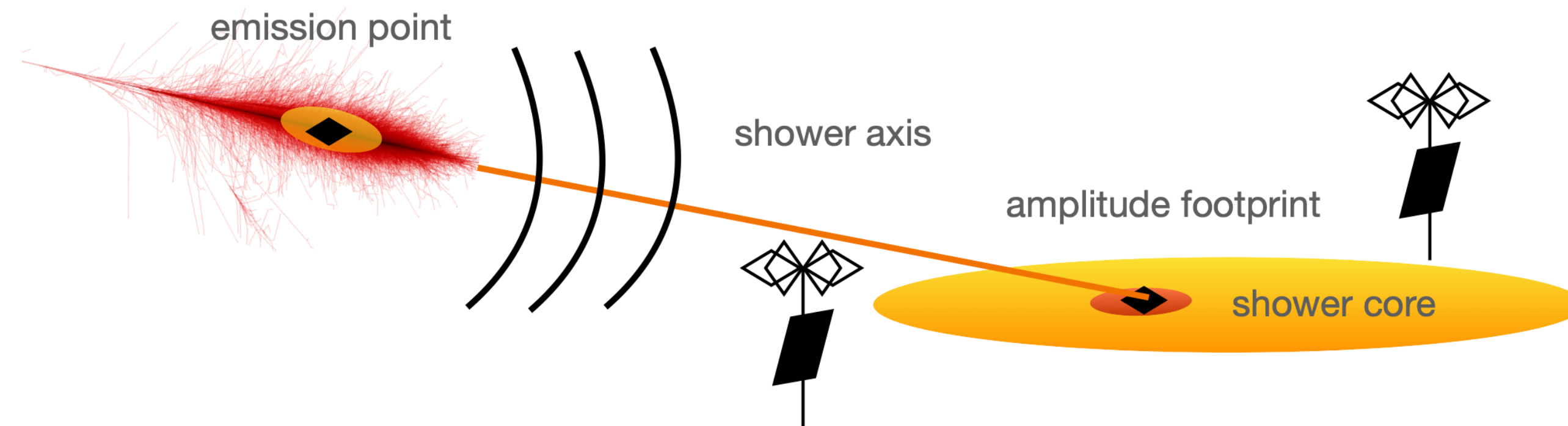
# EAS reconstruction

V.D., Martineau-Huynh and Tueros (published in Astroparticle Physics)

V.D., Martineau-Huynh, Tueros and Chiche (in prep.)

*Goal : develop a reconstruction procedure for very inclined EAS (UHE neutrino induced configuration)*

- **hybrid reconstruction** : combine arrival times and signal amplitude within the footprint
- modélisation sphérique du **front d'onde**
- **analytical description** of the footprint amplitude signal :
  - **signal asymmetries** (early-late / charge excess) and **Cherenkov asymmetry** (1<sup>st</sup> evidence !)





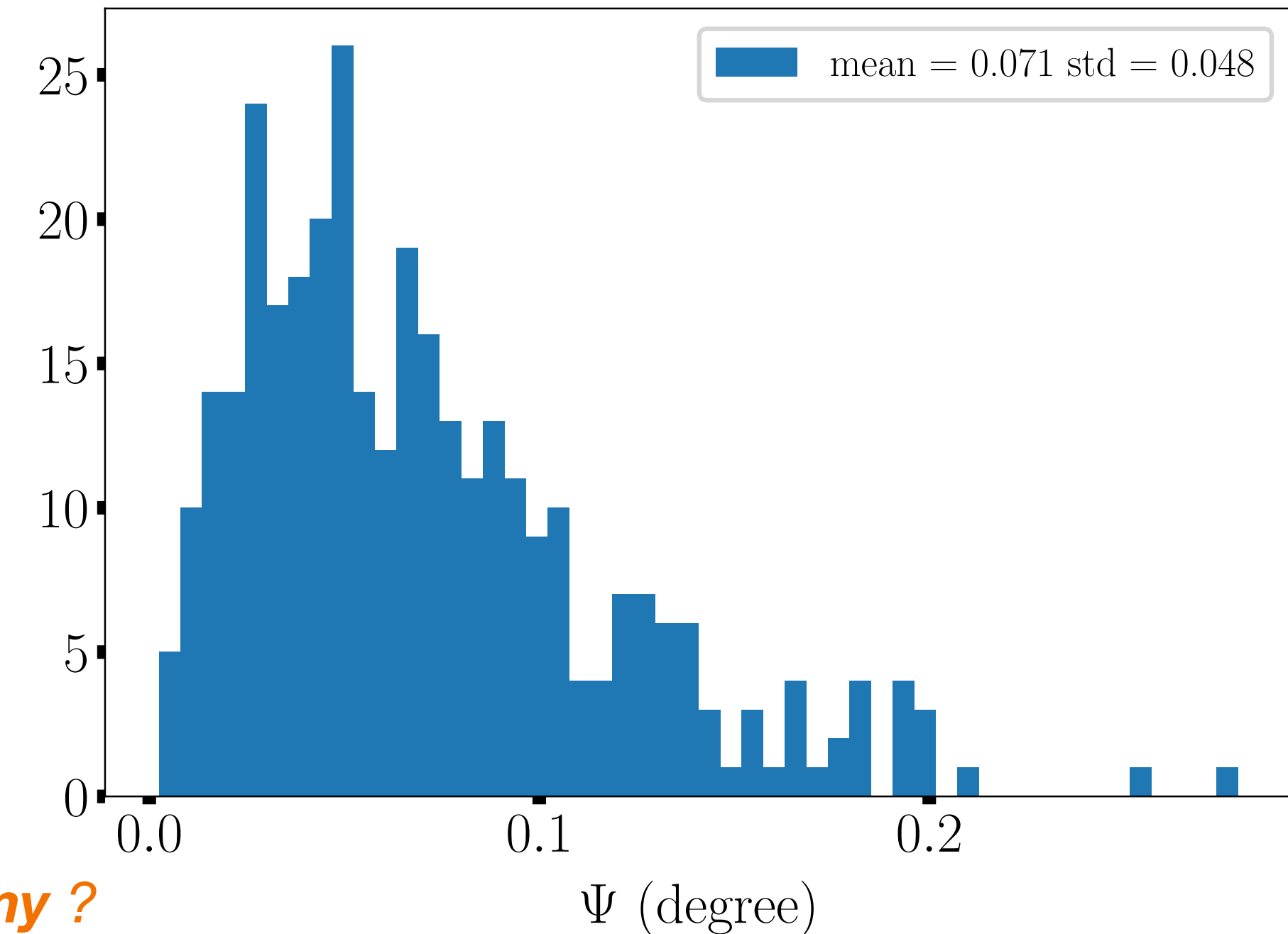
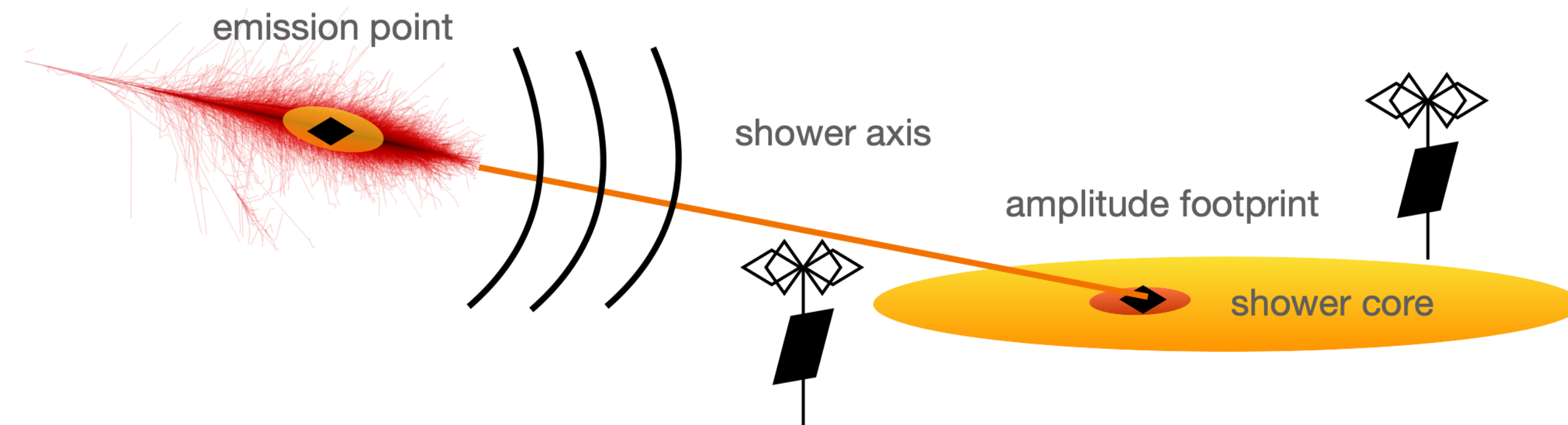
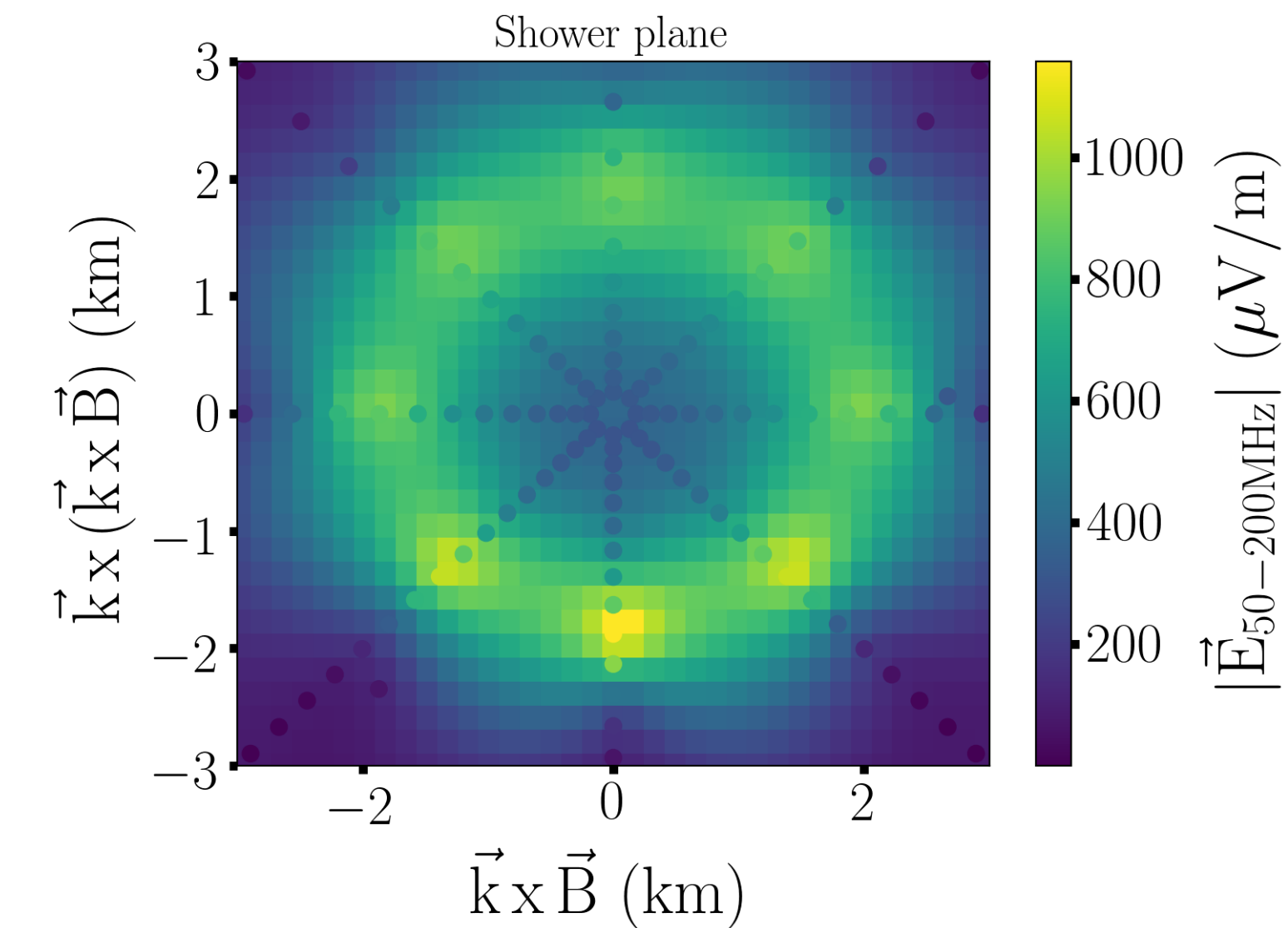
# EAS reconstruction

V.D., Martineau-Huynh and Tueros (published in Astroparticle Physics)

V.D., Martineau-Huynh, Tueros and Chiche (in prep.)

*Goal : develop a reconstruction procedure for very inclined EAS (UHE neutrino induced configuration)*

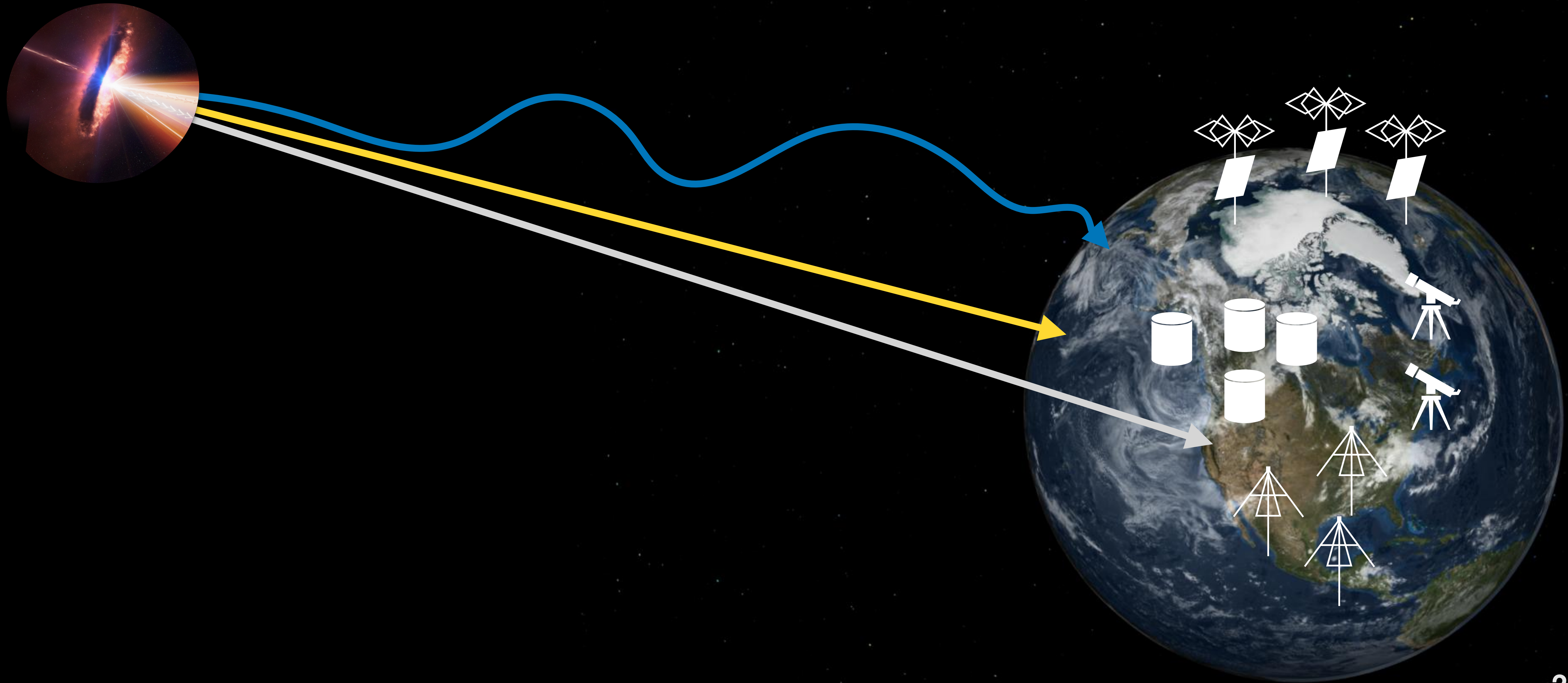
- **hybrid reconstruction** : combine arrival times and signal amplitude within the footprint
- modélisation sphérique du **front d'onde**
- **analytical description** of the footprint amplitude signal :
  - **signal asymmetries** (early-late / charge excess) and **Cherenkov asymmetry** (1<sup>st</sup> evidence !)



*Results : angular resolution of **0.1°** on average → possibility of **UHE neutrino astronomy** ?*

*+ composition and energy estimators*

# Summary of our journey with HE and UHE neutrinos

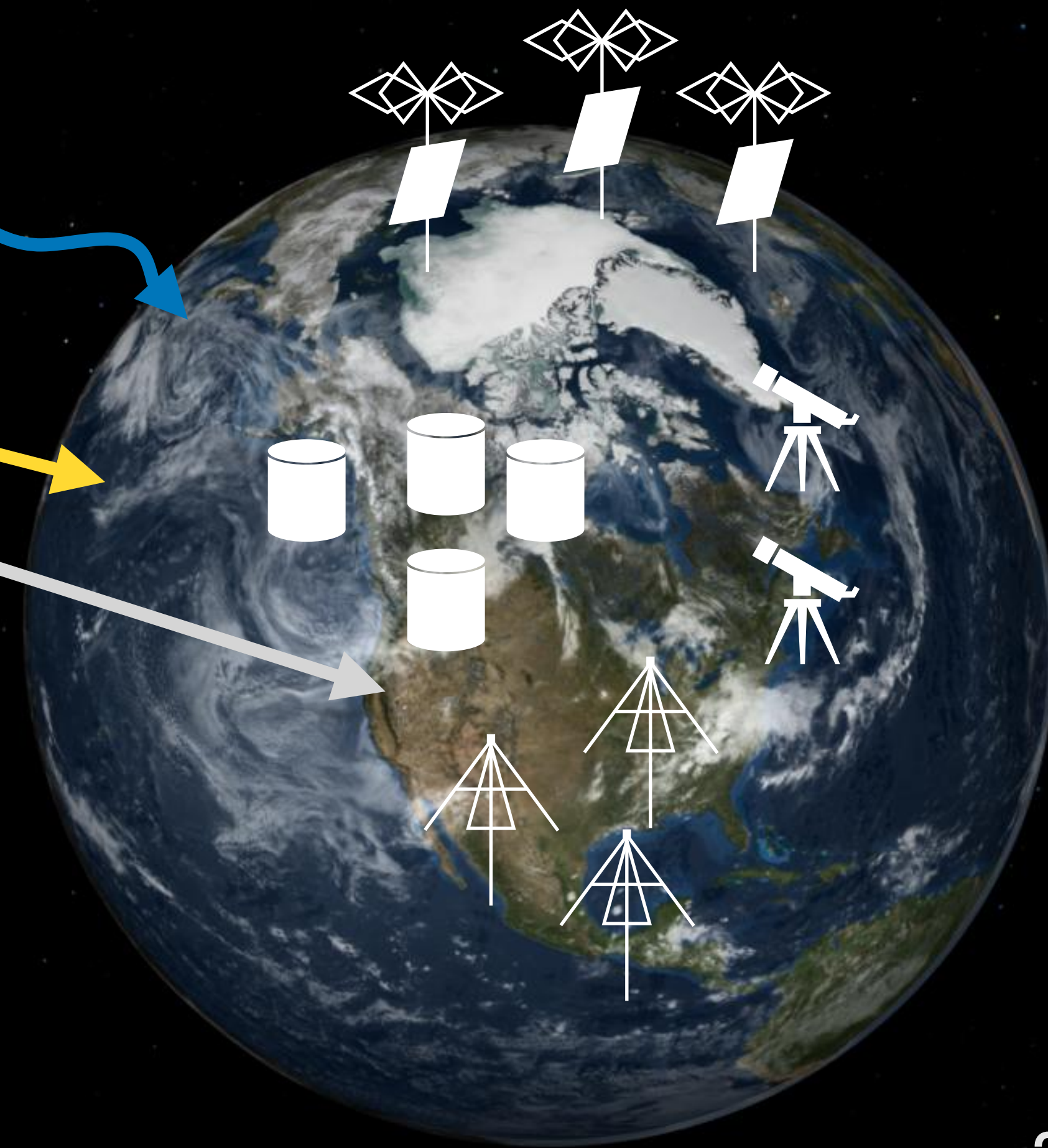




# Summary of our journey with HE and UHE neutrinos



- 3 candidates for point source emissions (all related to AGNs)
- No obvious source population for the diffuse emission
- Neutron star mergers can contribute (10%) to this diffuse neutrino flux
- We can combine multimessenger and experimental expectations to constrain UHE astroparticle sources

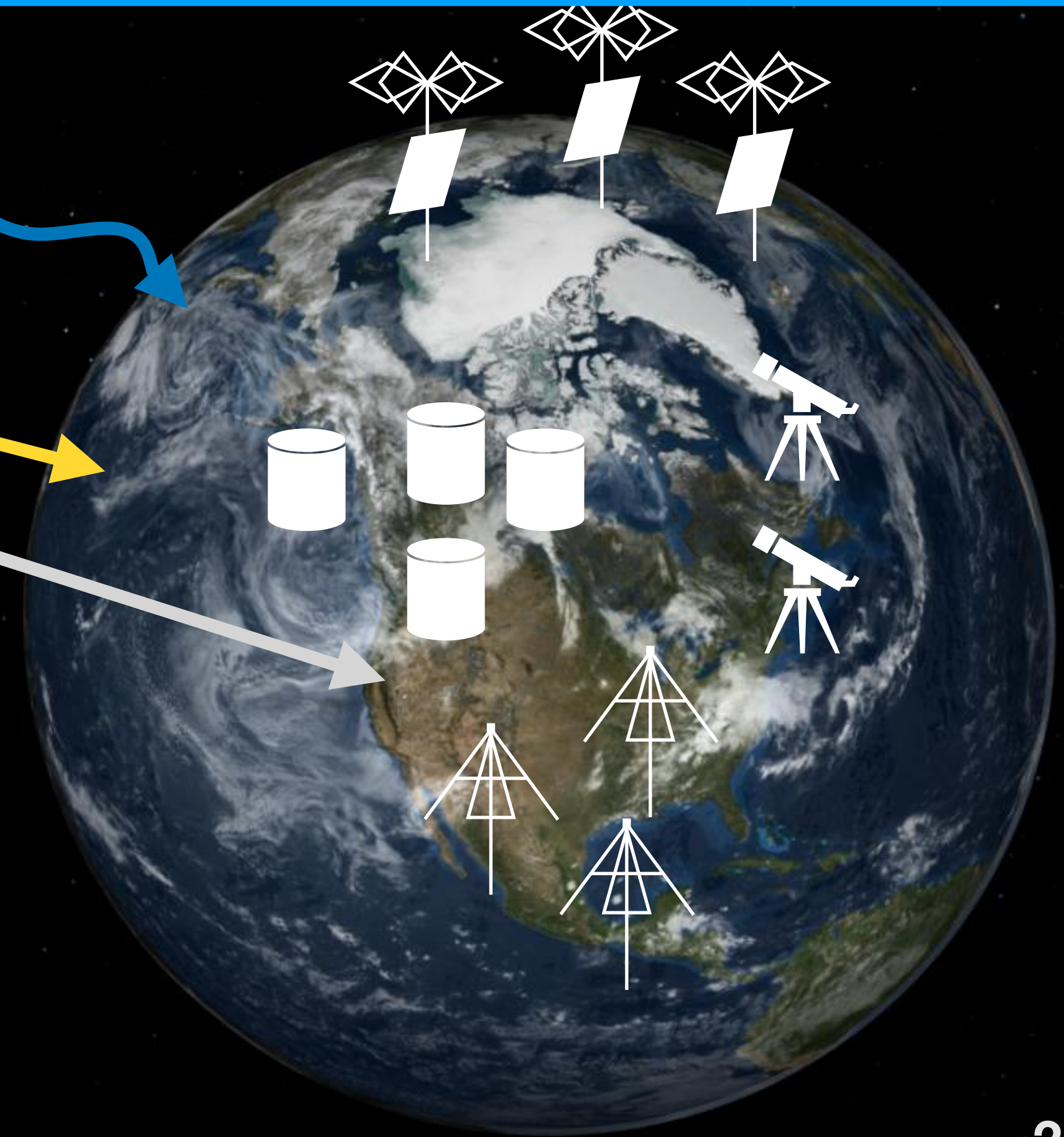
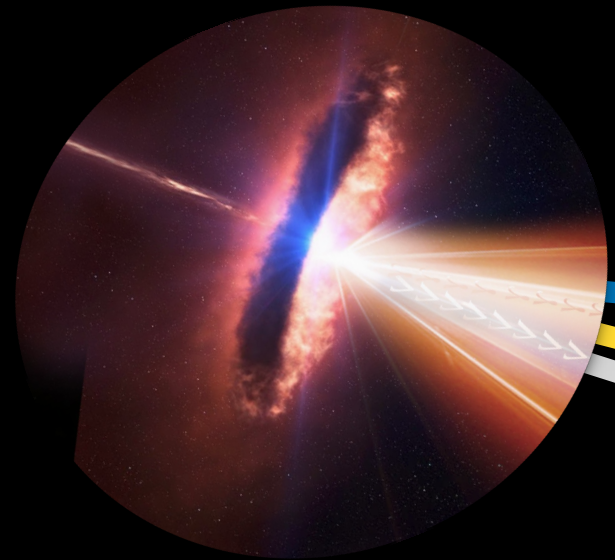




# Summary of our journey with HE and UHE neutrinos

- Identification of HE neutrino sources is challenging
- KM3NeT could make a difference (FoV, sensitivity, angular resolution)
- UHE neutrinos are theoretically predicted but with very low fluxes
- Radio-detection might be a solution (multiple designs envisioned)
- However radio-detection is also challenging (instruments/analysis/reconstruction)

- 3 candidates for point source emissions (all related to AGNs)
- No obvious source population for the diffuse emission
- Neutron star mergers can contribute (10%) to this diffuse neutrino flux
- We can combine multimessenger and experimental expectations to constrain UHE astroparticle sources





# Summary of our journey with HE and UHE neutrinos

- Identification of HE neutrino sources is challenging
- KM3NeT could make a difference (FoV, sensitivity, angular resolution)
- UHE neutrinos are theoretically predicted but with very low fluxes
- Radio-detection might be a solution (multiple designs envisioned)
- However radio-detection is also challenging (instruments/analysis/reconstruction)

- 3 candidates for point source emissions (all related to AGNs)
- No obvious source population for the diffuse emission
- Neutron star mergers can contribute (10%) to this diffuse neutrino flux
- We can combine multimessenger and experimental expectations to constrain UHE astroparticle sources

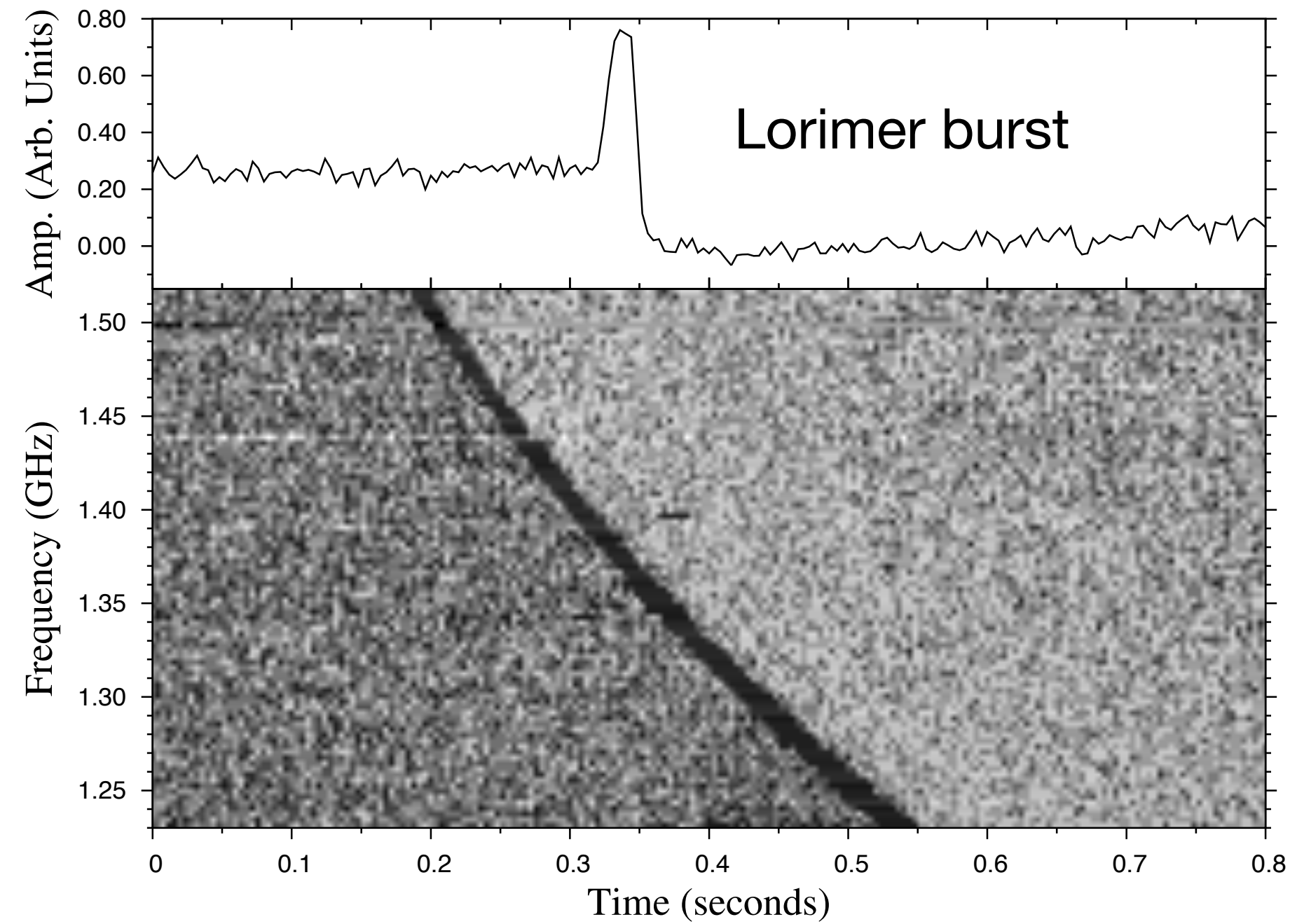
radio waves

radio transient events can also be detected with radio detector



# The Fast Radio Burst mystery

a new type of astrophysical radio transient!



Lorimer burst

FRB010724 - Keane from Lorimer 2018

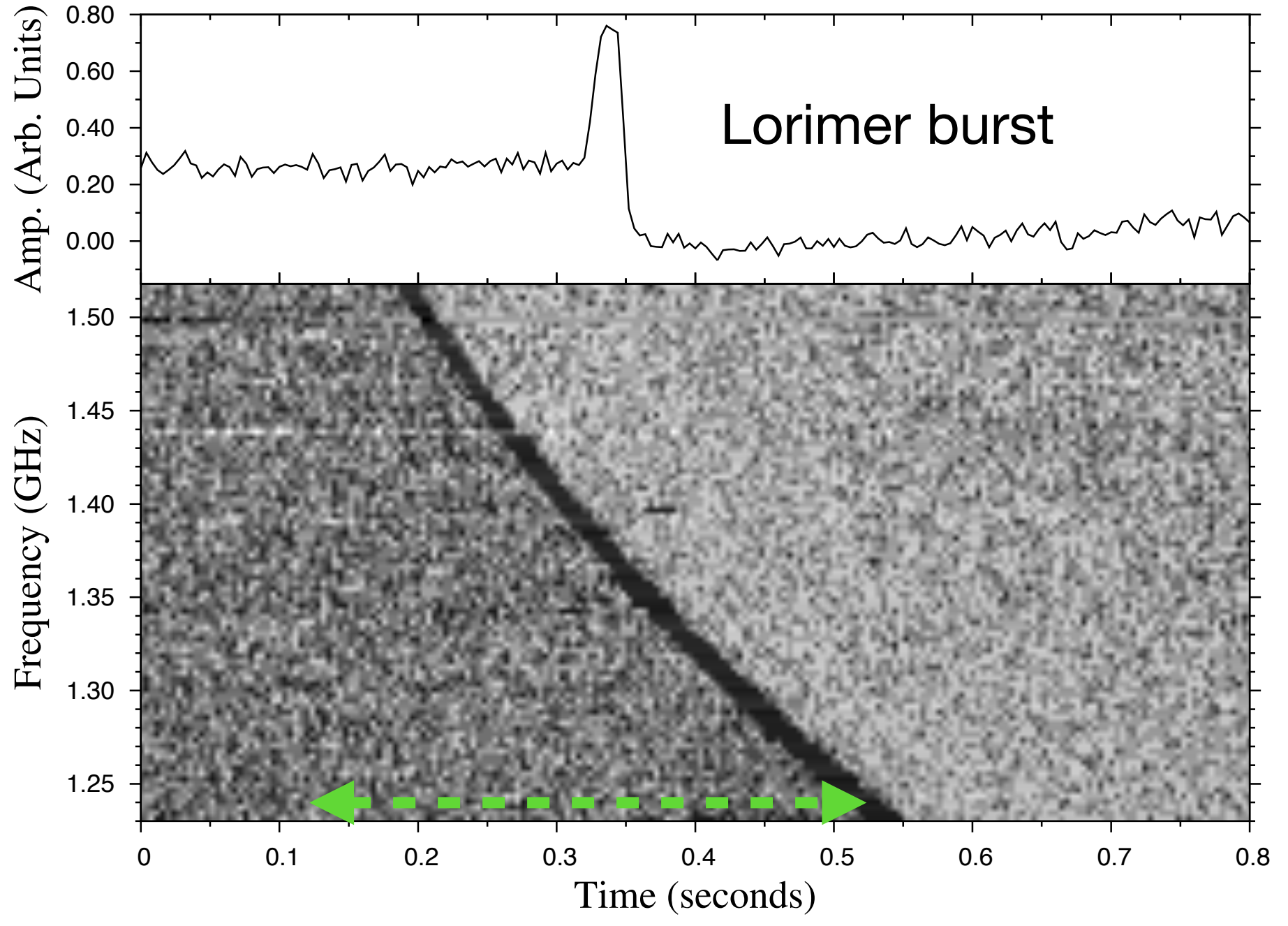
## Observed emission:

- Short radio pulses ( $\approx$ ms)
- Highly coherent
- Broad frequency band emissions
- Highly dispersed in arrival times



# The Fast Radio Burst mystery

a new type of astrophysical radio transient!



FRB010724 - Keane from Lorimer 2018

### Observed emission:

- Short radio pulses ( $\approx$ ms)
- Highly coherent
- Broad frequency band emissions
- Highly dispersed in arrival times

### Dispersion effects (propagation)

$$\Delta t \sim 4.15 \times 10^3 [\text{DM}] \nu^{-2}$$

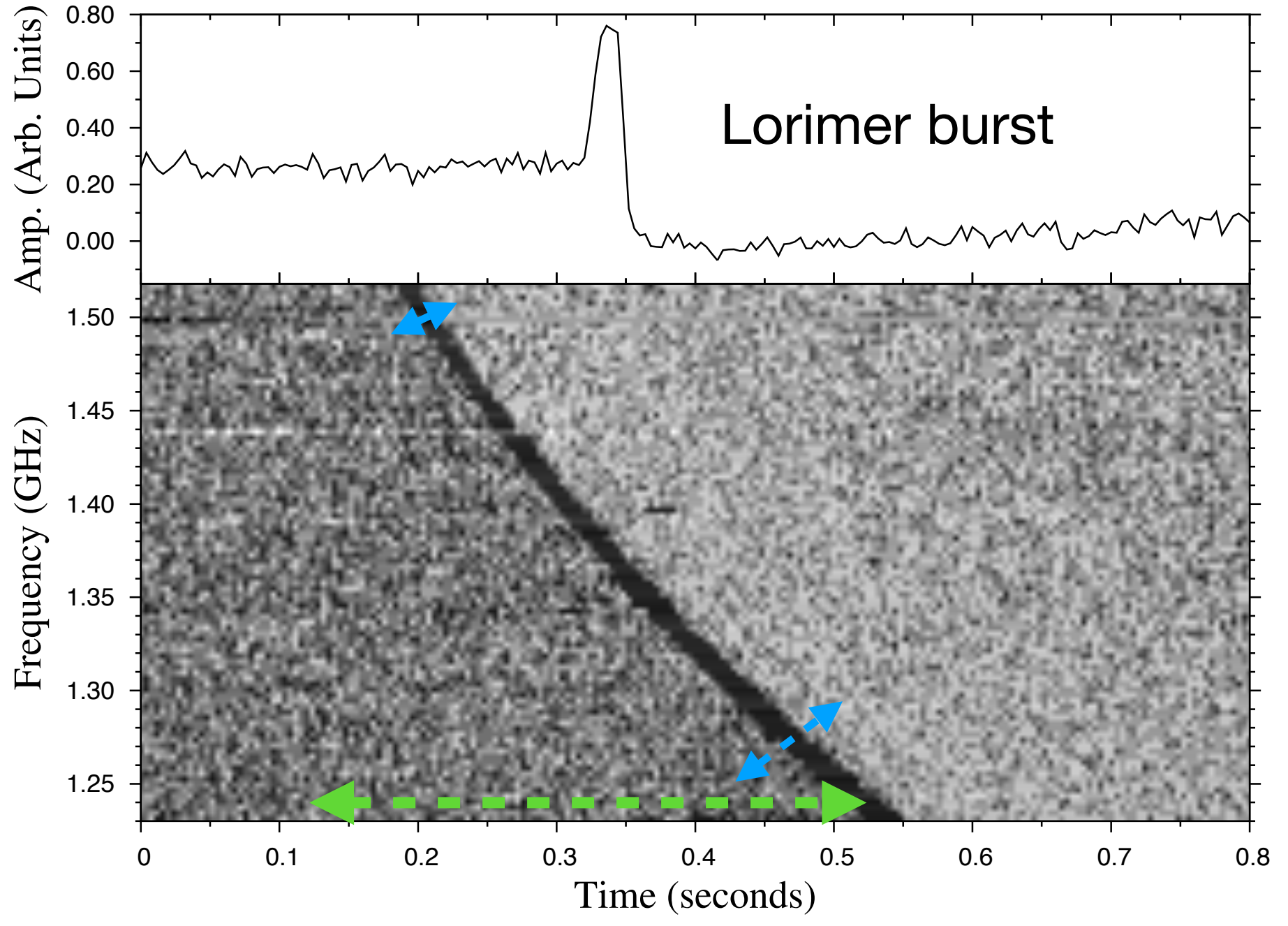
$$\Delta t(80 - 10\text{MHz}) \sim 40 \times [\text{DM}] \text{ s} \quad (\text{DM} > 100 \text{ for extra-galactic sources})$$

$$\rightarrow \text{DM} = \int_0^d n_e dl \quad \text{linked to distances}$$



# The Fast Radio Burst mystery

a new type of astrophysical radio transient!



FRB010724 - Keane from Lorimer 2018

## Observed emission:

- Short radio pulses ( $\approx$ ms)
- Highly coherent
- Broad frequency band emissions
- Highly dispersed in arrival times

### Dispersion effects (propagation)

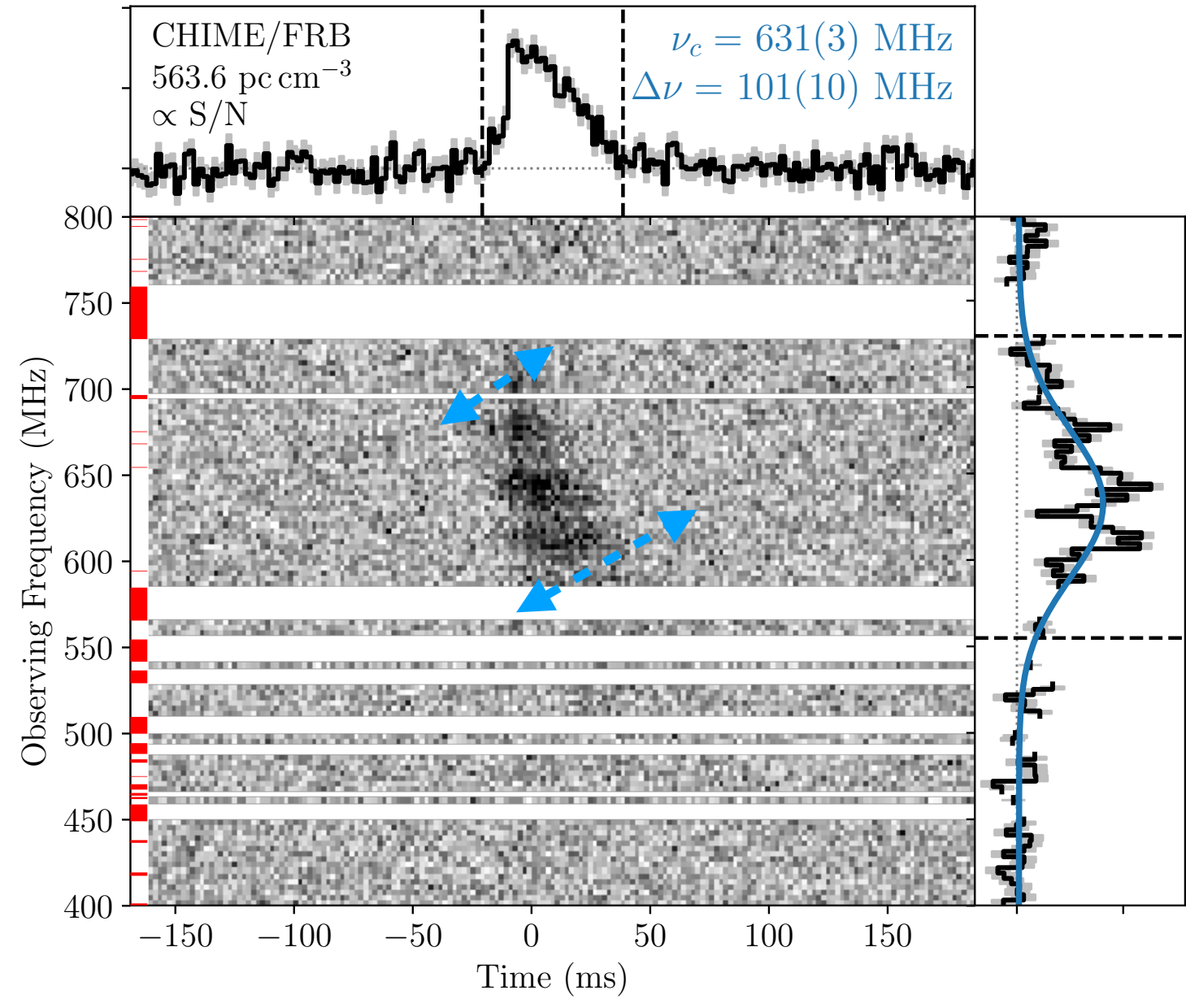
$$\Delta t \sim 4.15 \times 10^3 [\text{DM}] \nu^{-2}$$

$$\Delta t(80 - 10\text{MHz}) \sim 40 \times [\text{DM}] \text{ s} \quad (\text{DM} > 100 \text{ for extra-galactic sources})$$

$$\rightarrow \text{DM} = \int_0^d n_e dl \quad \text{linked to distances}$$

### Scattering effects (turbulences)

$$\delta t \propto \nu^{-4}$$

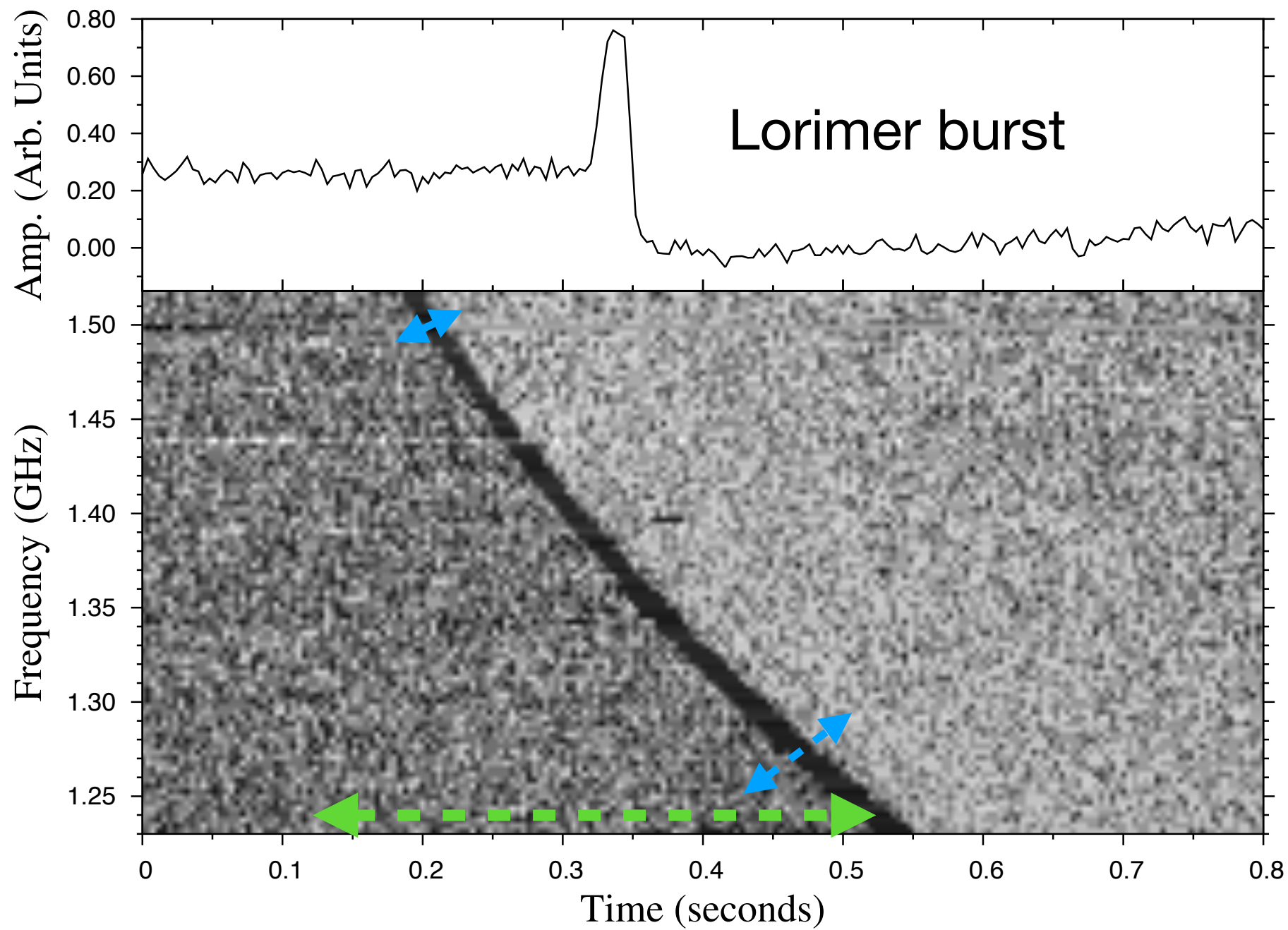


FRB121102: Arecibo repeater Josephy et al, 2019



# The Fast Radio Burst mystery

a new type of astrophysical radio transient!



FRB010724 - Keane from Lorimer 2018

## Observed emission:

- Short radio pulses ( $\approx$ ms)
- Highly coherent
- Broad frequency band emissions
- Highly dispersed in arrival times

## • Dispersion effects (propagation)

$$\Delta t \sim 4.15 \times 10^3 [\text{DM}] \nu^{-2}$$

$$\Delta t(80 - 10\text{MHz}) \sim 40 \times [\text{DM}] \text{ s} \quad (\text{DM} > 100 \text{ for extra-galactic sources})$$

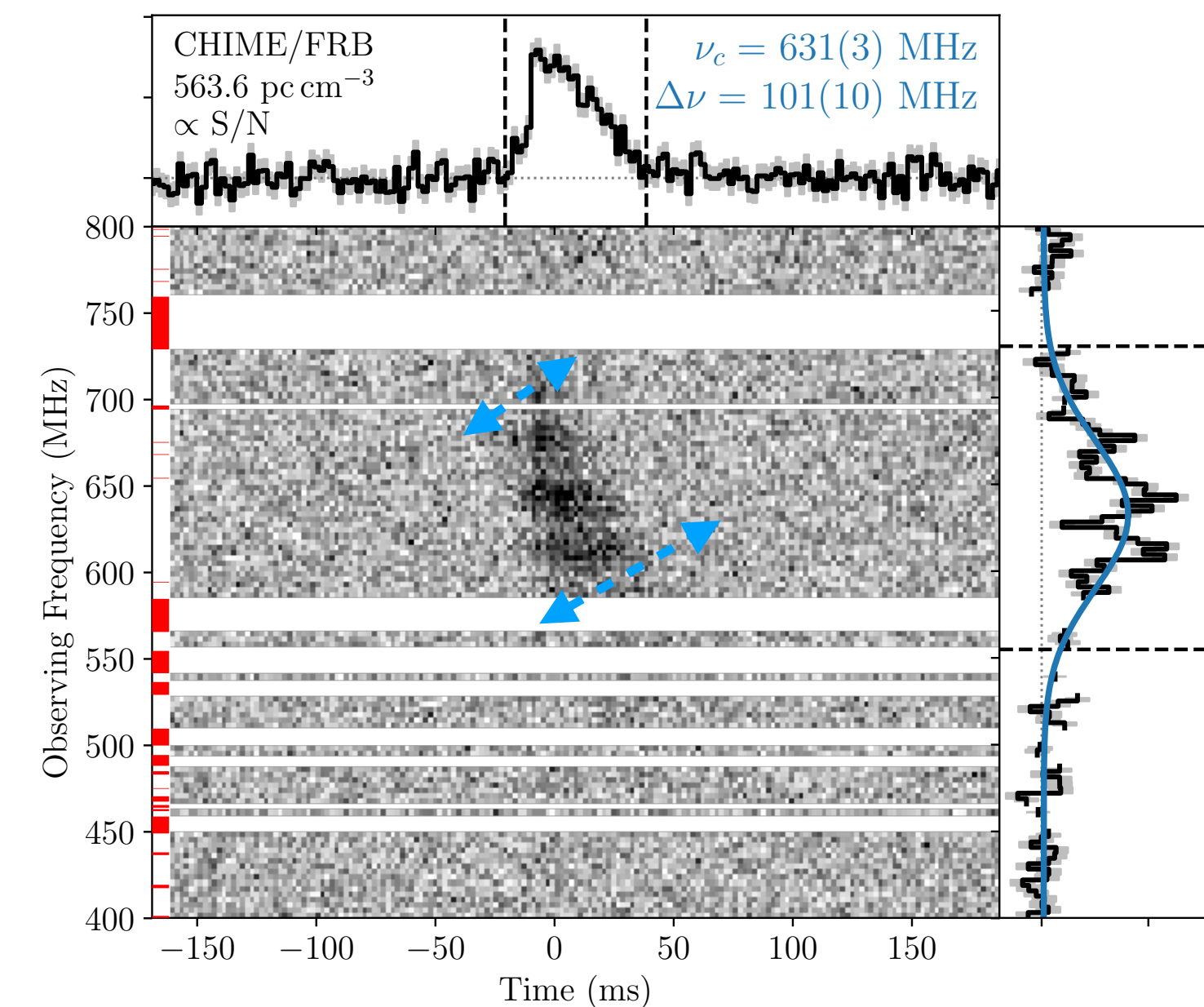
$$\rightarrow \text{DM} = \int_0^d n_e dl \quad \text{linked to distances}$$

## • Scattering effects (turbulences)

$$\delta t \propto \nu^{-4}$$

## Observed event characteristics:

- Cosmological distances: extragalactic origin (most likely)
- About 636 events observed
- 25 Repeaters (121102-Arecibo repeater, 180814 -CHIME, etc..)
- FRB fluencies up to 420 Jy.ms and steep spectra (ASKAP)
- Observations from 8 GHz down to 111MHz

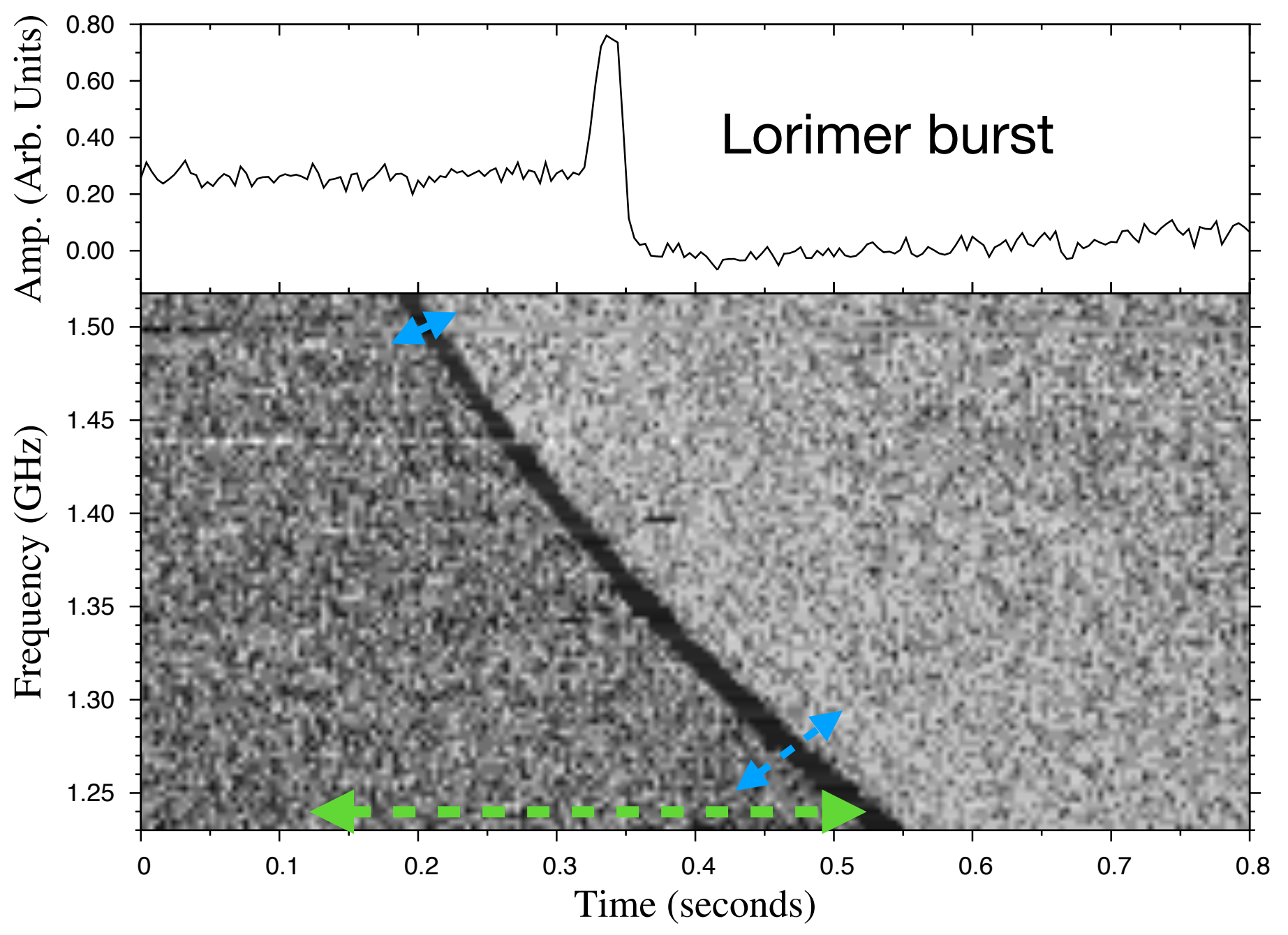


FRB121102: Arecibo repeater Josephy et al, 2019



# The Fast Radio Burst mystery

a new type of astrophysical radio transient!



FRB010724 - Keane from Lorimer 2018

## Observed emission:

- Short radio pulses ( $\approx$ ms)
- Highly coherent
- Broad frequency band emissions
- Highly dispersed in arrival times

emission mechanism?

## Dispersion effects (propagation)

$$\Delta t \sim 4.15 \times 10^3 [\text{DM}] \nu^{-2}$$

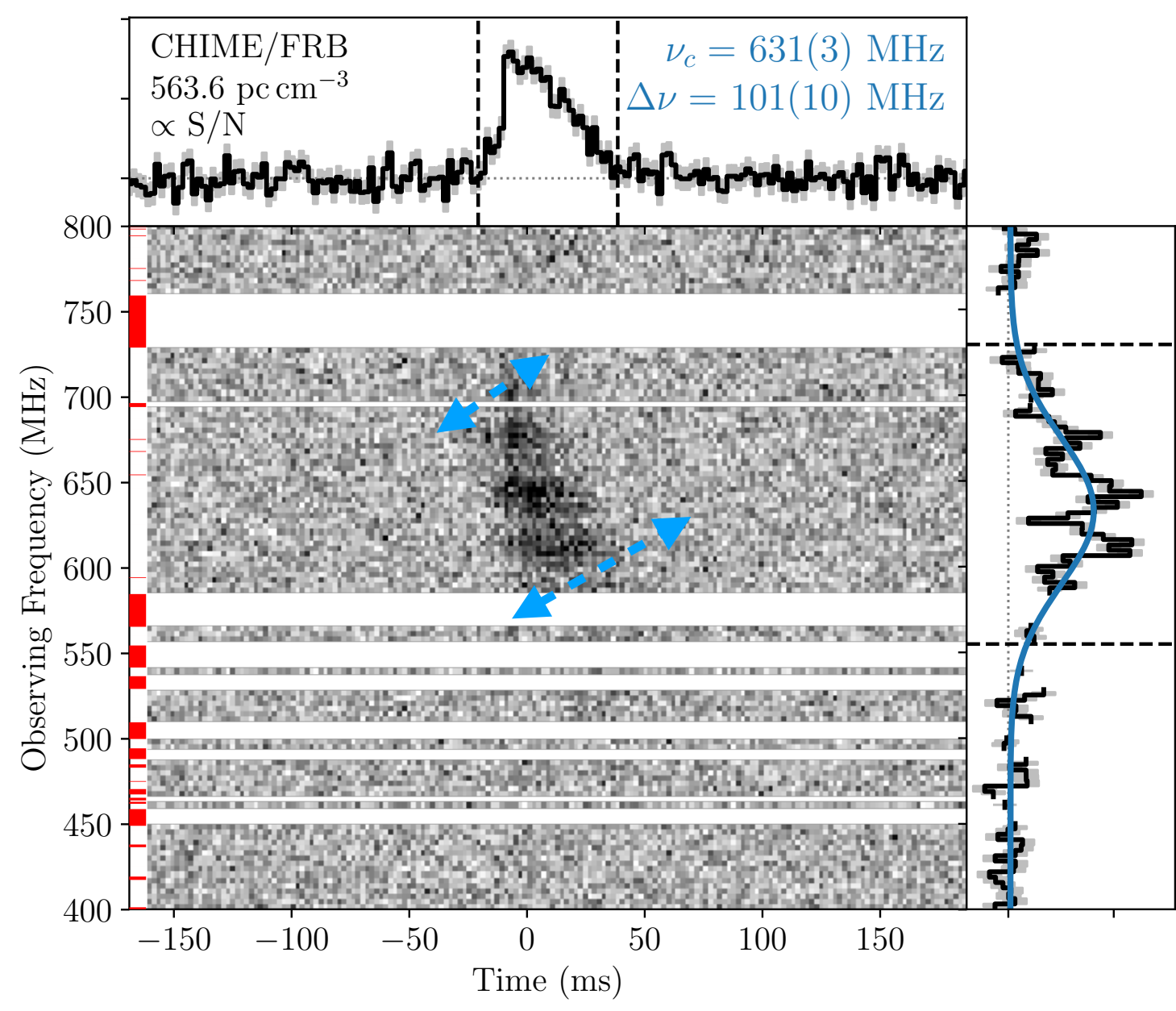
$$\Delta t(80 - 10\text{MHz}) \sim 40 \times [\text{DM}] \text{ s} \quad (\text{DM} > 100 \text{ for extra-galactic sources})$$

$$\rightarrow \text{DM} = \int_0^d n_e dl \quad \text{linked to distances}$$

## Scattering effects (turbulences)

$$\delta t \propto \nu^{-4}$$

source / population?



FRB121102: Arecibo repeater Josephy et al, 2019

## Observed event characteristics:

- Cosmological distances: extragalactic origin (most likely)
- About 636 events observed
- 25 Repeaters (121102-Arecibo repeater, 180814 -CHIME, etc..)
- FRB fluencies up to 420 Jy.ms and steep spectra (ASKAP)
- Observations from 8 GHz down to 111MHz

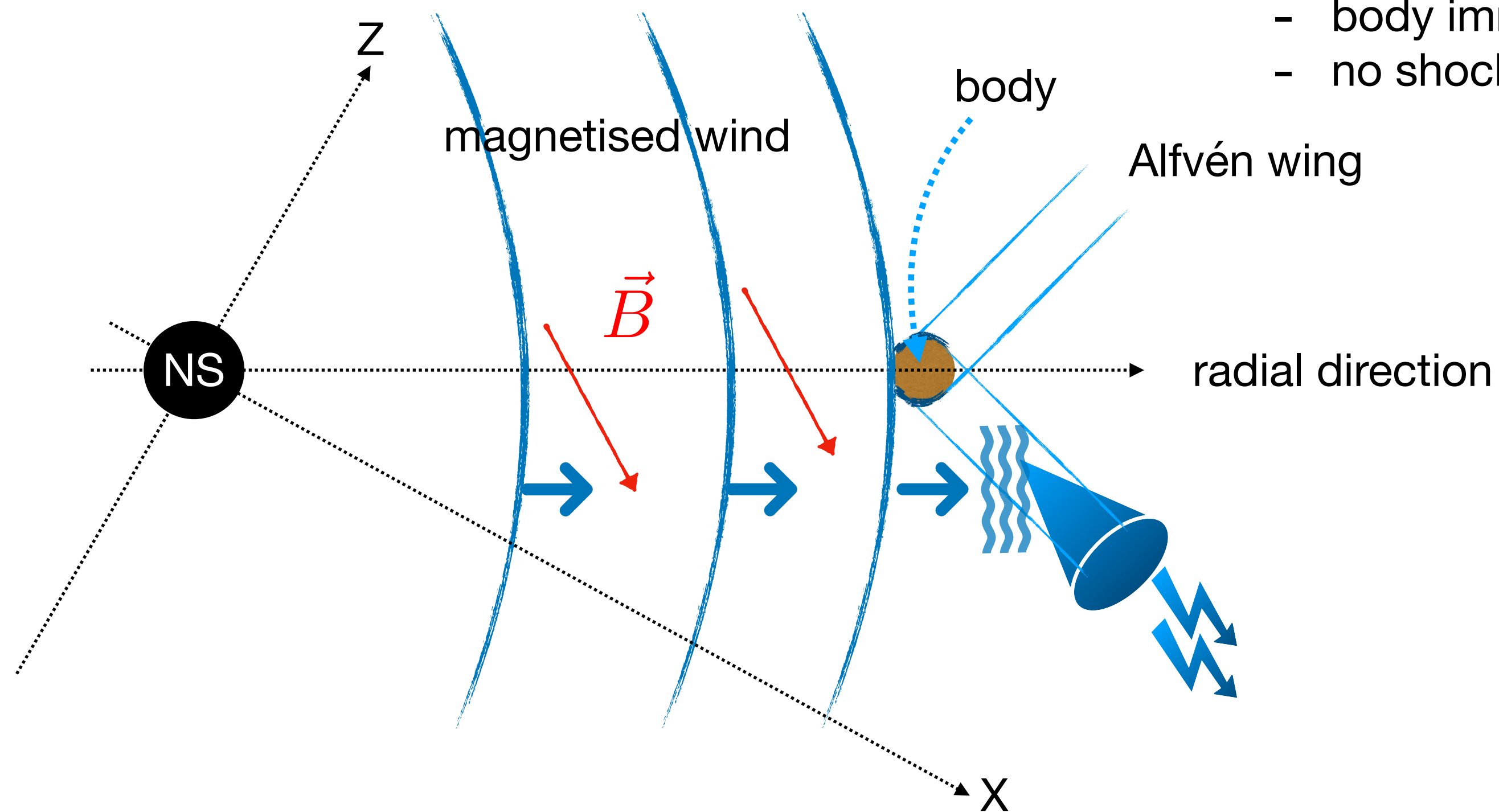


# A plausible emission model

among many other models: <https://frbtheorycat.org>

## The Alfvén wing emission mechanisms:

Mottez&Zarka 2014 / Mottez, Zarka, Voisin 2020



### 1) Magnetic coupling: Mottez&Heyvaerts 2012

- body immersed in magnetised plasma
- no shock required

### 2) Alfvén wings:

- potential drop induced by the conductive body
- two symmetrical current sheets

### 3) Radio emission:

- plasma excitations when crossing the Alfvén wings
- relativistic plasma -> beamed emission

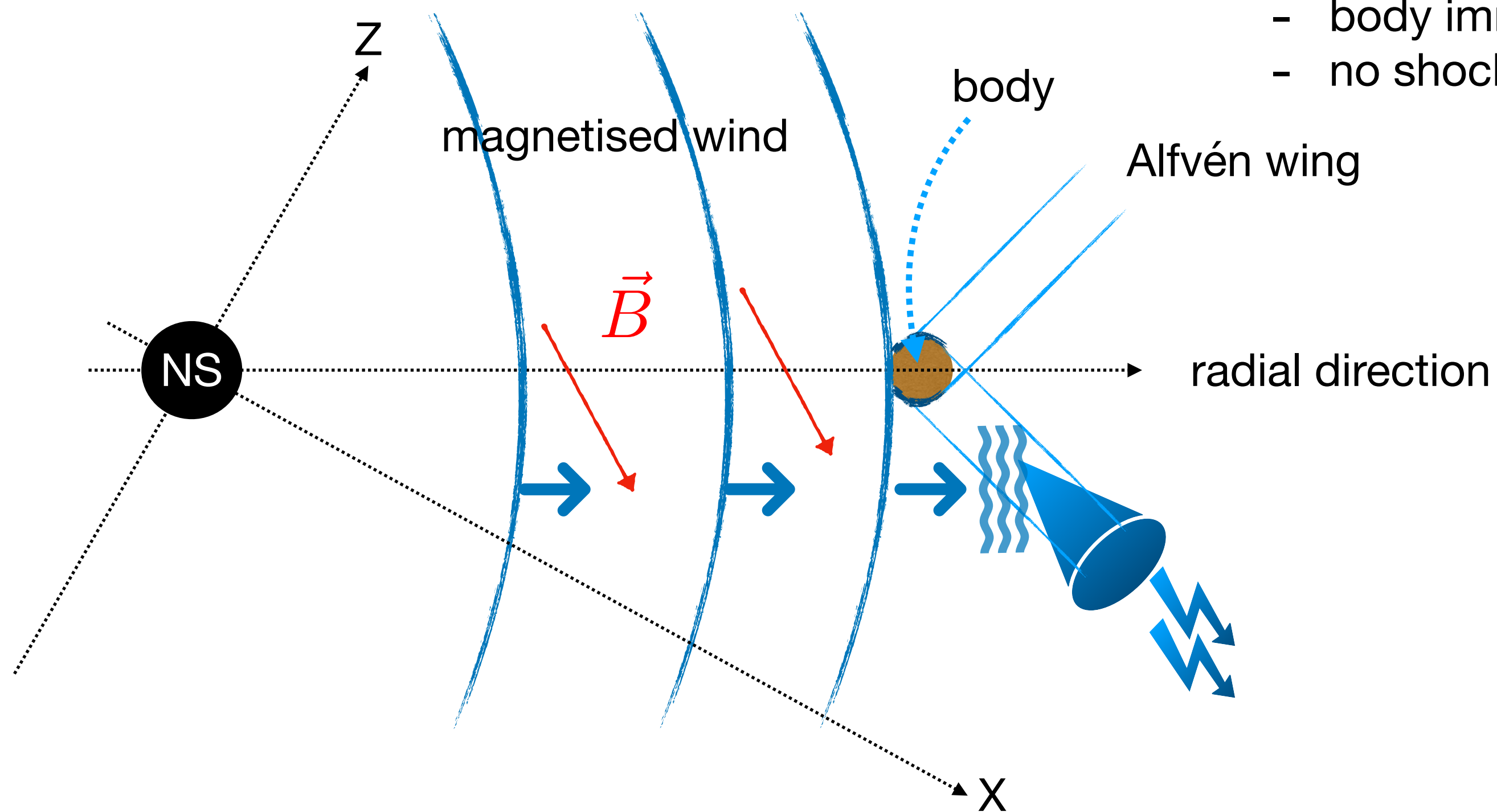


# A plausible emission model

among many other models: <https://frbtheorycat.org>

## The Alfvén wing emission mechanisms:

Mottez&Zarka 2014 / Mottez, Zarka, Voisin 2020



### 1) Magnetic coupling: Mottez&Heyvaerts 2012

- body immersed in magnetised plasma
- no shock required

### 2) Alfvén wings:

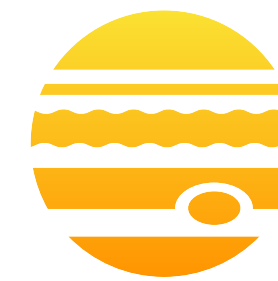
- potential drop induced by the conductive body
- two symmetrical current sheets

### 3) Radio emission:

- plasma excitations when crossing the Alfvén wings
- relativistic plasma -> beamed emission

## Pros:

- observed mechanism for non relativistic plasma (Jupiter-Io system for instance)
- reproduce FRB-like emission (lowest amount of energy involved)



## Cons:

- how to feed this mechanism with orbiting body immersed in the plasma with (observed) **non-periodical bursts**?
- how to observe such strongly beamed emissions?

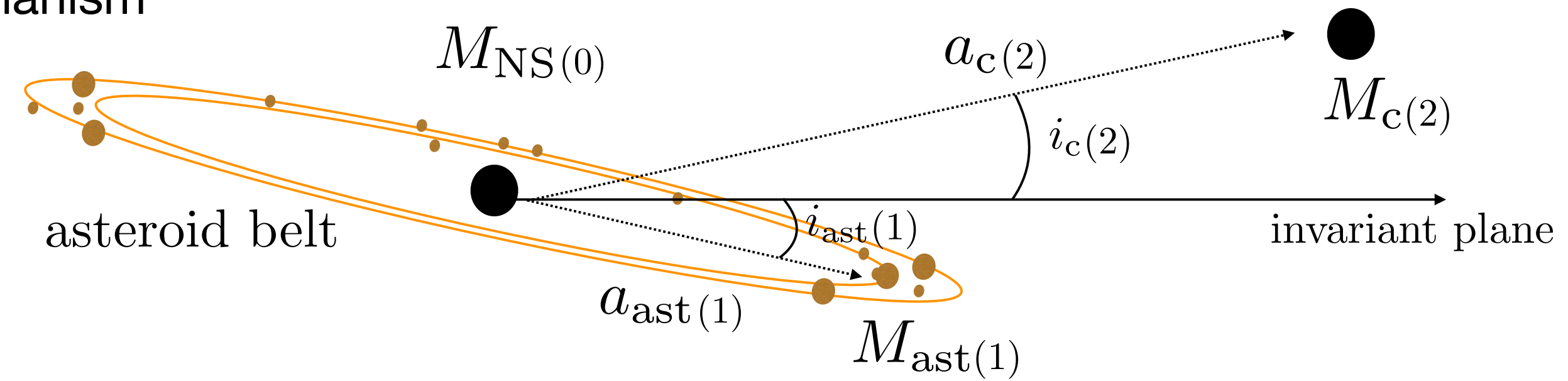
# A plausible source population model: Kozai-Lidov feeding of compact binary systems

V. D. , Kumiko Kotera (IAP), Joseph Silk (IAP, CEA, JHU, Oxford) (A&A 2021)

Goal: explain FRB repeating rates in the context of the Alfvén wing mechanism

- drive orbiting body as close as possible to the pulsar
- without periodical effects

Method: study the dynamical evolutions of asteroids in a 3 body system via Kozai-Lidov perturbations





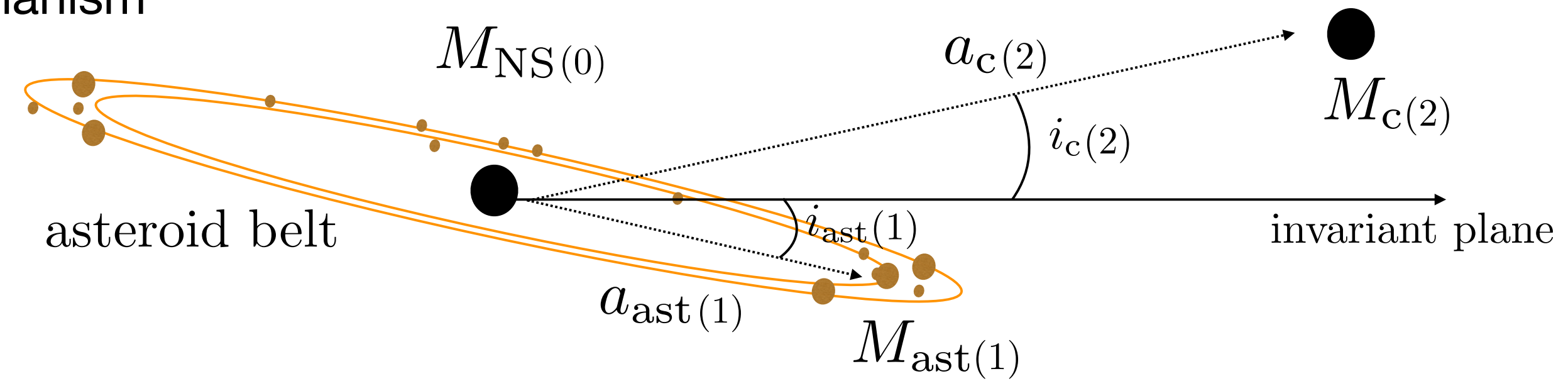
# A plausible source population model: Kozai-Lidov feeding of compact binary systems

V. D. , Kumiko Kotera (IAP), Joseph Silk (IAP, CEA, JHU, Oxford) (A&A 2021)

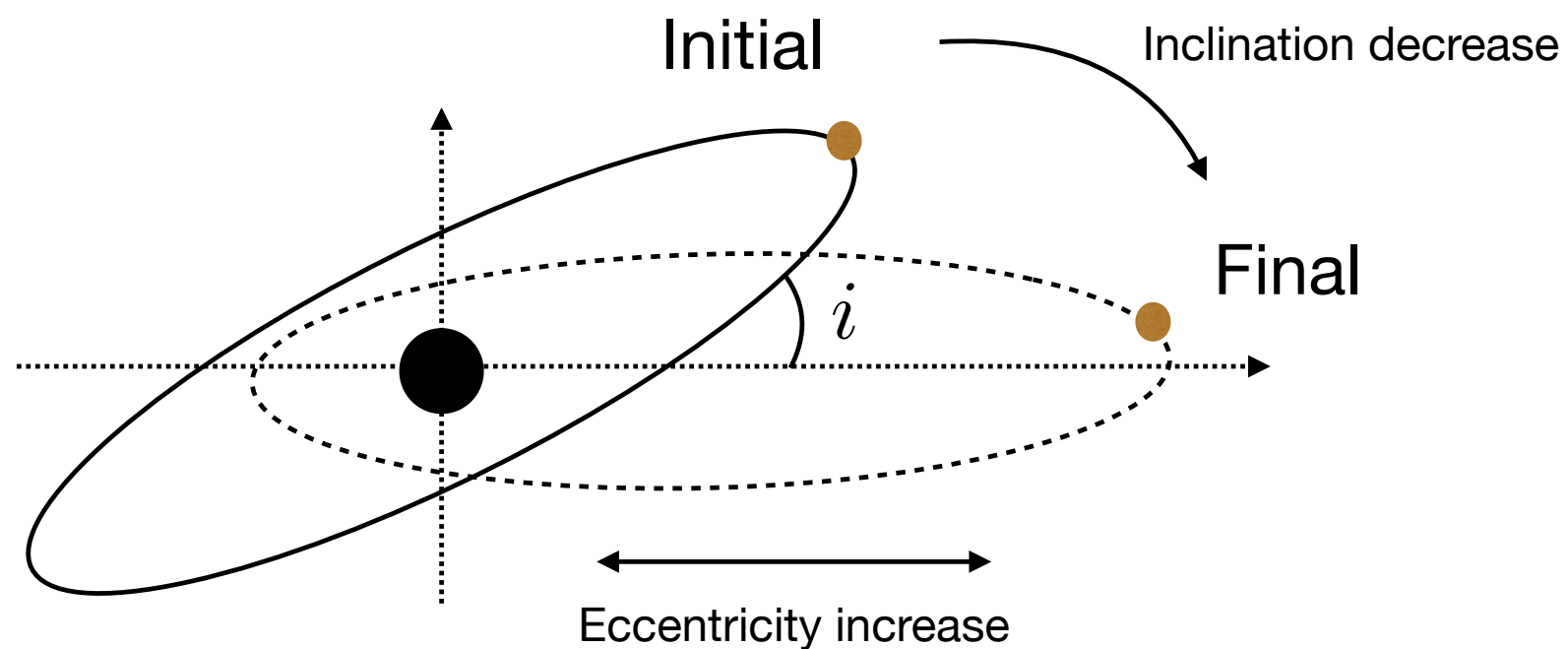
Goal: explain FRB repeating rates in the context of the Alfvén wing mechanism

- drive orbiting body as close as possible to the pulsar
- without periodical effects

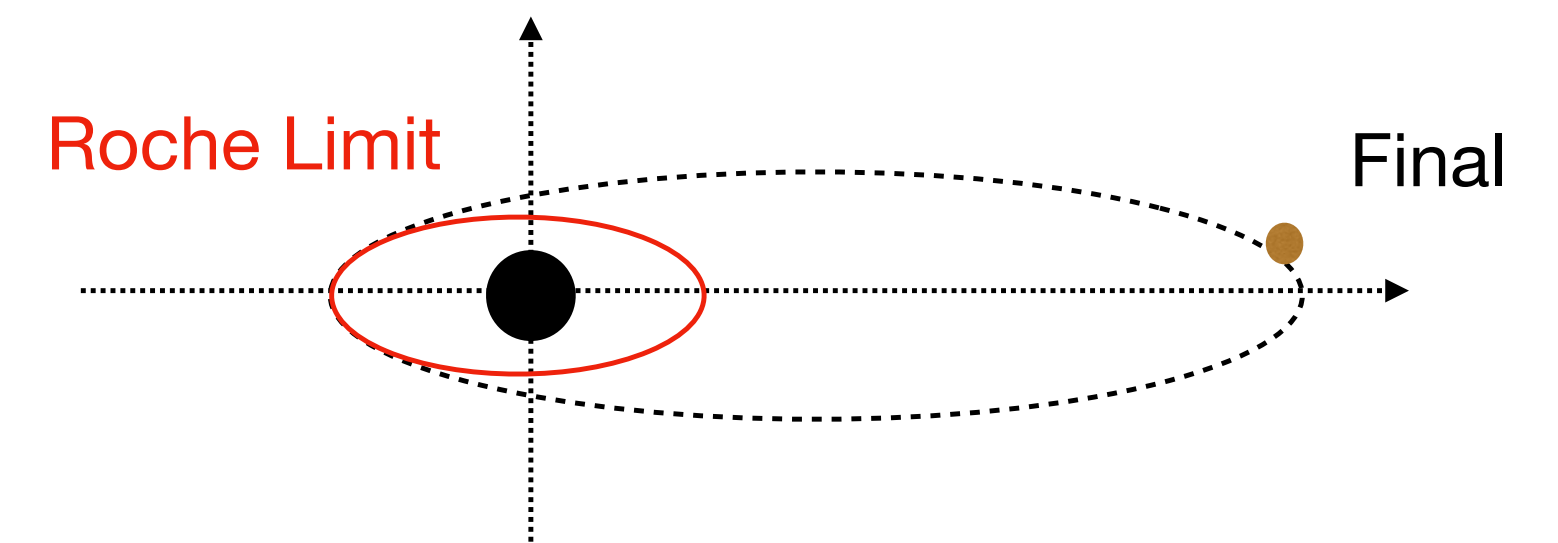
Method: study the dynamical evolutions of asteroids in a 3 body system via Kozai-Lidov perturbations



Kozai-Lidov effect: exchanges of orbital momentum → transfer of inclination to the eccentricity



the Roche limit is the closest position beyond which tidal effects disrupt the asteroid



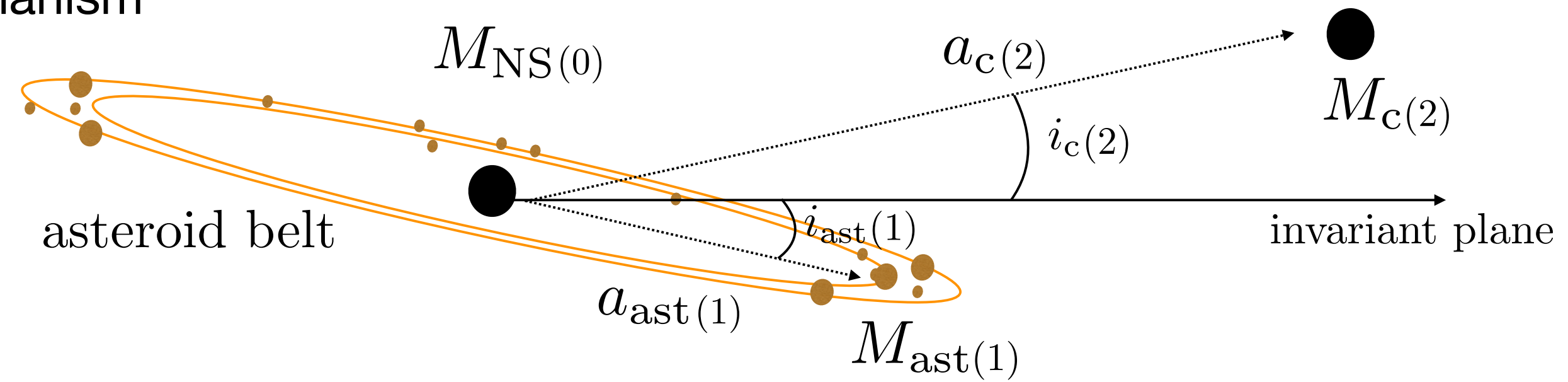
# A plausible source population model: Kozai-Lidov feeding of compact binary systems

V. D. , Kumiko Kotera (IAP), Joseph Silk (IAP, CEA, JHU, Oxford) (A&A 2021)

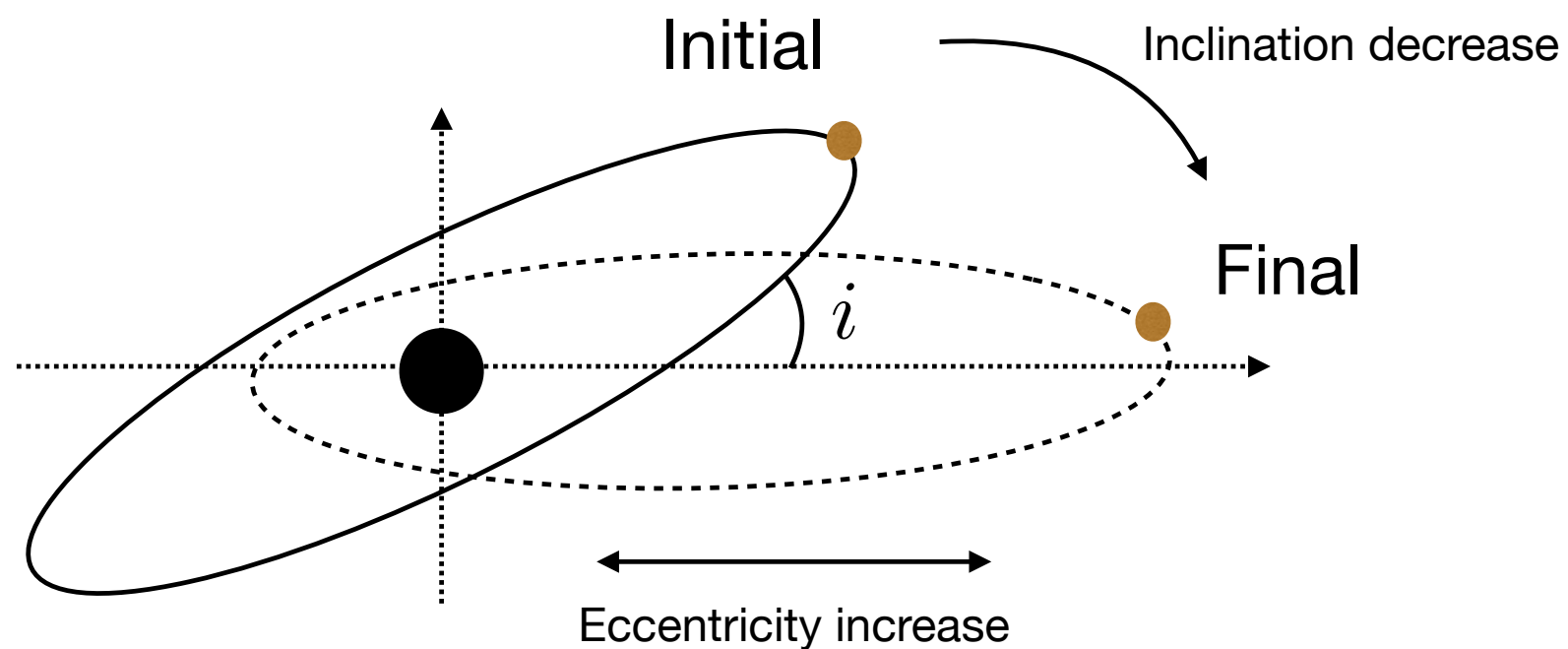
Goal: explain FRB repeating rates in the context of the Alfvén wing mechanism

- drive orbiting body as close as possible to the pulsar
- without periodical effects

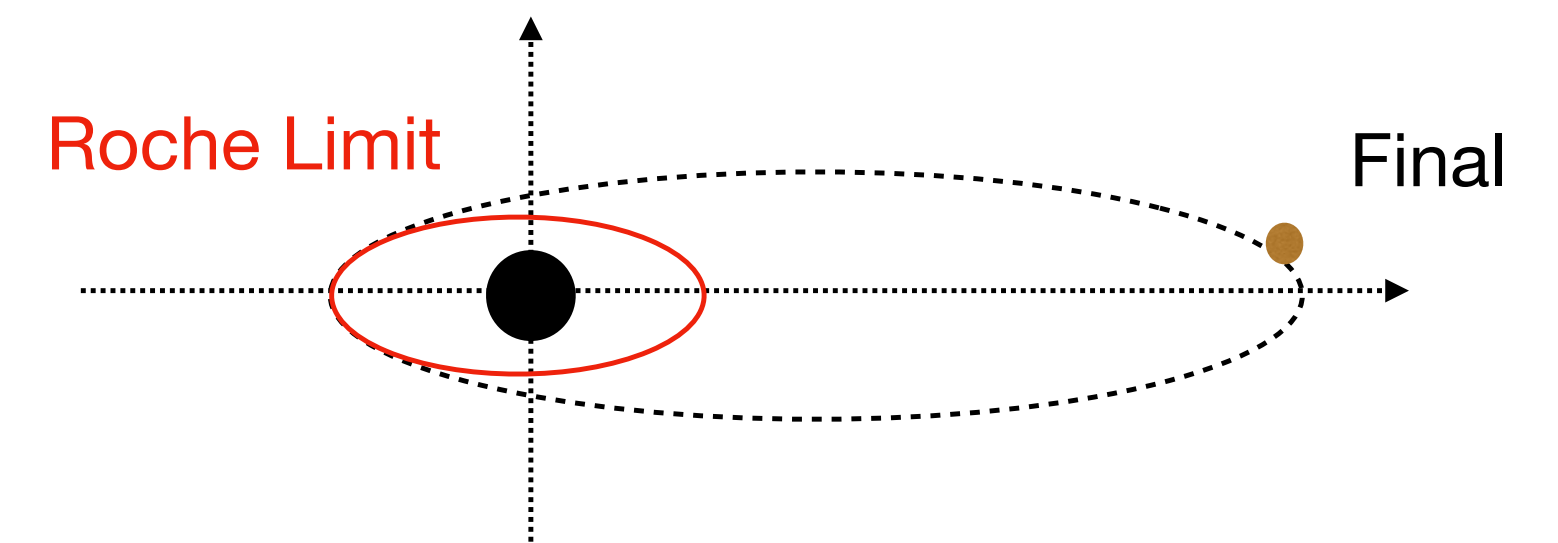
Method: study the dynamical evolutions of asteroids in a 3 body system via Kozai-Lidov perturbations



Kozai-Lidov effect: exchanges of orbital momentum → transfer of inclination to the eccentricity



the Roche limit is the closest position beyond which tidal effects disrupt the asteroid



Kozai-Lidov effects can drive the asteroids down to the Roche limit



# **A shot of Three-Body dynamics**

---

General Three-Body dynamics is complex with no general solution

However some effects such as Kozai-Lidov perturbations can be analytically derived

# A shot of Three-Body dynamics

General Three-Body dynamics is complex with no general solution

However some effects such as Kozai-Lidov perturbations can be analytically derived

Three-body Hamiltonian

$$\mathcal{H} = G \frac{m_0 m_1}{2a_1} + G \frac{(m_0 + m_1)m_2}{2a_2} + \mathcal{H}_{\text{pert}} \rightarrow \mathcal{H}_{\text{pert}} = \frac{G}{a_2} \sum_{j=2}^{\infty} \left(\frac{a_1}{a_2}\right)^j \mathcal{M}_j \left(\frac{r_1}{a_1}\right)^j \left(\frac{a_2}{r_2}\right)^{j+1} P_j[\cos(\Phi)]$$

$\rightarrow \mathcal{H}_{\text{pert}} \approx \mathcal{H}_{\text{quad}} + \epsilon \mathcal{H}_{\text{oct}} \quad \text{with} \quad \epsilon = \frac{a_1}{a_2} \frac{e_2}{1 - e_2^2}$

2 two-body system + interaction term

$\epsilon$  drives the dynamics between quadrupole effects and octupole effects



# A shot of Three-Body dynamics

General Three-Body dynamics is complex with no general solution

However some effects such as Kozai-Lidov perturbations can be analytically derived

Three-body Hamiltonian

$$\mathcal{H} = G \frac{m_0 m_1}{2a_1} + G \frac{(m_0 + m_1) m_2}{2a_2} + \mathcal{H}_{\text{pert}} \rightarrow \mathcal{H}_{\text{pert}} = \frac{G}{a_2} \sum_{j=2}^{\infty} \left( \frac{a_1}{a_2} \right)^j \mathcal{M}_j \left( \frac{r_1}{a_1} \right)^j \left( \frac{a_2}{r_2} \right)^{j+1} P_j[\cos(\Phi)]$$

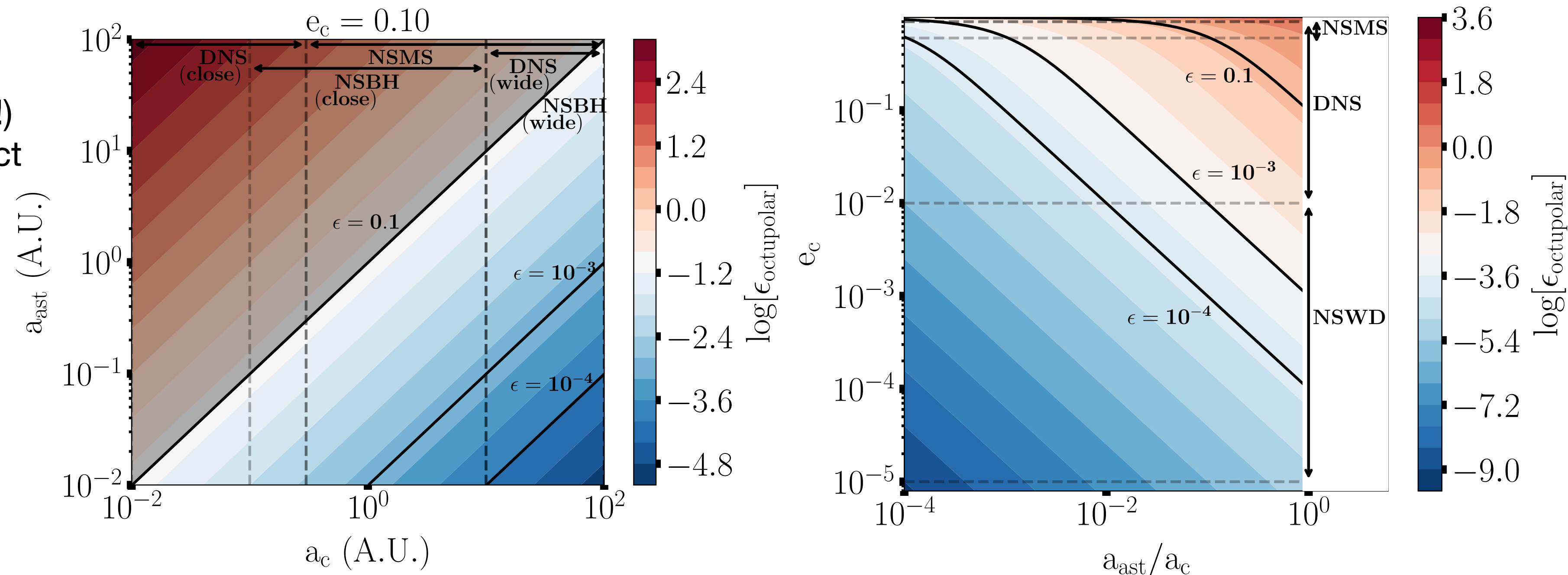
2 two-body system + interaction term

$$\rightarrow \mathcal{H}_{\text{pert}} \approx \mathcal{H}_{\text{quad}} + \epsilon \mathcal{H}_{\text{oct}} \quad \text{with} \quad \epsilon = \frac{a_1}{a_2} \frac{e_2}{1 - e_2^2}$$

$\epsilon$  drives the dynamics between quadrupole effects and octupole effects

Dynamical regimes:

- quadrupole → Kozai-Lidov effect
  - short timescales (still secular effect!)
- octupole → Excentric Kozai-Lidov effect
  - extreme eccentricity excitations



Parameter space for the different dynamical regimes

# **Kozai-Lidov times and repeating FRB rates**

---



# Kozai-Lidov times and repeating FRB rates

Kozai-Lidov effects happen over secular times  $\gg$  FRB repeaters occurrence times

$$t_{\text{KL}} \sim \frac{16}{15} \frac{a_2^3}{a_1^{3/2}} (1 - e_2^2)^{3/2} \frac{1}{\sqrt{G}} \frac{\sqrt{m_0 + m_1}}{m_2} \rightarrow t_{\text{EKL}} \sim \frac{128\sqrt{10}}{15\pi\sqrt{\epsilon}} t_{\text{KL},i=90^\circ} \sim \underline{4.8 \text{ yr}} \epsilon^{-1/2} \left(\frac{a_{\text{ast}}}{0.5 \text{ A.U.}}\right)^{-3/2} \left(\frac{a_c}{\text{A.U.}}\right)^3 \left(\frac{M_c}{1 M_\odot}\right)^{-1} \left(\frac{M_{\text{NS}}}{1.4 M_\odot}\right)^{1/2}$$

# Kozai-Lidov times and repeating FRB rates

Kozai-Lidov effects happen over secular times  $\gg$  FRB repeaters occurrence times

$$t_{\text{KL}} \sim \frac{16}{15} \frac{a_2^3}{a_1^{3/2}} (1 - e_2^2)^{3/2} \frac{1}{\sqrt{G}} \frac{\sqrt{m_0 + m_1}}{m_2} \rightarrow t_{\text{EKL}} \sim \frac{128\sqrt{10}}{15\pi\sqrt{\epsilon}} t_{\text{KL},i=90^\circ} \sim 4.8 \text{ yr } \epsilon^{-1/2} \left(\frac{a_{\text{ast}}}{0.5 \text{ A.U.}}\right)^{-3/2} \left(\frac{a_c}{\text{A.U.}}\right)^3 \left(\frac{M_c}{1 M_\odot}\right)^{-1} \left(\frac{M_{\text{NS}}}{1.4 M_\odot}\right)^{1/2}$$

**But:** relative delays between 2 consecutive asteroid infalls compatible!

$$\Delta t_{\text{KL}} = \frac{8}{5} \frac{a_2^3}{a_1^{5/2}} \Delta a_1 (1 - e_2^2)^{3/2} \frac{1}{\sqrt{G}} \frac{\sqrt{m_0 + m_1}}{m_2} \rightarrow \Delta t_{\text{EKL}} = \frac{256\sqrt{10}}{15\pi} \frac{t_{\text{KL},i=90^\circ}}{\sqrt{\epsilon}} \frac{\Delta a_1}{a_1}$$



# Kozai-Lidov times and repeating FRB rates

Kozai-Lidov effects happen over secular times  $\gg$  FRB repeaters occurrence times

$$t_{\text{KL}} \sim \frac{16}{15} \frac{a_2^3}{a_1^{3/2}} (1 - e_2^2)^{3/2} \frac{1}{\sqrt{G}} \frac{\sqrt{m_0 + m_1}}{m_2} \rightarrow t_{\text{EKL}} \sim \frac{128\sqrt{10}}{15\pi\sqrt{\epsilon}} t_{\text{KL},i=90^\circ} \sim 4.8 \text{ yr } \epsilon^{-1/2} \left(\frac{a_{\text{ast}}}{0.5 \text{ A.U.}}\right)^{-3/2} \left(\frac{a_c}{\text{A.U.}}\right)^3 \left(\frac{M_c}{1 M_\odot}\right)^{-1} \left(\frac{M_{\text{NS}}}{1.4 M_\odot}\right)^{1/2}$$

**But:** relative delays between 2 consecutive asteroid infalls compatible!

$$\Delta t_{\text{KL}} = \frac{8}{5} \frac{a_2^3}{a_1^{5/2}} \Delta a_1 (1 - e_2^2)^{3/2} \frac{1}{\sqrt{G}} \frac{\sqrt{m_0 + m_1}}{m_2} \rightarrow \Delta t_{\text{EKL}} = \frac{256\sqrt{10}}{15\pi} \frac{t_{\text{KL},i=90^\circ}}{\sqrt{\epsilon}} \frac{\Delta a_1}{a_1}$$

Assuming a “typical” asteroid belt  $\langle \Delta t_{\text{EKL}} \rangle \sim 2.7 \text{ days } \epsilon^{-1/2} \epsilon_{\text{eff}} \left[\frac{N_{\text{ast}}}{100}\right]^{-1} \frac{\epsilon_{\text{ast}}}{0.15} \left(\frac{\langle a_{\text{ast}} \rangle}{0.5 \text{ A.U.}}\right)^{-3/2} \left(\frac{a_c}{\text{A.U.}}\right)^3 \left(\frac{M_c}{10 M_\odot}\right)^{-1} \left(\frac{M_{\text{NS}}}{1.4 M_\odot}\right)^{1/2}$

# Kozai-Lidov times and repeating FRB rates

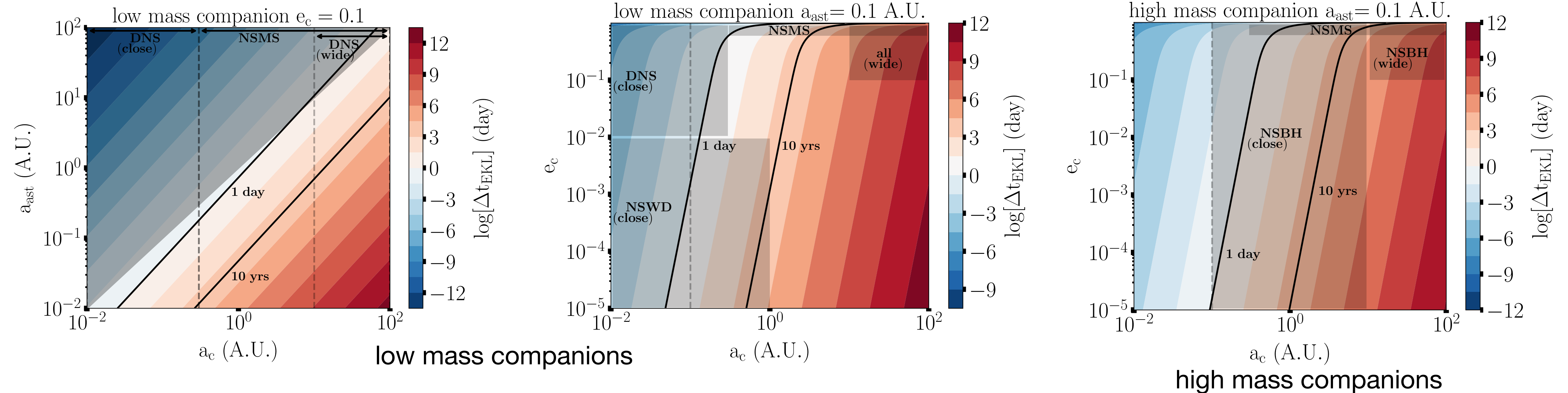
Kozai-Lidov effects happen over secular times  $\gg$  FRB repeaters occurrence times

$$t_{\text{KL}} \sim \frac{16}{15} \frac{a_2^3}{a_1^{3/2}} (1 - e_2^2)^{3/2} \frac{1}{\sqrt{G}} \frac{\sqrt{m_0 + m_1}}{m_2} \rightarrow t_{\text{EKL}} \sim \frac{128\sqrt{10}}{15\pi\sqrt{\epsilon}} t_{\text{KL},i=90^\circ} \sim 4.8 \text{ yr } \epsilon^{-1/2} \left(\frac{a_{\text{ast}}}{0.5 \text{ A.U.}}\right)^{-3/2} \left(\frac{a_c}{\text{A.U.}}\right)^3 \left(\frac{M_c}{1 M_\odot}\right)^{-1} \left(\frac{M_{\text{NS}}}{1.4 M_\odot}\right)^{1/2}$$

**But:** relative delays between 2 consecutive asteroid infalls compatible!

$$\Delta t_{\text{KL}} = \frac{8}{5} \frac{a_2^3}{a_1^{5/2}} \Delta a_1 (1 - e_2^2)^{3/2} \frac{1}{\sqrt{G}} \frac{\sqrt{m_0 + m_1}}{m_2} \rightarrow \Delta t_{\text{EKL}} = \frac{256\sqrt{10}}{15\pi} \frac{t_{\text{KL},i=90^\circ}}{\sqrt{\epsilon}} \frac{\Delta a_1}{a_1}$$

Assuming a “typical” asteroid belt  $\langle \Delta t_{\text{EKL}} \rangle \sim 2.7 \text{ days } \epsilon^{-1/2} \epsilon_{\text{eff}} \left[\frac{N_{\text{ast}}}{100}\right]^{-1} \frac{\epsilon_{\text{ast}}}{0.15} \left(\frac{\langle a_{\text{ast}} \rangle}{0.5 \text{ A.U.}}\right)^{-3/2} \left(\frac{a_c}{\text{A.U.}}\right)^3 \left(\frac{M_c}{10 M_\odot}\right)^{-1} \left(\frac{M_{\text{NS}}}{1.4 M_\odot}\right)^{1/2}$





# Kozai-Lidov times and repeating FRB rates

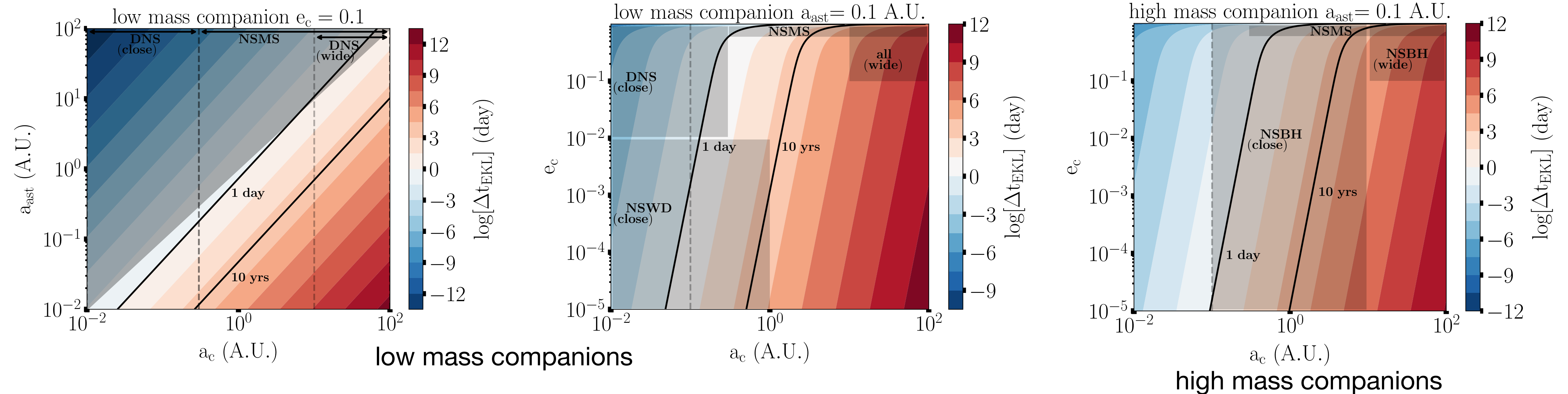
Kozai-Lidov effects happen over secular times  $\gg$  FRB repeaters occurrence times

$$t_{\text{KL}} \sim \frac{16}{15} \frac{a_2^3}{a_1^{3/2}} (1 - e_2^2)^{3/2} \frac{1}{\sqrt{G}} \frac{\sqrt{m_0 + m_1}}{m_2} \rightarrow t_{\text{EKL}} \sim \frac{128\sqrt{10}}{15\pi\sqrt{\epsilon}} t_{\text{KL},i=90^\circ} \sim 4.8 \text{ yr } \epsilon^{-1/2} \left(\frac{a_{\text{ast}}}{0.5 \text{ A.U.}}\right)^{-3/2} \left(\frac{a_c}{\text{A.U.}}\right)^3 \left(\frac{M_c}{1 M_\odot}\right)^{-1} \left(\frac{M_{\text{NS}}}{1.4 M_\odot}\right)^{1/2}$$

**But:** relative delays between 2 consecutive asteroid infalls compatible!

$$\Delta t_{\text{KL}} = \frac{8}{5} \frac{a_2^3}{a_1^{5/2}} \Delta a_1 (1 - e_2^2)^{3/2} \frac{1}{\sqrt{G}} \frac{\sqrt{m_0 + m_1}}{m_2} \rightarrow \Delta t_{\text{EKL}} = \frac{256\sqrt{10}}{15\pi} \frac{t_{\text{KL},i=90^\circ}}{\sqrt{\epsilon}} \frac{\Delta a_1}{a_1}$$

Assuming a “typical” asteroid belt  $\langle \Delta t_{\text{EKL}} \rangle \sim 2.7 \text{ days } \epsilon^{-1/2} \epsilon_{\text{eff}} \left[\frac{N_{\text{ast}}}{100}\right]^{-1} \frac{\epsilon_{\text{ast}}}{0.15} \left(\frac{\langle a_{\text{ast}} \rangle}{0.5 \text{ A.U.}}\right)^{-3/2} \left(\frac{a_c}{\text{A.U.}}\right)^3 \left(\frac{M_c}{10 M_\odot}\right)^{-1} \left(\frac{M_{\text{NS}}}{1.4 M_\odot}\right)^{1/2}$



both very short and long timescales can be reached depending on the system parameters

# Numerical results

---

Monte-Carlo simulations of asteroid infall relative time delays (with GR corrections):



# Numerical results

---

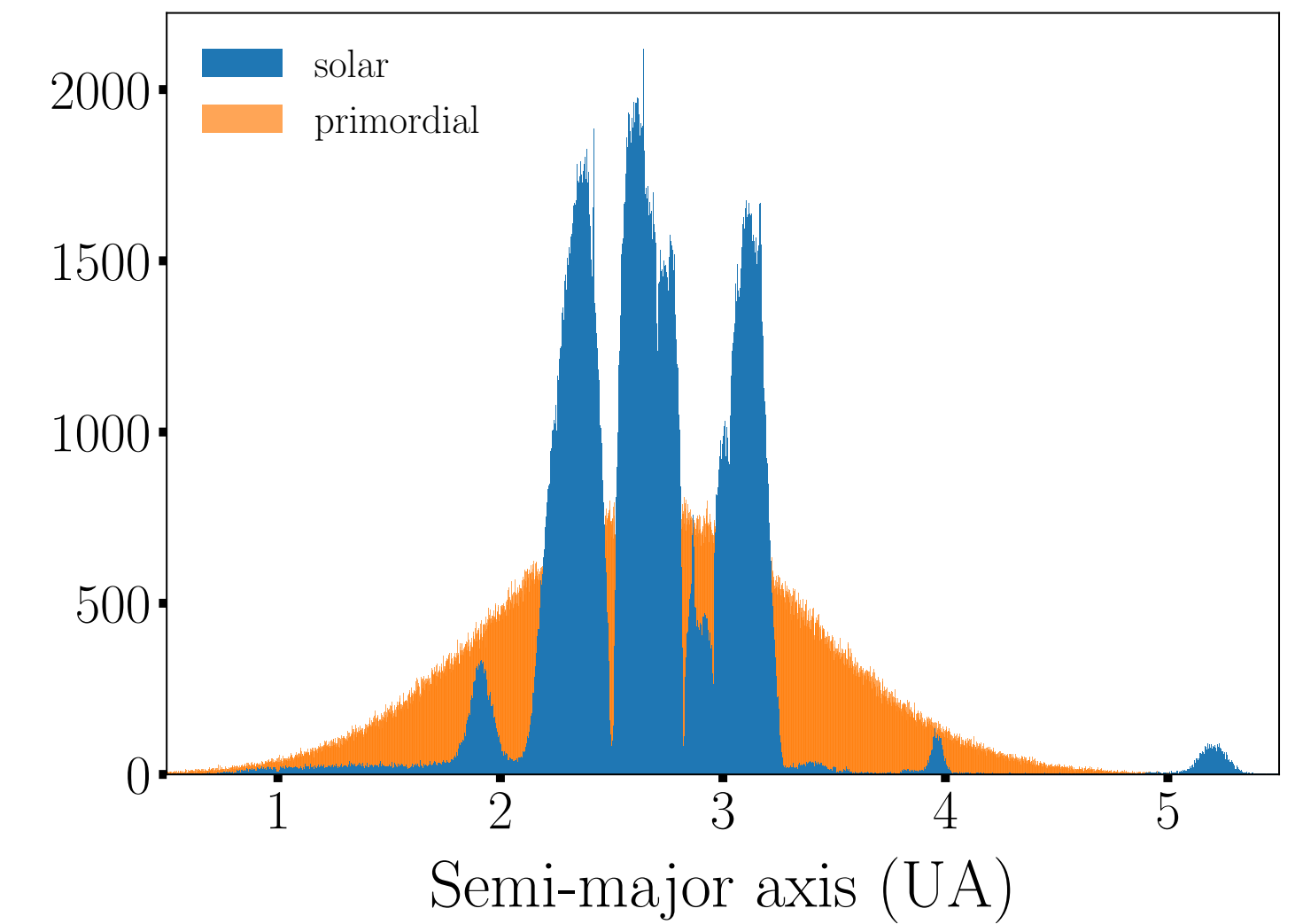
Monte-Carlo simulations of asteroid infall relative time delays (with GR corrections):

Primordial asteroid belt simulation based on the Solar asteroid belt:

- size / extension
- asteroid masses

Method:

- asteroids randomly draw from the primordial belt
- selection on initial conditions that can trigger Kozai-Lidov effects
- selection on asteroids that reaches the Roche limit
- Kozai-Lidov times are computed
- relative times are extracted from the infall timelines



# Numerical results

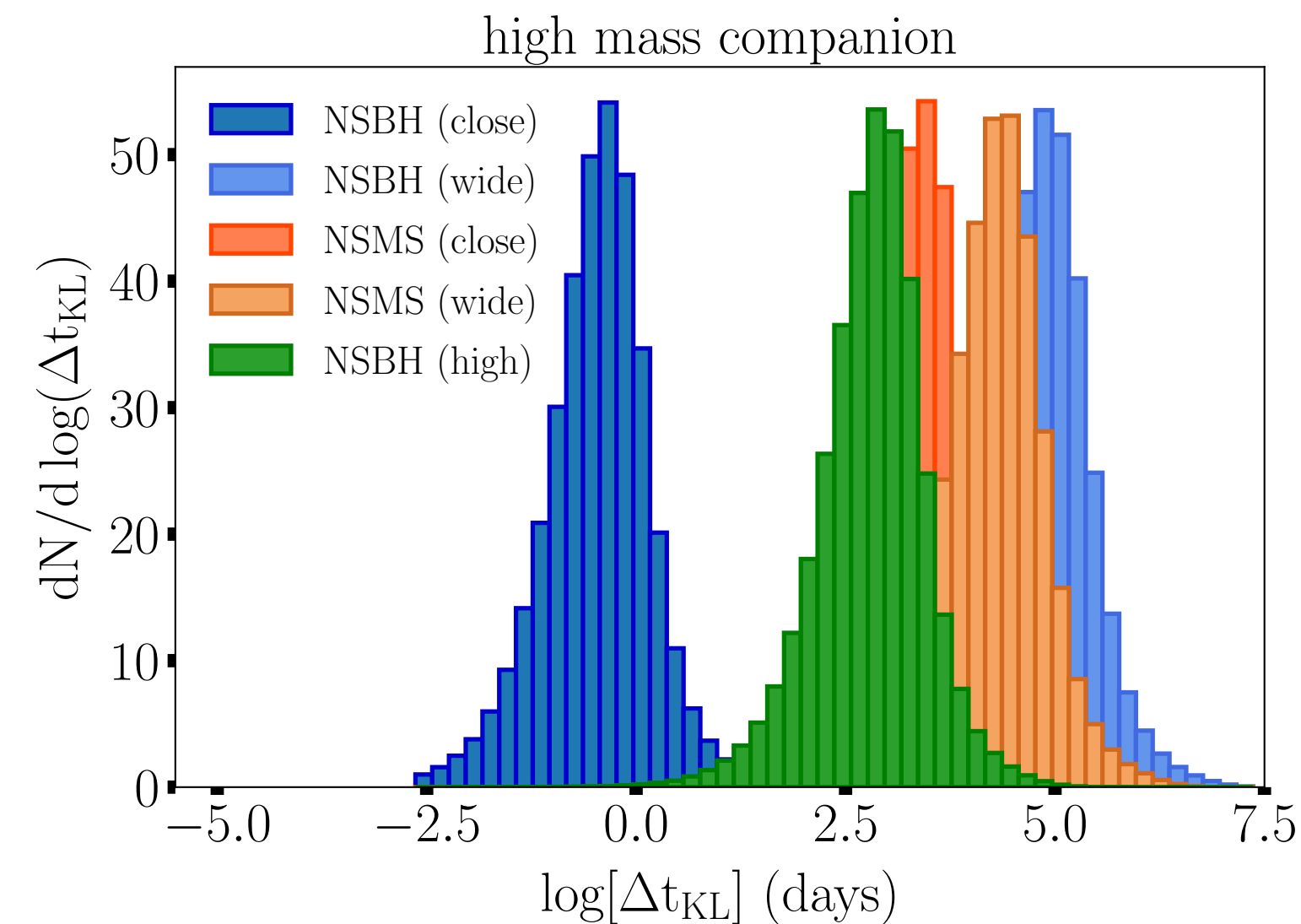
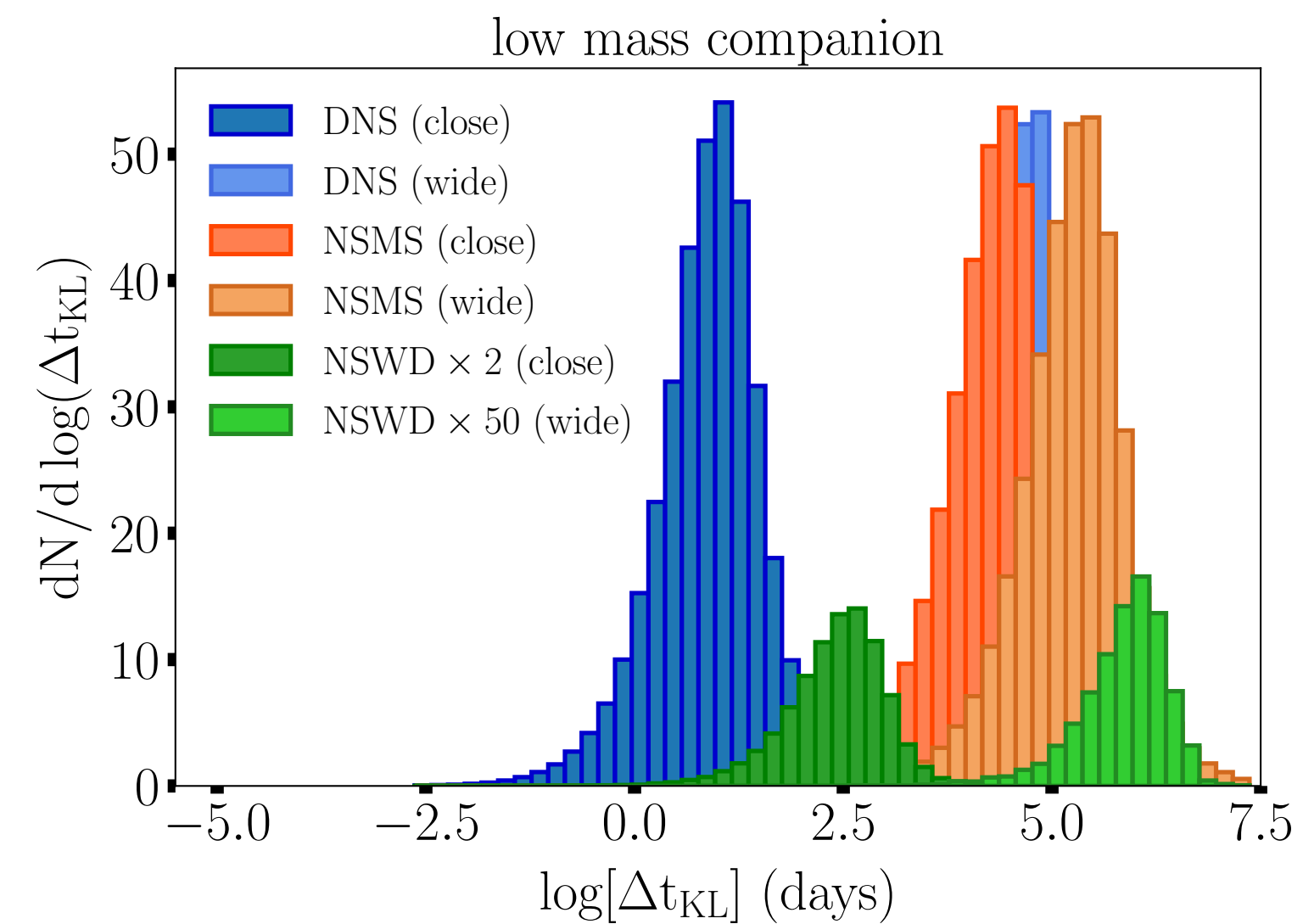
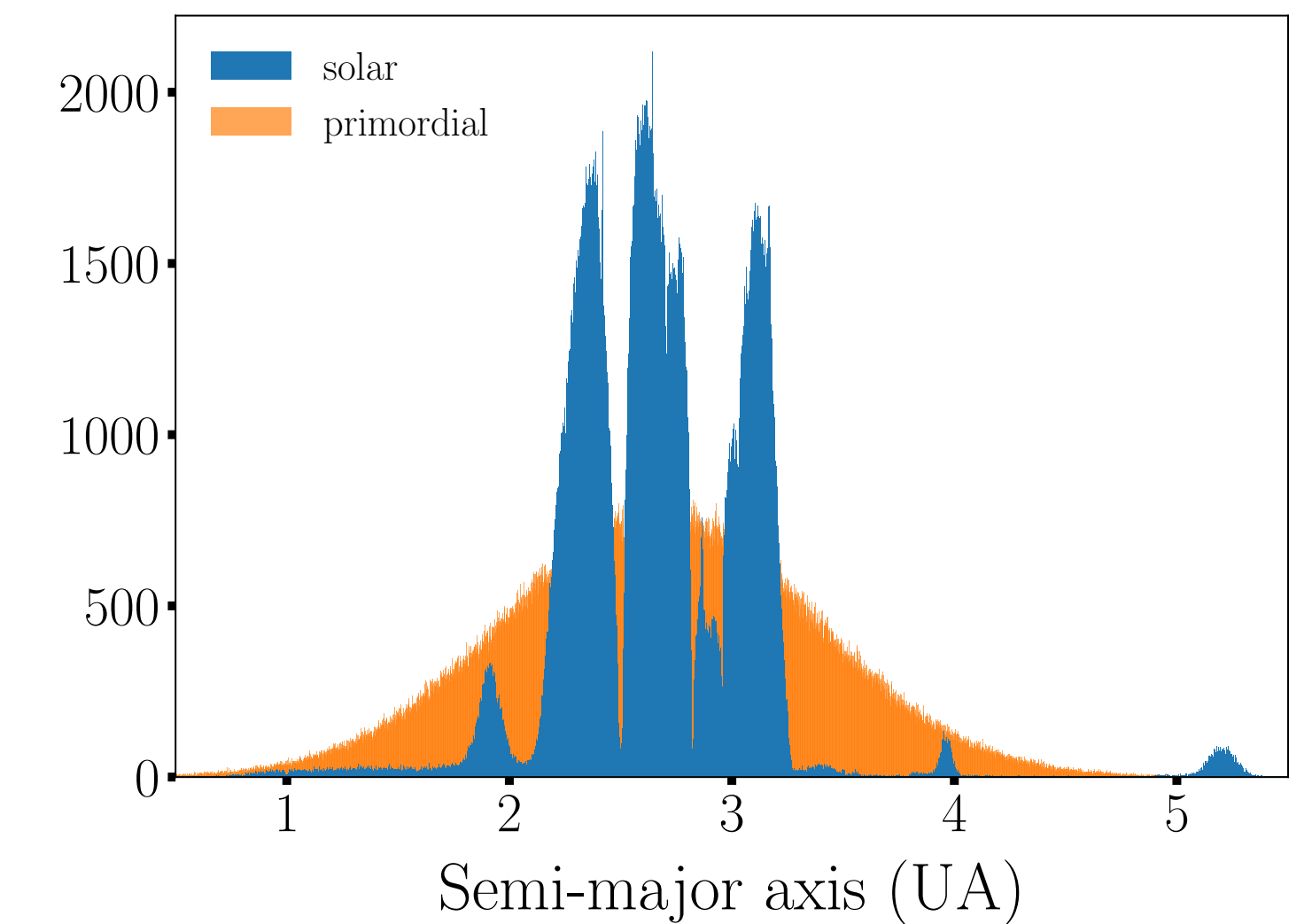
Monte-Carlo simulations of asteroid infall relative time delays (with GR corrections):

Primordial asteroid belt simulation based on the Solar asteroid belt:

- size / extension
- asteroid masses

Method:

- asteroids randomly draw from the primordial belt
- selection on initial conditions that can trigger Kozai-Lidov effects
- selection on asteroids that reaches the Roche limit
- Kozai-Lidov times are computed
- relative times are extracted from the infall timelines



**Results:** The dichotomy between the two populations is solved via the companion parameters of the systems:

- all FRB are repeaters
- mildly close system  $\rightarrow$  day/month repeaters with lifetime  $\sim 10$ s of years
- wide system are steady sources that will be observed as non repeaters



# Dichotomy of repeating and non-repeating FRB

FRB rates from the model (accounting for populations):

$$\begin{aligned} \text{non repeaters: } \dot{n}_{\text{FRB,nrep}} &\sim \frac{t_{\text{EKL}}}{\langle \Delta t_{\text{EKL}} \rangle} \epsilon_{\text{nrep}} \epsilon_{\text{wide}} \dot{n}_{\text{c}} = \frac{1}{2} N_{\text{ast}} \epsilon_{\text{ast}}^{-1} \epsilon_{\text{eff}} \epsilon_{\text{nrep}} \epsilon_{\text{wide}} \dot{n}_{\text{c}} \sim \underline{4 \times 10^3 \text{ Gpc}^{-3} \text{ yr}^{-1}} \frac{N_{\text{ast}}}{100} \frac{\epsilon_{\text{eff}}}{0.2} \left( \frac{\epsilon_{\text{ast}}}{0.15} \right)^{-1} \frac{\epsilon_{\text{wide}}}{0.3} \frac{\epsilon_{\text{nrep}} \dot{n}_{\text{c}}}{0.2 \text{ Mpc}^{-3} \text{ Myr}^{-1}} \\ \text{repeaters: } \dot{n}_{\text{FRB,rep}} &\sim \underline{200 \text{ Gpc}^{-3} \text{ yr}^{-1}} \frac{\epsilon_{\text{rep}} \epsilon_{\text{mild-close}} \dot{n}_{\text{c}}}{0.2 \text{ Mpc}^{-3} \text{ Myr}^{-1}} \end{aligned}$$

FRB rates inferred from observations:

$$\dot{n}_{\text{FRB,obs}} \sim \underline{2 \times 10^3 \text{ Gpc}^{-3} \text{ yr}^{-1}} \text{ E. Petroff et al 2019}$$

# Dichotomy of repeating and non-repeating FRB

FRB rates from the model (accounting for populations):

$$\begin{aligned} \text{non repeaters: } \dot{n}_{\text{FRB,nrep}} &\sim \frac{t_{\text{EKL}}}{\langle \Delta t_{\text{EKL}} \rangle} \epsilon_{\text{nrep}} \epsilon_{\text{wide}} \dot{n}_{\text{c}} = \frac{1}{2} N_{\text{ast}} \epsilon_{\text{ast}}^{-1} \epsilon_{\text{eff}} \epsilon_{\text{nrep}} \epsilon_{\text{wide}} \dot{n}_{\text{c}} \sim \underline{4 \times 10^3 \text{ Gpc}^{-3} \text{ yr}^{-1}} \frac{N_{\text{ast}}}{100} \frac{\epsilon_{\text{eff}}}{0.2} \left( \frac{\epsilon_{\text{ast}}}{0.15} \right)^{-1} \frac{\epsilon_{\text{wide}}}{0.3} \frac{\epsilon_{\text{nrep}} \dot{n}_{\text{c}}}{0.2 \text{ Mpc}^{-3} \text{ Myr}^{-1}} \\ \text{repeaters: } \dot{n}_{\text{FRB,rep}} &\sim \underline{200 \text{ Gpc}^{-3} \text{ yr}^{-1}} \frac{\epsilon_{\text{rep}} \epsilon_{\text{mild-close}} \dot{n}_{\text{c}}}{0.2 \text{ Mpc}^{-3} \text{ Myr}^{-1}} \end{aligned}$$

FRB rates inferred from observations:

$$\dot{n}_{\text{FRB,obs}} \sim \underline{2 \times 10^3 \text{ Gpc}^{-3} \text{ yr}^{-1}} \quad \text{E. Petroff et al 2019}$$

➔ A subset (<10%) of NS-BH population could explain the observed FRB rates (repeaters + non-repeaters)!

**Consequences:** this model can be discriminated against others through:

- the characterisation of the Alfvén wing mechanism
- the population dynamics:
  - most repeaters should stop after 10s of years as their asteroid belt becomes depleted
  - some non repeaters could occasionally repeat
  - series of sub-Jansky level short radio burst be observed as EM counterparts from NSWD, DNS, NSMS and NSBH mergers



# Dichotomy of repeating and non-repeating FRB

FRB rates from the model (accounting for populations):

$$\begin{aligned} \text{non repeaters: } \dot{n}_{\text{FRB,nrep}} &\sim \frac{t_{\text{EKL}}}{\langle \Delta t_{\text{EKL}} \rangle} \epsilon_{\text{nrep}} \epsilon_{\text{wide}} \dot{n}_{\text{c}} = \frac{1}{2} N_{\text{ast}} \epsilon_{\text{ast}}^{-1} \epsilon_{\text{eff}} \epsilon_{\text{nrep}} \epsilon_{\text{wide}} \dot{n}_{\text{c}} \sim 4 \times 10^3 \text{ Gpc}^{-3} \text{ yr}^{-1} \frac{N_{\text{ast}}}{100} \frac{\epsilon_{\text{eff}}}{0.2} \left( \frac{\epsilon_{\text{ast}}}{0.15} \right)^{-1} \frac{\epsilon_{\text{wide}}}{0.3} \frac{\epsilon_{\text{nrep}} \dot{n}_{\text{c}}}{0.2 \text{ Mpc}^{-3} \text{ Myr}^{-1}} \\ \text{repeaters: } \dot{n}_{\text{FRB,rep}} &\sim 200 \text{ Gpc}^{-3} \text{ yr}^{-1} \frac{\epsilon_{\text{rep}} \epsilon_{\text{mild-close}} \dot{n}_{\text{c}}}{0.2 \text{ Mpc}^{-3} \text{ Myr}^{-1}} \end{aligned}$$

FRB rates inferred from observations:

$$\dot{n}_{\text{FRB,obs}} \sim 2 \times 10^3 \text{ Gpc}^{-3} \text{ yr}^{-1} \quad \text{E. Petroff et al 2019}$$

➔ A subset (<10%) of NS-BH population could explain the observed FRB rates (repeaters + non-repeaters)!

**Consequences:** this model can be discriminated against others through:

- the characterisation of the Alfvén wing mechanism
- the population dynamics:
  - most repeaters should stop after 10s of years as their asteroid belt becomes depleted
  - some non repeaters could occasionally repeat
  - series of sub-Jansky level short radio burst be observed as EM counterparts from NSWD, DNS, NSMS and NSBH mergers

Situation similar to GRB community 50 yrs ago:  
the lack of observational constraints does not allow to discriminate between the great number of models

# The low frequency quest: do FRBs exist at low frequencies (below 111MHz) ?

At low frequencies → signal intensity is reduced (scattering effects) → low frequency hunter needed



# The low frequency quest: do FRBs exist at low frequencies (below 111MHz) ?

At low frequencies → signal intensity is reduced (scattering effects) → low frequency hunter needed

## The New Extension in Nançay Upgrading LOFAR(NenuFAR):

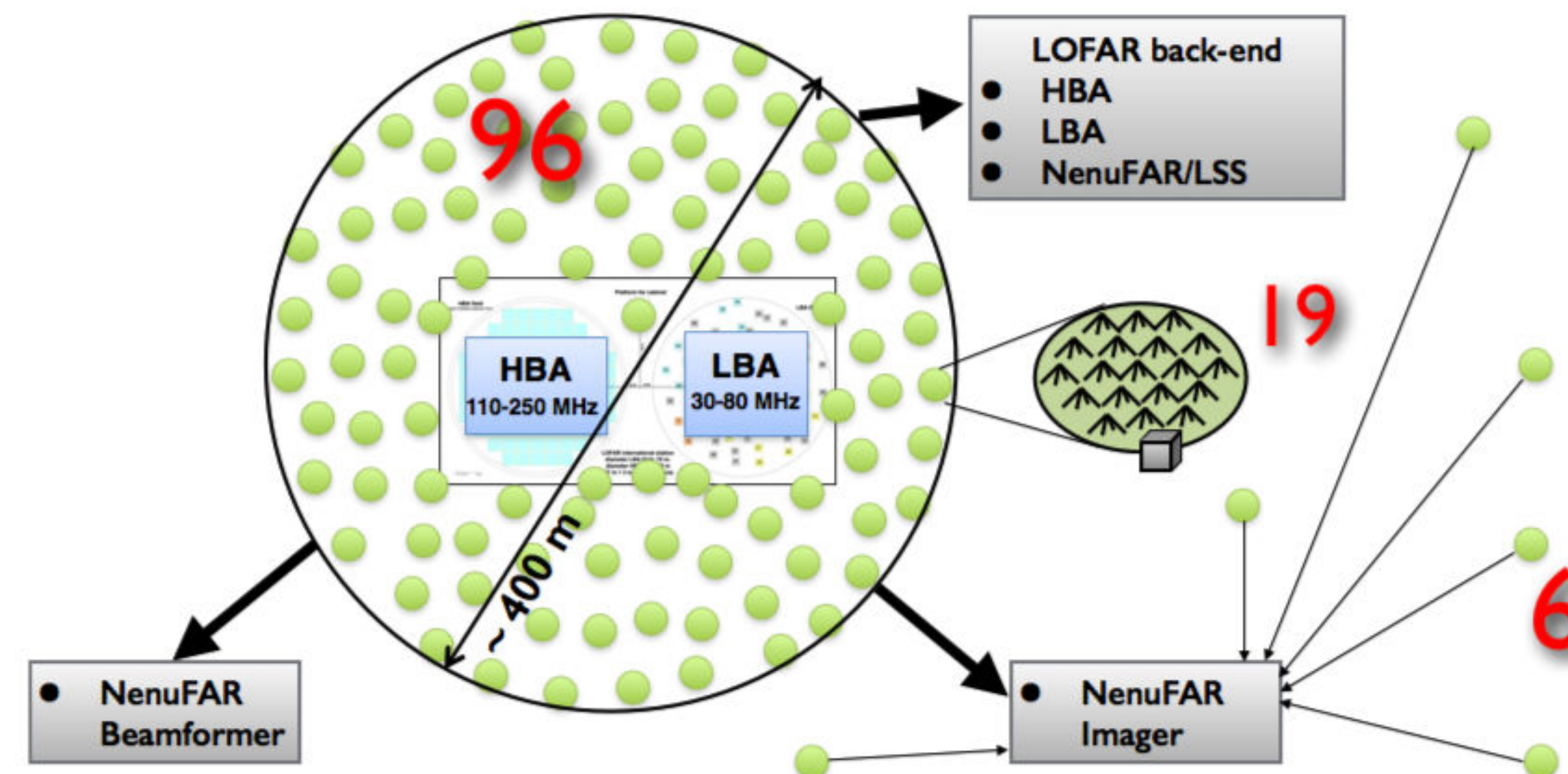




# The low frequency quest: do FRBs exist at low frequencies (below 111MHz) ?

At low frequencies → signal intensity is reduced (scattering effects) → low frequency hunter needed

## The New Extension in Nançay Upgrading LOFAR(NenuFAR):



- Core of  $\approx 400$  m diameter
- + 6 MA at distances up to 3km

- SKA pathfinder partly constructed and in commissioning in the Nançay Radioastronomy Station
- 1938 dual polarisation antennas, hierarchically distributed in Mini-Arrays (MA)
- 10-85 MHz ( from Earth's ionospheric cut-off to radio broadcast FM band)



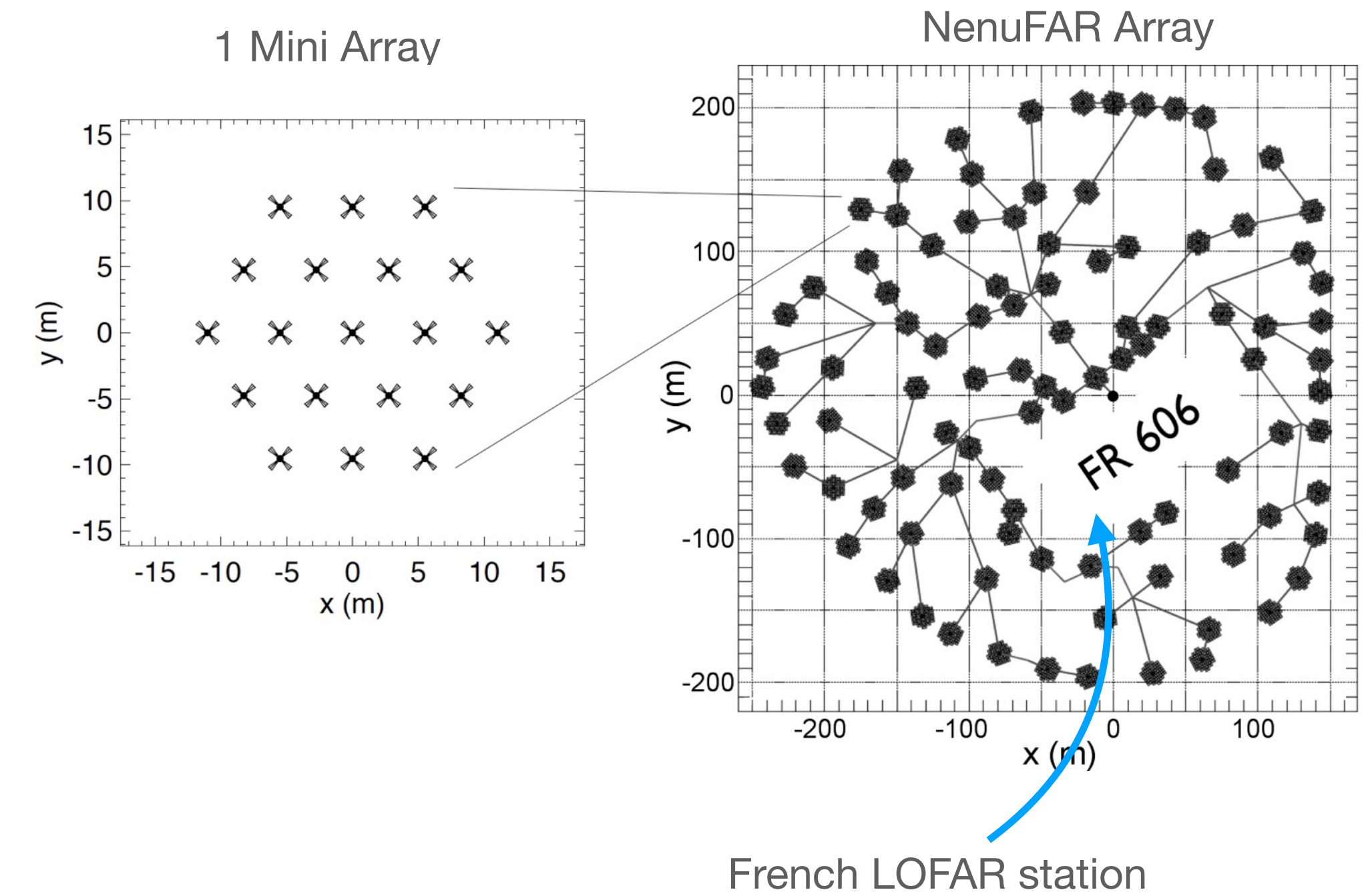
# NenuFAR configuration

---

# NenuFAR configuration

## Array:

- Antennas grouped in **mini-arrays of 19** crossed-dipoles → **SNR**
- **Baselines from 400m to 3km** → **angular resolution**
- Up to **88000m<sup>2</sup>** of collecting area





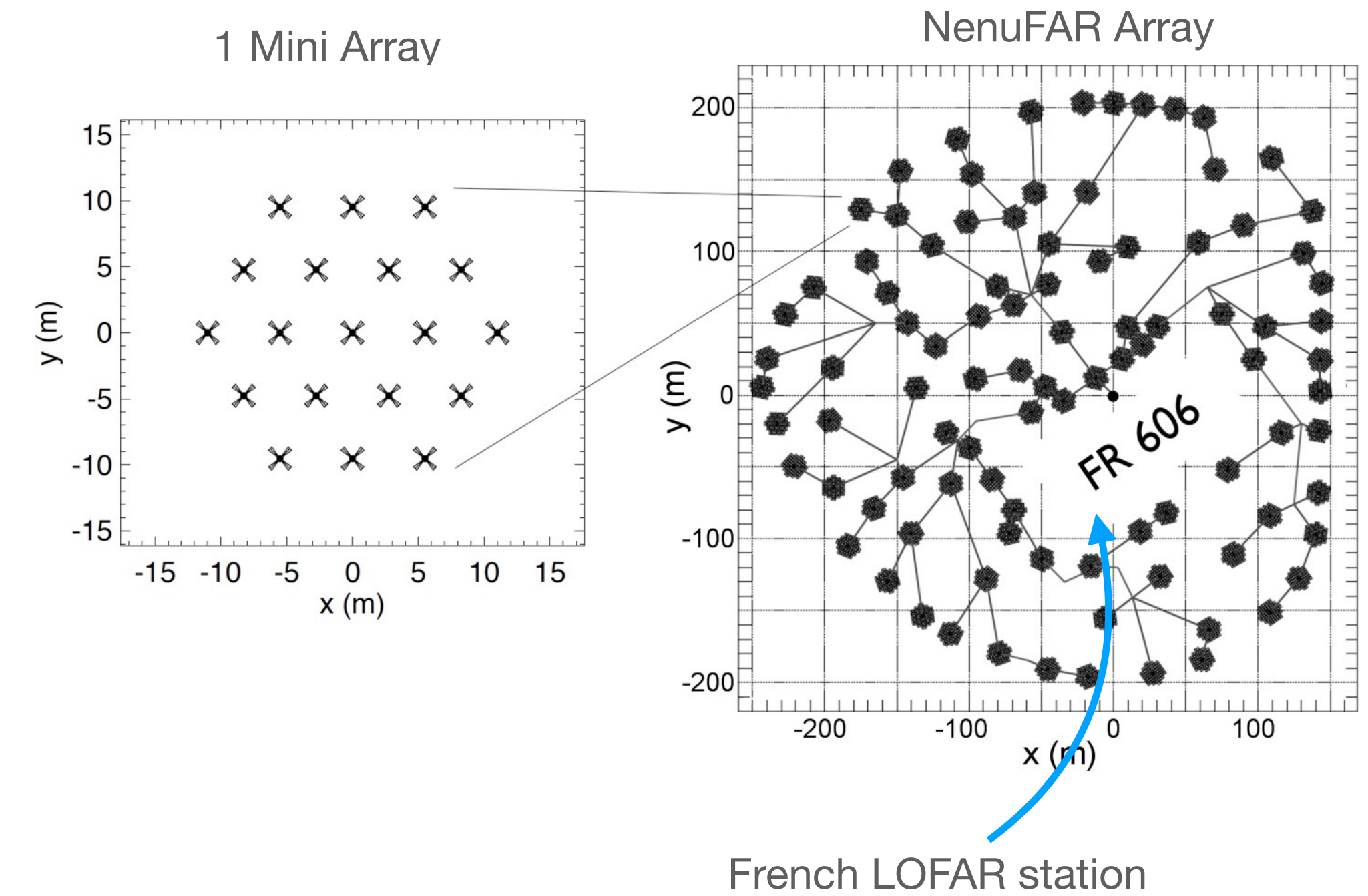
# NenuFAR configuration

## Array:

- Antennas grouped in **mini-arrays of 19** crossed-dipoles → **SNR**
- **Baselines from 400m to 3km** → **angular resolution**
- Up to **88000m<sup>2</sup>** of collecting area

## Signals:

- Time-frequency resolution → **df~195kHz** and **dt~5μs**
- With channelisation **df->3kHz** with **dt~1ms** → **very fine spectral resolution**
- Waveforms at **5ns** time resolution



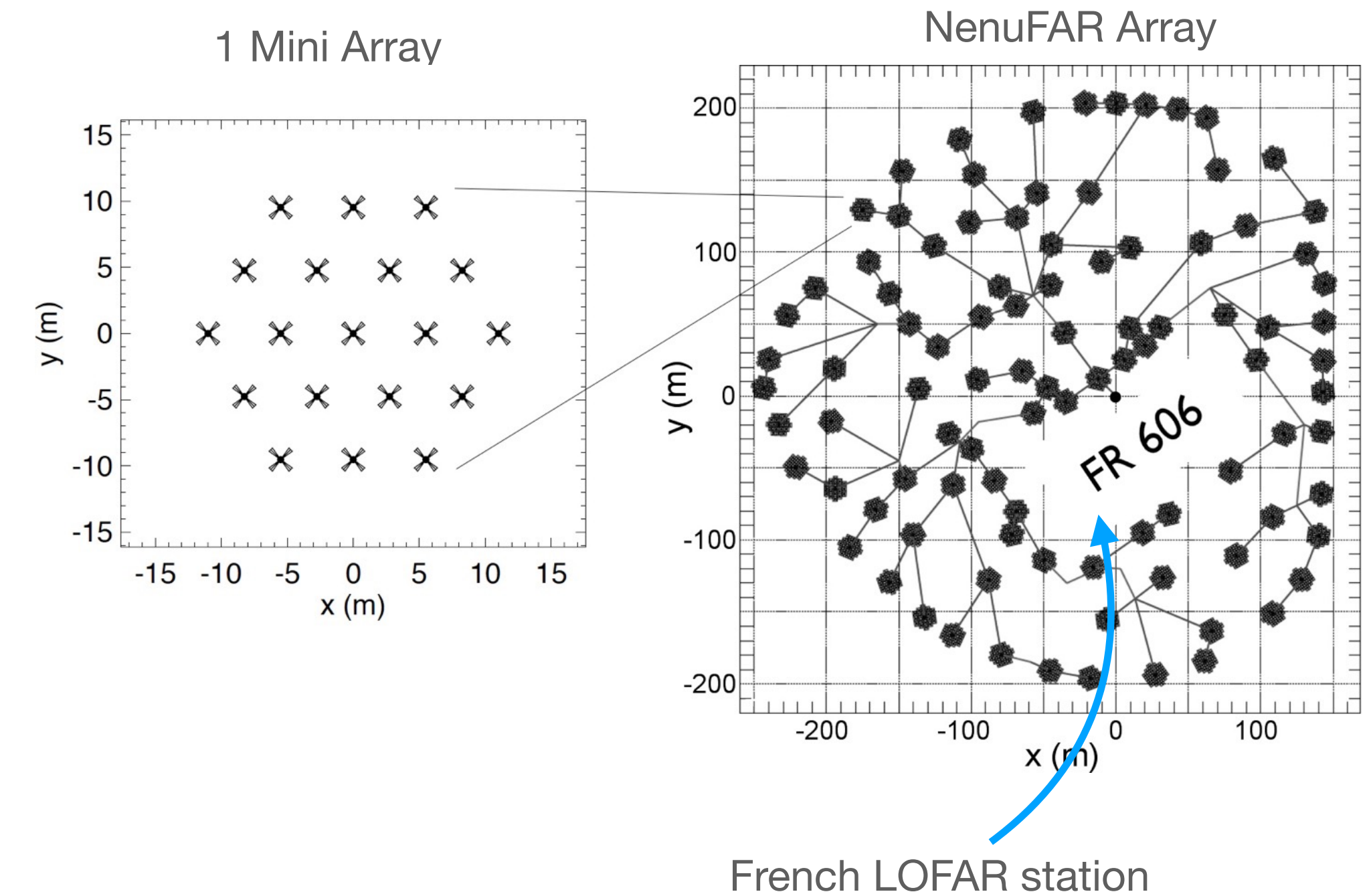
# NenuFAR configuration

## Array:

- Antennas grouped in **mini-arrays of 19** crossed-dipoles → **SNR**
- **Baselines from 400m to 3km** → **angular resolution**
- Up to **88000m<sup>2</sup>** of collecting area

## Signals:

- Time-frequency resolution → **df~195kHz** and **dt~5μs**
- With channelisation **df->3kHz** with **dt~1ms** → **very fine spectral resolution**
- Waveforms at **5ns** time resolution



Can operate in 4 distinct modes:

- **standalone beam former** → **FRB observation**
- capturing waveform → transient buffer
- standalone imager
- Upgraded LOFAR station (low frequency)



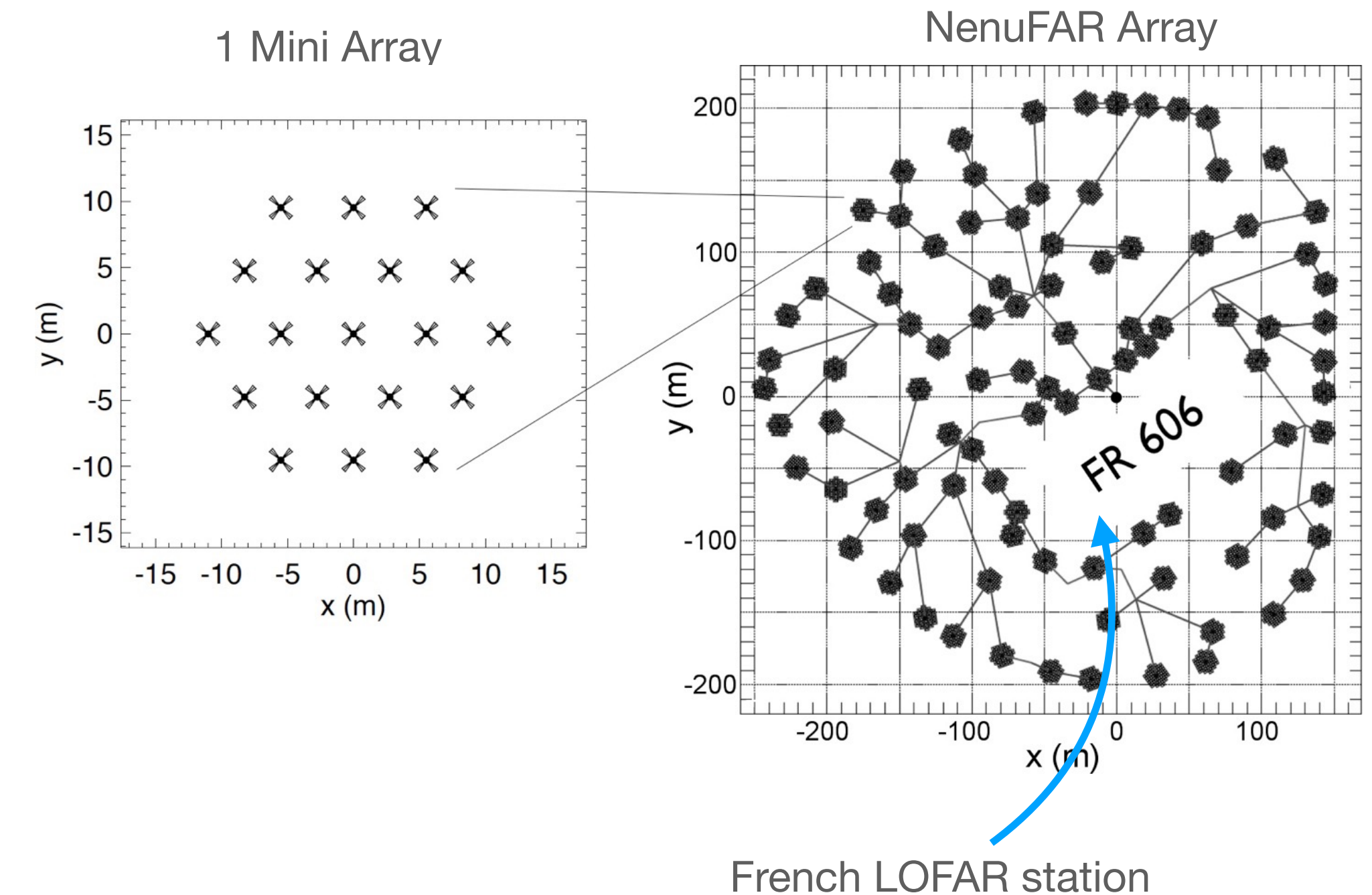
# NenuFAR configuration

## Array:

- Antennas grouped in **mini-arrays of 19** crossed-dipoles → SNR
- **Baselines from 400m to 3km** → angular resolution
- Up to **88000m<sup>2</sup>** of collecting area

## Signals:

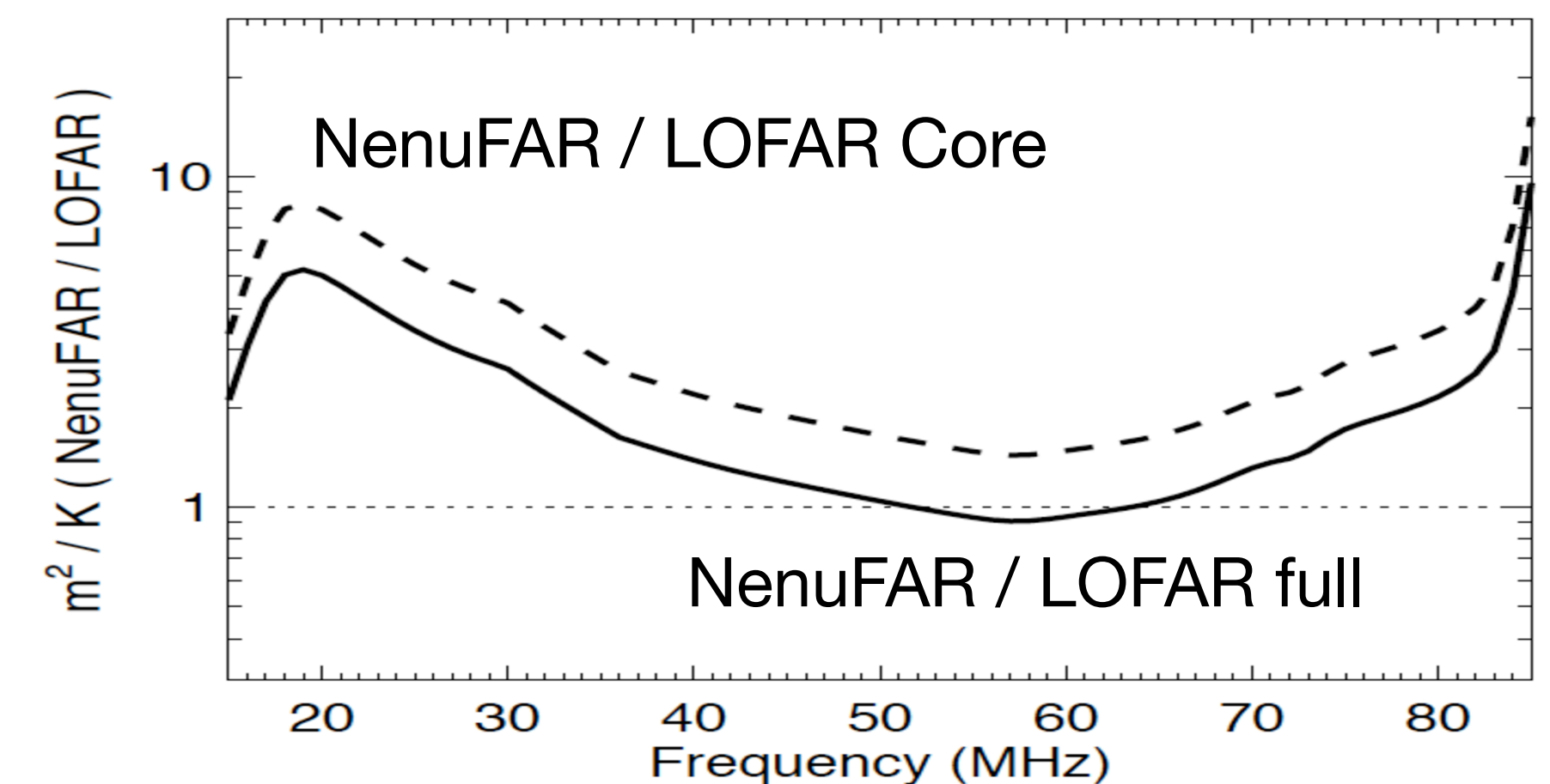
- Time-frequency resolution → **df~195kHz** and **dt~5μs**
- With channelisation **df->3kHz** with **dt~1ms** → very fine spectral resolution
- Waveforms at **5ns** time resolution



Can operate in 4 distinct modes:

- **standalone beam former** → FRB observation
- capturing waveform → transient buffer
- standalone imager
- Upgraded LOFAR station (low frequency)

**NenuFAR has been designed to reach the highest sensitivity at lowest frequencies**



# NenuFAR activities

---

|                   |      |                                      |
|-------------------|------|--------------------------------------|
| Long Term Program | LT01 | Cosmic Dawn                          |
|                   | LT02 | Exoplanets & Stars                   |
|                   | LT03 | Pulsars                              |
|                   | LT04 | Transients                           |
|                   | LT05 | Fast Radio Bursts                    |
|                   | LT06 | Planetary Lightning                  |
|                   | LT07 | Jupiter joint studies                |
|                   |      |                                      |
|                   | LT09 | Galaxies                             |
|                   | LT10 | Radio recombination lines            |
|                   | LT11 | Sun                                  |
|                   | LT12 | Radio Gamma                          |
|                   | LT13 | SETI                                 |
| Research Program  | RP1A | Faraday tomography of 3C196 field    |
|                   | RP1B | NenuFAR Low-Frequency Sky Survey     |
|                   | RP1C | Free-free absorption in Cassiopeia A |
|                   | SP16 | Student training                     |
|                   | SP17 | Radio-Amateurs                       |



# NenuFAR activities

---

Long Term Program

LT01

Cosmic Dawn

LT02

Exoplanets & Stars

LT03

Pulsars

LT04

Transients

LT05

Fast Radio Bursts

LT06

Planetary Lightning

LT07

Jupiter joint studies

LT09

Galaxies

LT10

Radio recombination lines

LT11

Sun

LT12

Radio Gamma

LT13

SETI

Research Program

RP1A

Faraday tomography of 3C196 field

RP1B

NenuFAR Low-Frequency Sky Survey

RP1C

Free-free absorption in Cassiopeia A

SP16

Student training

SP17

Radio-Amateurs



# NenuFAR activities

---

|                                     |                                      |                                      |                       |
|-------------------------------------|--------------------------------------|--------------------------------------|-----------------------|
| Long Term Program                   | LT01                                 | Cosmic Dawn                          |                       |
|                                     | LT02                                 | Exoplanets & Stars                   |                       |
|                                     | LT03                                 | Pulsars                              |                       |
|                                     | LT04                                 | Transients                           |                       |
|                                     | Work lead by <b>Valentin Decoene</b> | LT05                                 | Fast Radio Bursts     |
|                                     |                                      | LT06                                 | Planetary Lightning   |
|                                     |                                      | LT07                                 | Jupiter joint studies |
|                                     | LT09                                 | Galaxies                             |                       |
|                                     | LT10                                 | Radio recombination lines            |                       |
|                                     | LT11                                 | Sun                                  |                       |
| Work lead by <b>Richard Dallier</b> | LT12                                 | Radio Gamma                          |                       |
|                                     | LT13                                 | SETI                                 |                       |
| Research Program                    | RP1A                                 | Faraday tomography of 3C196 field    |                       |
|                                     | RP1B                                 | NenuFAR Low-Frequency Sky Survey     |                       |
|                                     | RP1C                                 | Free-free absorption in Cassiopeia A |                       |
|                                     | SP16                                 | Student training                     |                       |
|                                     | SP17                                 | Radio-Amateurs                       |                       |





# The Long Term LT05 program

---

**V.D.**, Zarka (LESIA), Ng (LPC2E), Mottez (LUTh), Voisin (LUTh), Griessmier (LPC2E), Cognard (LPC2E), Dallier (Subatech), Martin (Subatech)

Goal: discover and characterise FRB signals at low frequency or derive strong constraints

# The Long Term LT05 program

---

V.D., Zarka (LESIA), Ng (LPC2E), Mottez (LUTh), Voisin (LUTh), Griessmier (LPC2E), Cognard (LPC2E), Dallier (Subatech), Martin (Subatech)

Goal: discover and characterise FRB signals at low frequency or derive strong constraints

**Observation strategy:**





# The Long Term LT05 program

---

V.D., Zarka (LESIA), Ng (LPC2E), Mottez (LUTh), Voisin (LUTh), Griessmier (LPC2E), Cognard (LPC2E), Dallier (Subatech), Martin (Subatech)

Goal: discover and characterise FRB signals at low frequency or derive strong constraints

## Observation strategy:

### Target selection:

- already observed FRBs
- repeating sources (mostly)
- observed at close frequencies  
(in the MHz range)
- close-by sources (low DM)

# The Long Term LT05 program

---

V.D., Zarka (LESIA), Ng (LPC2E), Mottez (LUTh), Voisin (LUTh), Griessmier (LPC2E), Cognard (LPC2E), Dallier (Subatech), Martin (Subatech)

Goal: discover and characterise FRB signals at low frequency or derive strong constraints

## Observation strategy:

### Target selection:

- already observed FRBs
- repeating sources (mostly)
- observed at close frequencies (in the MHz range)
- close-by sources (low DM)



### Simulation study:

- observation parameters
- data reduction
- burst search



# The Long Term LT05 program

V.D., Zarka (LESIA), Ng (LPC2E), Mottez (LUTh), Voisin (LUTh), Griessmier (LPC2E), Cognard (LPC2E), Dallier (Subatech), Martin (Subatech)

Goal: discover and characterise FRB signals at low frequency or derive strong constraints

## Observation strategy:

### Target selection:

- already observed FRBs
- repeating sources (mostly)
- observed at close frequencies (in the MHz range)
- close-by sources (low DM)

### Optimised observation parameters:

- beam forming mode (one beam with full array)
- source tracking
- commensal observation time dedicated to each target
- optimised frequency and time integration parameters

### Simulation study:

- observation parameters
- data reduction
- burst search





# The Long Term LT05 program

V.D., Zarka (LESIA), Ng (LPC2E), Mottez (LUTh), Voisin (LUTh), Griessmier (LPC2E), Cognard (LPC2E), Dallier (Subatech), Martin (Subatech)

Goal: discover and characterise FRB signals at low frequency or derive strong constraints

## Observation strategy:

### Target selection:

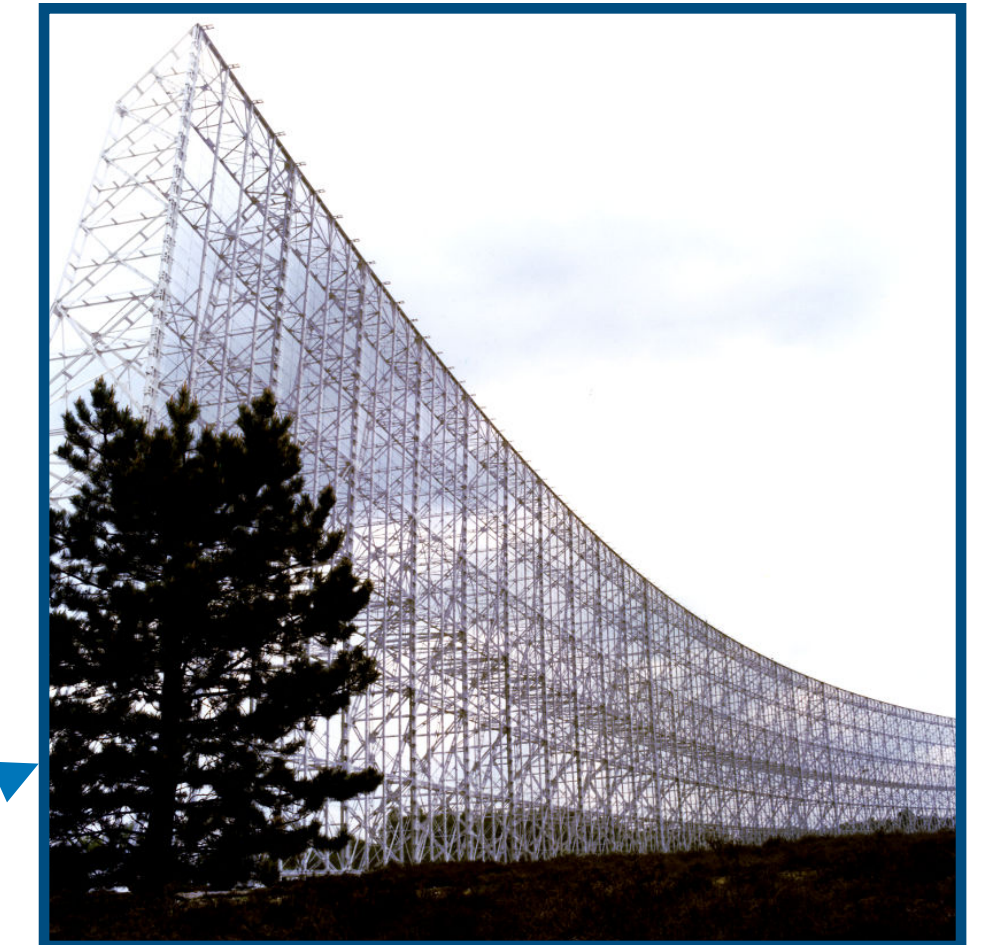
- already observed FRBs
- repeating sources (mostly)
- observed at close frequencies (in the MHz range)
- close-by sources (low DM)

### Optimised observation parameters:

- beam forming mode (one beam with full array)
- source tracking
- commensal observation time dedicated to each target
- optimised frequency and time integration parameters

### Simulation study:

- observation parameters
- data reduction
- burst search



**Joint observations:**  
when possible with the NRT  
at higher frequencies  
(if observable target)

**+LOFAR survey:**  
multi-wavelength campaign  
for FRB180916



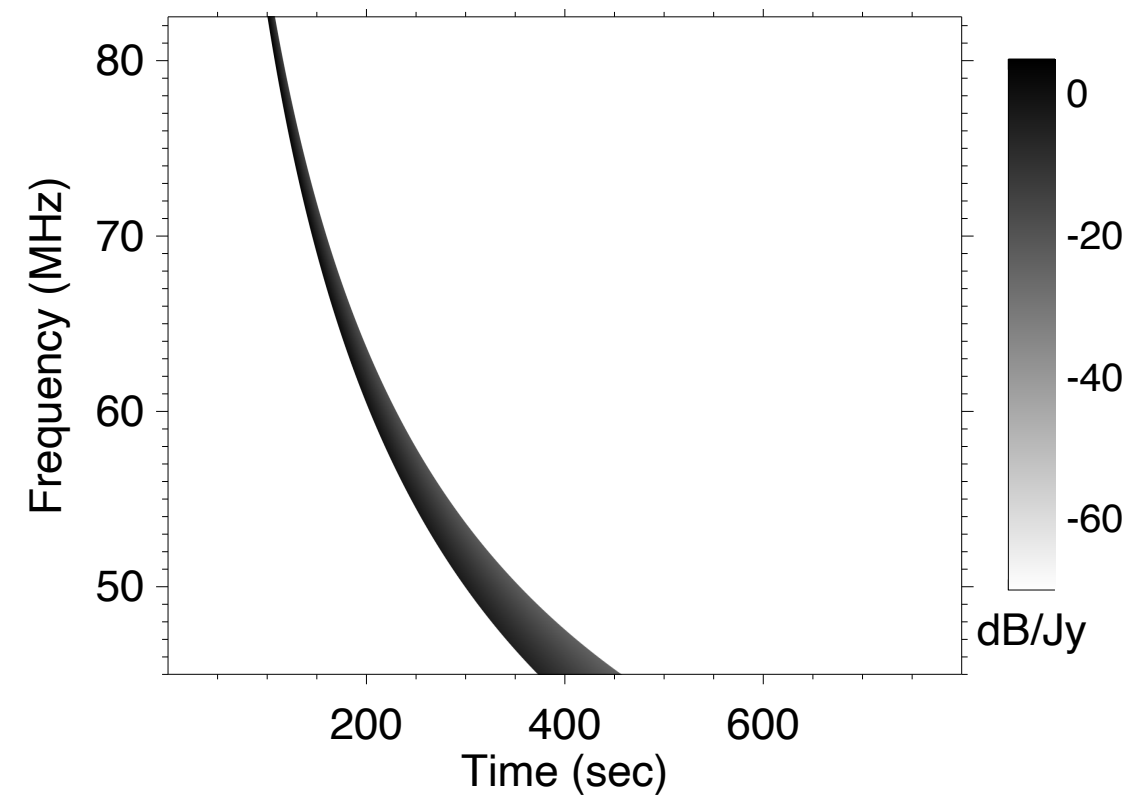


# Simulation study

**Idea:** simulate FRB signals of **already observed sources** with prior knowledge on the parameters to extrapolate at low frequency with the NenuFAR telescope

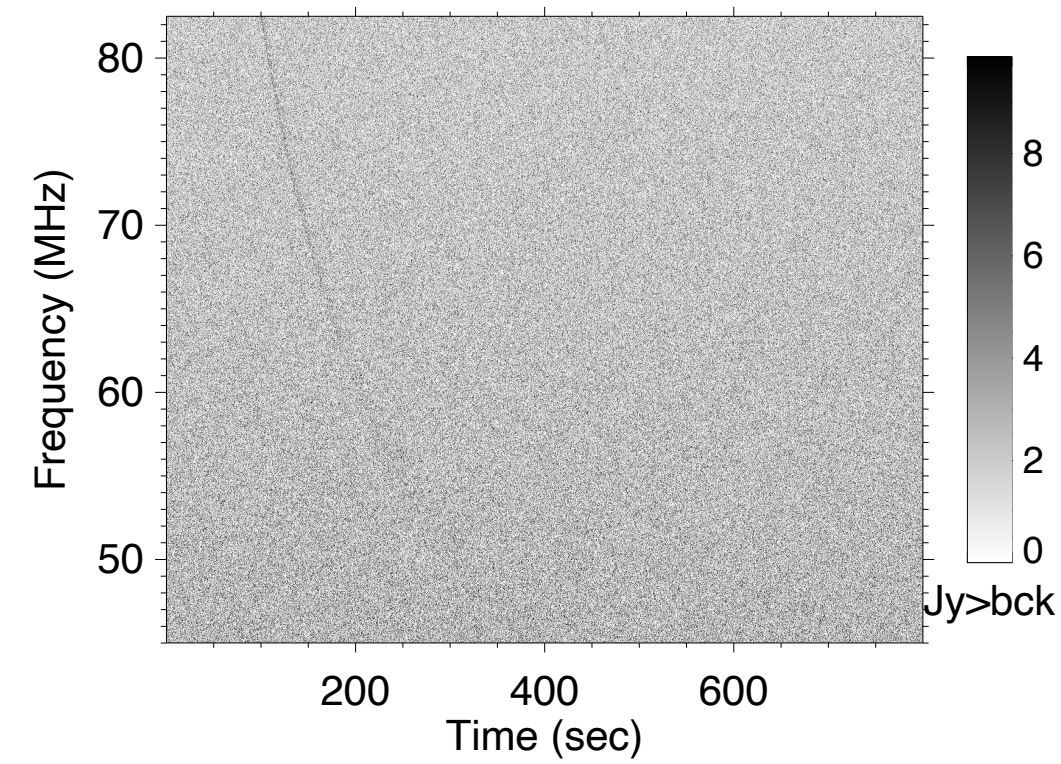
**Method:**

(1)



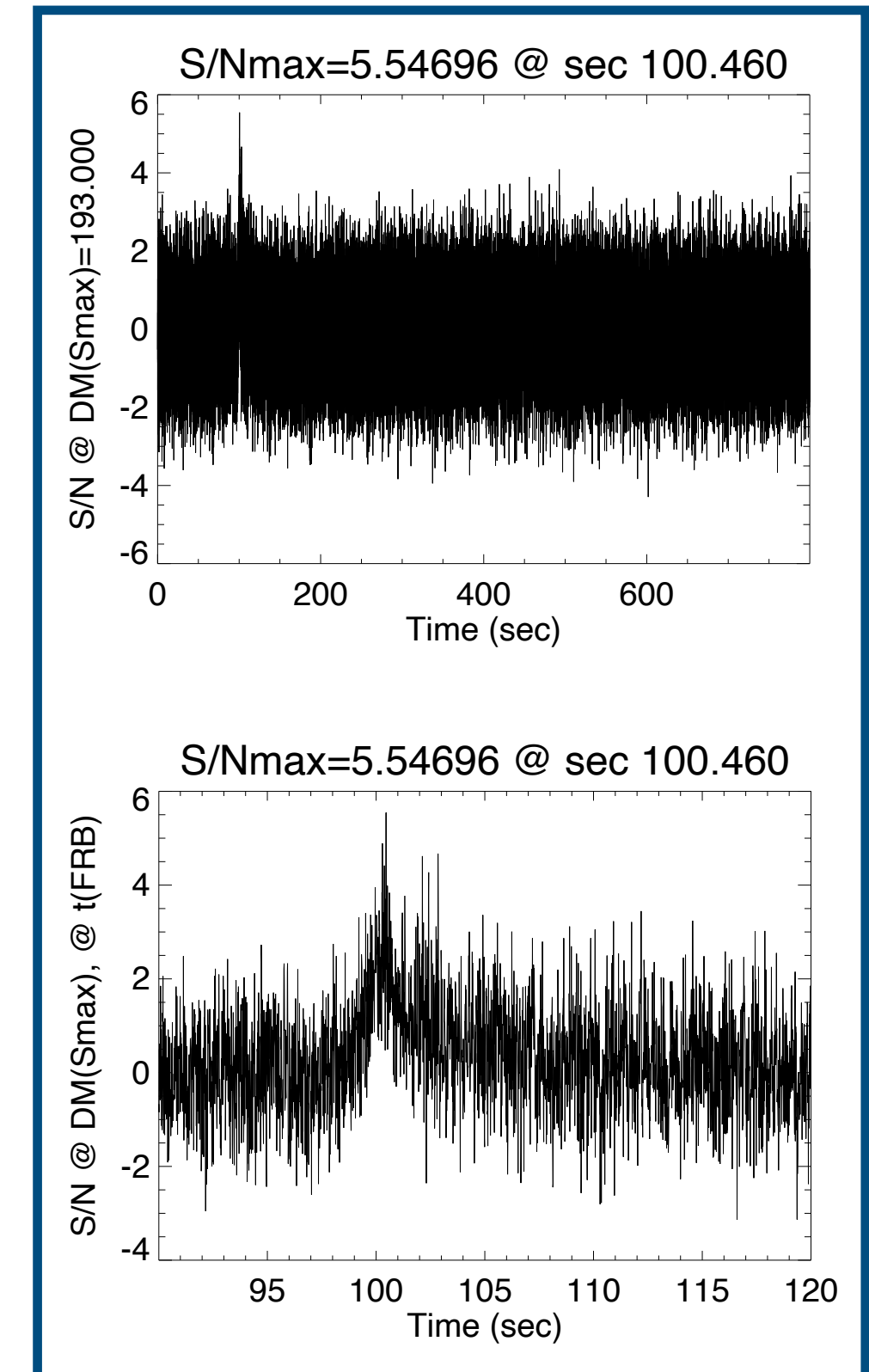
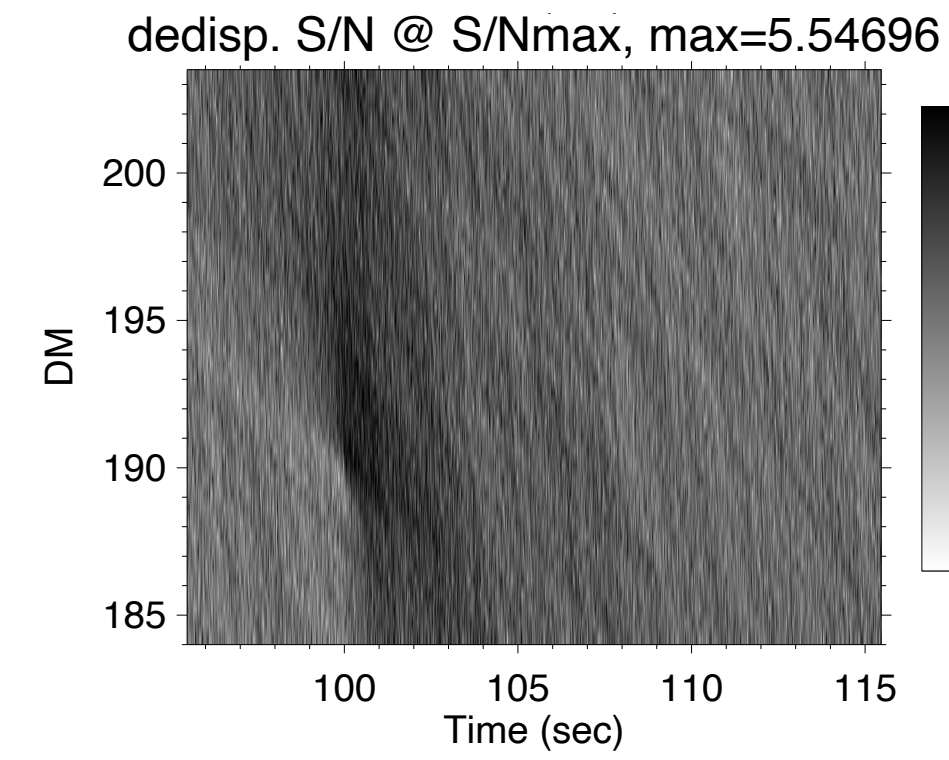
Simulate a FRB dynamical spectrum

(2)



Dilute the signal in the sky background

(3)



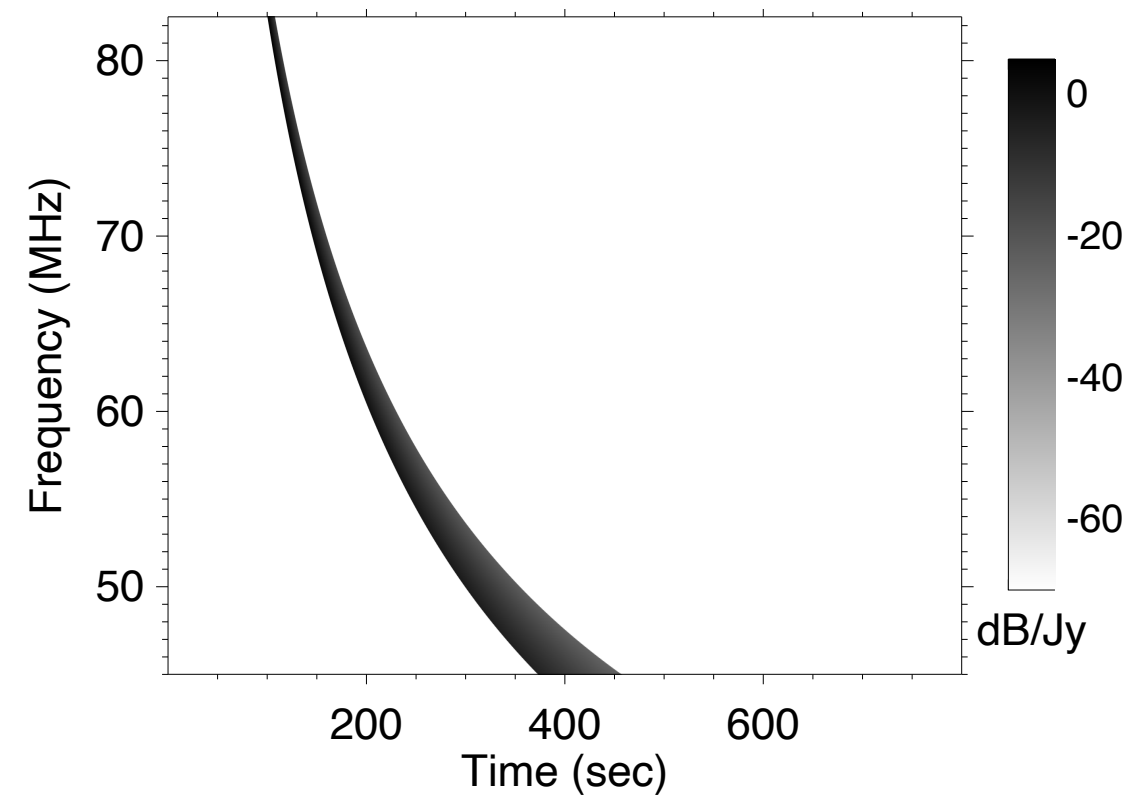


# Simulation study

**Idea:** simulate FRB signals of **already observed sources** with prior knowledge on the parameters to extrapolate at low frequency with the NenuFAR telescope

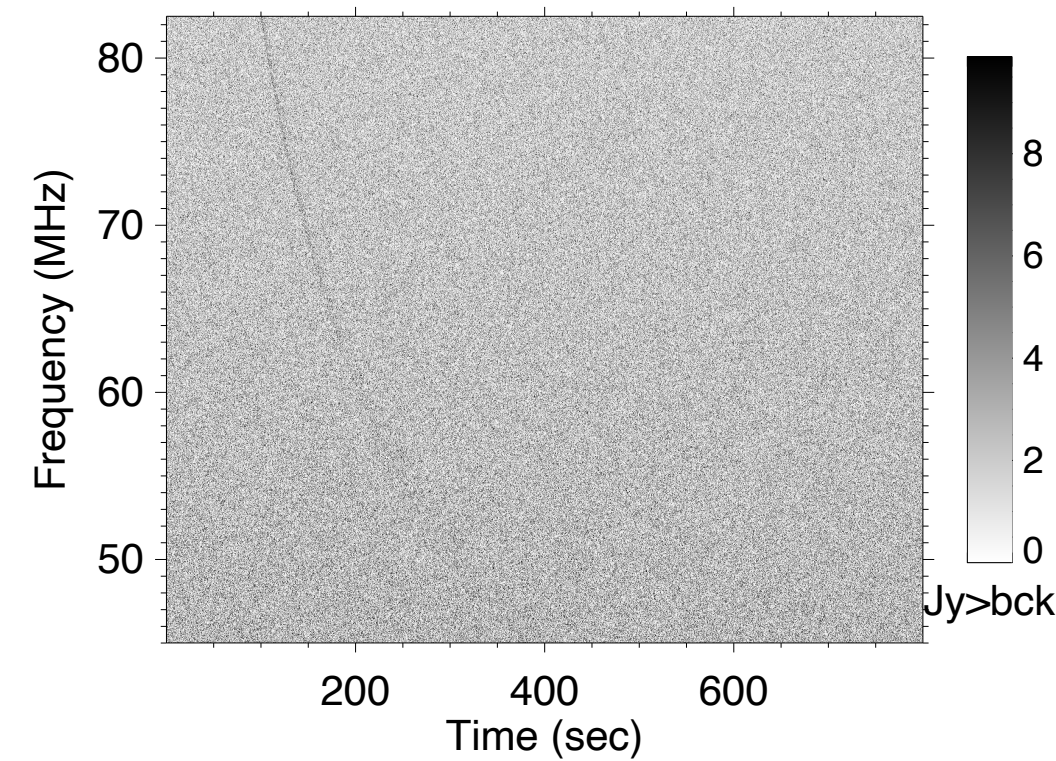
## Method:

(1)



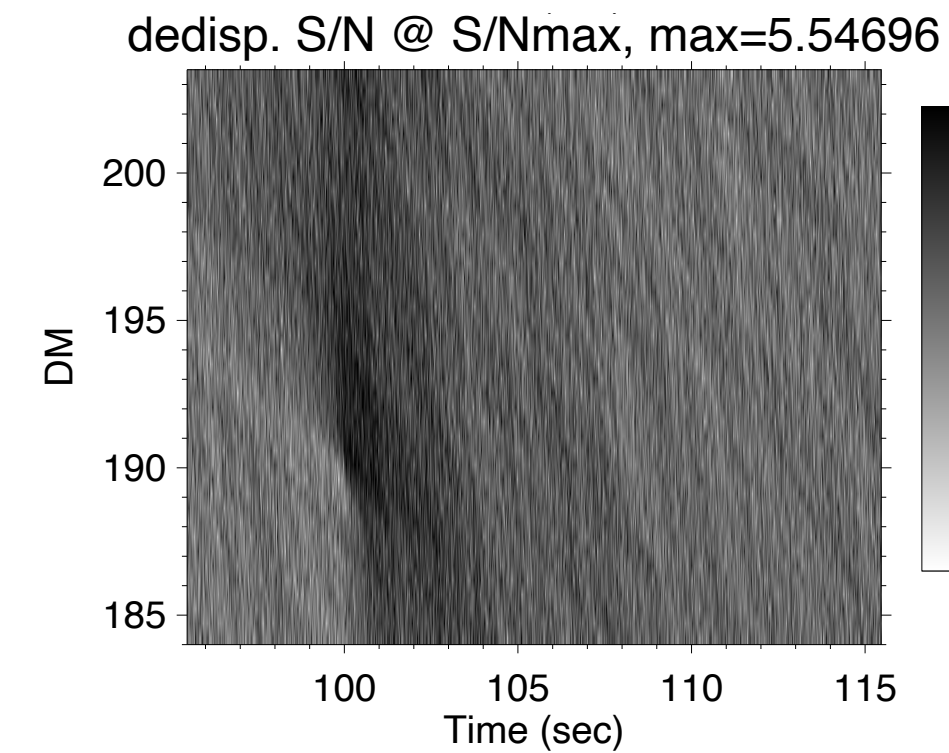
Simulate a FRB dynamical spectrum

(2)

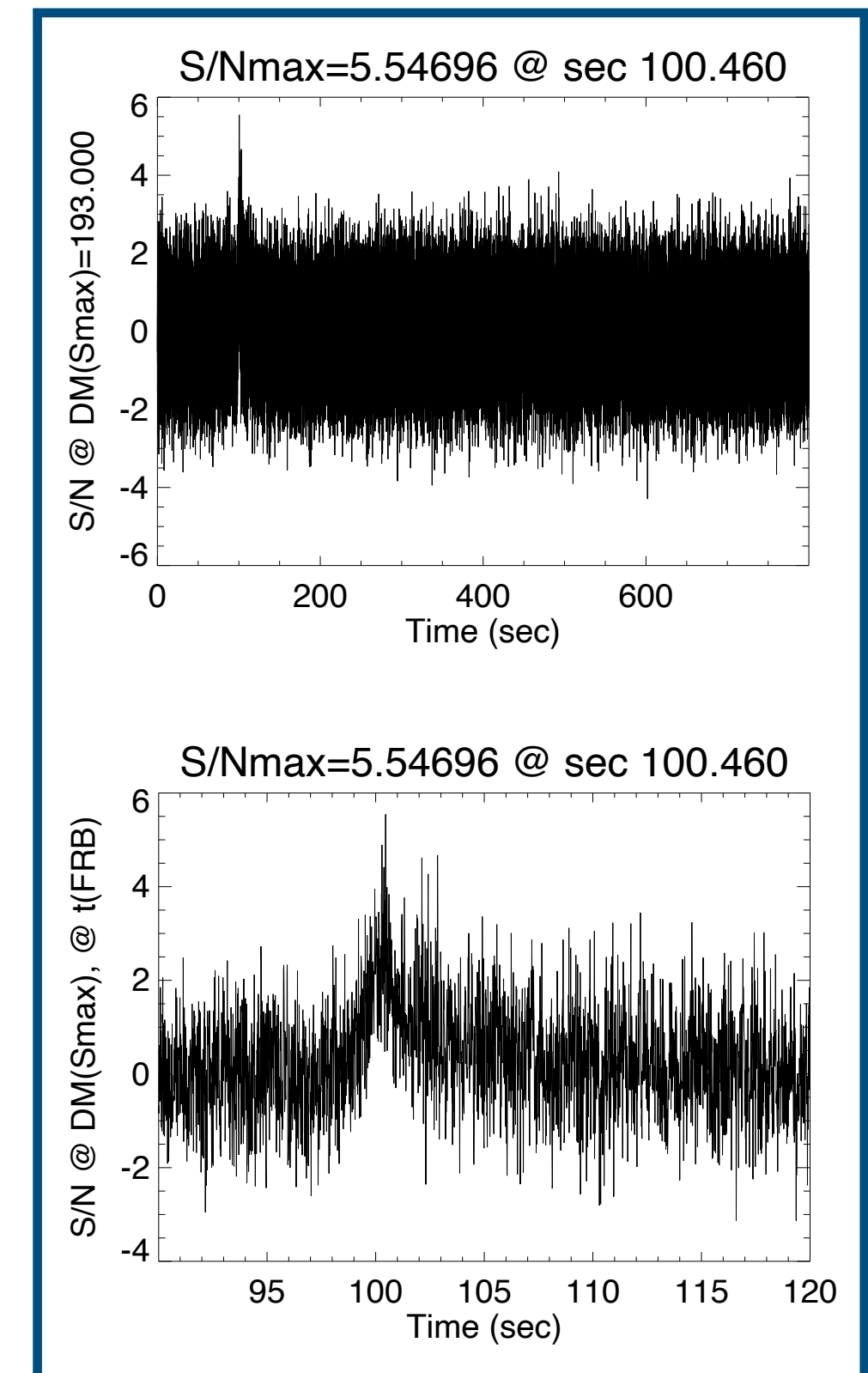


Dilute the signal in the sky background

(3)



Proceed to a parametric search of the DM within the time and frequency resolution parameters of NenuFAR



Prior knowledge of the DM allows to reduce significantly the parametric search

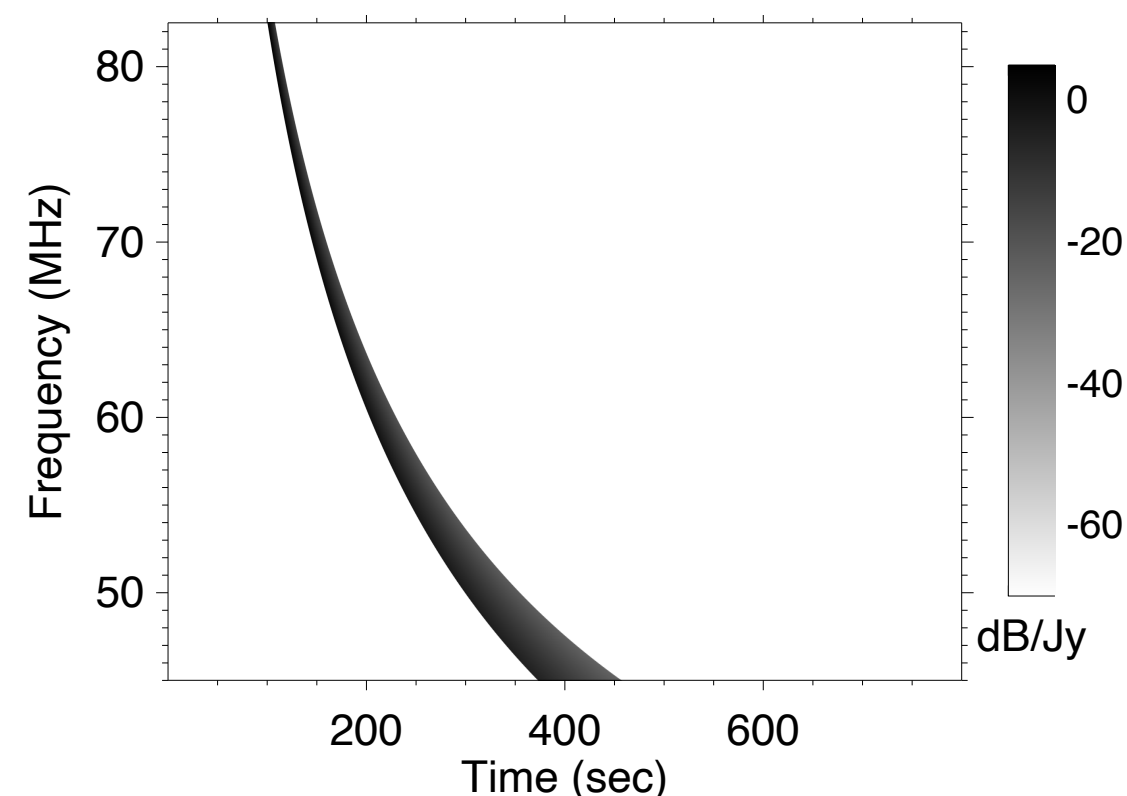


# Simulation study

**Idea:** simulate FRB signals of **already observed sources** with prior knowledge on the parameters to extrapolate at low frequency with the NenuFAR telescope

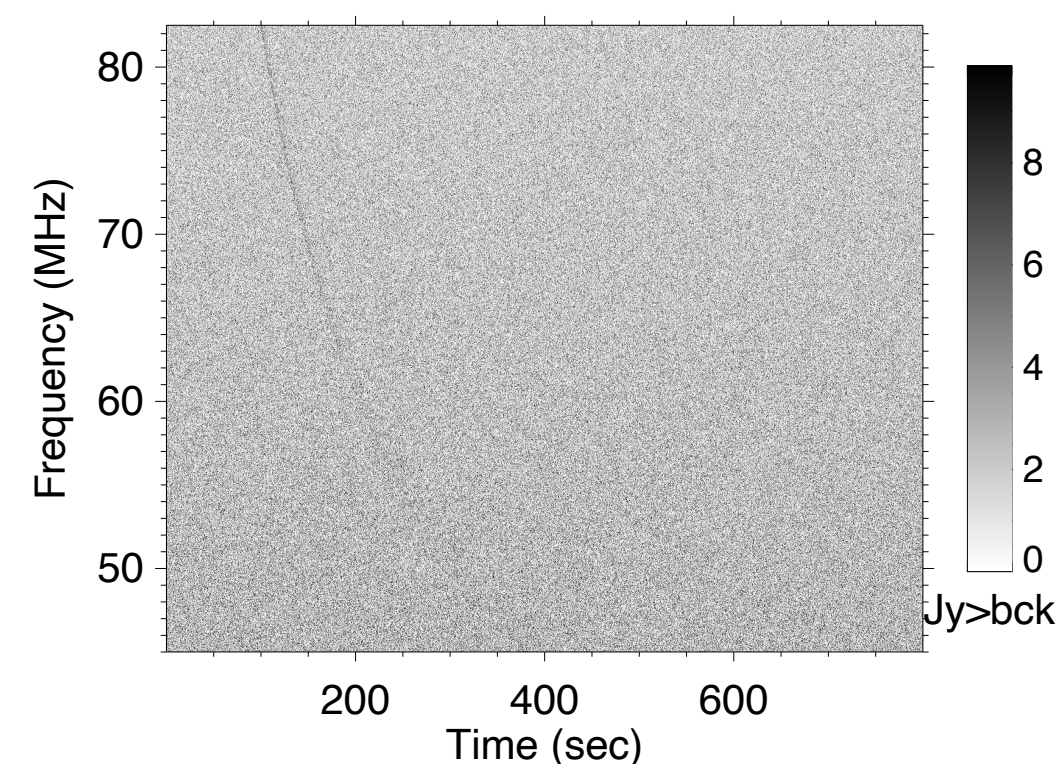
## Method:

(1)



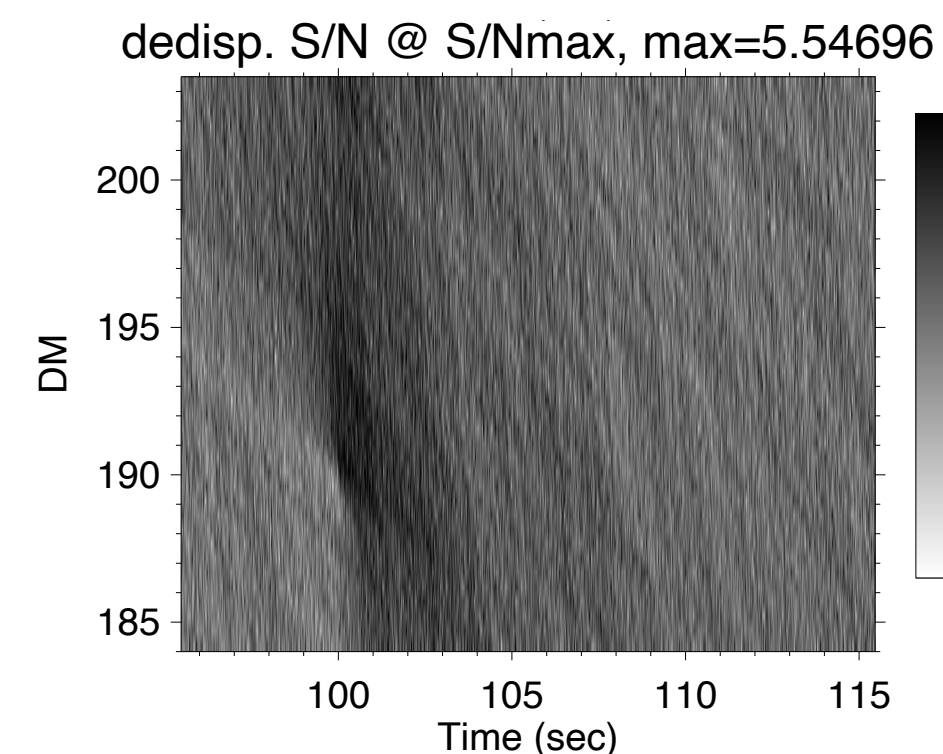
Simulate a FRB dynamical spectrum

(2)

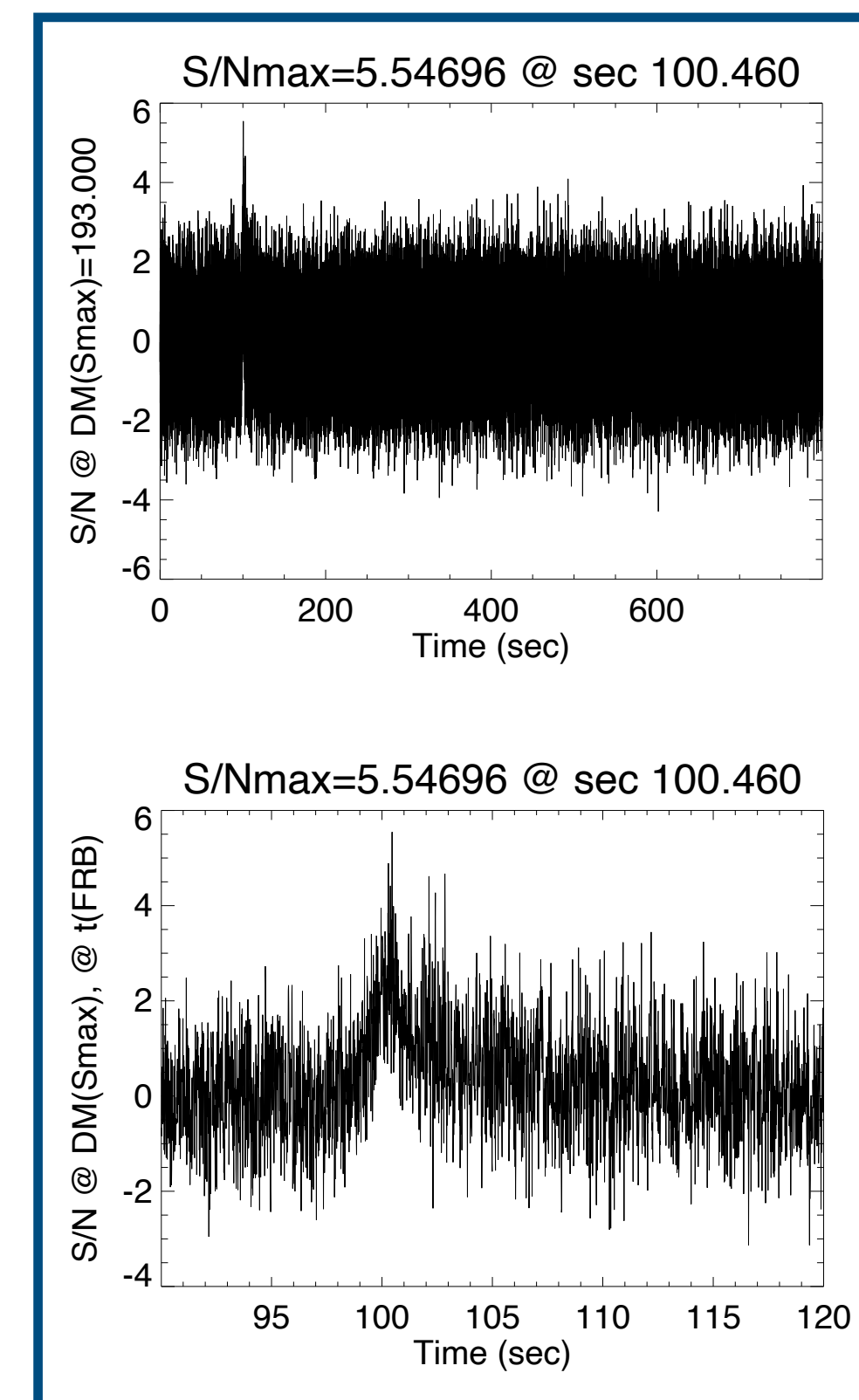


Dilute the signal in the sky background

(3)



Proceed to a parametric search of the DM within the time and frequency resolution parameters of NenuFAR



Maximise the SNR

Prior knowledge of the DM allows to reduce significantly the parametric search

Fine tuning of the resolution parameters of NenuFAR

The optimal parameter set used is given by a 1.5kHz frequency resolution and a 21ms integration time to combine flexibility for the analysis and storage gain

# Pre-processing and data reduction strategy

**Goals:** remove noise signals from external interferences and instrumental effects and reduce as much as possible the data volume

**Motivation:** the data rate at the output of NenuFAR given the resolution parameters chosen is about 60GB/h → reaching a few tens of TBs per semester!

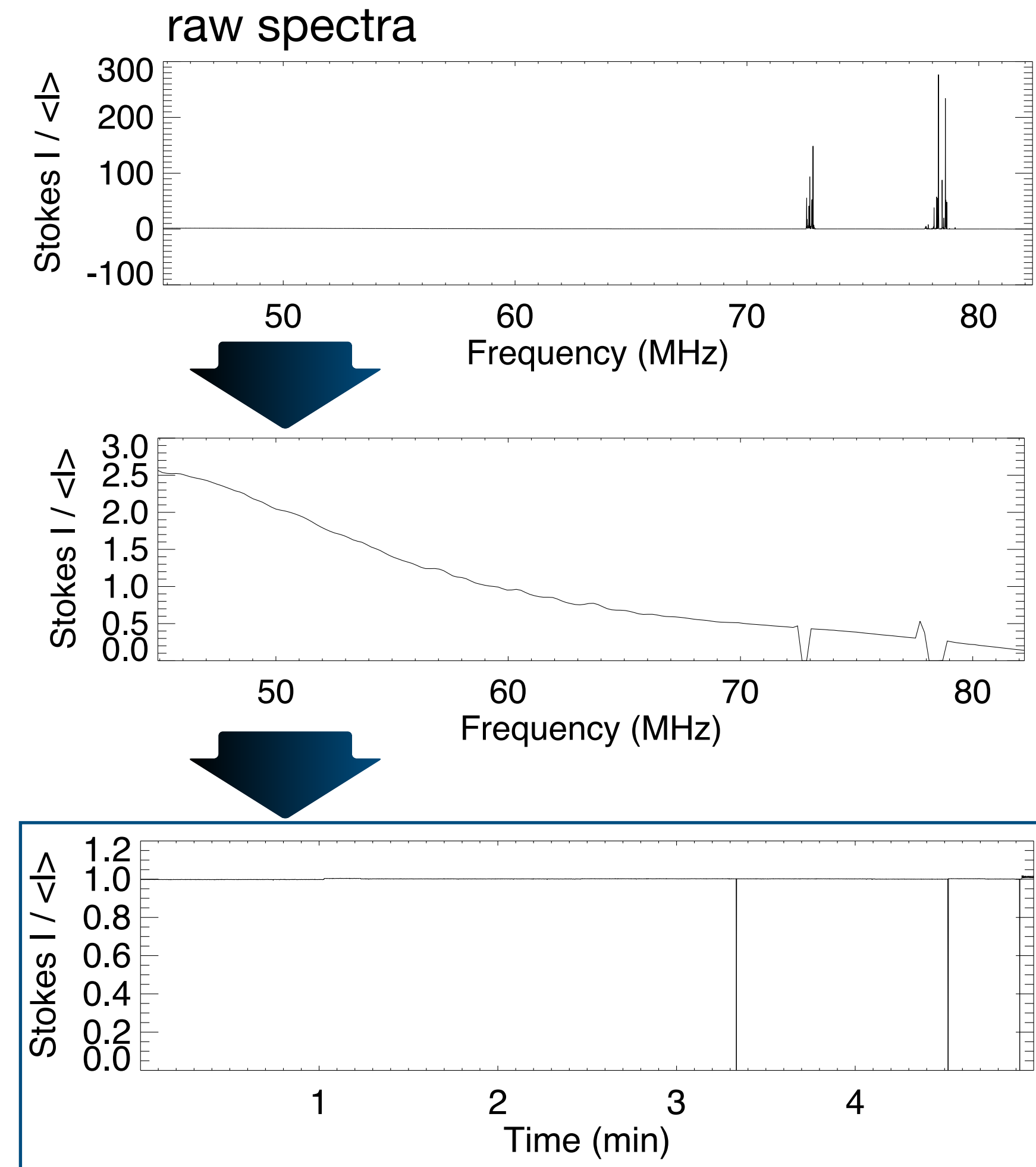
## Method:

data cleaning

1. identify and remove Radio Frequency Interferences (RFI):
  1. mask frequency channels fully polluted
  2. proceed to a search in the time integrated plane for frequency spikes
  3. proceed to a search in the frequency integrated plane for narrow broad band emissions
  4. correct for time-frequency slopes

2. De-disperse the signal inside each channel at the expected DM (but not over all channels) and integrate channels up to 2-4 remaining channels
3. Additionally a post integration over time can be applied for a reduction of a factor 2

data reduction



clean spectra

Ongoing work: ~1500 hours of observations to be analysed



# Pre-processing and data reduction strategy

**Goals:** remove noise signals from external interferences and instrumental effects and reduce as much as possible the data volume

**Motivation:** the data rate at the output of NenuFAR given the resolution parameters chosen is about 60GB/h → reaching a few tens of TBs per semester!

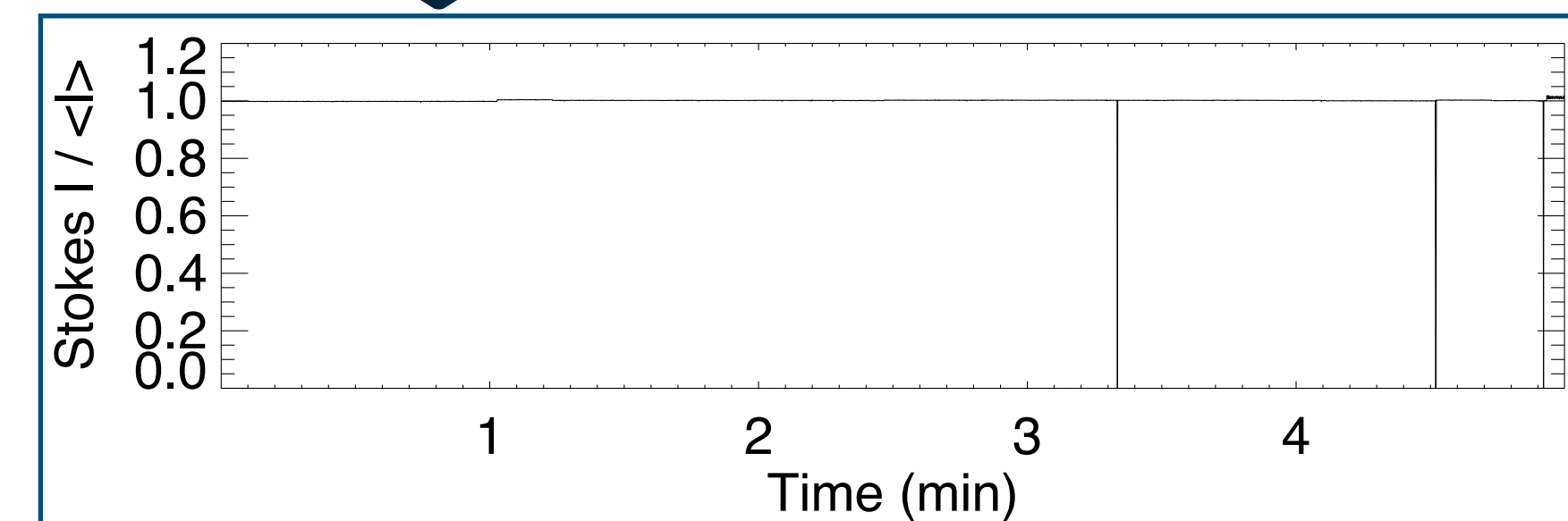
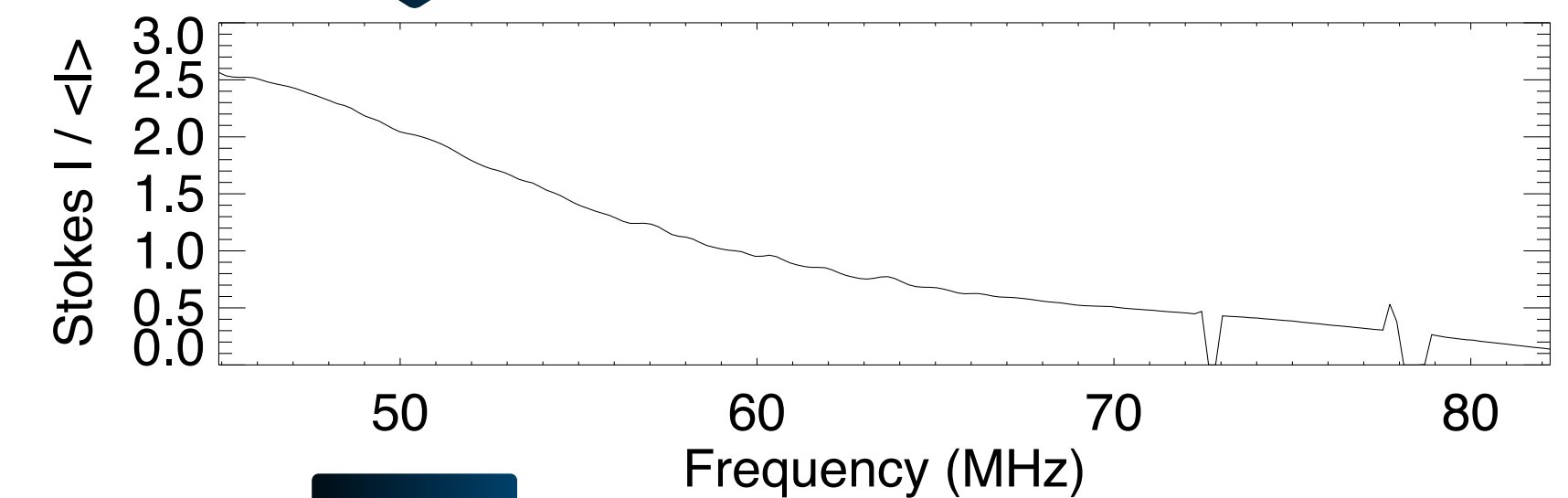
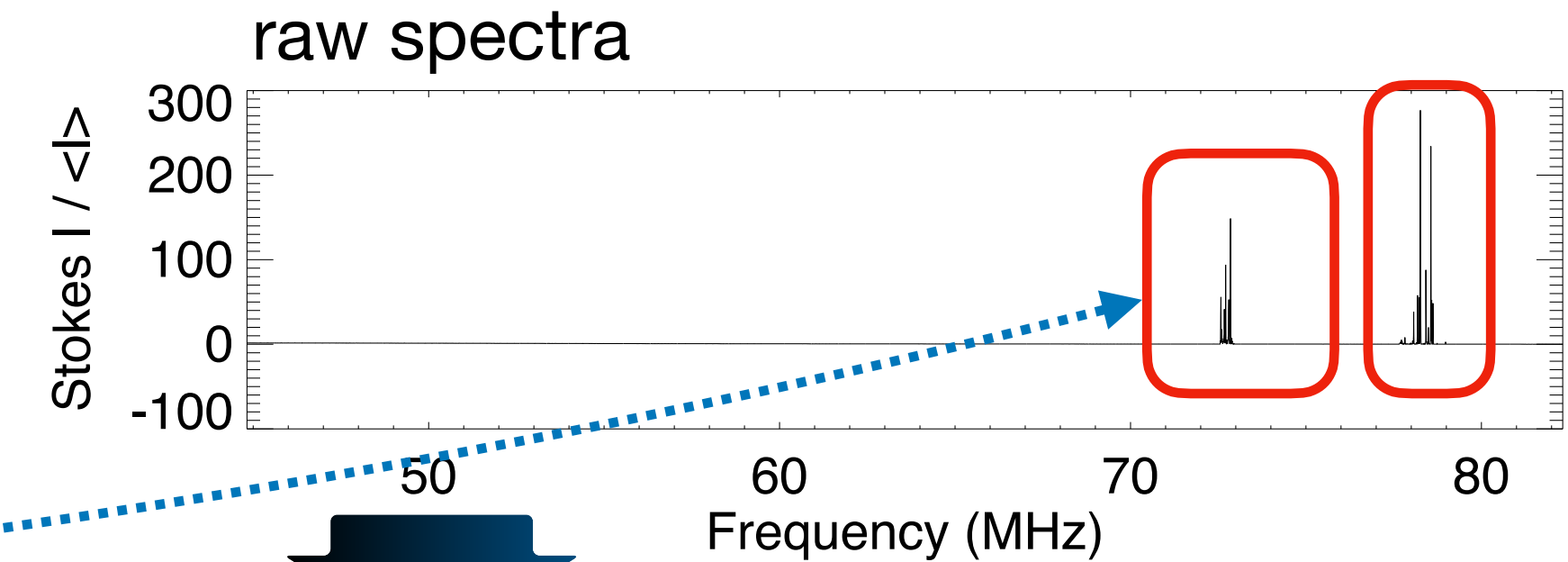
## Method:

data cleaning

1. identify and remove Radio Frequency Interferences (RFI):
  1. mask frequency channels fully polluted
  2. proceed to a search in the time integrated plane for frequency spikes
  3. proceed to a search in the frequency integrated plane for narrow broad band emissions
  4. correct for time-frequency slopes

data reduction

2. De-disperse the signal inside each channel at the expected DM (but not over all channels) and integrate channels up to 2-4 remaining channels
3. Additionally a post integration over time can be applied for a reduction of a factor 2



clean spectra

Ongoing work: ~1500 hours of observations to be analysed

# Pre-processing and data reduction strategy

**Goals:** remove noise signals from external interferences and instrumental effects and reduce as much as possible the data volume

**Motivation:** the data rate at the output of NenuFAR given the resolution parameters chosen is about 60GB/h → reaching a few tens of TBs per semester!

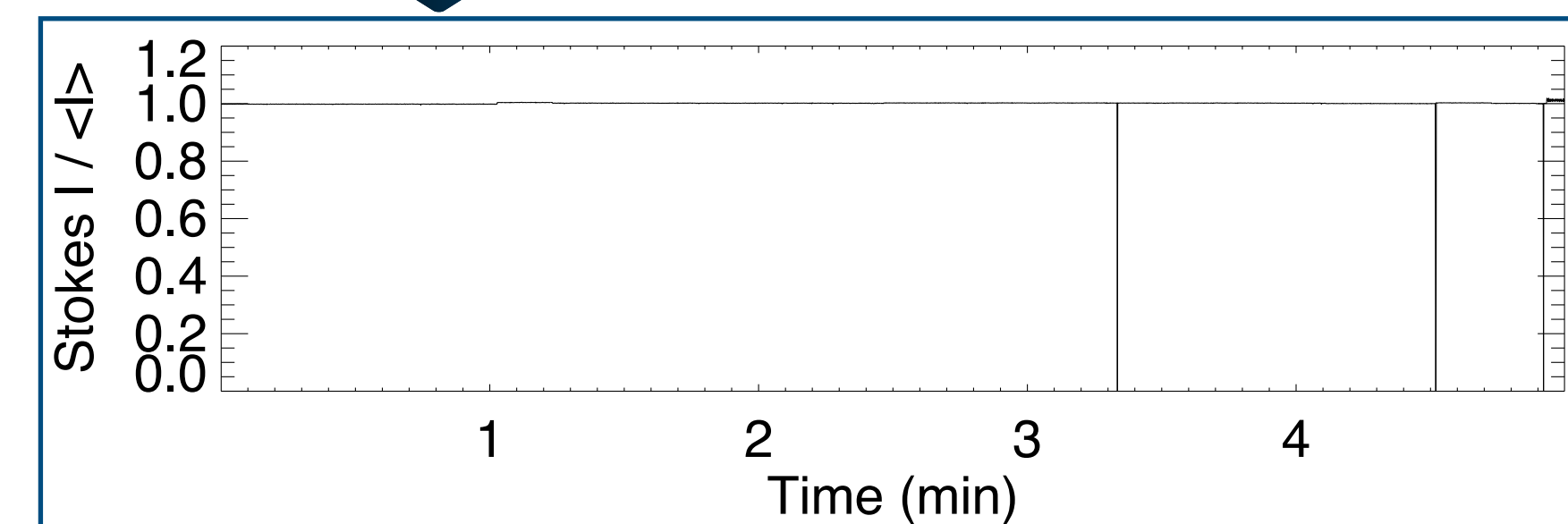
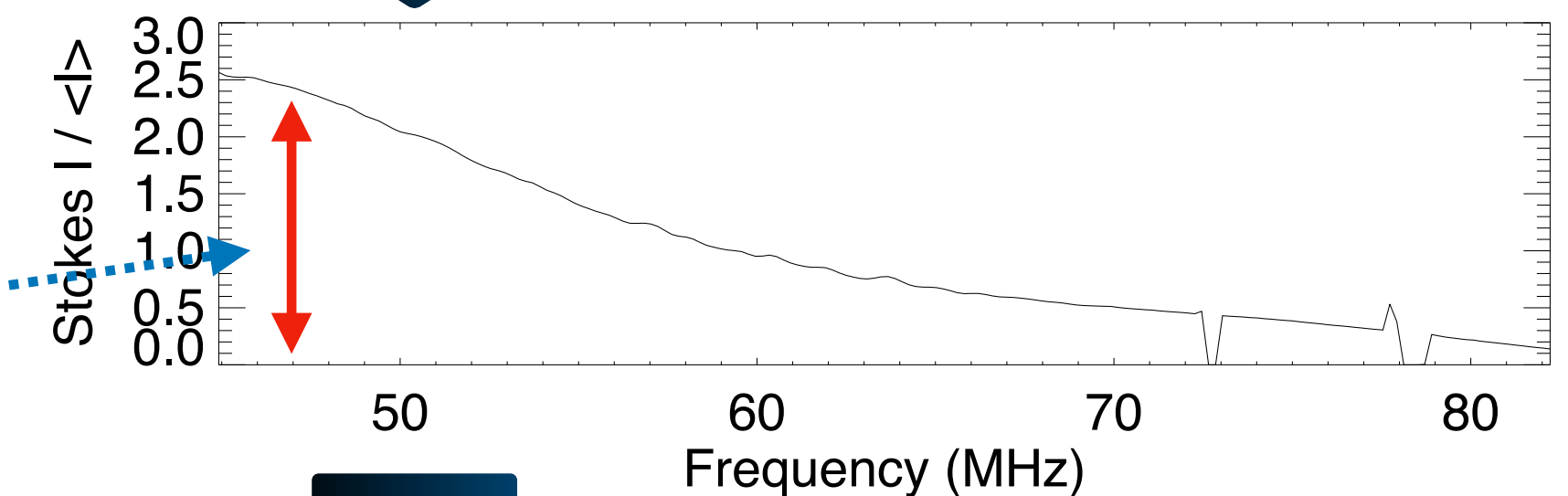
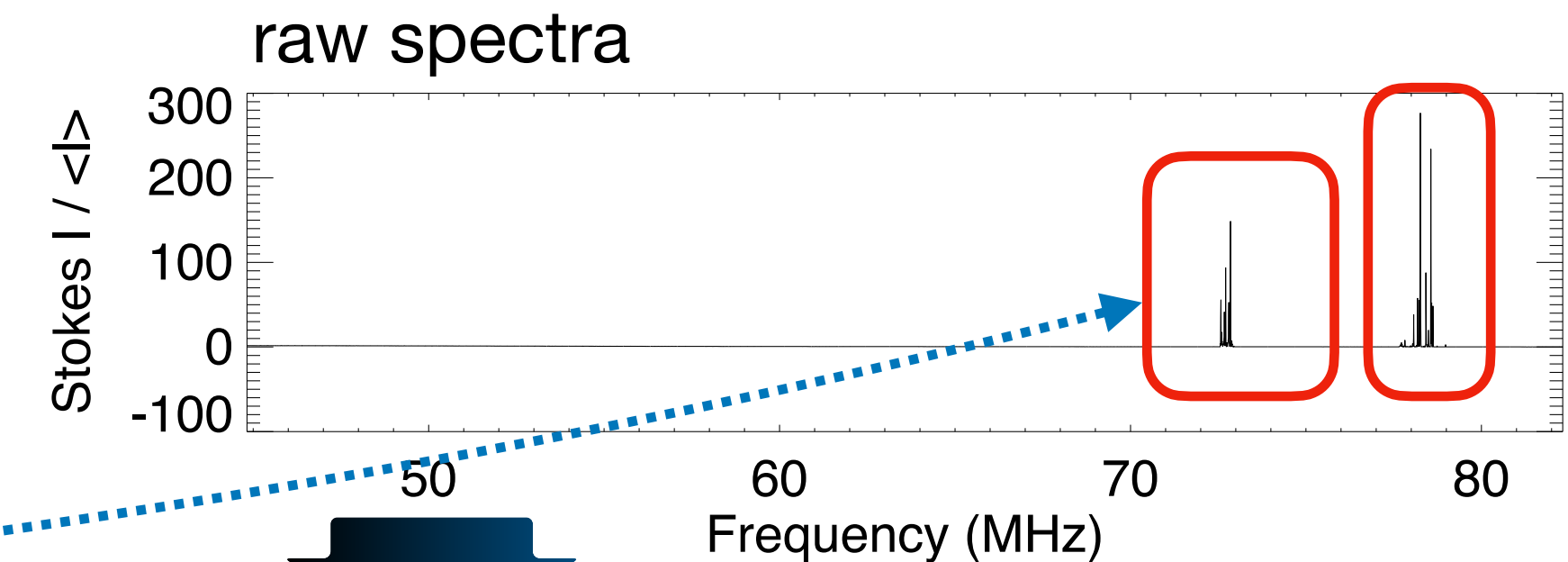
## Method:

data cleaning

1. identify and remove Radio Frequency Interferences (RFI):
  1. mask frequency channels fully polluted
  2. proceed to a search in the time integrated plane for frequency spikes
  3. proceed to a search in the frequency integrated plane for narrow broad band emissions
  4. correct for time-frequency slopes

data reduction

2. De-disperse the signal inside each channel at the expected DM (but not over all channels) and integrate channels up to 2-4 remaining channels
3. Additionally a post integration over time can be applied for a reduction of a factor 2



clean spectra

Ongoing work: ~1500 hours of observations to be analysed

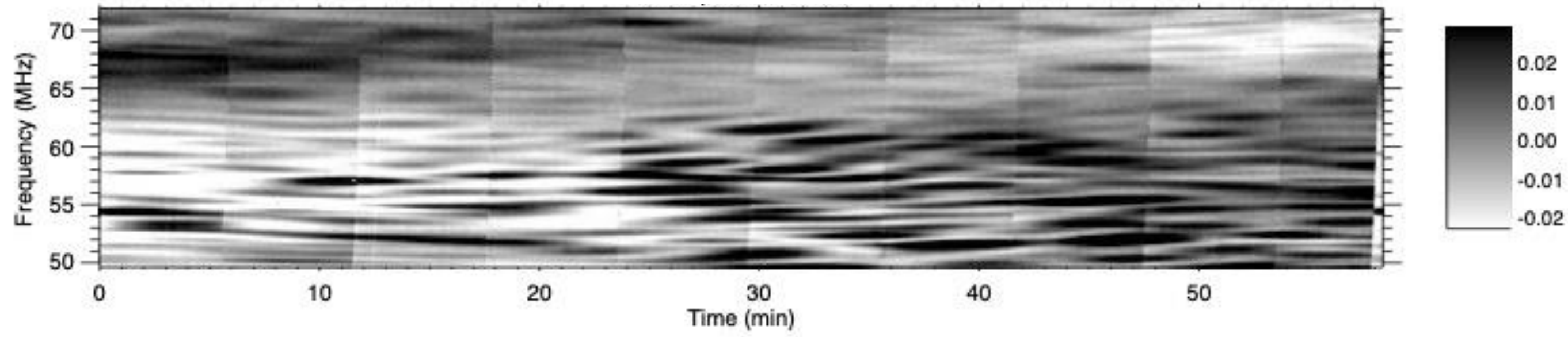


# Analysis method on pulsar observations

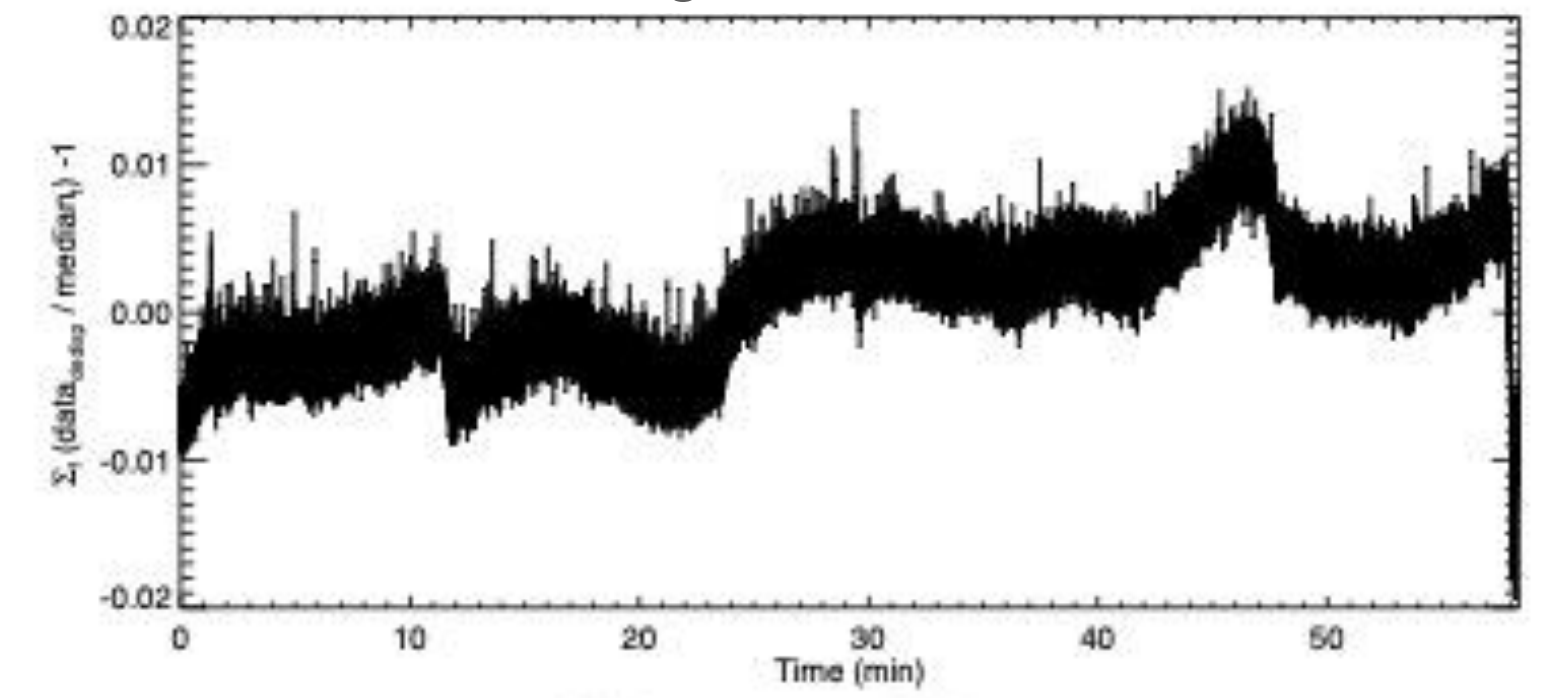
The idea is to clean the time-frequency data in the Fourier domain

test on observations PSRB0329+54

time-frequency plane



integrated time series

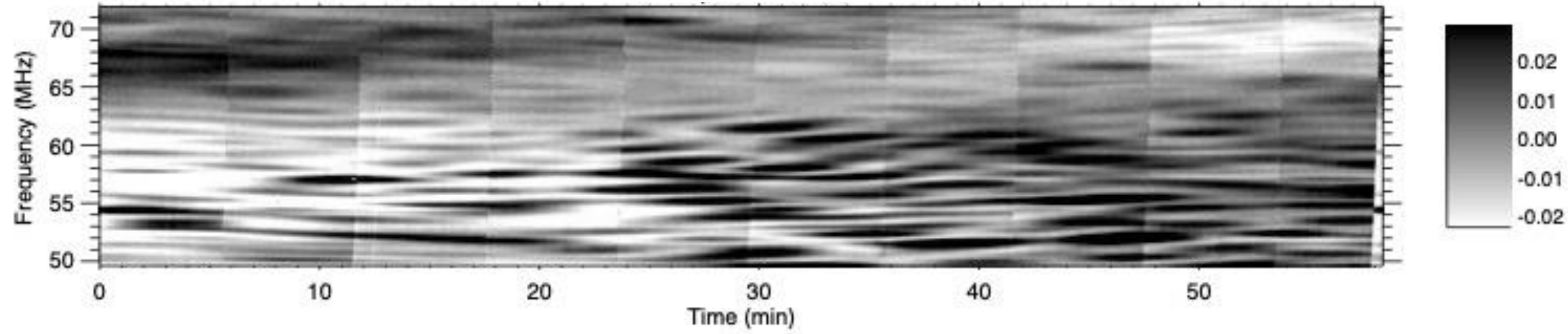


# Analysis method on pulsar observations

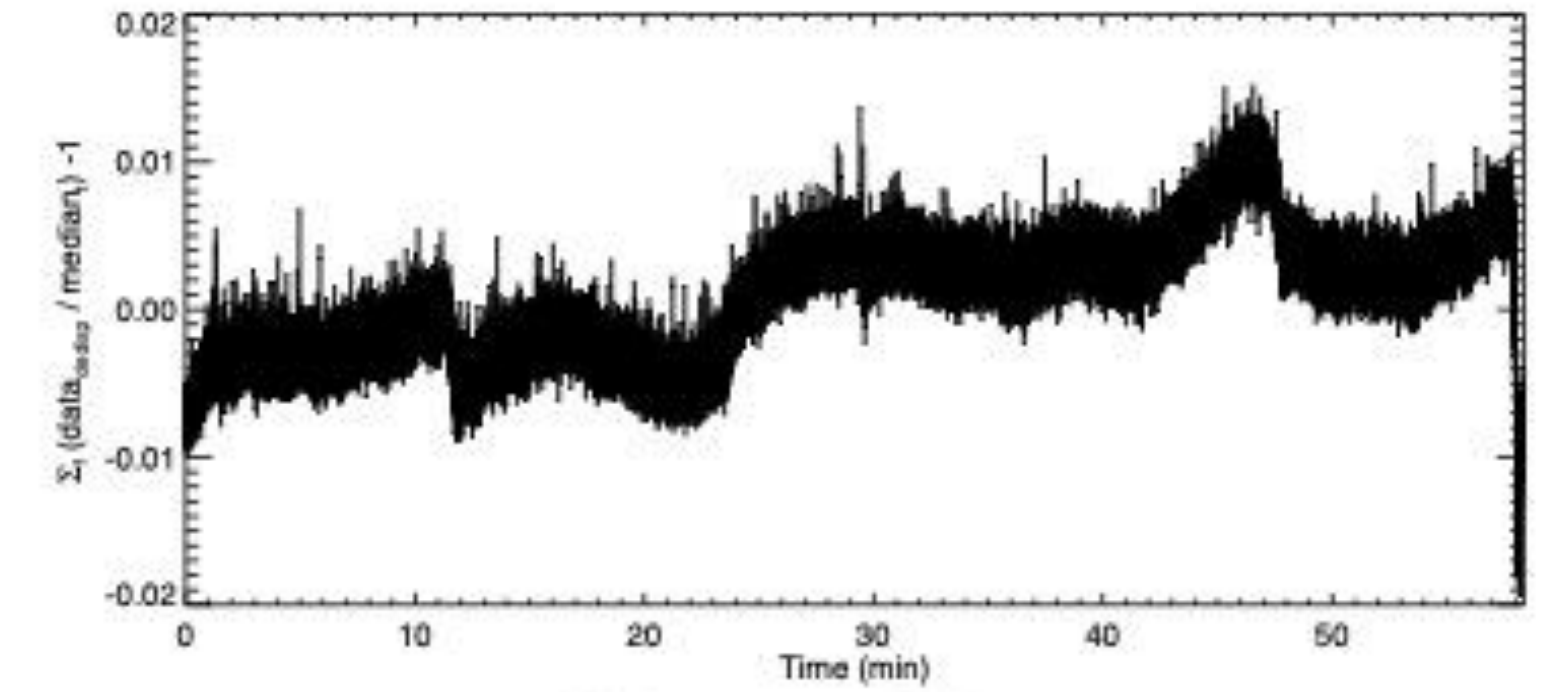
The idea is to clean the time-frequency data in the Fourier domain

test on observations PSRB0329+54

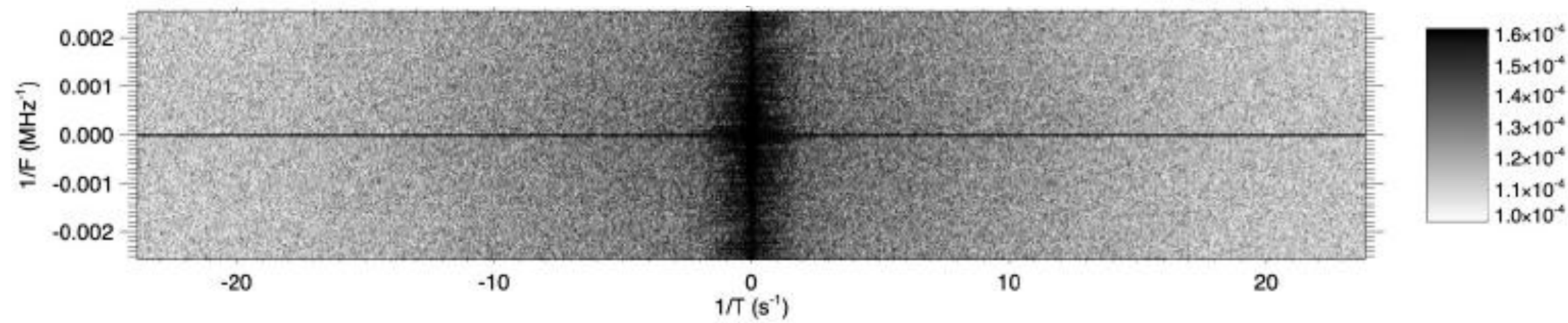
time-frequency plane



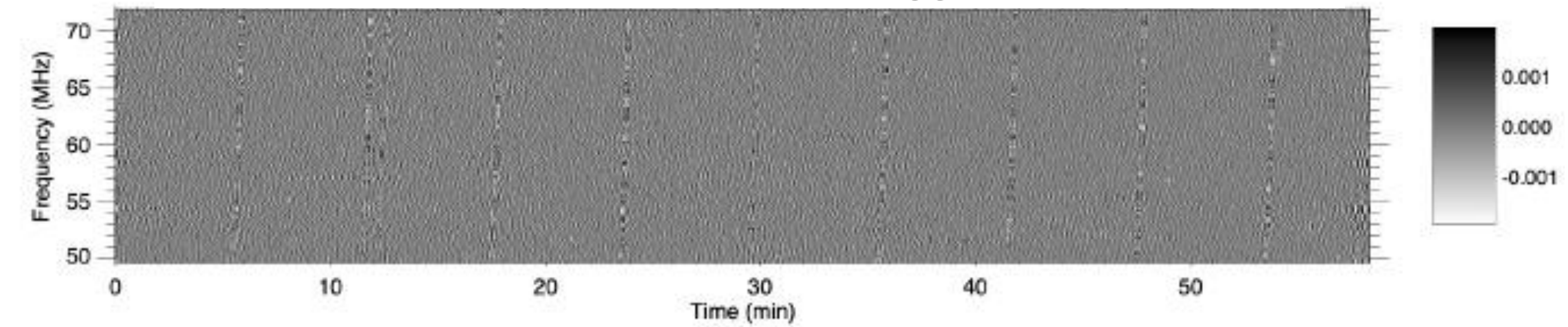
integrated time series



2D Fourier plane of the power spectrum



inverse 2D Fourier transform of the flagged power spectrum



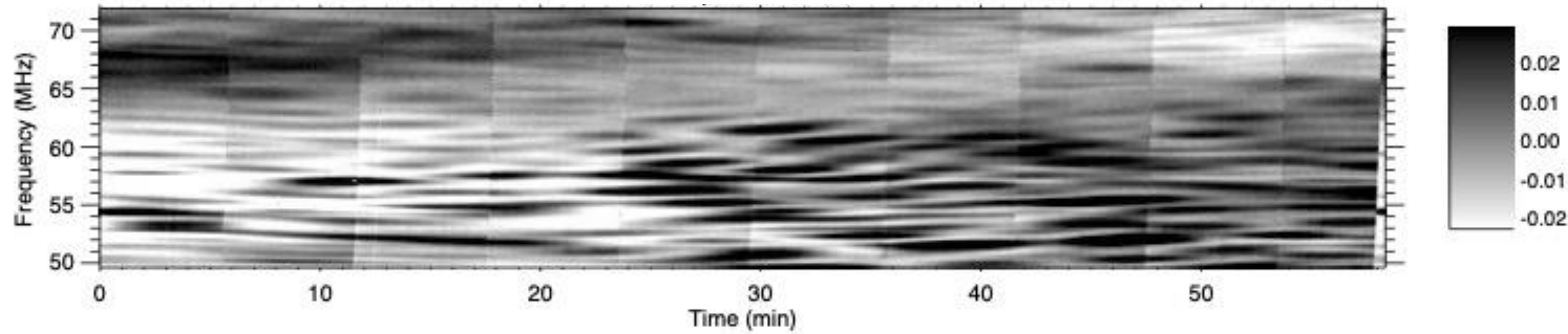


# Analysis method on pulsar observations

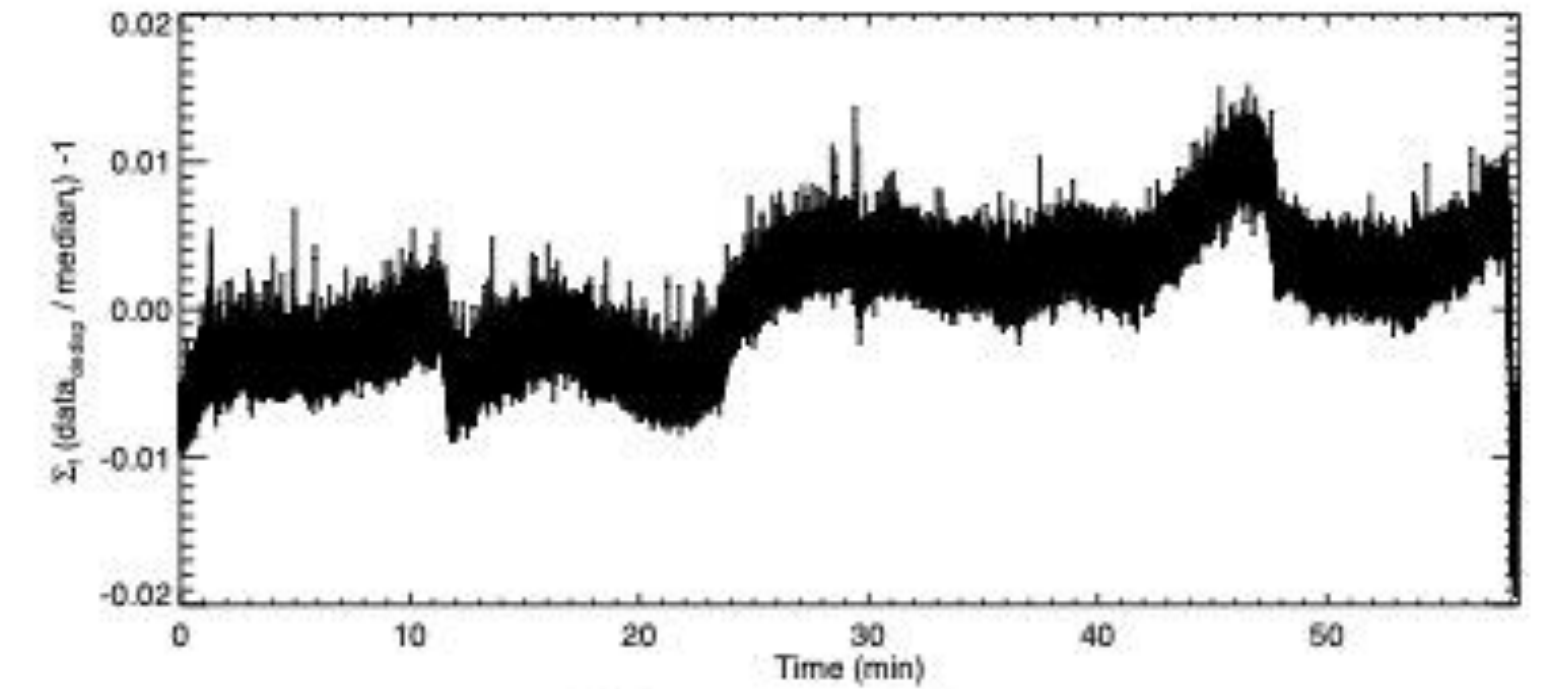
The idea is to clean the time-frequency data in the Fourier domain

test on observations PSRB0329+54

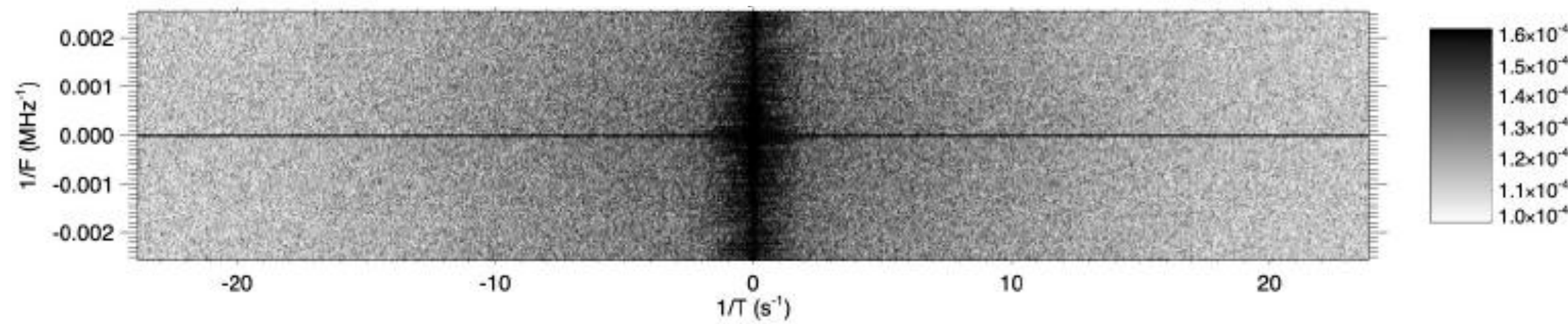
time-frequency plane



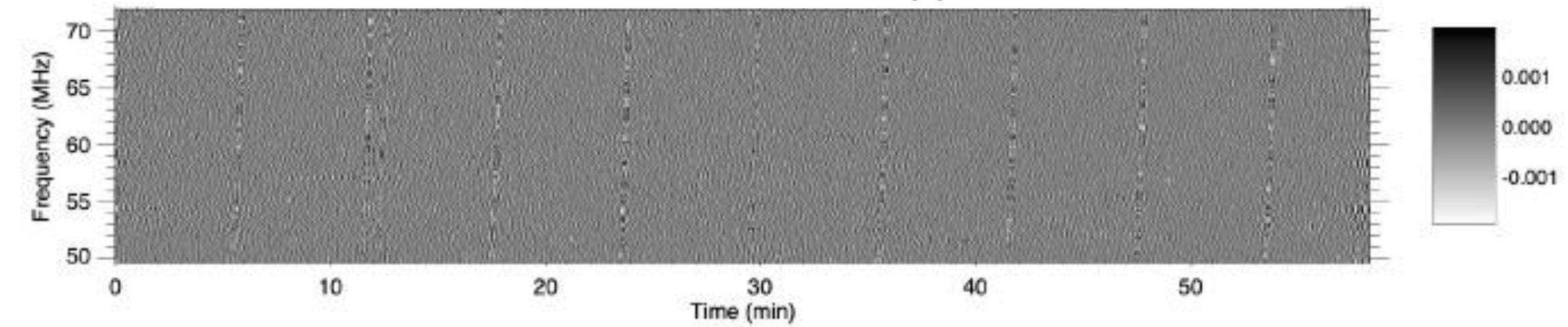
integrated time series



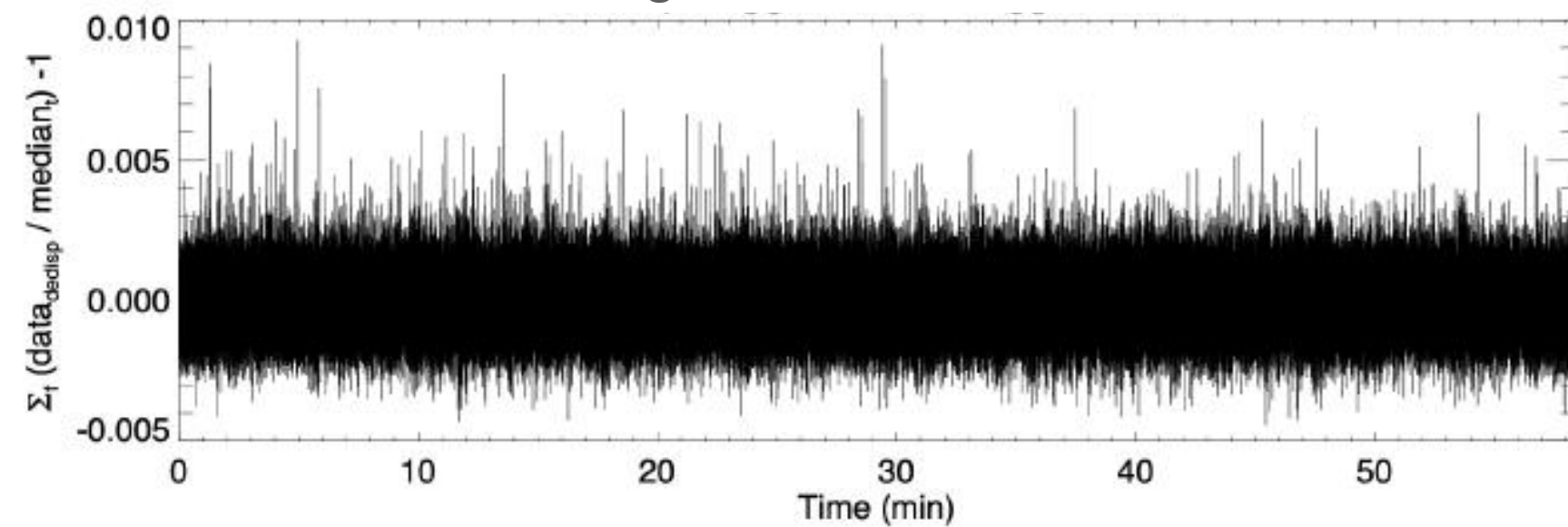
2D Fourier plane of the power spectrum



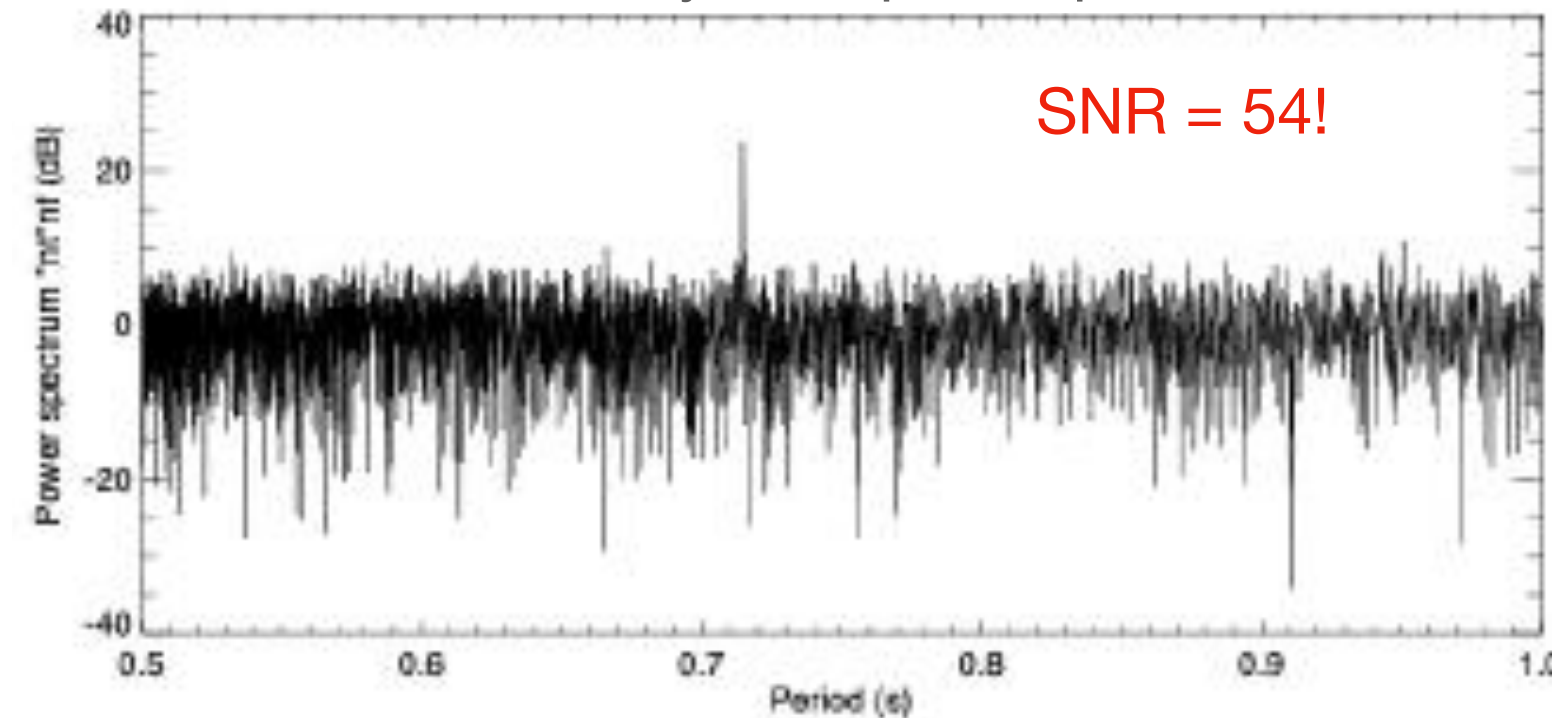
inverse 2D Fourier transform of the flagged power spectrum



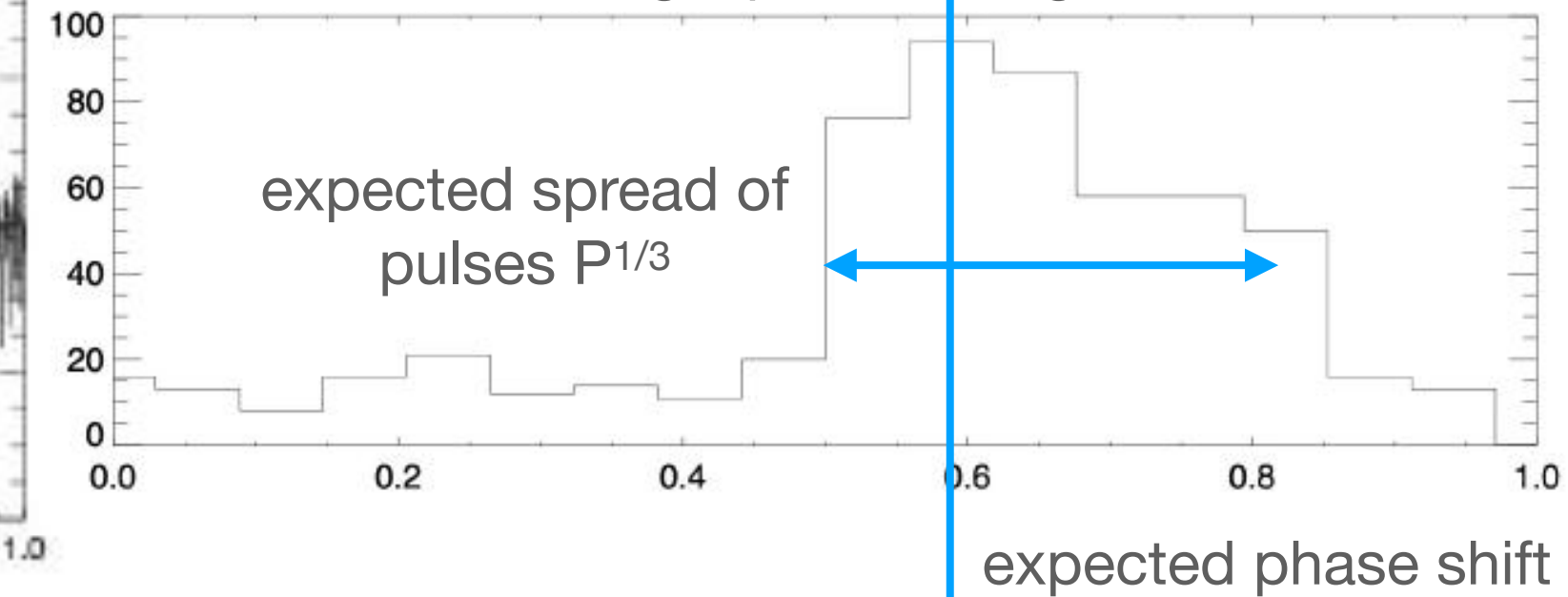
integrated time series



Fourier analysis of pulsar period



single pulse histogram



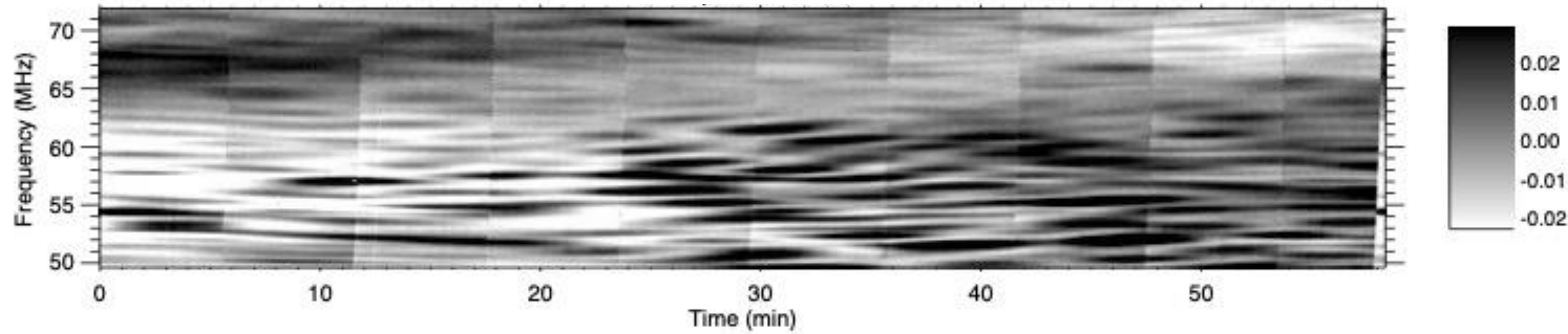


# Analysis method on pulsar observations

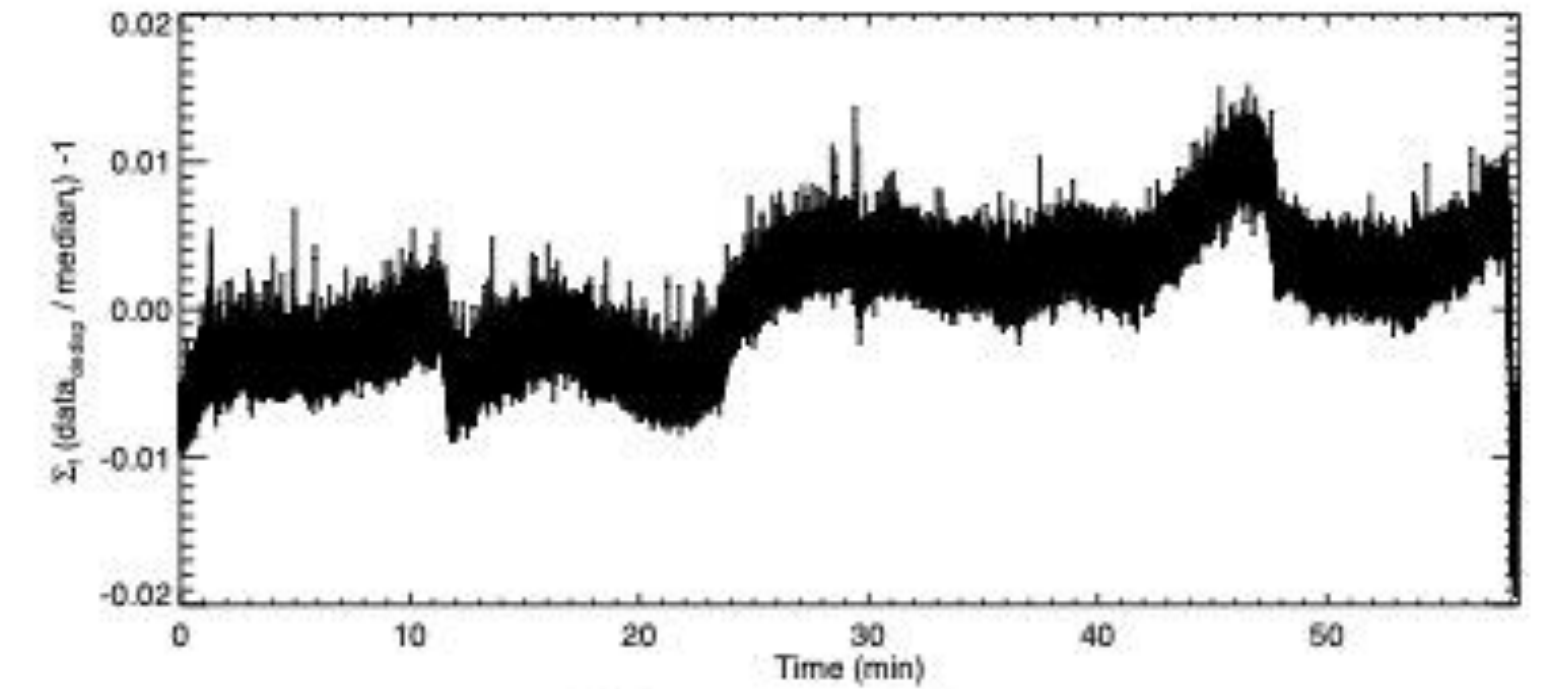
The idea is to clean the time-frequency data in the Fourier domain

test on observations PSRB0329+54

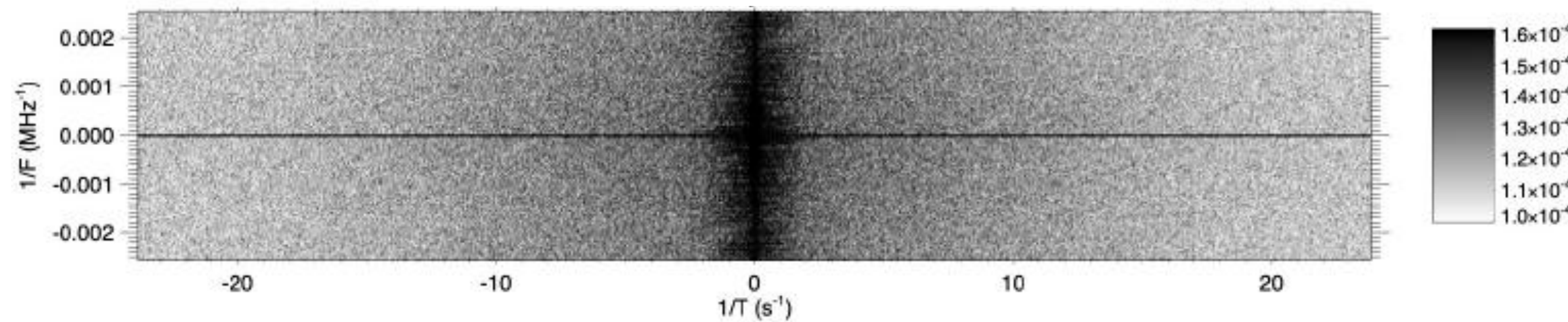
time-frequency plane



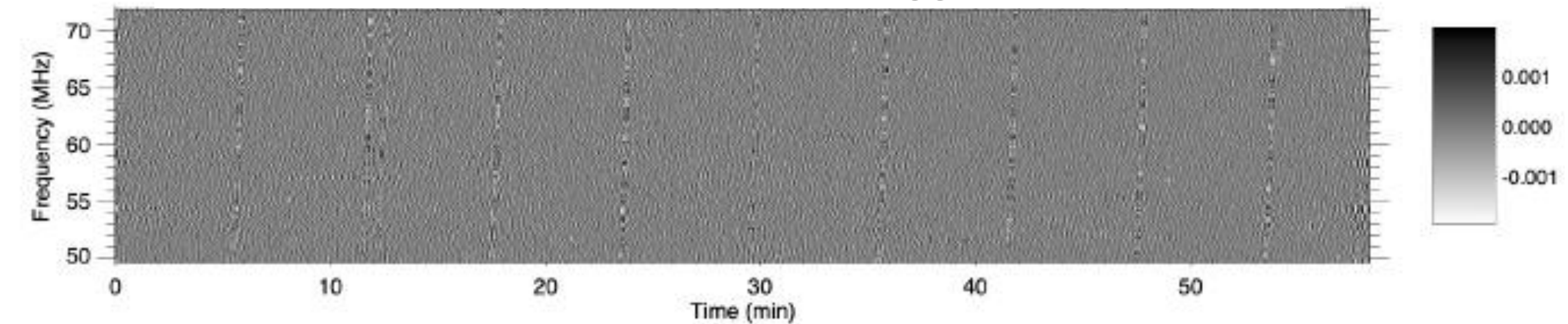
integrated time series



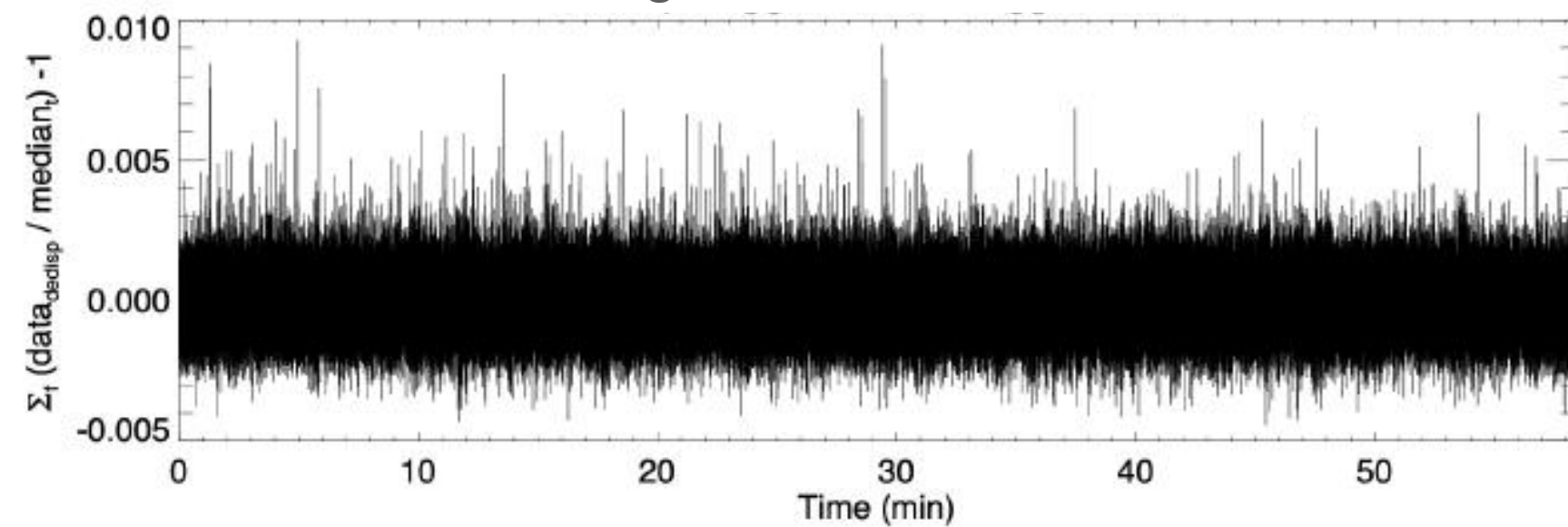
2D Fourier plane of the power spectrum



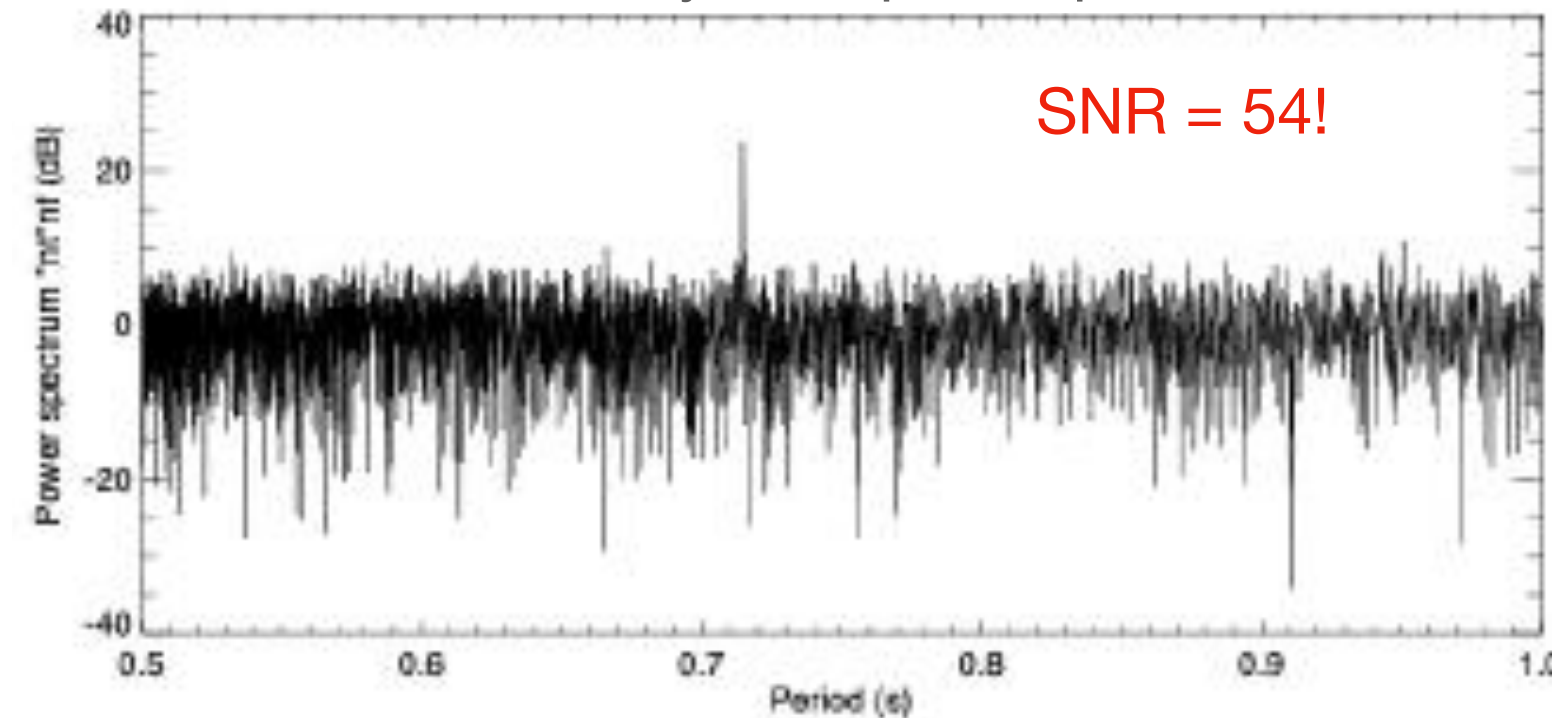
inverse 2D Fourier transform of the flagged power spectrum



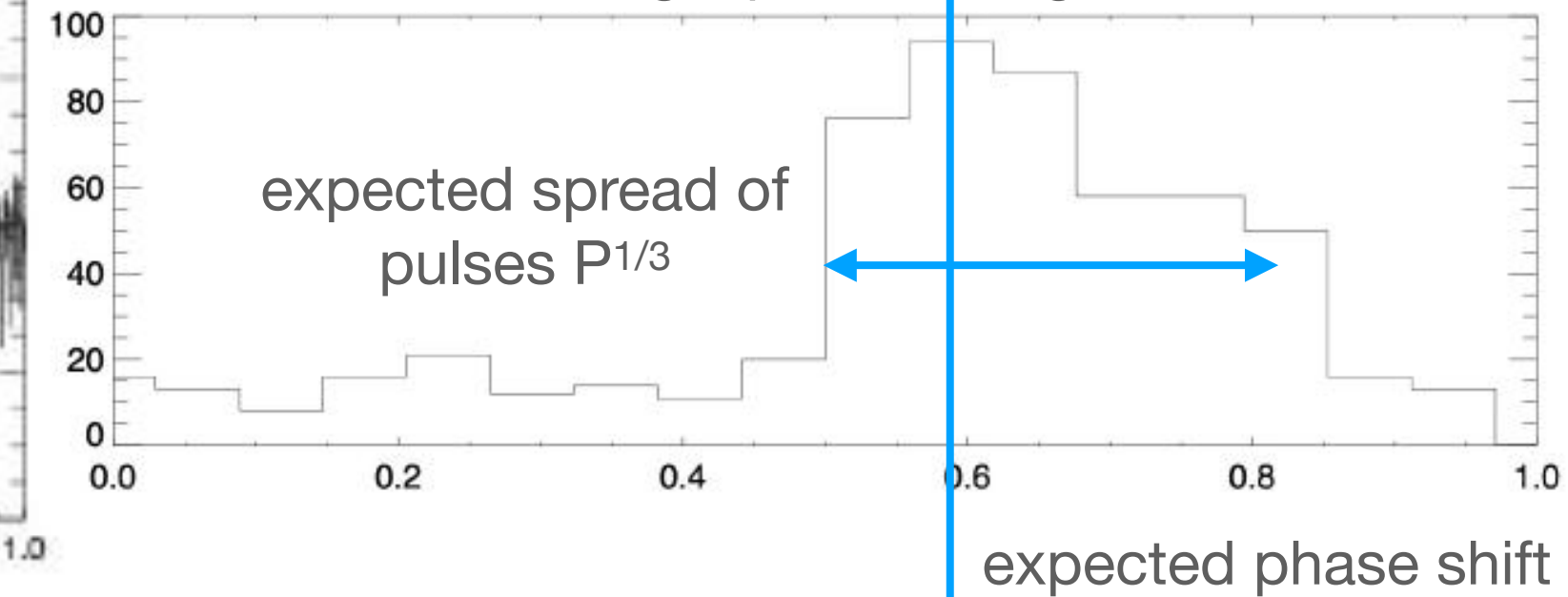
integrated time series



Fourier analysis of pulsar period



single pulse histogram

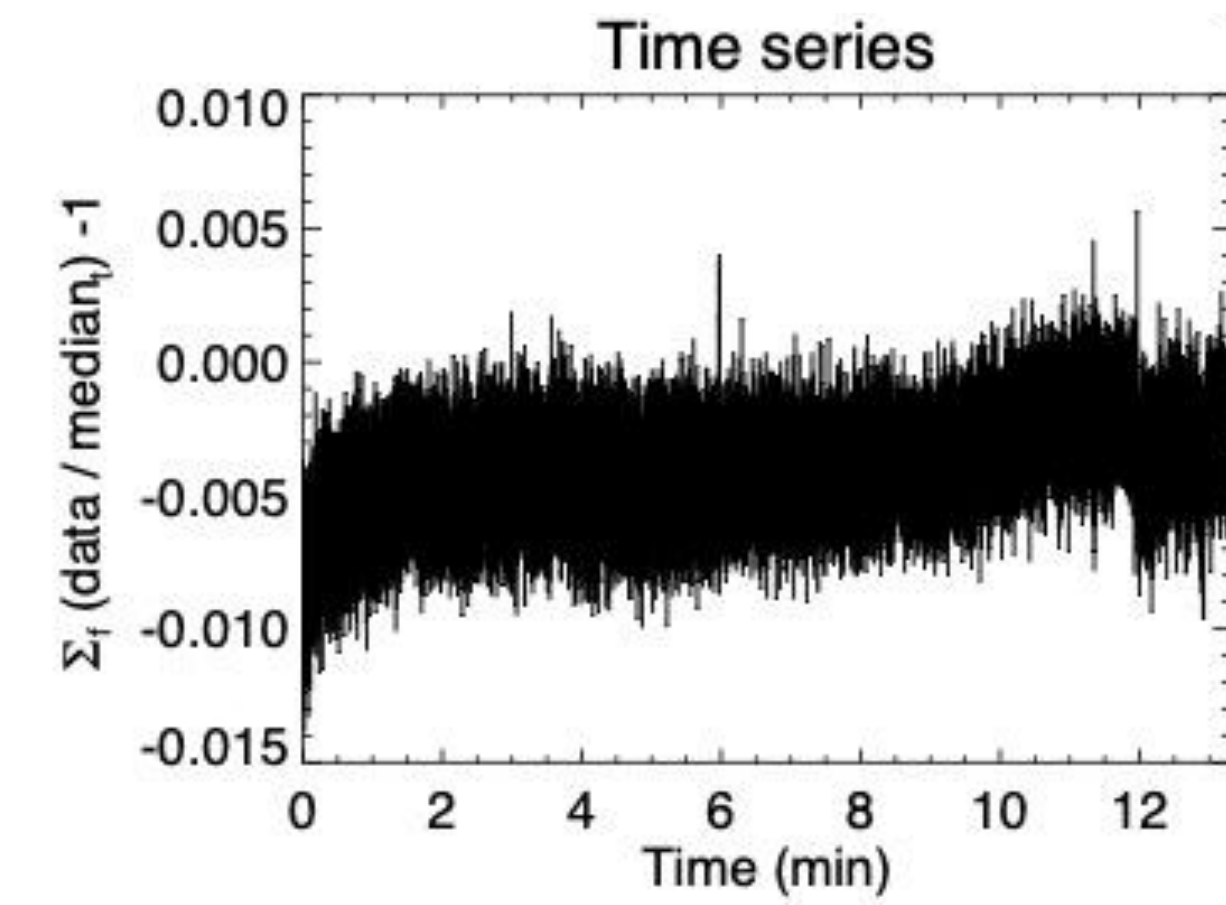
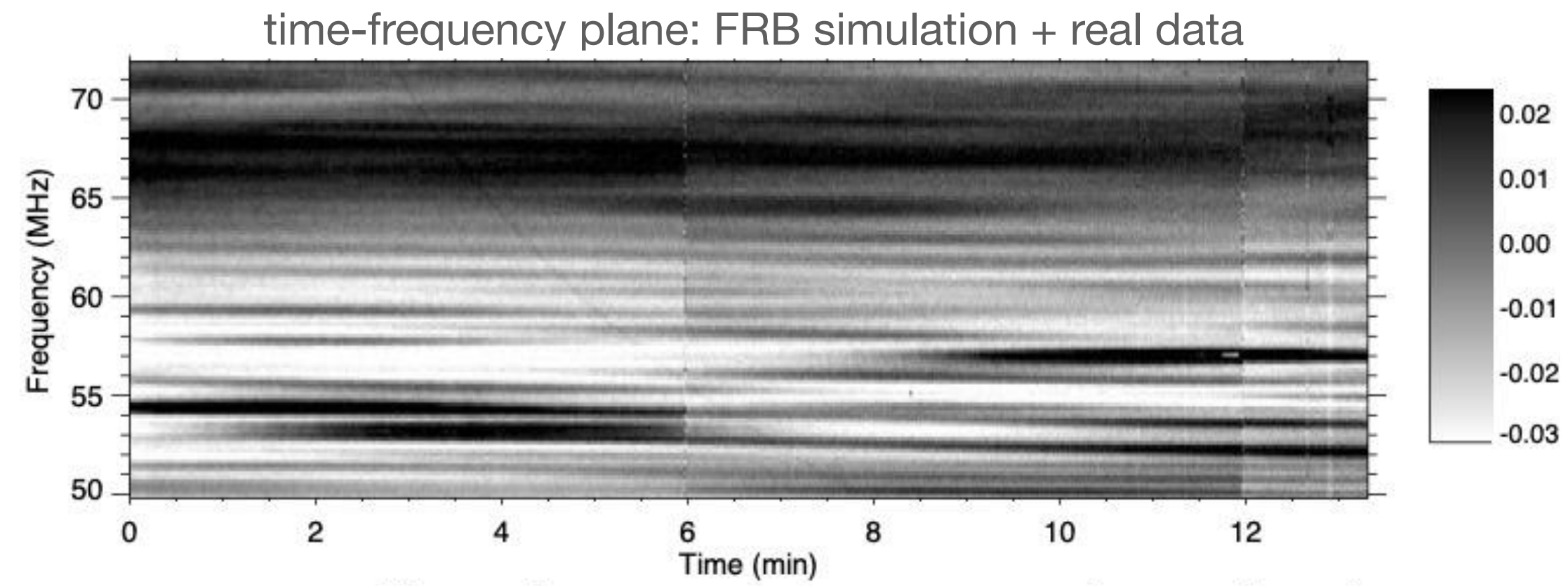


High pass Fourier filtering allows to clean the data efficiently enough to detect single pulses!



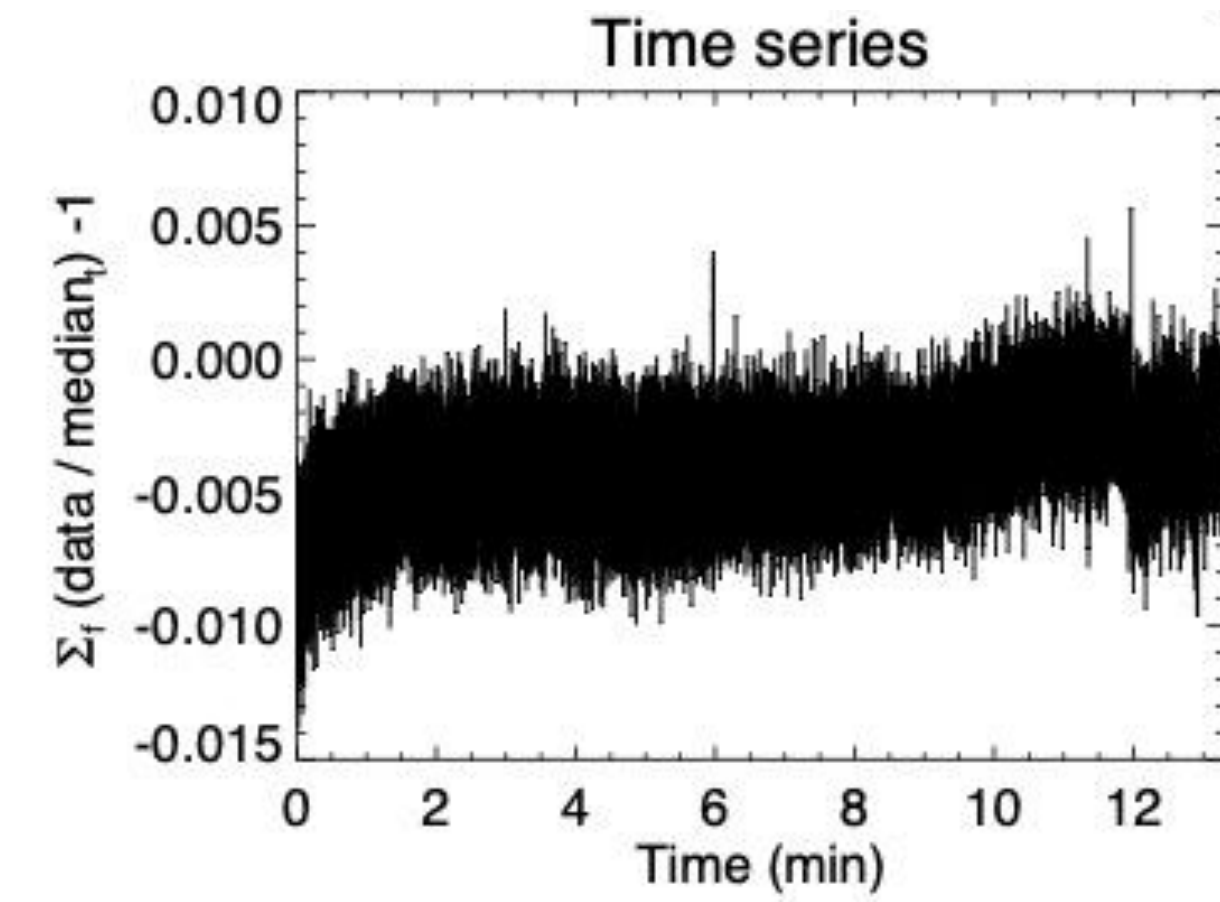
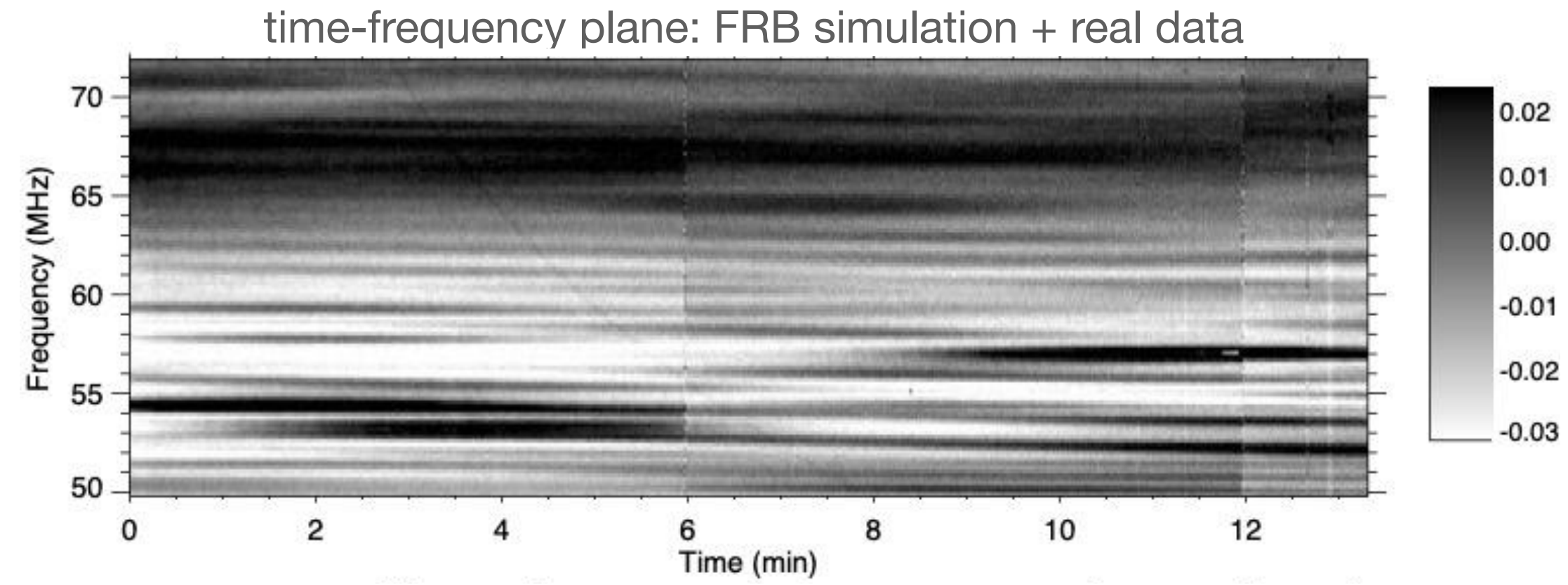
# Analysis method on FRB simulations with real noise

Test the method on a simulated FRB signal embedded into real observation data

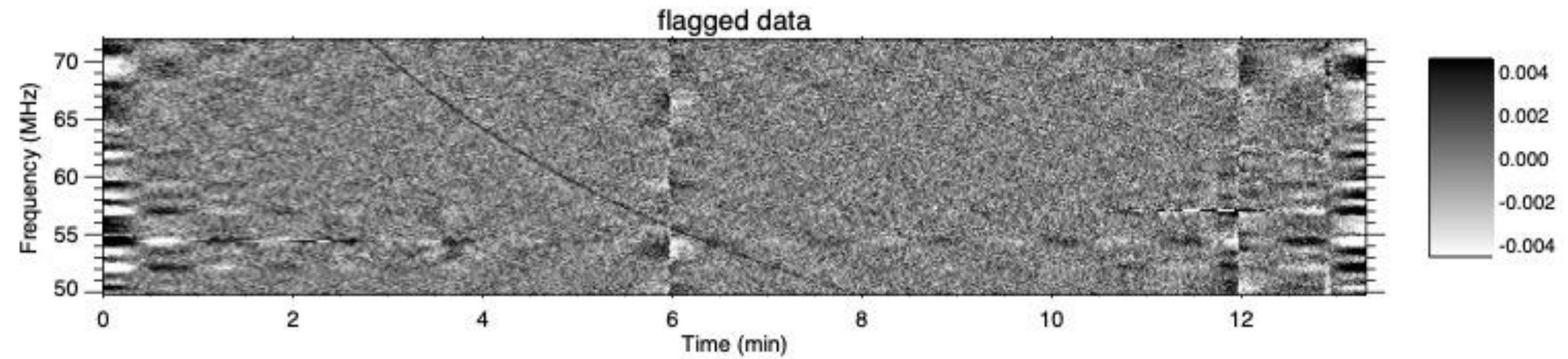


# Analysis method on FRB simulations with real noise

Test the method on a simulated FRB signal embedded into real observation data



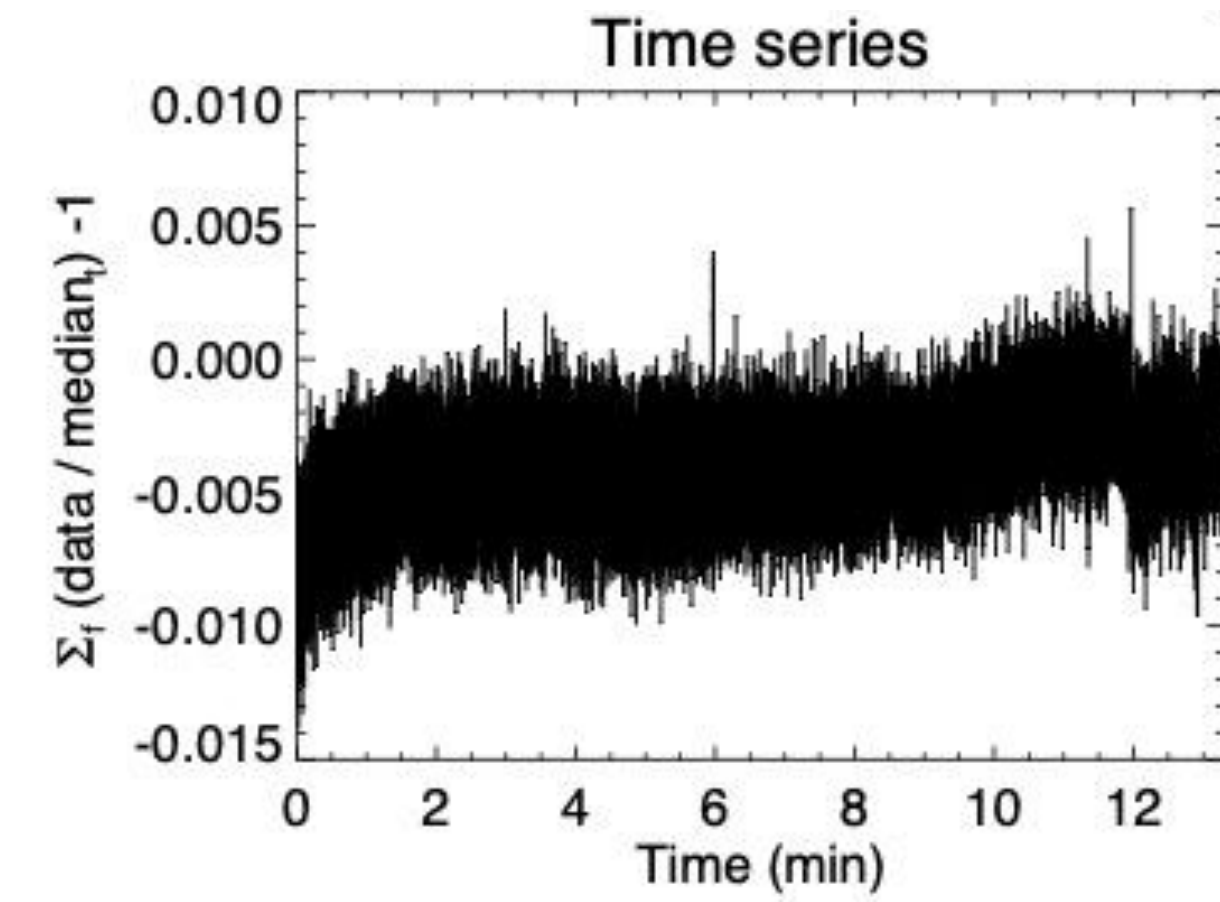
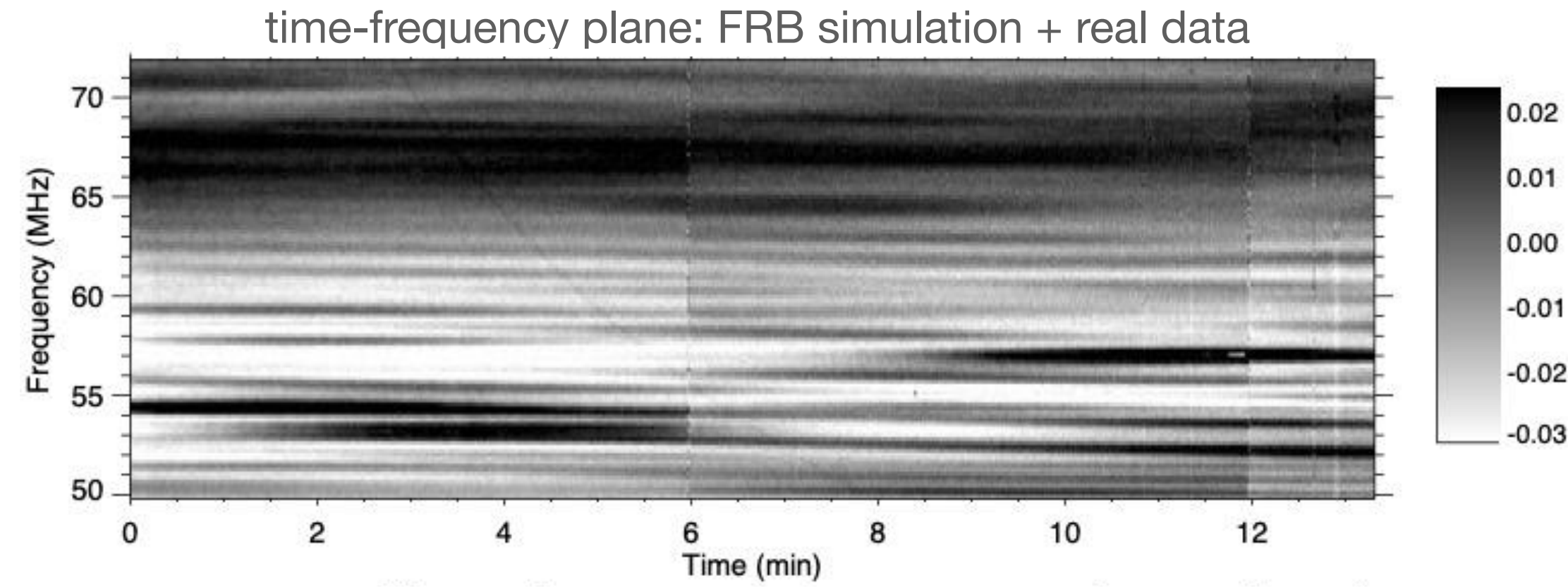
 we apply the high pass 2D Fourier filter



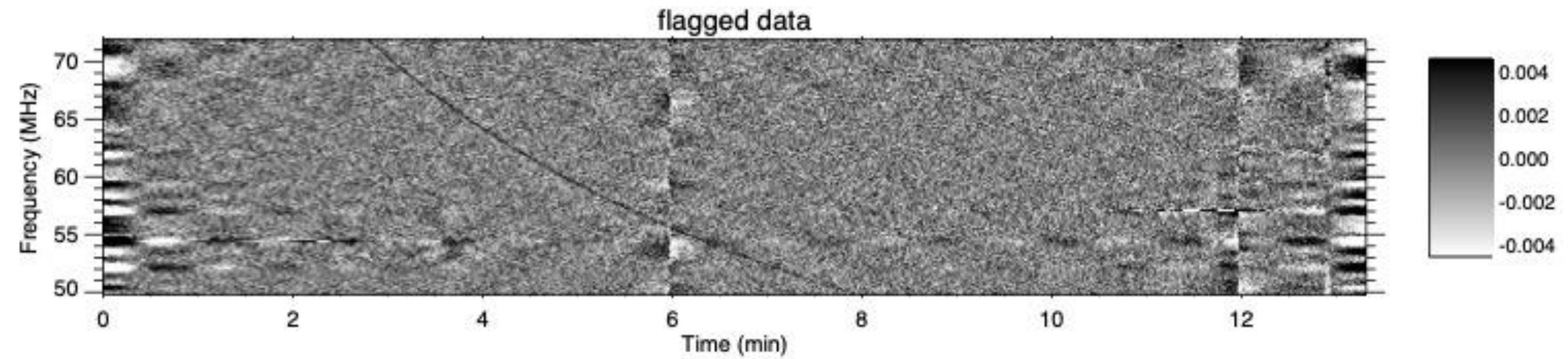


# Analysis method on FRB simulations with real noise

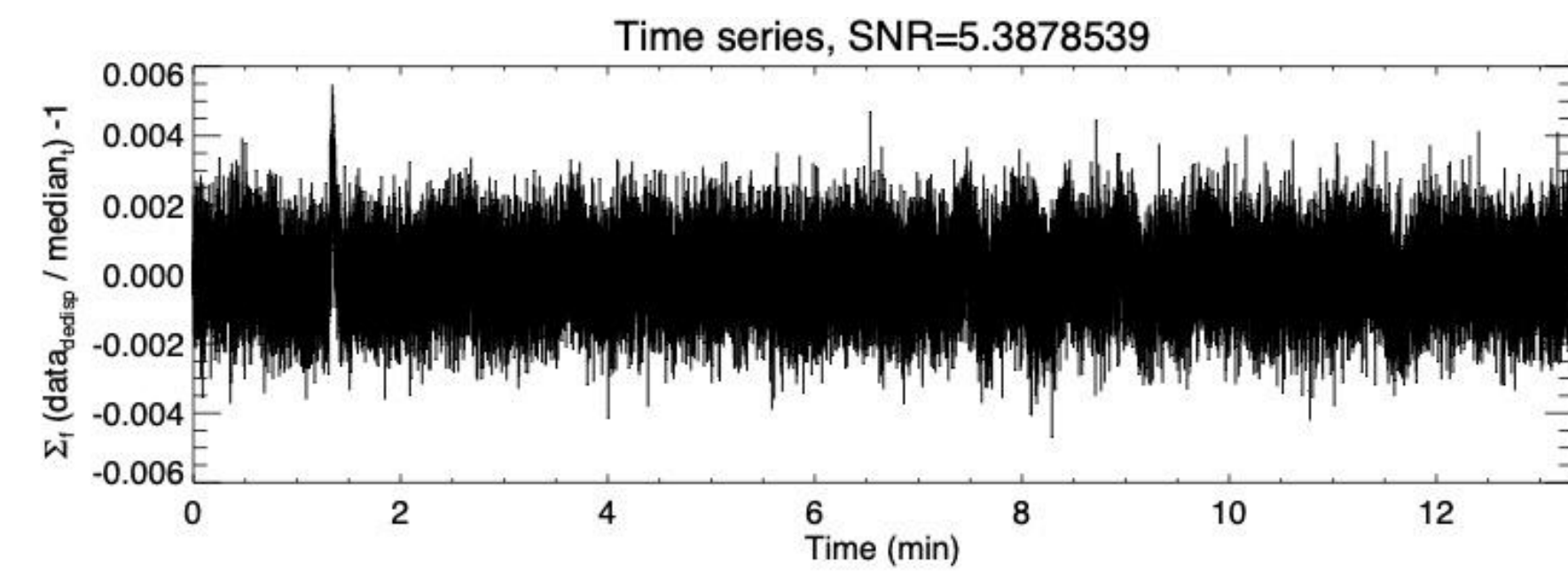
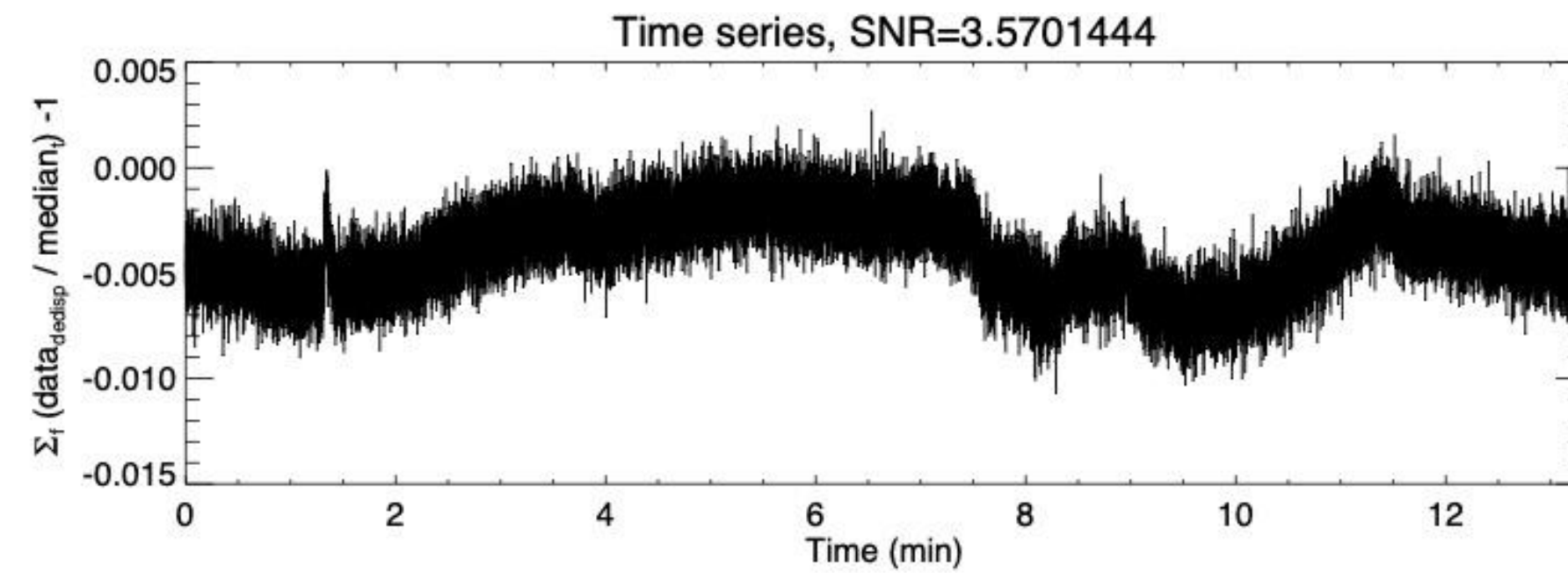
Test the method on a simulated FRB signal embedded into real observation data



we apply the high pass 2D Fourier filter



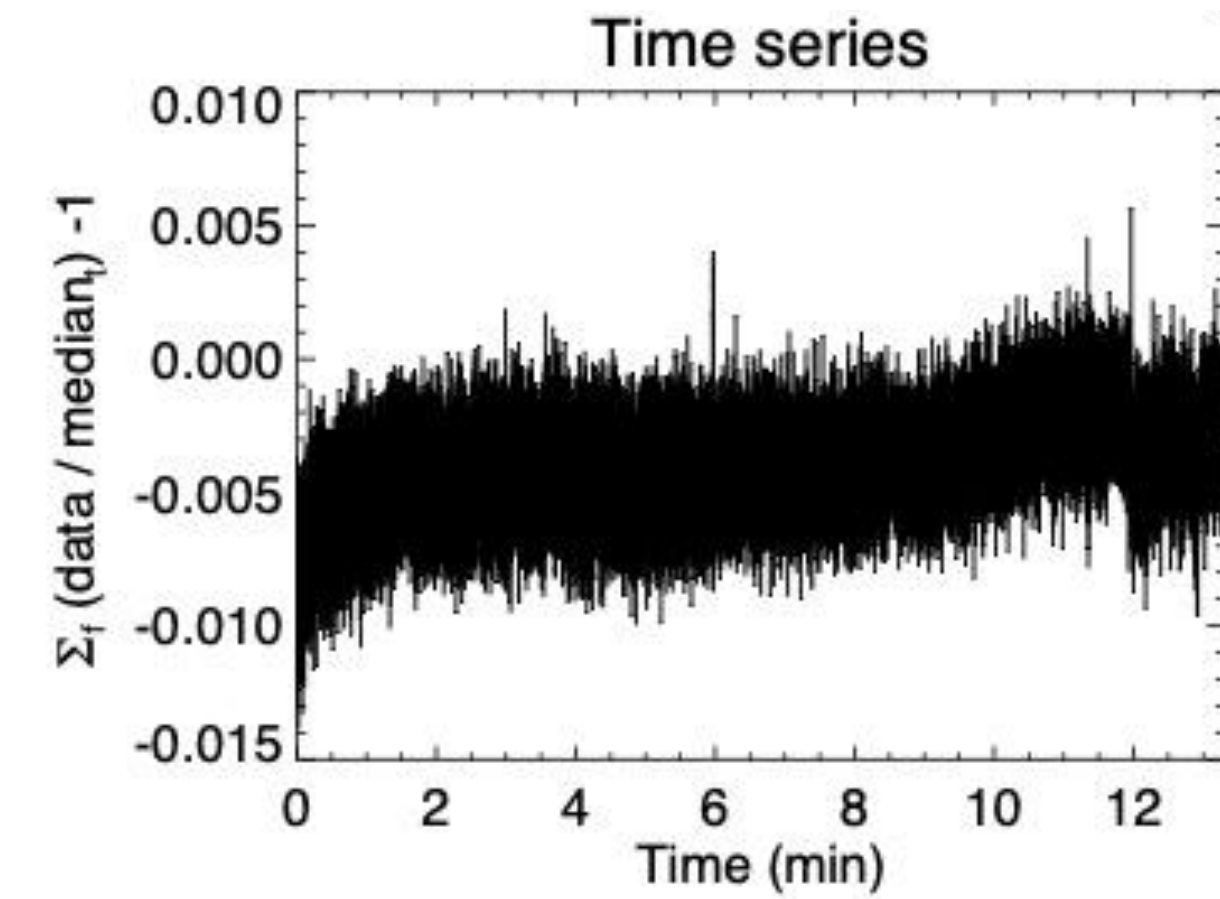
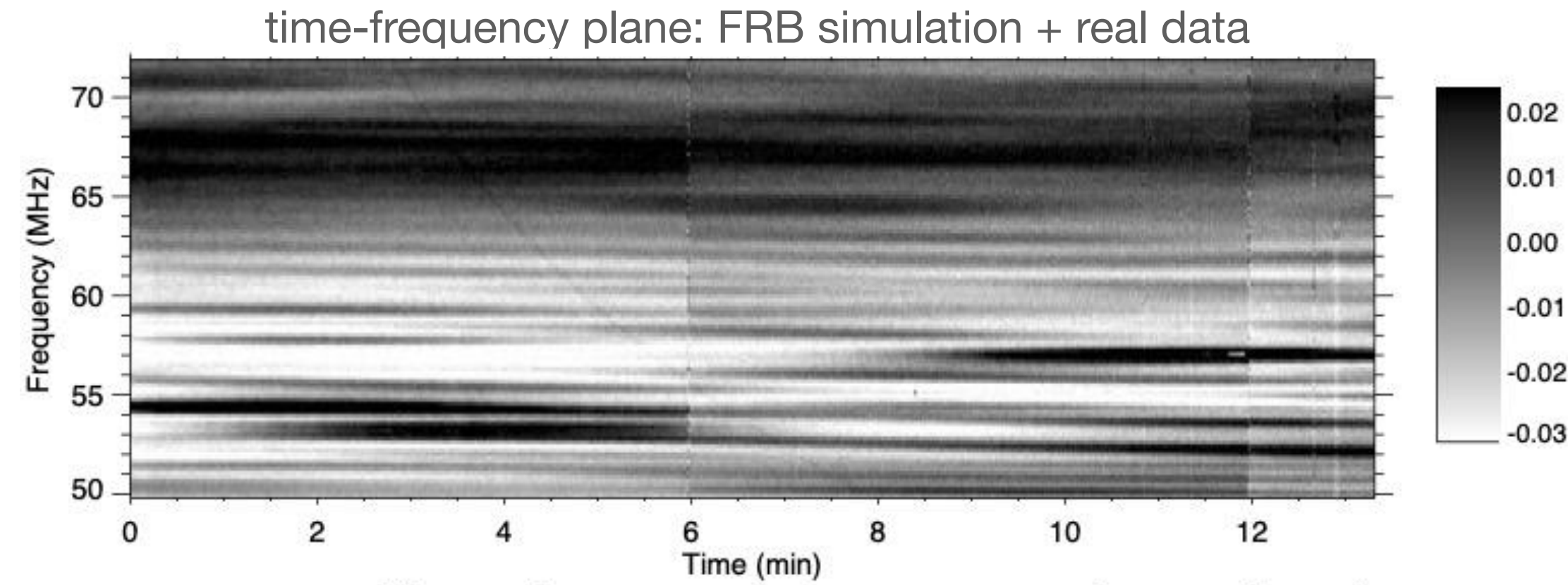
Comparison without and with filtering:



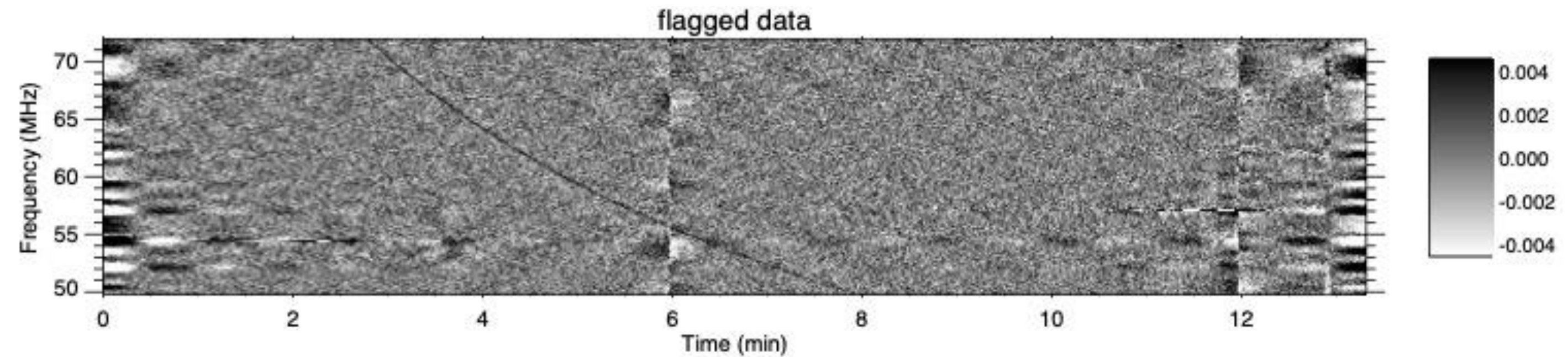


# Analysis method on FRB simulations with real noise

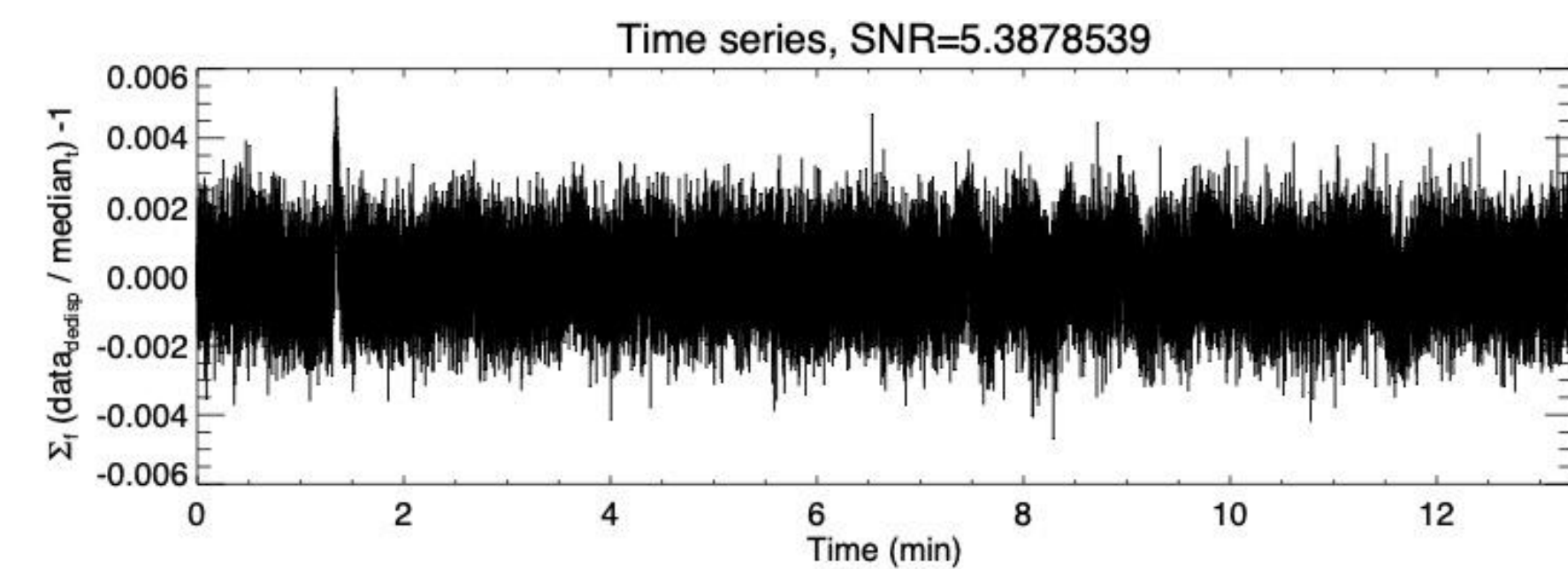
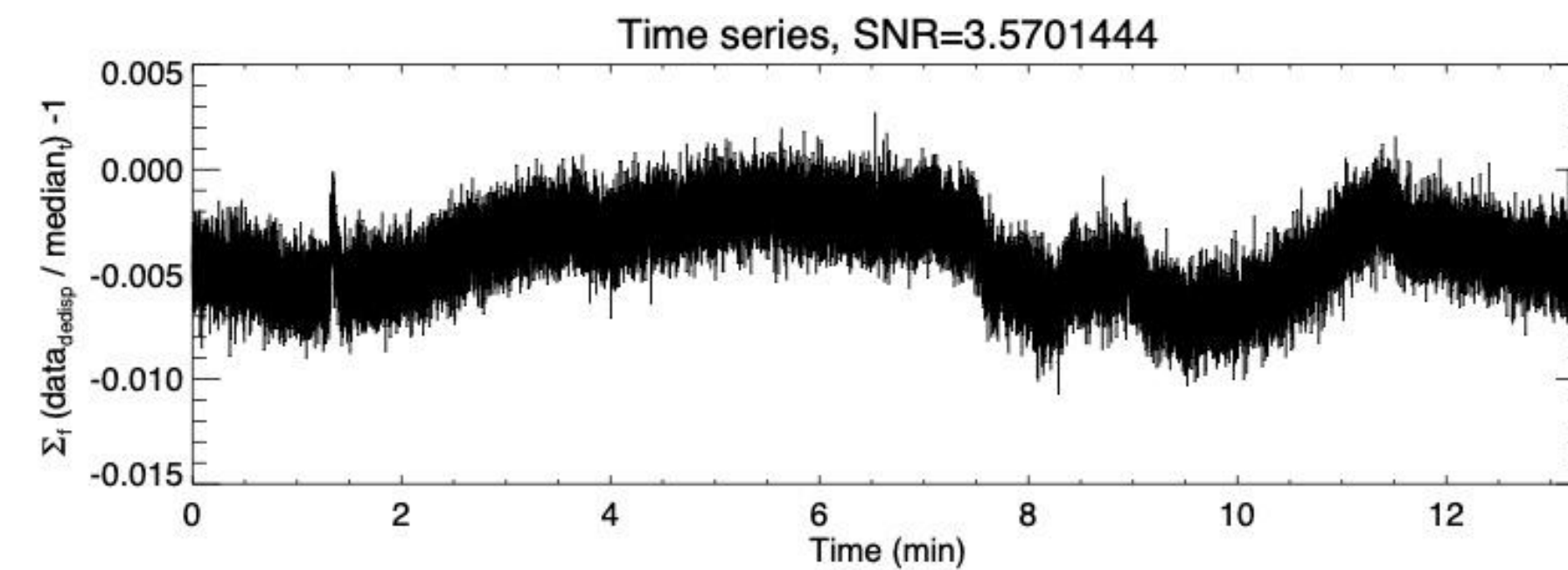
Test the method on a simulated FRB signal embedded into real observation data



we apply the high pass 2D Fourier filter



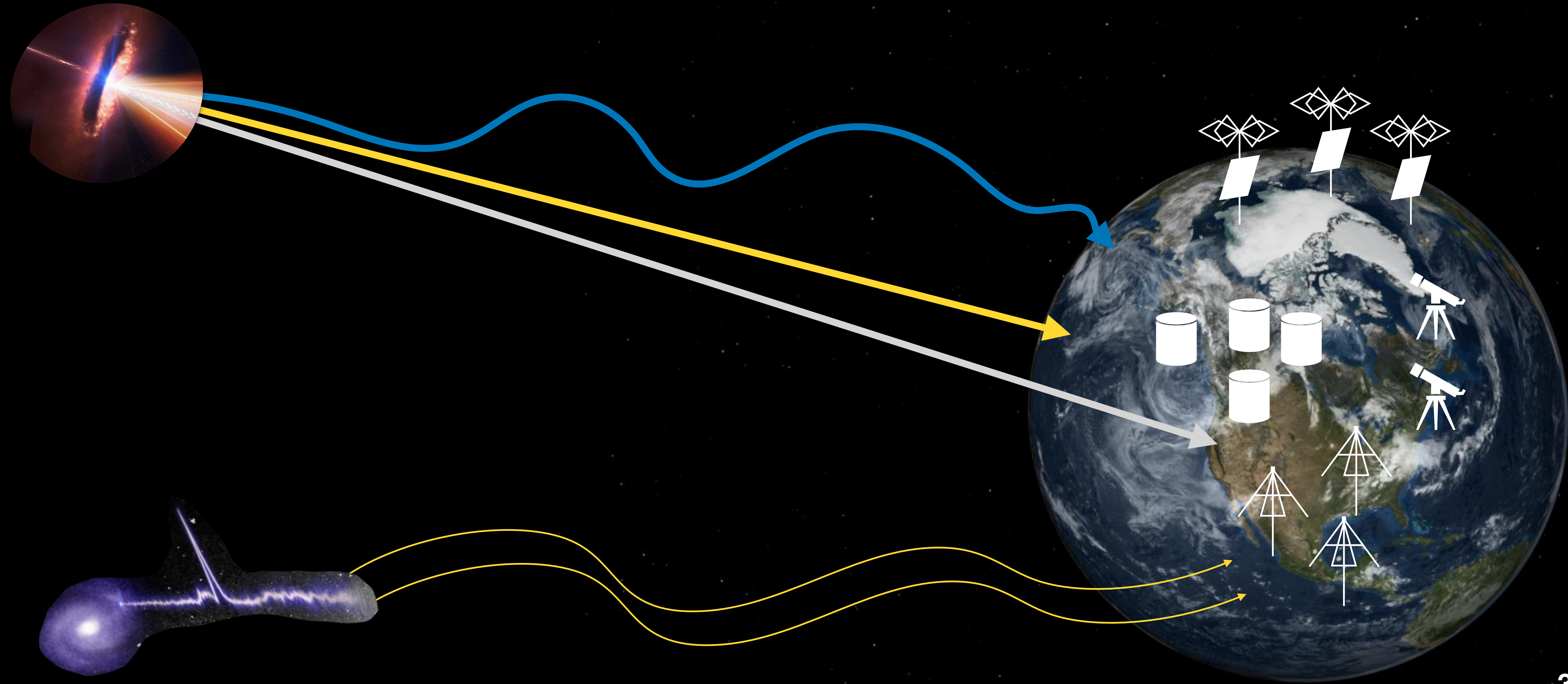
Comparison without and with filtering:



The high pass 2D Fourier filtering allows to increase the SNR by a factor  $\sim 1.5!$



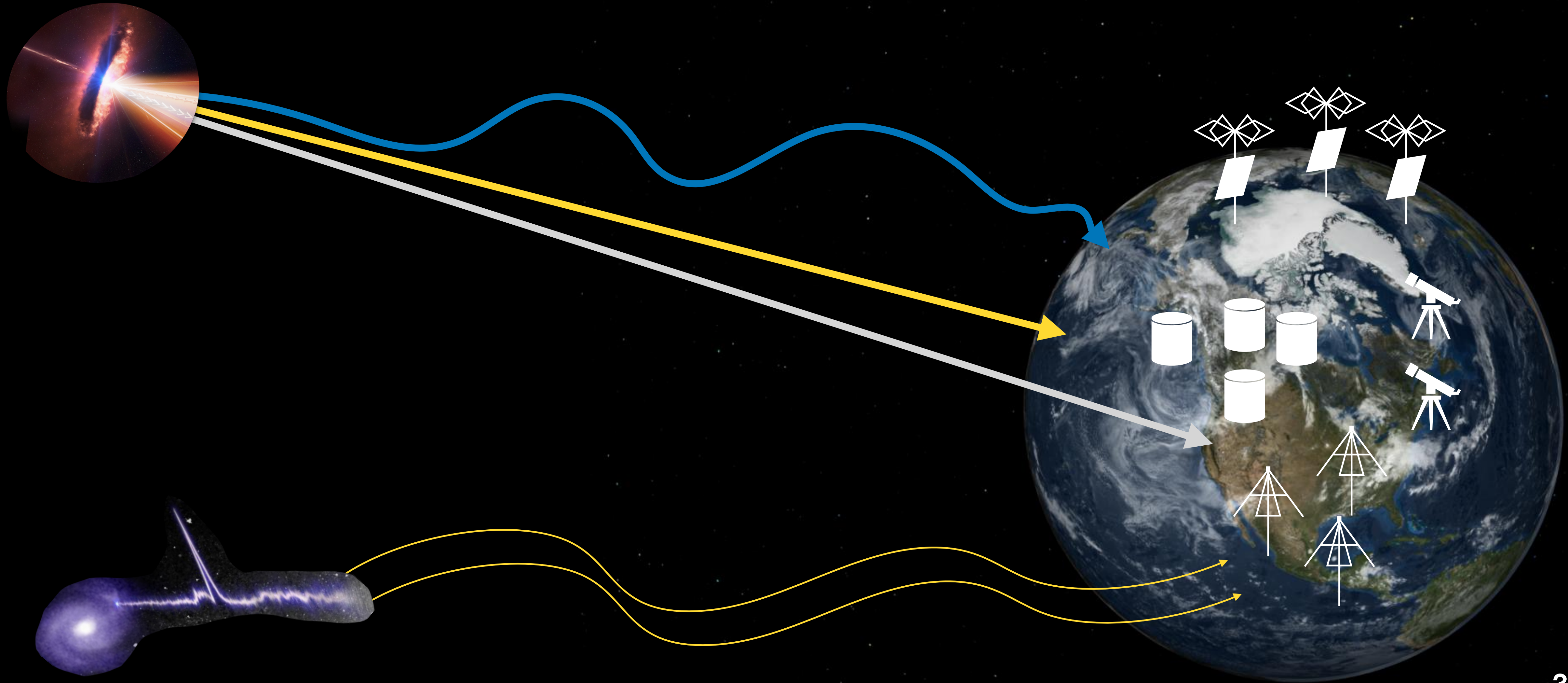
# Summary of our journey with FRBs





# Summary of our journey with FRBs

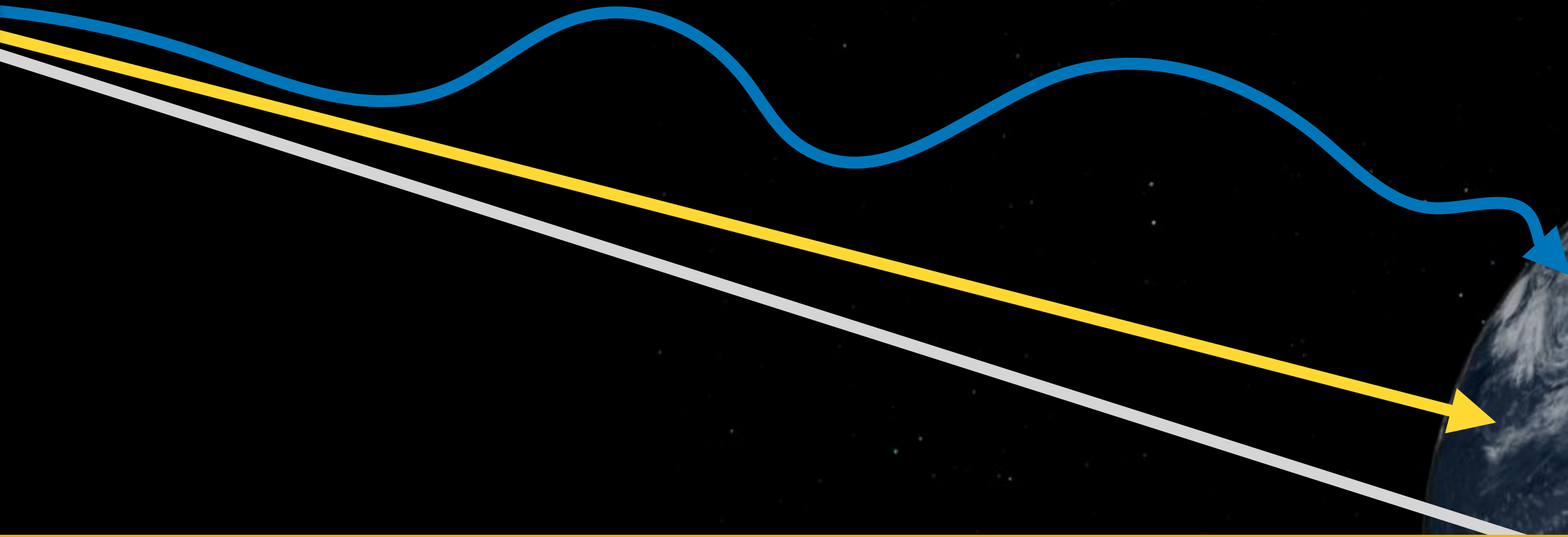
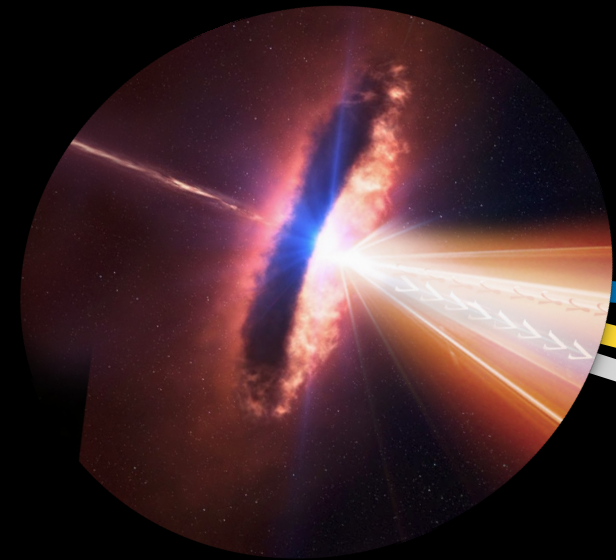
- FRBs are a new type of fast radio transients
- There is very sparse information on them yet
- NenuFAR conducts observations at low frequencies on repeaters
- The existence (or not) of FRBs at low frequencies is critical for the emission models and source candidates



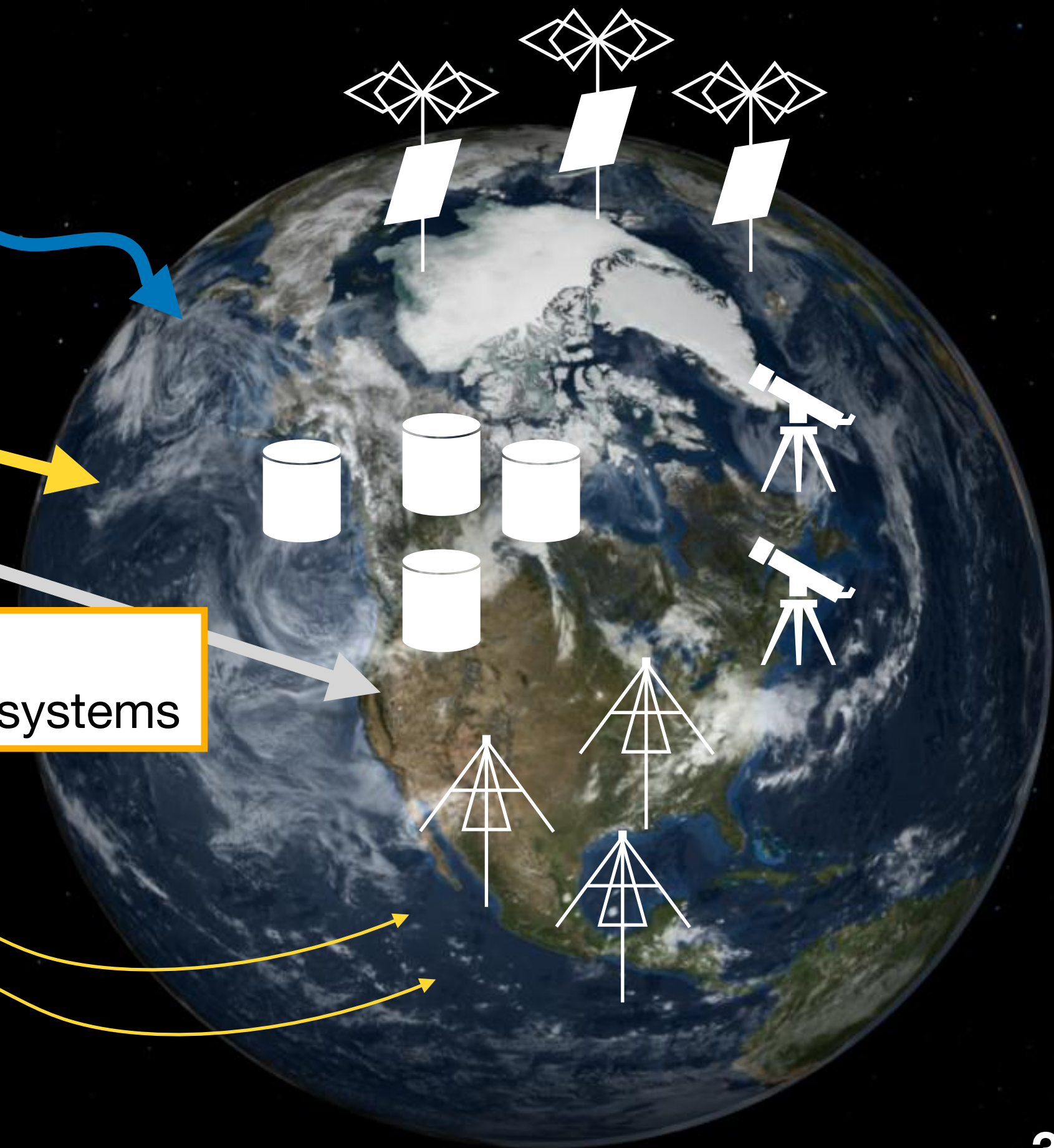
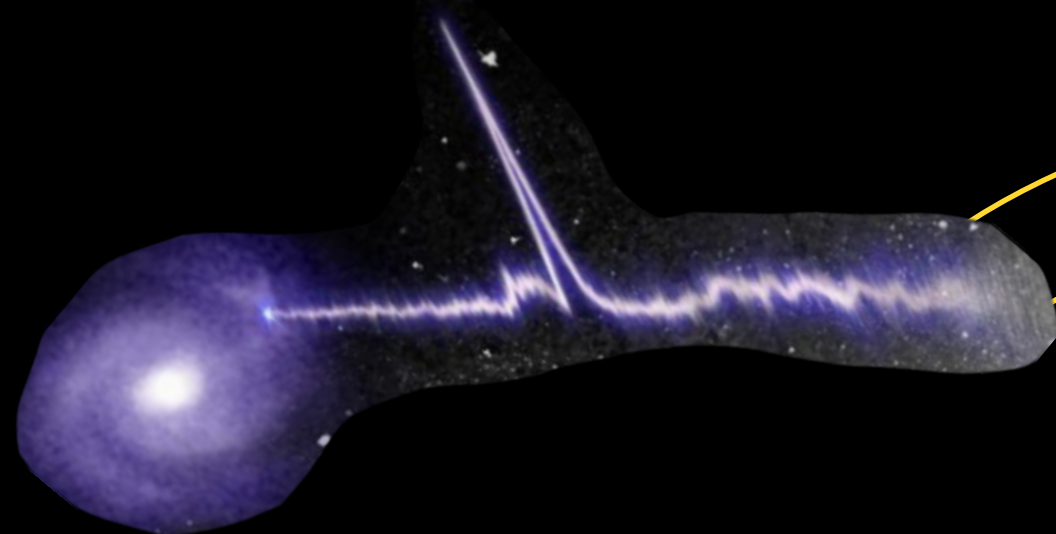


# Summary of our journey with FRBs

- FRBs are a new type of fast radio transients
- There is very sparse information on them yet
- NenuFAR conducts observations at low frequencies on repeaters
- The existence (or not) of FRBs at low frequencies is critical for the emission models and source candidates

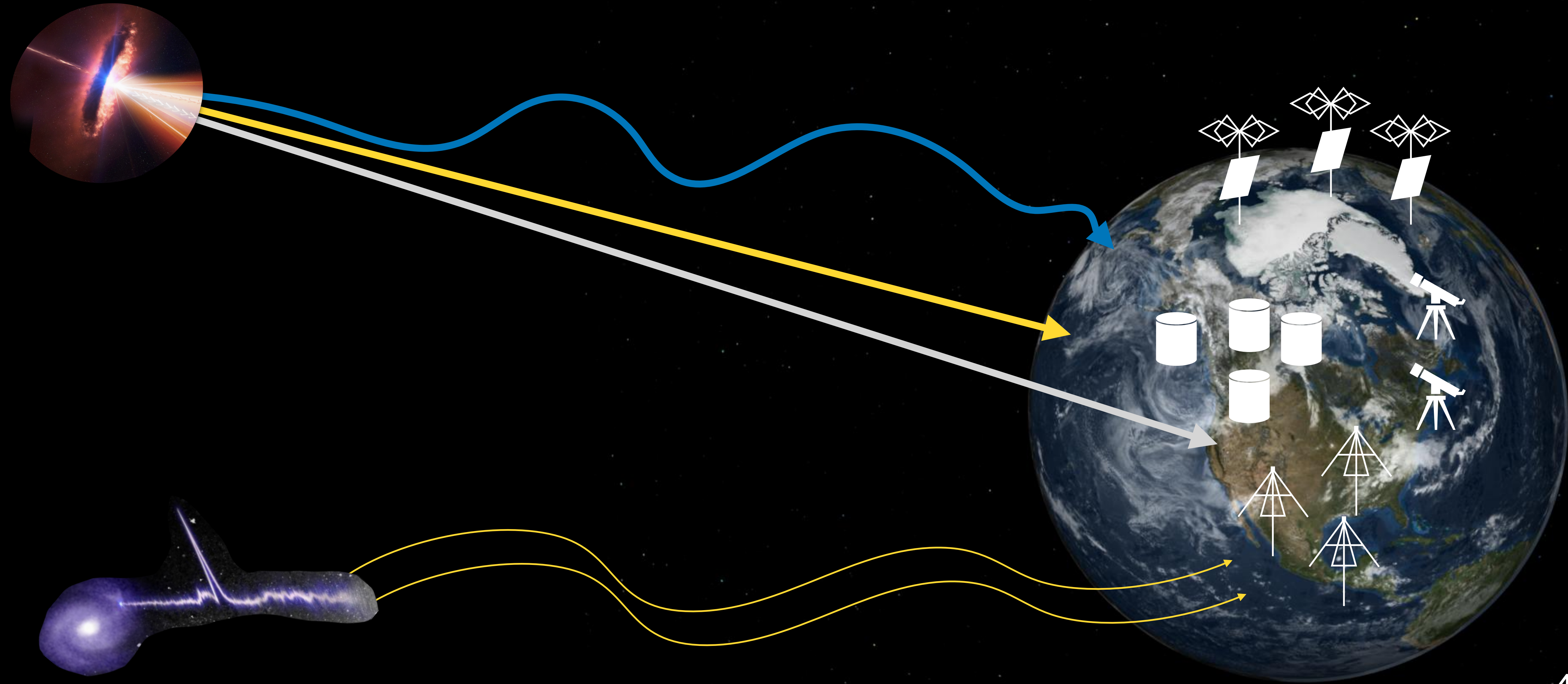


- FRB emissions can be explained via the Alfvén wing model
- Repeaters and non-repeaters can be explained thanks three-body dynamics inside binary systems



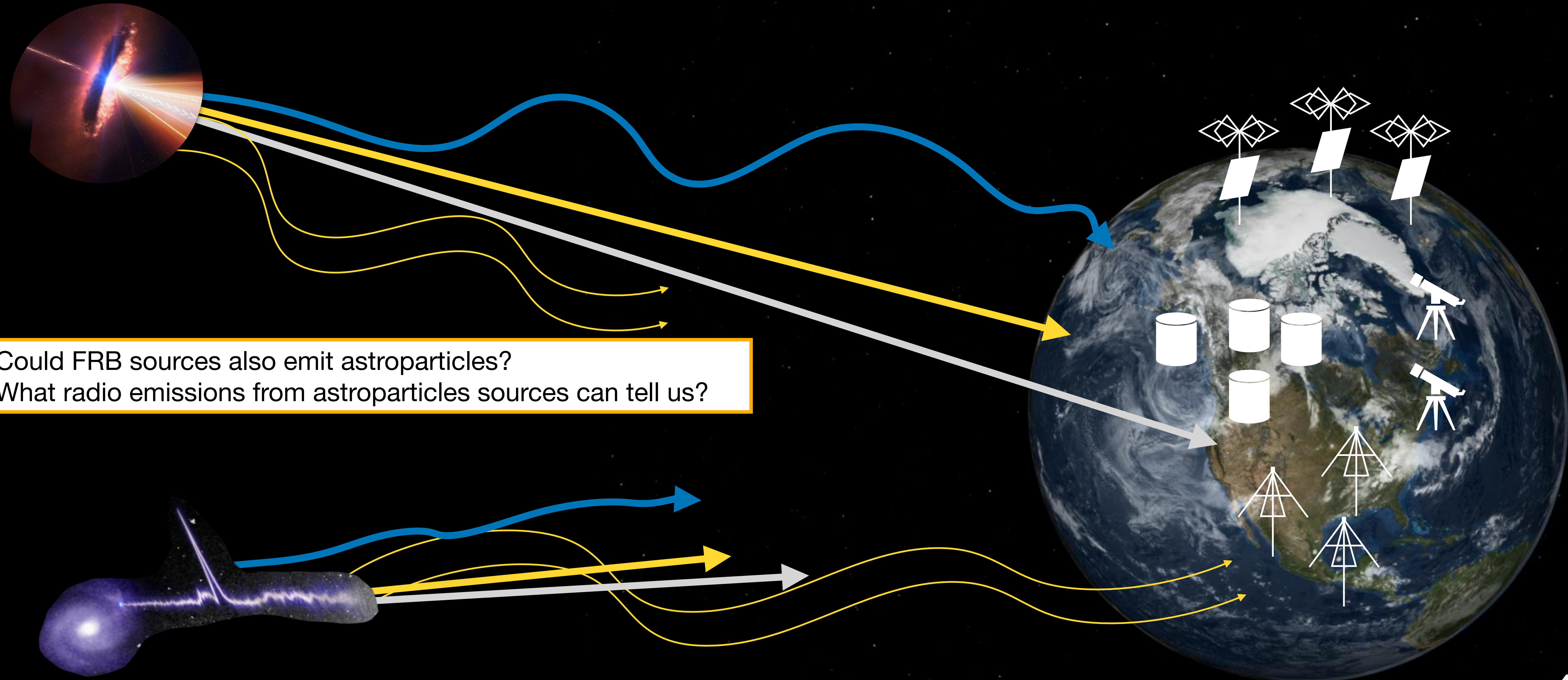


# The journey doesn't end here...





# The journey doesn't end here...



- Could FRB sources also emit astroparticles?
- What radio emissions from astroparticles sources can tell us?

# **Multi-messenger (MM) and multi-wavelength (MW) high energy sources**

**There is already many hints toward the connections between radio transients and MM emissions**



# **Multi-messenger (MM) and multi-wavelength (MW) high energy sources**

**There is already many hints toward the connections between radio transients and MM emissions**

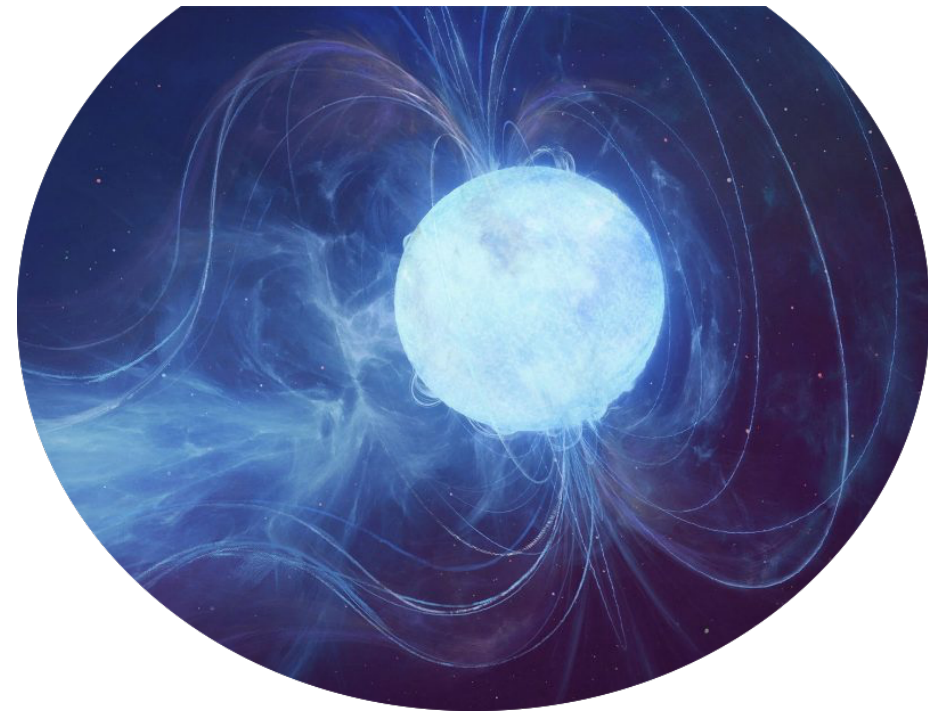
- jets/accretion-disks and kilonova
- highly magnetic environments / winds / outflows

# Multi-messenger (MM) and multi-wavelength (MW) high energy sources

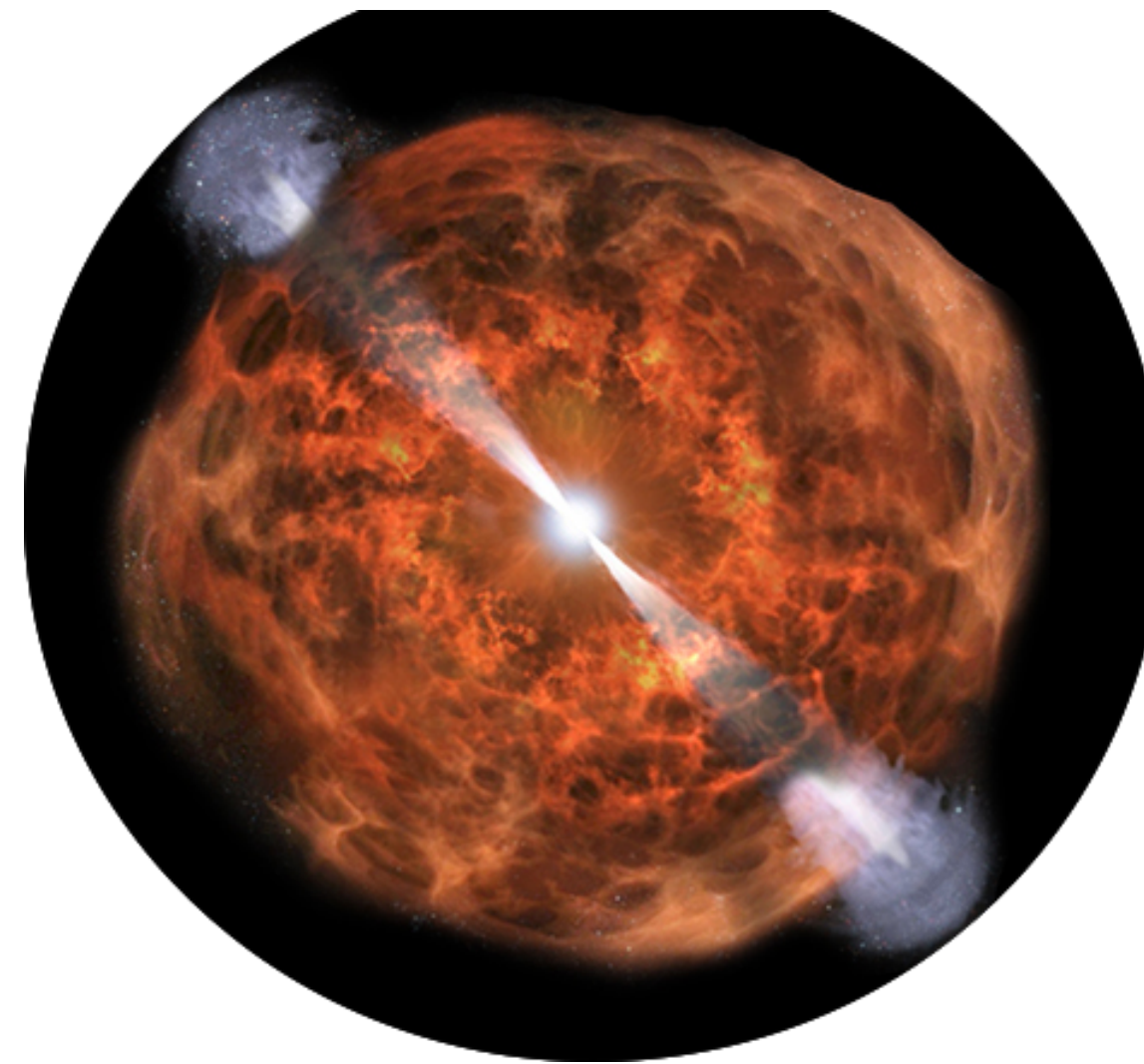
There is already many hints toward the connections between radio transients and MM emissions

- jets/accretion-disks and kilonova
- highly magnetic environments / winds / outflows

**Magnetars**



**Kilonova**



**Coalescence**



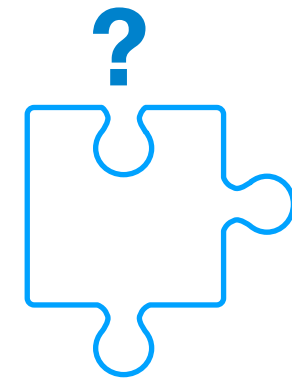
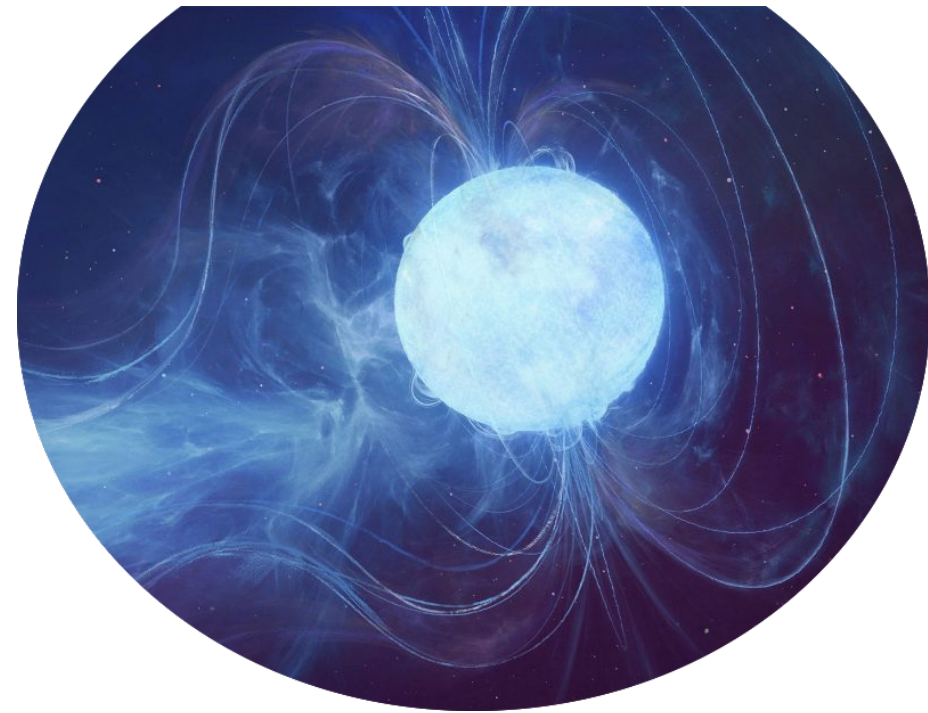


# Multi-messenger (MM) and multi-wavelength (MW) high energy sources

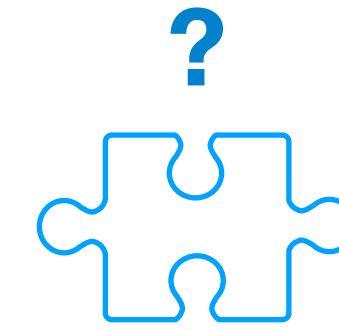
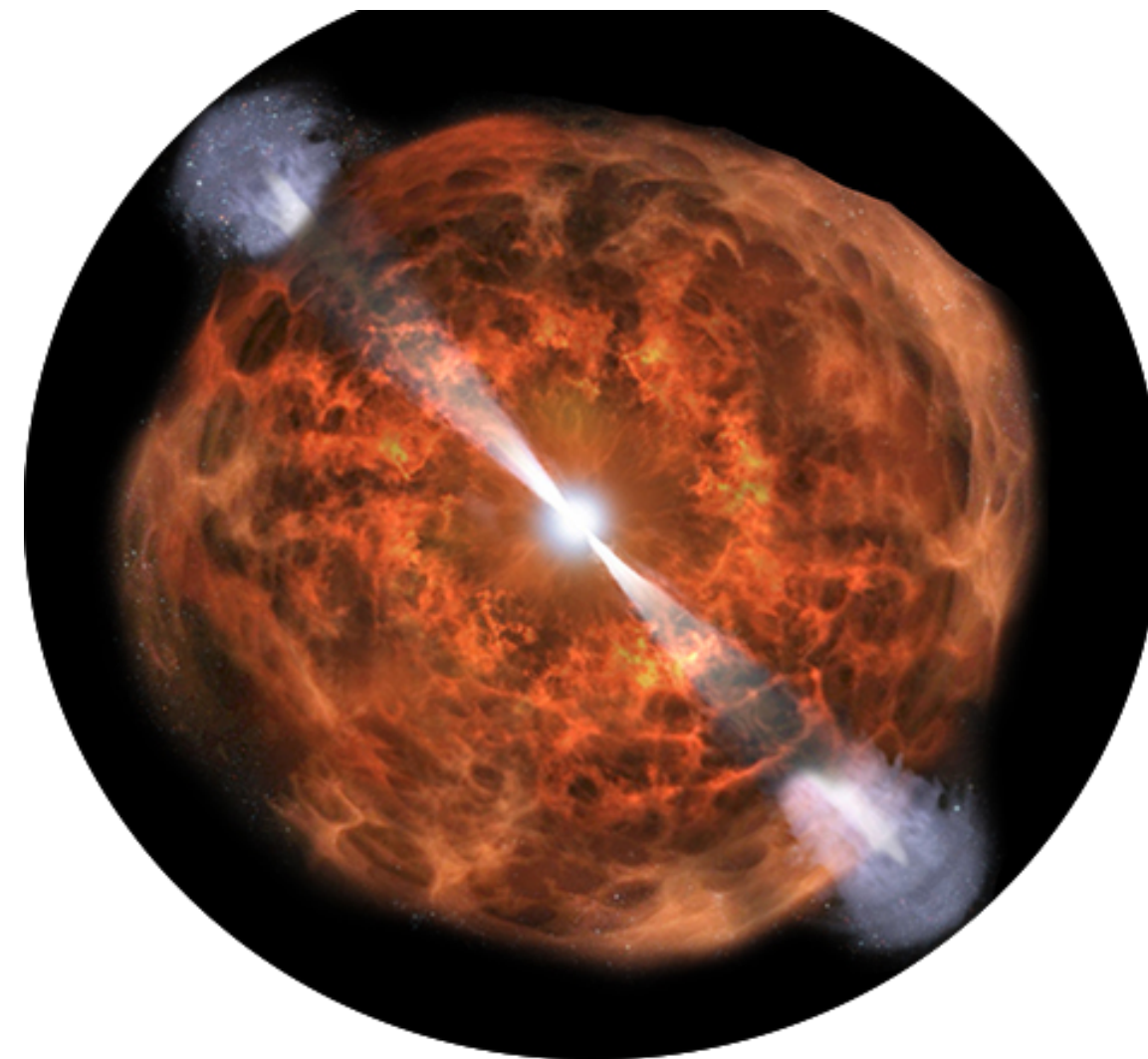
There is already many hints toward the connections between radio transients and MM emissions

- jets/accretion-disks and kilonova
- highly magnetic environments / winds / outflows

**Magnetars**



**Kilonova**



**Coalescence**



**We need to have MM and MW models in order to probe the physics consistently**

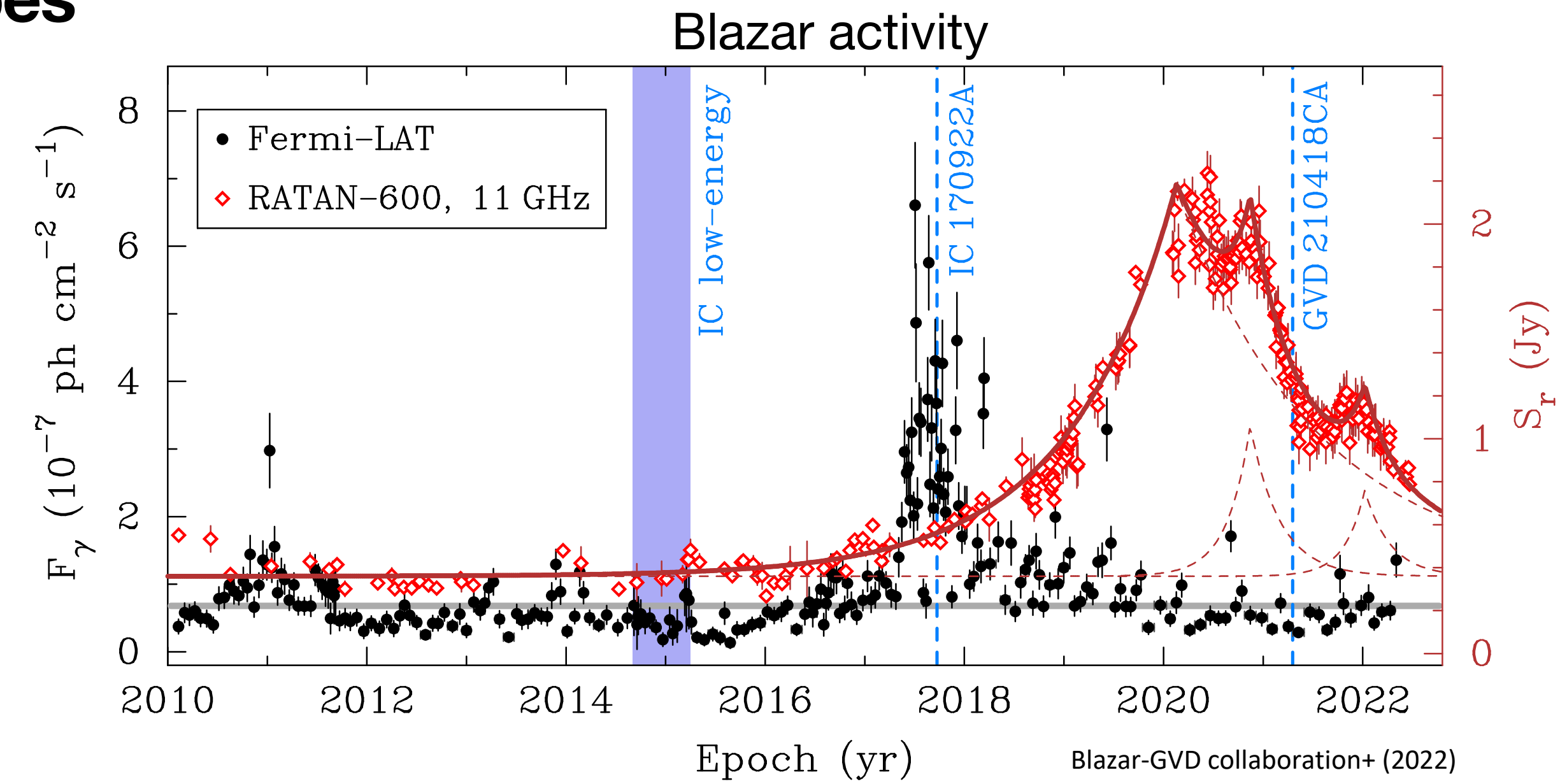
# **Combining astroparticle detectors and radio-telescopes**

---



# Combining astroparticle detectors and radio-telescopes

- **Observation strategies** → joint observations
  - improve alert strategies
  - bring unique insight for models
- **Alert strategies** → tuned thanks to model predictions and experimental feedbacks



# Combining astroparticle detectors and radio-telescopes

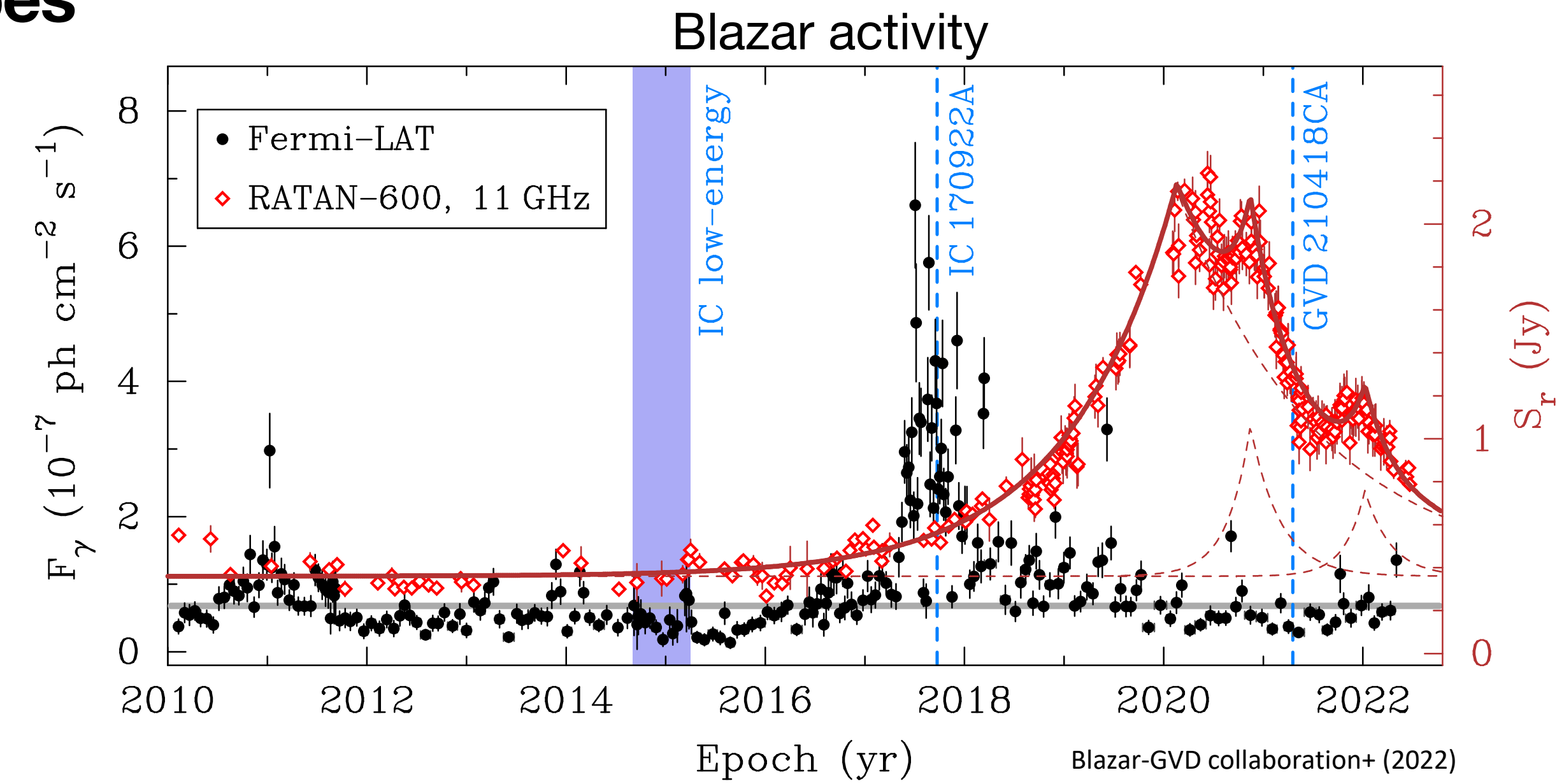
- **Observation strategies** → joint observations
  - improve alert strategies
  - bring unique insight for models
- **Alert strategies** → tuned thanks to model predictions and experimental feedbacks

**Transverse experiments:** radio-astronomy / radio-detectors

- high background rejection expertise (astroparticle community)
- high radio sensitivity (radio-astronomy community)



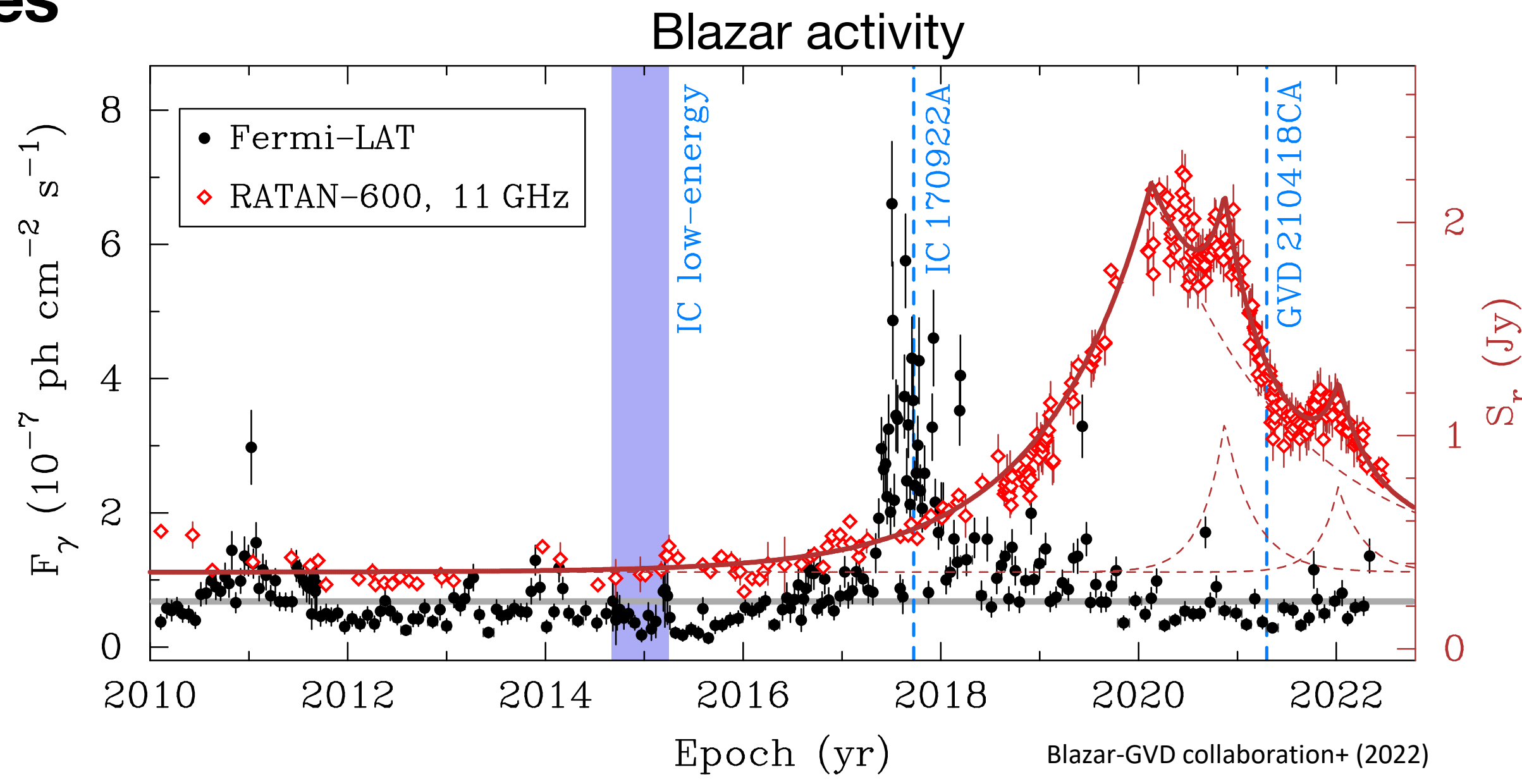
RadioGaGa:  
beamformed radio arrays for EAS gamma ray detection



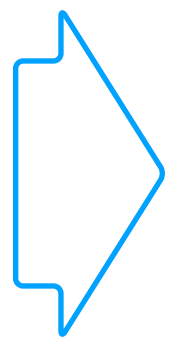


# Combining astroparticle detectors and radio-telescopes

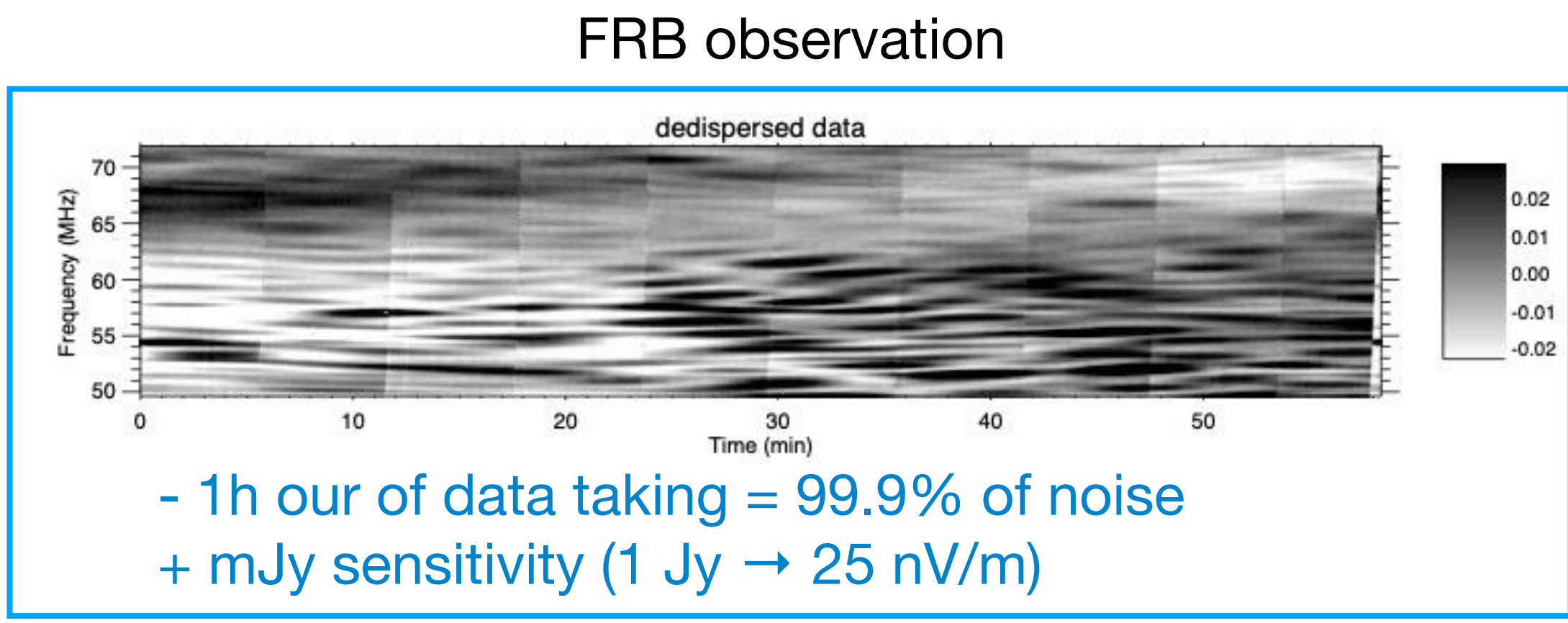
- **Observation strategies** → joint observations
  - improve alert strategies
  - bring unique insight for models
- **Alert strategies** → tuned thanks to model predictions and experimental feedbacks



- Transverse experiments:** radio-astronomy / radio-detectors
- high background rejection expertise (astroparticle community)
  - high radio sensitivity (radio-astronomy community)



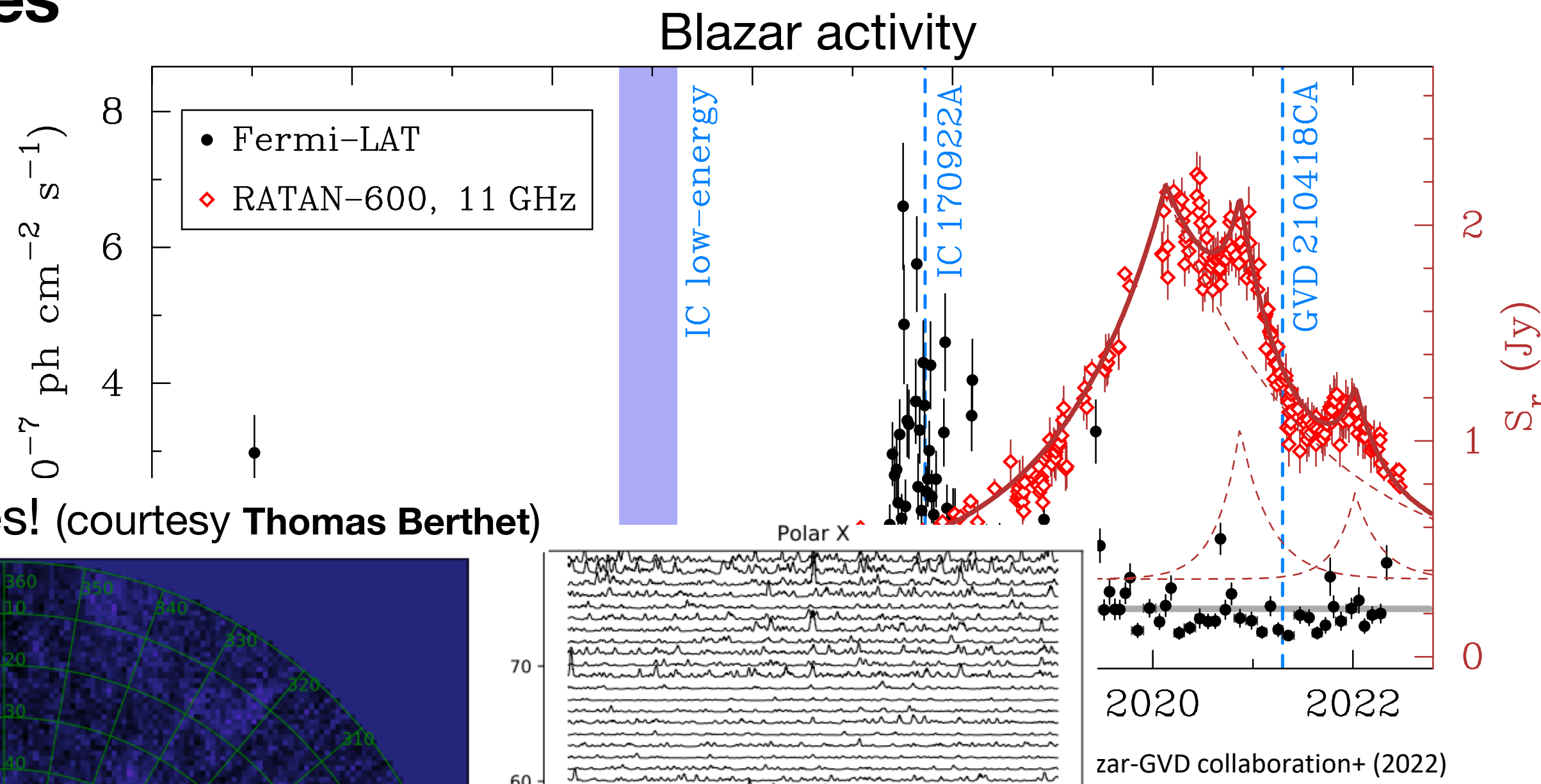
RadioGaGa:  
beamformed radio arrays for EAS gamma ray detection



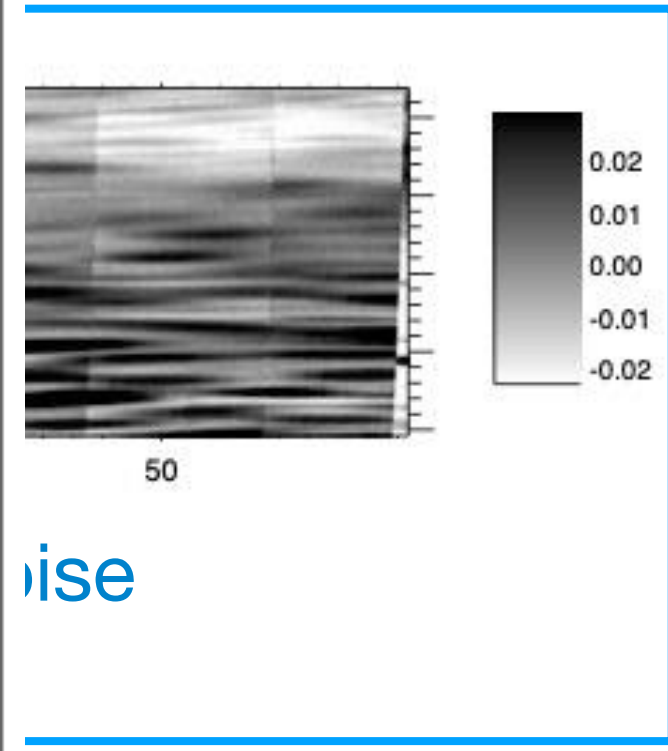
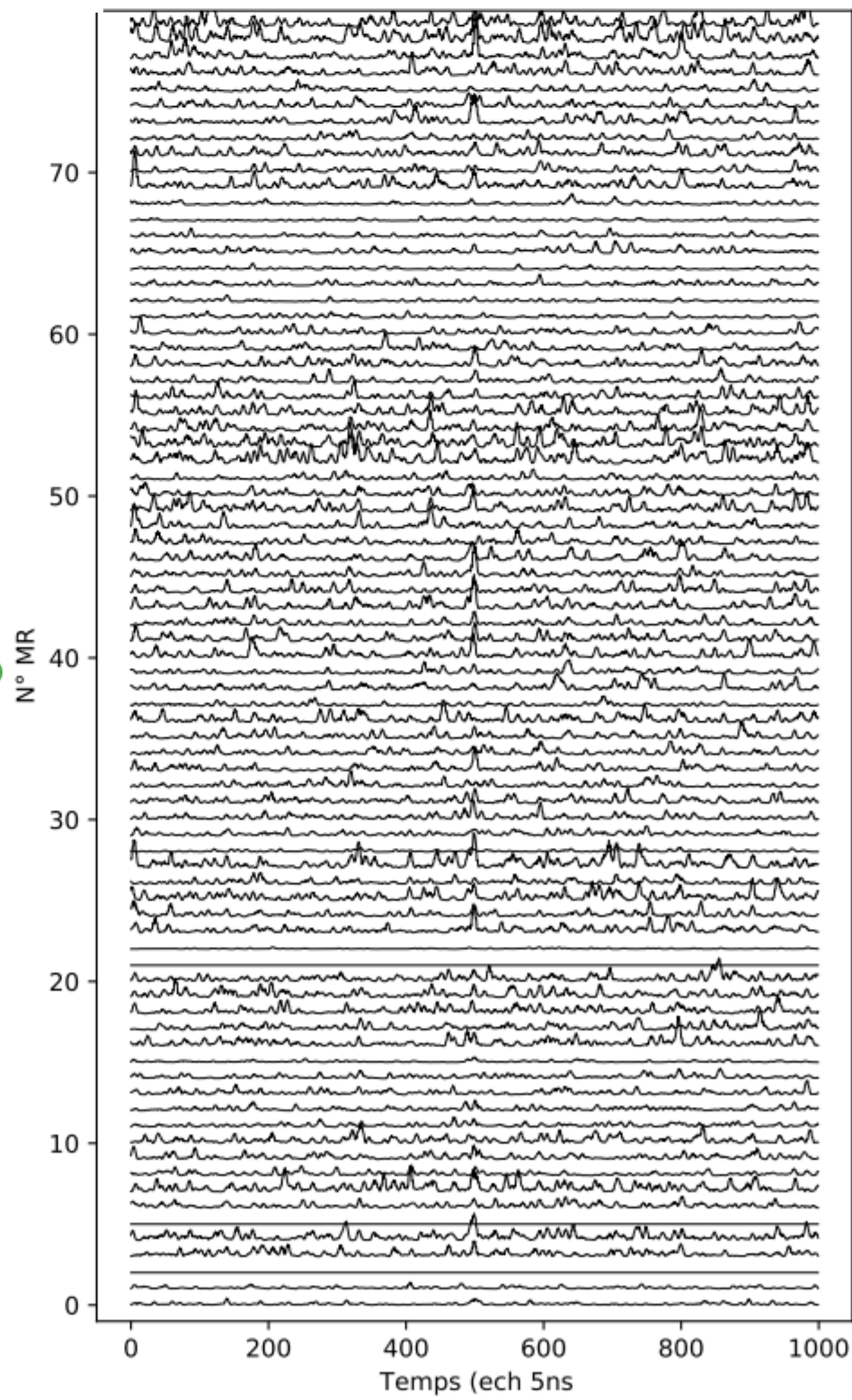
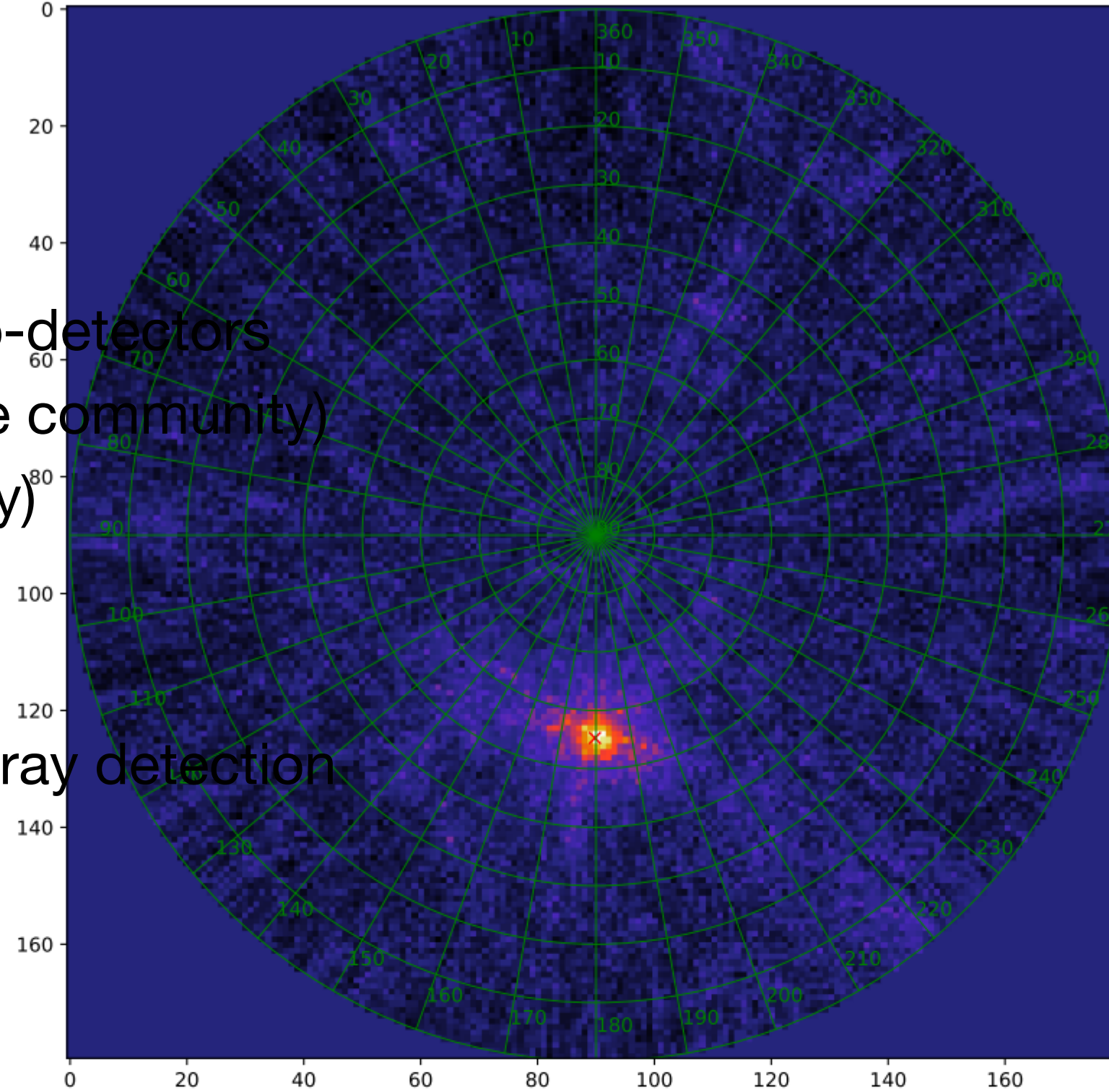


# Combining astroparticle detectors and radio-telescopes

- **Observation strategies** → joint observations
  - improve alert strategies
  - bring unique insight for models
- **Alert strategies** → tuned thanks to model predictions and experimental feedbacks



Solar nano pulses! (courtesy Thomas Berthet)



**Transverse experiments:** radio-astronomy / radio-detectors

- high background rejection expertise (astroparticle community)
- high radio sensitivity (radio-astronomy community)

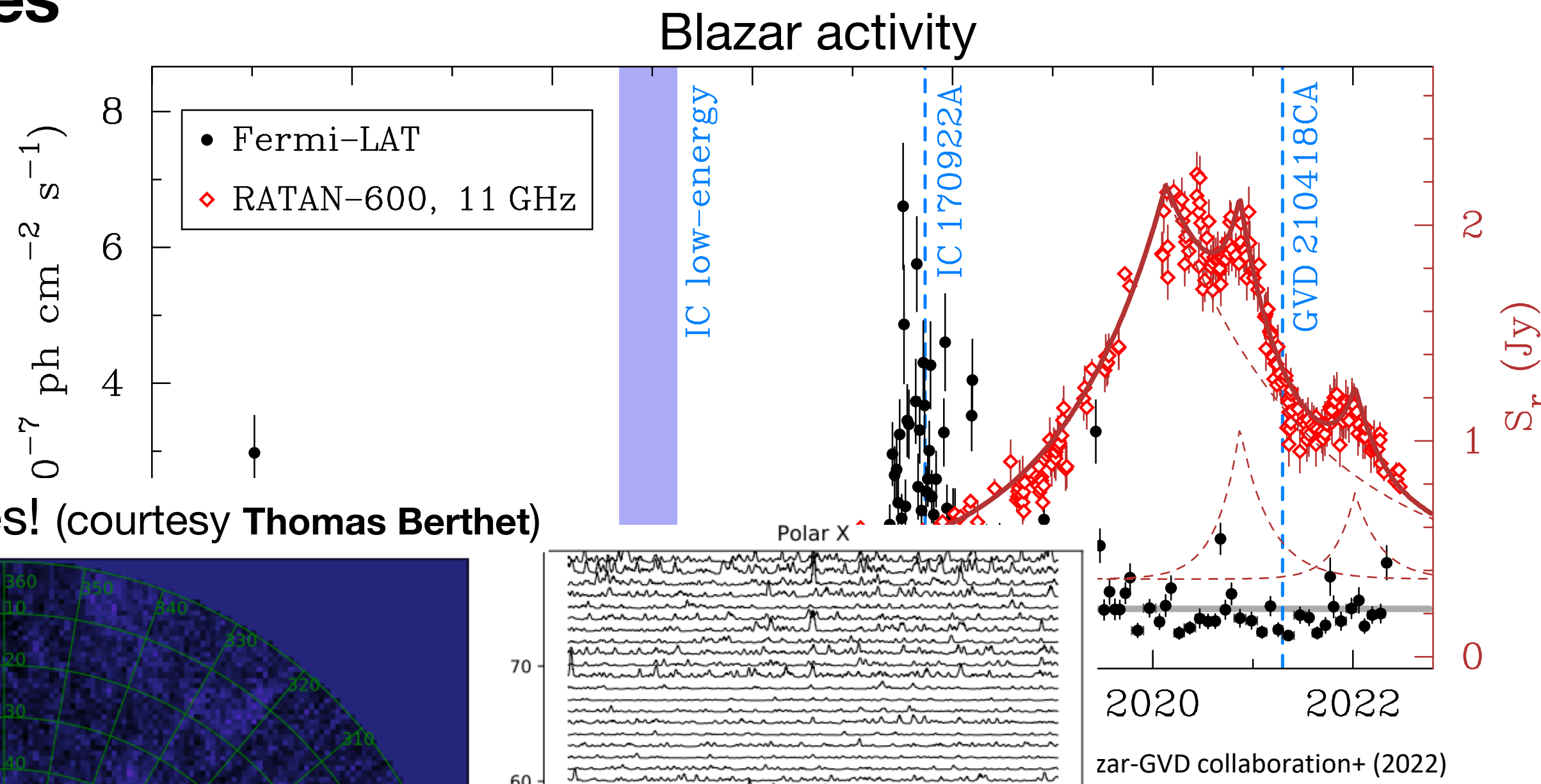
➤ RadioGaGa:  
beamformed radio arrays for EAS gamma ray detection

➤ RadioGaGa trigger:  
develop for gamma-ray EAS and to be used for FRB

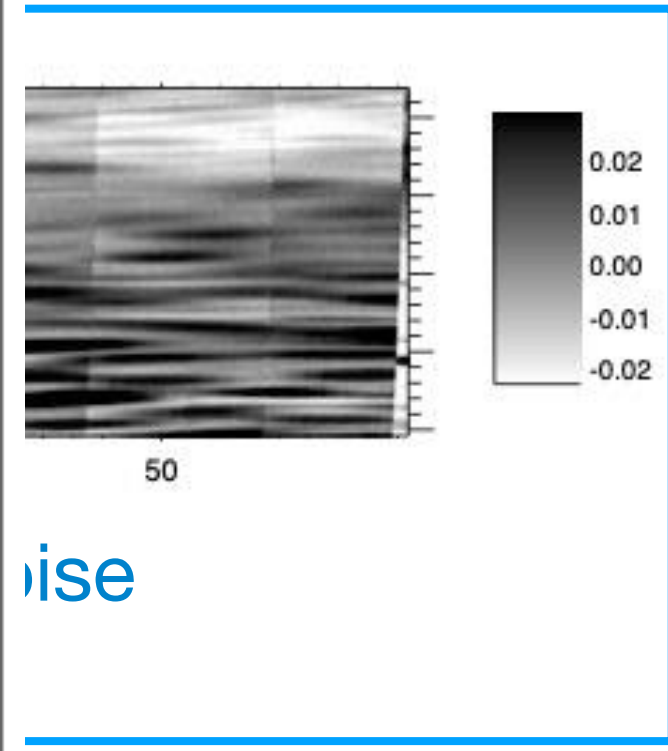
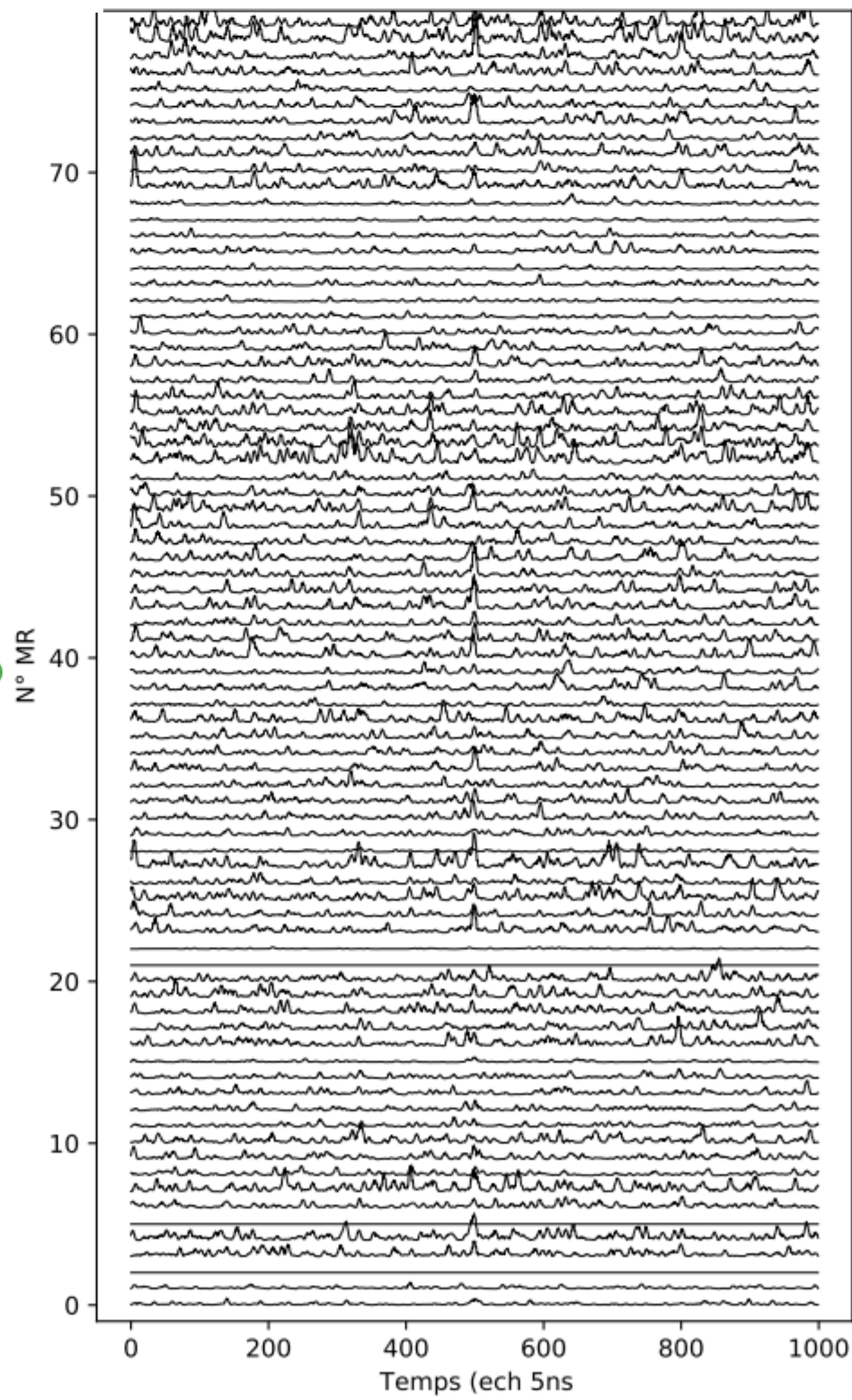
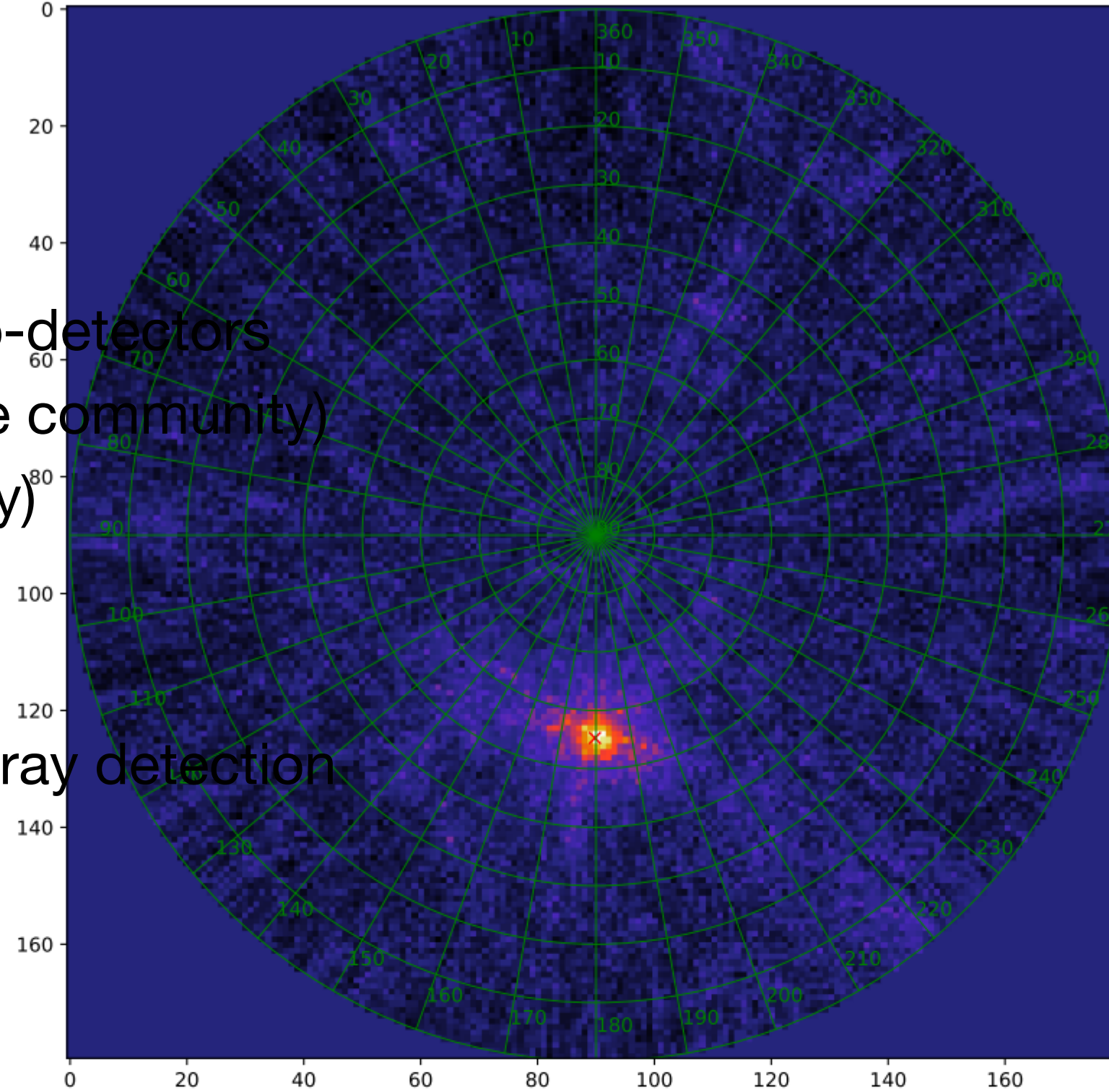


# Combining astroparticle detectors and radio-telescopes

- **Observation strategies** → joint observations
  - improve alert strategies
  - bring unique insight for models
- **Alert strategies** → tuned thanks to model predictions and experimental feedbacks



Solar nano pulses! (courtesy Thomas Berthet)



**Transverse experiments:** radio-astronomy / radio-detectors

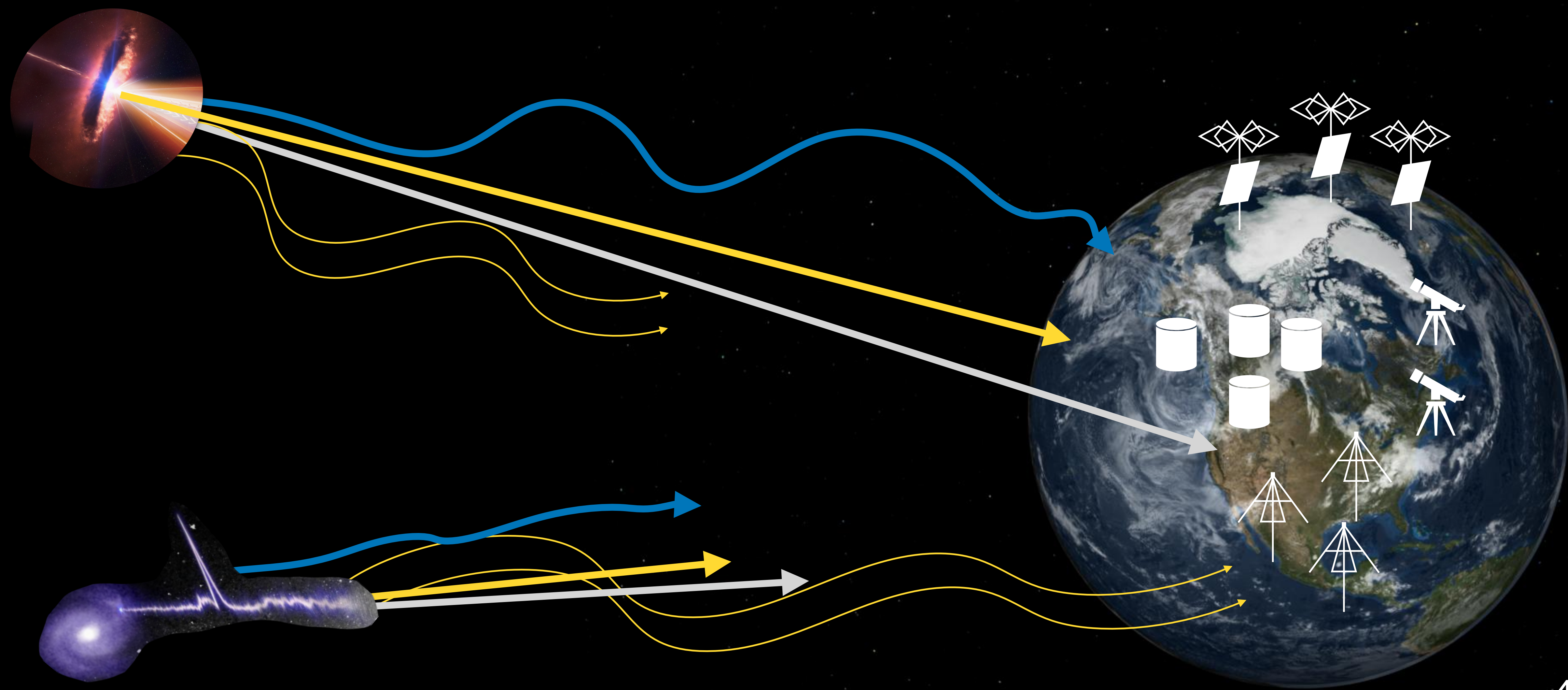
- high background rejection expertise (astroparticle community)
- high radio sensitivity (radio-astronomy community)

➤ RadioGaGa: beamformed radio arrays for EAS gamma ray detection

➤ RadioGaGa trigger: develop for gamma-ray EAS and to be used for FRB



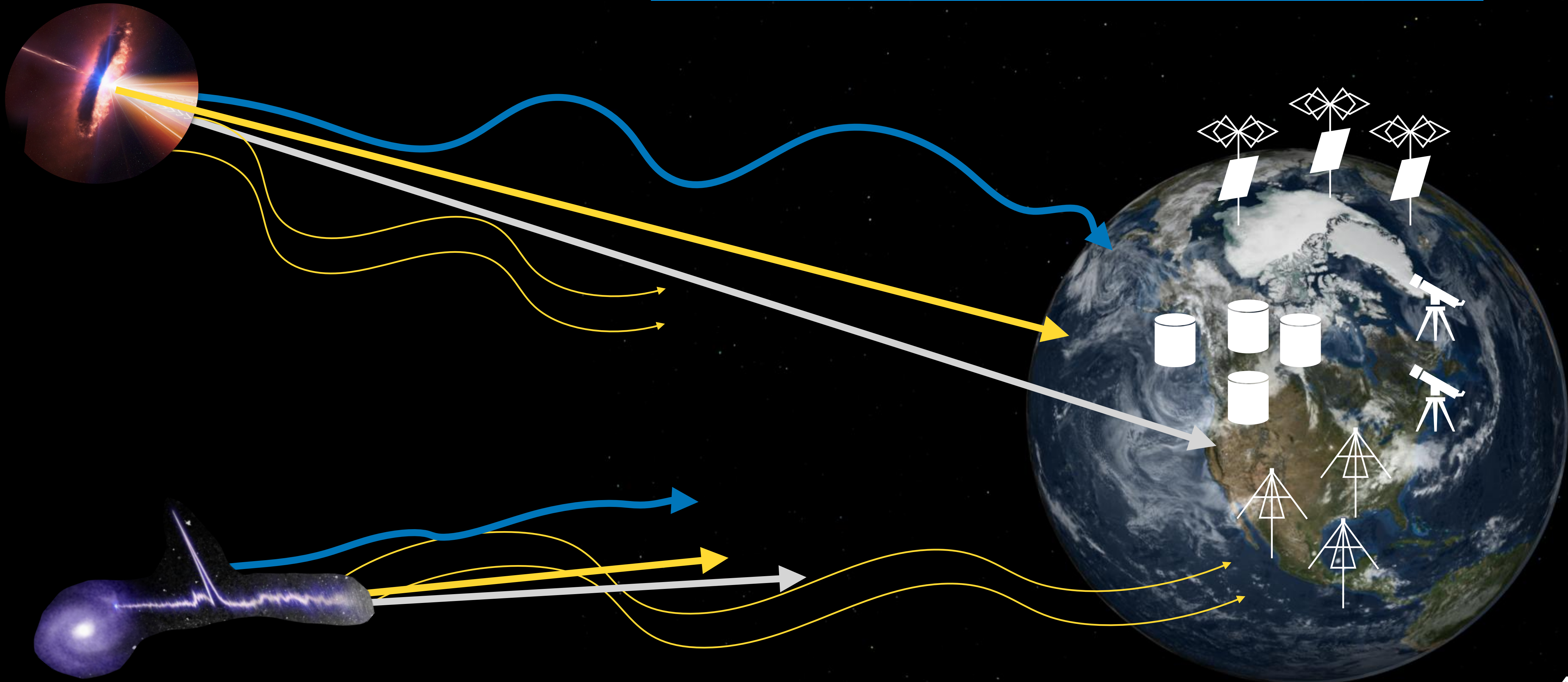
# Conclusion





# Conclusion

The advent of the multi messenger astronomy mixed the frontiers between astroparticles and radioastronomy sources

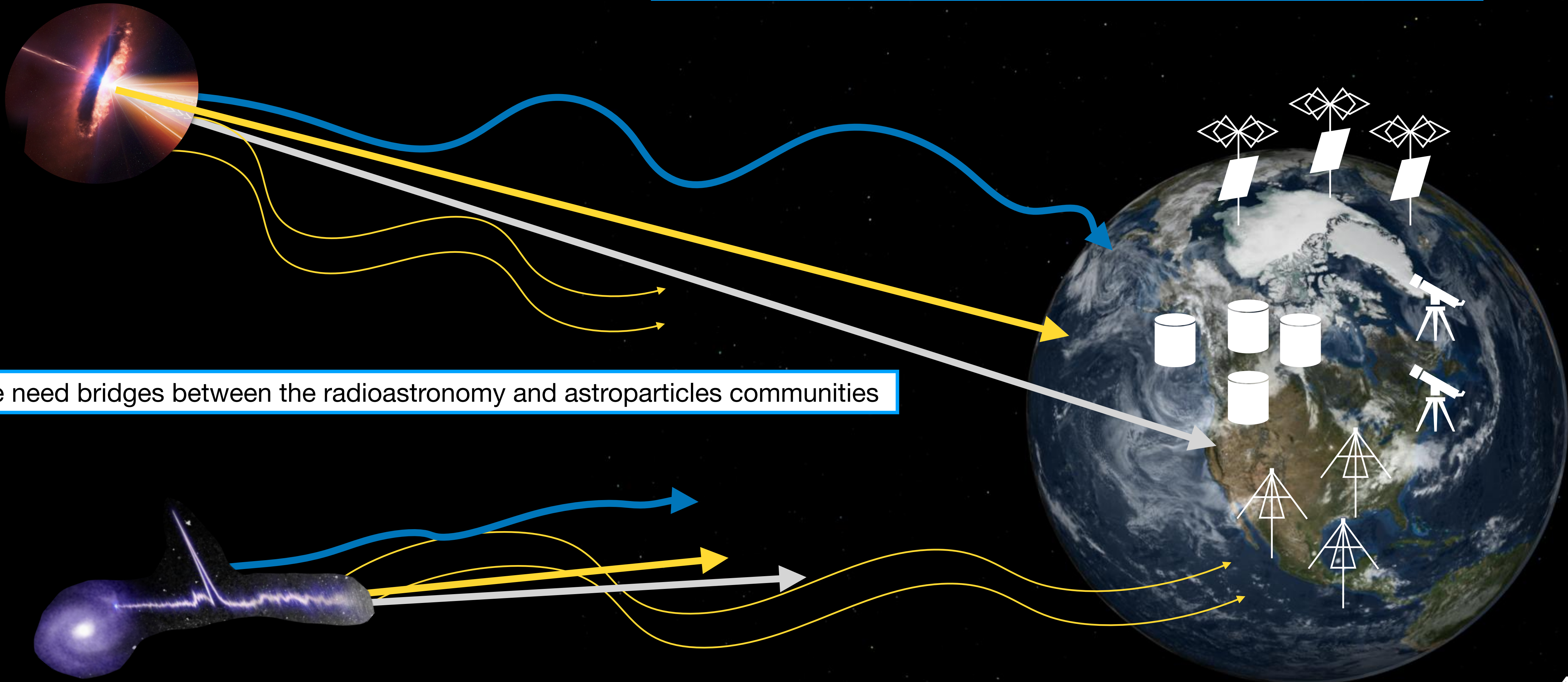




# Conclusion

The advent of the multi messenger astronomy mixed the frontiers between astroparticles and radioastronomy sources

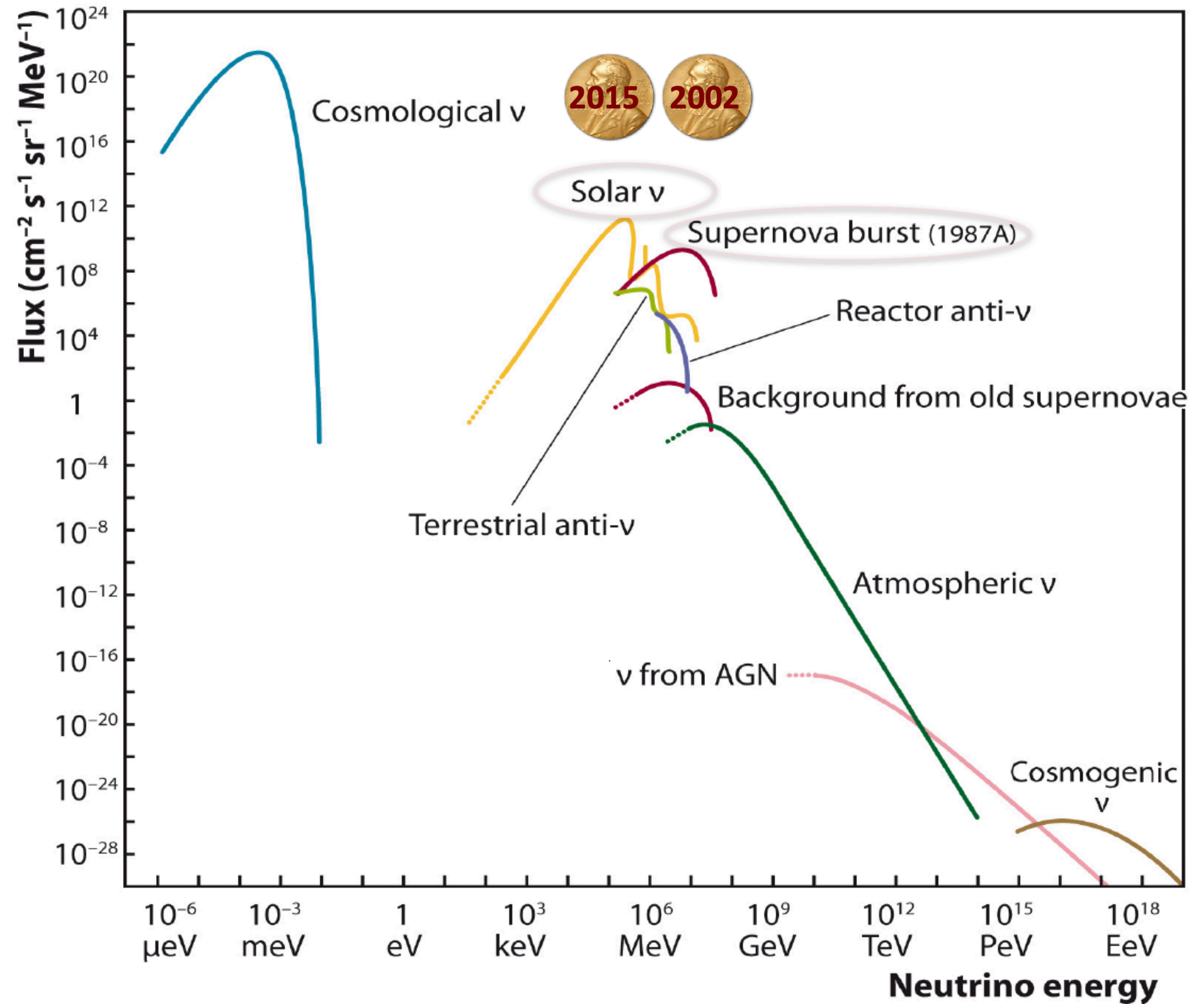
We need bridges between the radioastronomy and astroparticles communities





**Backup slides**

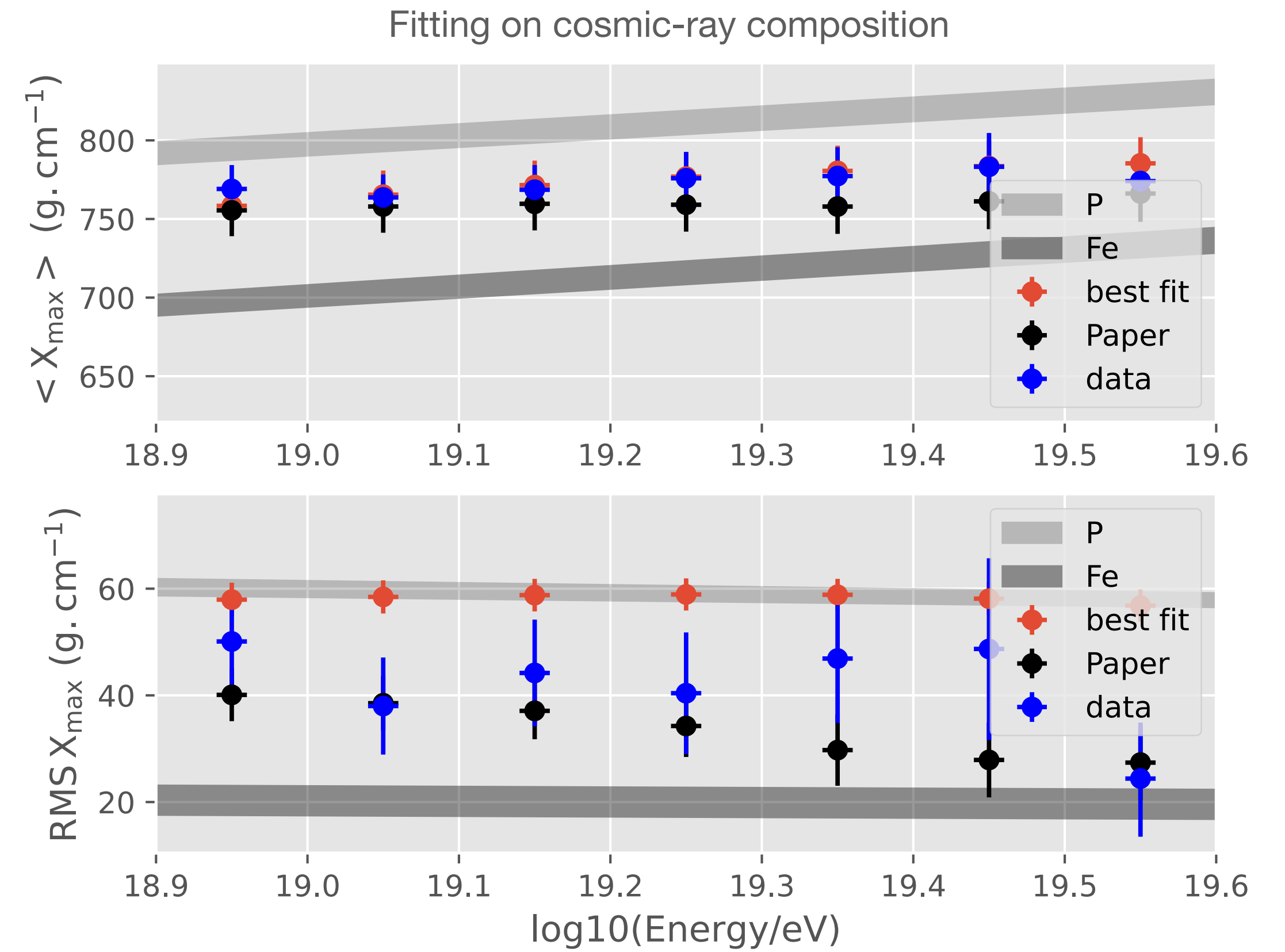
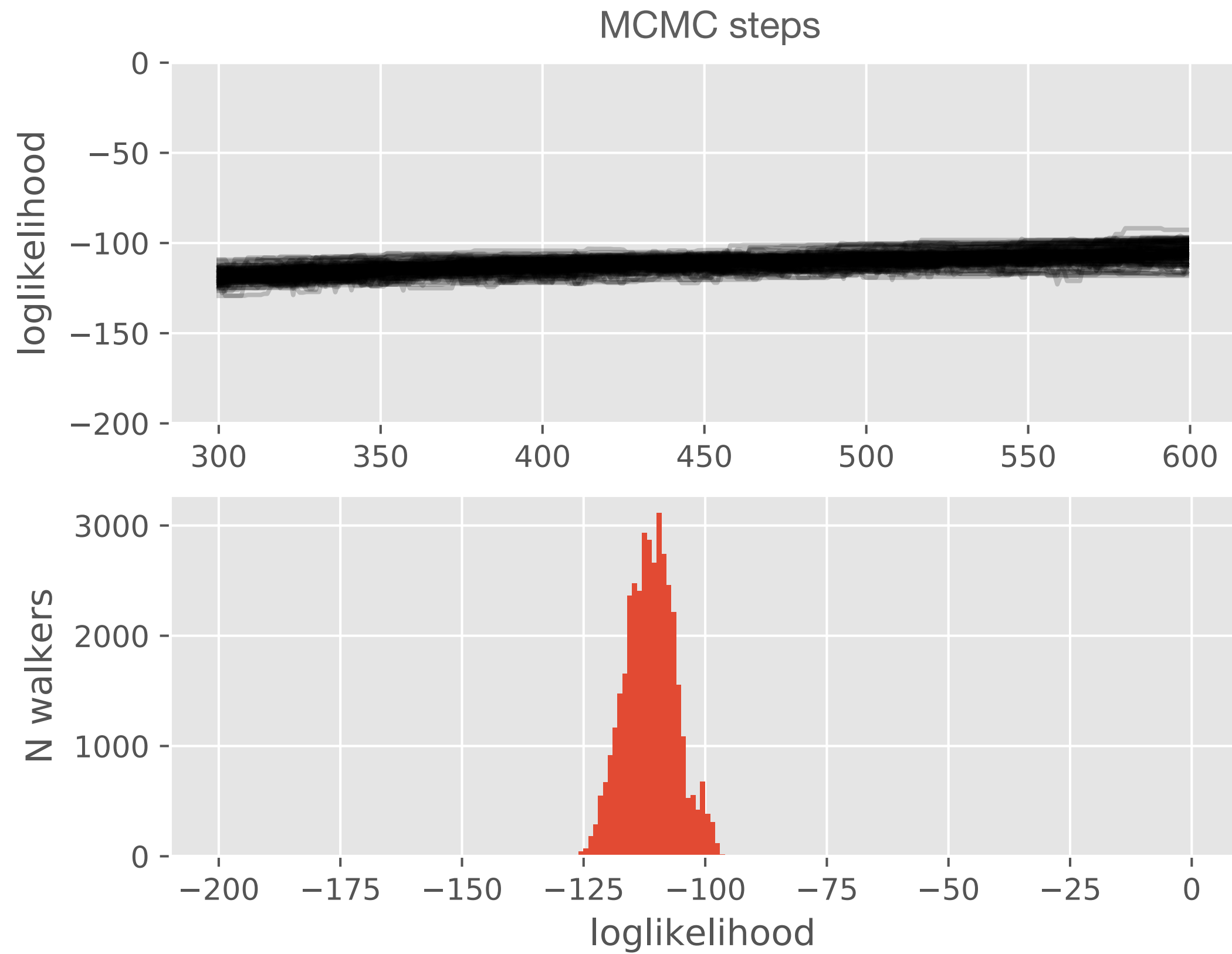
# Neutrino landscape





# Constraining the possible sources of cosmogenic neutrinos

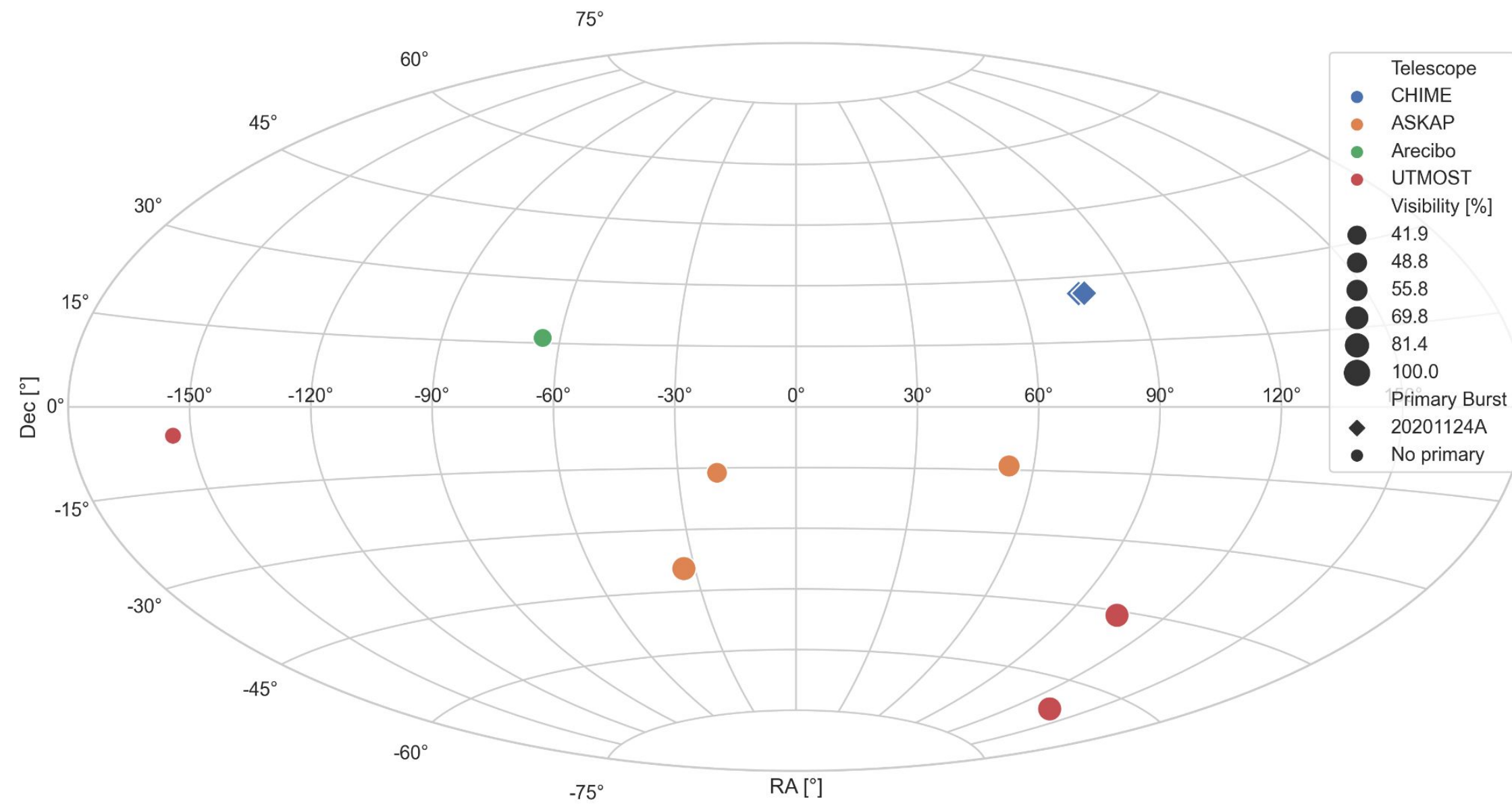
Parameter space exploration with MCMC methods



# KM3NeT activities at Subatech : FRB analysis

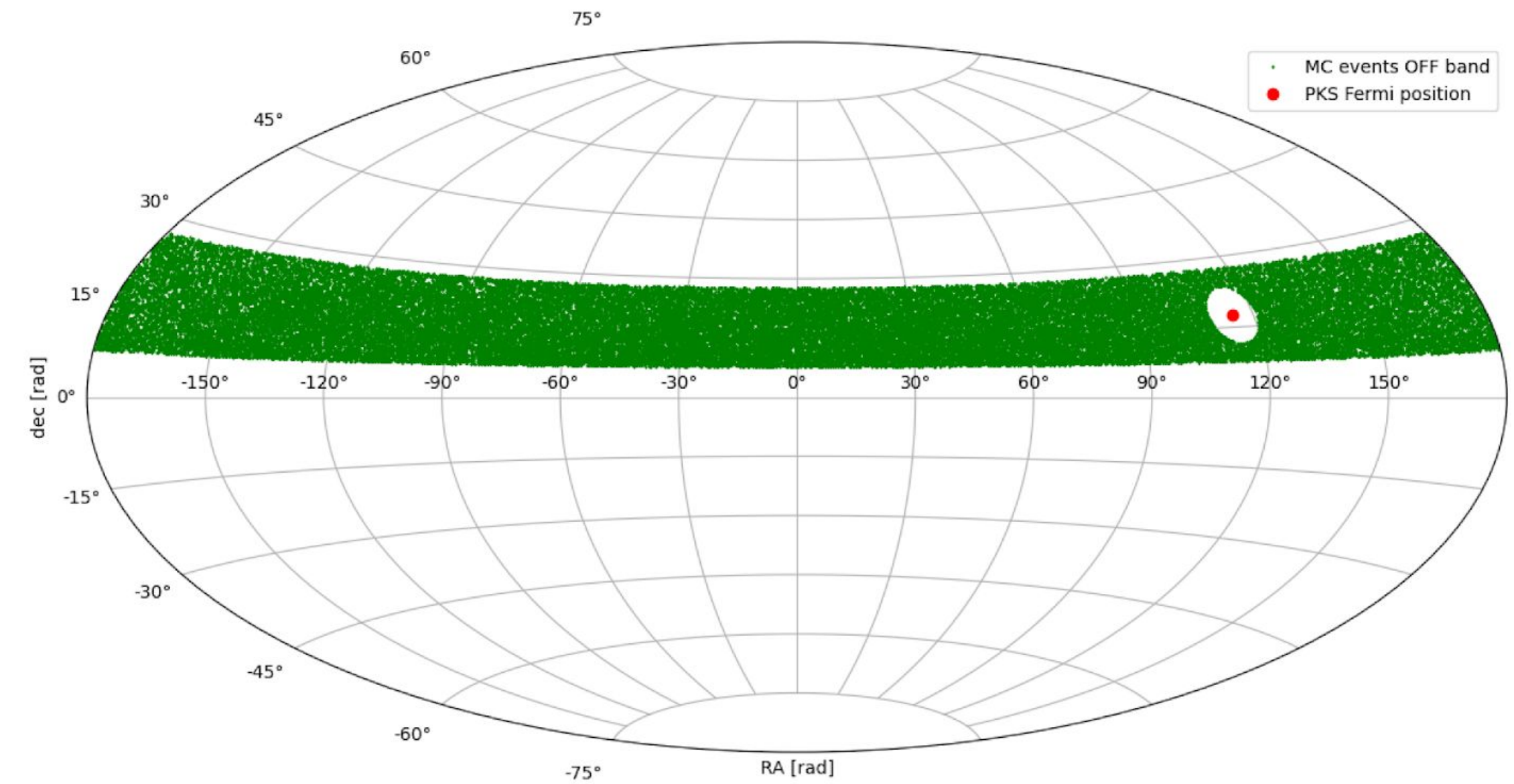


Sky map of FRBs observed during ORCA6  
with a visibility over 39% in a +/- 6h time window around the detection



43 targets observed by ORCA6 & Nançay  
12 targets with visibility > 39%

ON-OFF definition Arca MC

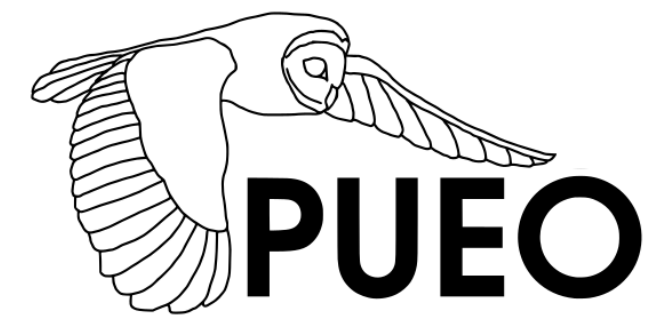


Région OFF délimitée par la bande de déclinaison de +/- 10° autour de la position de PKS 0735 [KM3NeT collaboration, 2022]

ON/OFF example

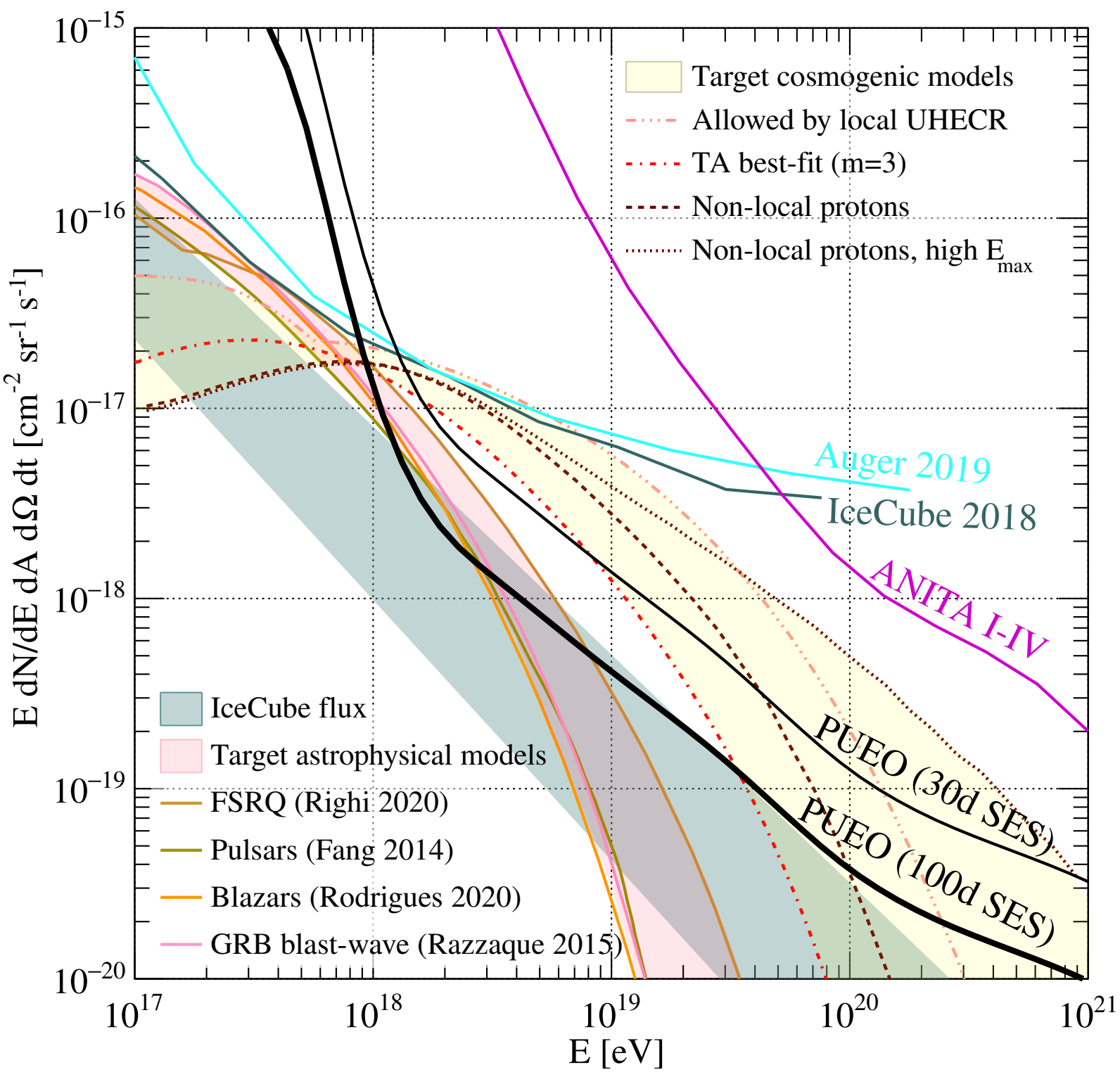


# Payload for Ultrahigh Energy Observations (PUEO)

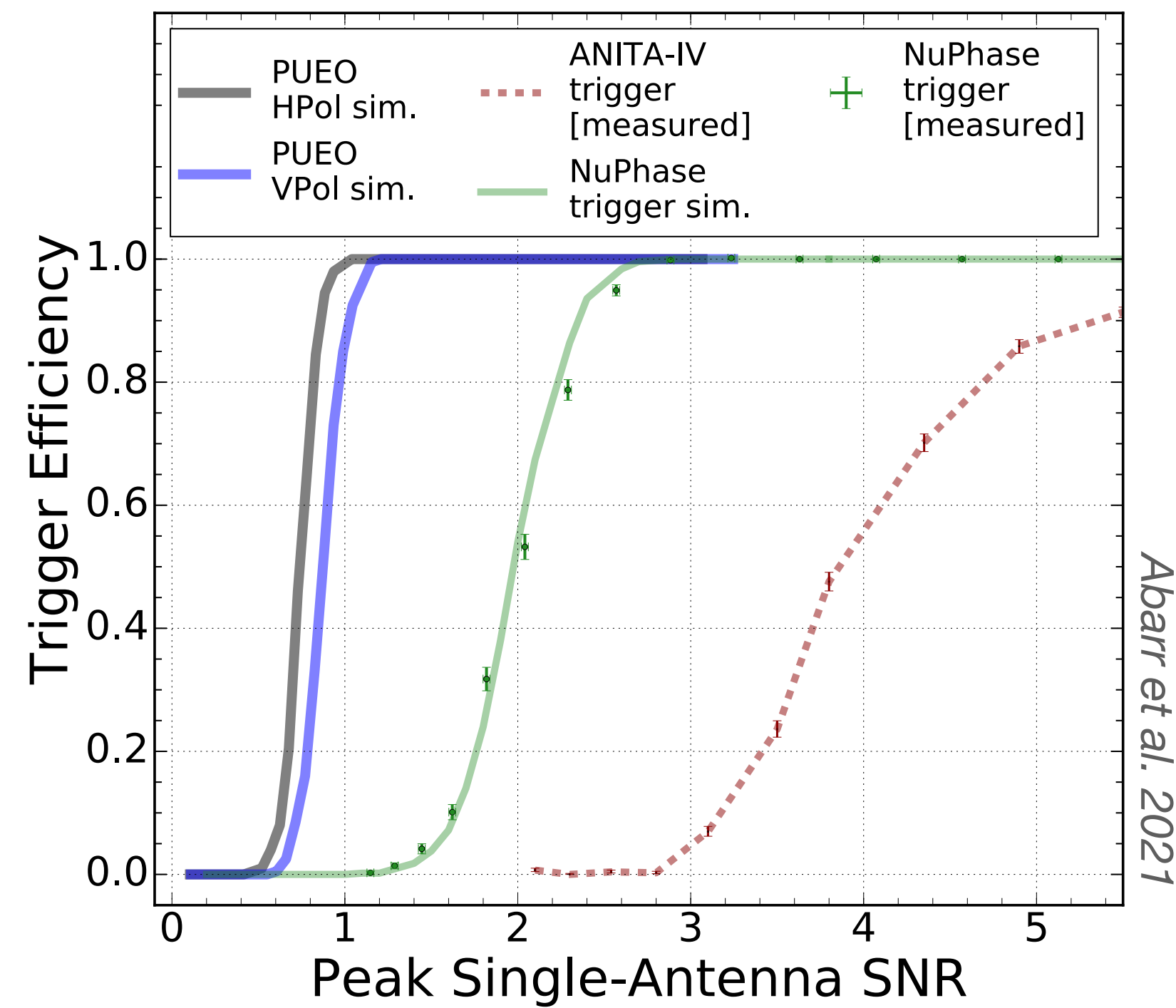


How to do better with same size constraints?

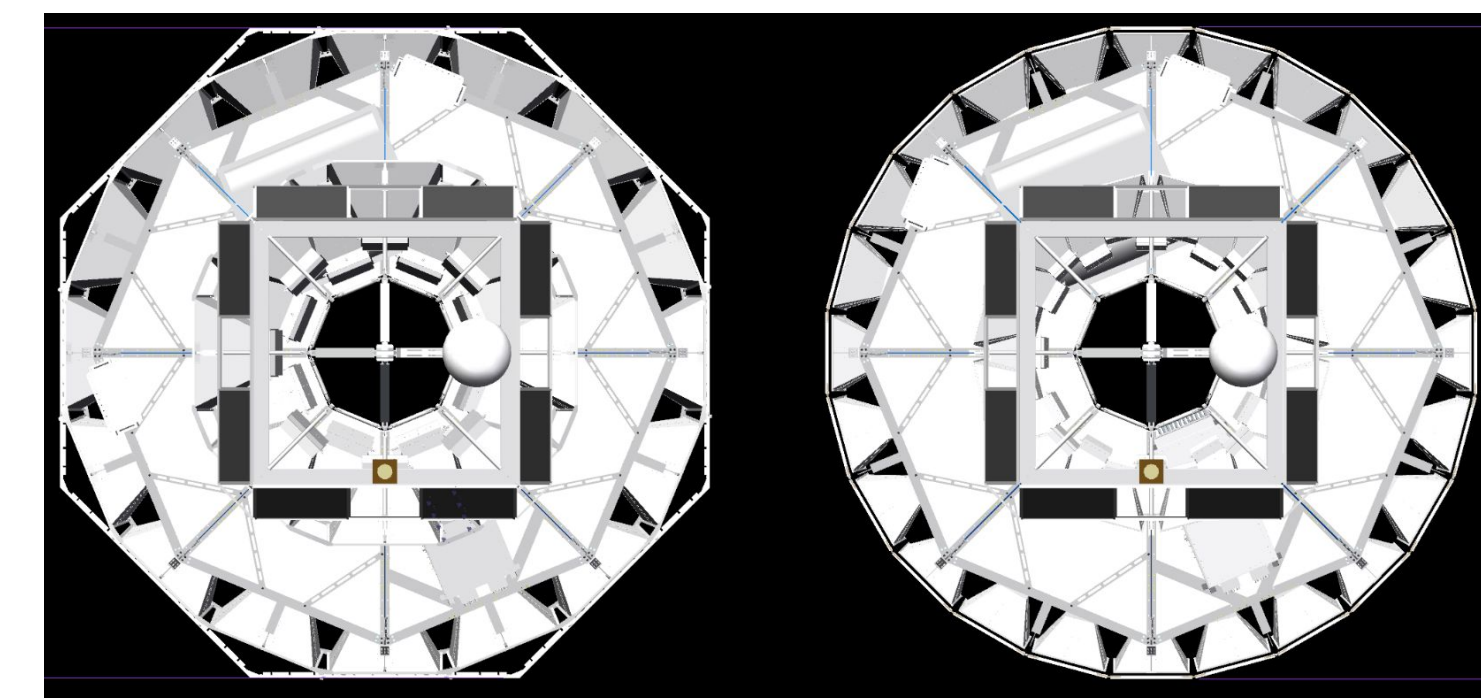
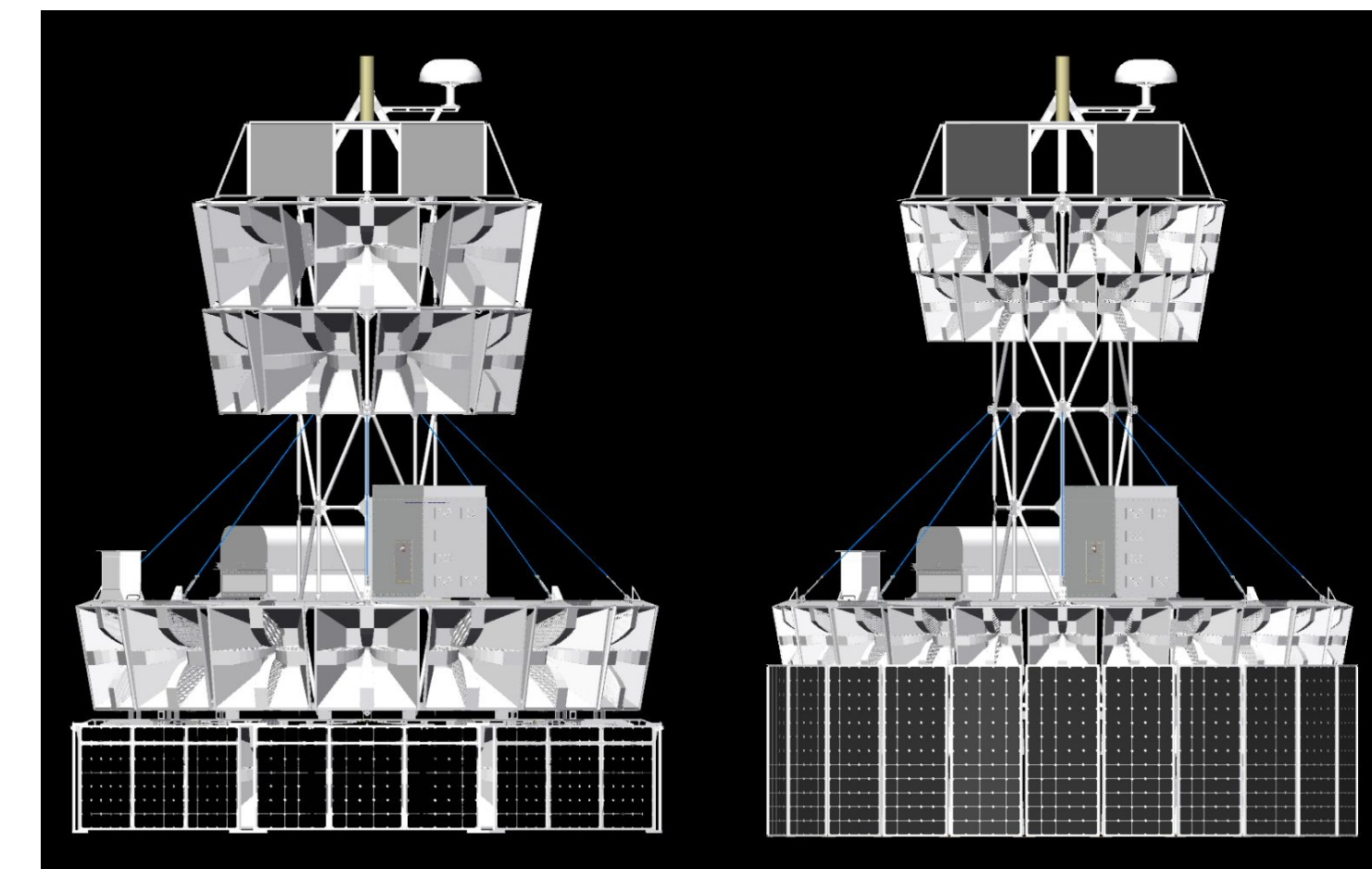
Predicted sensitivity for PUEO



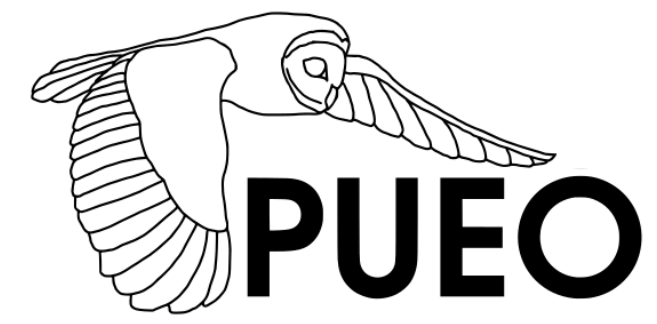
Increase of the detection threshold



Comparison ANITA IV / PUEO

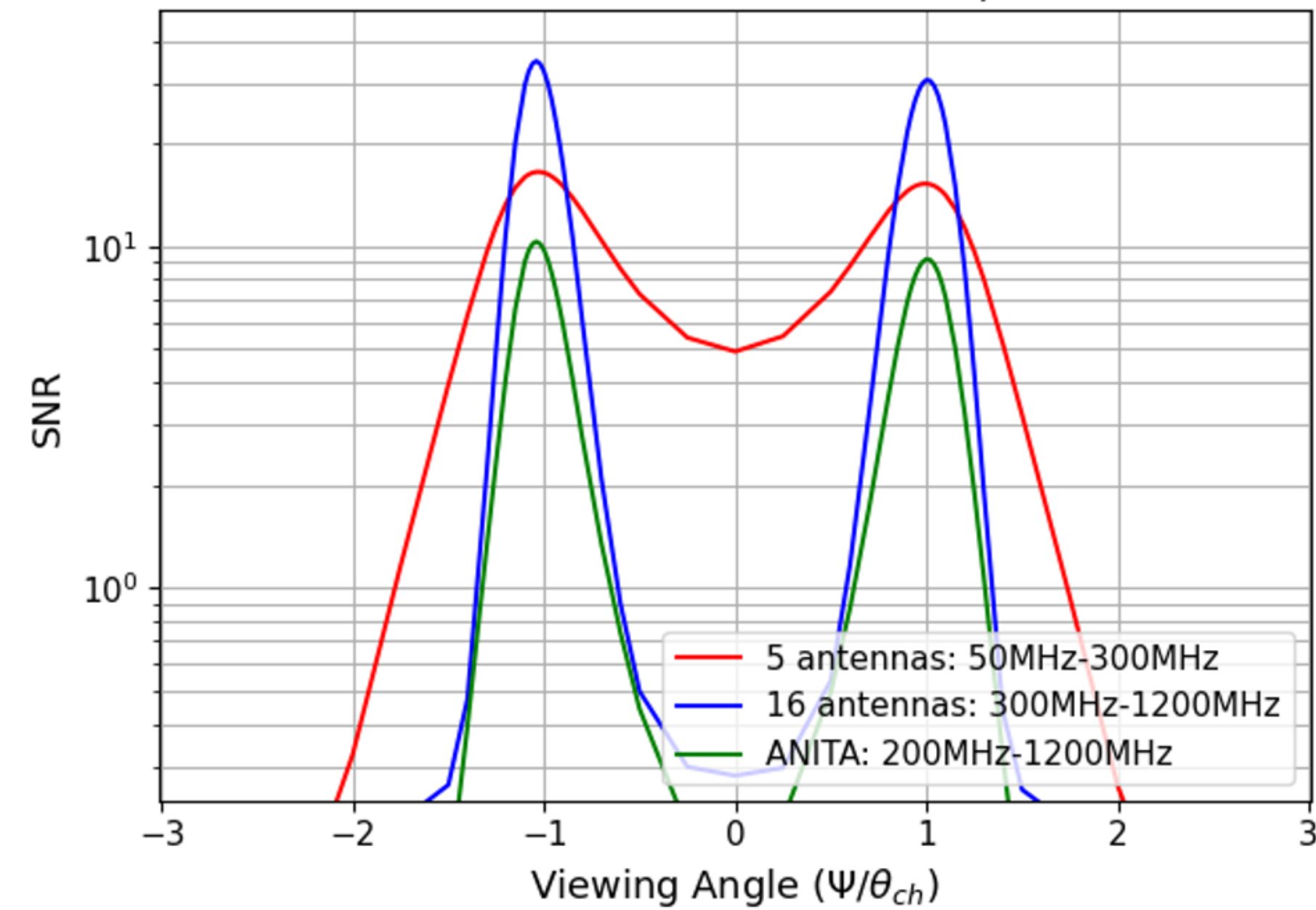


# Goal of the Low Frequency Instrument

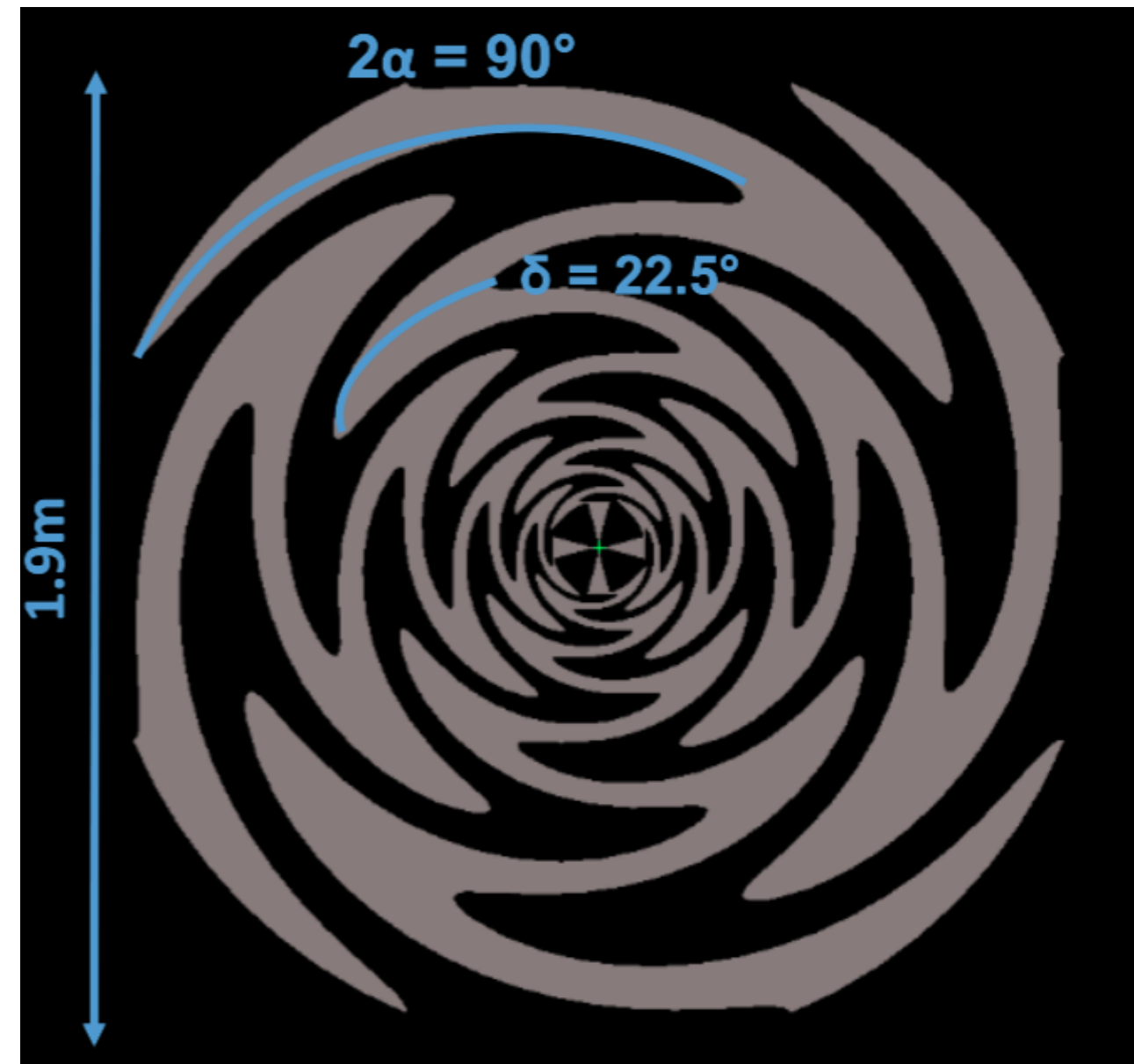


At low frequency the FoV increases hence the sensitivity

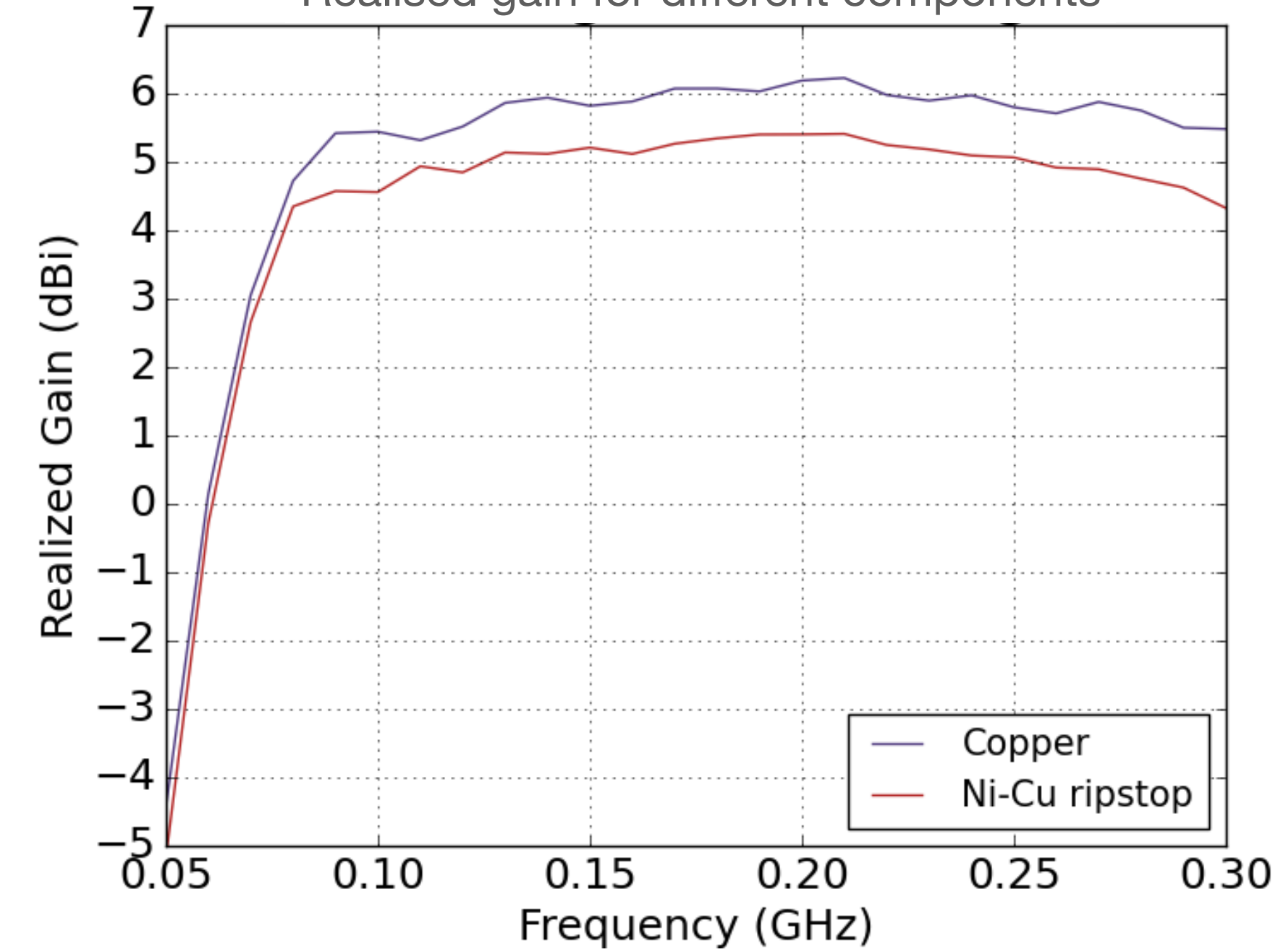
radio beam for EAS  
Reflected CR:  $E = 1\text{EeV}$ ,  $\theta = 80.0^\circ$ ,  $\phi = 0.0^\circ$



Sinuuous antenna



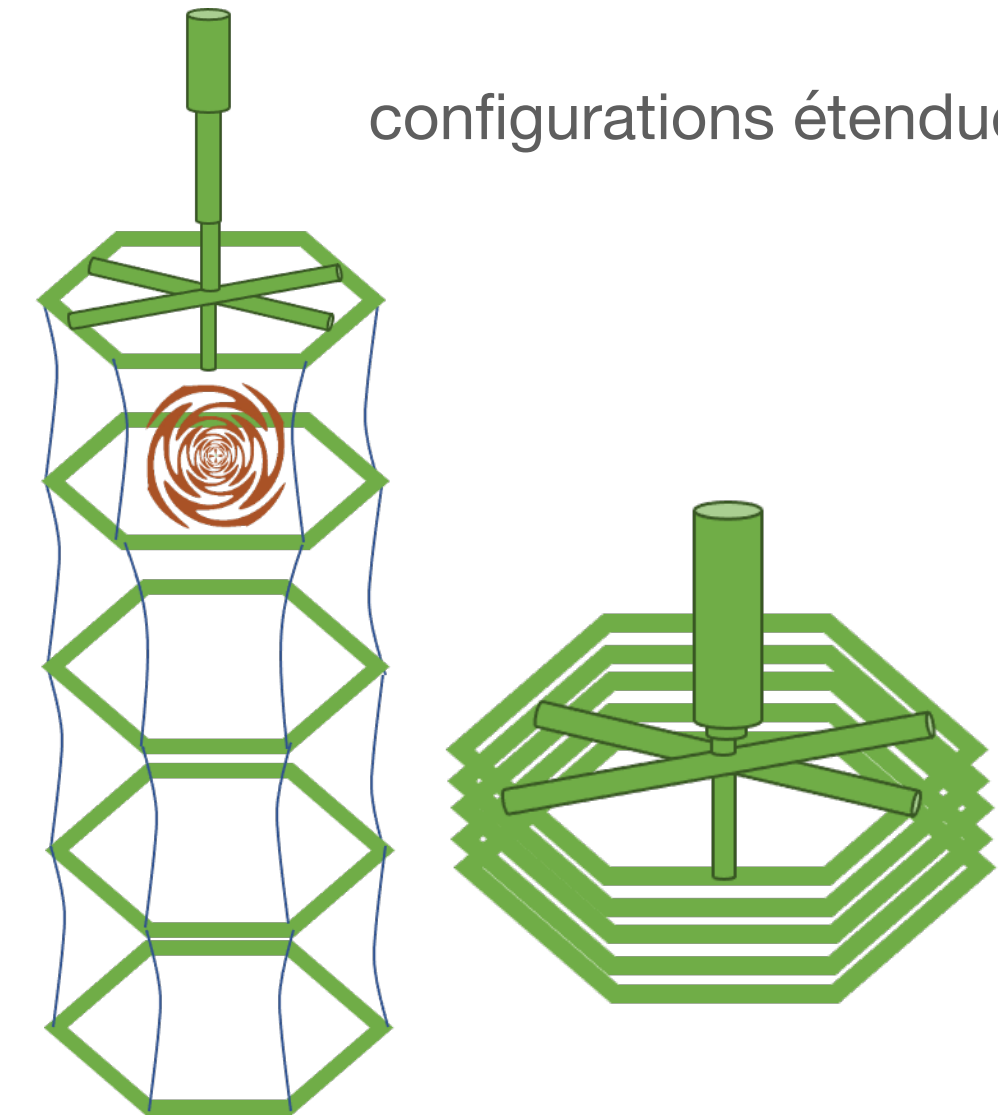
Realised gain for different components



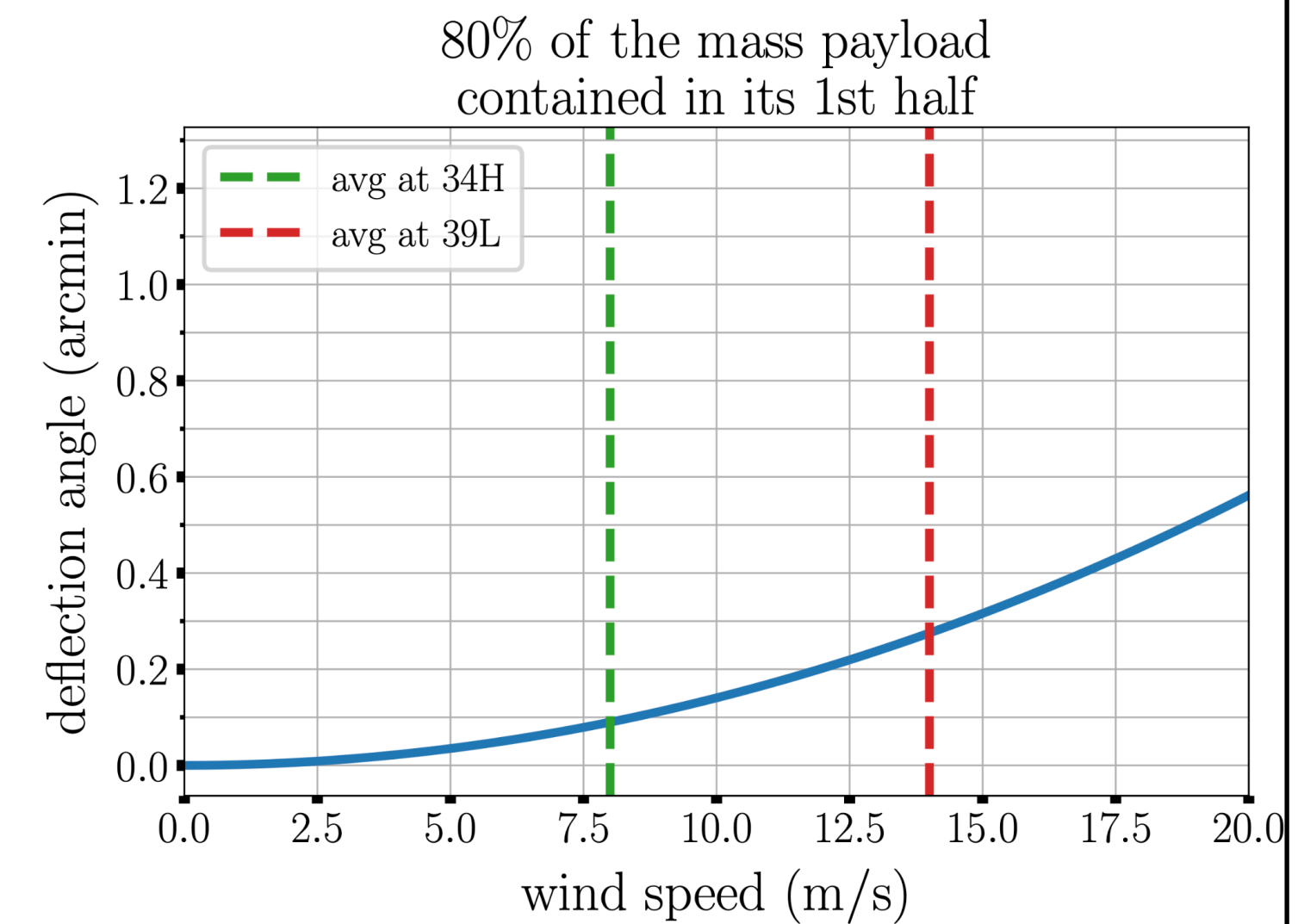
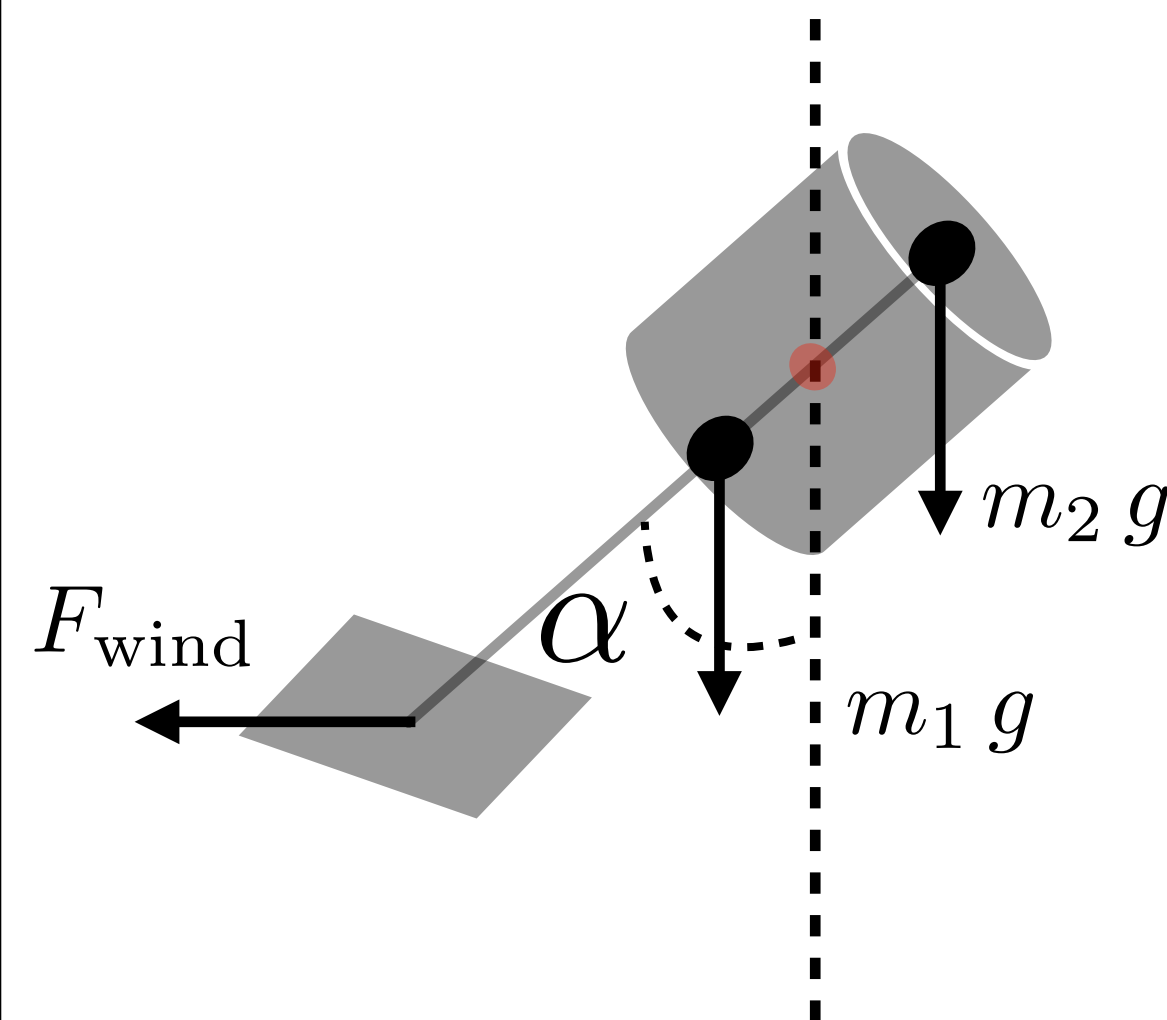
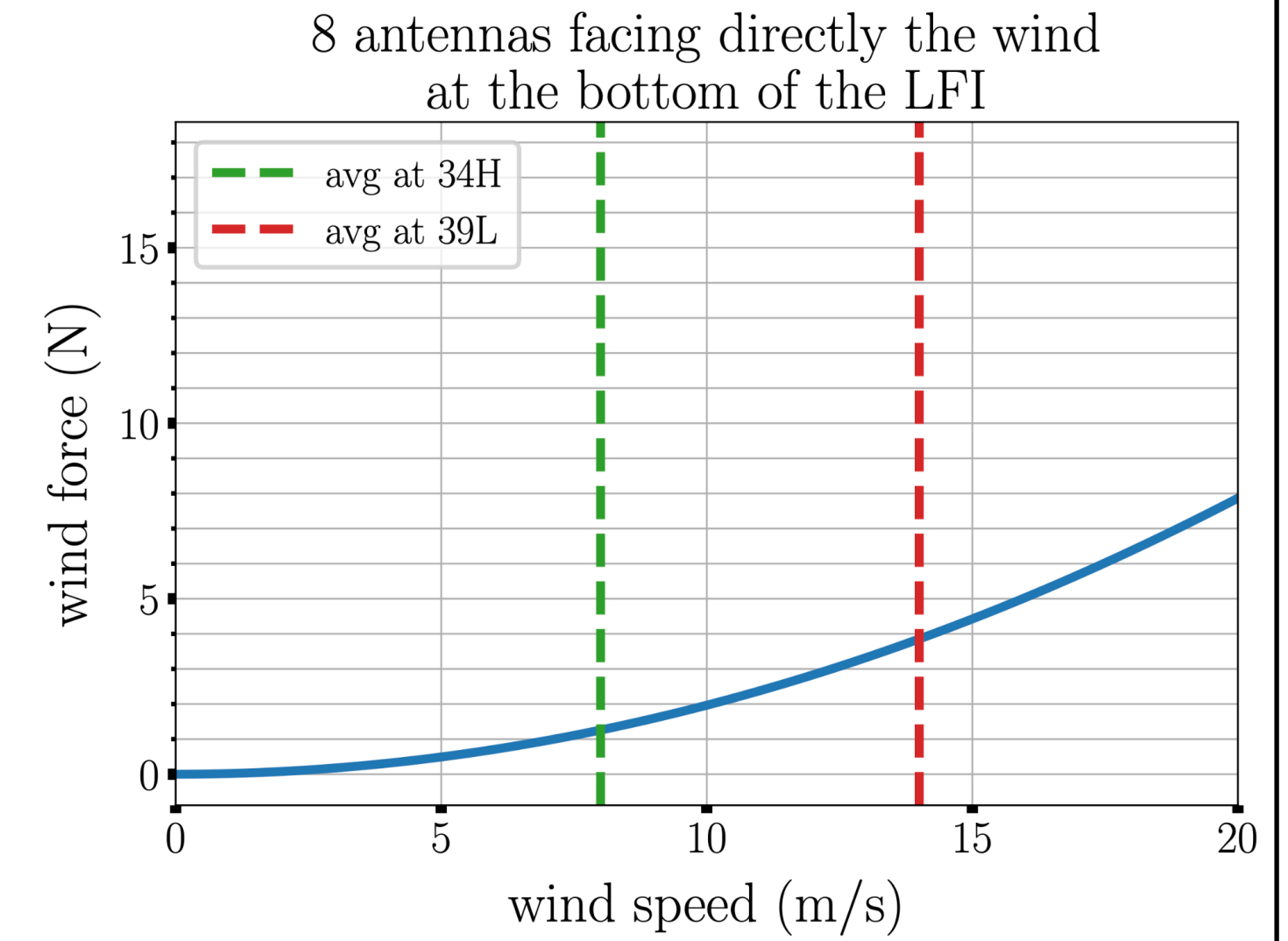
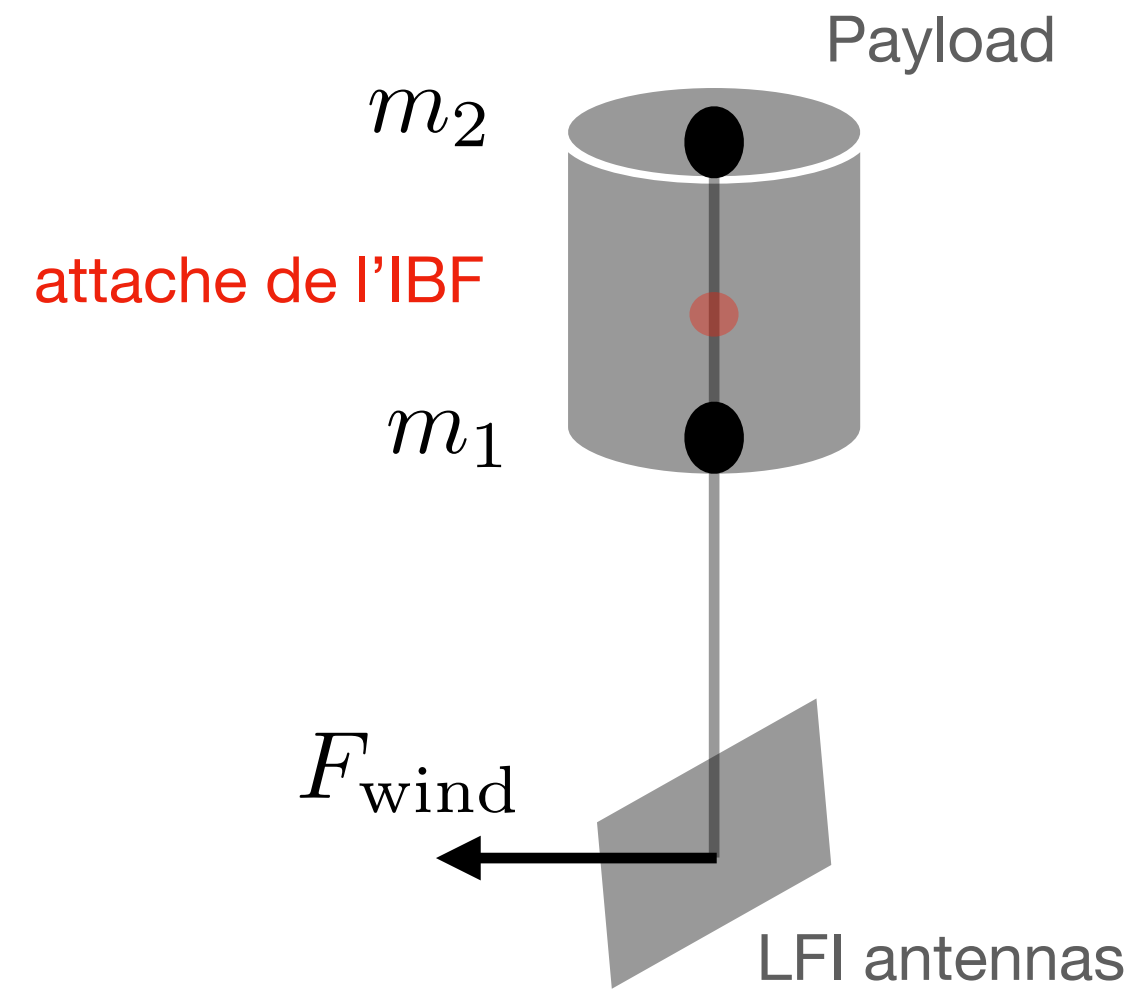


# LFI: risk assessment

configurations étendue et compacte

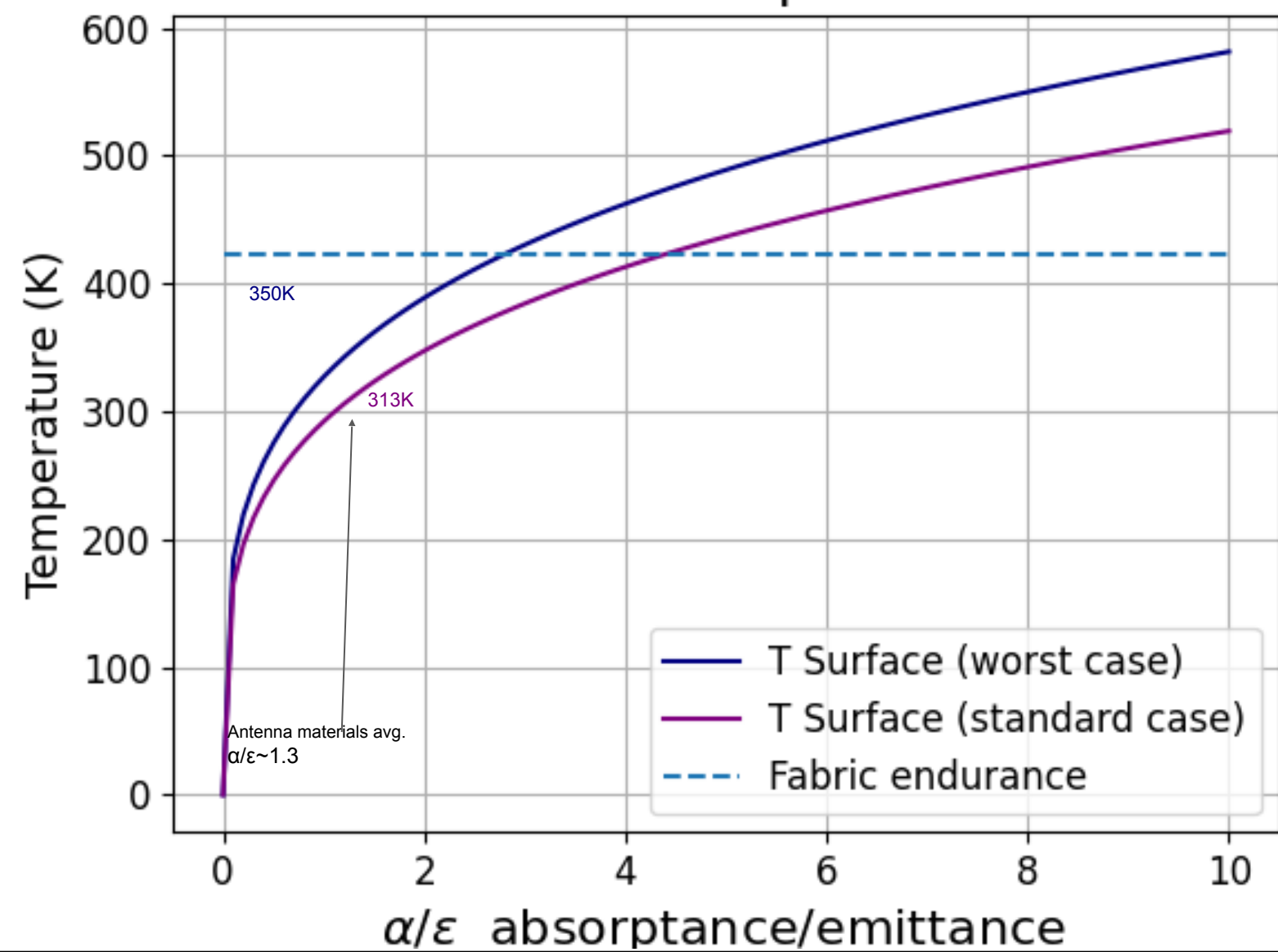


## Modélisation des effets du vents



## Modélisation des effets thermiques

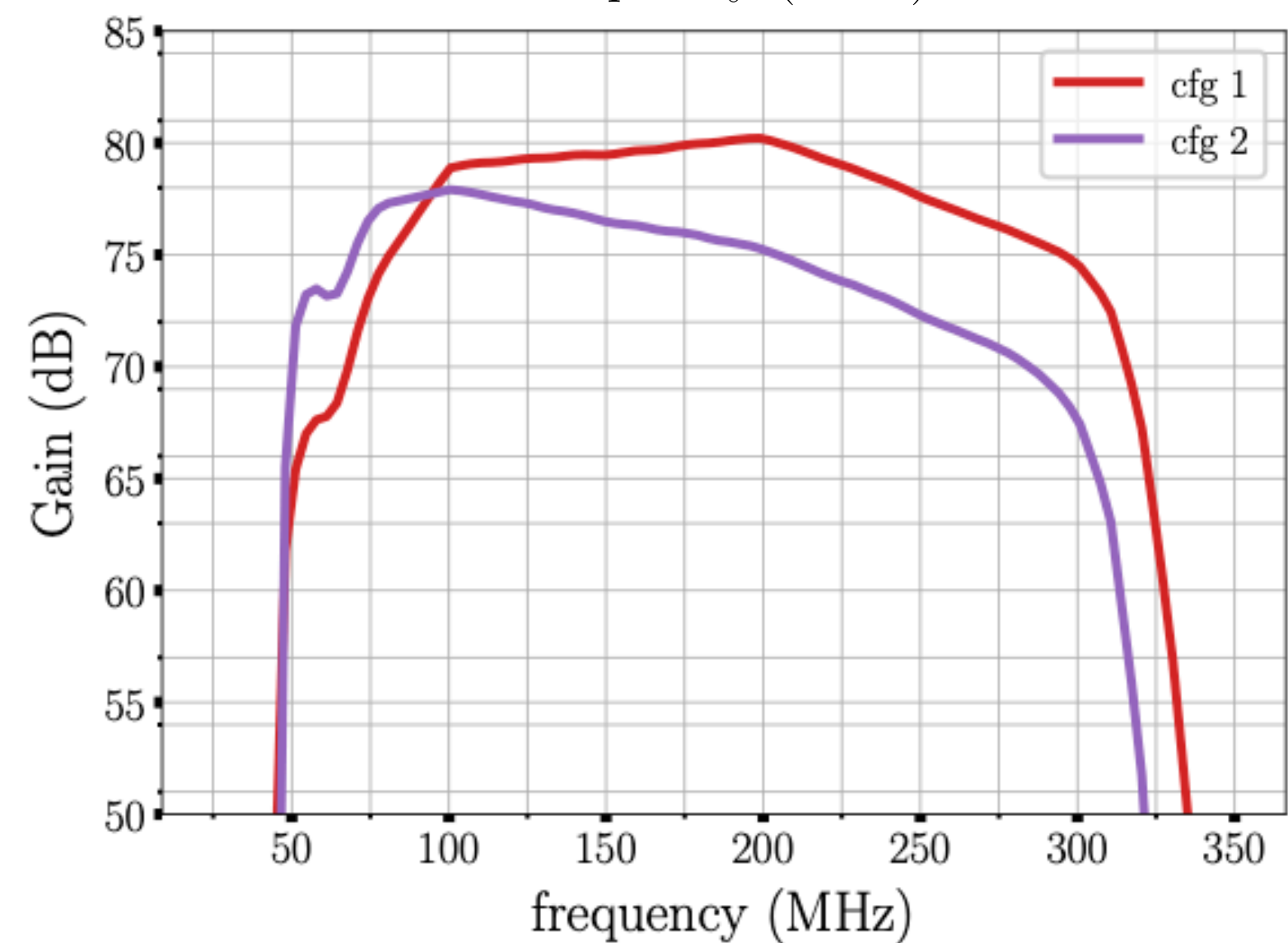
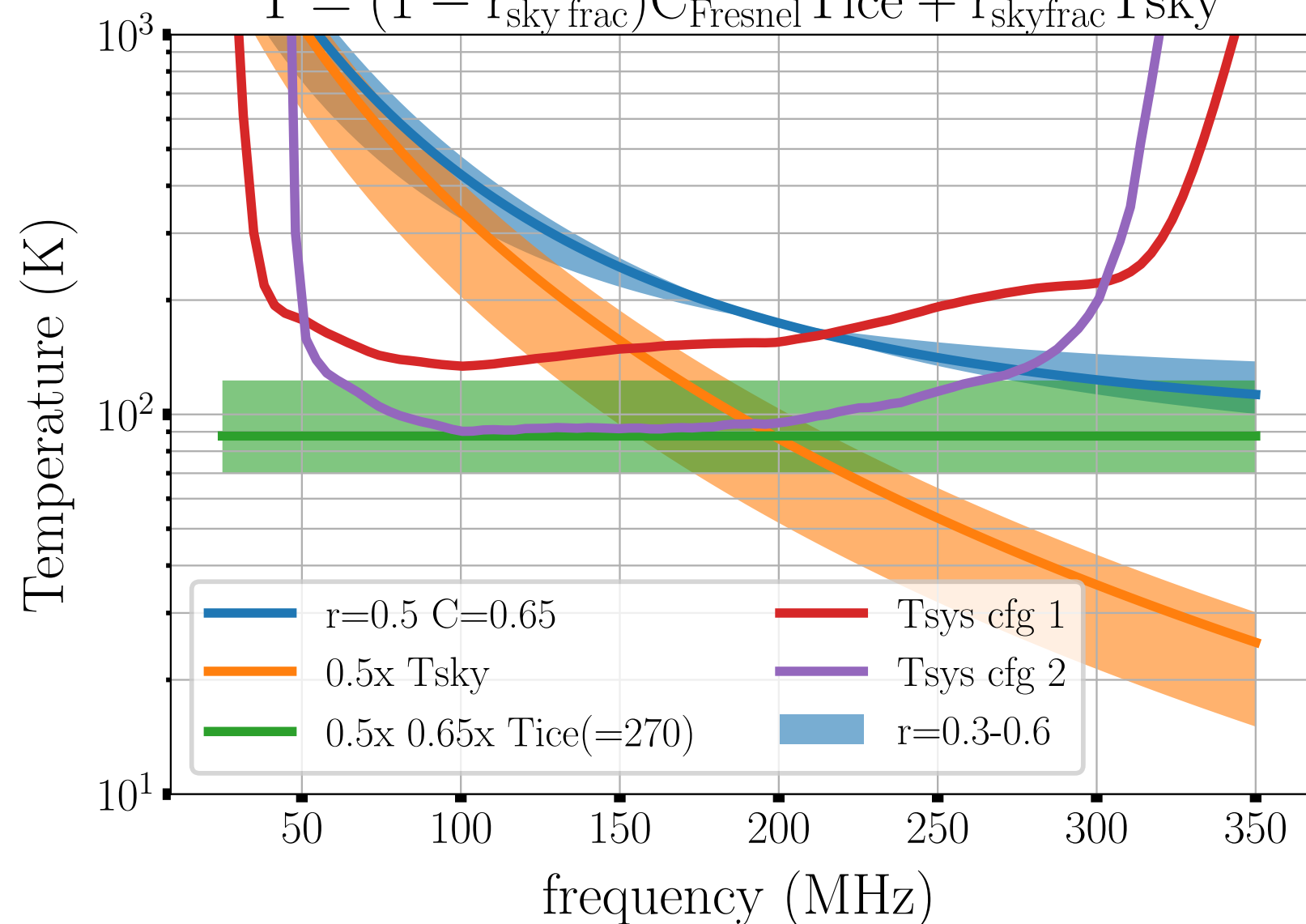
Surface temperature



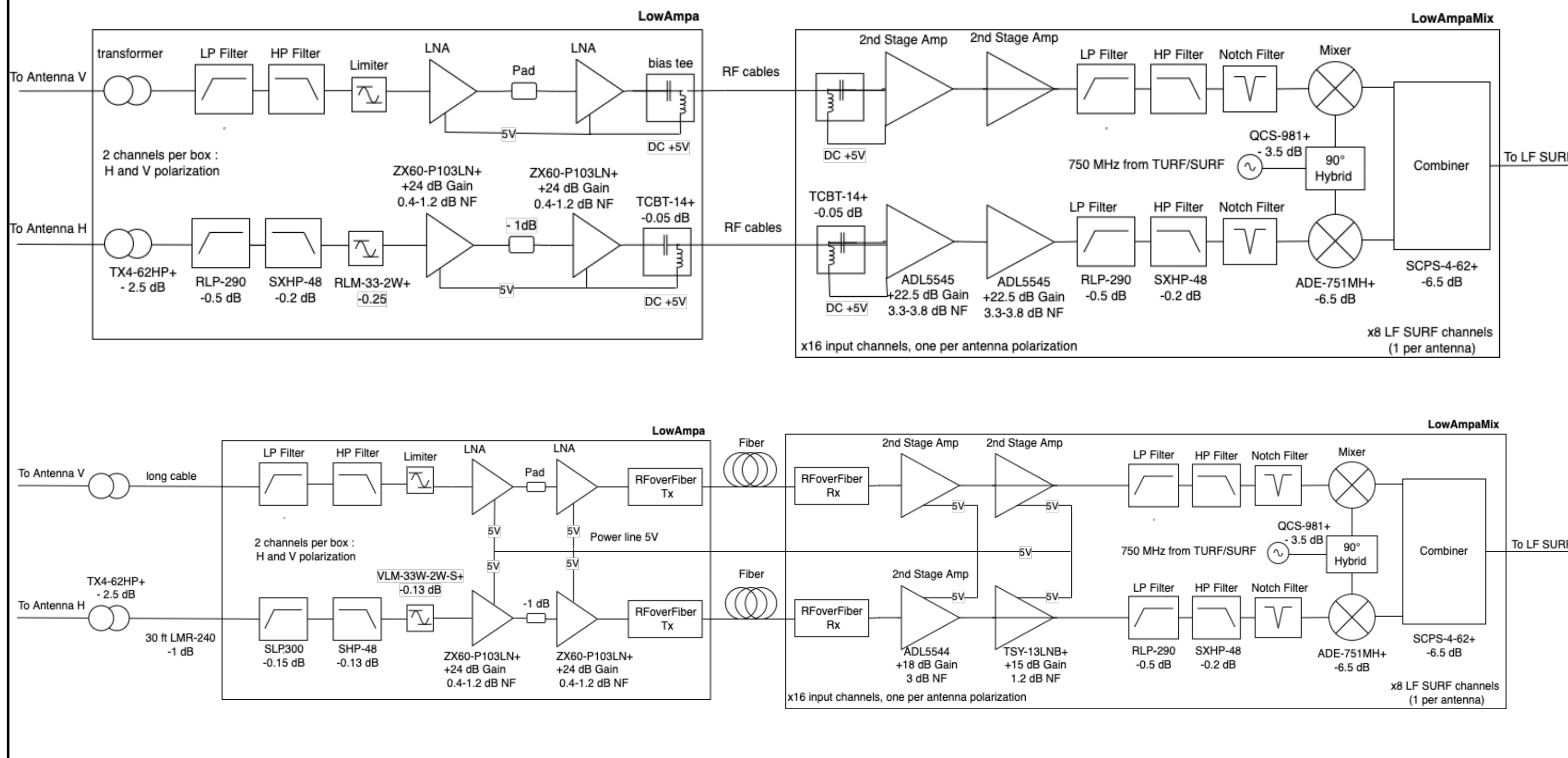
# LFI RF chain

## Simulated noise and expected gain

$$T = (1 - r_{\text{sky frac}}) C_{\text{Fresnel}} T_{\text{ice}} + r_{\text{sky frac}} T_{\text{sky}}$$



## Studied configuration for the full RF chain of the LFI





## Prototypes and TRL6 flight requirements

Scaled model (1/4)

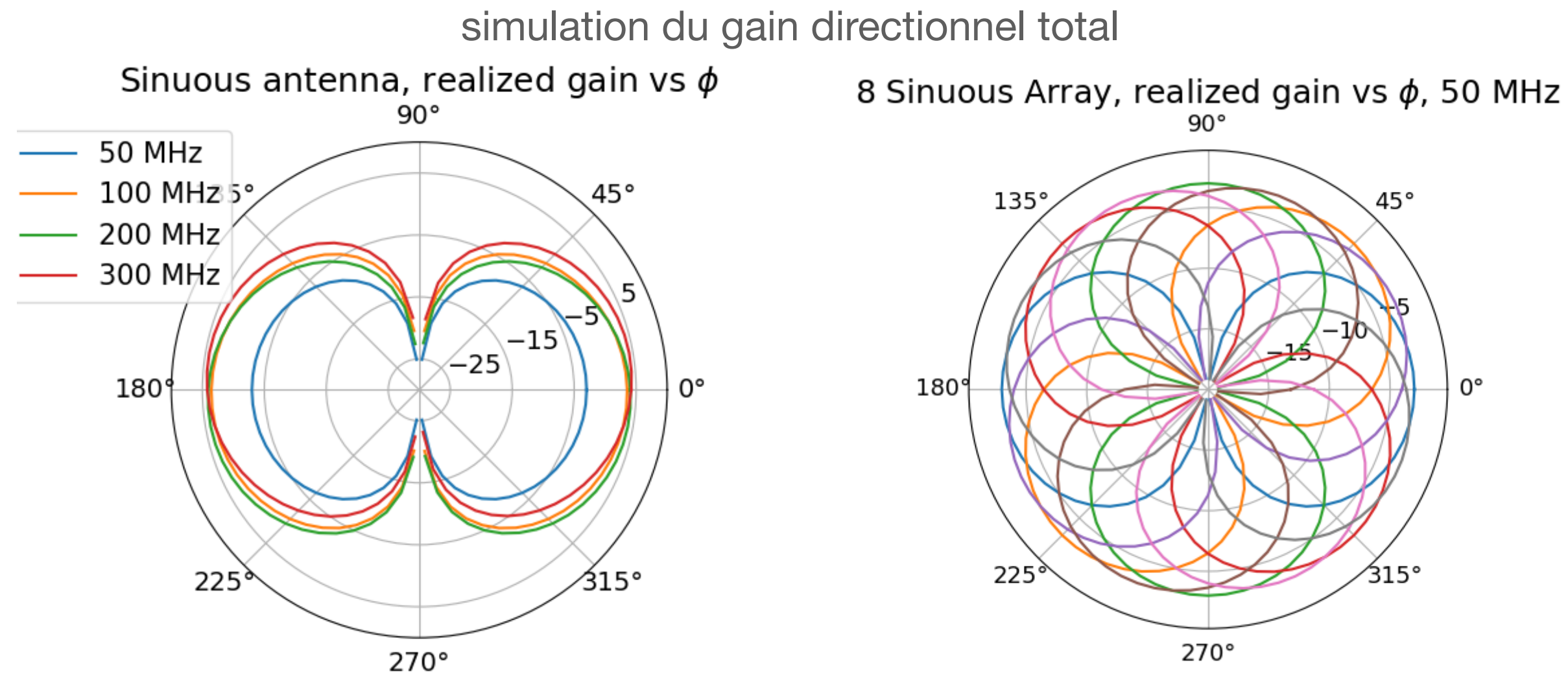


Thermal vacuum chamber

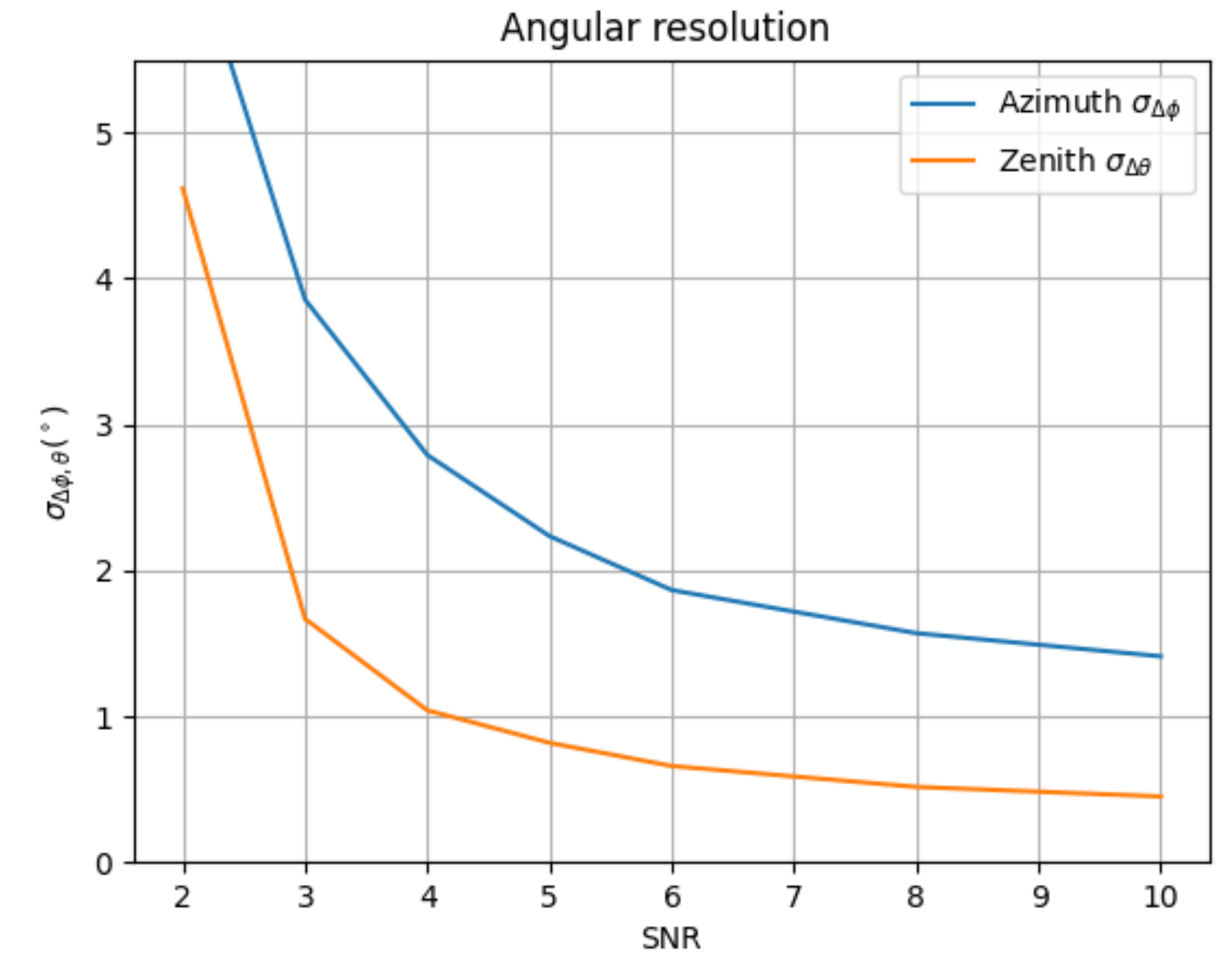




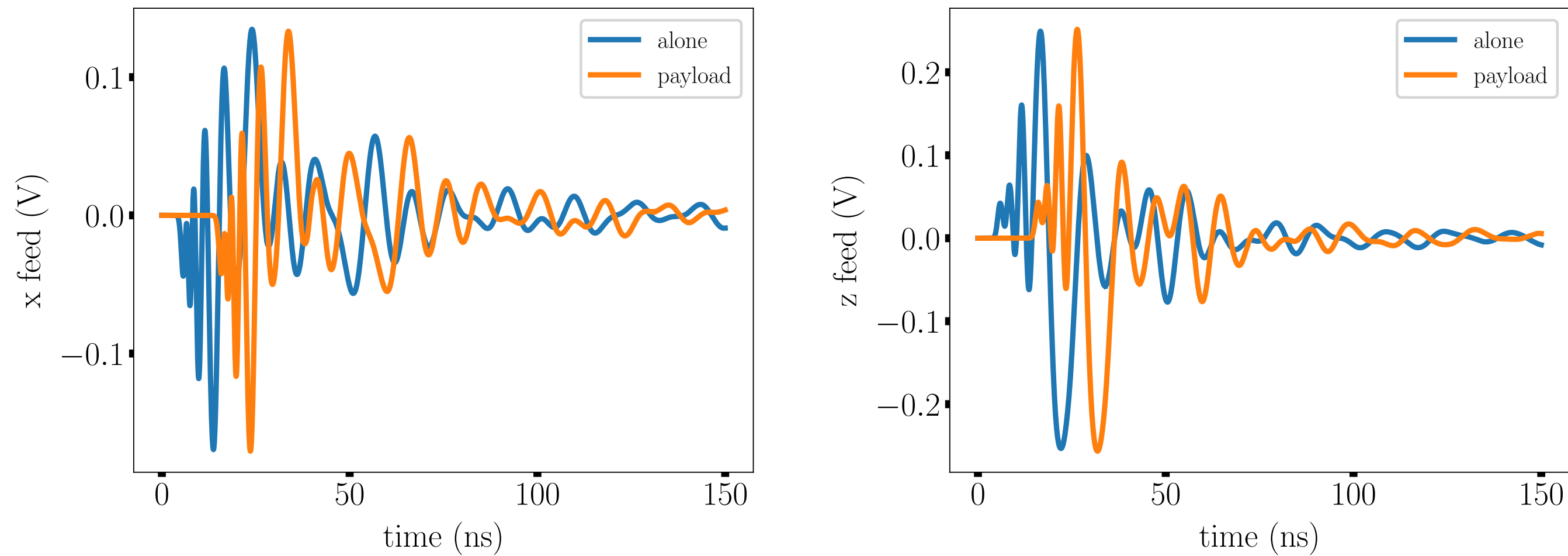
## Simulations of the LFI performances



## Simulations of the angular reconstruction



## Simulations of the possible interferences with the payload (XFDTD)

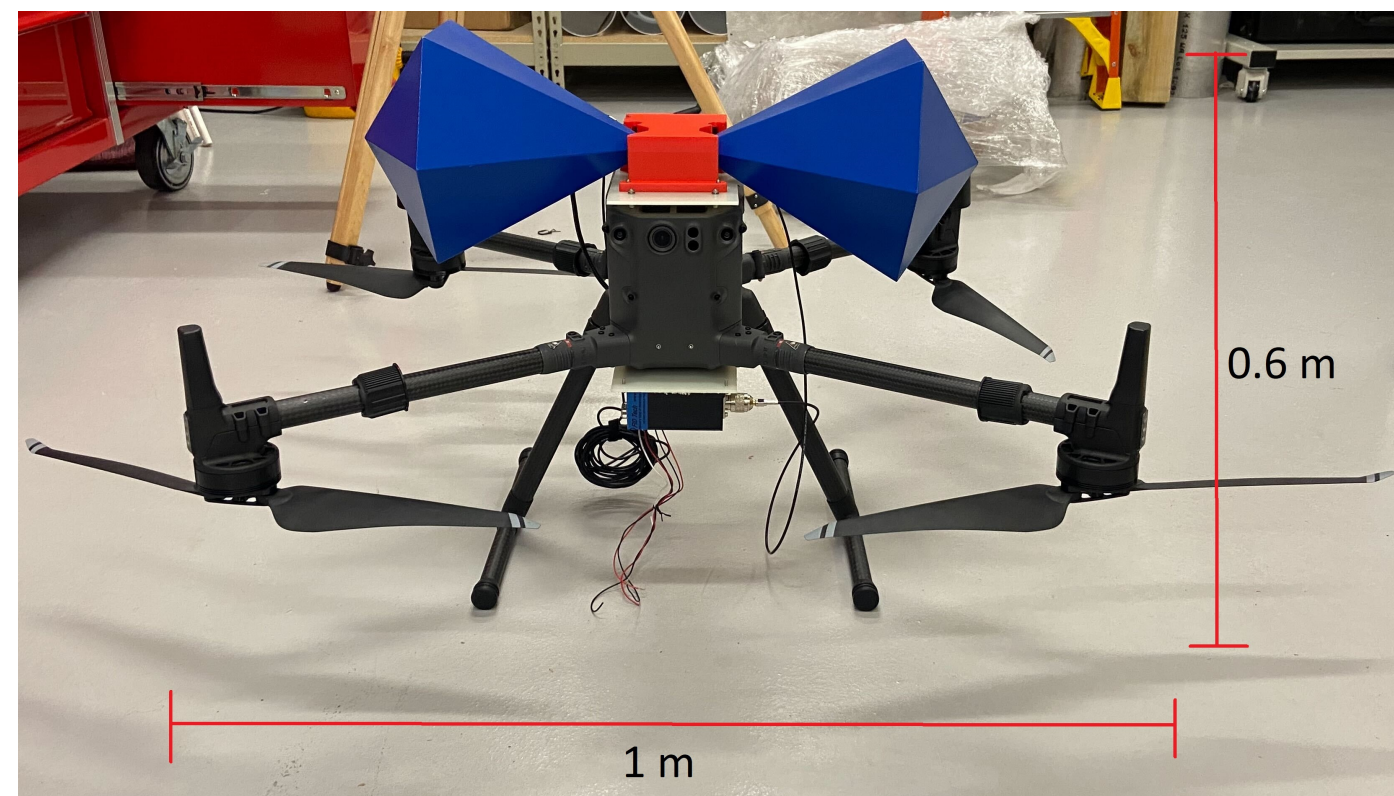
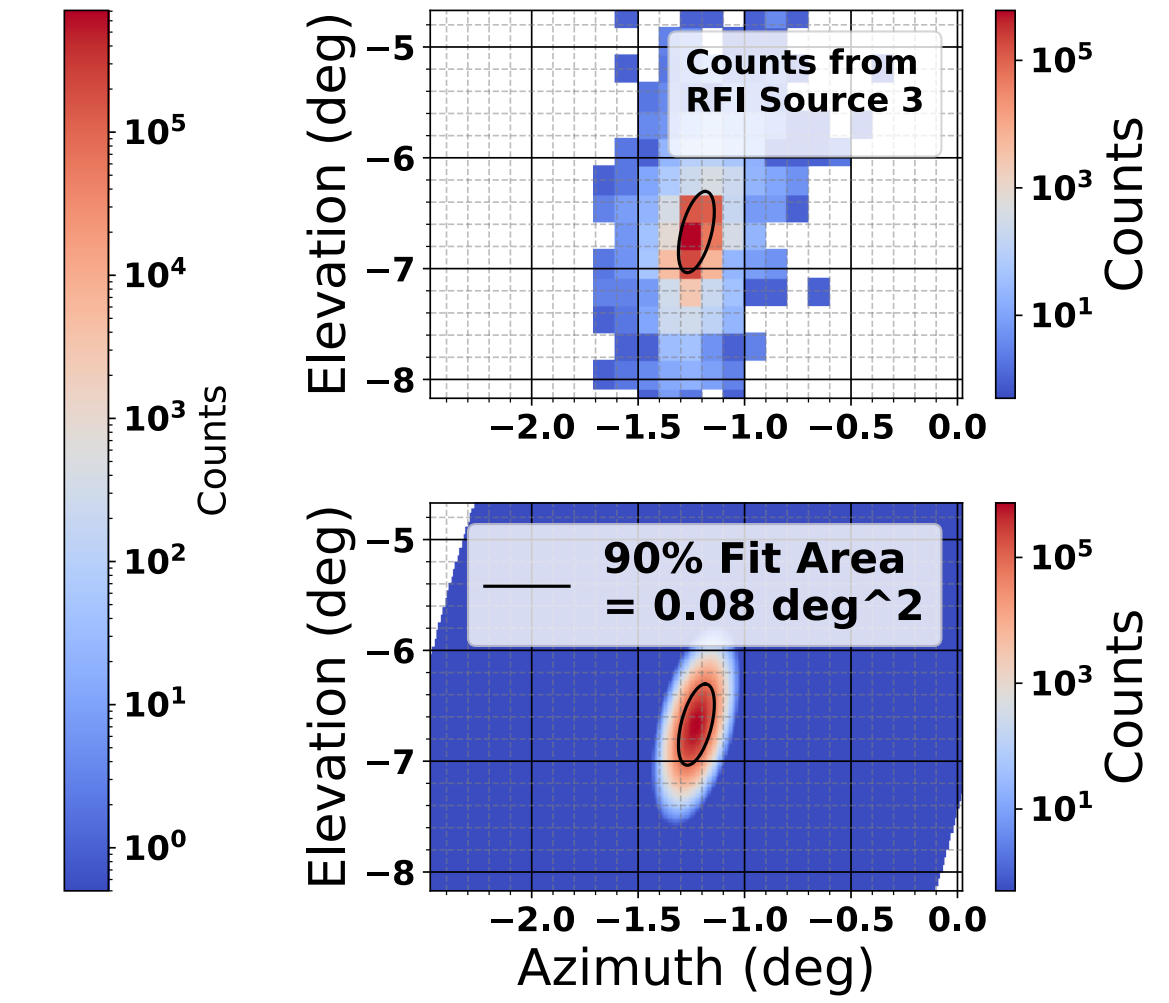
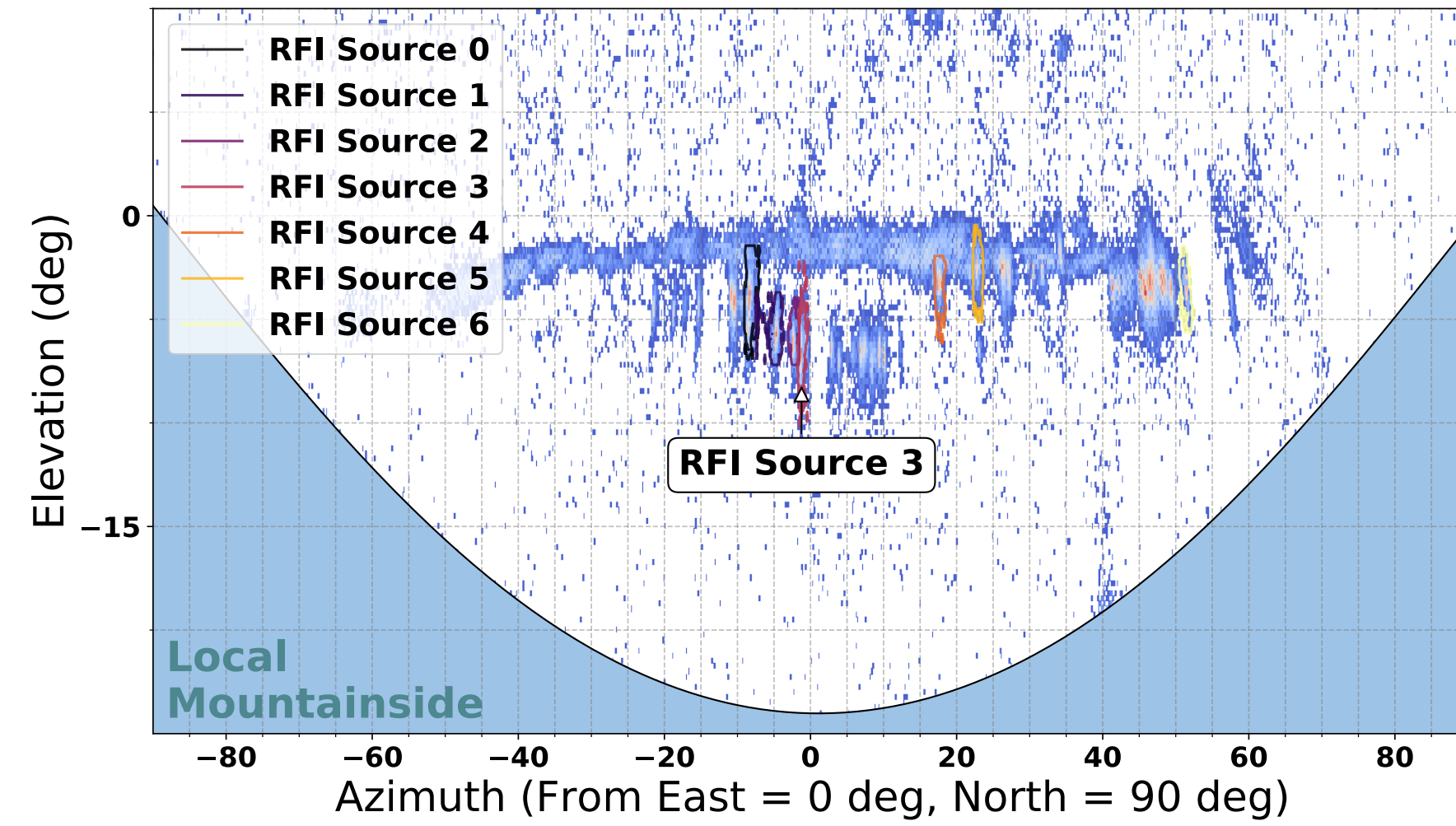
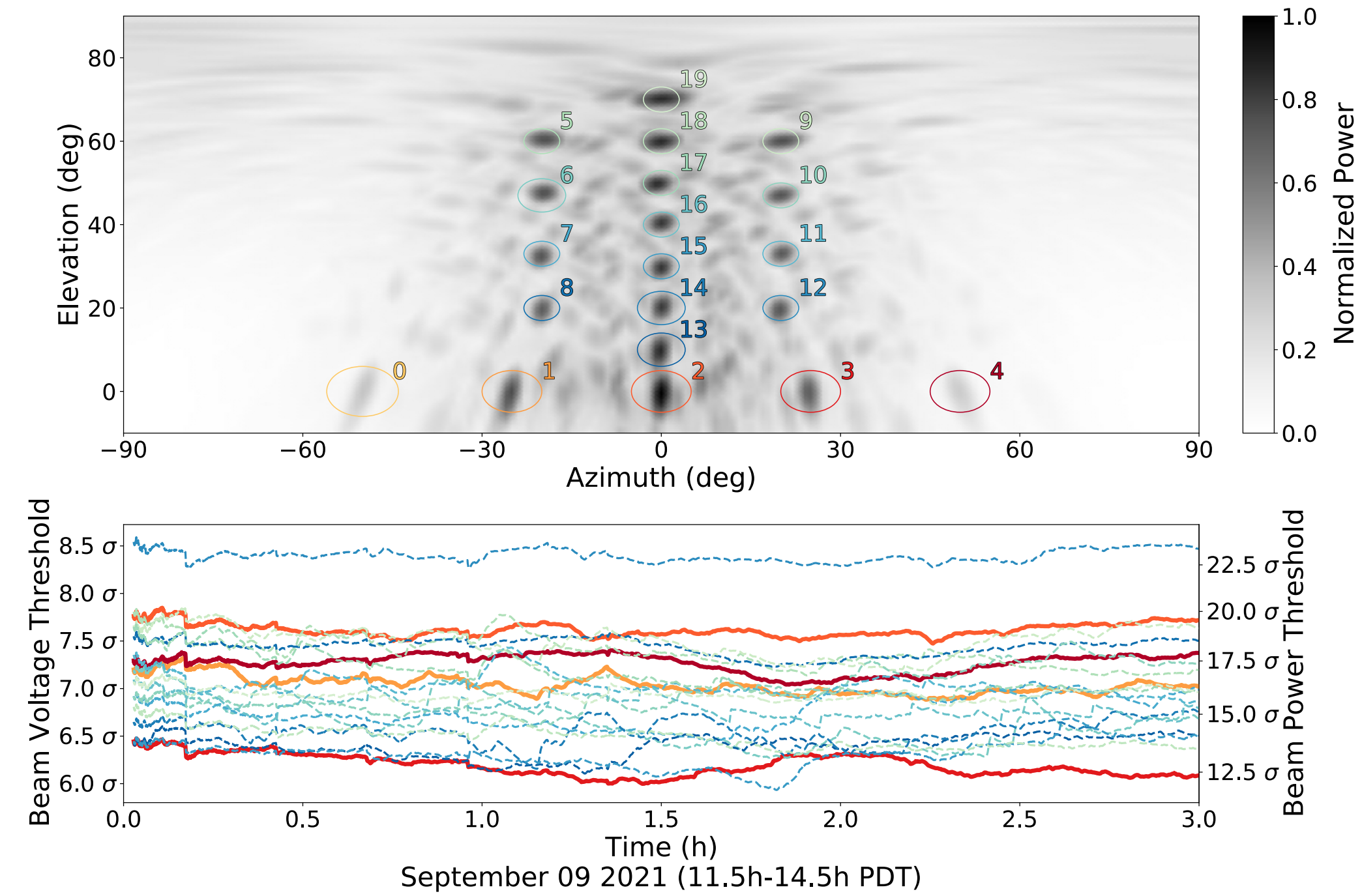




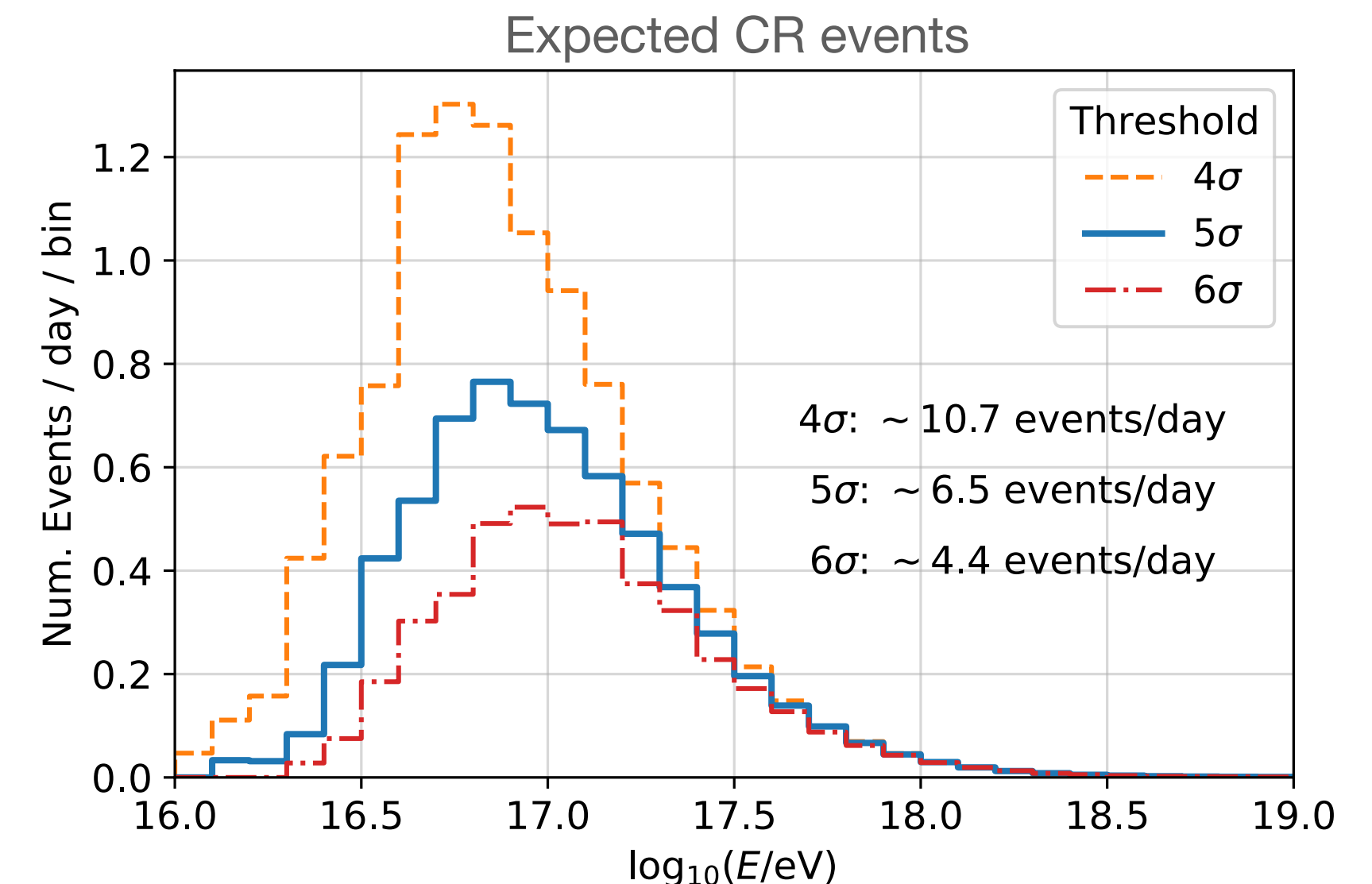
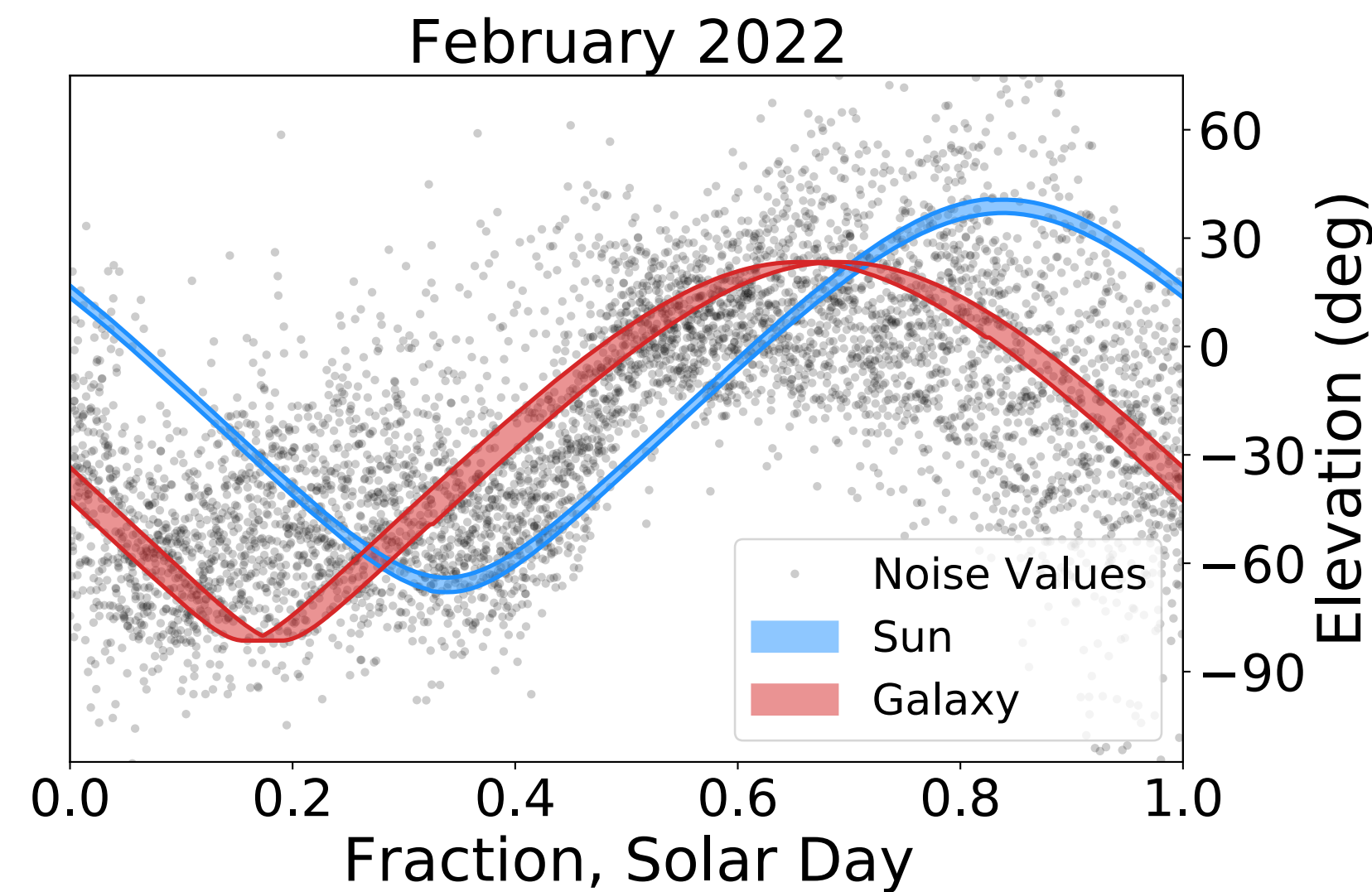


# The BEACON prototype

Southall (UChicago), Deaconu (UChicago), V. D., et al. (submitted to NIMA)



Calibration drone



Andrew Zeolla (Grad. student @PSU)

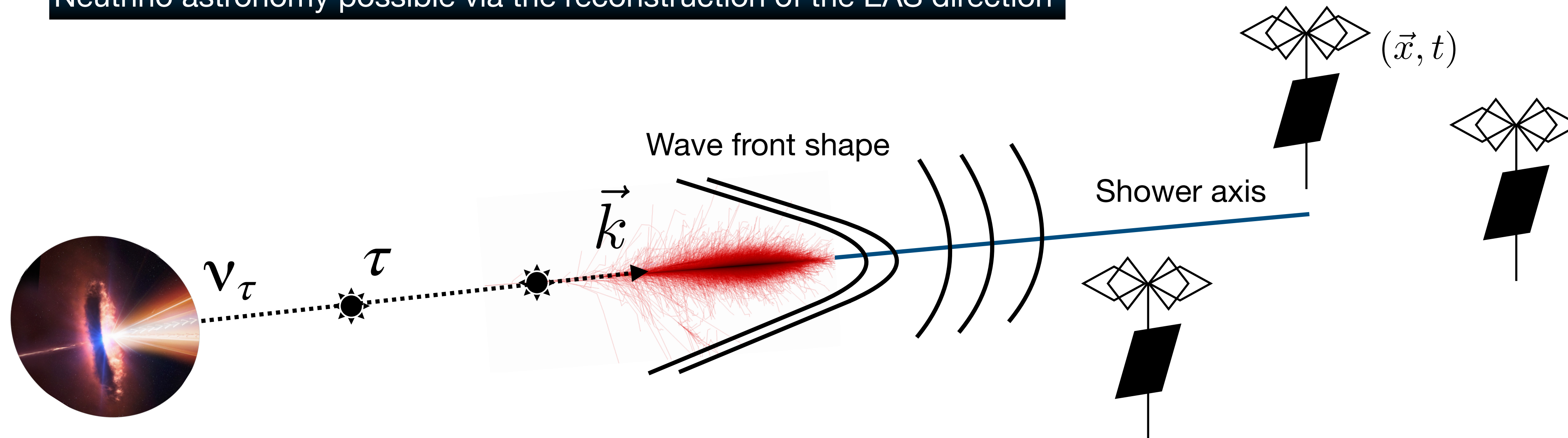


# Reconstruction of radio detected extensive air showers

Goal: Neutrino astronomy requires reconstruction of the arrival direction (target of  $0.1^\circ$  of accuracy)

Lorentz boosts  $\longrightarrow$  EAS direction = neutrino direction

Neutrino astronomy possible via the reconstruction of the EAS direction



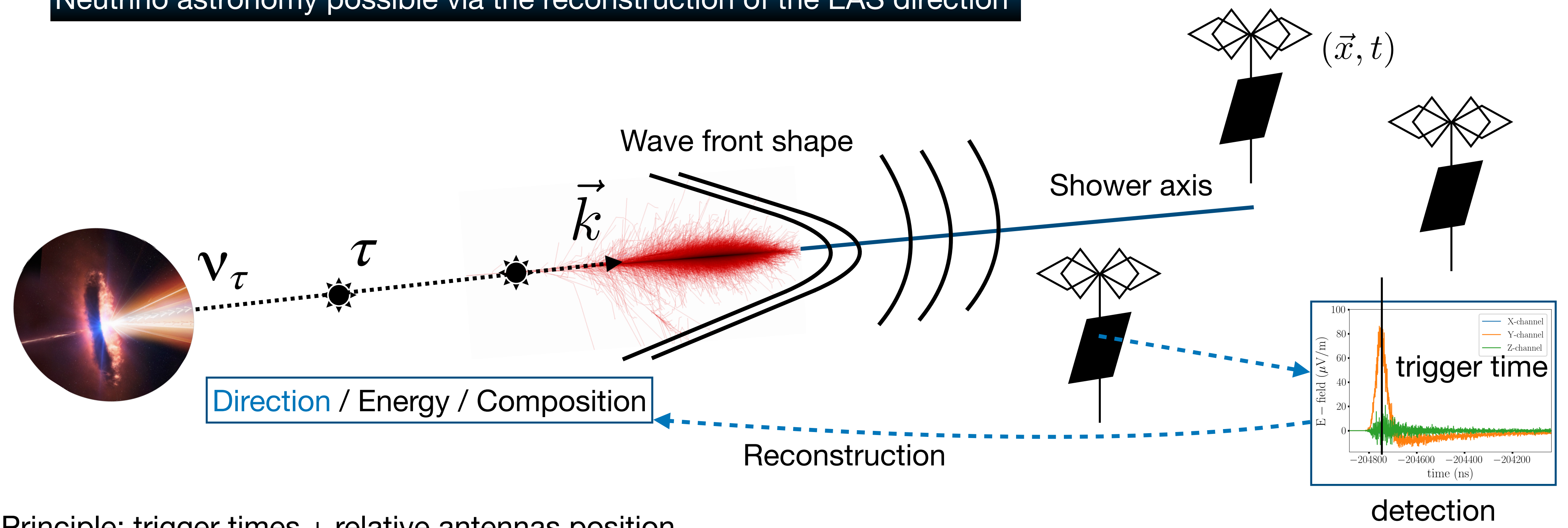


# Reconstruction of radio detected extensive air showers

Goal: Neutrino astronomy requires reconstruction of the arrival direction (target of  $0.1^\circ$  of accuracy)

Lorentz boosts  $\rightarrow$  EAS direction = neutrino direction

Neutrino astronomy possible via the reconstruction of the EAS direction



Principle: trigger times + relative antennas position  
 $\rightarrow$  information on the EAS direction

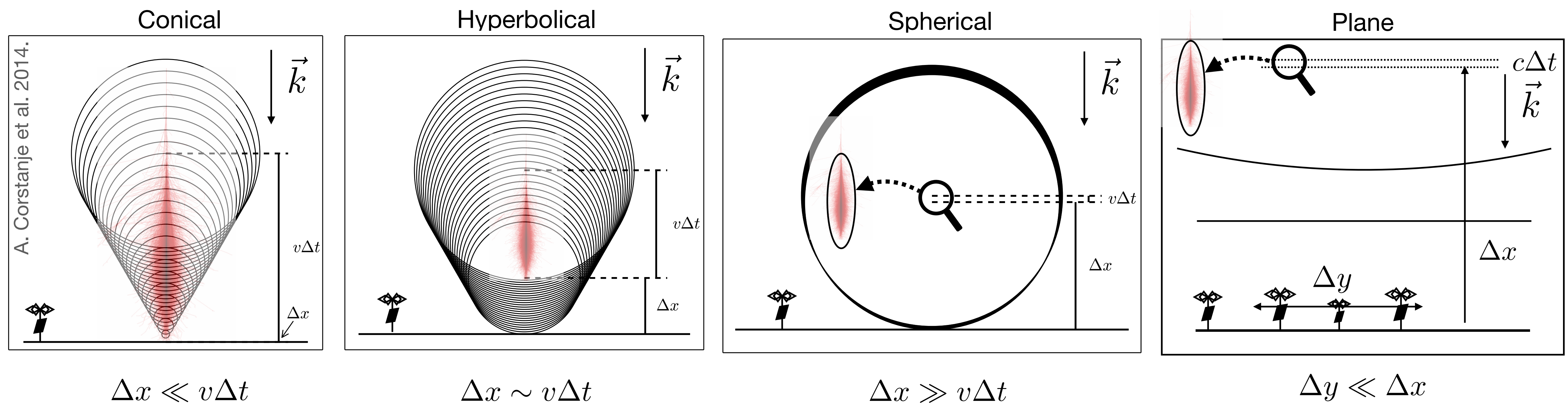
Method: adjust the wave front model to the trigger times  $\rightarrow$  neutrino astronomy accuracy = wave front shape correctness

# Wave front shape descriptions: state of the art

LOPES and LOFAR measured an hyperbolic wave front shape F.G. Schröder et al, 2014. A. Corstanje et al. 2014.

Wave front shape description depends on:

- distance to ground
- emission extension
- detector size



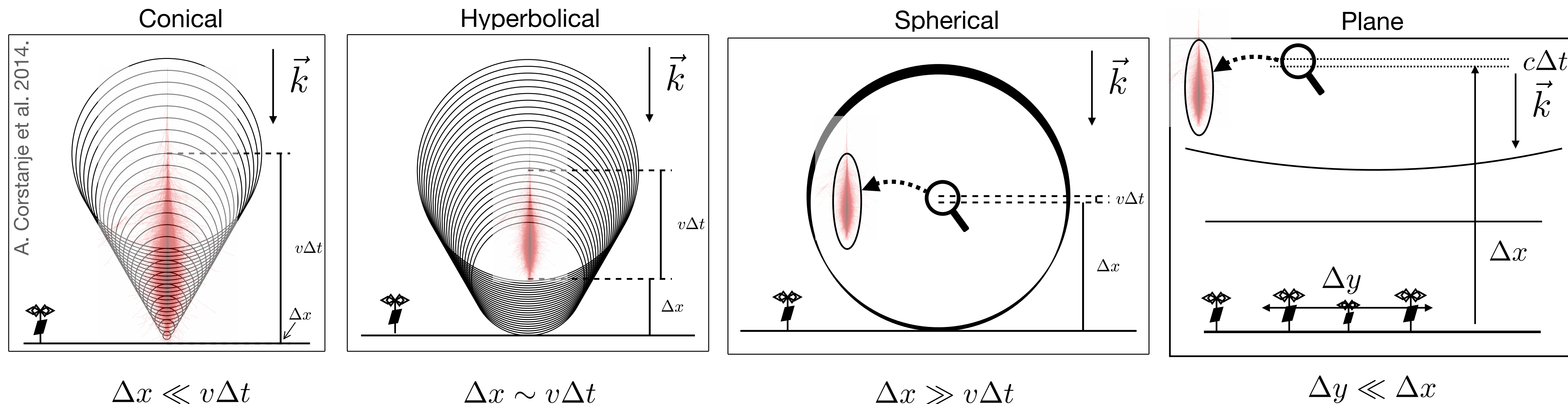


# Wave front shape descriptions: state of the art

LOPES and LOFAR measured an hyperbolic wave front shape F.G. Schröder et al, 2014. A. Corstanje et al. 2014.

Wave front shape description depends on:

- distance to ground
- emission extension
- detector size



**But** in the case of GRAND:

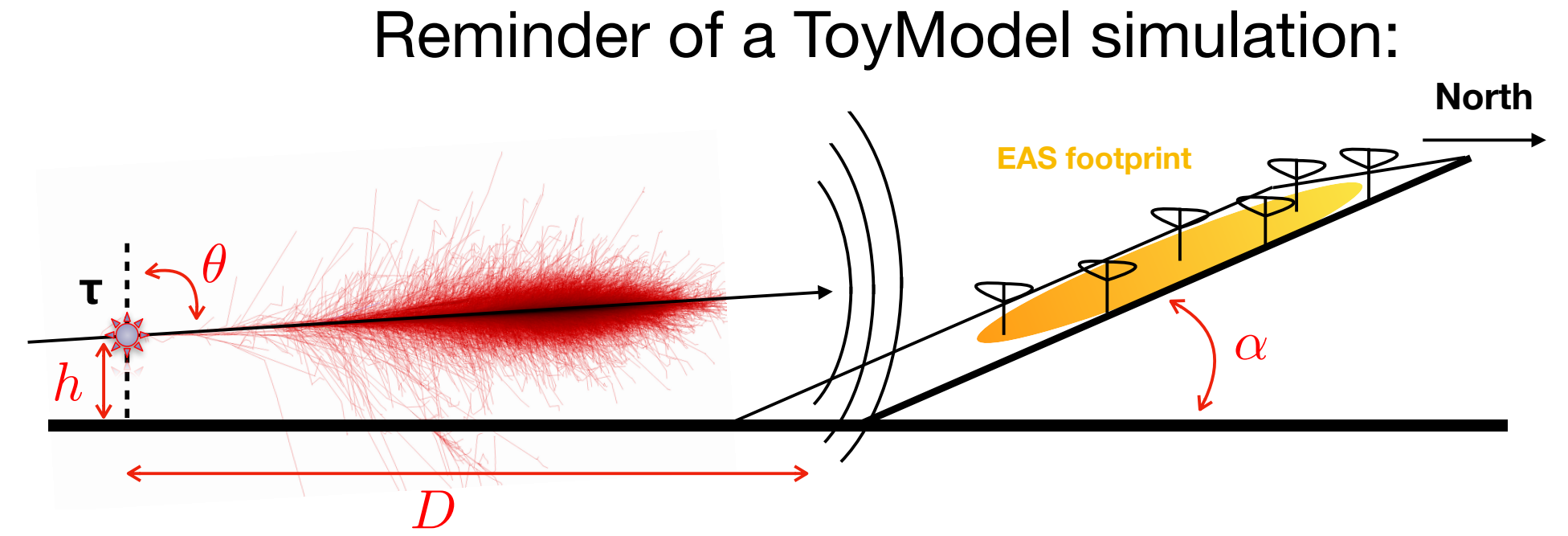
- very inclined EAS → extended emission zone
- very large array → emission changes

A detailed study of GRAND measured wave front shape needed

# Hyperbolic wavefront model

Standard approach: study the wave front curvature

- on simulations
- GRAND-like layout



residuals = trigger time - wave front model

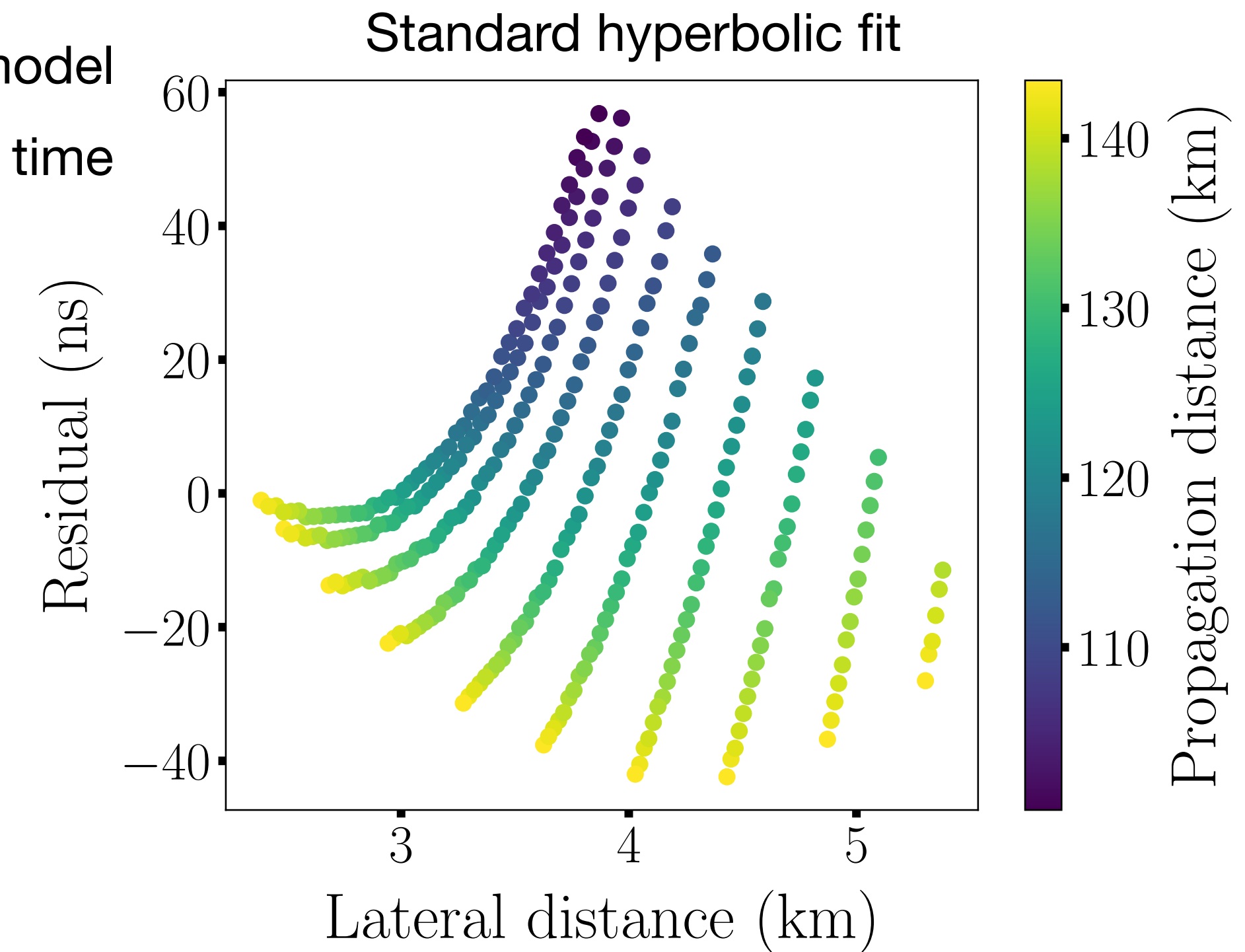
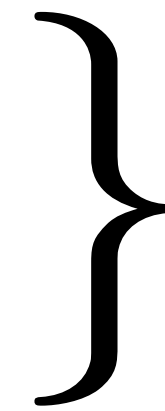
1 dot = 1 antenna trigger time

Standard definition

$$ct^{\text{hyp}} = -a + \sqrt{a^2 + b^2 r^2}$$

$r$  = lateral distance

$(a, b)$  = hyperbolic parameters



Very inclined showers: evolution of the wave front is visible

Fixed hyperbolic parameters → snapshot of the emission (LOFAR/LOPES)

Hyperbolic parameters physical meaning ?

How does the wave front evolve?

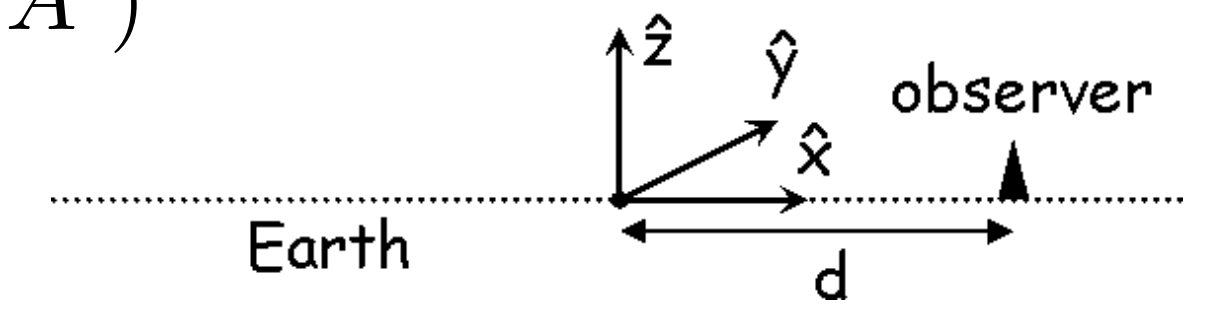
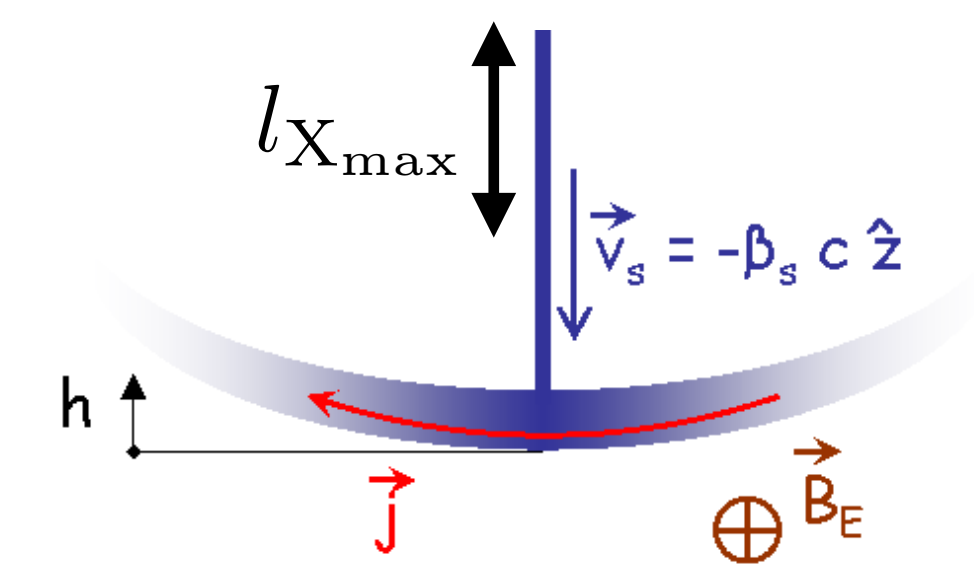


# Macroscopic approach of the EAS emission

Can we derive the wave front shape from physical principles ?

- Model the charge current induced by the particle  $J^\mu(\vec{x}, t)$  in terms of particle density and repartition

Potential-vector (classical electrodynamics)  $A^\mu(\vec{x}, t) \longrightarrow$  Electric field  $\vec{E}(\vec{x}, t) = -(\partial_i A^0 + \partial_0 A^i)$



Scholten et al. (2008)

Too many parameters to adjust in this model

# Macroscopic approach of the EAS emission

Can we derive the wave front shape from physical principles ?

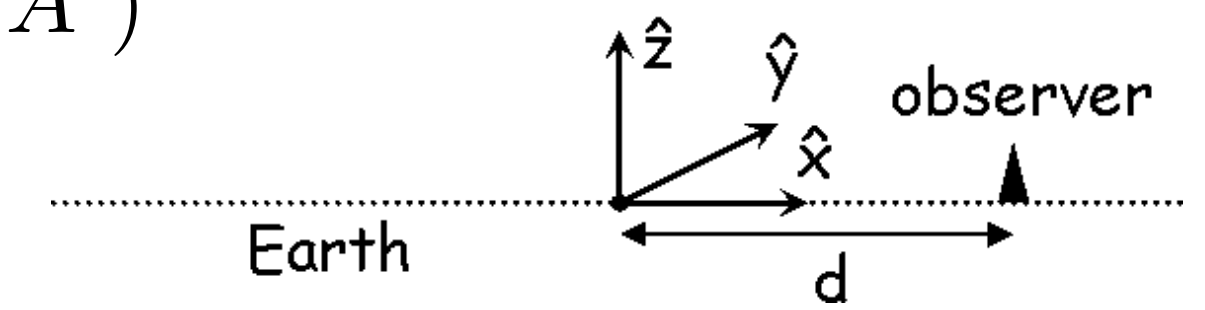
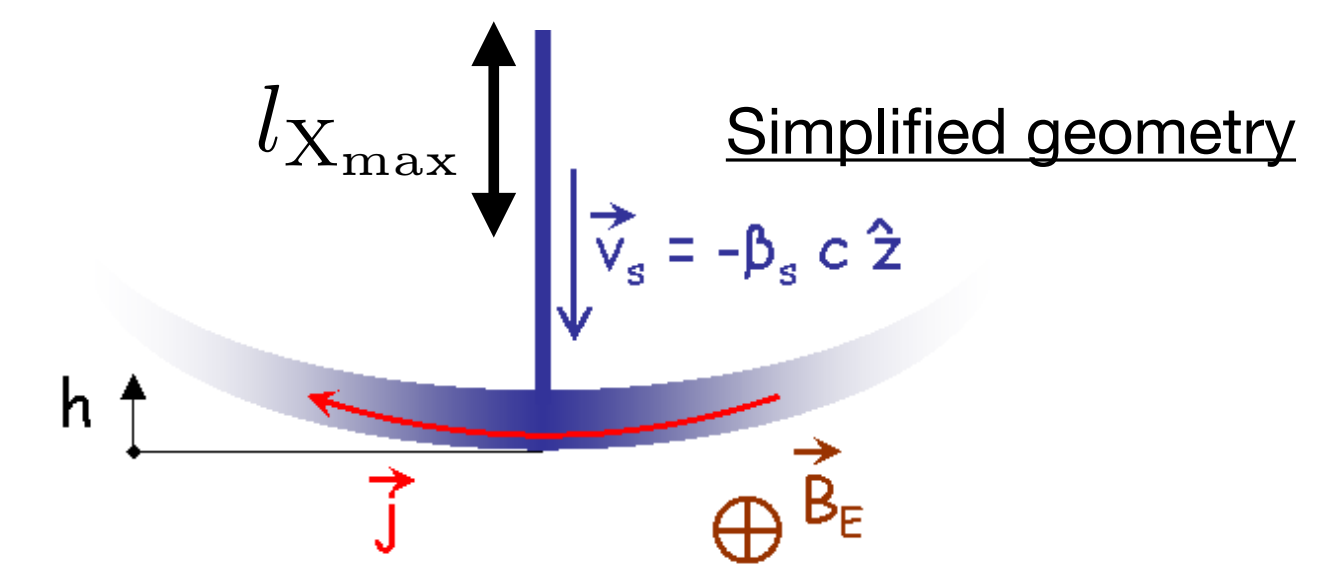
- Model the charge current induced by the particle  $J^\mu(\vec{x}, t)$  in terms of particle density and repartition

Potential-vector (classical electrodynamics)  $A^\mu(\vec{x}, t) \longrightarrow$  Electric field  $\vec{E}(\vec{x}, t) = -(\partial_i A^0 + \partial_0 A^i)$

- In the “Limiting case” and in a simplified geometry

$$E_x(t, r) = -J \frac{n^2 \Delta}{c \mathcal{D}^2} \frac{df_t(t_r)}{dt_r} + J f_t(t_r) \frac{c \beta_s^2 t}{\mathcal{D}^3}$$

where  $\left\{ \begin{array}{l} n = \text{index of refraction} \\ \Delta = \text{geometrical distance} \\ \mathcal{D} = \text{observer distance} \end{array} \right.$



Limiting case:

- shower particle front thickness is neglected
- Index of refraction is close to unity

Too many parameters to adjust in this model



# Macroscopic approach of the EAS emission

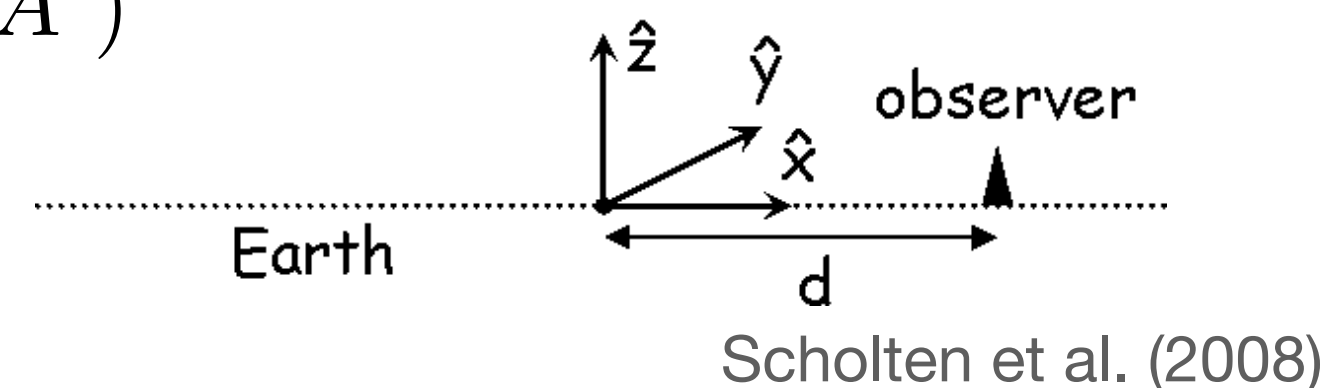
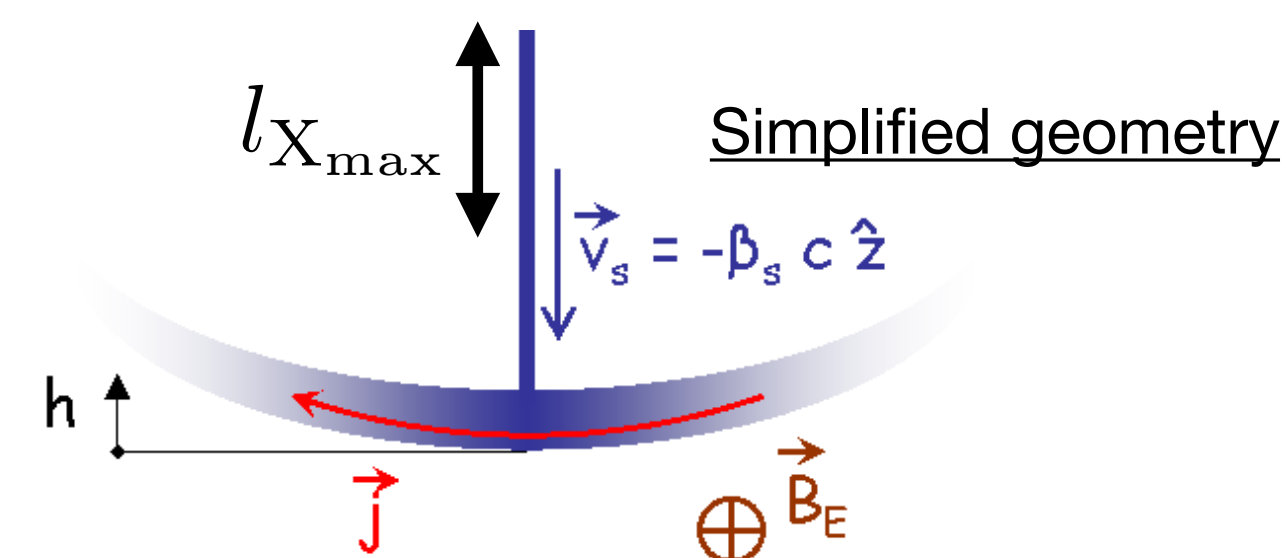
Can we derive the wave front shape from physical principles ?

- Model the charge current induced by the particle  $J^\mu(\vec{x}, t)$  in terms of particle density and repartition

Potential-vector (classical electrodynamics)  $A^\mu(\vec{x}, t) \longrightarrow$  Electric field  $\vec{E}(\vec{x}, t) = -(\partial_i A^0 + \partial_0 A^i)$

- In the "Limiting case" and in a simplified geometry

$$E_x(t, r) = -J \frac{n^2 \Delta}{c \mathcal{D}^2} \frac{df_t(t_r)}{dt_r} + J f_t(t_r) \frac{c \beta_s^2 t}{\mathcal{D}^3} \quad \text{where} \quad \begin{cases} n = \text{index of refraction} \\ \Delta = \text{geometrical distance} \\ \mathcal{D} = \text{observer distance} \end{cases}$$



- Limiting case:
- shower particle front thickness is neglected
  - Index of refraction is close to unity

- The wave front corresponds to  $\frac{dE_x(t, r)}{dt} = 0$  maximum of the emission

$$\longrightarrow t = -\frac{(1 + \beta_s)(1 + \delta)}{T(\delta + \chi)} \mp \sqrt{\frac{(1 + \beta_s)^2(1 + \delta)^2}{T^2(\delta + \chi)^2} - \frac{\tau(1 + \beta_s)}{T(\delta + \chi)}} \sim -a + \sqrt{a^2 + b^2 r^2}$$

with  $a = \frac{(1 + \beta_s)(1 + \delta)}{T(\delta + \chi)}$

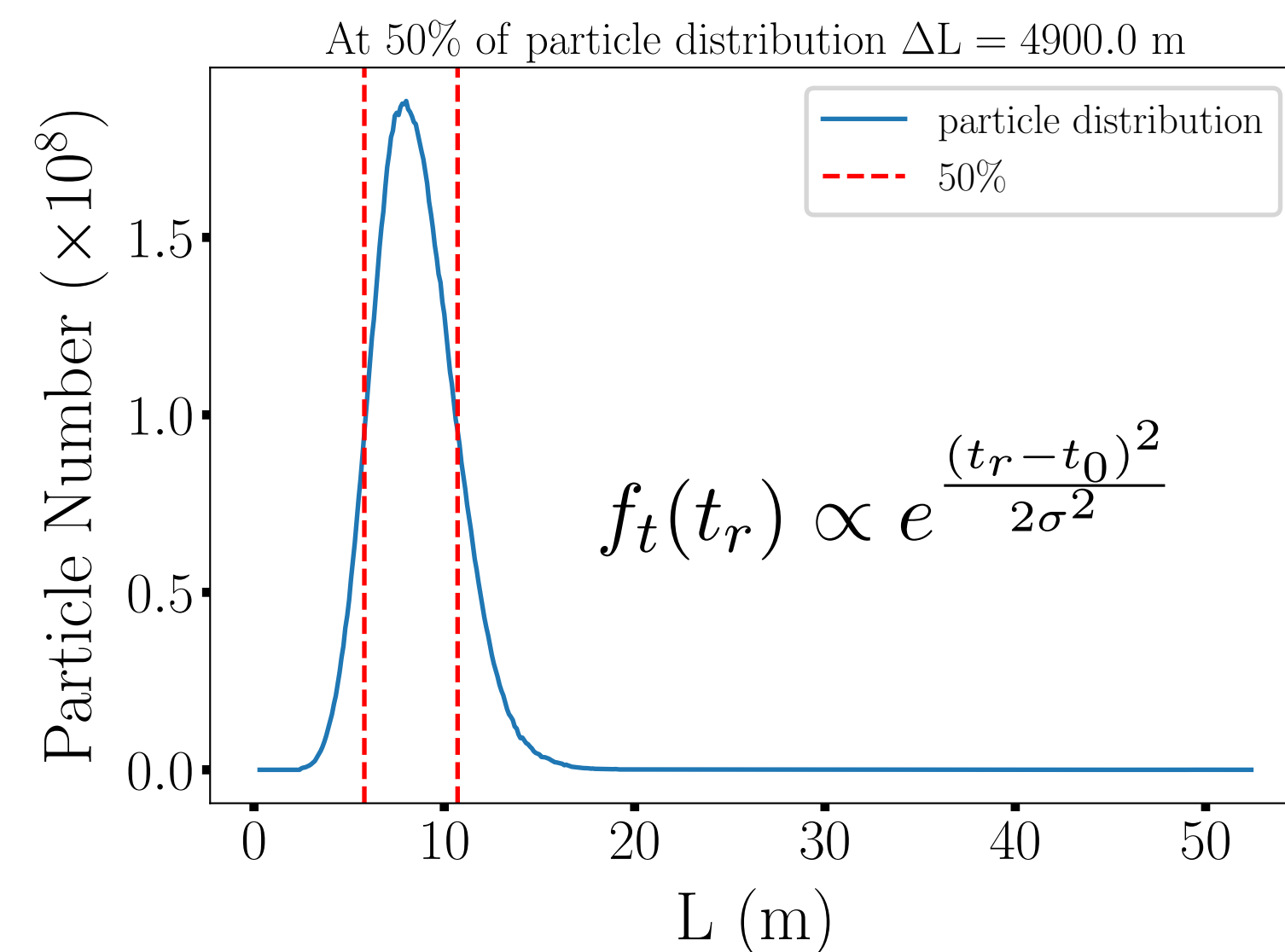
and

$$b = \frac{(1 + \beta_s)}{T(\delta + \chi)} \frac{l}{\beta_s^2 c^3 \sigma^2}$$

$$\begin{cases} \tau = \frac{l r^2}{\beta_s^2 c^3 \sigma^2} & T = \frac{l}{\beta_s c \sigma^2} \\ \delta = \frac{l n^2 \Delta}{\beta_s^2 c^2 \sigma^2} & \chi = 1 - \frac{n^2 (l - l_{X_{max}})}{\Delta} \end{cases}$$

only physical parameters of the shower

Assuming a gaussian particle distribution

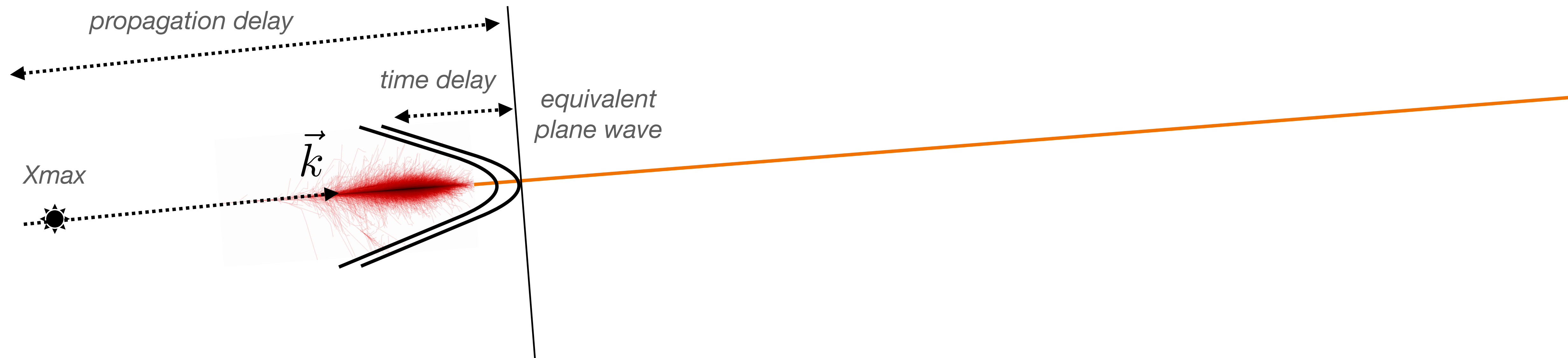


Too many parameters to adjust in this model

# Study of the wavefront shape: method

V. D (PSU), Olivier Martineau-Huynh (LPNHE) and Matias Tueros (CONICET) (Astroparticle Physics, 2022)

What time delays tell us about the curvature of the wavefront?



Wavefront shape modelling:

wavefront = propagation + curvature

propagation delay = plane wave propagation at speed  $c/n$

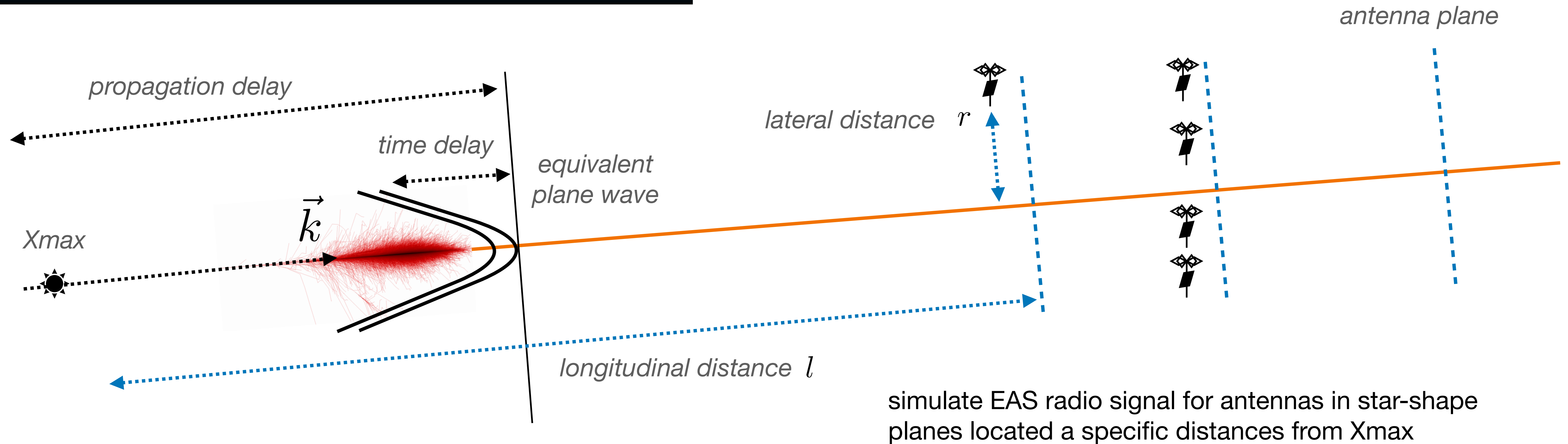
time delay = intrinsic curvature of the wavefront



# Study of the wavefront shape: method

V. D (PSU), Olivier Martineau-Huynh (LPNHE) and Matias Tueros (CONICET) (Astroparticle Physics, 2022)

What time delays tell us about the curvature of the wavefront?



## Wavefront shape modelling:

wavefront = propagation + curvature

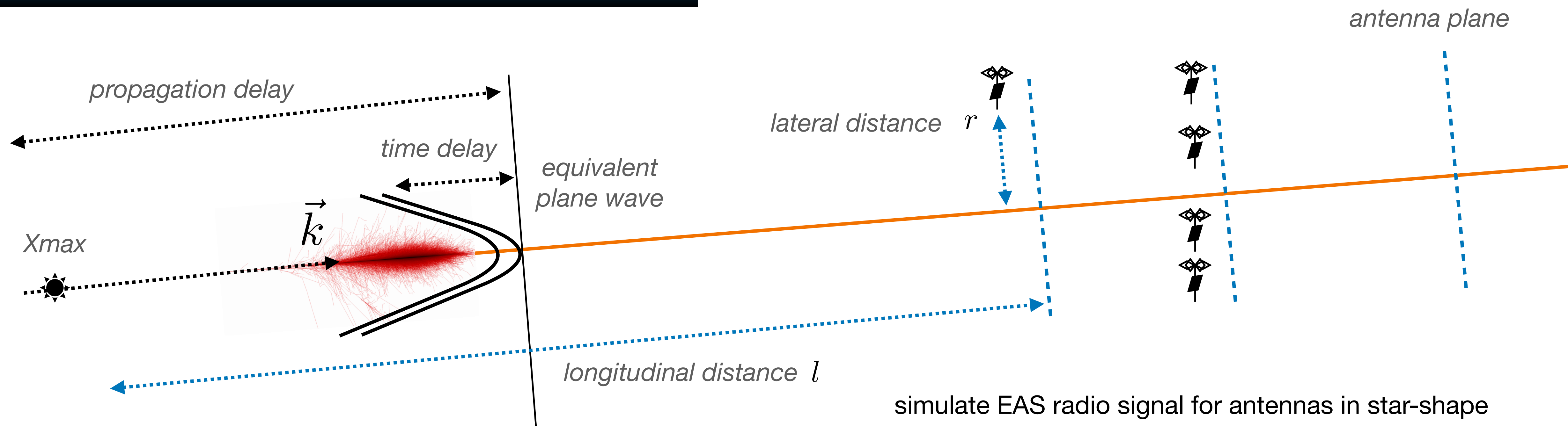
propagation delay = plane wave propagation at speed  $c/n$

time delay = intrinsic curvature of the wavefront

# Study of the wavefront shape: method

V. D (PSU), Olivier Martineau-Huynh (LPNHE) and Matias Tueros (CONICET) (Astroparticle Physics, 2022)

What time delays tell us about the curvature of the wavefront?



simulate EAS radio signal for antennas in star-shape planes located a specific distances from  $X_{max}$

ZHAireS simulation:

- 7 planes from 17km to 200km
- zenith between  $63^\circ$  and  $88^\circ$
- energies between 0.02EeV and 4EeV
- azimuth values =  $0^\circ$ ,  $180^\circ$  and  $270^\circ$  w.r.t. magnetic North

→ sample the wavefront along radial and longitudinal distances

Wavefront shape modelling:

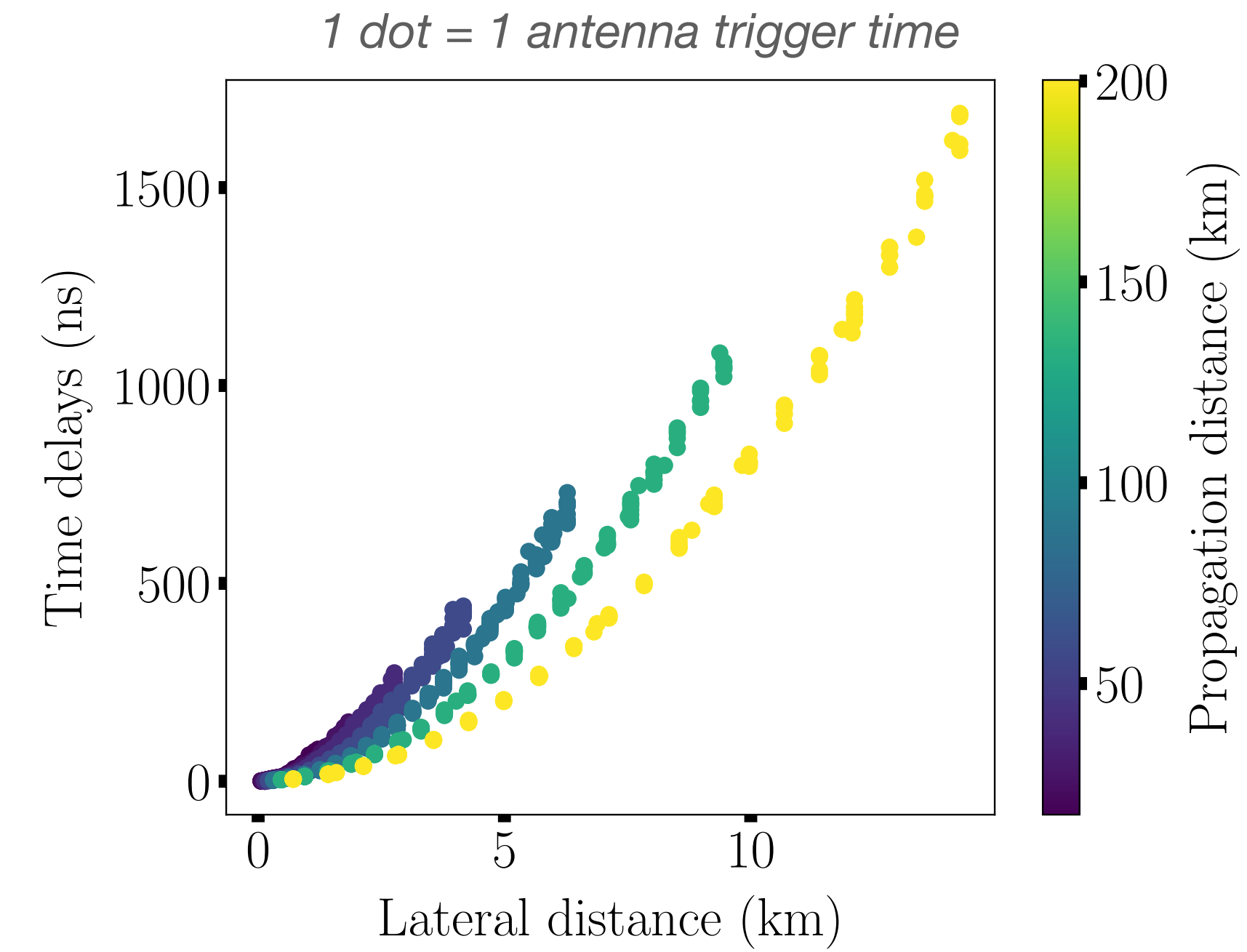
wavefront = propagation + curvature

propagation delay = plane wave propagation at speed  $c/n$

time delay = intrinsic curvature of the wavefront



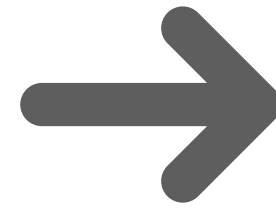
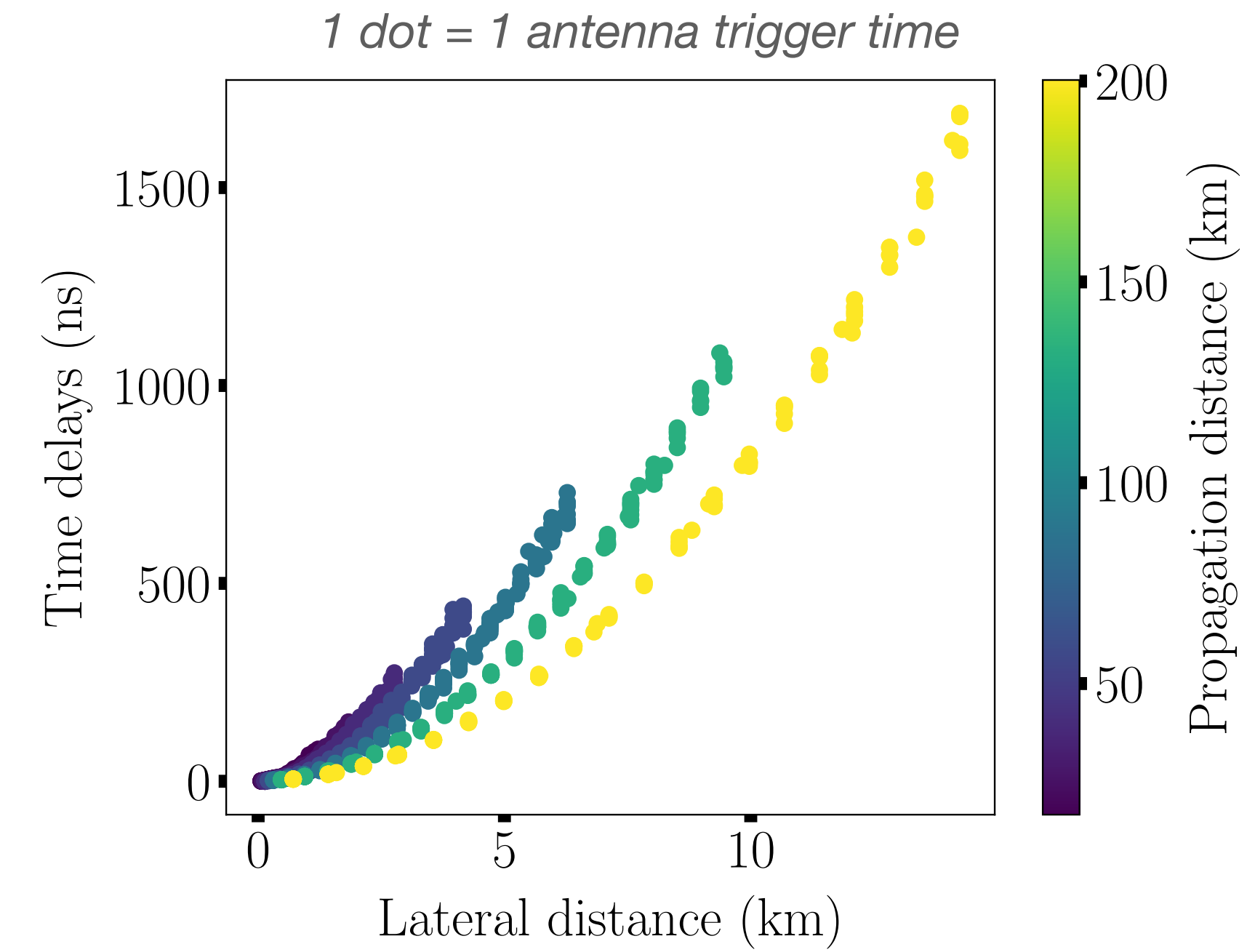
# Study of the wavefront shape: results



- time delays increase with lateral distance
- curvature reduces with propagation distance

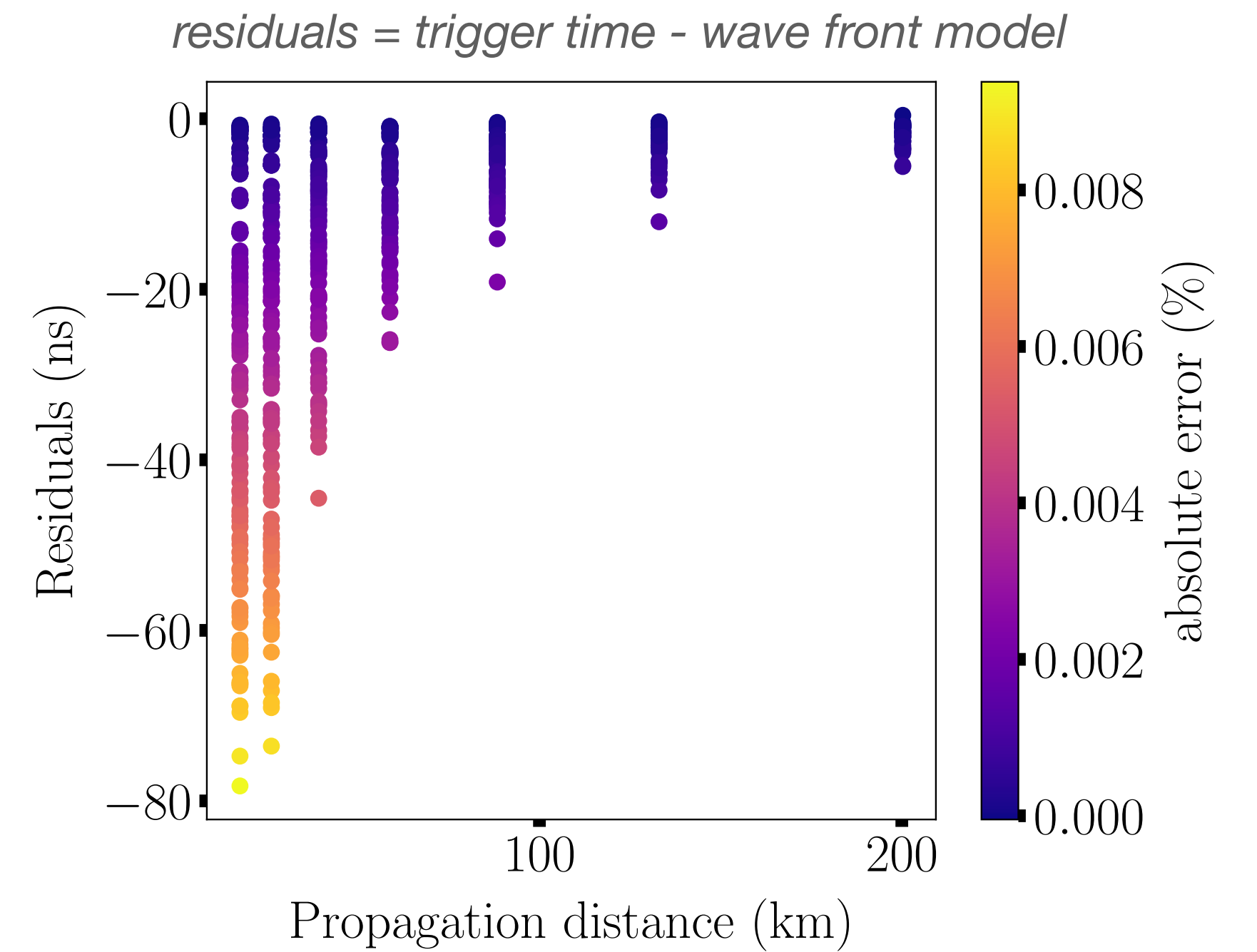
what model describes best this curvature ?

# Study of the wavefront shape: results



spherical wavefront model

$$ct^{\text{sph}} = n\sqrt{l^2 + r^2}$$

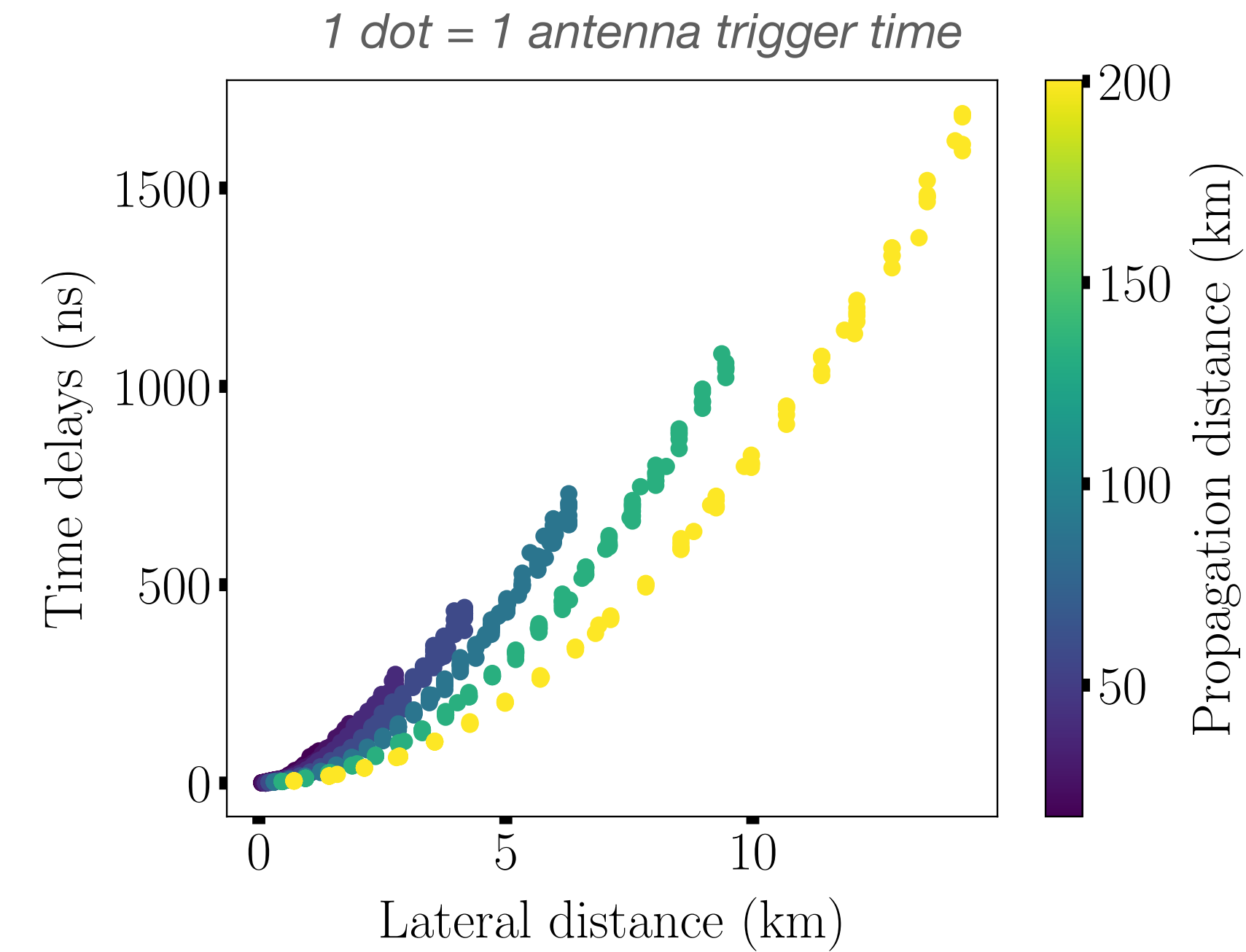


- time delays increase with lateral distance
- curvature reduces with propagation distance

what model describes best this curvature ?

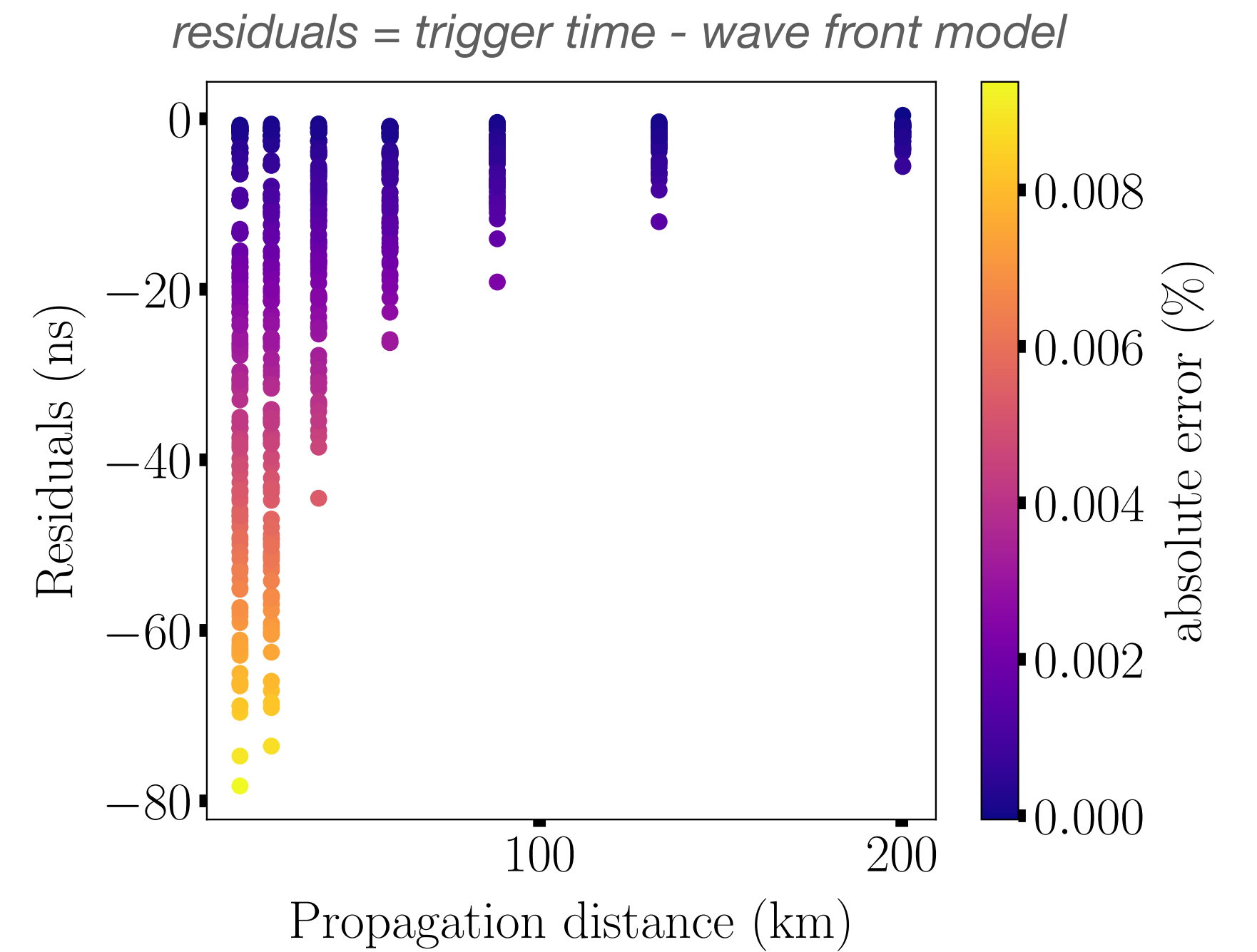


# Study of the wavefront shape: results



spherical wavefront model

$$ct^{\text{sph}} = n\sqrt{l^2 + r^2}$$



- time delays increase with lateral distance
- curvature reduces with propagation distance

what model describes best this curvature ?

## Results:

- residuals < experimental time resolution
- arrival times undistinguishable between spherical model and more complex model

# Consequences for reconstruction

---



# Consequences for reconstruction

---

Results: spherical wavefront model offers a very good level of description

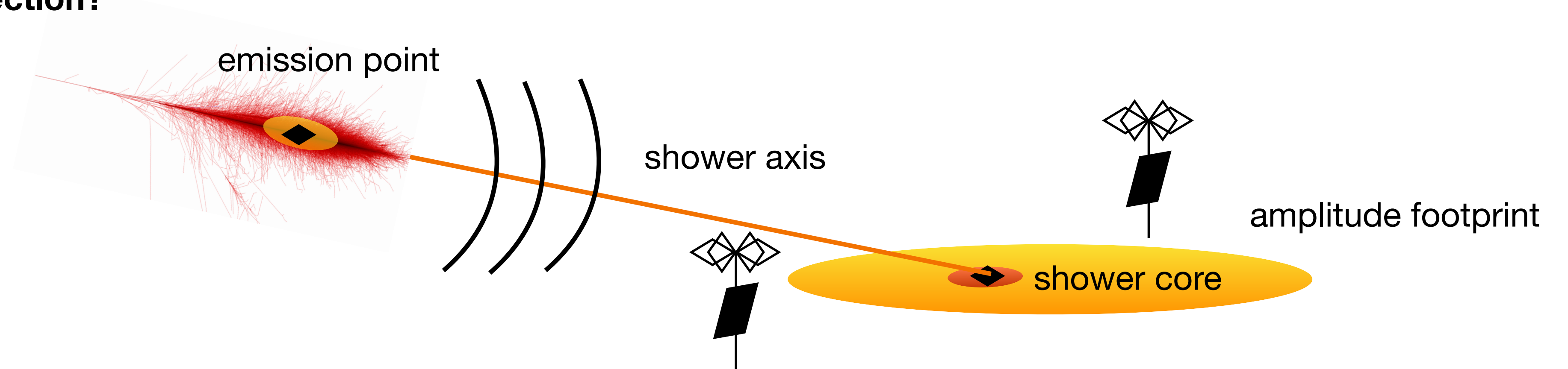
Consequences: impossible to reconstruct the arrival direction: spherical wave front model → point-like emission = no favoured direction

# Consequences for reconstruction

**Results:** spherical wavefront model offers a very good level of description

**Consequences:** impossible to reconstruct the arrival direction: spherical wave front model → point-like emission = no favoured direction

**How to reconstruct the arrival direction?**



**A second natural point along the shower propagation: shower core**



# Information content in the amplitude distribution of the radiation

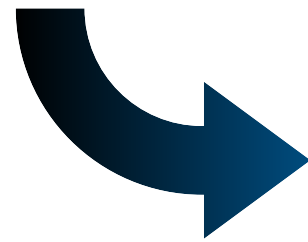
**Amplitude distribution (pattern) = antennas measurements → straightforward handle on the core position**

Beaming of the emission + Cerenkov effect (signal coherence + compression)



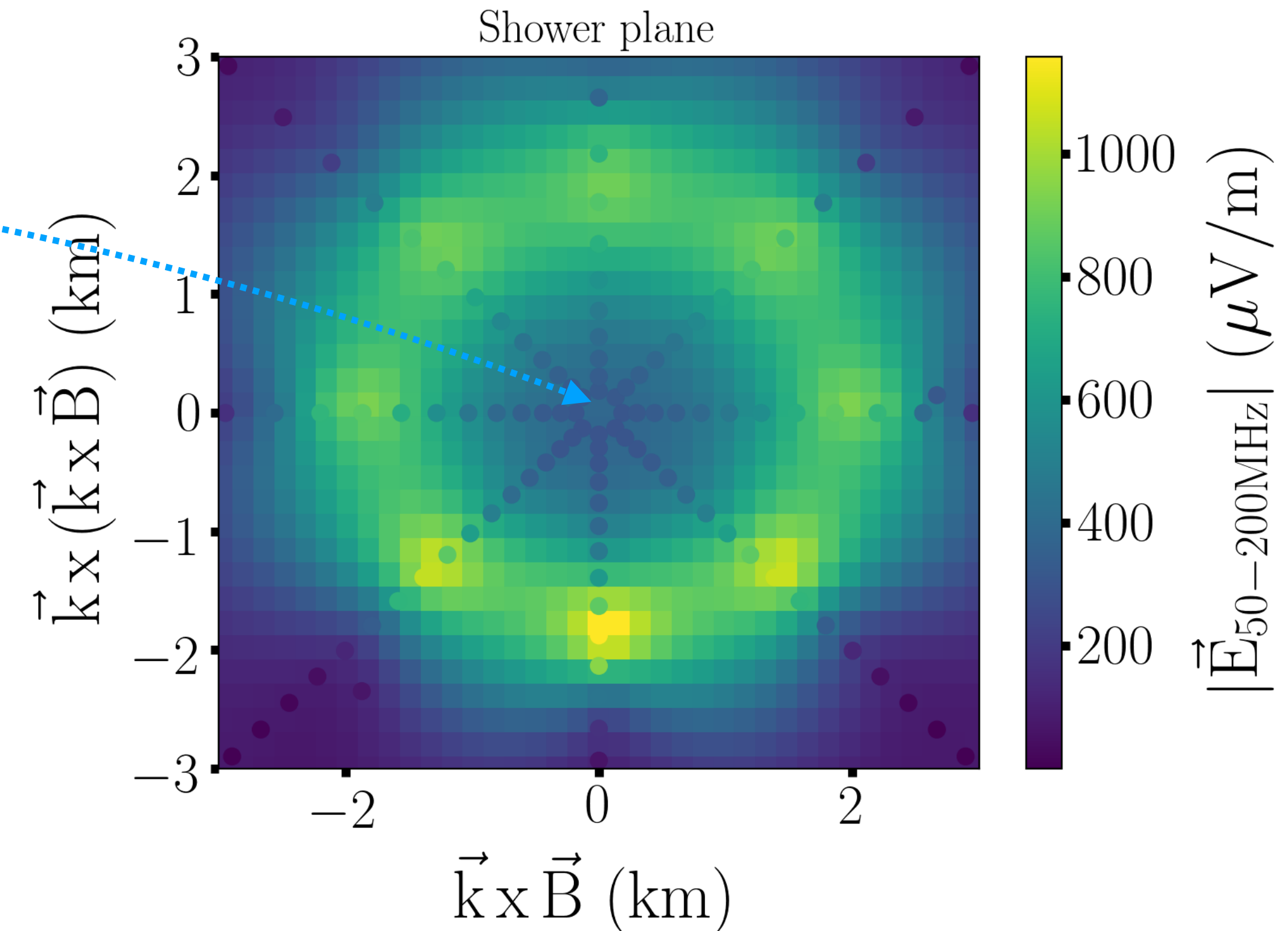
Distinct signature of the core position  
in the signal amplitude

Geomagnetic emission + Askaryan emission = asymmetry features



depends on:

- geomagnetic field orientation
- observer position



**Correctness of the amplitude model → accuracy of the reconstruction of the arrival direction**

# Information content in the amplitude distribution of the radiation

Amplitude distribution (pattern) = antennas measurements → straightforward handle on the core position

Beaming of the emission + Cerenkov effect (signal coherence + compression)

→ Distinct signature of the core position in the signal amplitude

Geomagnetic emission + Askaryan emission = asymmetry features

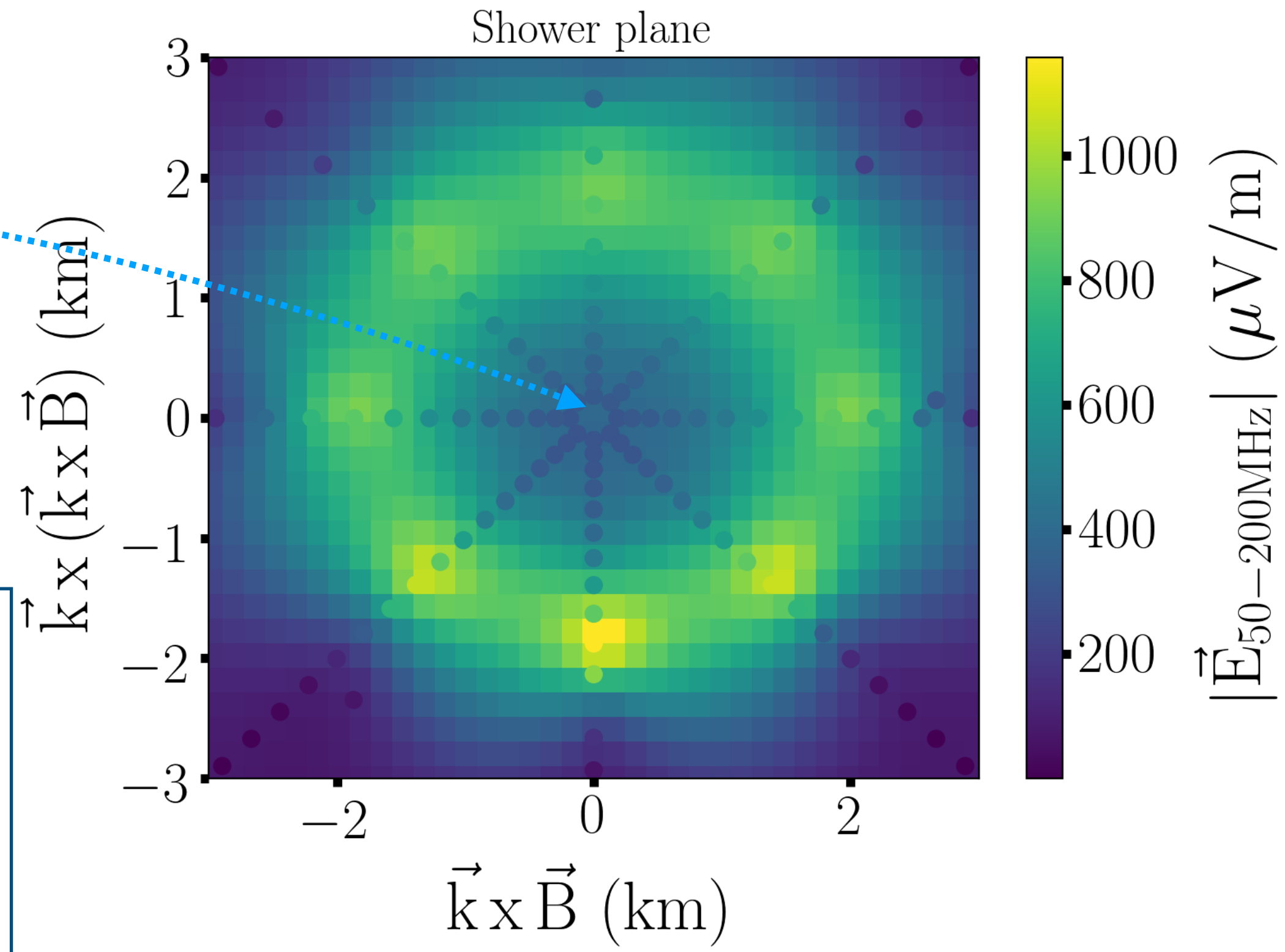
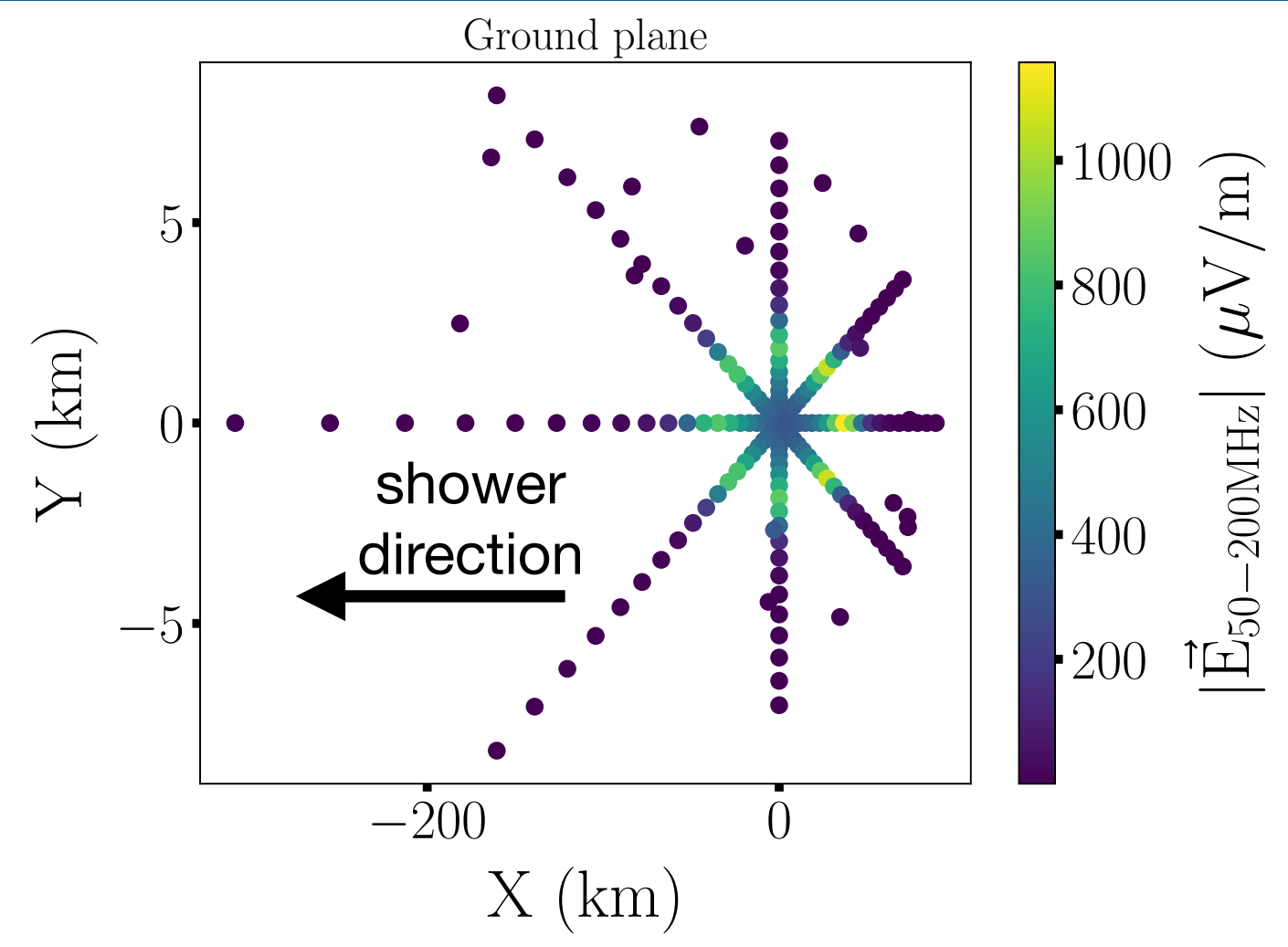
↪ depends on:

- geomagnetic field orientation
- observer position

New simulation set used: “StarShape”

- centered on the shower core
- Star shaped

→ better sampling of the amplitude



Correctness of the amplitude model → accuracy of the reconstruction of the arrival direction



# Phenomenological description of the amplitude pattern

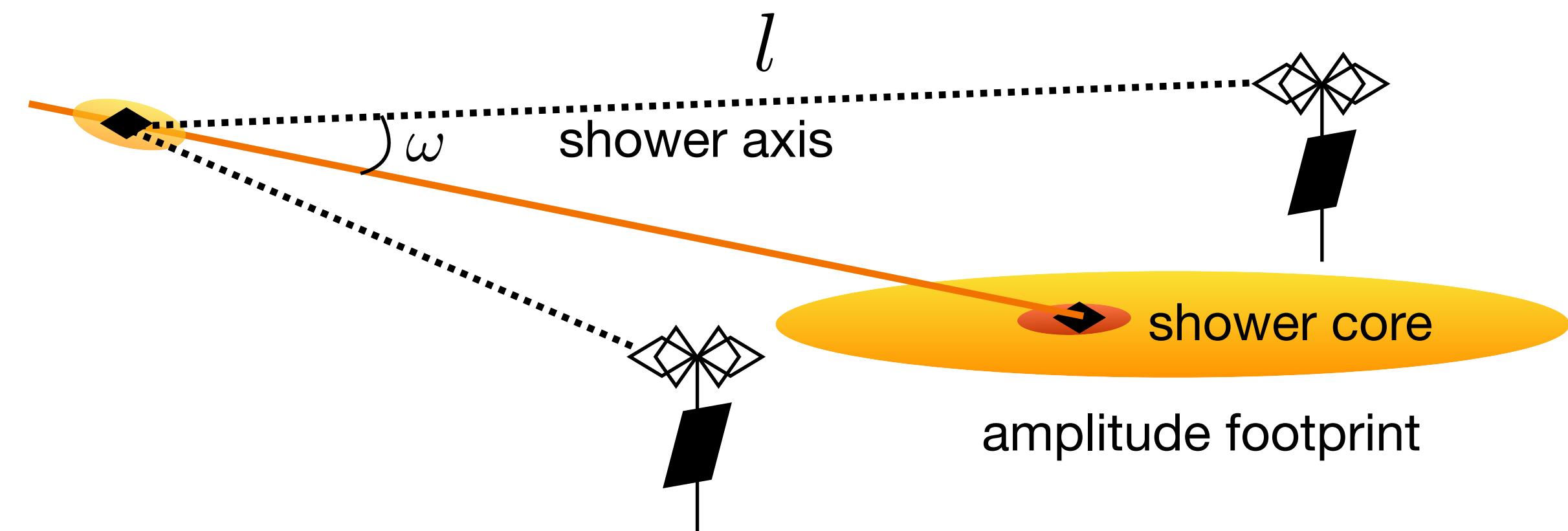
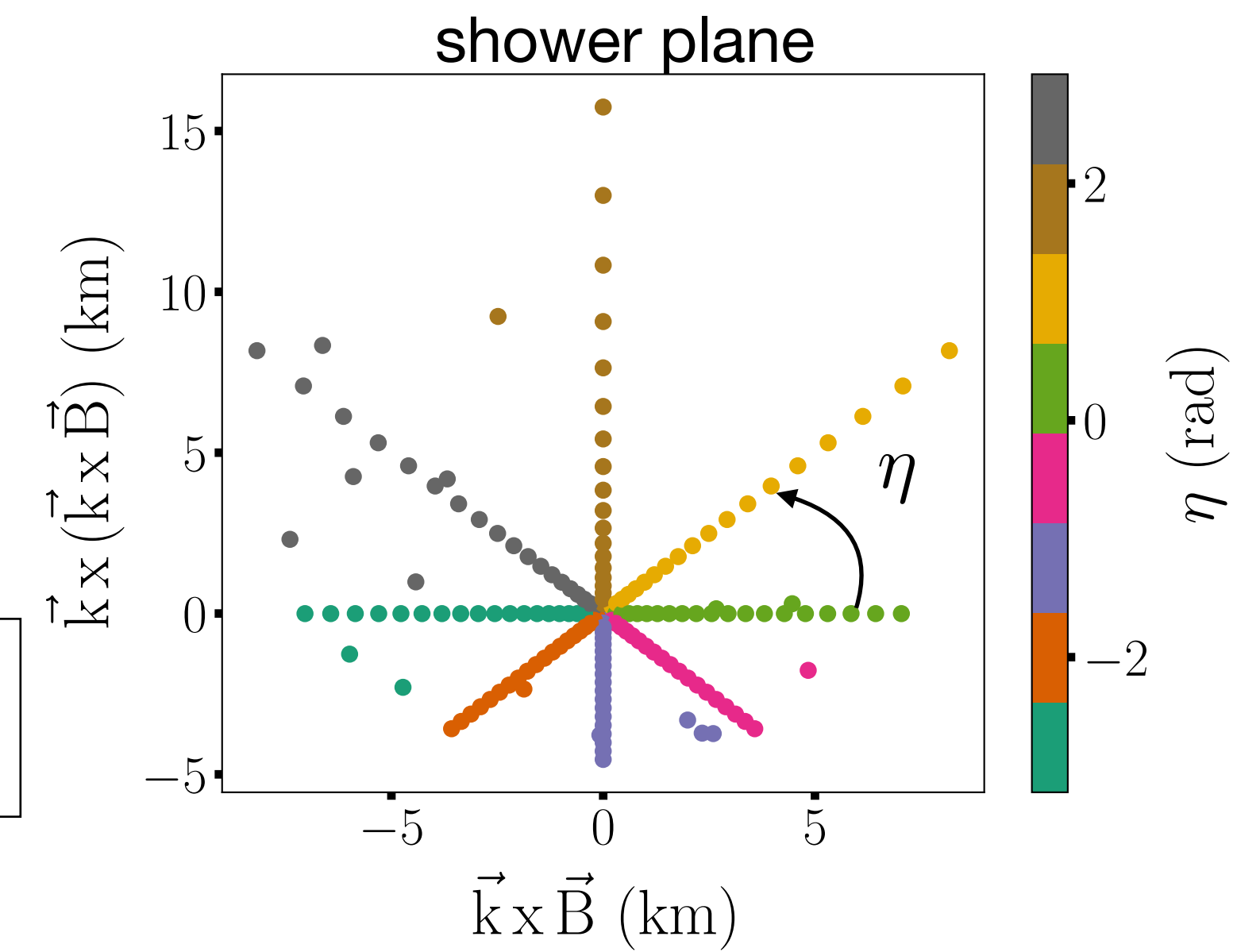
**Goal:** analytical description of the amplitude:

- shower direction
- all the asymmetries effects

**Method:** phenomenological description as a function of the angular position of the observer

**Angular Distribution Function:  
(ADF)**

$$f^{\text{ADF}}(\omega, \eta, \alpha, l; \delta\omega, \mathcal{A}) = \frac{\mathcal{A}}{l} f^{\text{GeoM}}(\alpha, \eta, \mathcal{B}) f^{\text{Cerenkov}}(\omega, \delta\omega)$$



# Phenomenological description of the amplitude pattern

**Goal:** analytical description of the amplitude:

- shower direction
- all the asymmetries effects

**Method:** phenomenological description as a function of the angular position of the observer

**Angular Distribution Function:**  
(ADF)

$$f^{\text{ADF}}(\omega, \eta, \alpha, l; \delta\omega, \mathcal{A}) = \frac{\mathcal{A}}{l} f^{\text{GeoM}}(\alpha, \eta, \mathcal{B}) f^{\text{Cerenkov}}(\omega, \delta\omega)$$

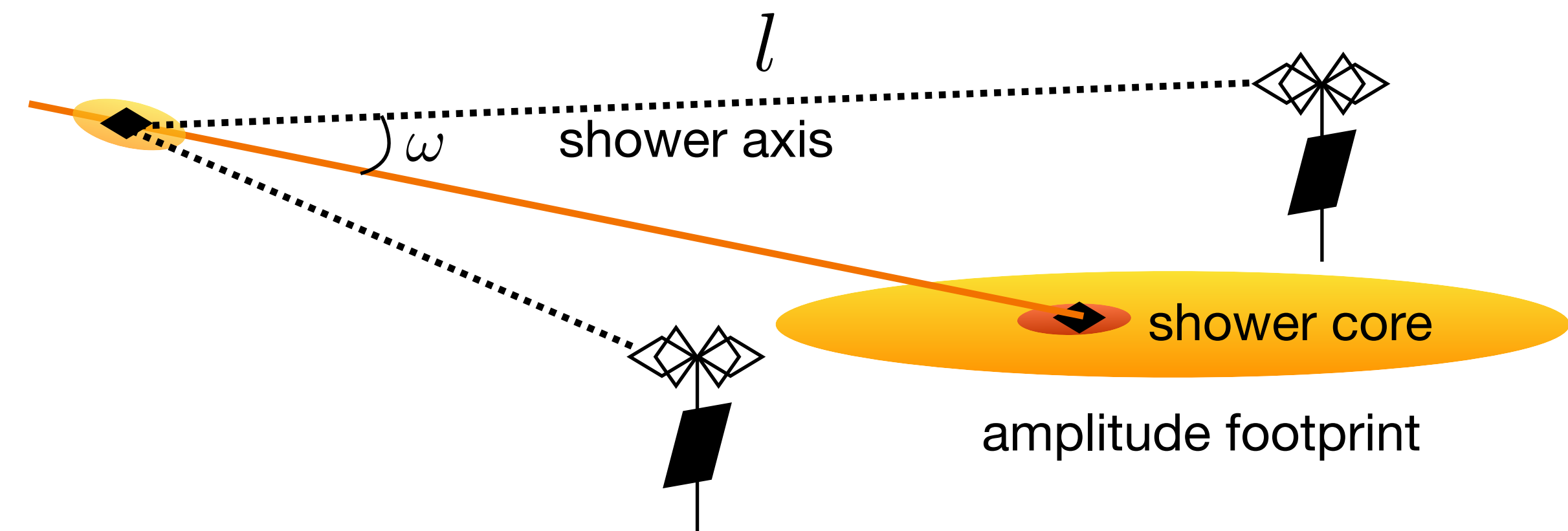
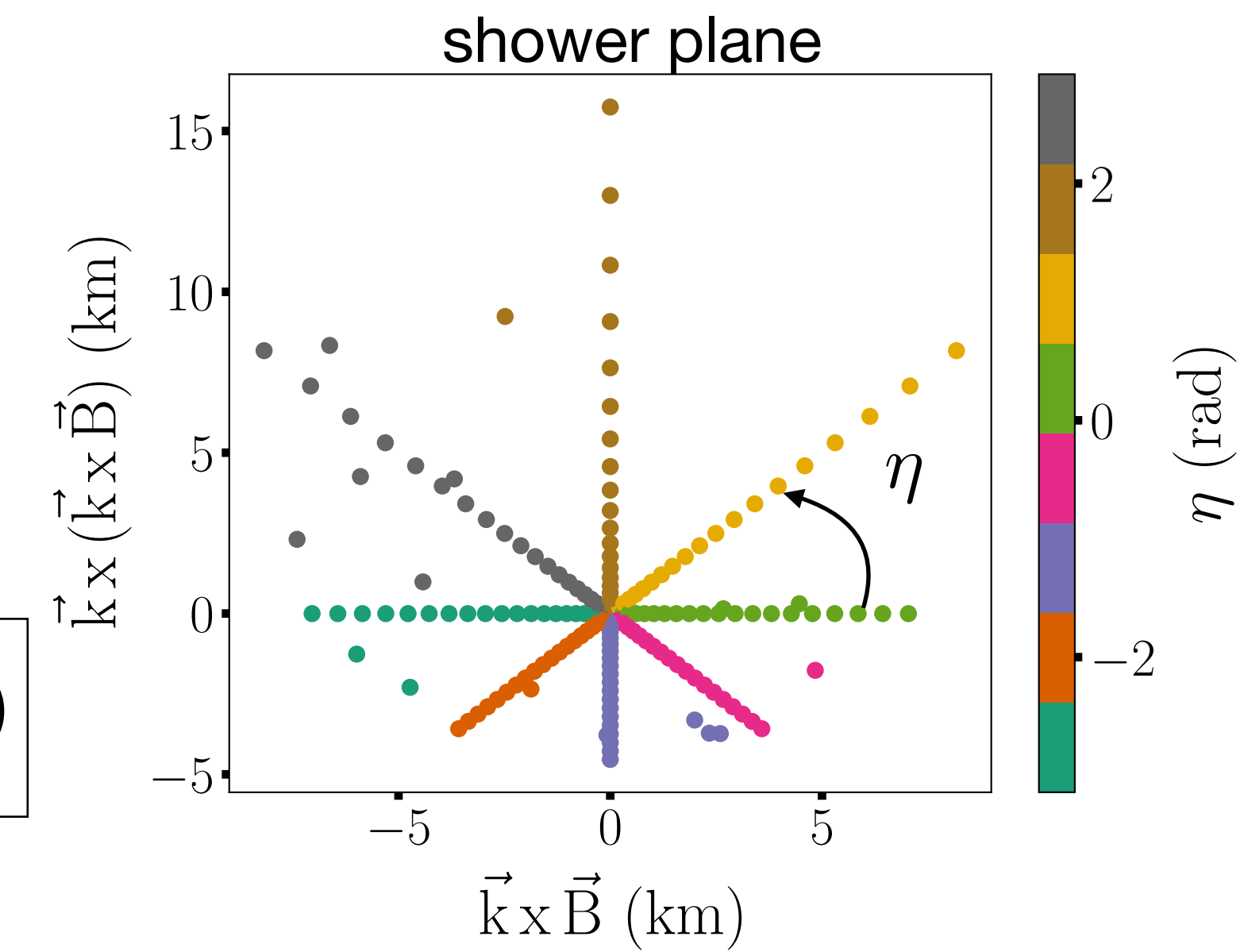
- Geomagnetic asymmetry  $f^{\text{GeoM}}(\alpha, \eta, \mathcal{B}) = 1 + \mathcal{B} \sin(\alpha)^2 \cos(\eta)$

$\alpha$  magnetic field inclination

$\mathcal{B}$  geomagnetic strength



interplay between emission mechanisms  
→ signal excess along the Lorentz force direction





# Phenomenological description of the amplitude pattern

**Goal:** analytical description of the amplitude:

- shower direction
- all the asymmetries effects

**Method:** phenomenological description as a function of the angular position of the observer

**Angular Distribution Function: (ADF)**

$$f^{\text{ADF}}(\omega, \eta, \alpha, l; \delta\omega, \mathcal{A}) = \frac{\mathcal{A}}{l} f^{\text{GeoM}}(\alpha, \eta, \mathcal{B}) f^{\text{Cerenkov}}(\omega, \delta\omega)$$

- Geomagnetic asymmetry  $f^{\text{GeoM}}(\alpha, \eta, \mathcal{B}) = 1 + \mathcal{B} \sin(\alpha)^2 \cos(\eta)$

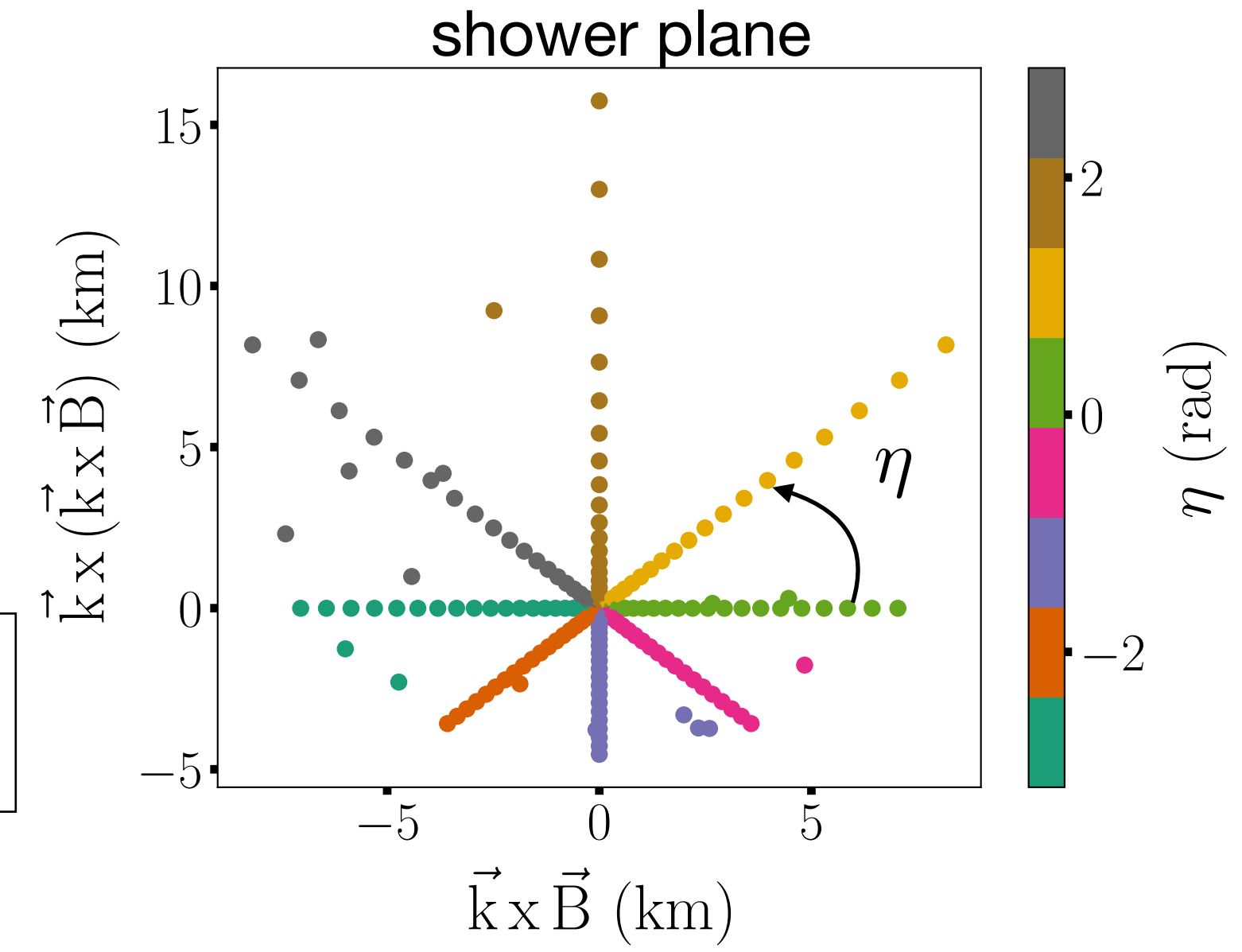
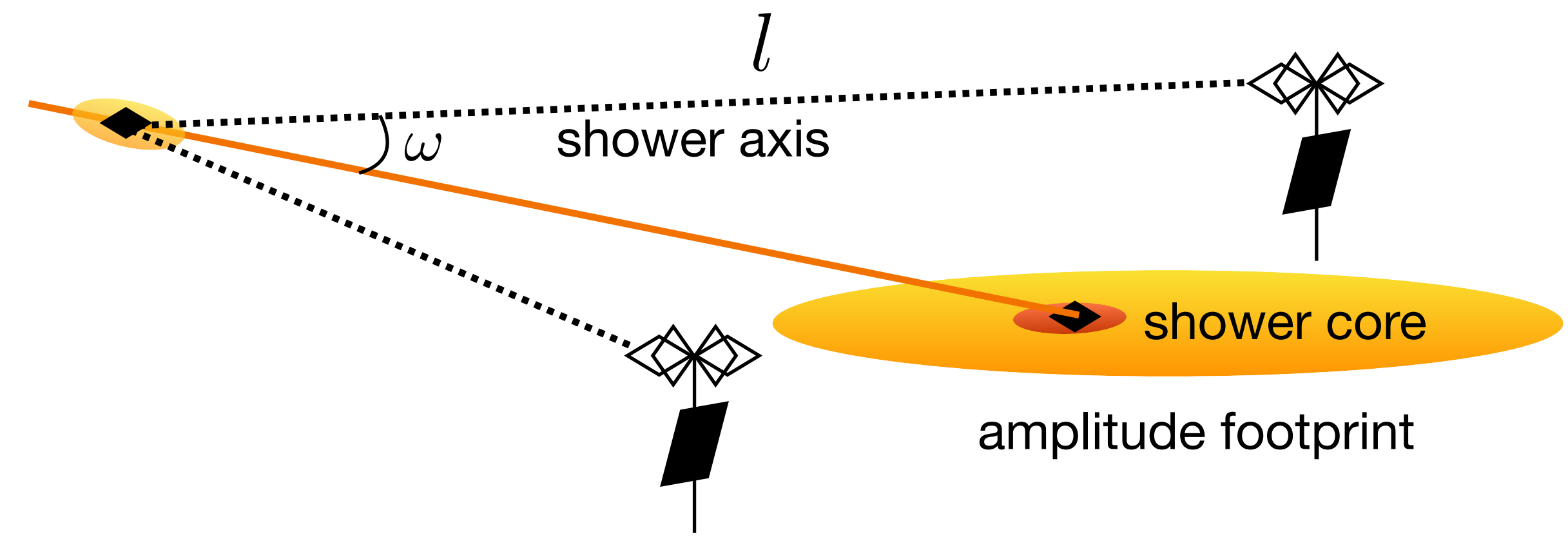
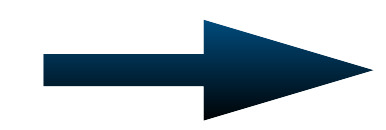
$\alpha$  magnetic field inclination       $\mathcal{B}$  geomagnetic strength



interplay between emission mechanisms  
→ signal excess along the Lorentz force direction

- Early-late asymmetry  $\frac{\mathcal{A}}{l}$  → energy dilution

$$\frac{\mathcal{A}}{l}$$



# Phenomenological description of the amplitude pattern

**Goal:** analytical description of the amplitude:

- shower direction
- all the asymmetries effects

**Method:** phenomenological description as a function of the angular position of the observer

**Angular Distribution Function:**  
(ADF)

$$f^{\text{ADF}}(\omega, \eta, \alpha, l; \delta\omega, \mathcal{A}) = \frac{\mathcal{A}}{l} f^{\text{GeoM}}(\alpha, \eta, \mathcal{B}) f^{\text{Cerenkov}}(\omega, \delta\omega)$$

- Geomagnetic asymmetry

$$f^{\text{GeoM}}(\alpha, \eta, \mathcal{B}) = 1 + \mathcal{B} \sin(\alpha)^2 \cos(\eta)$$

$\alpha$  magnetic field inclination

$\mathcal{B}$  geomagnetic strength



interplay between emission mechanisms  
→ signal excess along the Lorentz force direction

- Early-late asymmetry

$$\frac{\mathcal{A}}{l}$$



energy dilution

- Cerenkov cone

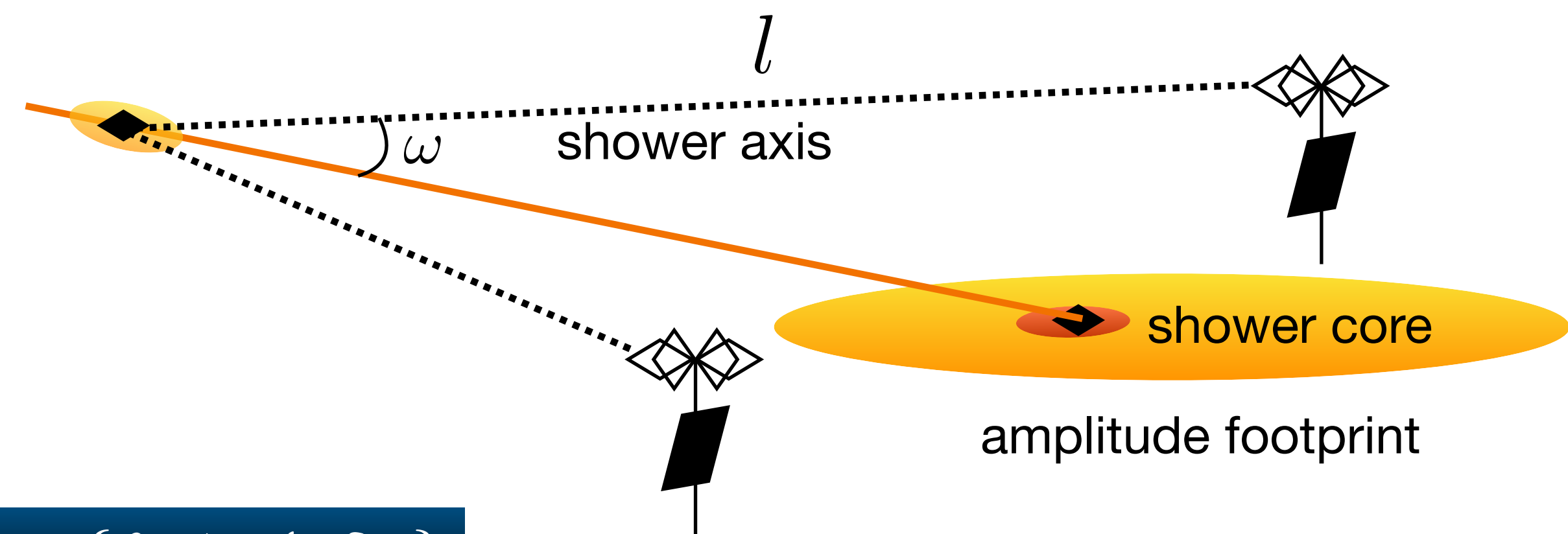
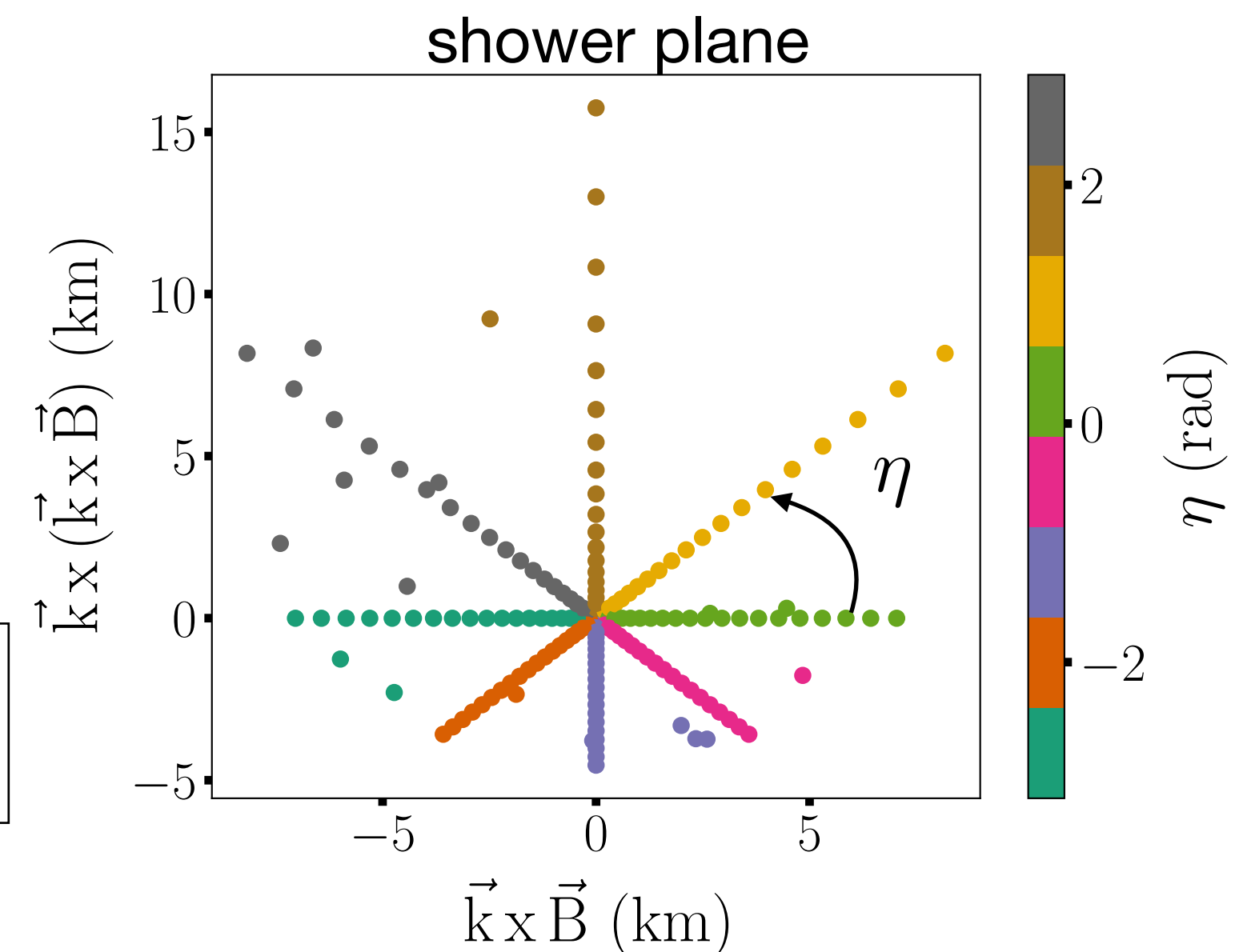
$$f^{\text{Cerenkov}}(\omega, \delta\omega) = \frac{1}{1 + 4 \left[ \frac{(\tan(\omega) / \tan(\omega_C))^2 - 1}{\delta\omega} \right]^2}$$



geometrical Cerenkov effect description



$\omega_C$



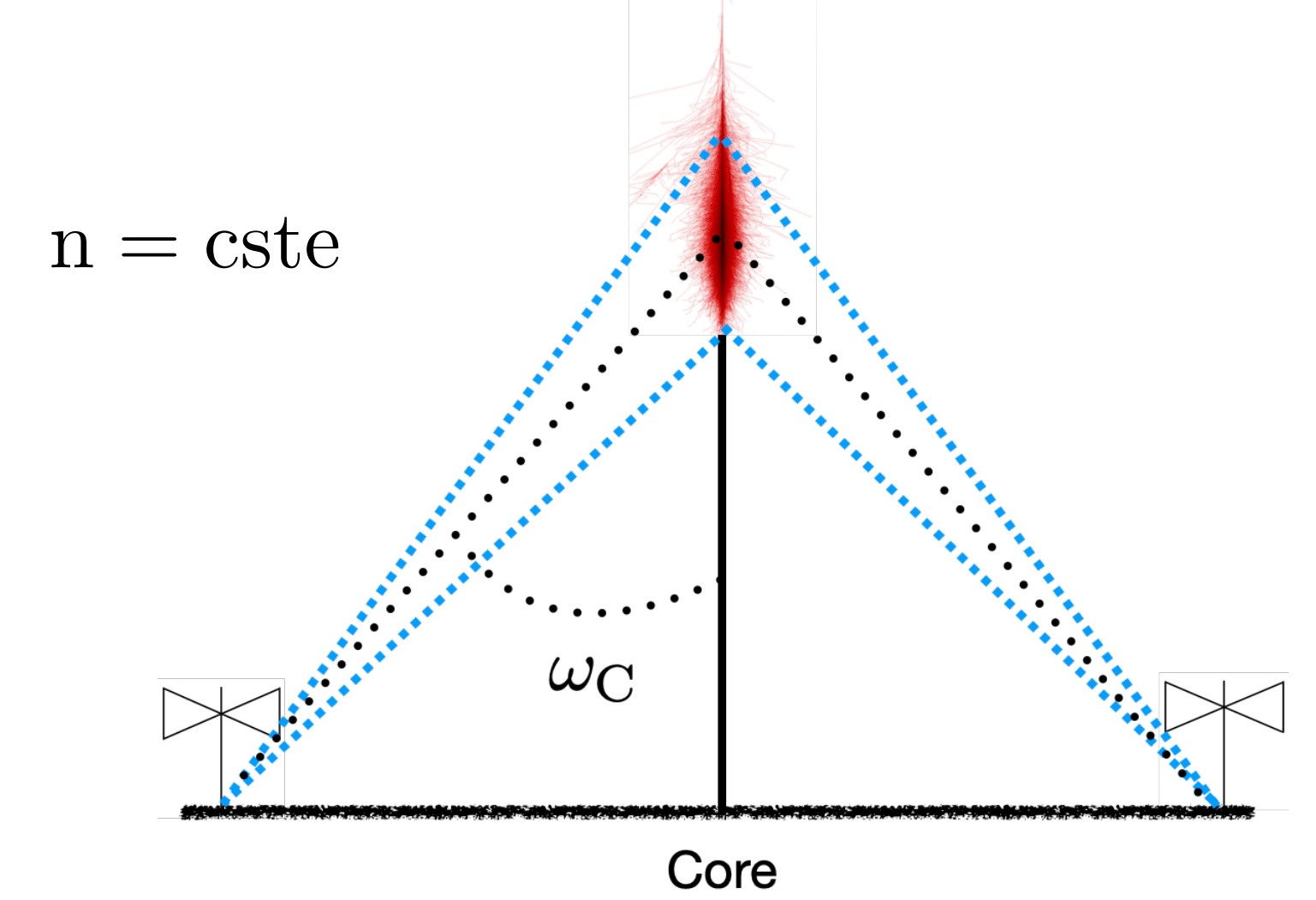
4 fitting parameters only:  $\{\theta, \phi, \mathcal{A}, \delta\omega\}$



# A side result: Cerenkov cone asymmetry

## Cerenkov cone:

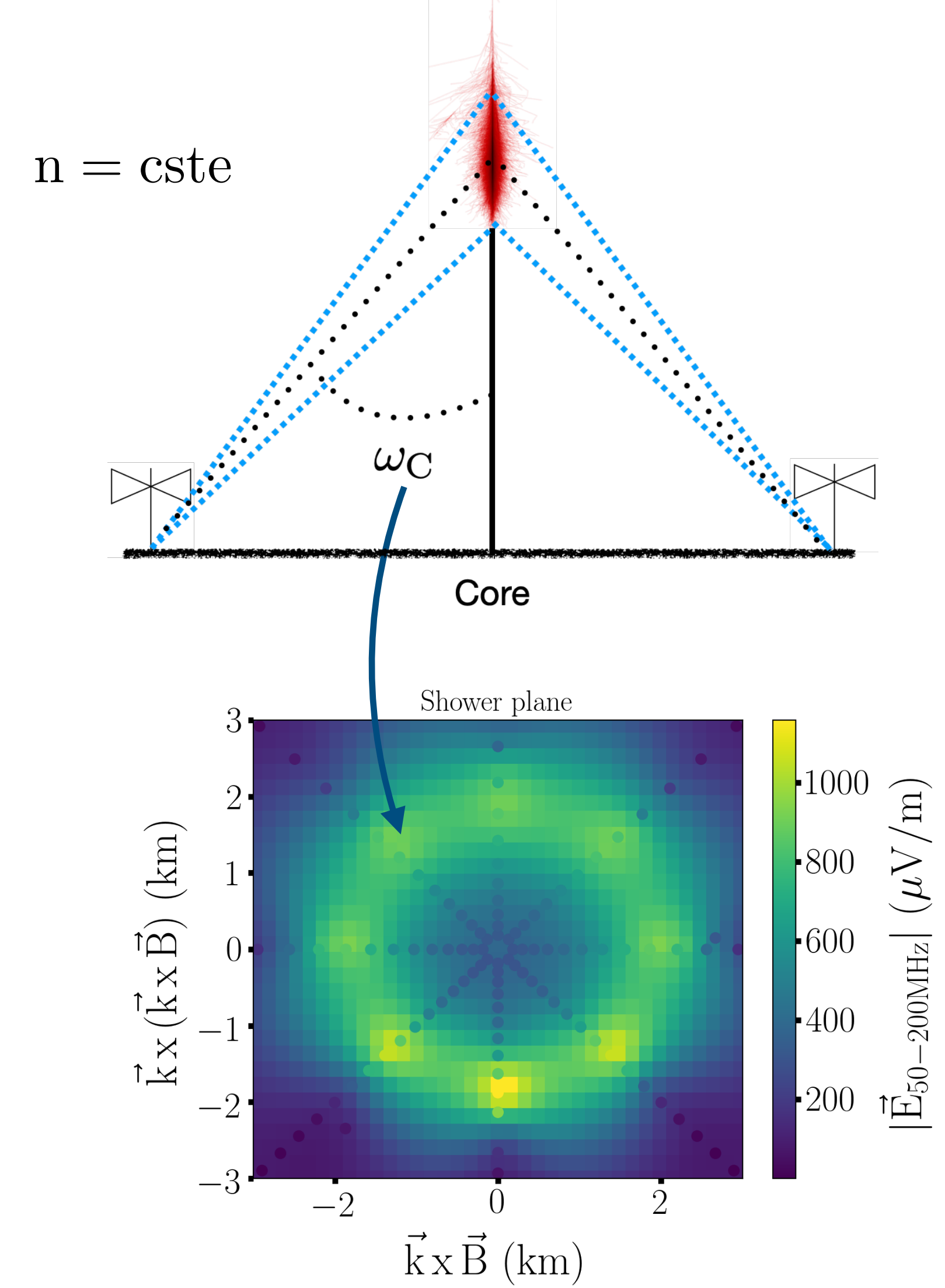
- geometrical effect → angle where all emissions arrive at same time
- signal compression → high amplitudes
- standard computation:  $\omega_C = \arccos(1/n)$  (equal optical paths = constant n)



# A side result: Cerenkov cone asymmetry

## Cerenkov cone:

- geometrical effect → angle where all emissions arrive at same time
- signal compression → high amplitudes
- standard computation:  $\omega_C = \arccos(1/n)$  (equal optical paths = constant n)



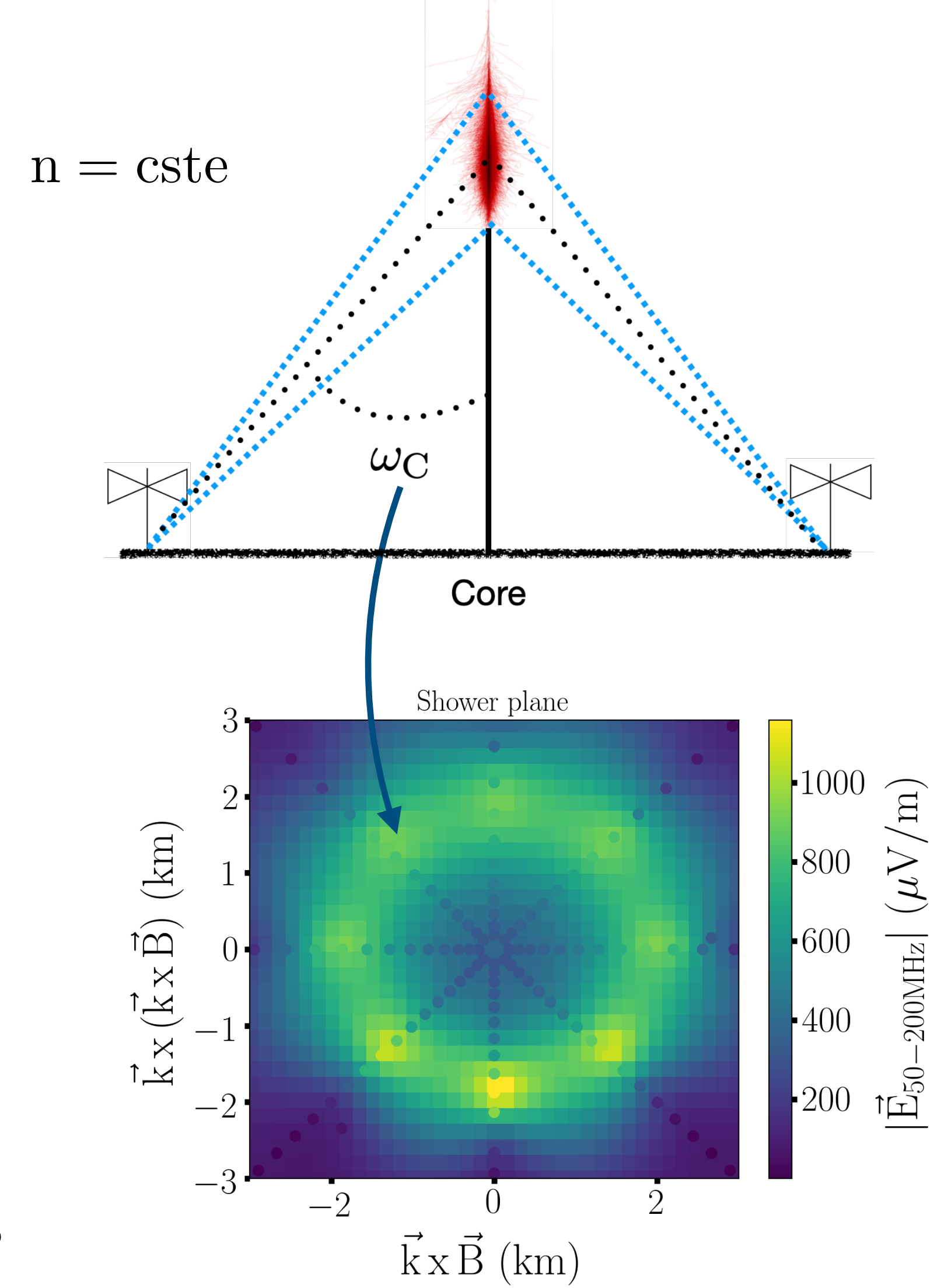
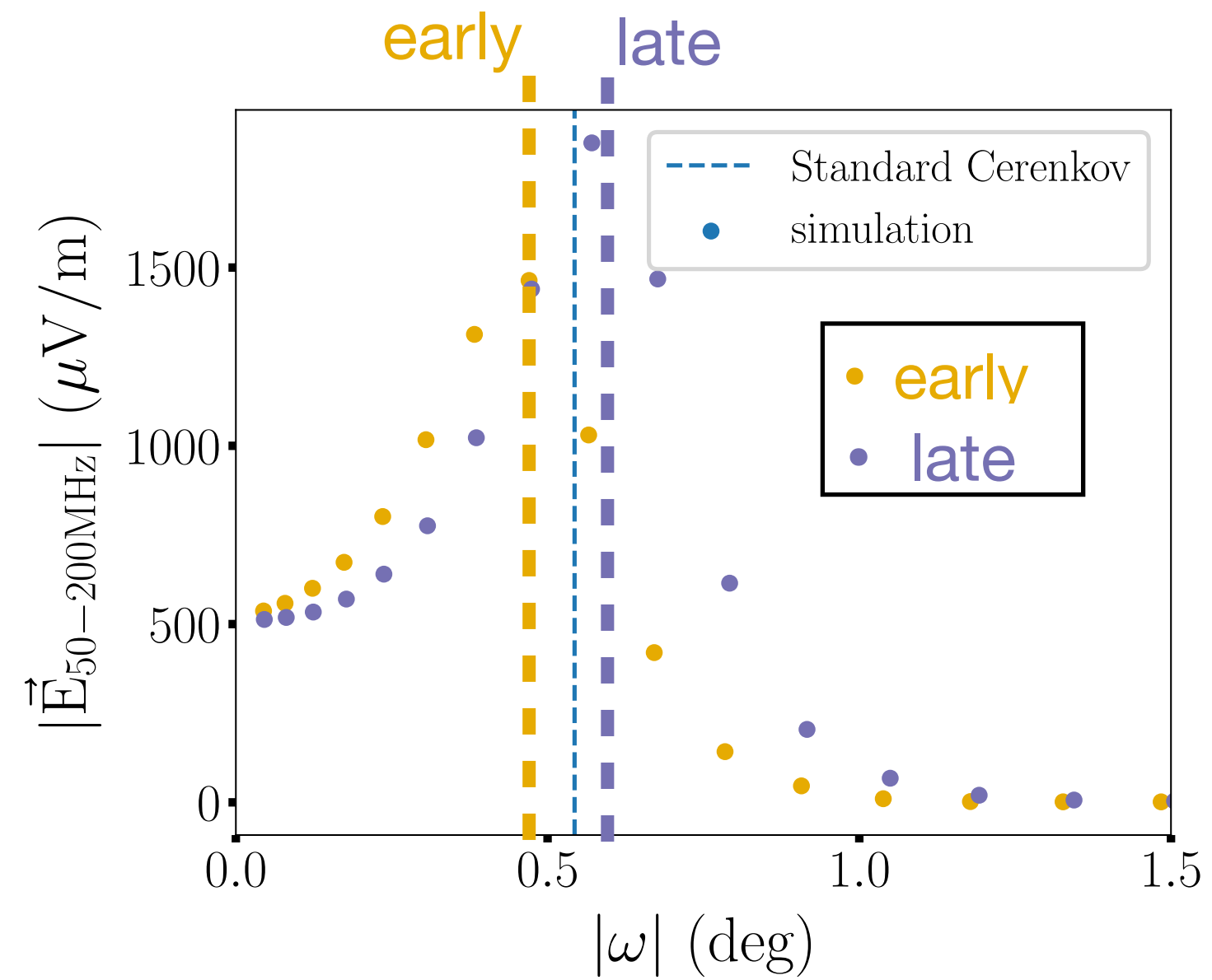
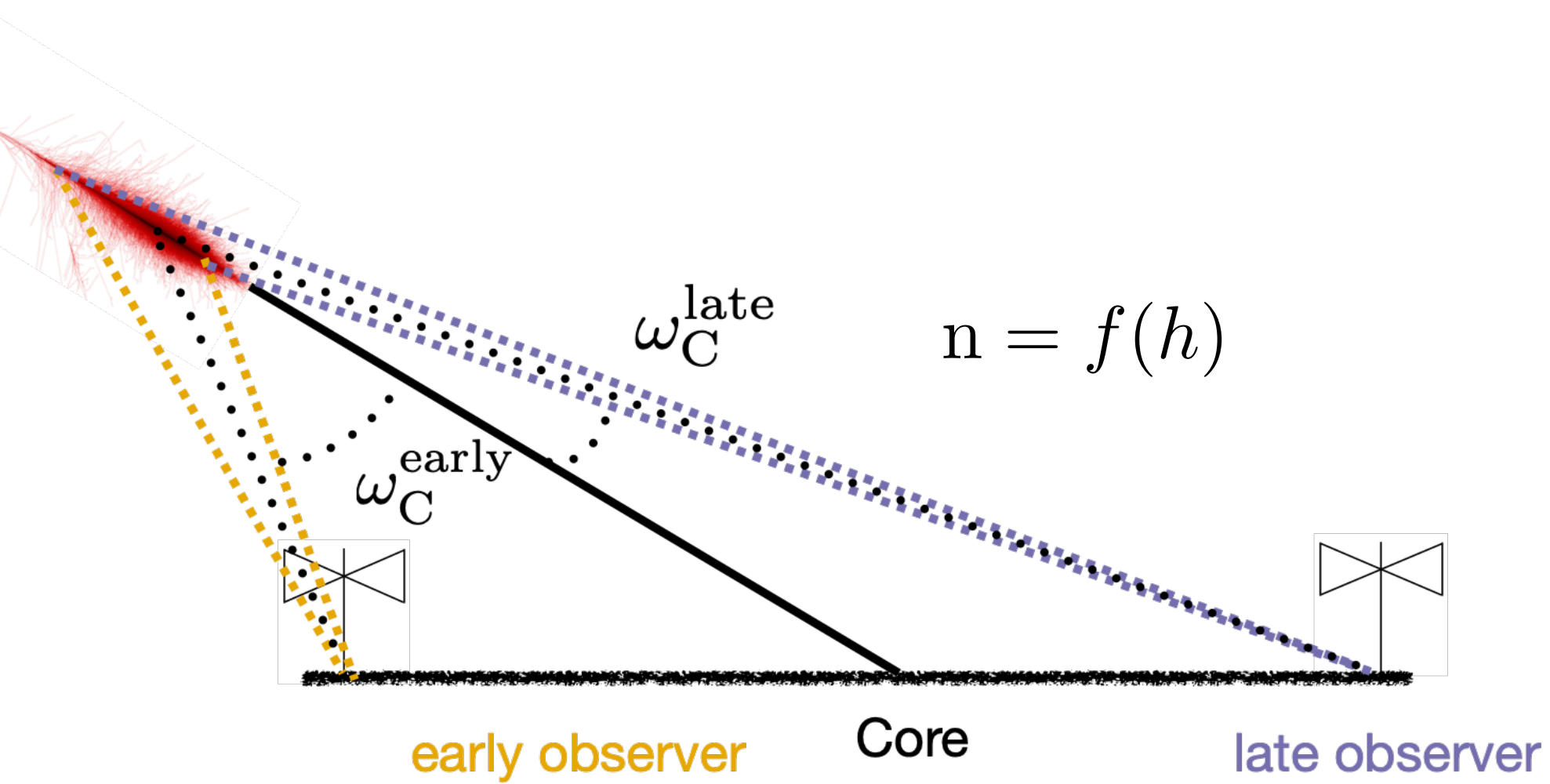


# A side result: Cerenkov cone asymmetry

## Cerenkov cone:

- geometrical effect → angle where all emissions arrive at same time
- signal compression → high amplitudes
- standard computation:  $\omega_C = \arccos(1/n)$  (equal optical paths = constant  $n$ )

**But** if optical paths are different (varying  $n$ )  $\omega_C = f(\vec{x}, \theta, \phi)$

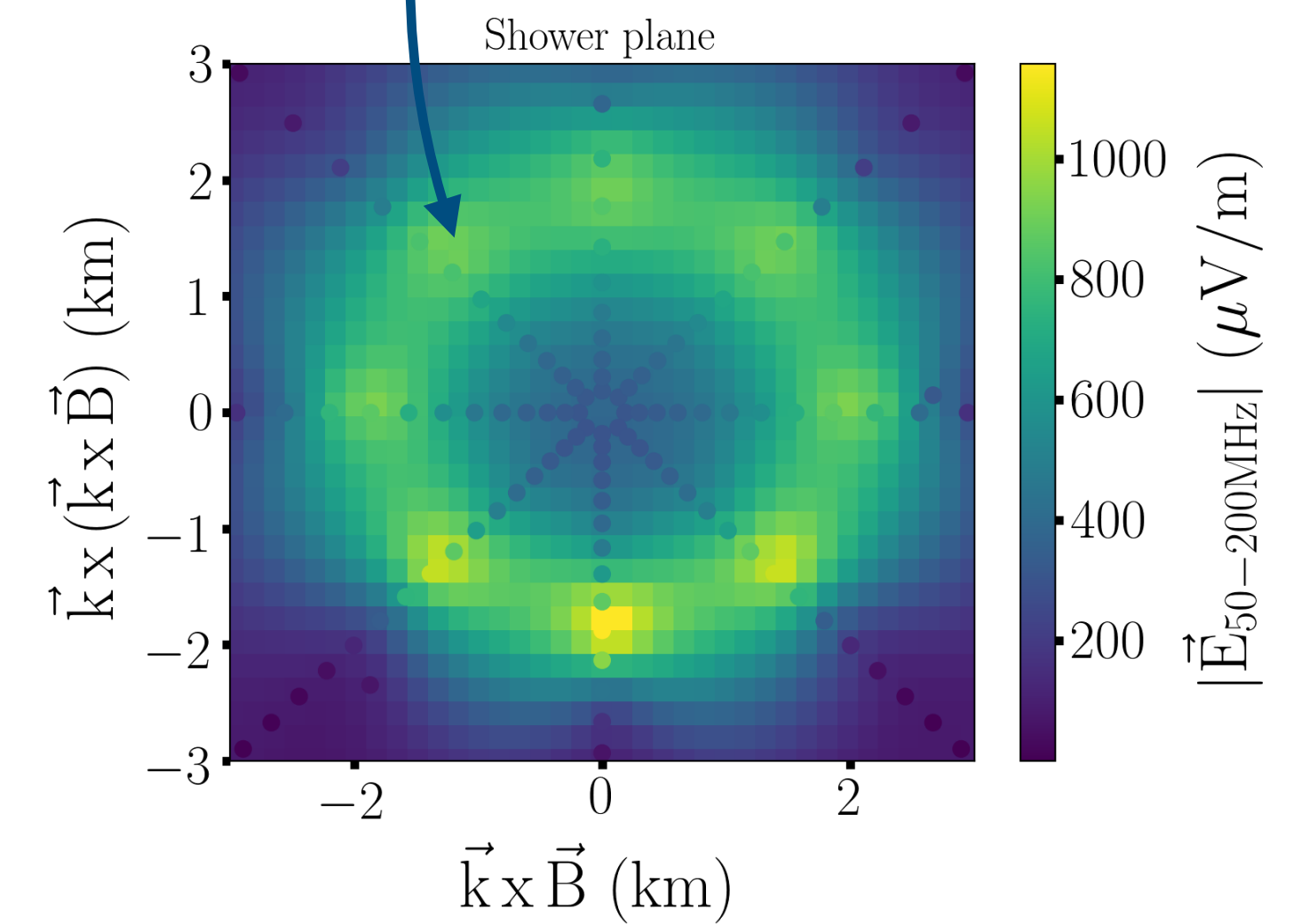
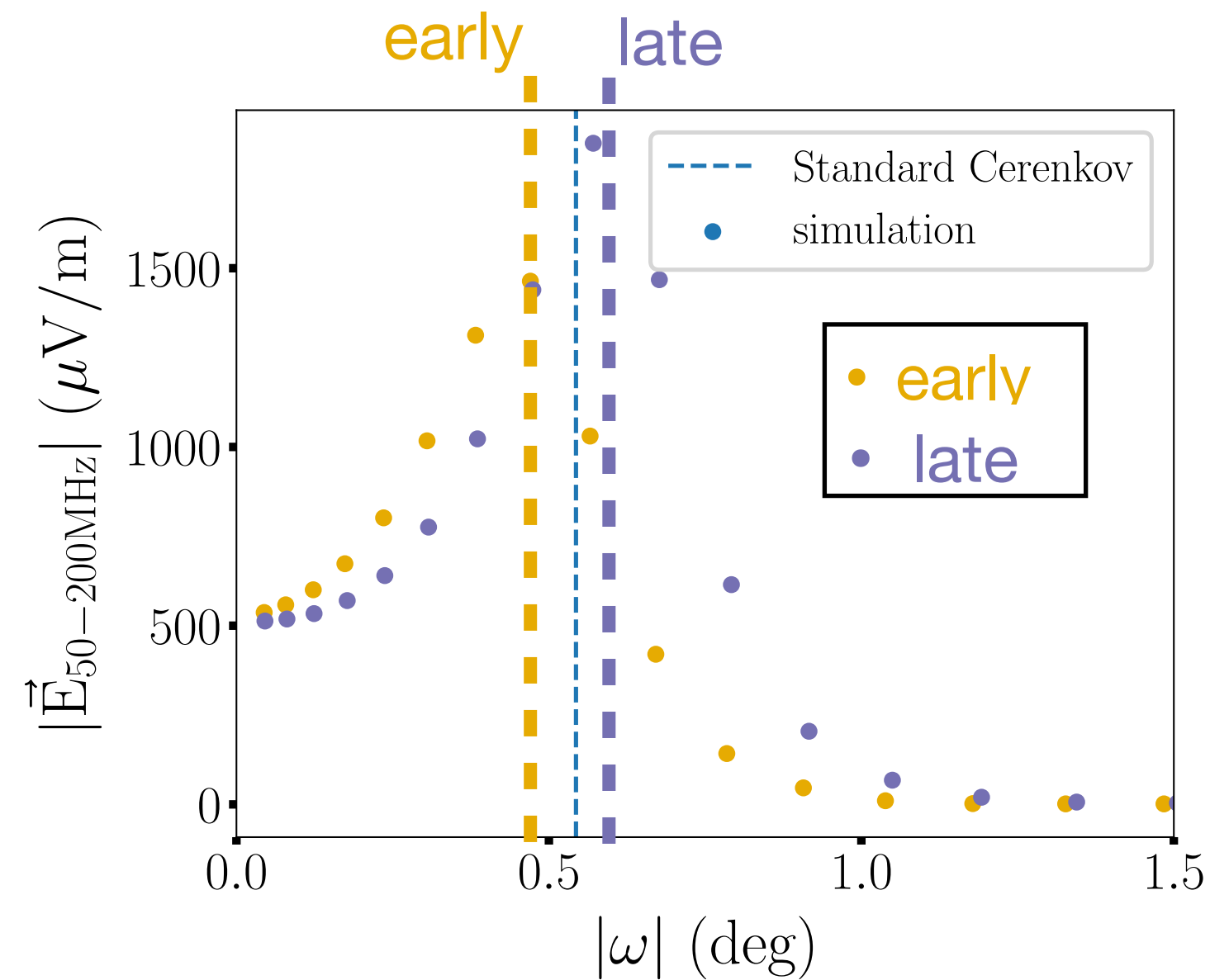
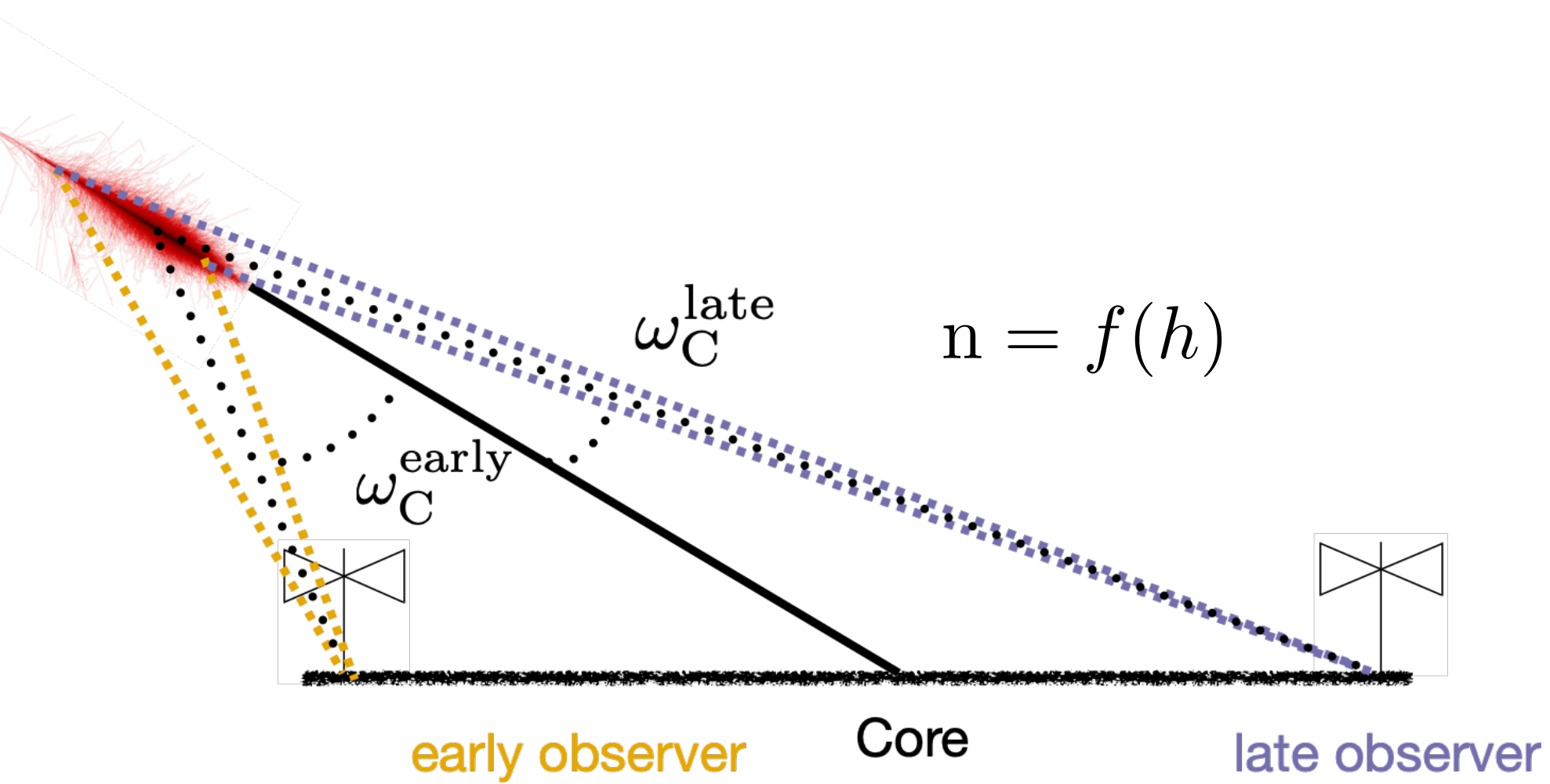
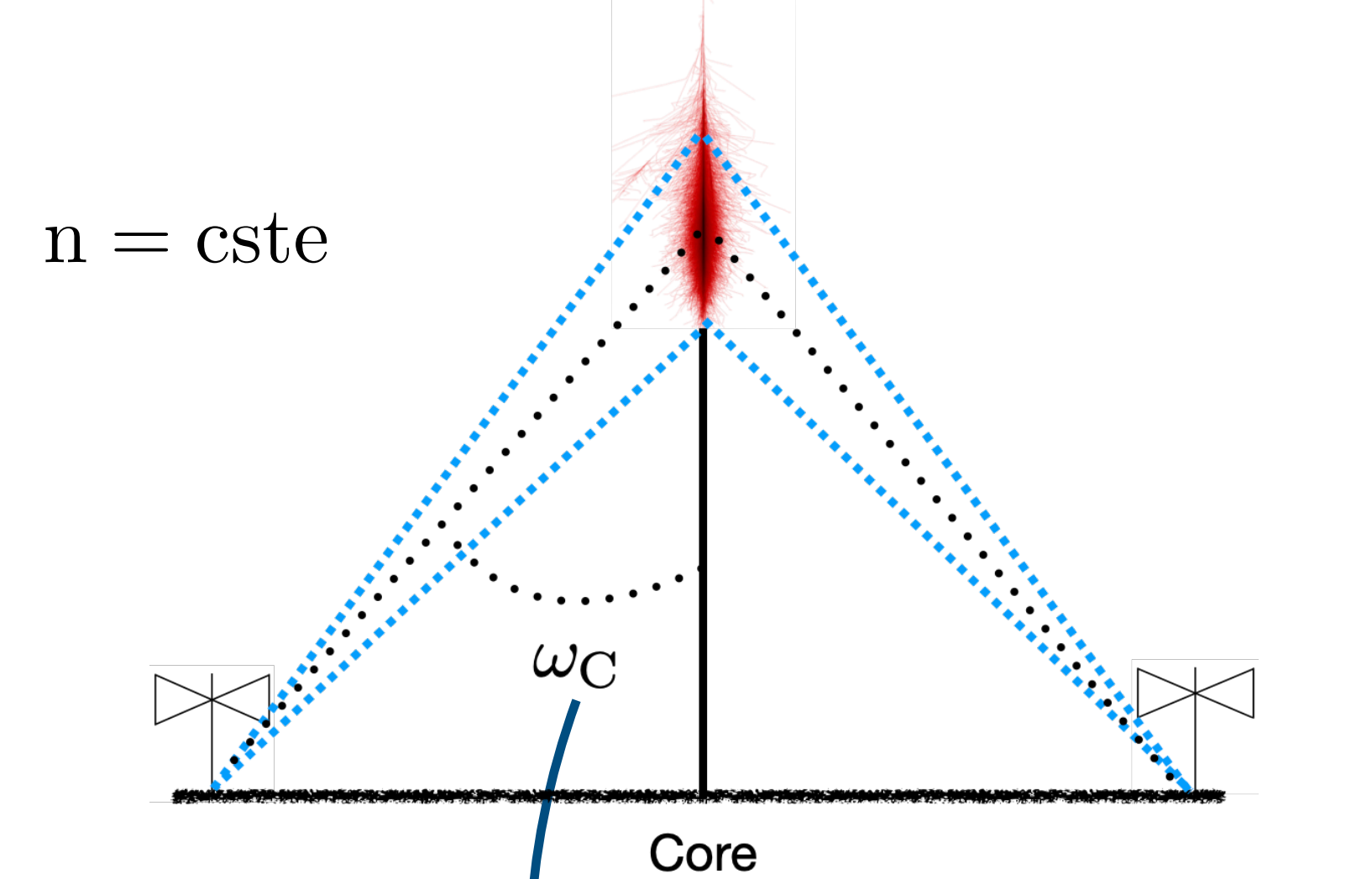


# A side result: Cerenkov cone asymmetry

## Cerenkov cone:

- geometrical effect → angle where all emissions arrive at same time
- signal compression → high amplitudes
- standard computation:  $\omega_C = \arccos(1/n)$  (equal optical paths = constant  $n$ )

**But** if optical paths are different (varying  $n$ )  $\omega_C = f(\vec{x}, \theta, \phi)$



analytical description of  
 $\omega_C = f(\vec{x}, \theta, \phi)$

used into the amplitude model:  
each antenna “sees” a different  
Cerenkov cone

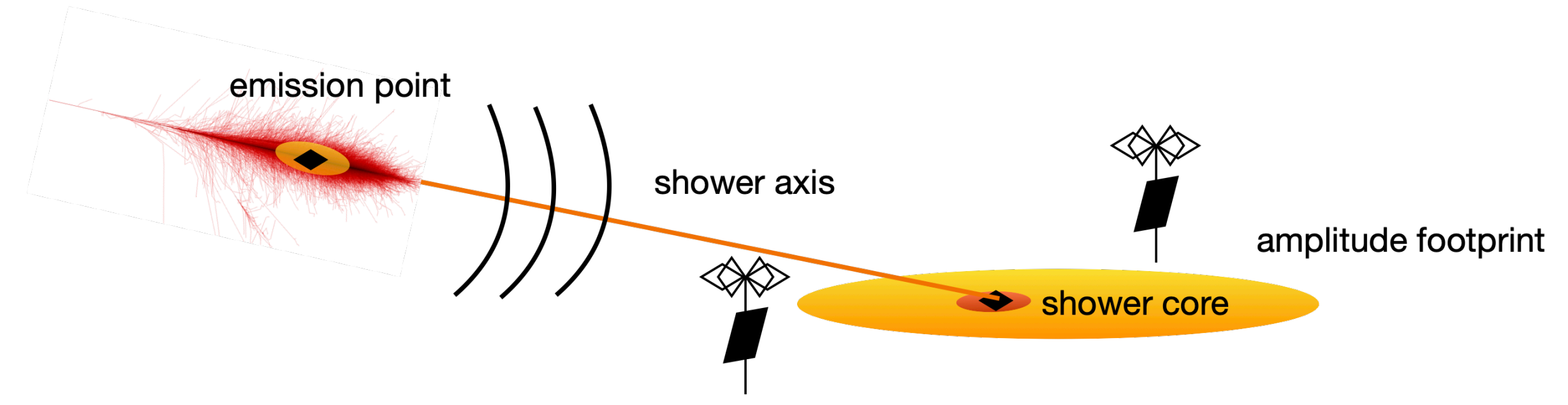
The analytical description of the Cerenkov  
asymmetry matches the simulated data



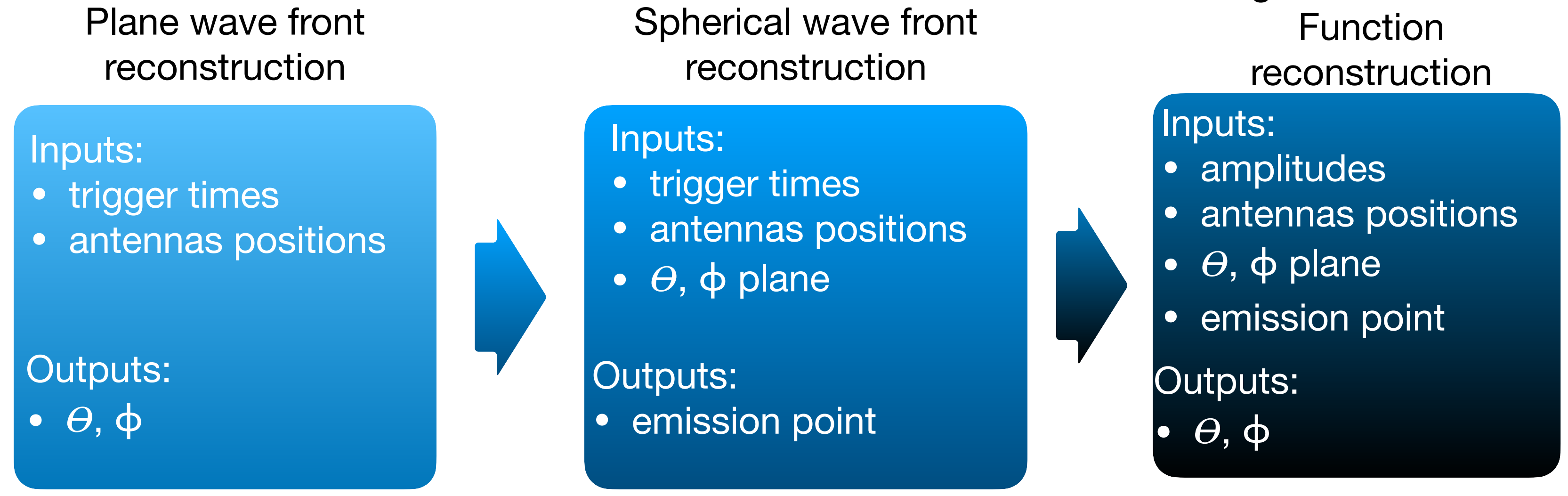
# Arrival direction reconstruction procedure

**Principles:** reconstruction of two points along the extensive air shower:

- emission point
- Cerenkov cone (signal “valley” around the core)



**Procedure:**



same weight for all antennas

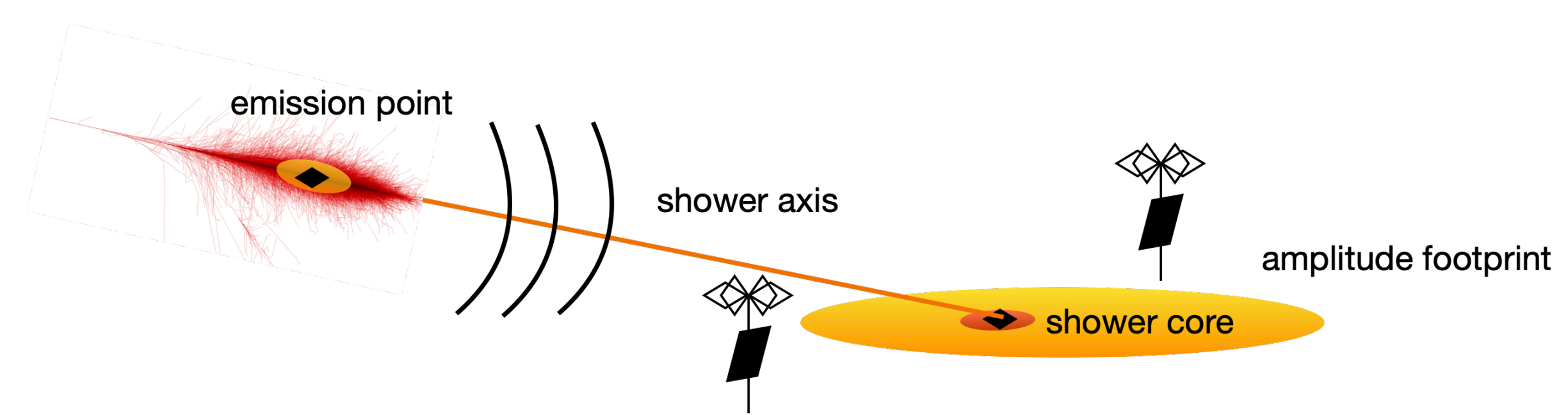
- measured quantities
- $t$  trigger times
  - $A$  amplitudes
  - $\vec{x}$  antenna positions

- adjusted quantities
- $\vec{k}$  shower direction
  - $(x_{source}, y_{source}, z_{source}, t_{source})$  emission point

**Tests on a stationary noise model:**

- gaussian time GPS jitter of rms=5ns
- two gaussian amplitude errors of 10% and 20% (aggressive and conservative)

# Arrival direction reconstruction procedure



**Principles:** reconstruction of two points along the extensive air shower:

- emission point
- Cerenkov cone (signal “valley” around the core)

## Procedure:

Plane wave front reconstruction

Inputs:

- trigger times
- antennas positions

Outputs:

- $\theta, \phi$

Spherical wave front reconstruction

Inputs:

- trigger times
- antennas positions
- $\theta, \phi$  plane

Outputs:

- emission point

Angular Distribution Function reconstruction

Inputs:

- amplitudes
- antennas positions
- $\theta, \phi$  plane
- emission point

Outputs:

- $\theta, \phi$

measured quantities

- $t$  trigger times
- $A$  amplitudes
- $\vec{x}$  antenna positions

adjusted quantities

- $\vec{k}$  shower direction
- $(x_{\text{source}}, y_{\text{source}}, z_{\text{source}}, t_{\text{source}})$  emission point

same weight for all antennas

## Tests on a stationary noise model:

- gaussian time GPS jitter of rms=5ns
- two gaussian amplitude errors of 10% and 20% (aggressive and conservative)

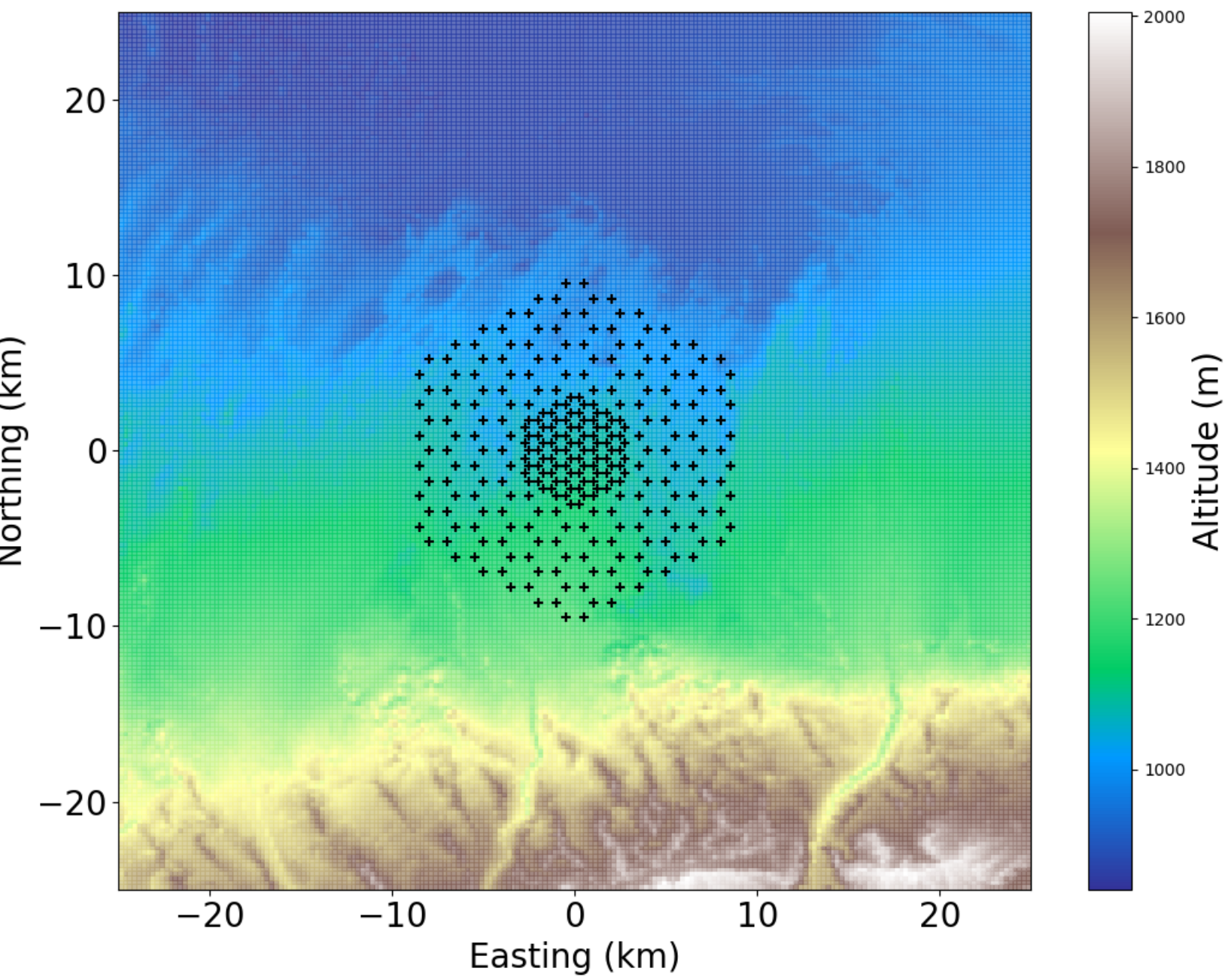
reconstruction procedure validated on StarShape simulations and performances obtained on realistic arrays



# Reconstruction performances for GRANDProto300 (GP300)

---

The 300 antennas GRAND prototype



## GP300 layout:

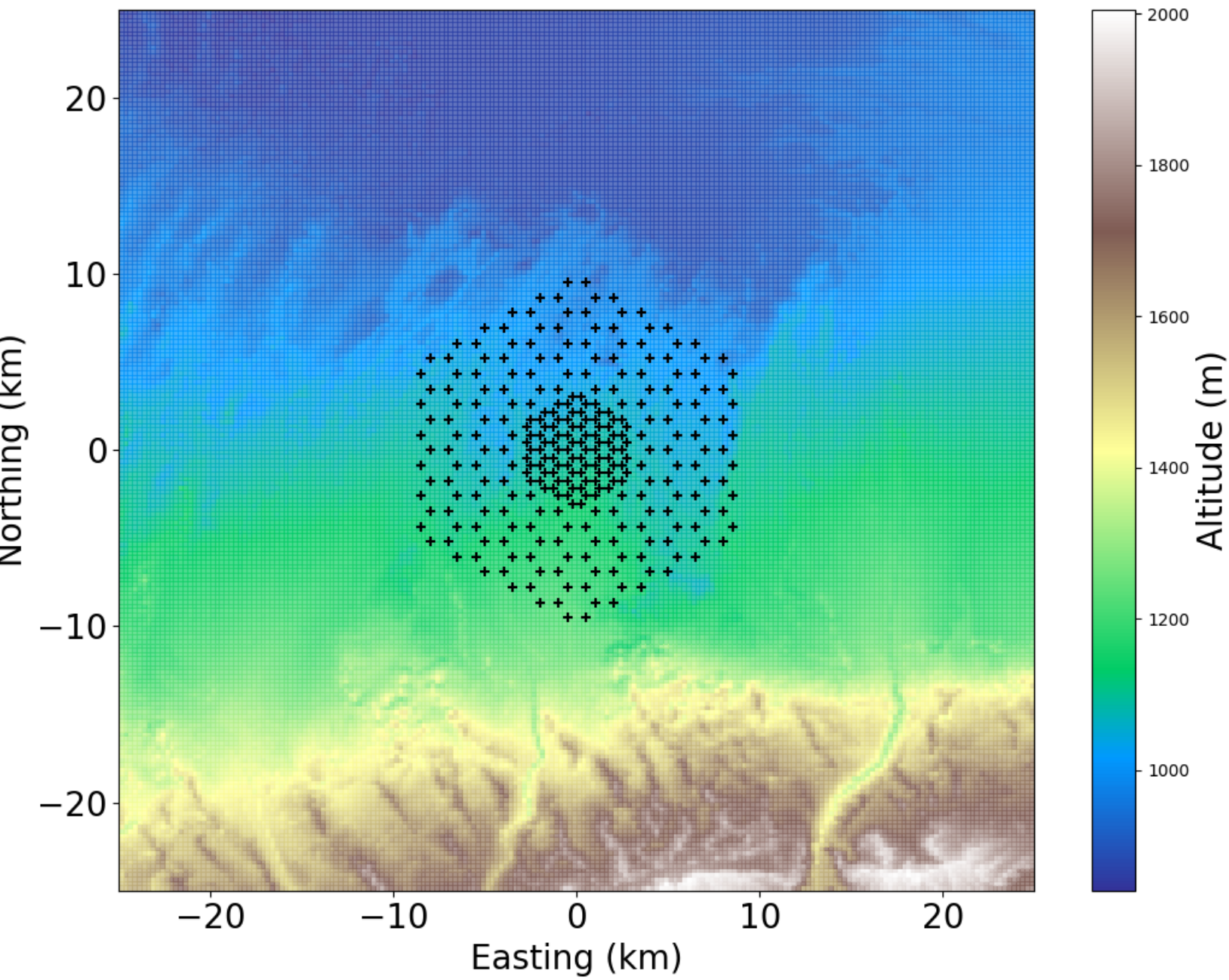
- ~300 antennas over ~200 km<sup>2</sup>
- detection of cosmic rays and gamma rays

## GP300 simulations:

- real topography
- primaries: proton, iron and gamma

# Reconstruction performances for GRANDProto300 (GP300)

The 300 antennas GRAND prototype

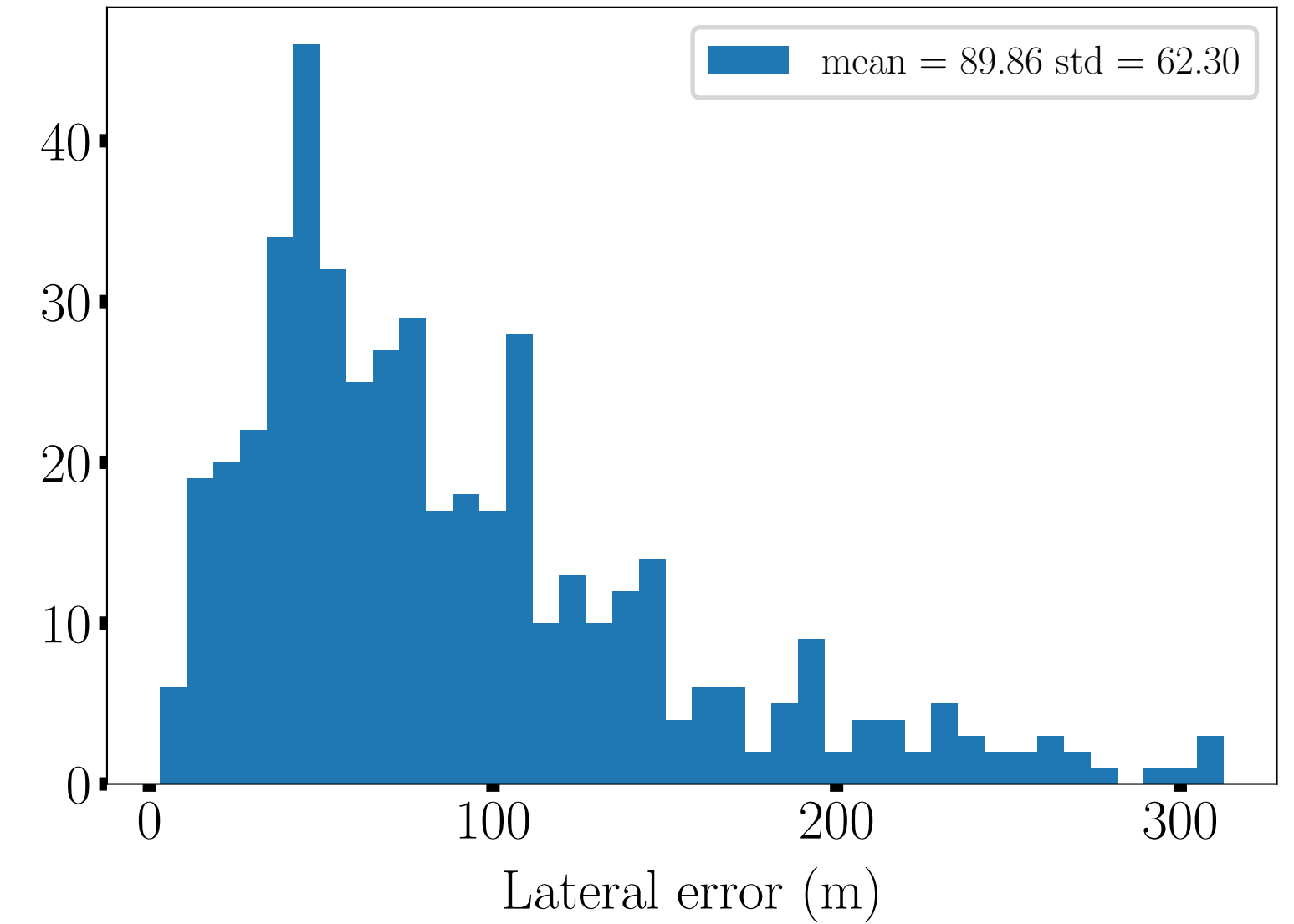
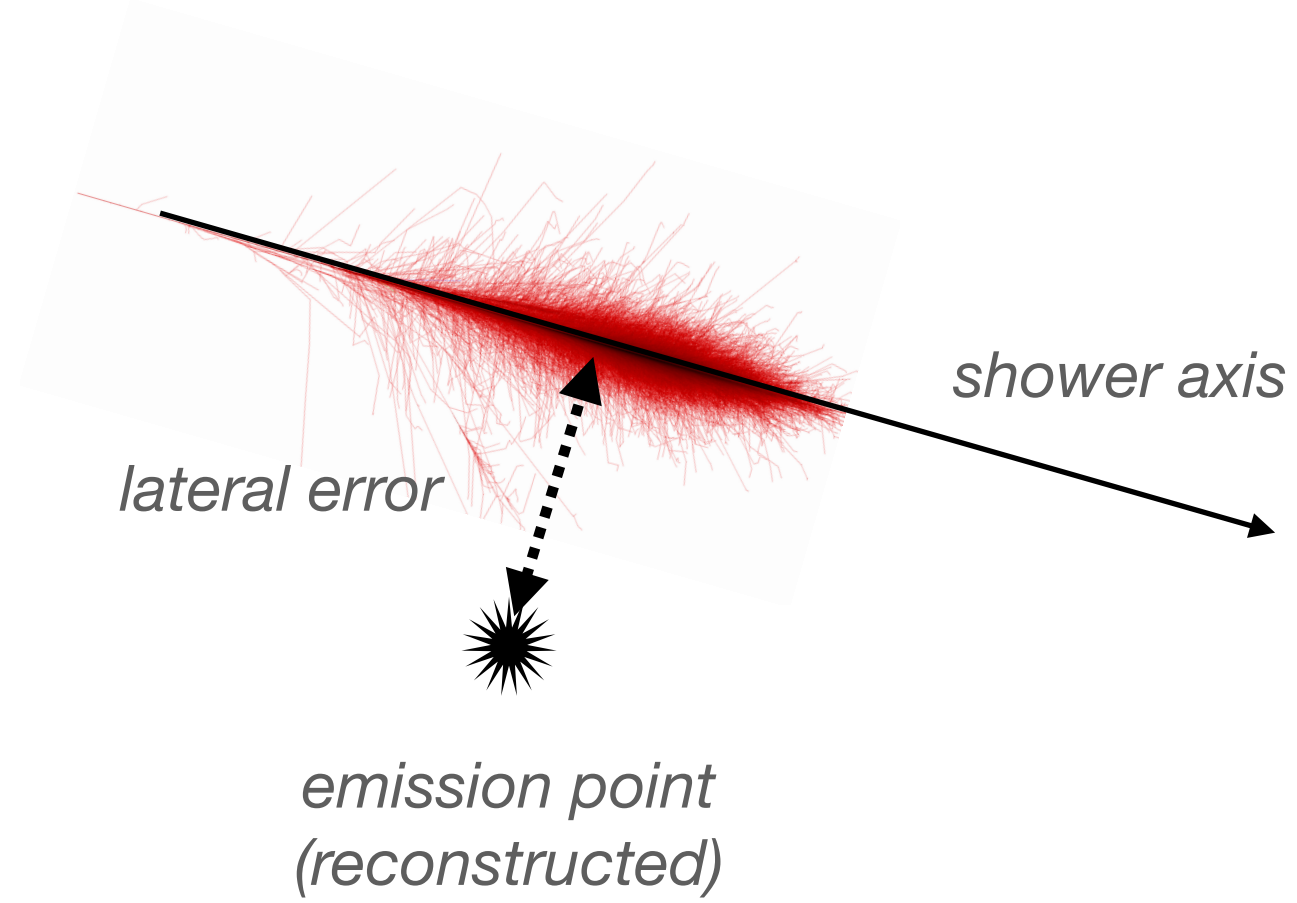


## GP300 layout:

- ~300 antennas over ~200 km<sup>2</sup>
- detection of cosmic rays and gamma rays

## GP300 simulations:

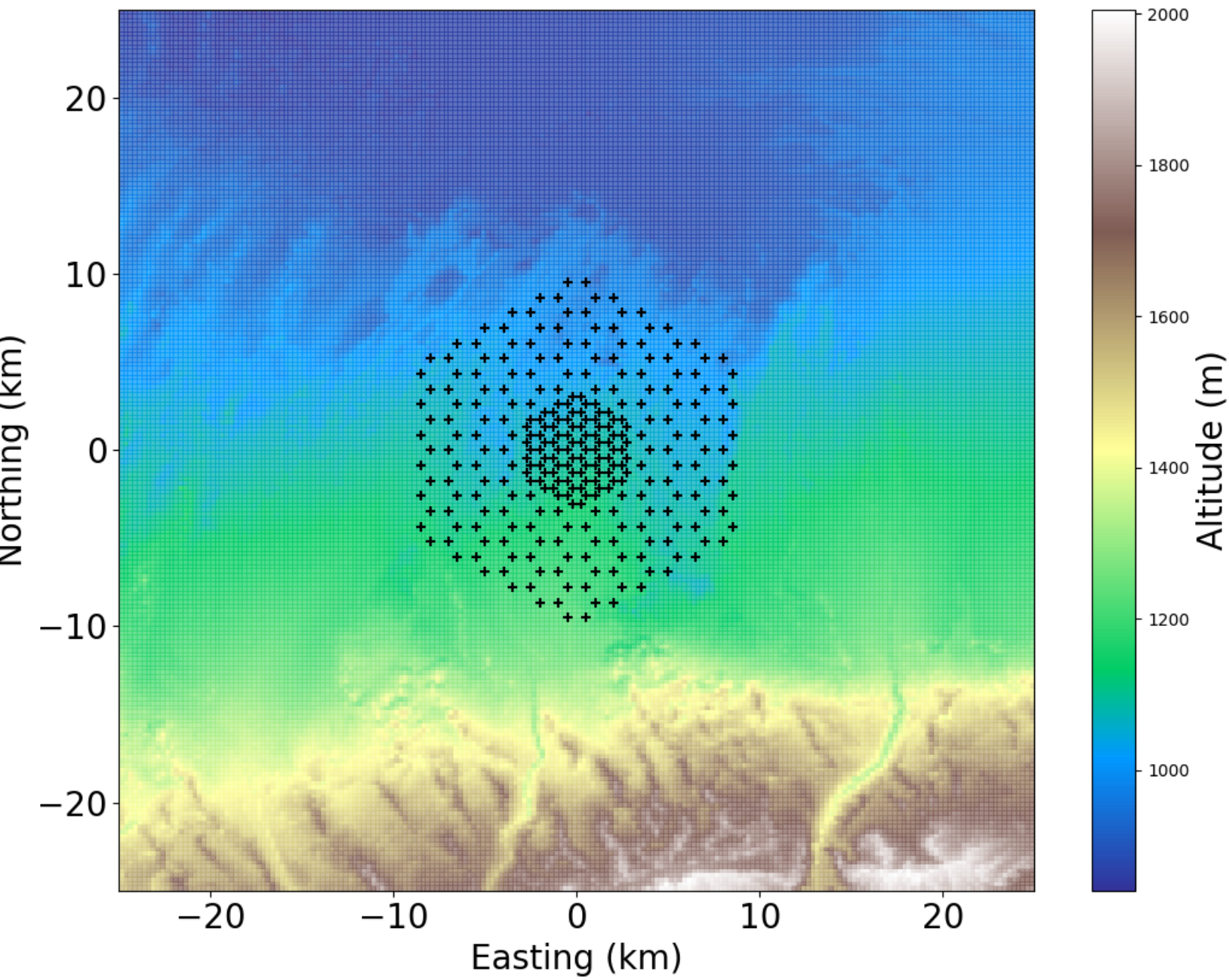
- real topography
- primaries: proton, iron and gamma





# Reconstruction performances for GRANDProto300 (GP300)

The 300 antennas GRAND prototype

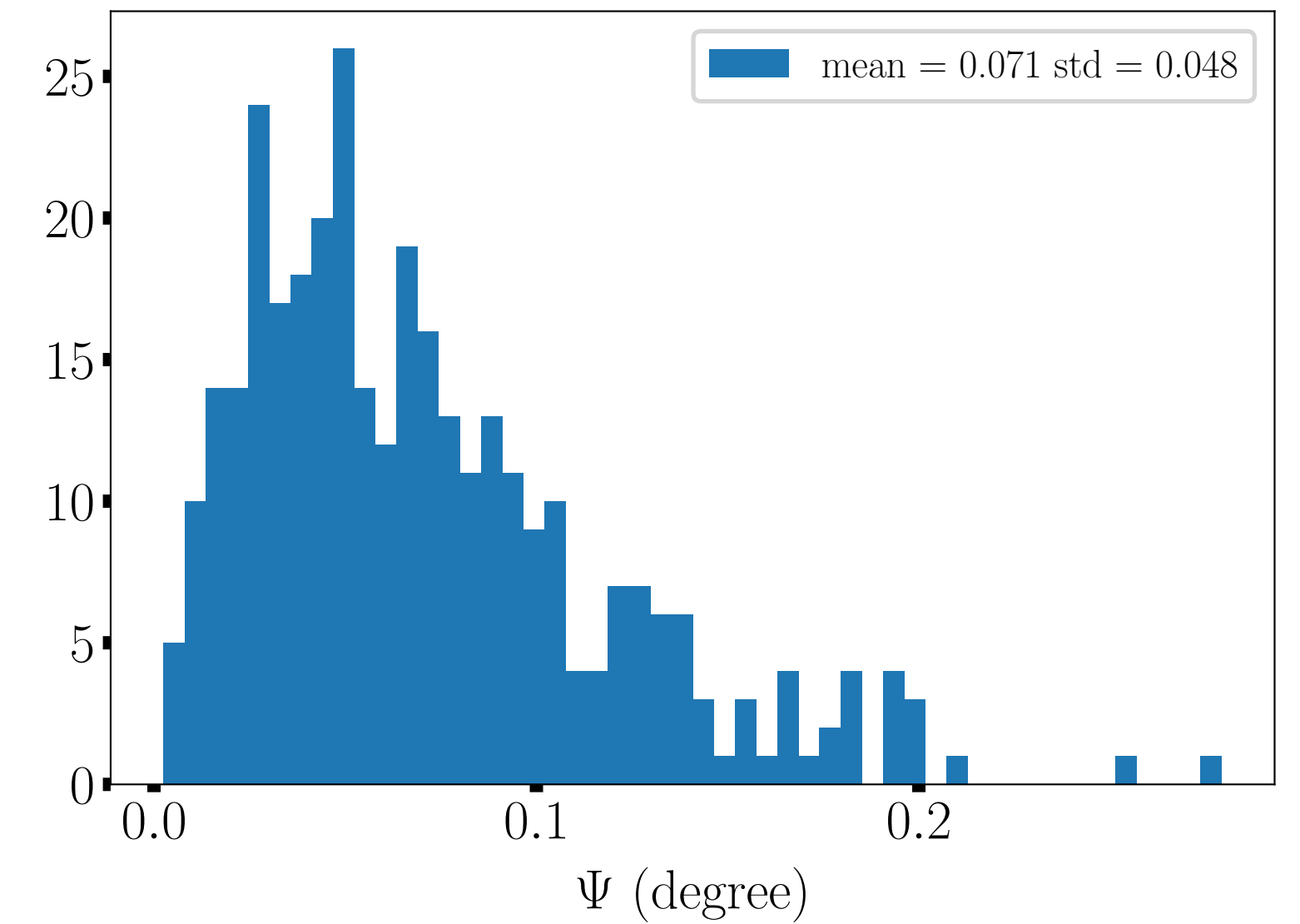
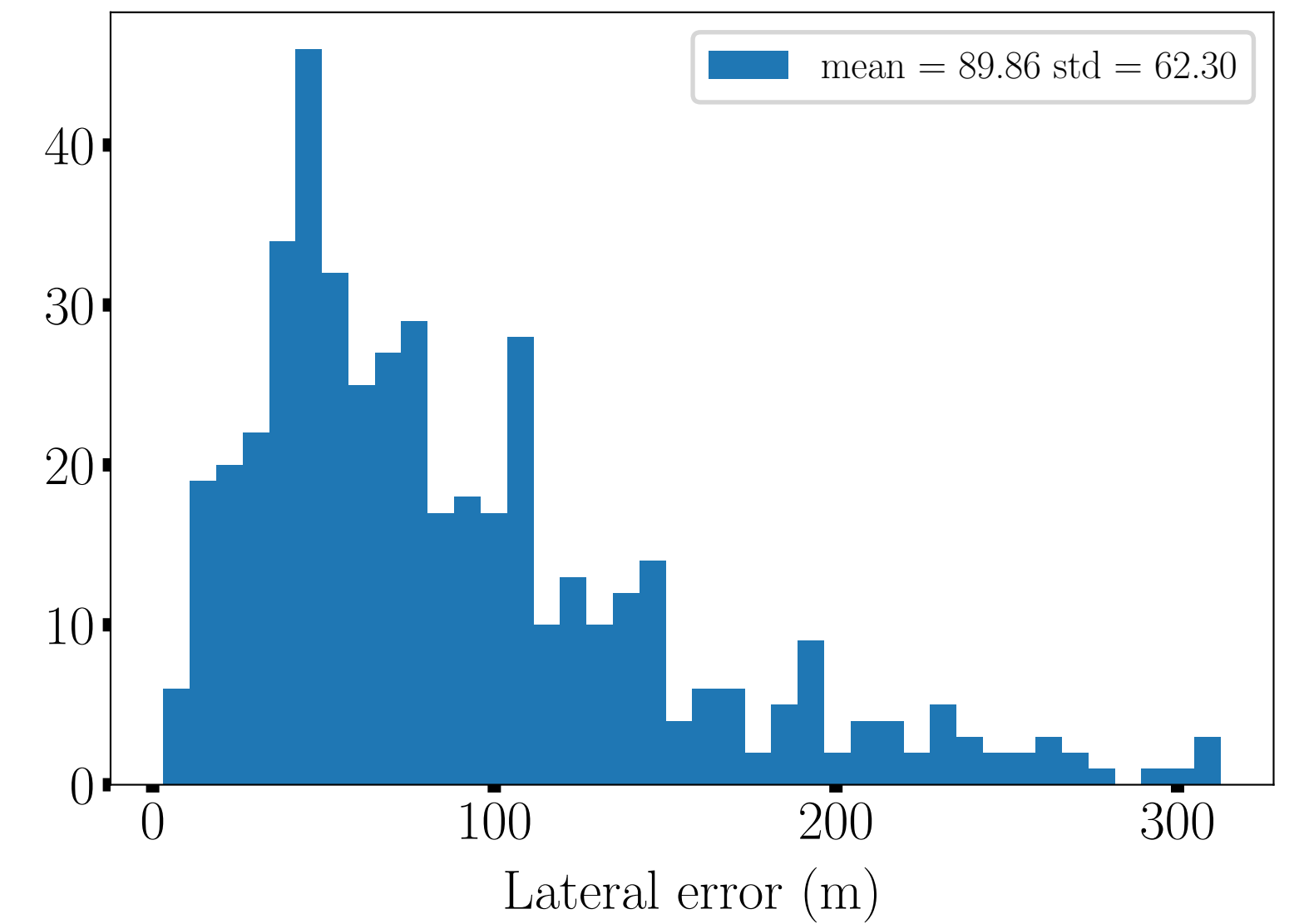
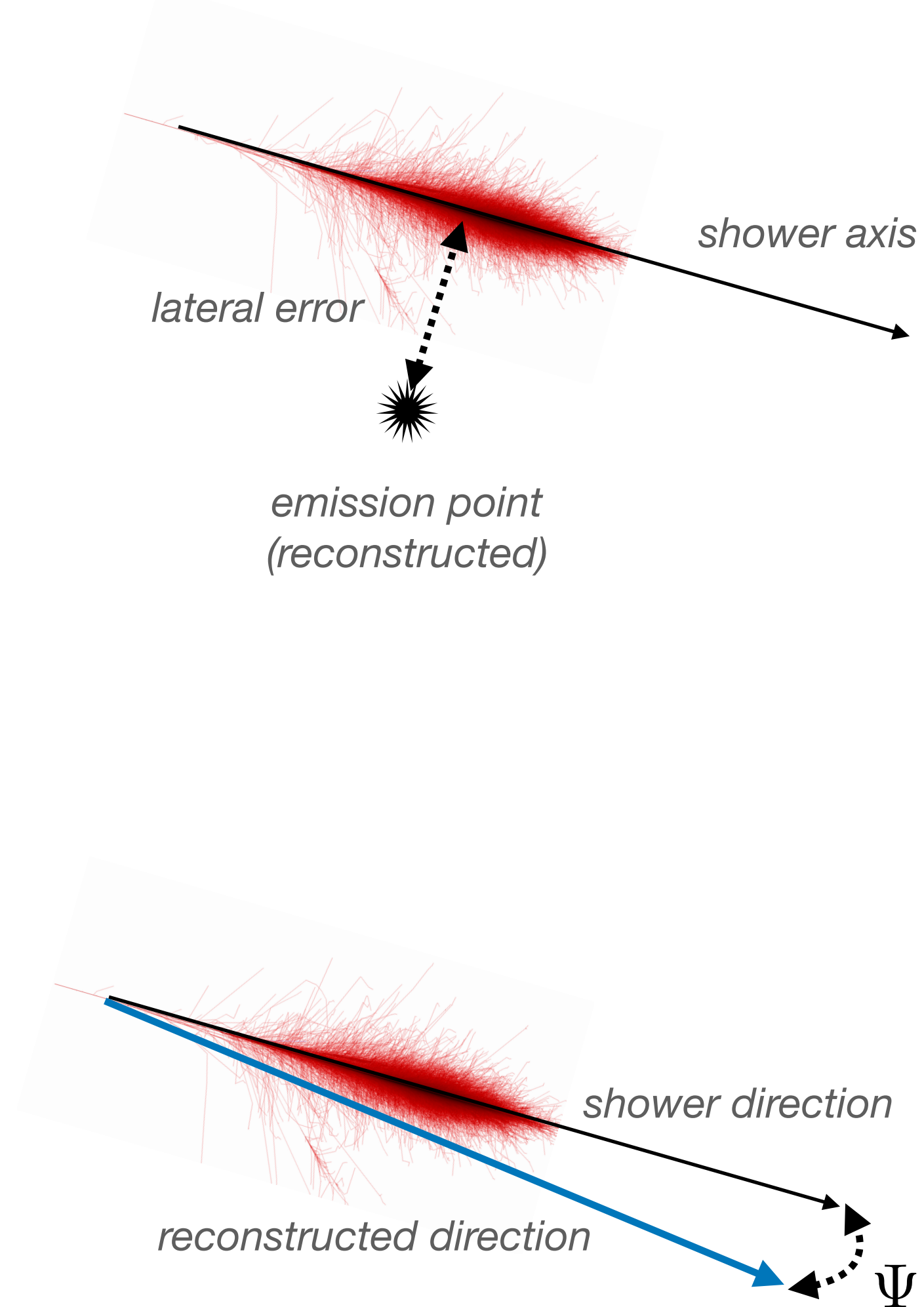


## GP300 layout:

- ~300 antennas over ~200 km<sup>2</sup>
- detection of cosmic rays and gamma rays

## GP300 simulations:

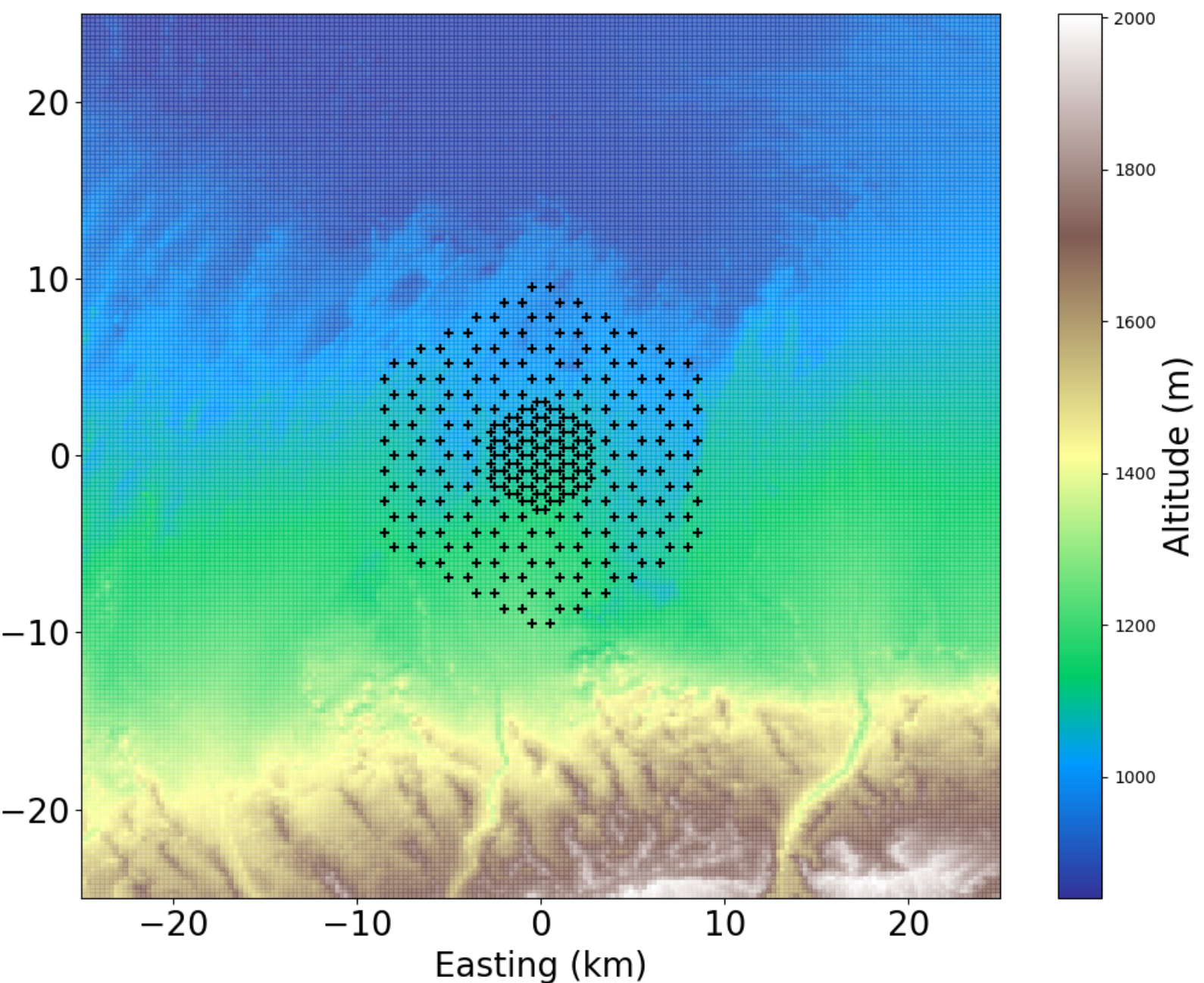
- real topography
- primaries: proton, iron and gamma





# Reconstruction performances for GRANDProto300 (GP300)

The 300 antennas GRAND prototype

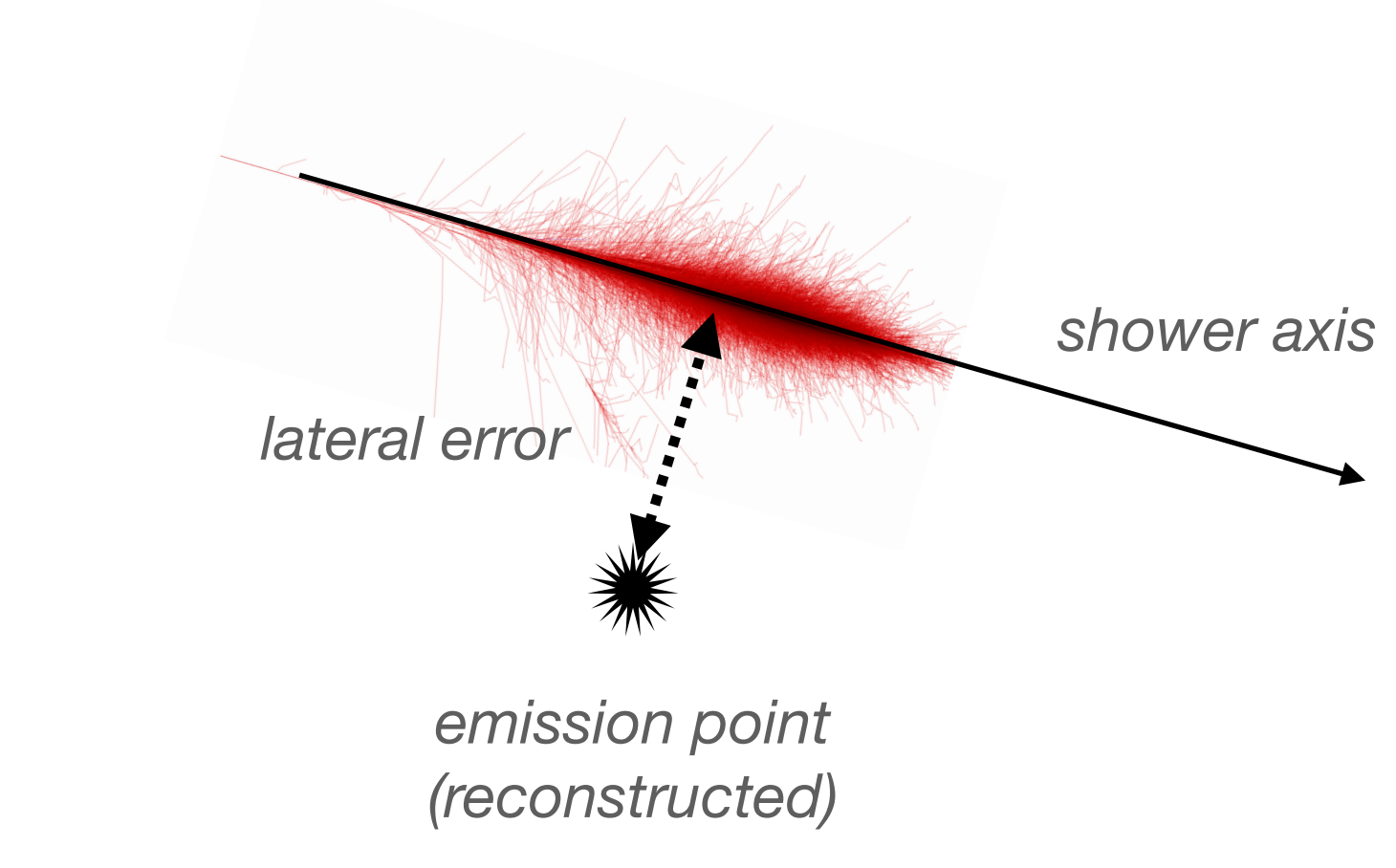


GP300 layout:

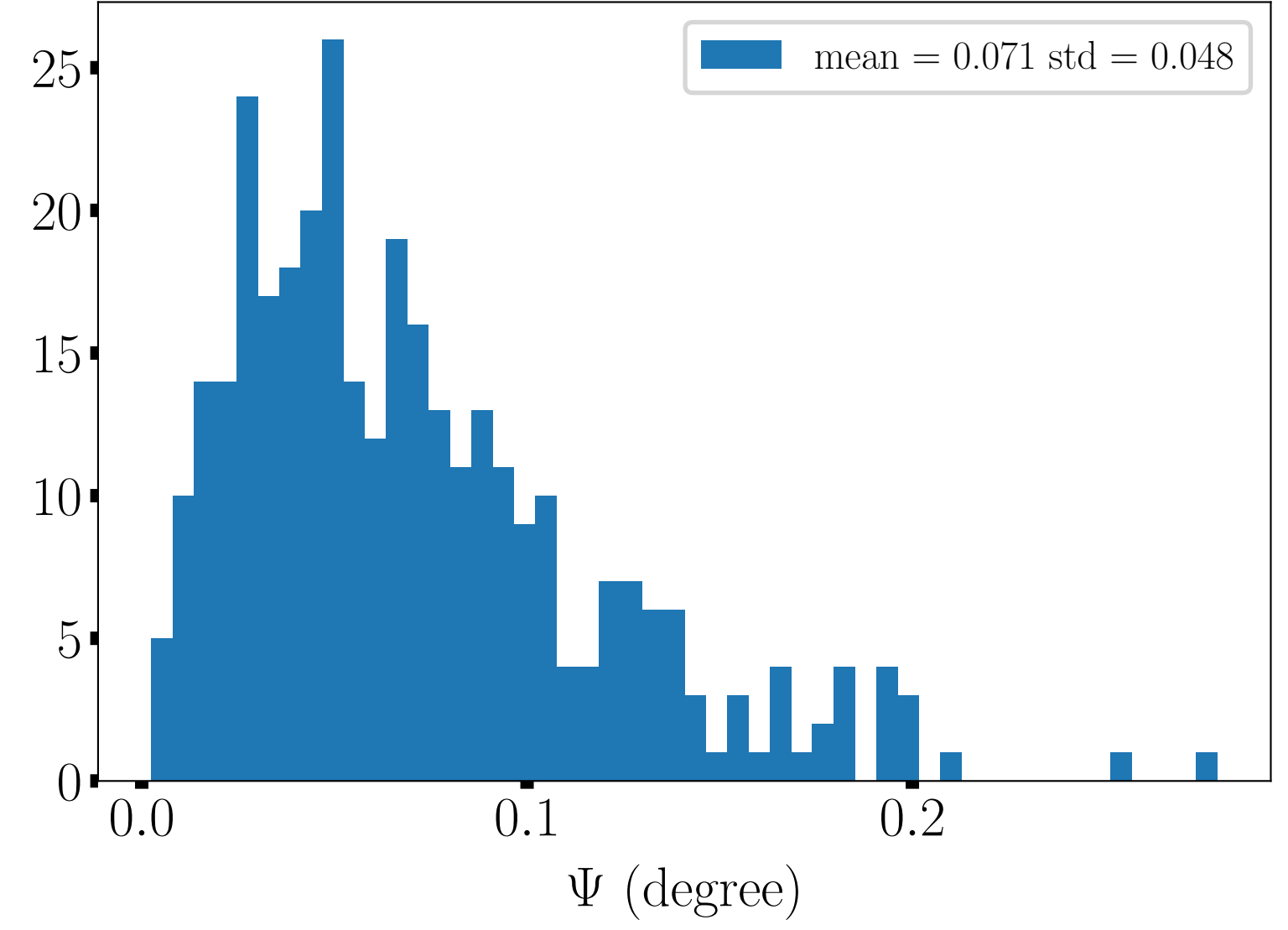
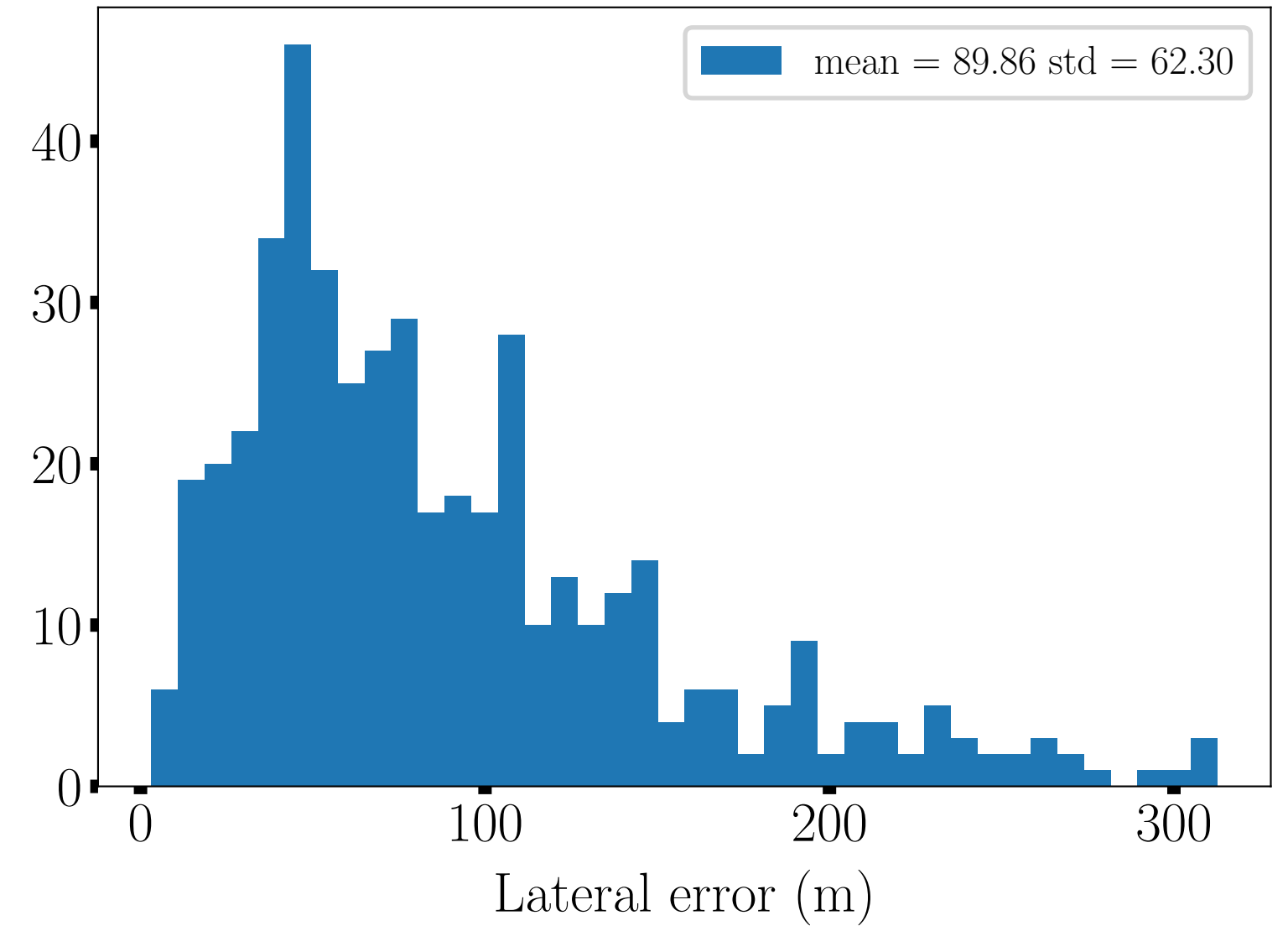
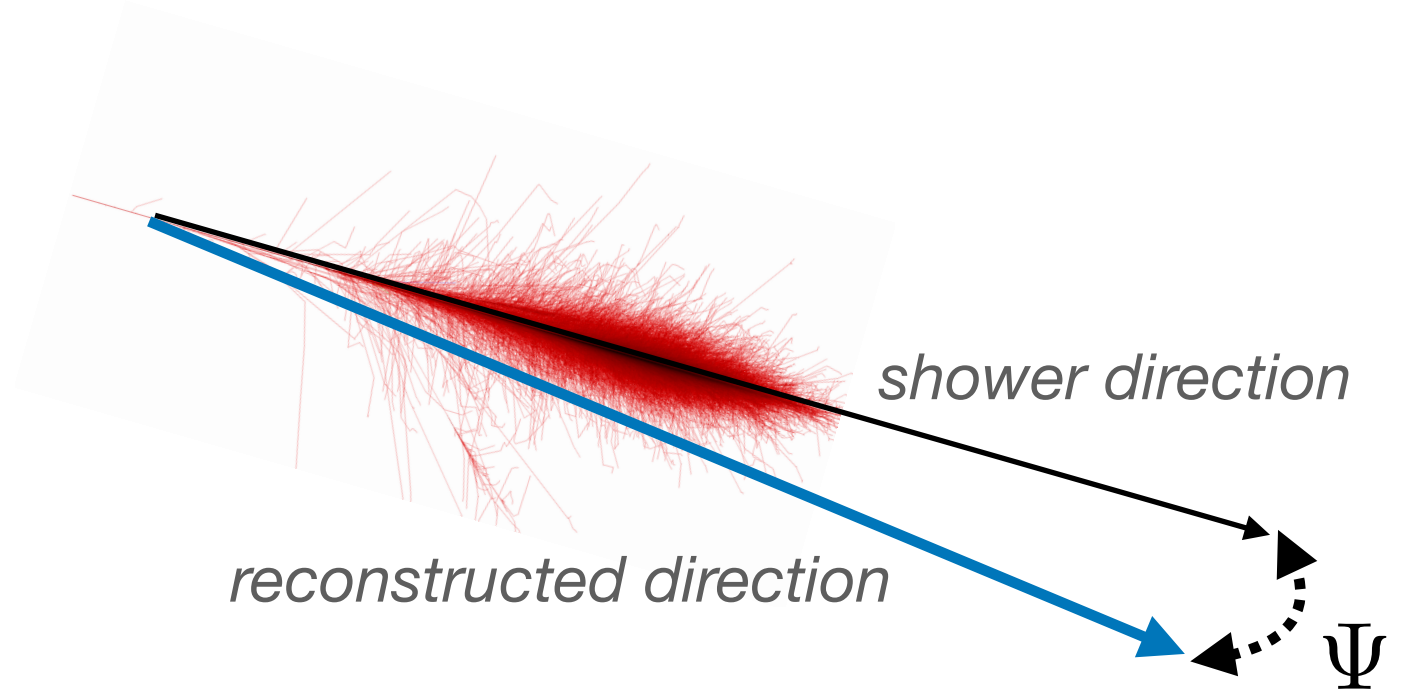
- ~300 antennas over ~200 km<sup>2</sup>
- detection of cosmic rays and gamma rays

GP300 simulations:

- real topography
- primaries: proton, iron and gamma



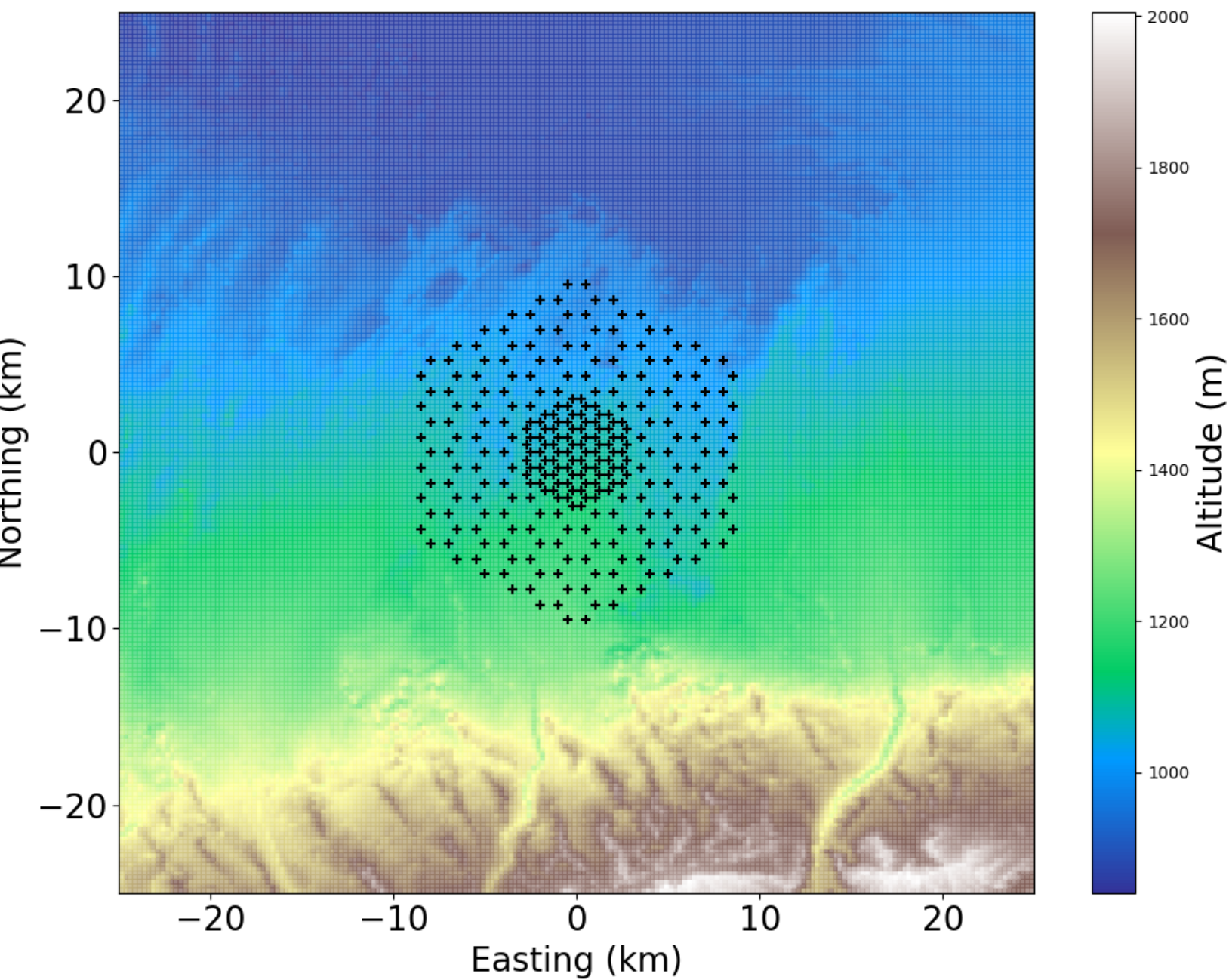
Constraint on the lateral position ~90 m  
Angular resolution ~0.07°





# Reconstruction performances for GRANDProto300 (GP300)

The 300 antennas GRAND prototype

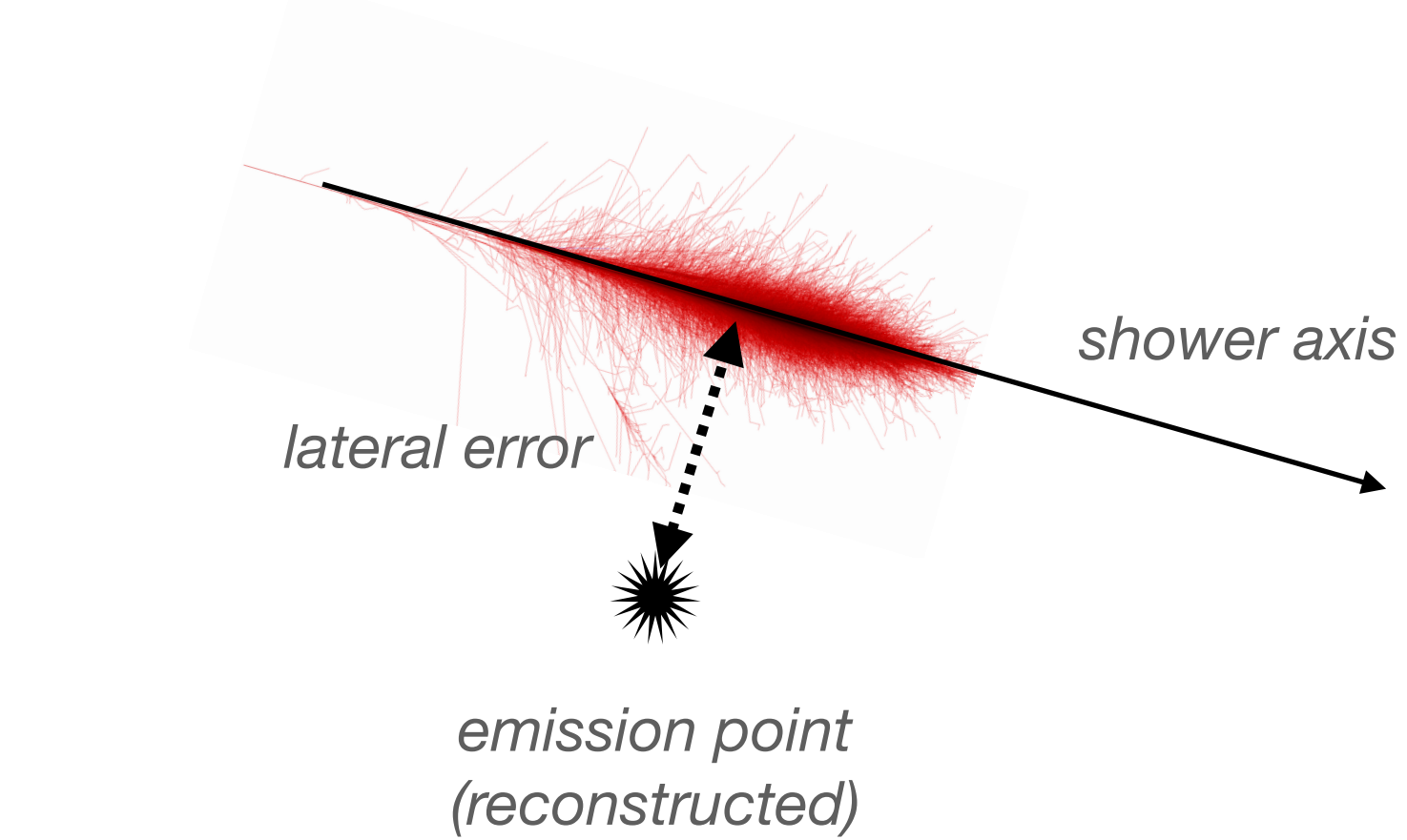


## GP300 layout:

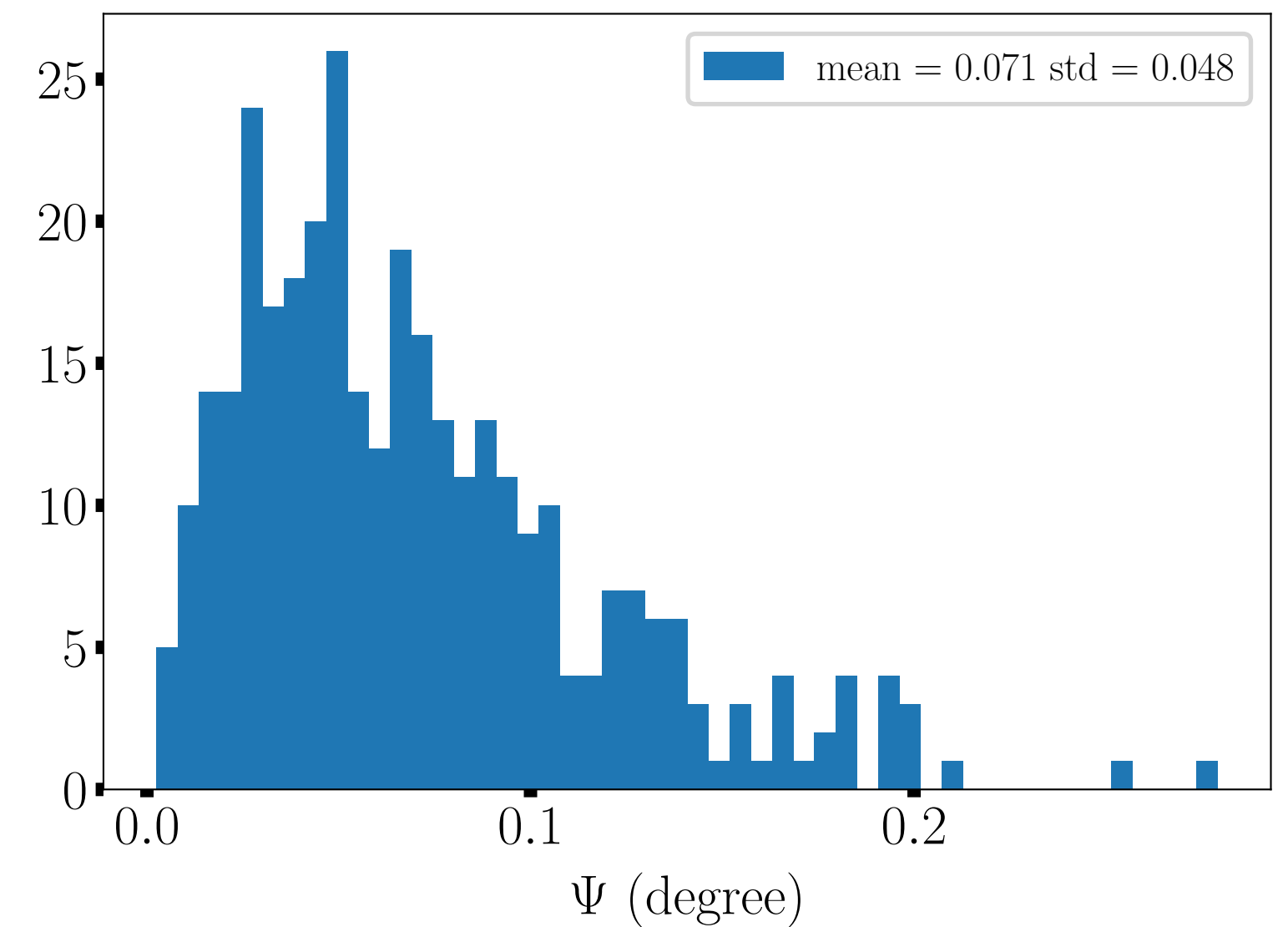
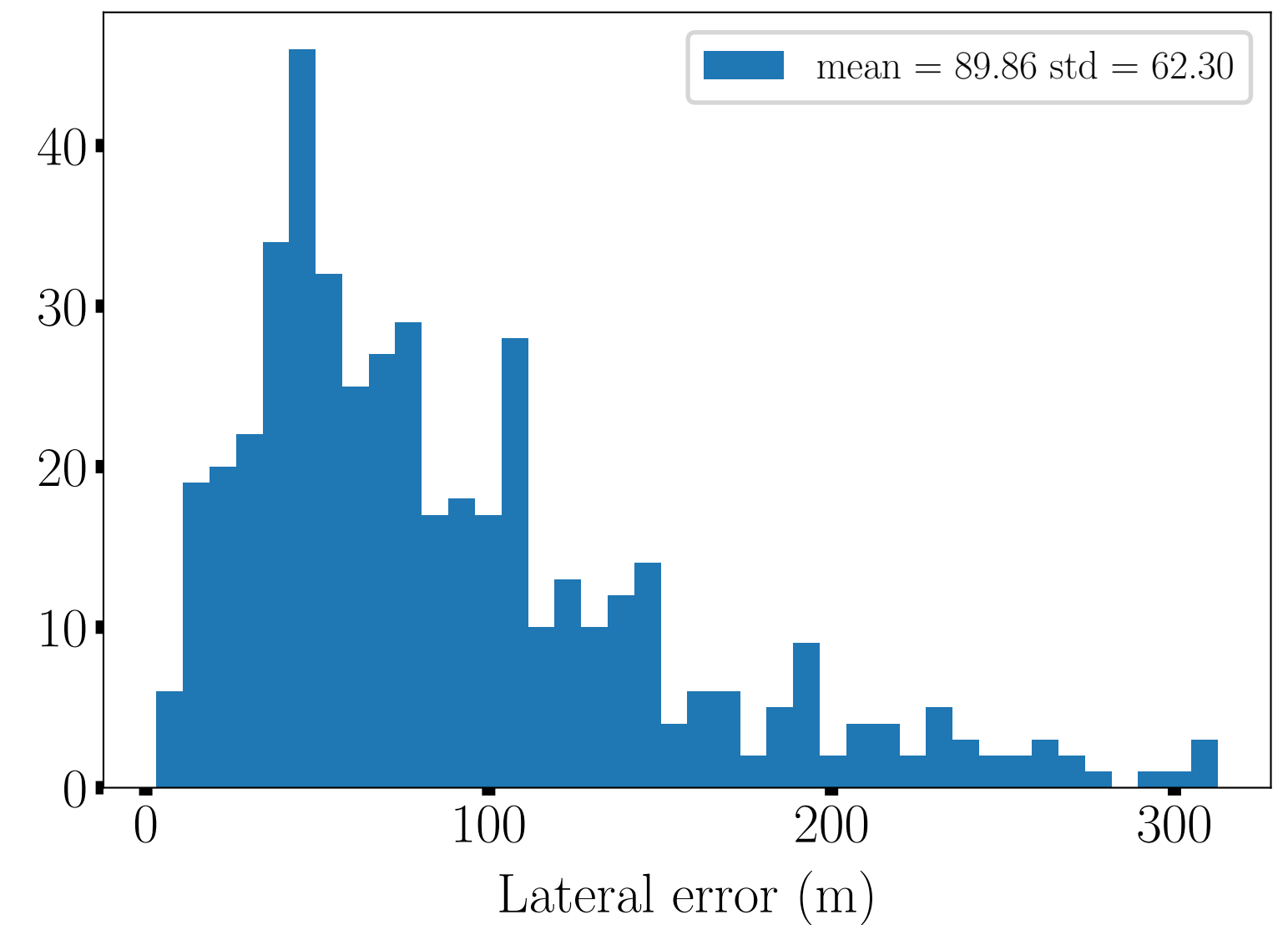
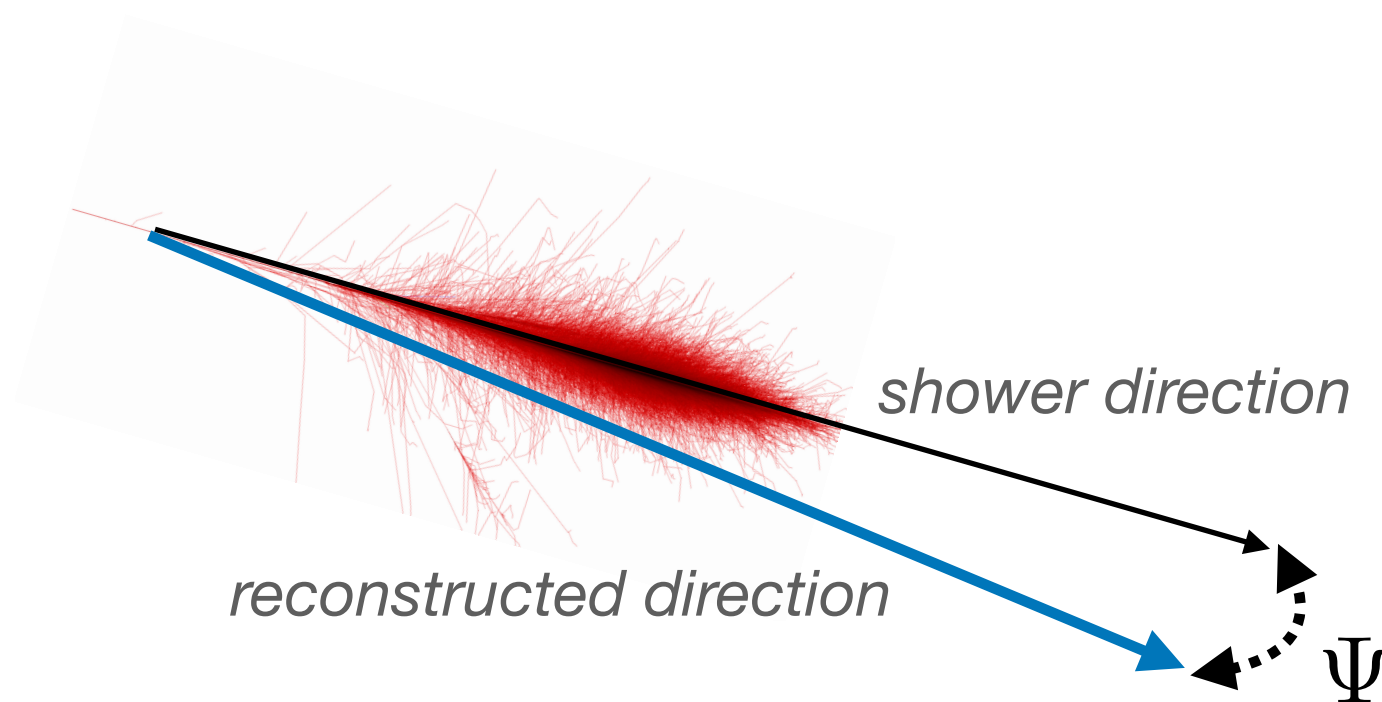
- ~300 antennas over ~200 km<sup>2</sup>
- detection of cosmic rays and gamma rays

## GP300 simulations:

- real topography
- primaries: proton, iron and gamma



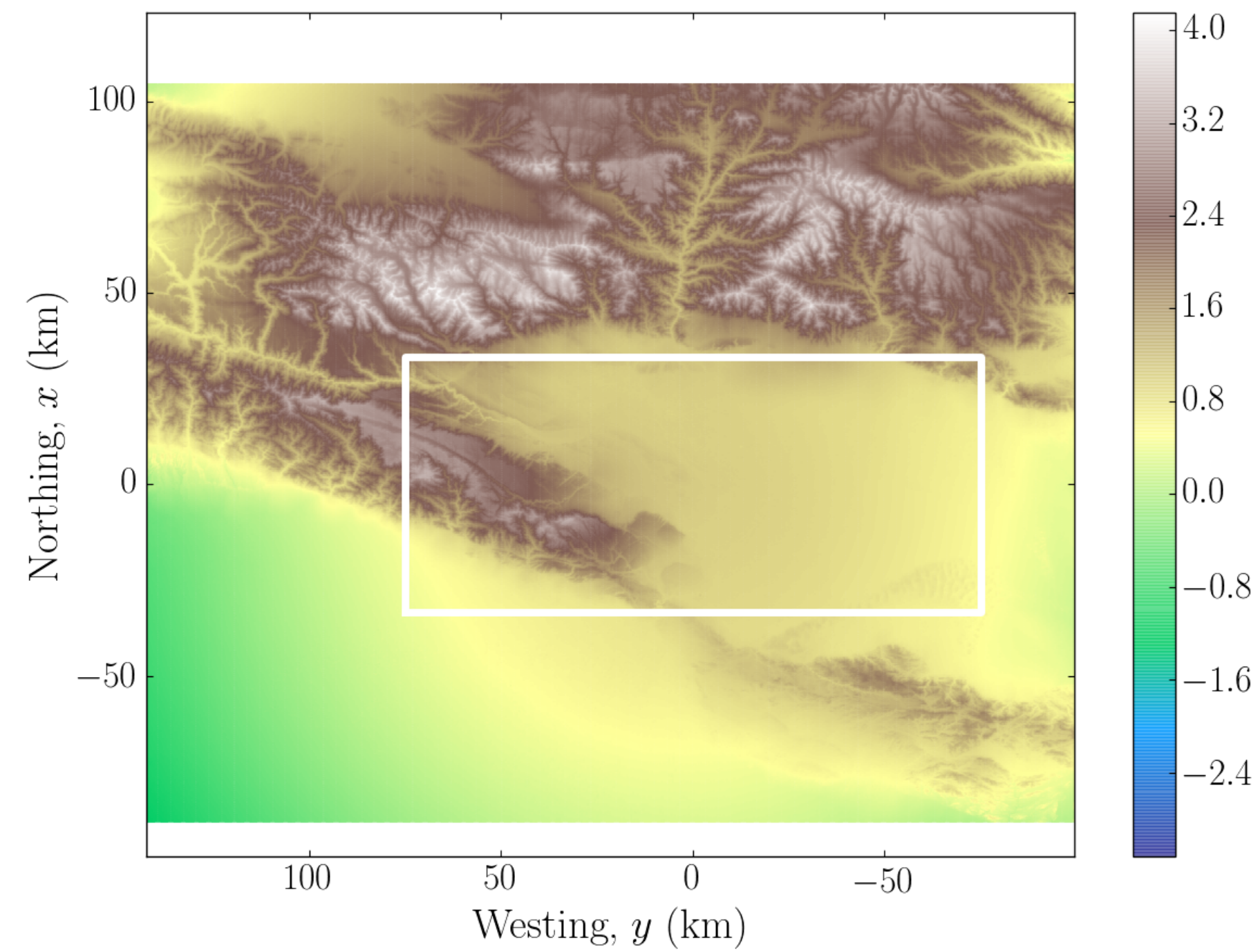
Constraint on the lateral position ~90 m  
Angular resolution ~0.07°



The arrival direction can be reconstructed on average below 0.1°  
and the emission point can be localised with precision

# Reconstruction performances for Hot Spot 1 (HS1)

HS1: a sensitivity principle study on a realistic topography of a sub-array



## HS1 layout:

- 10 000 antennas over a 10 000 km<sup>2</sup>
- square grid array with a 1 km spacing
- neutrino induced EAS from realistic isotropic flux

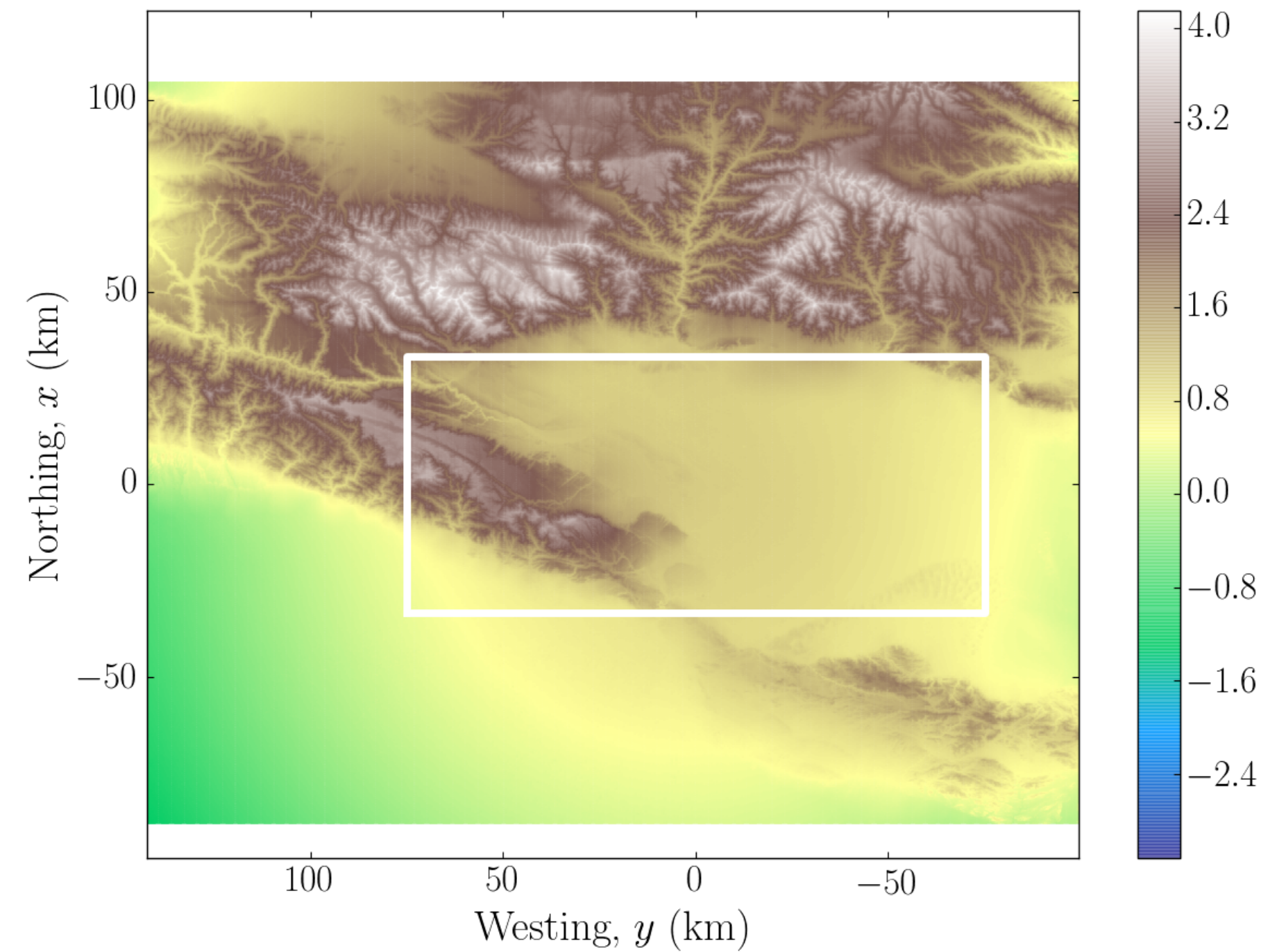
## HS1 simulations:

- real topography
- primaries: neutrino



# Reconstruction performances for Hot Spot 1 (HS1)

HS1: a sensitivity principle study on a realistic topography of a sub-array

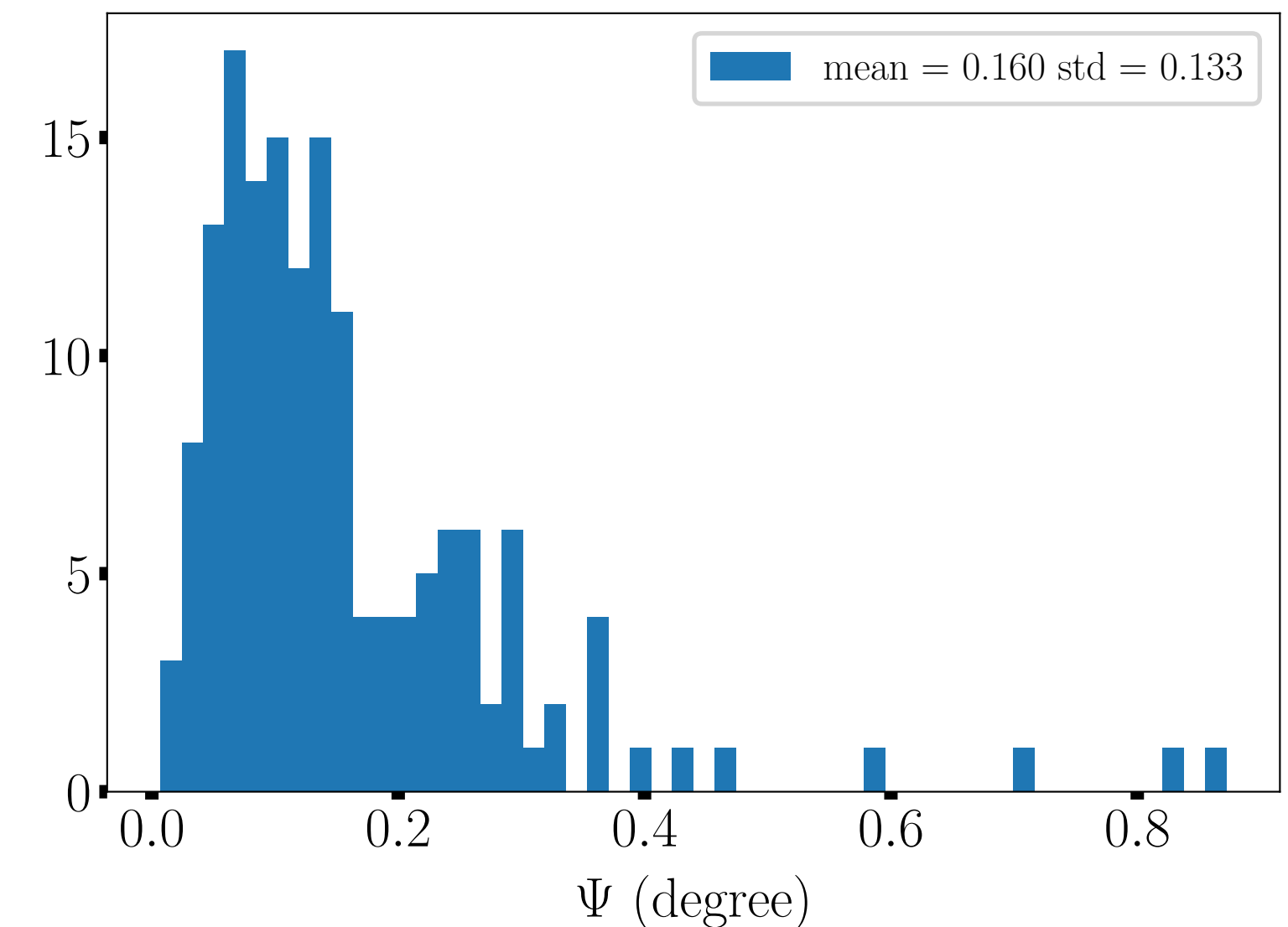
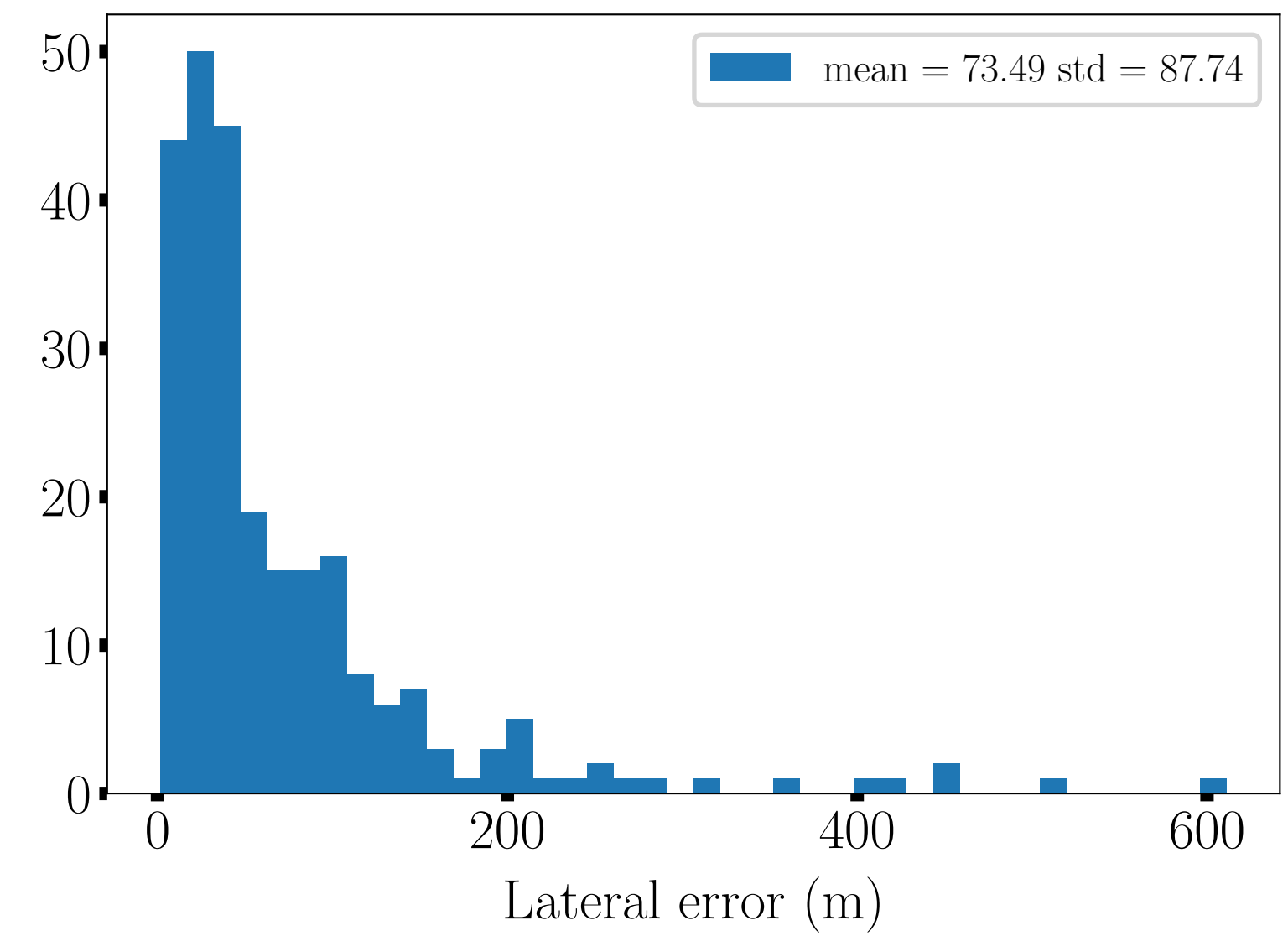
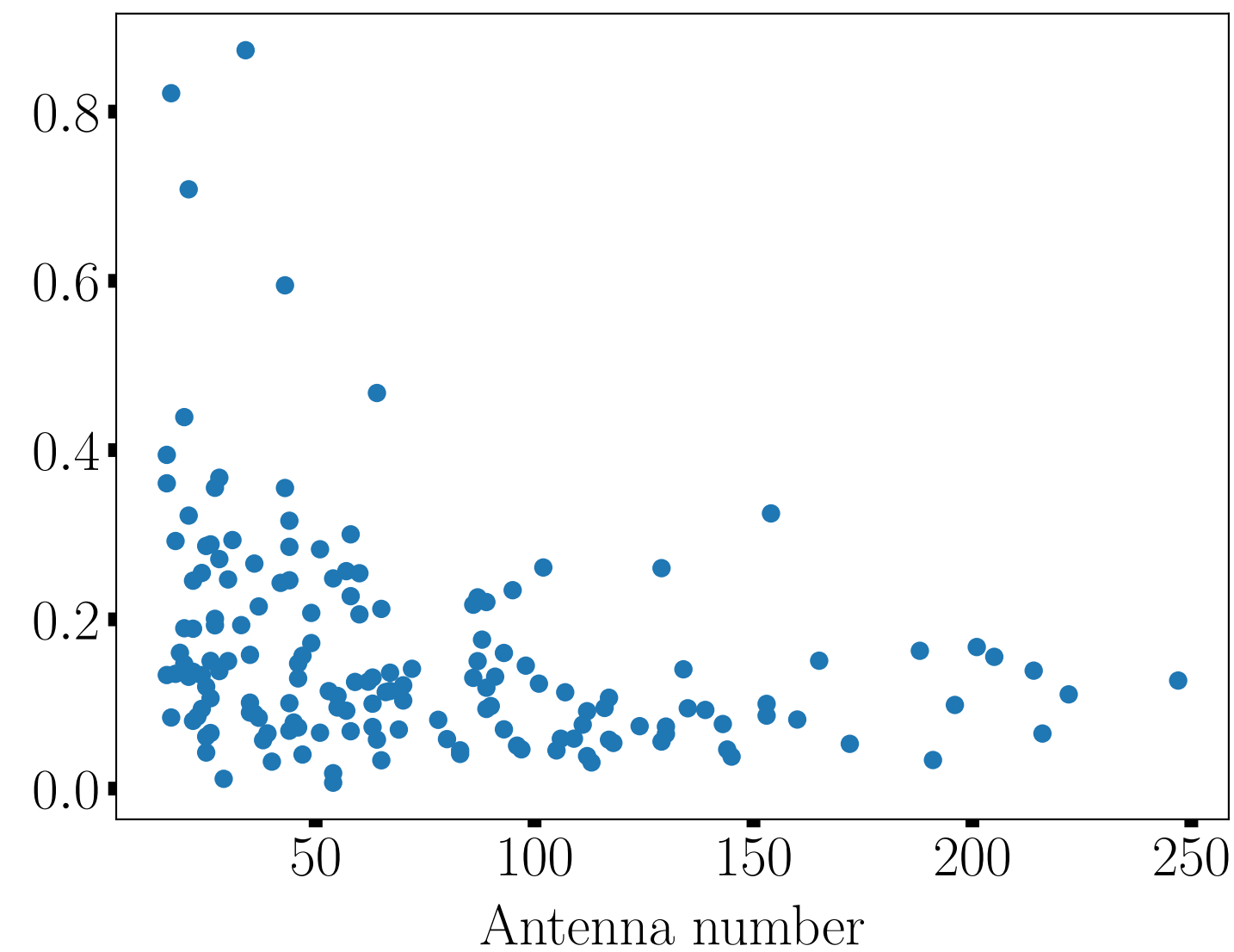


## HS1 layout:

- 10 000 antennas over a 10 000 km<sup>2</sup>
- square grid array with a 1 km spacing
- neutrino induced EAS from realistic isotropic flux

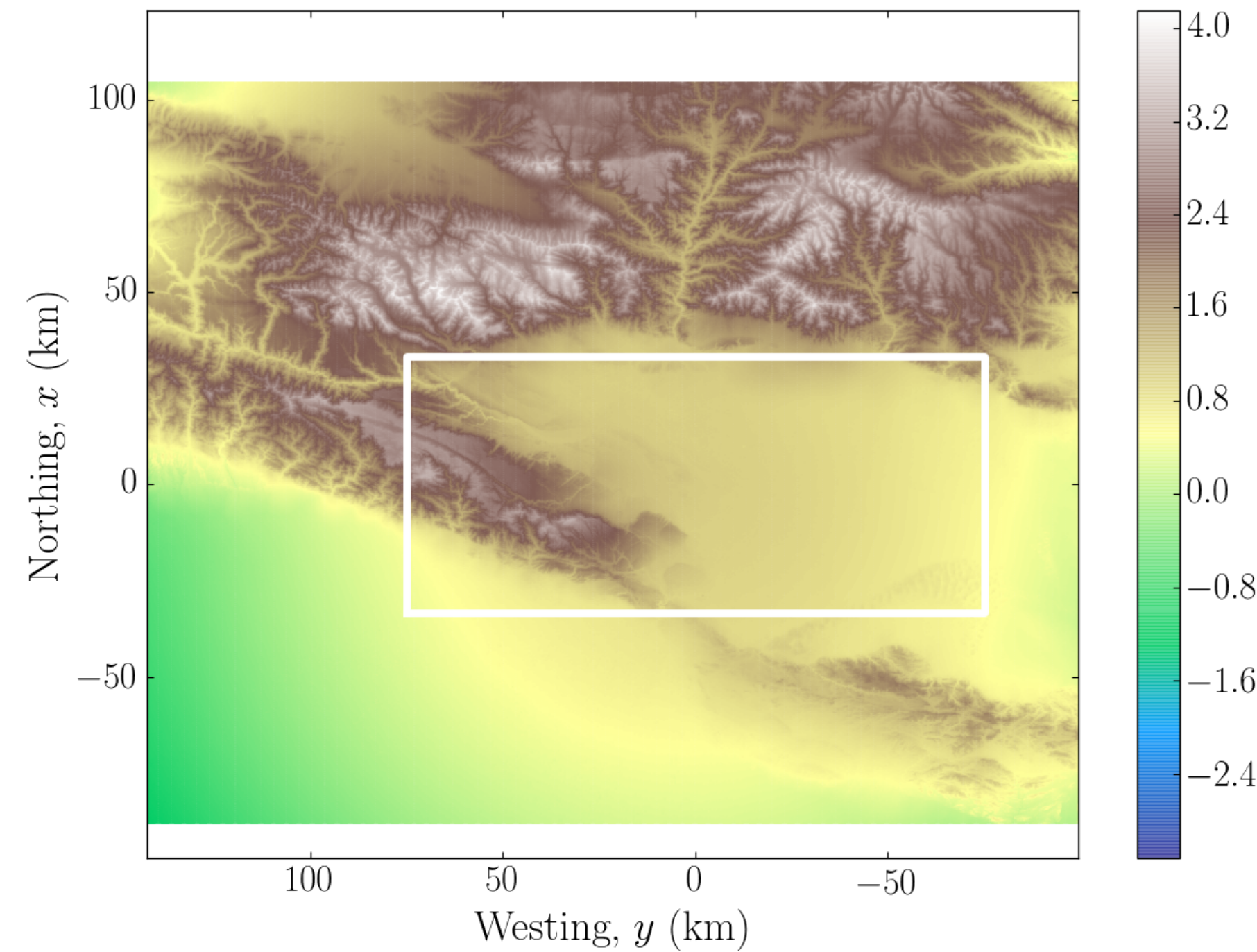
## HS1 simulations:

- real topography
- primaries: neutrino



# Reconstruction performances for Hot Spot 1 (HS1)

HS1: a sensitivity principle study on a realistic topography of a sub-array



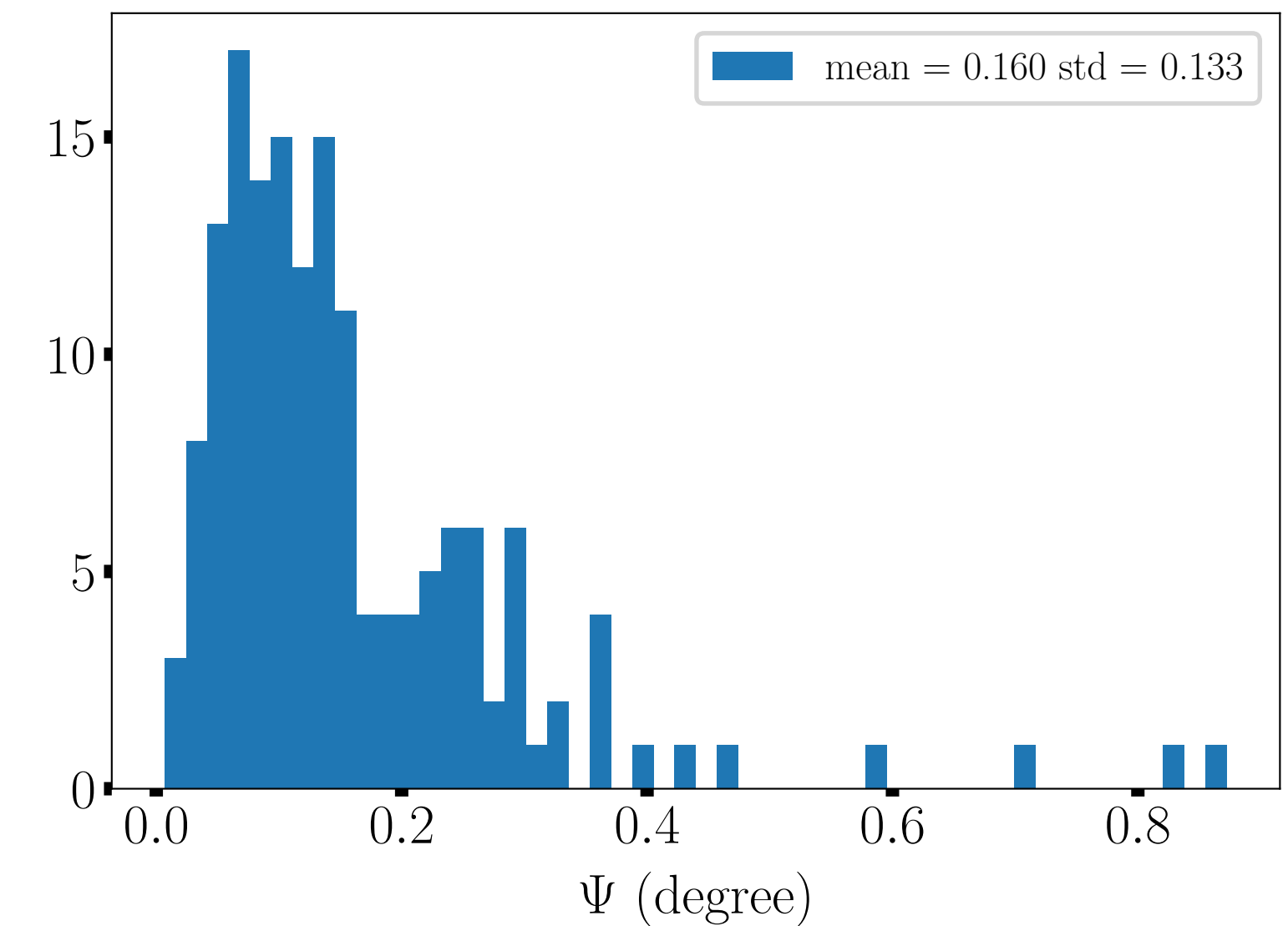
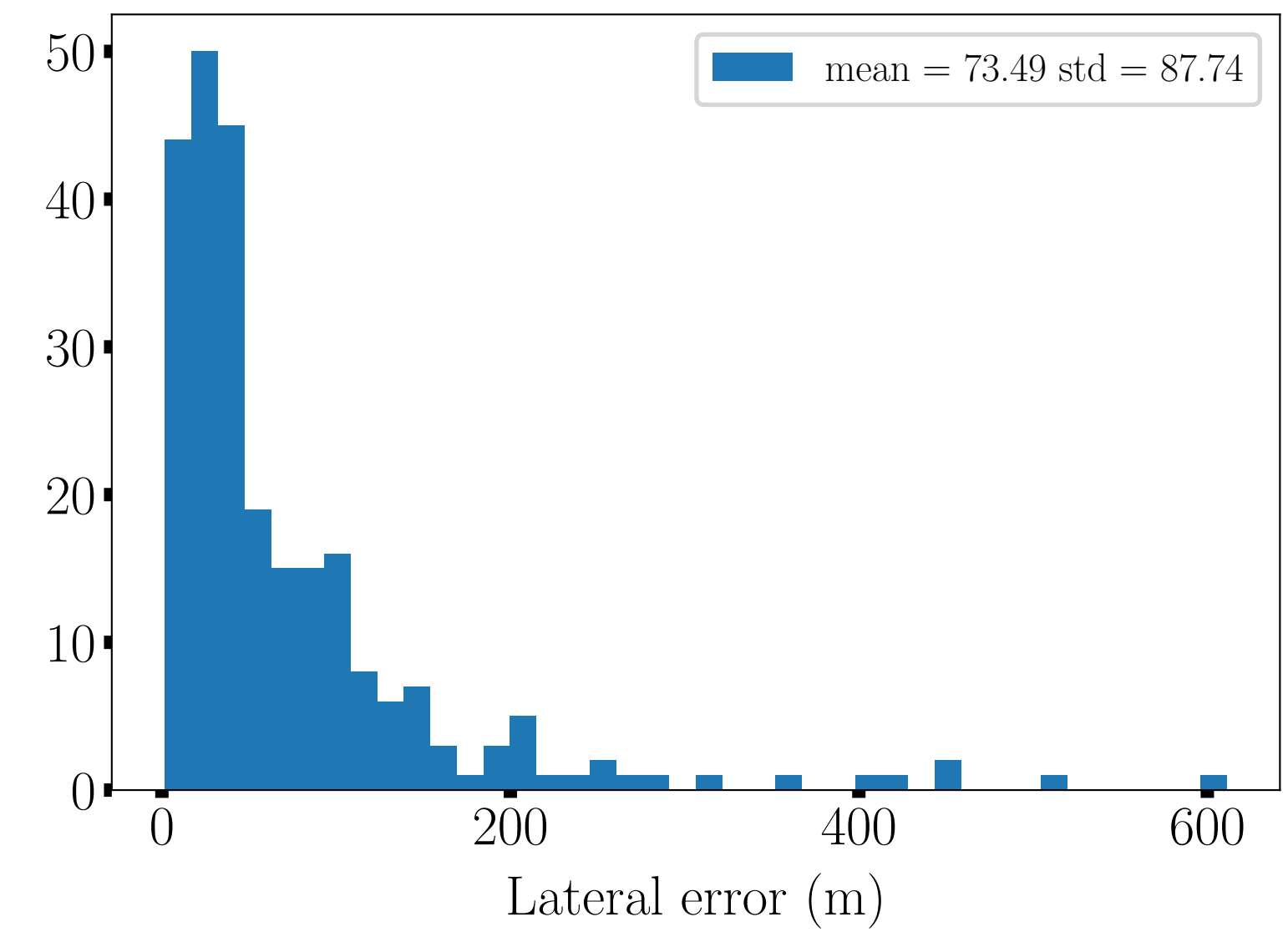
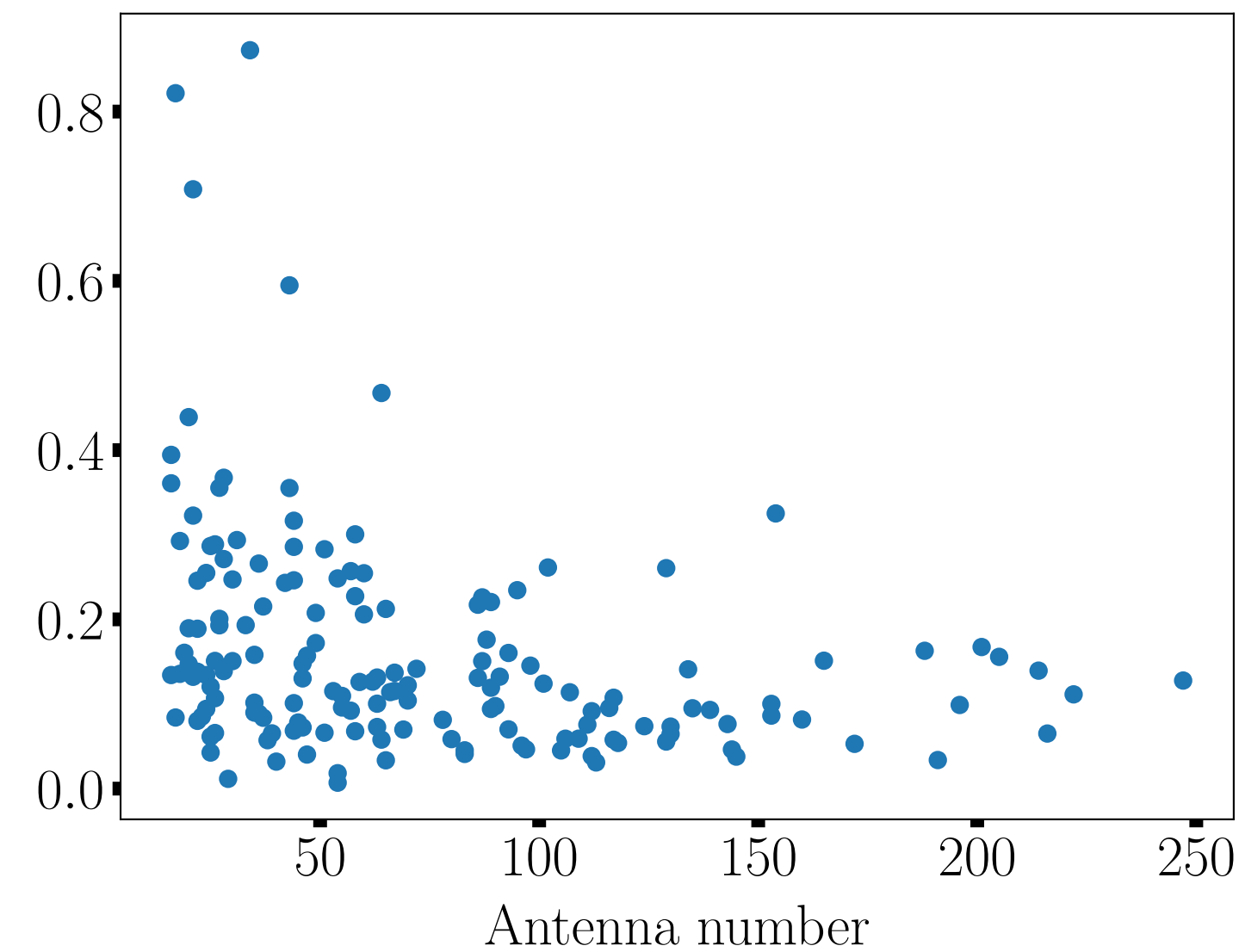
## HS1 layout:

- 10 000 antennas over a 10 000 km<sup>2</sup>
- square grid array with a 1 km spacing
- neutrino induced EAS from realistic isotropic flux

## HS1 simulations:

- real topography
- primaries: neutrino

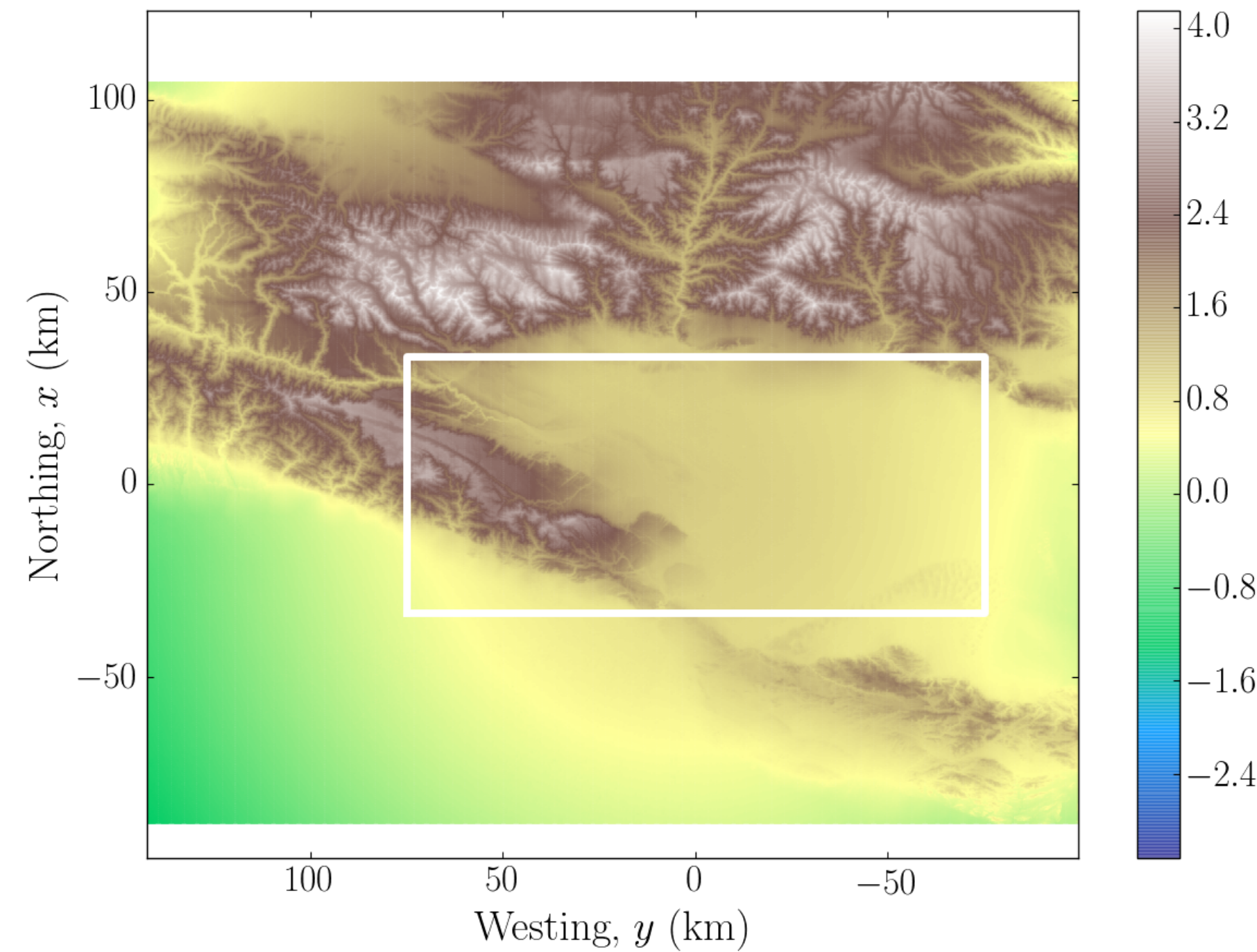
Constraint on the lateral position  $\sim 70$  m  
Angular resolution  $\sim 0.1^\circ$





# Reconstruction performances for Hot Spot 1 (HS1)

HS1: a sensitivity principle study on a realistic topography of a sub-array



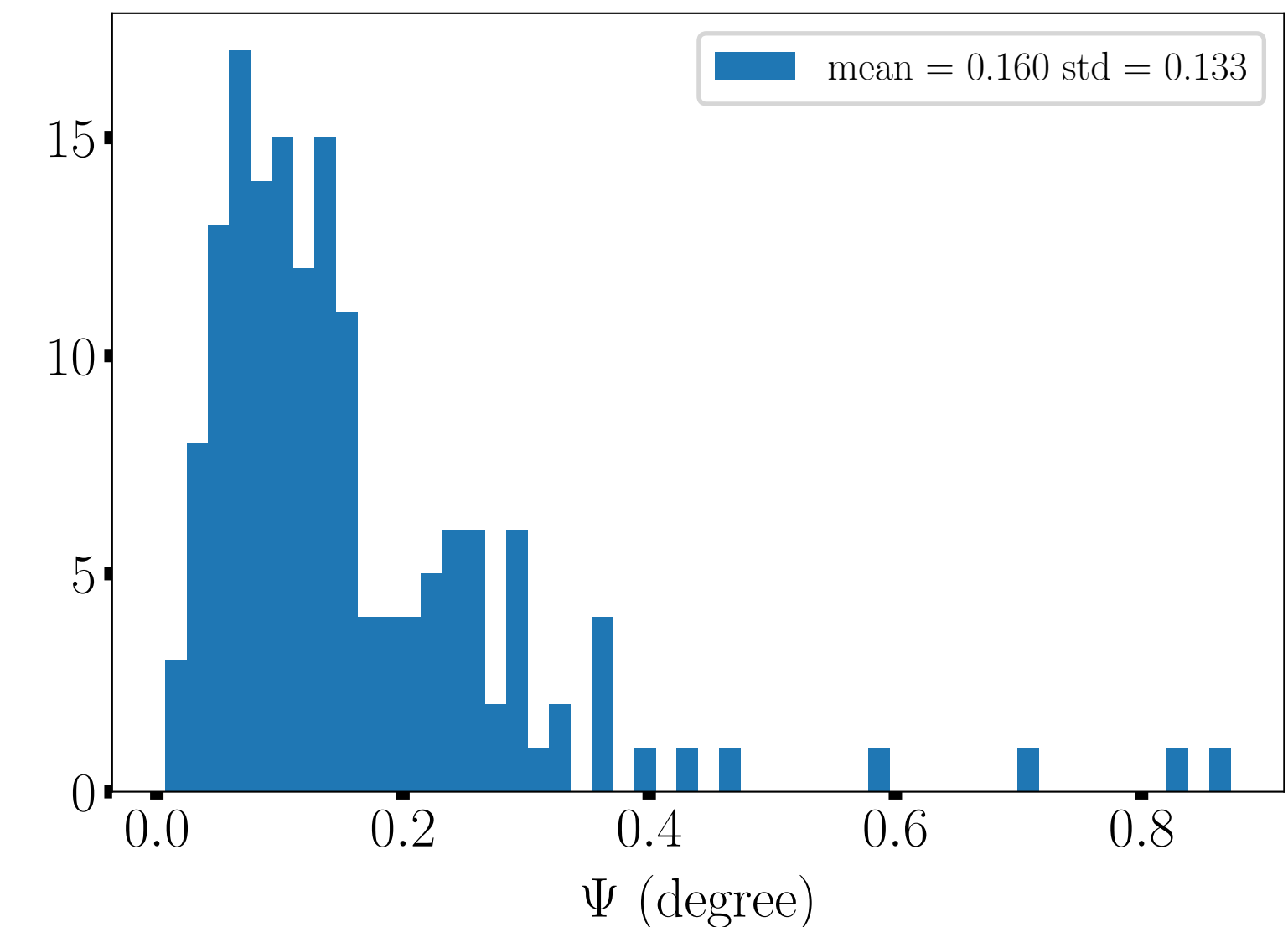
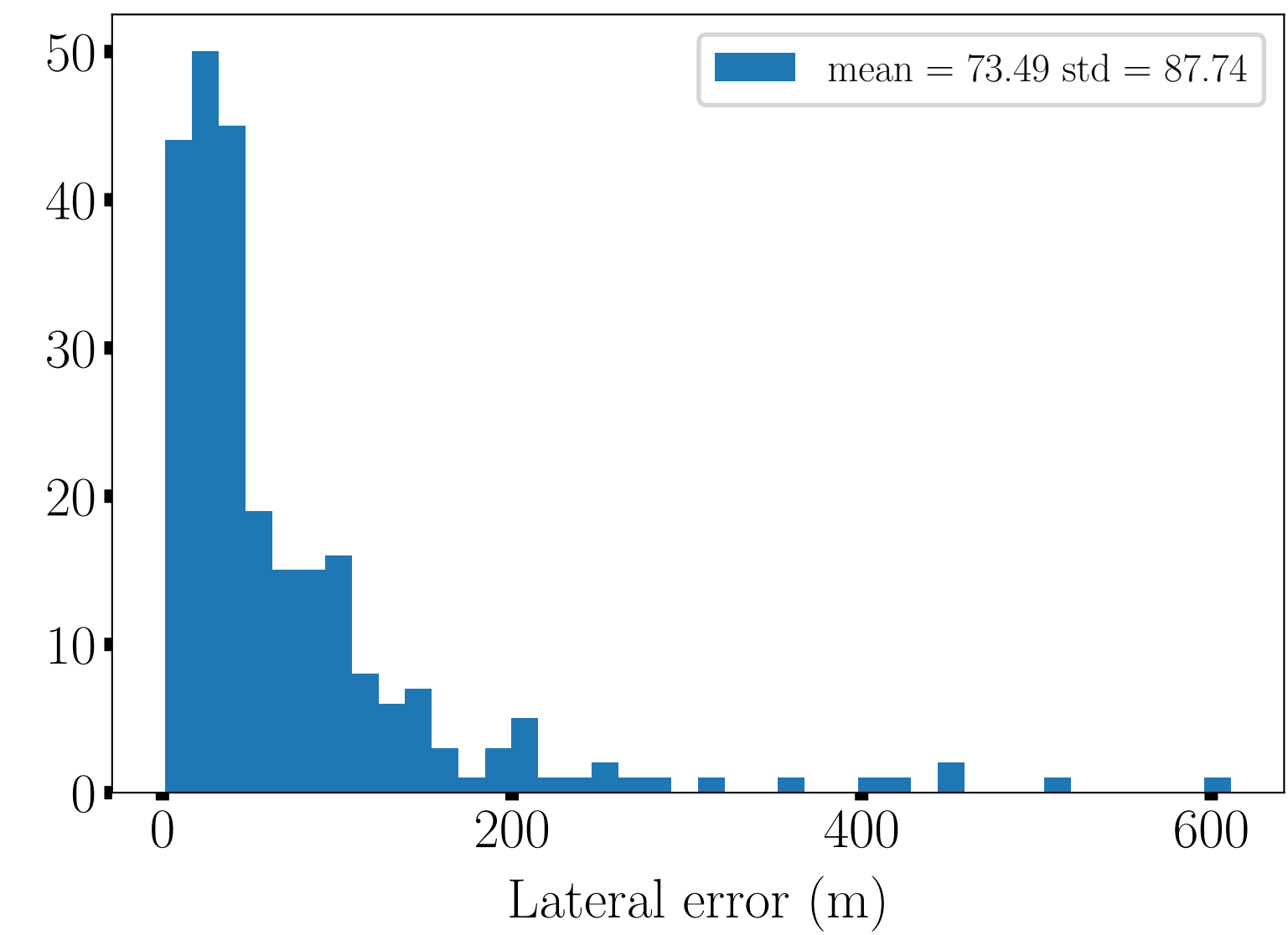
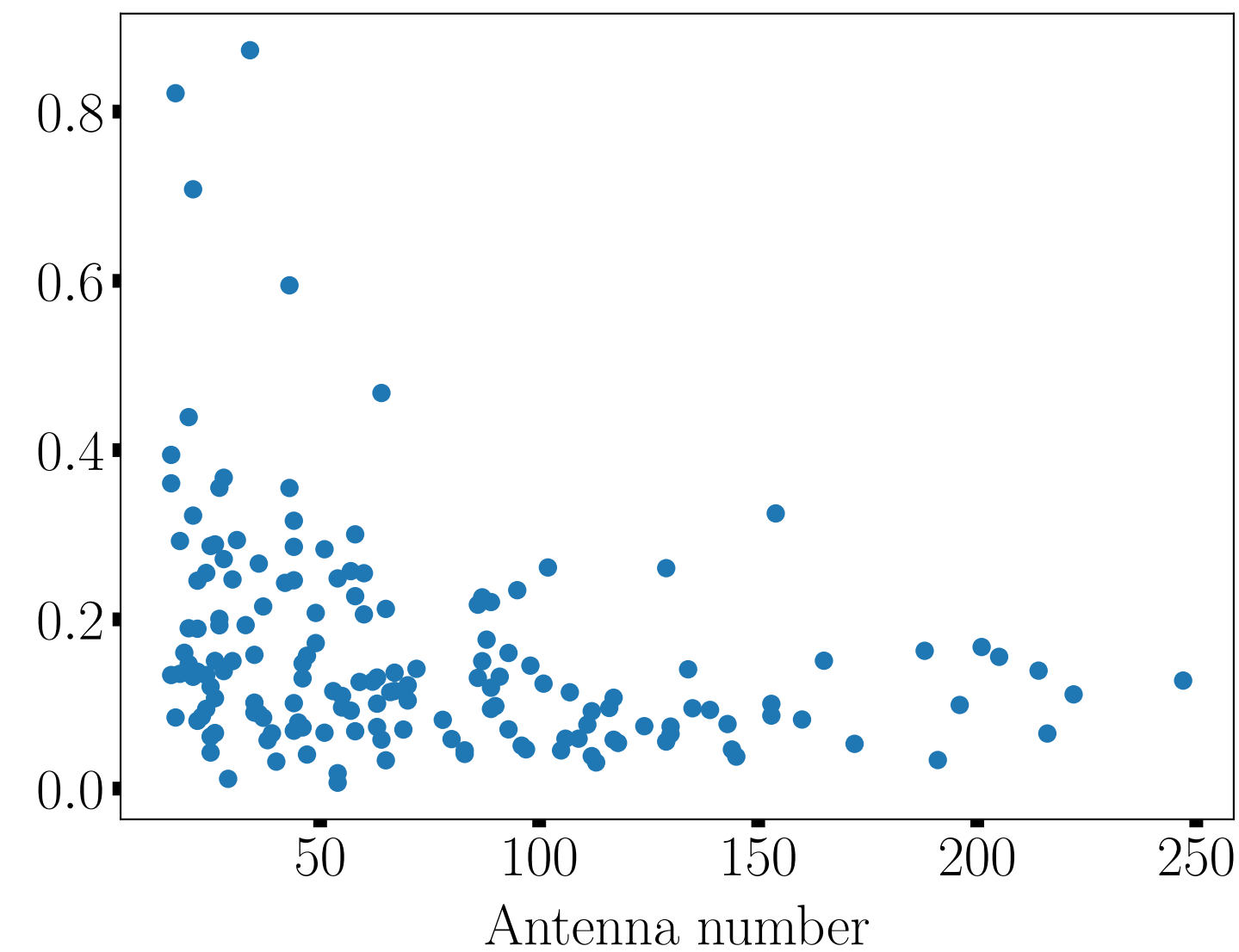
## HS1 layout:

- 10 000 antennas over a 10 000 km<sup>2</sup>
- square grid array with a 1 km spacing
- neutrino induced EAS from realistic isotropic flux

## HS1 simulations:

- real topography
- primaries: neutrino

Constraint on the lateral position  $\sim 70$  m  
Angular resolution  $\sim 0.1^\circ$

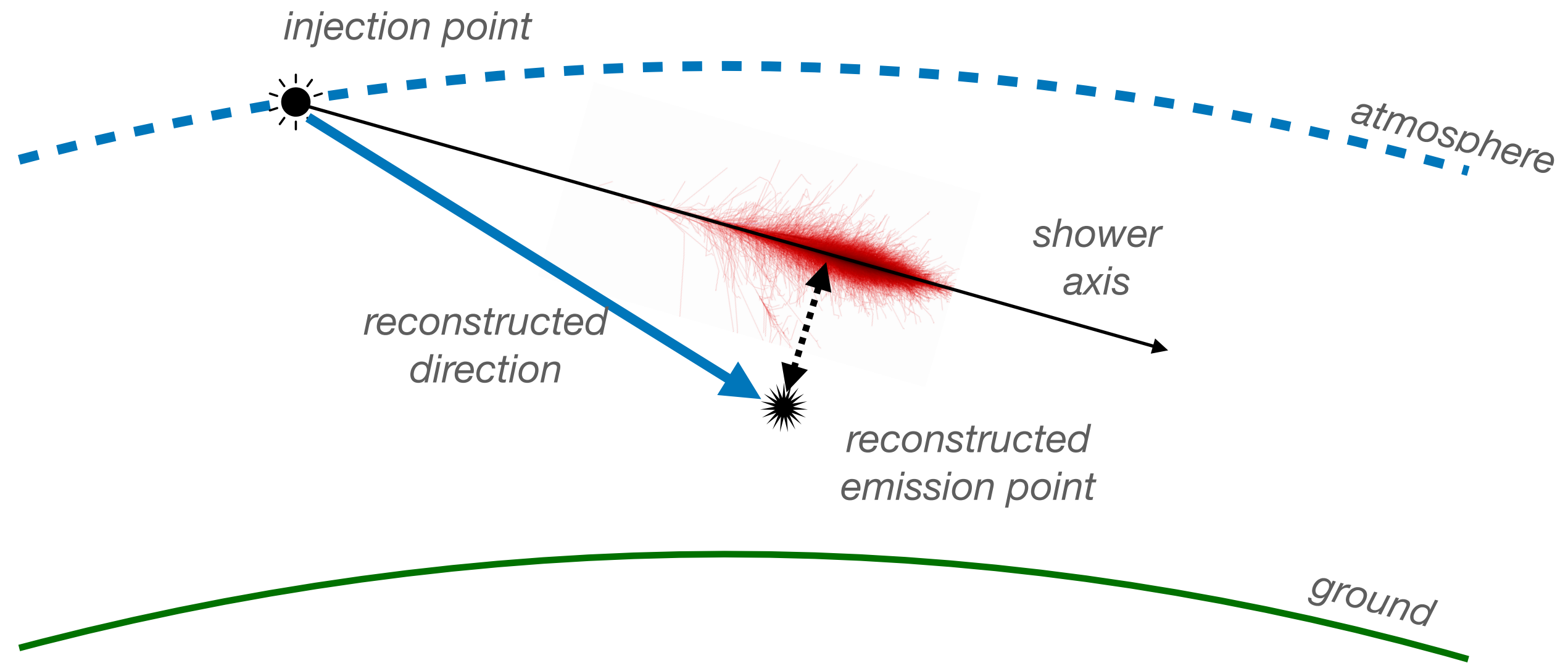


## Validation of the reconstruction for the neutrinos:

- source emission very well constrained
- arrival direction within the targeted goal of  $0.1^\circ$

# Constraining the composition?

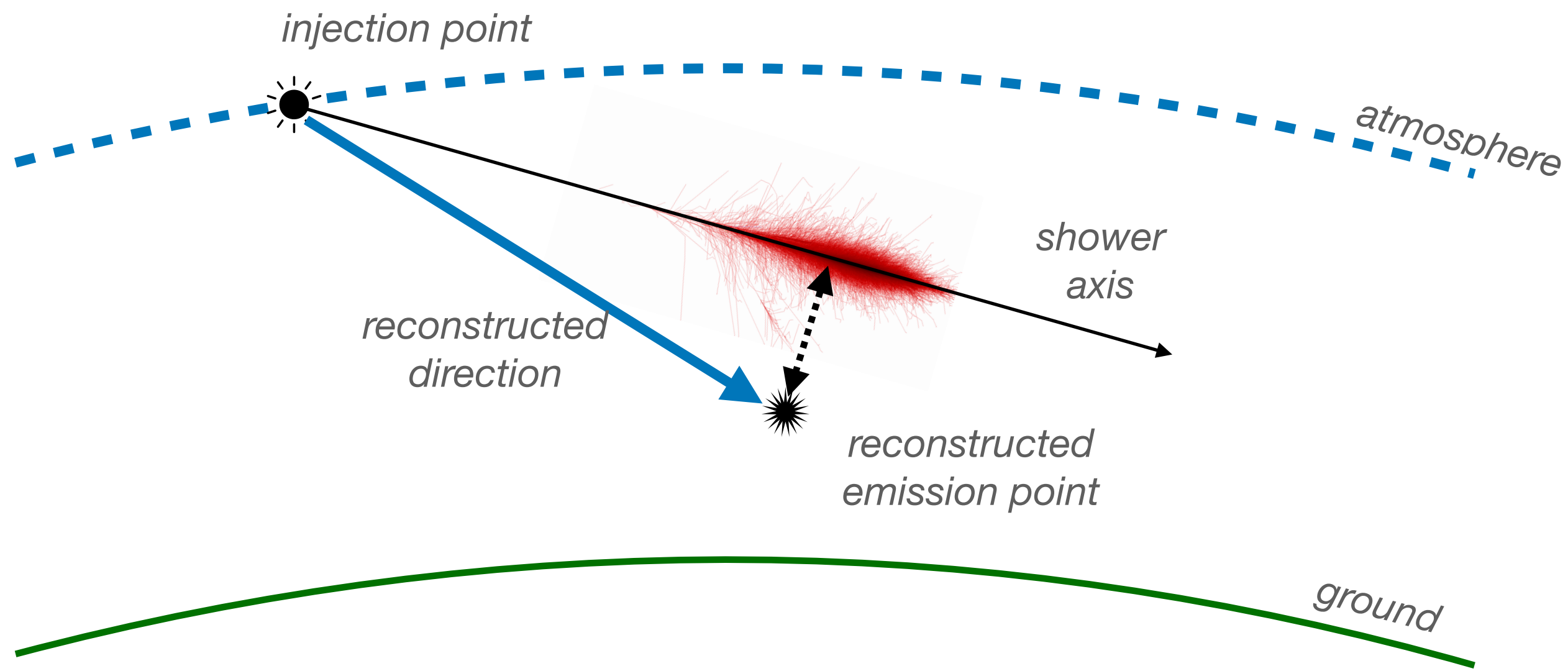
Indirectly we can compute:  
the atmosphere column density integral from injection to reconstructed emission point



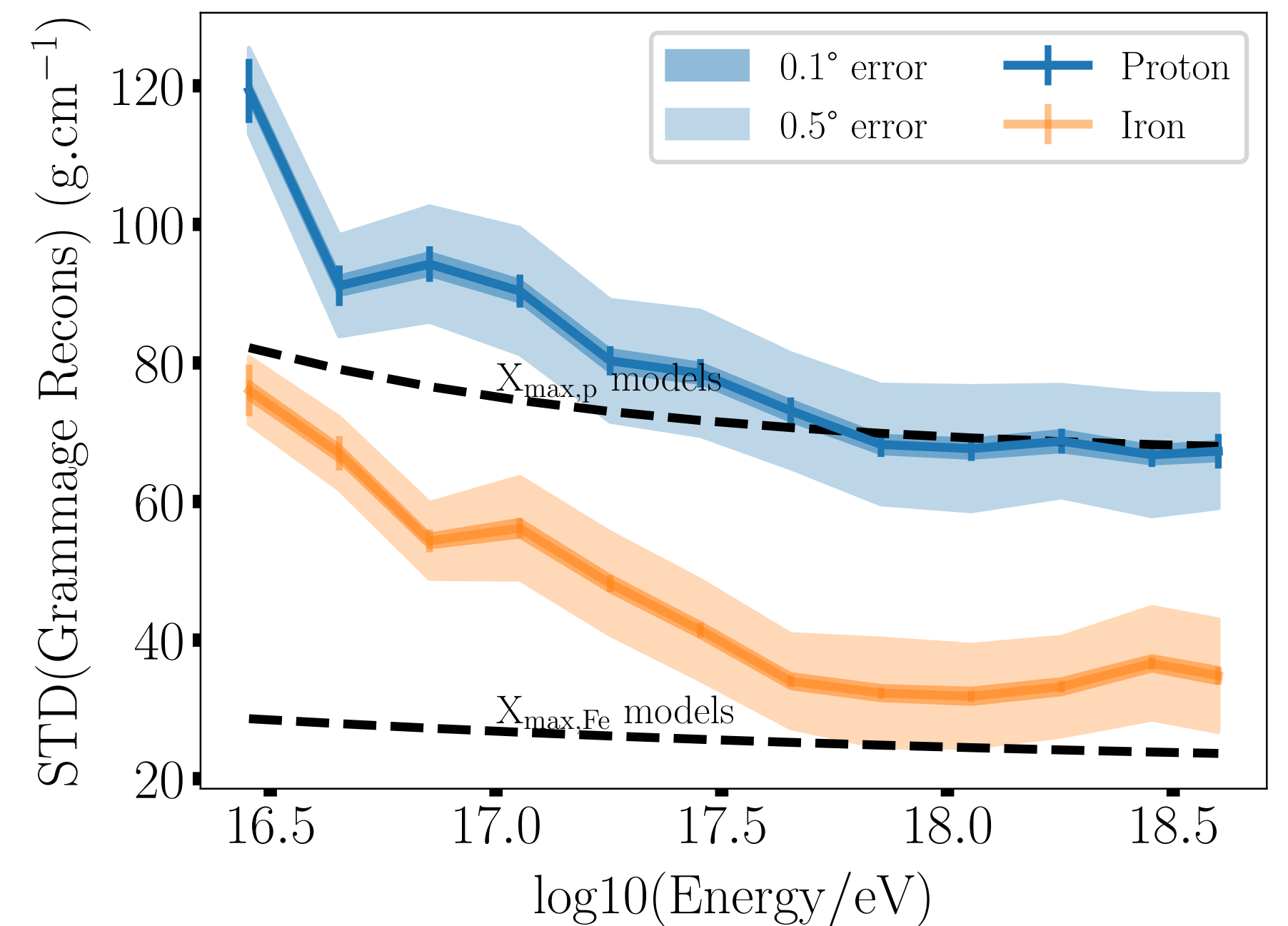
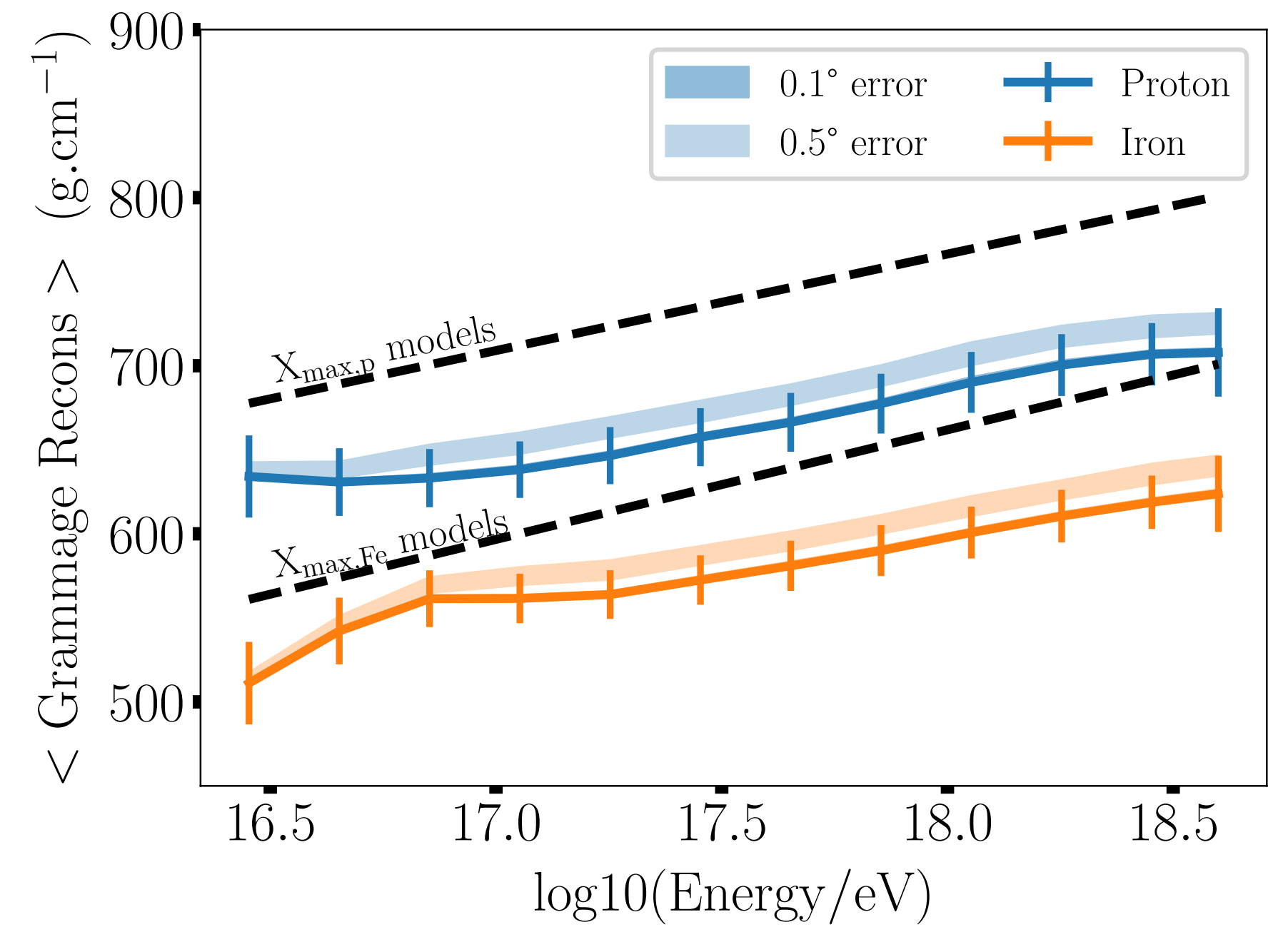


# Constraining the composition?

Indirectly we can compute:  
the atmosphere column density integral from injection to reconstructed emission point

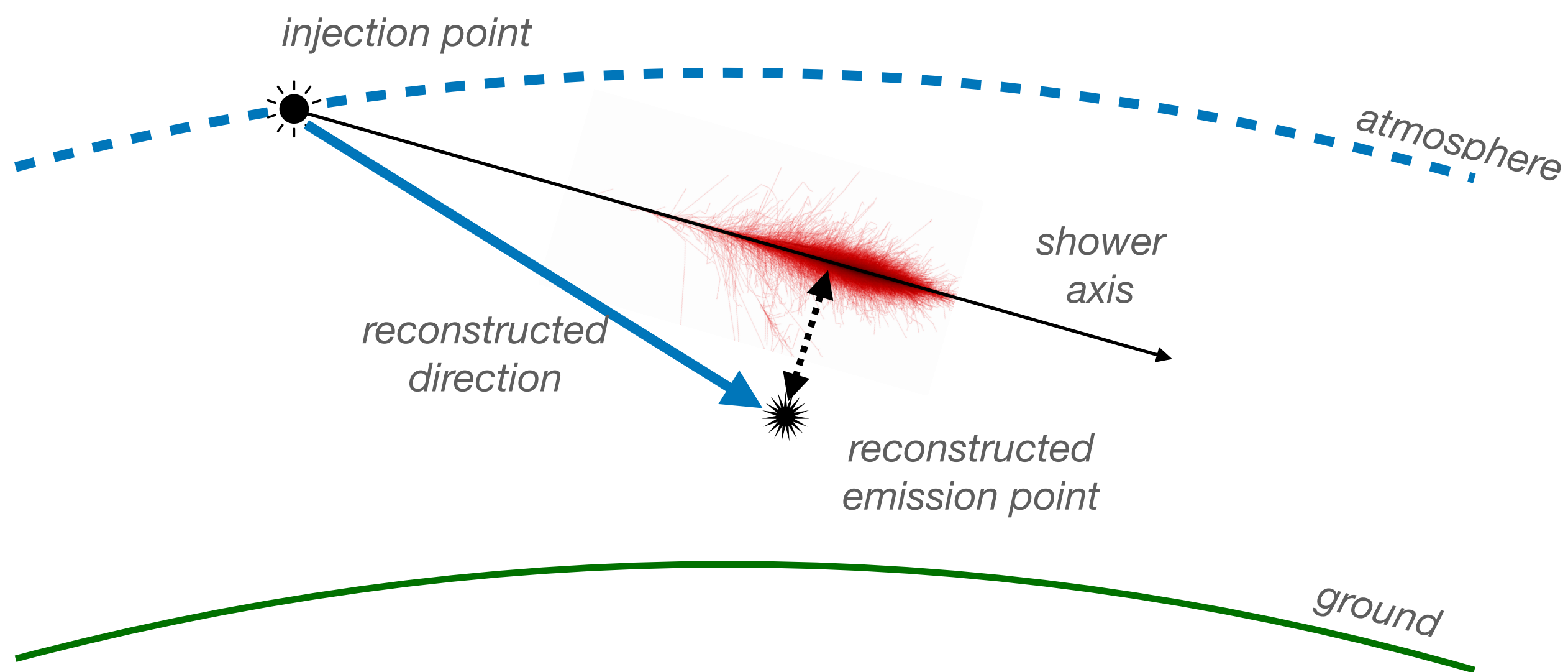


- valid proxy on the mass composition **but** different from  $X_{\max}$
- nevertheless results are compatible with standard reconstruction of  $X_{\max}$



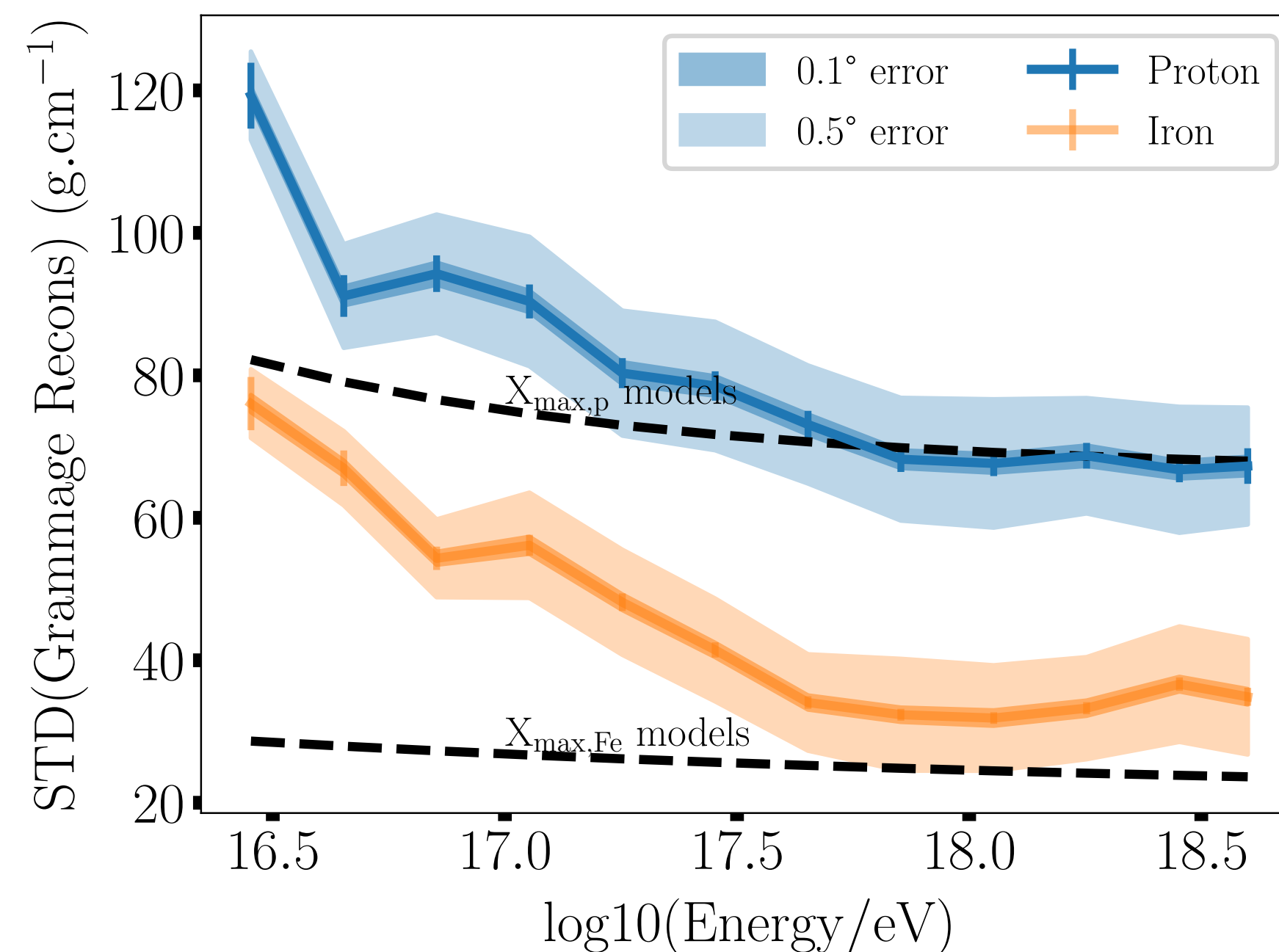
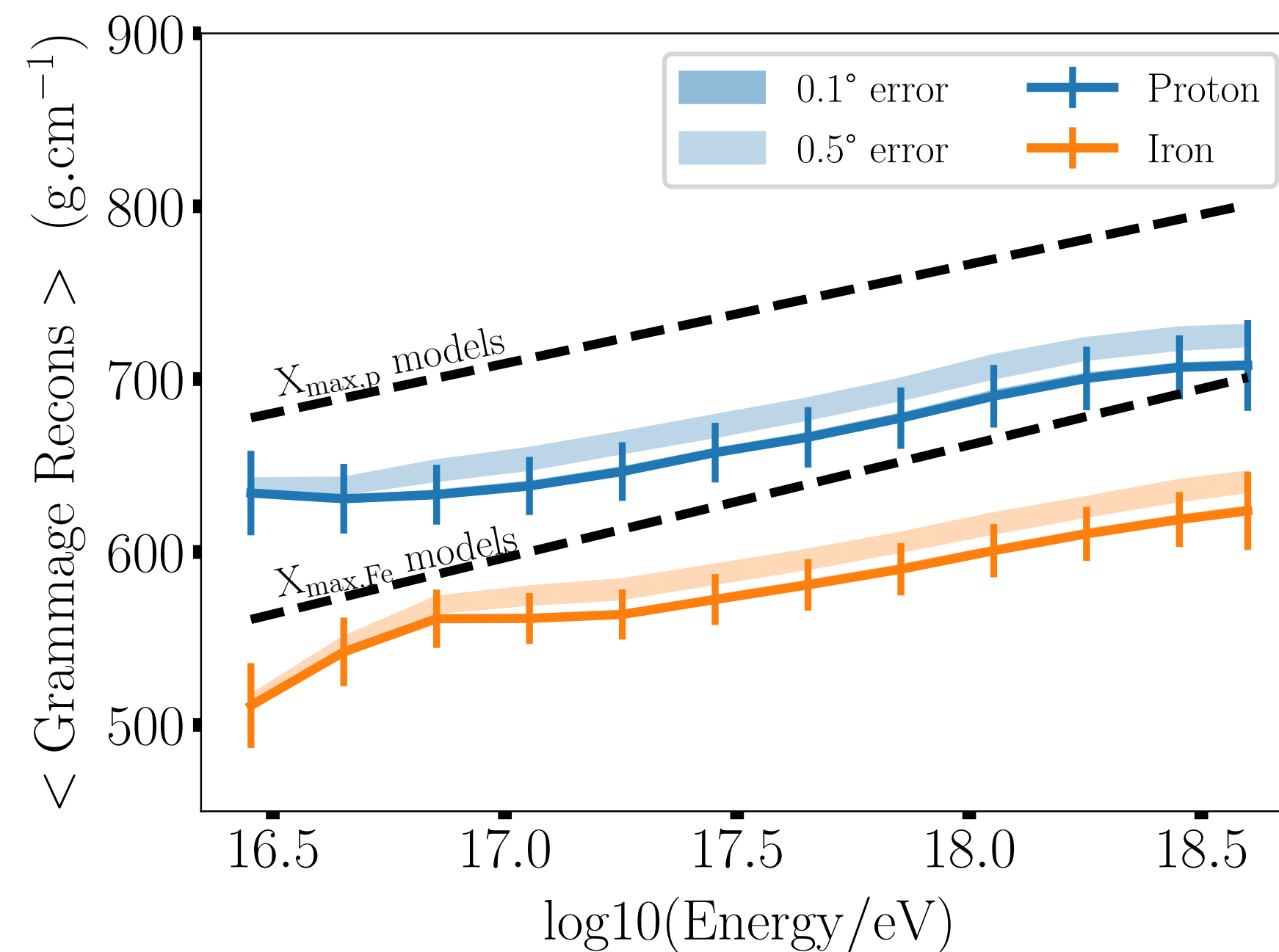
# Constraining the composition?

Indirectly we can compute:  
the atmosphere column density integral from injection to reconstructed emission point



- valid proxy on the mass composition **but** different from  $X_{\max}$
- nevertheless results are compatible with standard reconstruction of  $X_{\max}$

constraints on primary identifications comparable to particle  $X_{\max}$  method





# **Towards energy reconstruction?**

Idea is to correlate one of the fit parameter to the shower energy

# Towards energy reconstruction?

Idea is to correlate one of the fit parameter to the shower energy

From the ADF fit we directly obtain:

$$f^{\text{ADF}}(\omega, \eta, \alpha, l; \delta\omega, \mathcal{A}) = \frac{\mathcal{A}}{l} f^{\text{GeoM}}(\alpha, \eta, \mathcal{B}) f^{\text{Cerenkov}}(\omega, \delta\omega)$$



# Towards energy reconstruction?

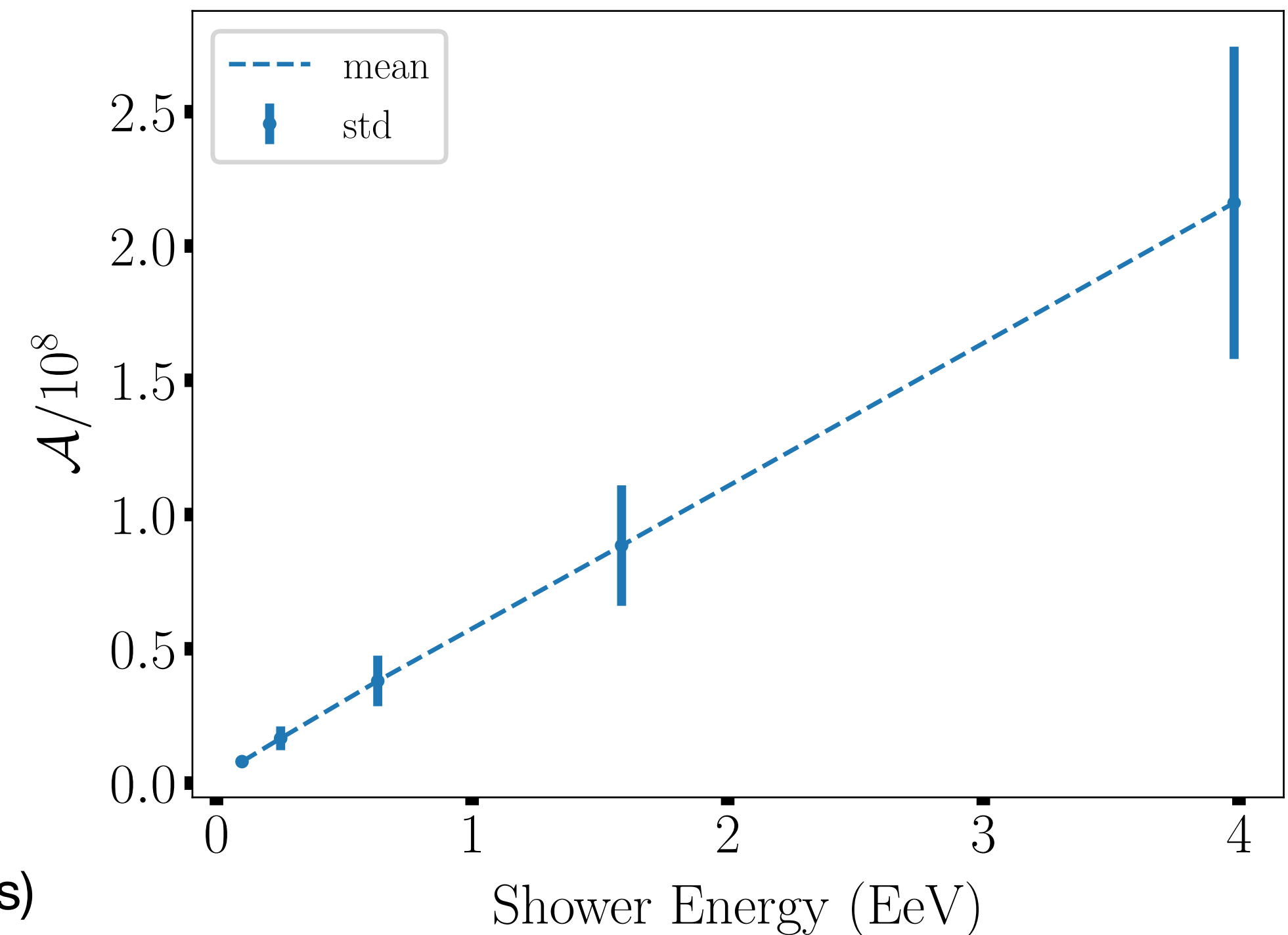
Idea is to correlate one of the fit parameter to the shower energy

From the ADF fit we directly obtain:

$$f^{\text{ADF}}(\omega, \eta, \alpha, l; \delta\omega, \mathcal{A}) = \frac{\mathcal{A}}{l} f^{\text{GeoM}}(\alpha, \eta, \mathcal{B}) f^{\text{Cerenkov}}(\omega, \delta\omega)$$

Very preliminary work:

- no detailed study done yet
- ADF refinement probably necessary to increase accuracy (cf asymmetries)



strong correlation between the amplitude term of the ADF and the energy

# Towards energy reconstruction?

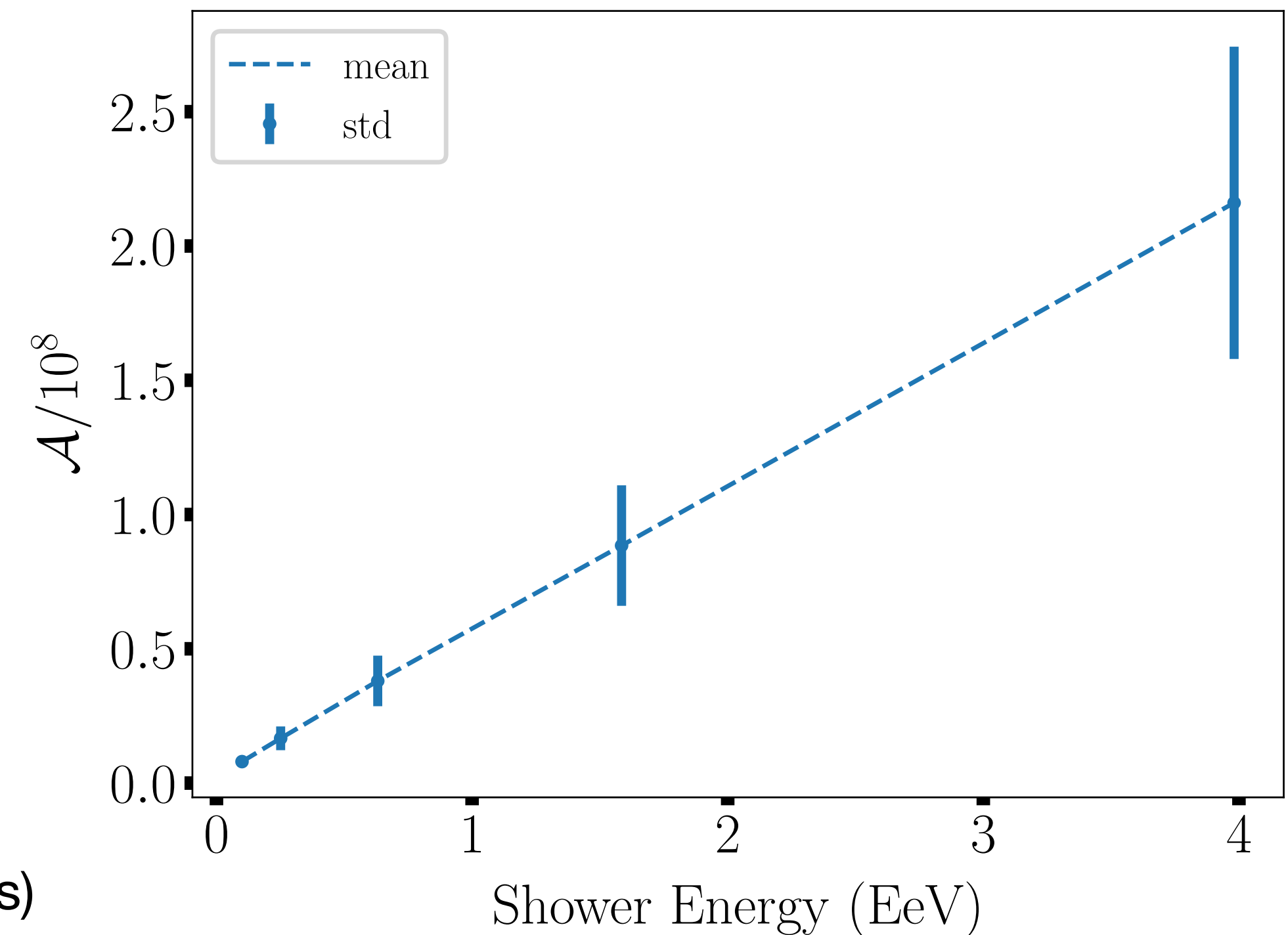
Idea is to correlate one of the fit parameter to the shower energy

From the ADF fit we directly obtain:

$$f^{\text{ADF}}(\omega, \eta, \alpha, l; \delta\omega, \mathcal{A}) = \frac{\mathcal{A}}{l} f^{\text{GeoM}}(\alpha, \eta, \mathcal{B}) f^{\text{Cerenkov}}(\omega, \delta\omega)$$

Very preliminary work:

- no detailed study done yet
- ADF refinement probably necessary to increase accuracy (cf asymmetries)



strong correlation between the amplitude term of the ADF and the energy

Good potential for energy reconstruction



# NenuFAR full spec sheet

## Array:

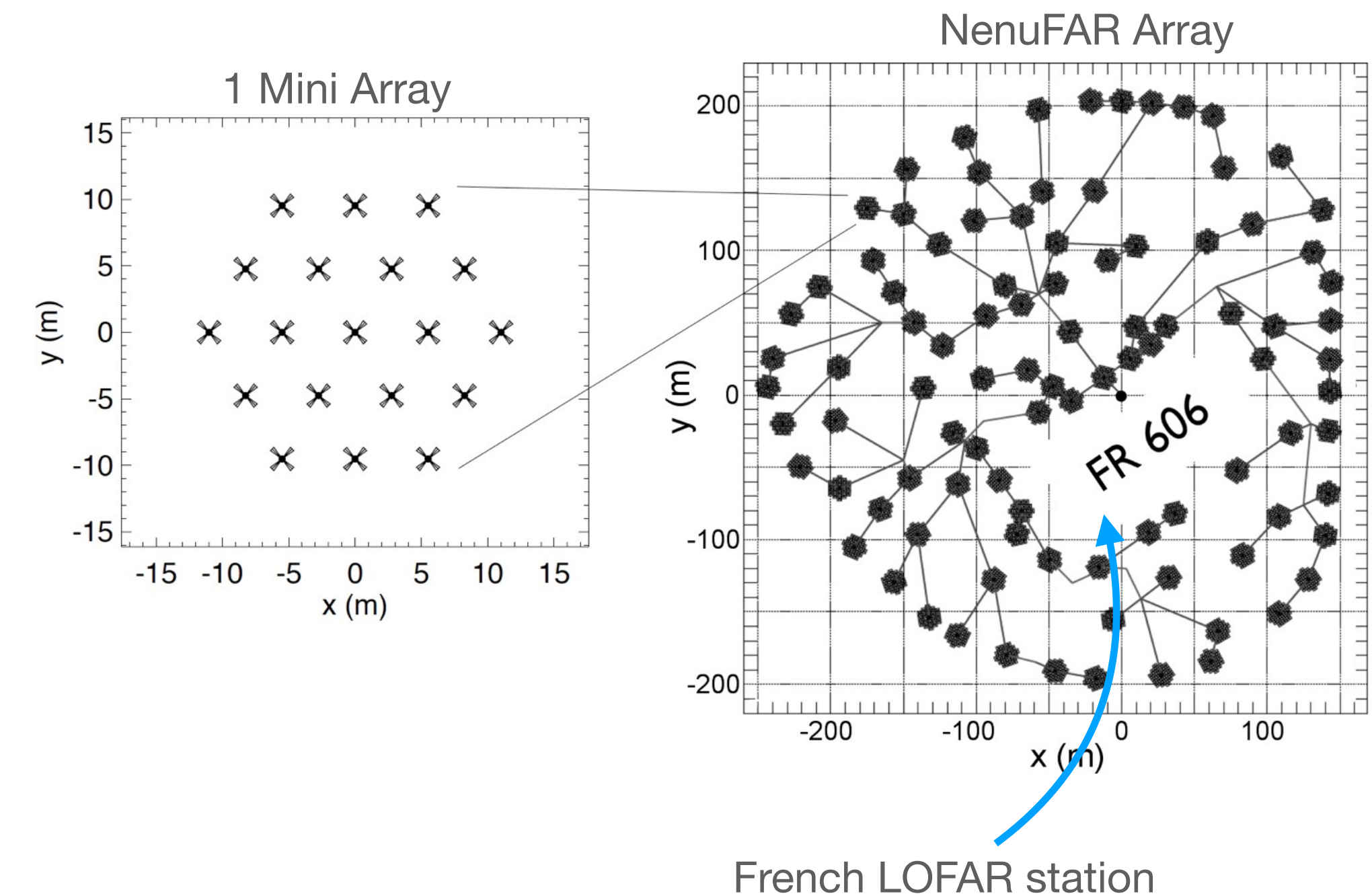
- Antennas grouped in hexagonal tiles of 19 crossed-dipoles  
→ **Mini-Arrays** -MA (5.5m antenna step)
- 4560 baselines from 25m to 400M + 591 **baselines from 400m to 3km**
- Collecting area from 88000m<sup>2</sup> at 15MHz to 8000m<sup>2</sup> at 85MHz

## Signals:

- Each MA delivers two linearly polarised signals (NE and NW) to receivers
- **Time-frequency resolution** →  $df \sim 195\text{kHz}$  and  $dt \sim 5\mu\text{s}$
- **With channelisation**  $df \rightarrow 3\text{kHz}$  with  $dt \sim 1\text{ms}$
- Waveforms at 5ns time resolution  
→ Sensitivity  $\sim 130\text{ mJy}$  at 15MHz to  $9\text{ mJy}$  at 85 MHz for  $df=10\text{MHz}$  x  $dt=1\text{h}$

Can operate in 4 distinct modes:

- **standalone beam former** → [FRB observation](#)
- capturing waveform → transient buffer
- standalone imager
- Upgraded LOFAR station (low frequency)



# NenuFAR full spec sheet

## Array:

- Antennas grouped in hexagonal tiles of 19 crossed-dipoles  
→ **Mini-Arrays** -MA (5.5m antenna step)
- 4560 baselines from 25m to 400M + 591 **baselines from 400m to 3km**
- Collecting area from 88000m<sup>2</sup> at 15MHz to 8000m<sup>2</sup> at 85MHz

## Signals:

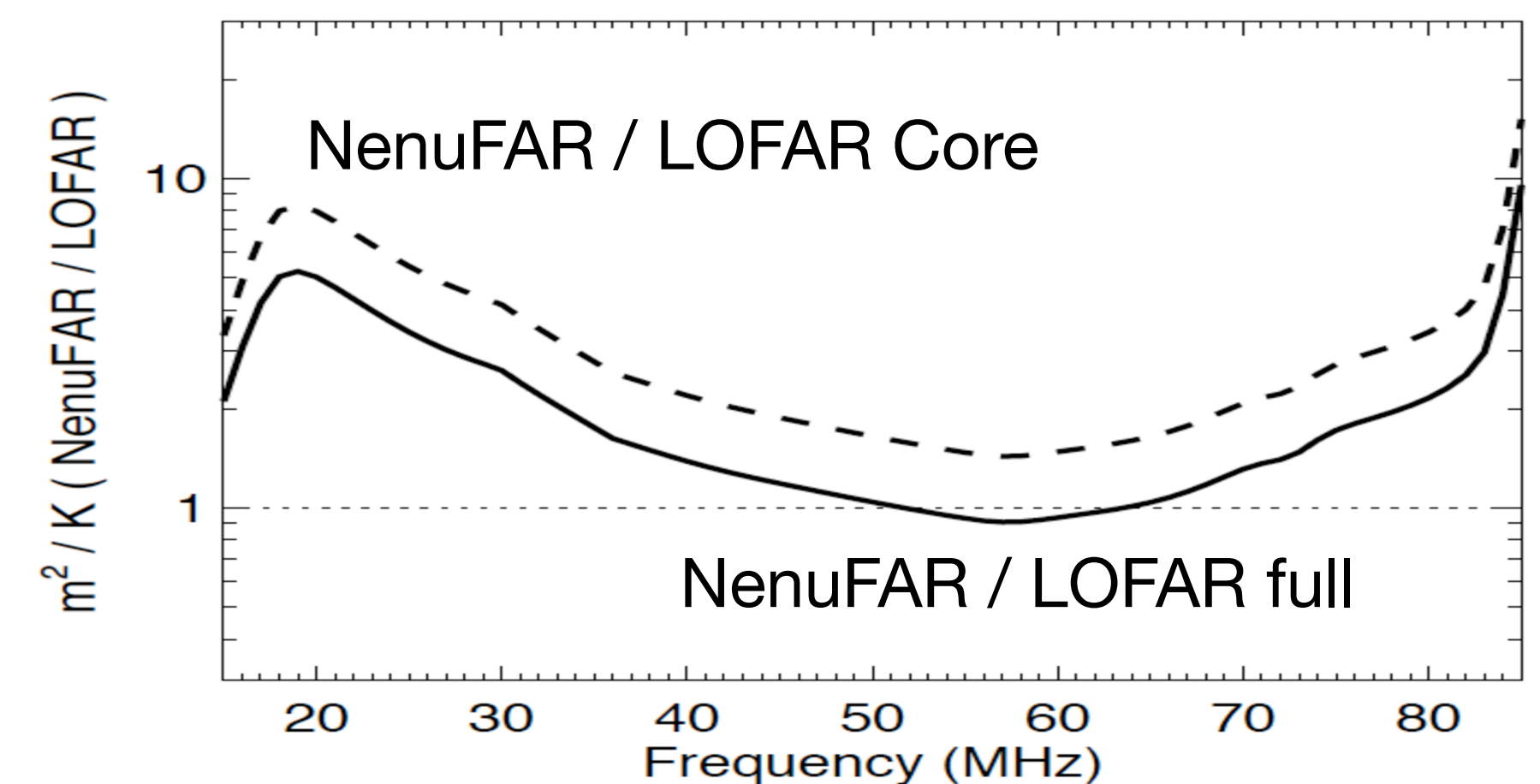
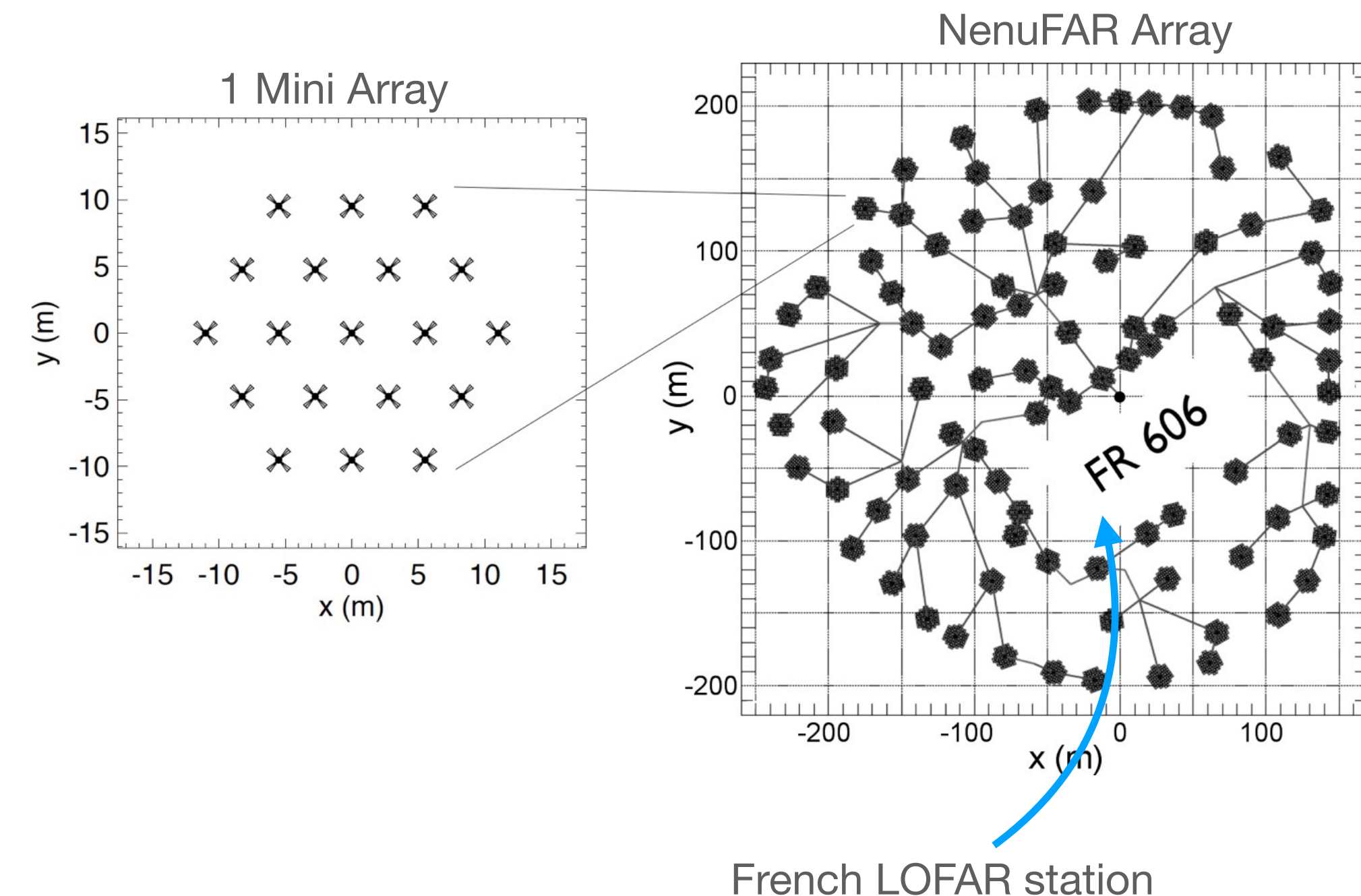
- Each MA delivers two linearly polarised signals (NE and NW) to receivers
- **Time-frequency resolution** →  $df \sim 195\text{kHz}$  and  $dt \sim 5\mu\text{s}$
- **With channelisation**  $df \rightarrow 3\text{kHz}$  with  $dt \sim 1\text{ms}$
- Waveforms at 5ns time resolution

→ Sensitivity  $\sim 130$  mJy at 15MHz to 9 mJy at 85 MHz for  $df=10\text{MHz}$  x  $dt=1\text{h}$

Can operate in 4 distinct modes:

- **standalone beam former** → [FRB observation](#)
- capturing waveform → transient buffer
- standalone imager
- Upgraded LOFAR station (low frequency)

**NenuFAR has been designed to reach the highest sensitivity at low frequencies**

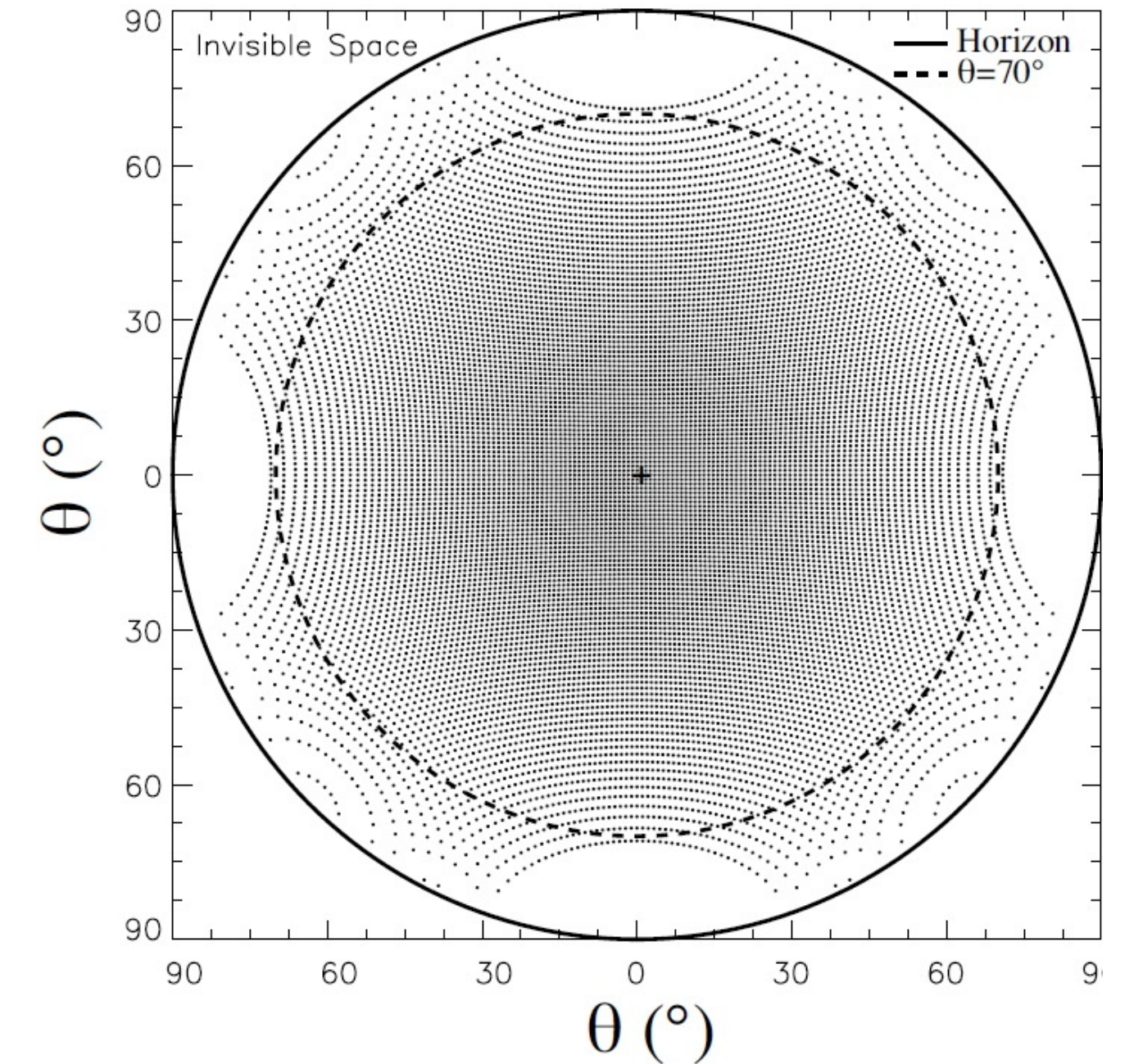
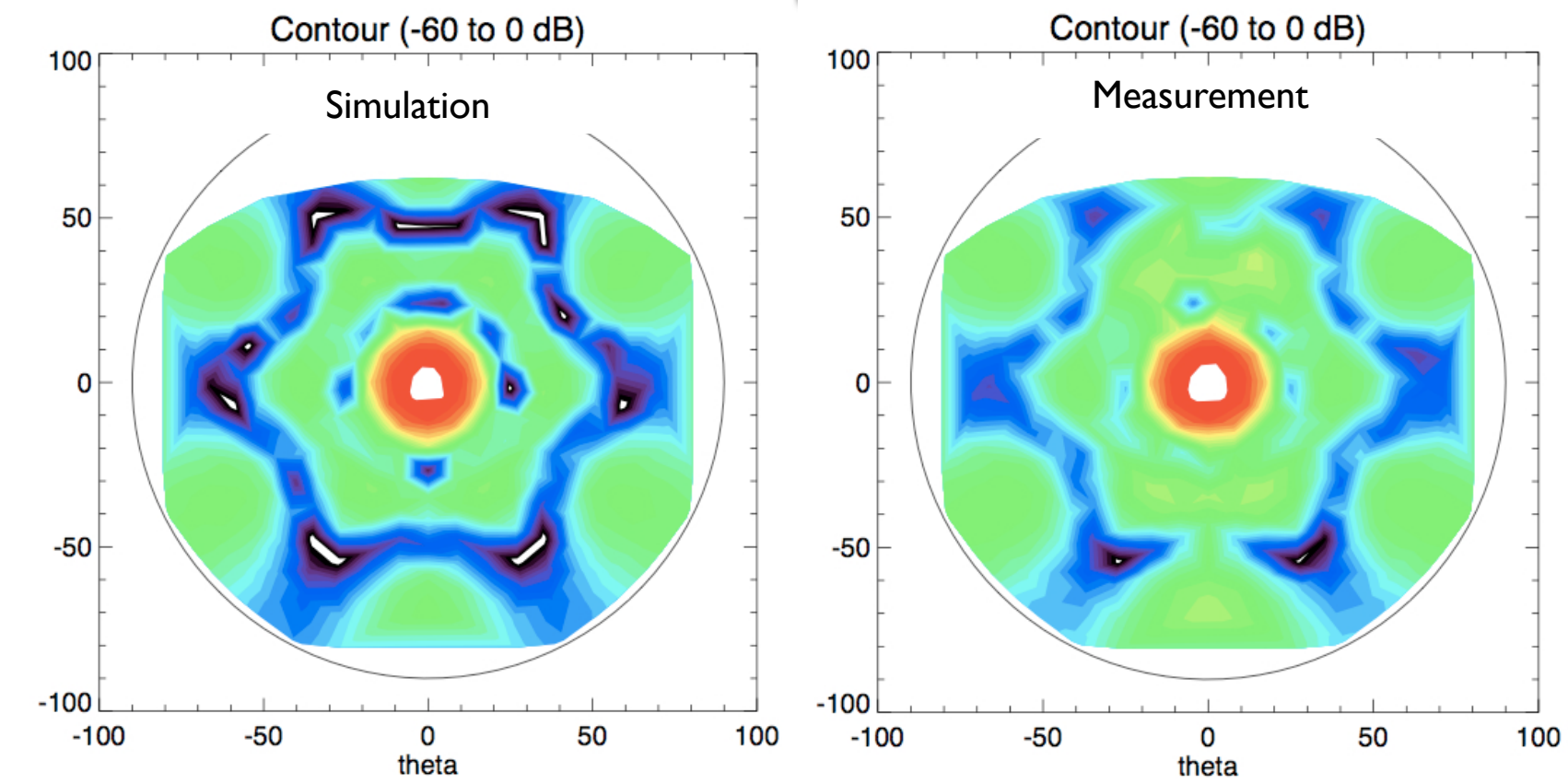
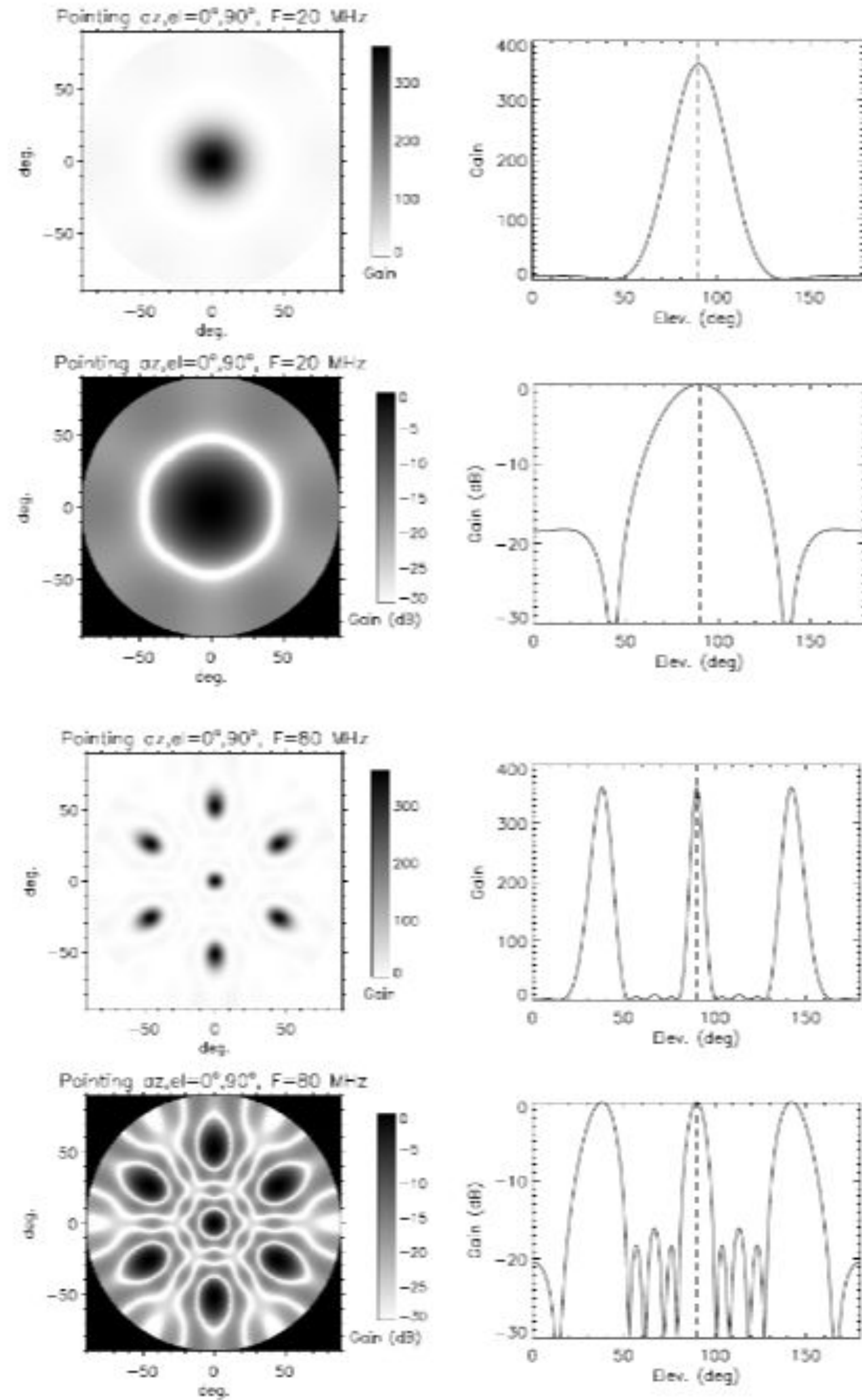




# NenuFAR interferometric mode

## Interferometric measurements:

- In each MA signals are combined through analog phasing + summation system → beam (restrict FoV but higher sensitivity)
- MA are analog phased with delay lines → achromatic
- Delay lines are 7-bit systems of switchable cables → 16384 pointable directions (128x128 = EW x NS) in the sky
- Pointing from declination  $-23^\circ$  to  $+90^\circ$
- FoV  $\sim 46^\circ$  at 15MHz to  $\sim 8^\circ$  at 85MHz
- Angular resolution 23' at 15MHz to 4' at 85MHz (down to 0.4" in LSS mode)





# NenuFAR computing and data storage

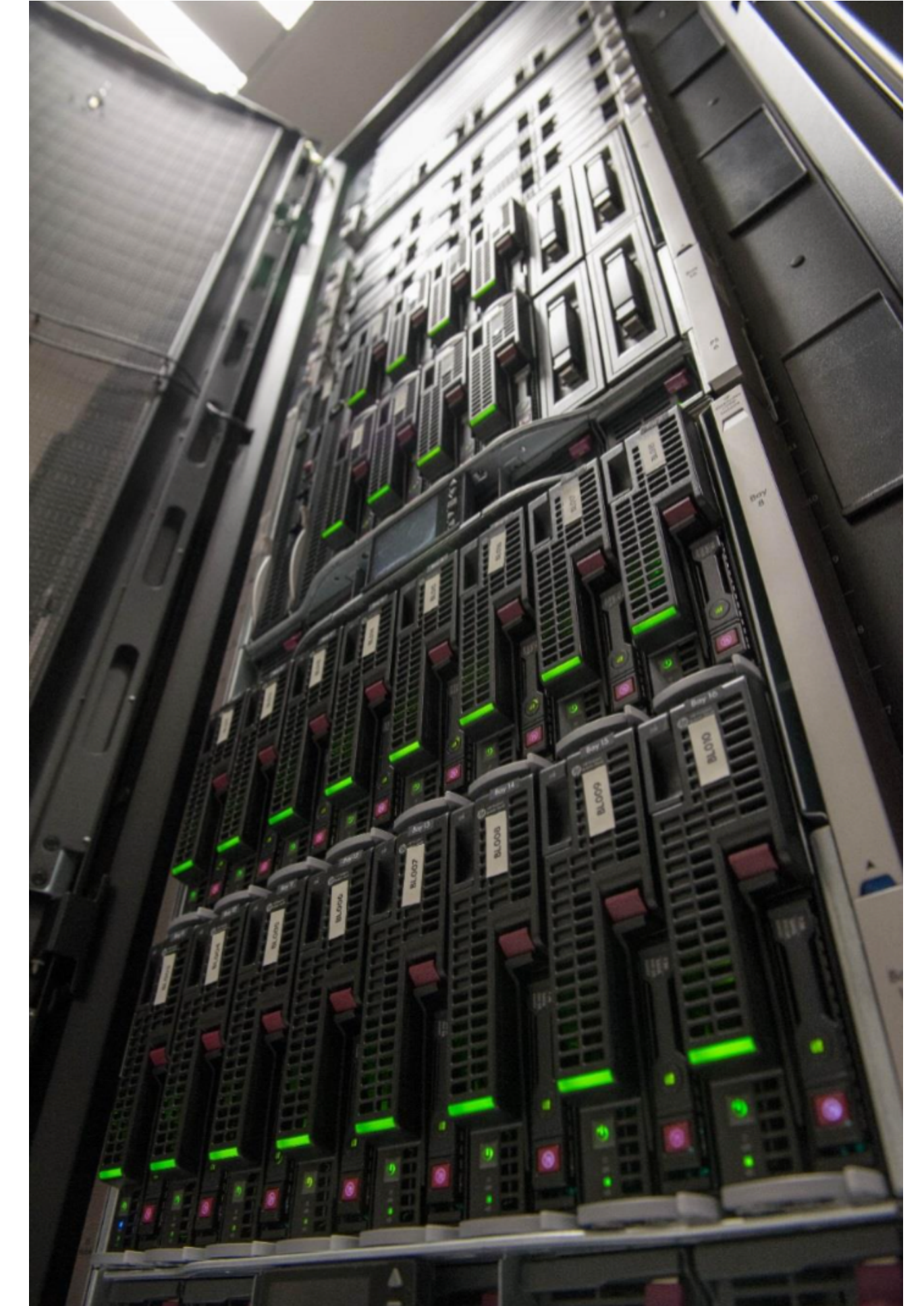
---

## Data Centers:

- L0 data ~5-10To/day → Nancay data center (1Po) for reduction
- L1 data ~1-2Po/year → NenuFAR data center (10Po) for analysis and final storage (L2 data)

## NenuFAR data center:

- BRGM cloud technology
- Virtual machine/virtual observatory/GUI NenuFAR
- Space storage and computing power extensions
- Connection to high performance computation centers
- Cost ~2.2M€
- Test bench for SKA-Regional-Center

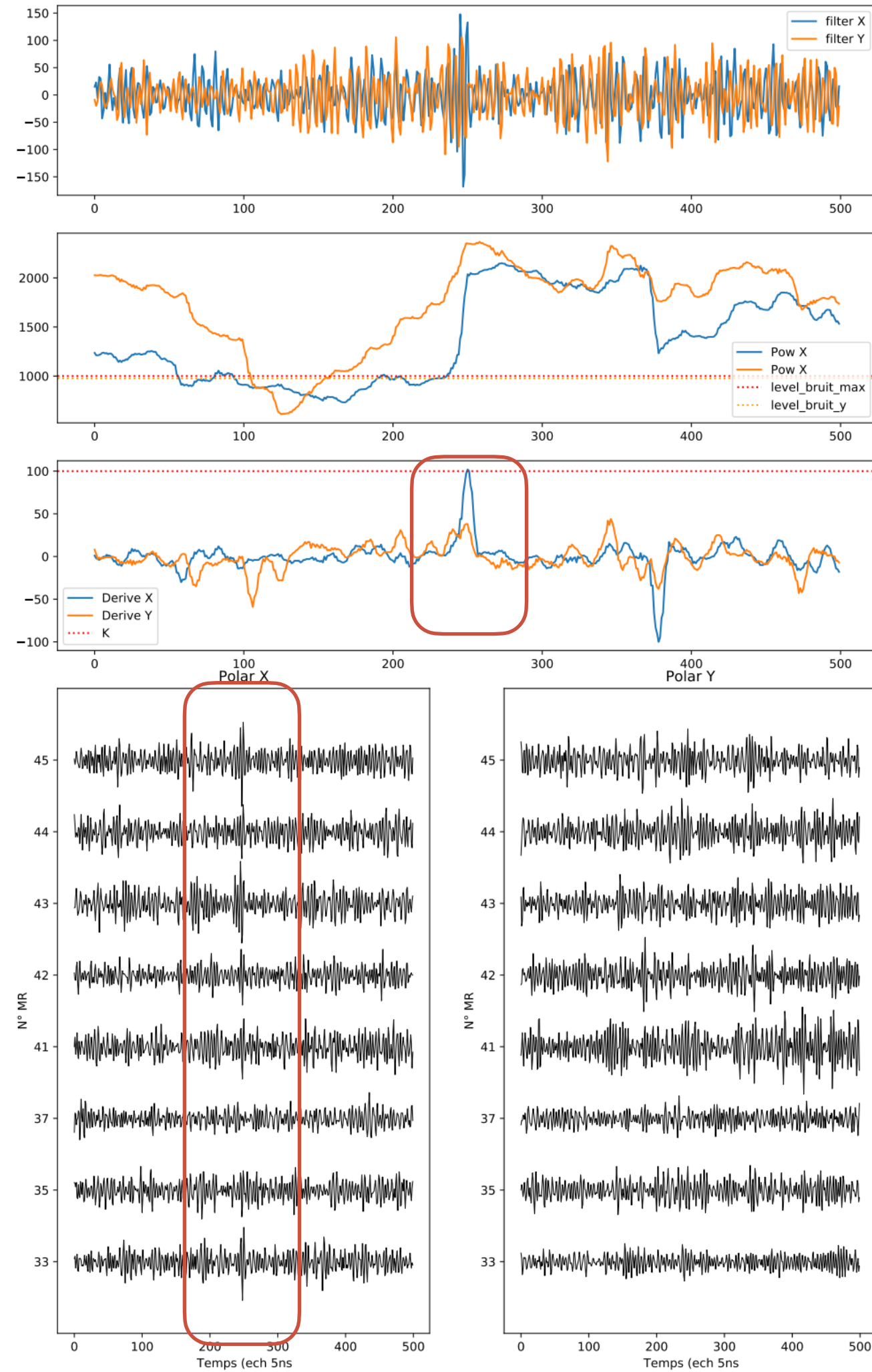




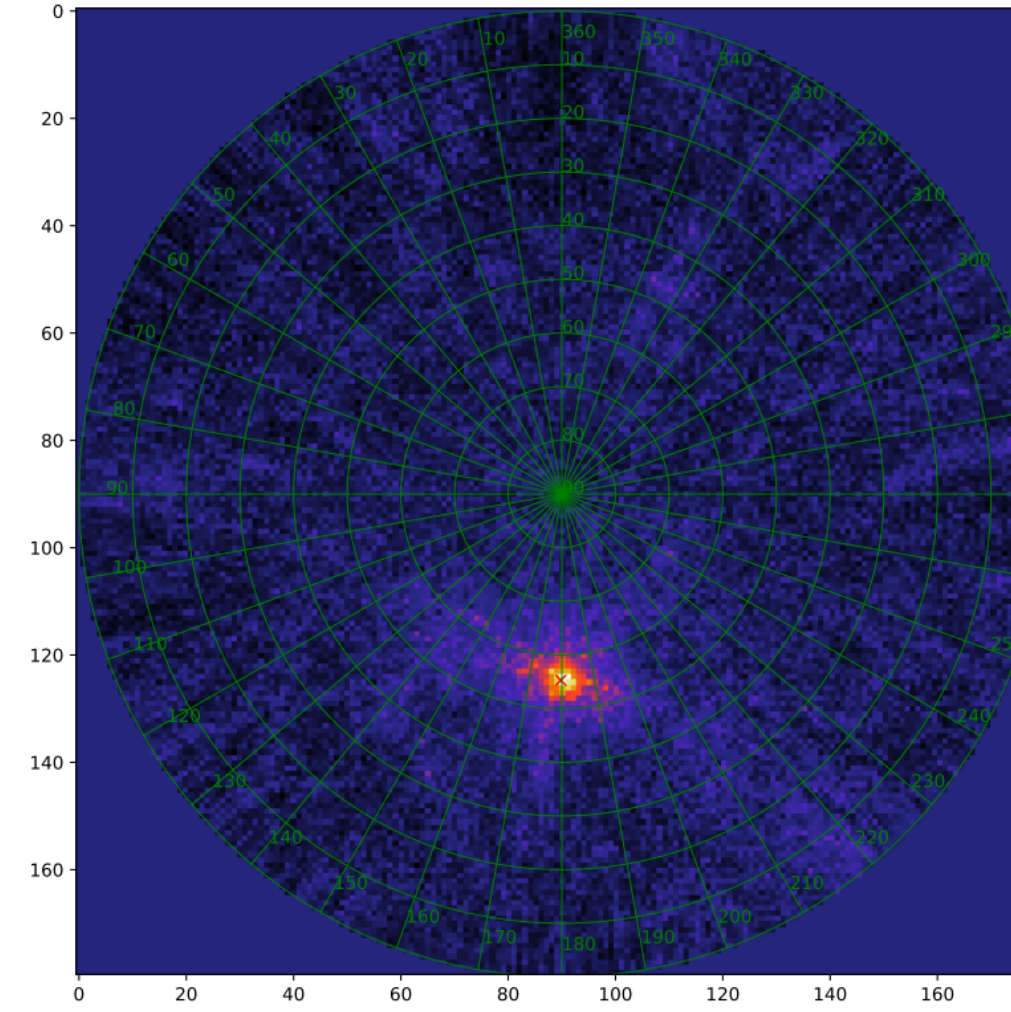
# RadioGaGa: radio detection of gamma-ray EAS

Idea:

- use a subset of MA
- to survey the sky
- trigger on impulsive signals
- retrieve all MA signals



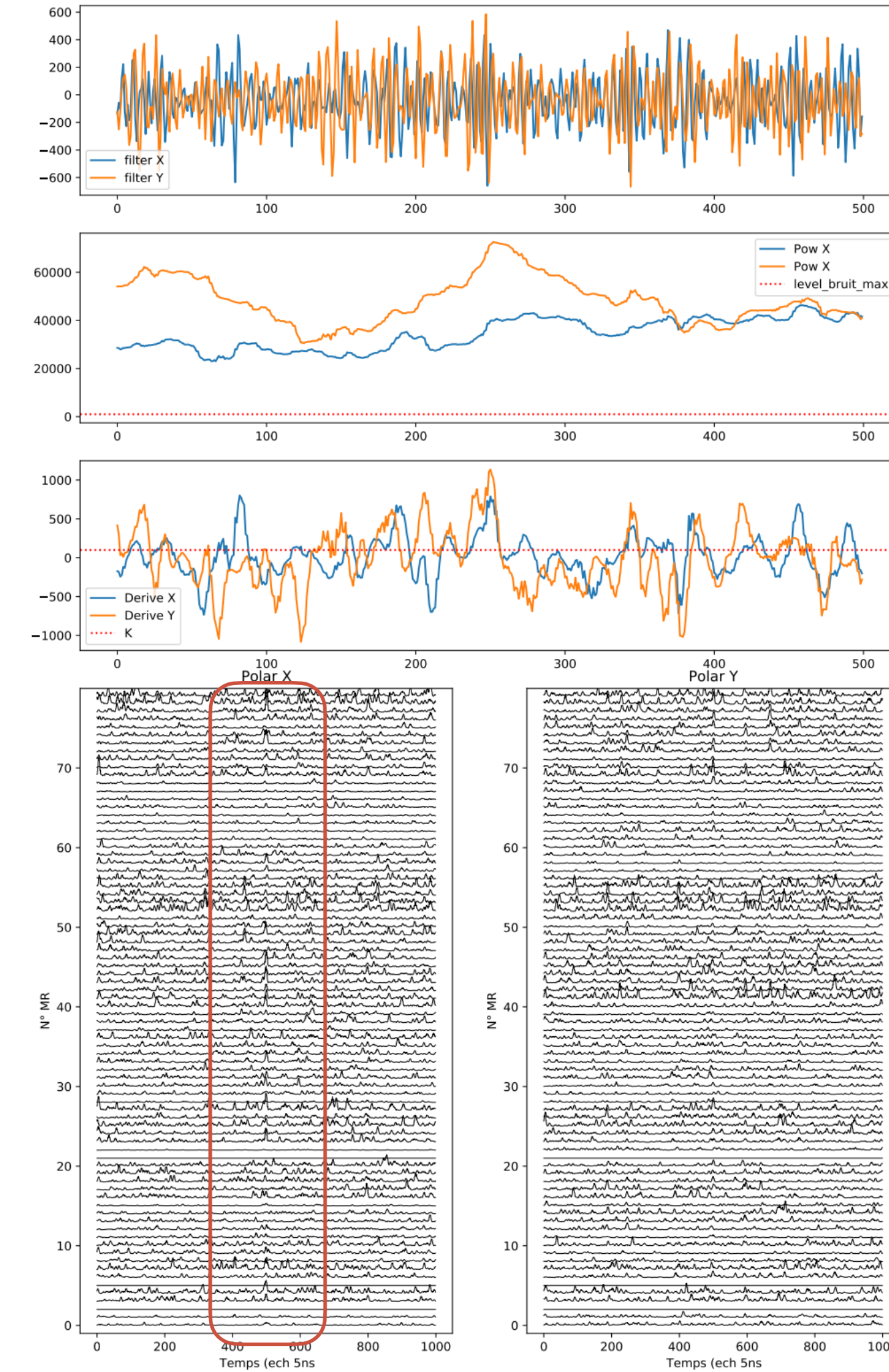
MA used for trigger



```
#####PARAMETERS#####
'k1': [100, 100]
'k2': [0, 0]
'rising_time_min': [1, 1]
'rising_time_max': [5, 5]
>window_w': 128
'level_bruit_max': 1000
'pourcent_20': [18.75, 18.75]
'pourcent_80': [87.5, 87.5]
'polar_min': 0
'polar_max': 0
'binary_test': 0

#####PROCESSED#####
'max': [0, 2106]
'max_20': [0, 1187]
'max_80': [0, 1964]
'level_bruit': [0, 976]
'rising_time': [0, 5]
'polar_rapport': 0

#####INFOS#####
'hdr': b"!T4!"
'cnt': 492033
'gps_second': 1660823592
'gps_nano': 877827790
'utc_second': 1660823592
'utc_nano': 877824790
'tbb_second': 1660823592
'tbb_nano': 877819780
'nb_ech': 16384
'FPGA_ver': '0x20210615'
'struc_ver': '1.00'
'MR_list': (33, 35, 37, 41, 42, 43, 44, 45)
```



all MA



# **Multi-messenger (MM) and multi-wavelength (MW) high energy sources**

**There is already many hints toward the connections between radio transients and MM emissions**



# **Multi-messenger (MM) and multi-wavelength (MW) high energy sources**

**There is already many hints toward the connections between radio transients and MM emissions**

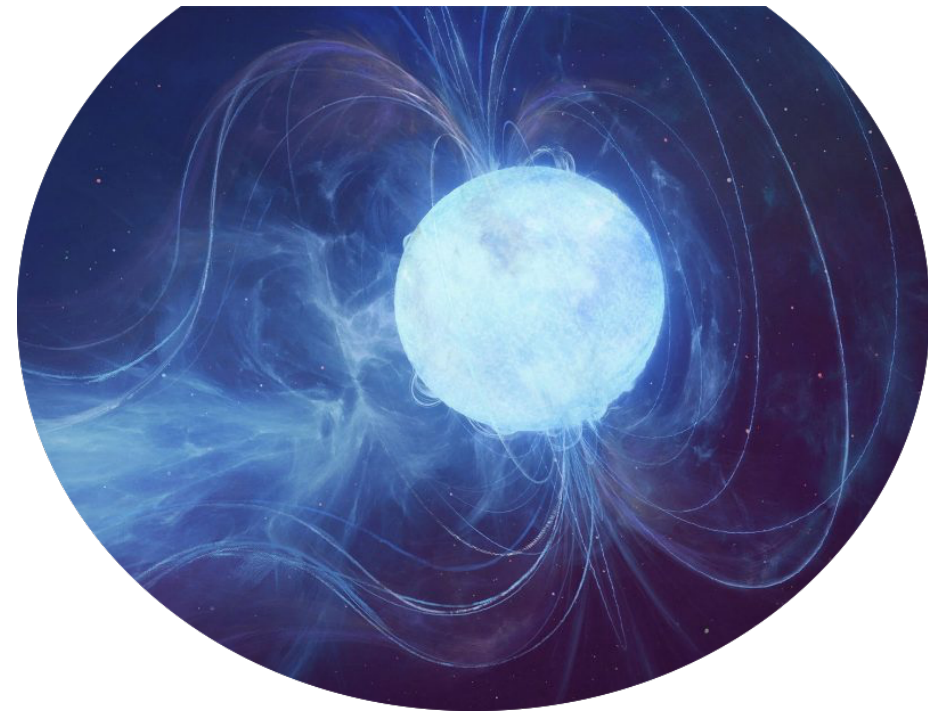
- jets/accretion-disks and kilonova**
- highly magnetic environments / winds / outflows**

# Multi-messenger (MM) and multi-wavelength (MW) high energy sources

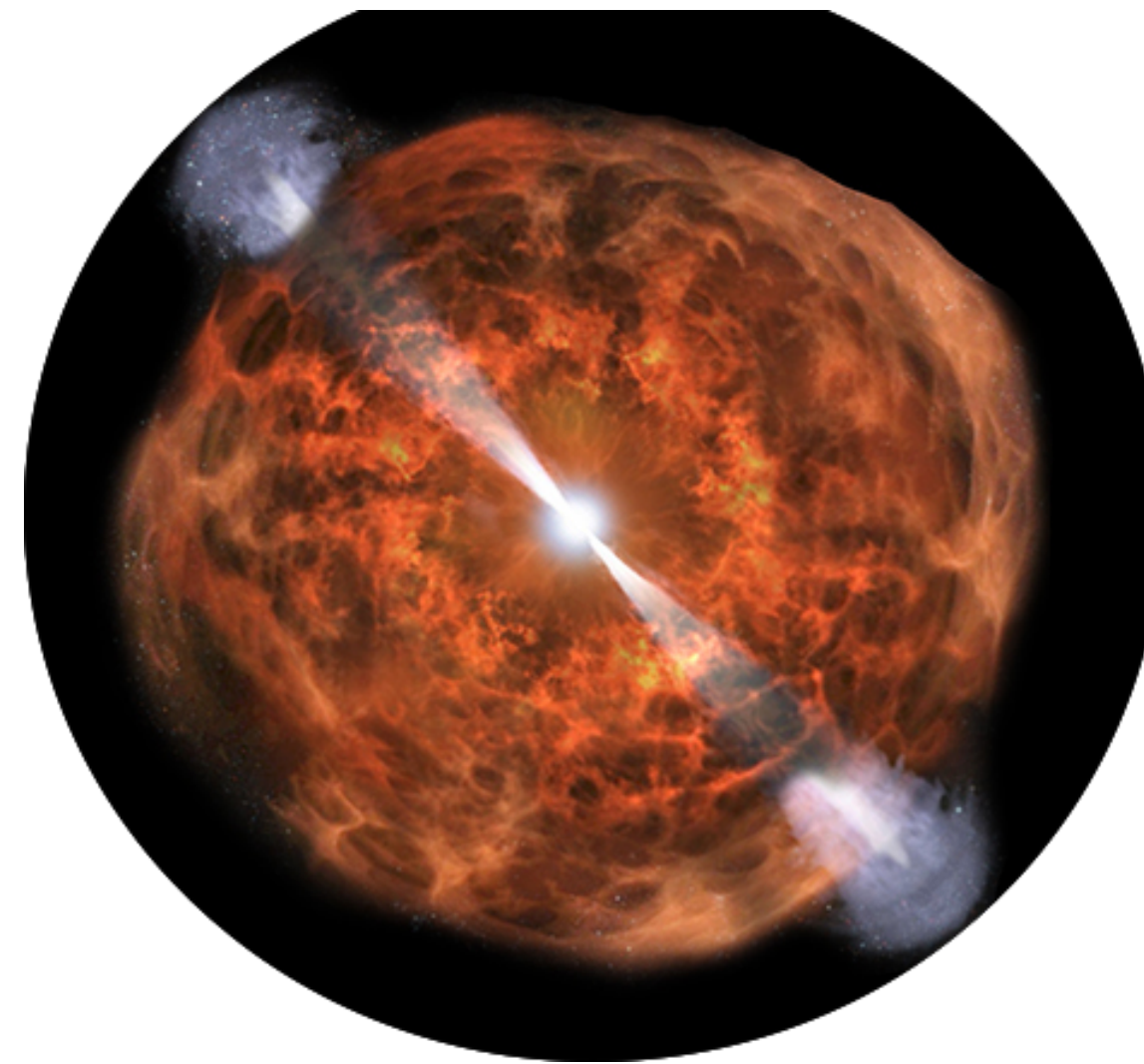
There is already many hints toward the connections between radio transients and MM emissions

- jets/accretion-disks and kilonova
- highly magnetic environments / winds / outflows

**Magnetars**



**Kilonova**



**Coalescence**



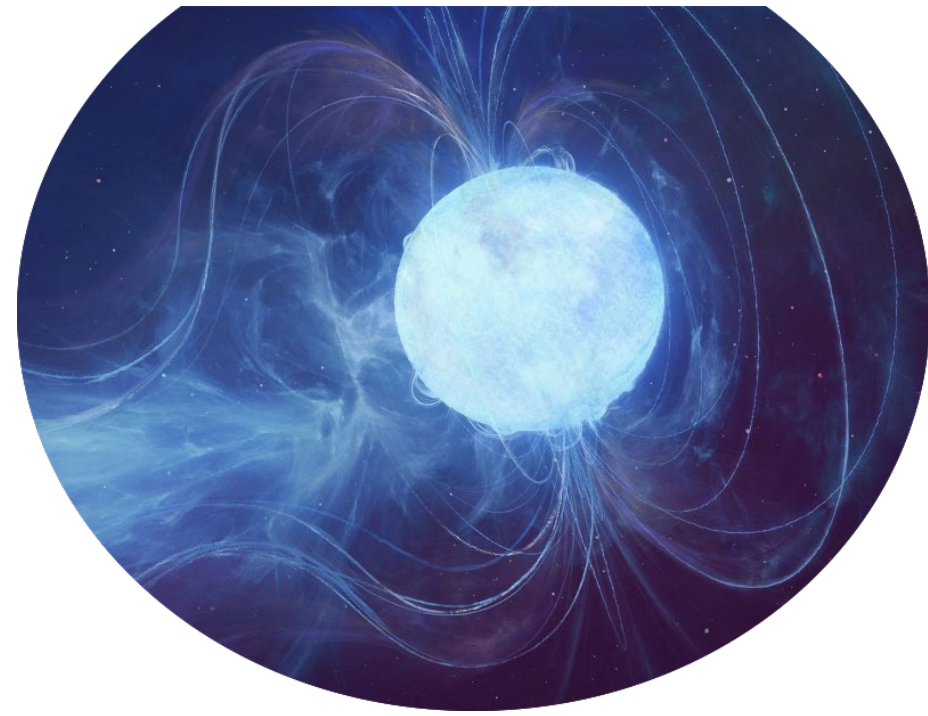


# Multi-messenger (MM) and multi-wavelength (MW) high energy sources

There is already many hints toward the connections between radio transients and MM emissions

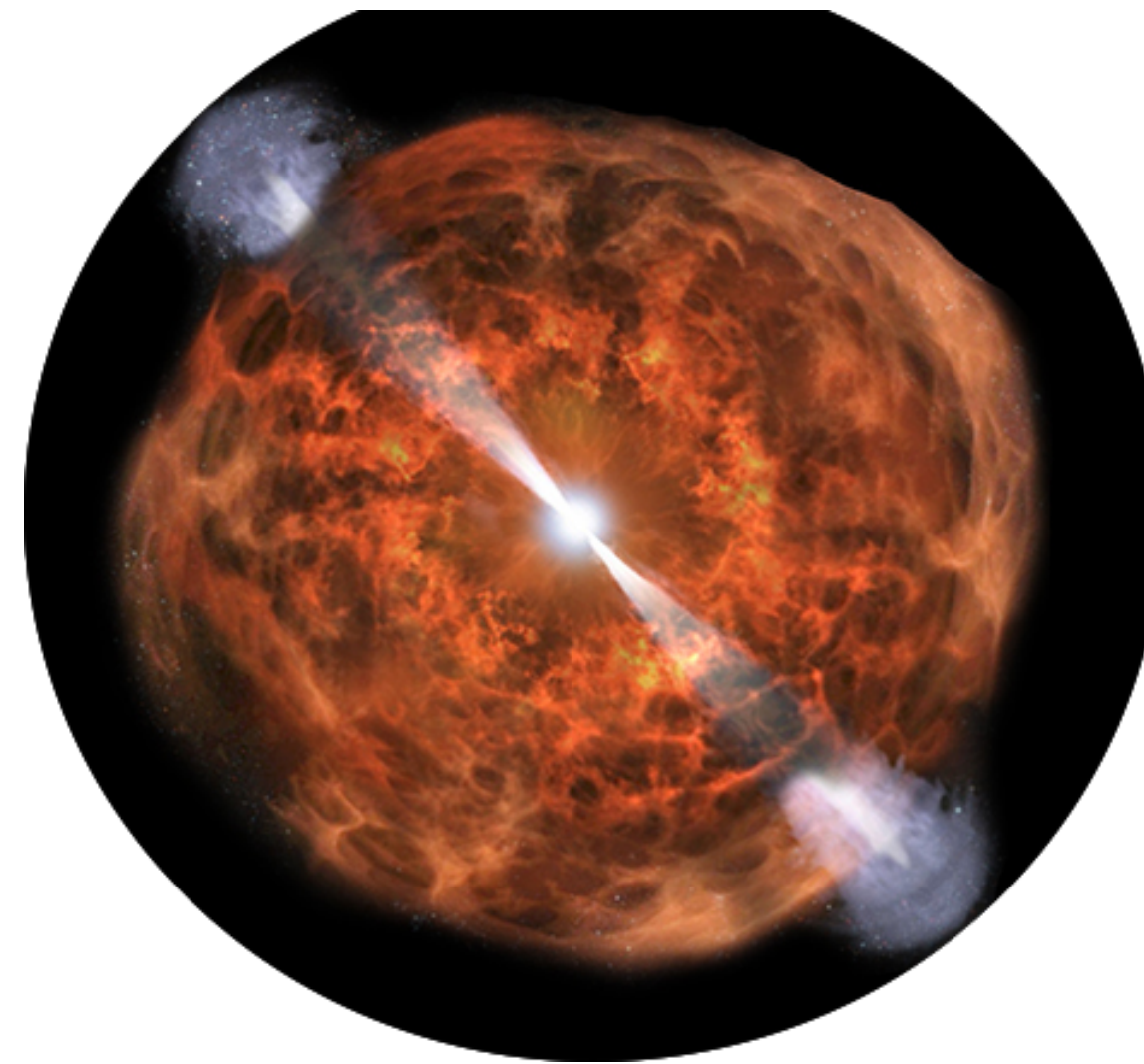
- jets/accretion-disks and kilonova
- highly magnetic environments / winds / outflows

## Magnetars



- Progenitors: neutron stars
- Models: Gamma-rays/radio
- observations: X-ray/radio

## Kilonova



- Progenitors: DNS, WD mergers, NS-WD, NS-BH
- Models: GW/Gamma-rays/neutrinos
- Observations: GW/Gamma-rays

## Coalescence



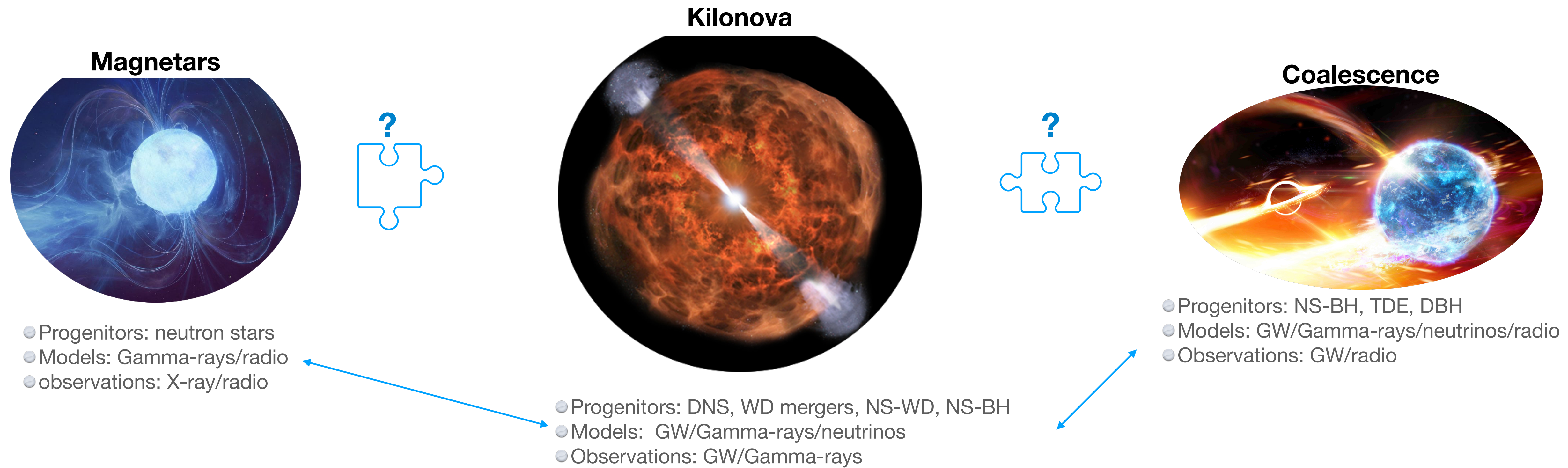
- Progenitors: NS-BH, TDE, DBH
- Models: GW/Gamma-rays/neutrinos/radio
- Observations: GW/radio



# Multi-messenger (MM) and multi-wavelength (MW) high energy sources

There is already many hints toward the connections between radio transients and MM emissions

- jets/accretion-disks and kilonova
- highly magnetic environments / winds / outflows



We need to have MM and MW models in order to probe the physics consistently